



United States Department of Agriculture

**Agricultural
Research
Service**

**Agriculture Handbook
Number 727**

August 2020

Wind Erosion Prediction System (WEPS): Technical Documentation

Wind Erosion Prediction System (WEPS): Technical Documentation

United States Department of Agriculture

Agricultural Research Service

Agriculture Handbook Number 727

August 2020

Volume Citation:

USDA-ARS. 2020. The Wind Erosion Prediction System (WEPS): Technical Documentation, J. Tatarko (Ed.). USDA Agriculture Handbook 727. United States Department of Agriculture, Agricultural Research Service, Beltsville, MD. 533 pp. Available in digital only.

Chapter Citation (example):

Tatarko, J. and L.E. Wagner. 2020. Introduction to the Wind Erosion Prediction System (WEPS). In: The Wind Erosion Prediction System (WEPS): Technical Documentation, J. Tatarko (Ed.). USDA Agriculture Handbook 727:1-12. United States Department of Agriculture, Agricultural Research Service, Beltsville, MD. Available in digital only.

Preface

The Wind Erosion Prediction System (WEPS) is a computer model designed to simulate wind erosion processes on cultivated agricultural lands. WEPS incorporates nearly 70 years of wind erosion research by the U.S. Department of Agriculture (USDA) to provide accurate and universal simulations of soil loss by wind and represents superior wind erosion prediction technology over previous prediction methods. In addition to providing improved estimates of soil loss, WEPS partitions loss, transport, and deposition into coarse (creep + saltation) and fine (suspension) size classes to account for the unique characteristics of each size to enable evaluations of their respective effects on the soil and surrounding environment. It also provides the amounts of loss by direction for each size class for offsite soil, air, and water quality assessments. WEPS models the field surface state and wind erosion as physically based processes as much as possible. It operates on a daily-time step to simulate soil surface erodibility as affected by soil, land management, and stochastically simulated weather. The strongest utility of WEPS is its ability to apply different “what-if” management scenarios to the land to develop alternatives for wind erosion control.

WEPS is a critical component of the USDA strategy to reduce particulate emissions from cultivated agricultural lands and was designed primarily for use by USDA Natural Resources Conservation Service (NRCS) to (1) assist land managers in developing farming systems to control wind erosion, (2) establish acceptable field-level conservation plans, and (3) determine wind erosion susceptibility as part of the Conservation Reserve Program (CRP) and other national programs. NRCS uses the model to evaluate erosion potential on 14 million hectares (35 million acres) of land where conservation practices are applied. Other users of WEPS include national, State, and local government agencies, universities, scientists, managers of disturbed lands, and individual farmers. WEPS has been applied in a variety of research studies including predicting the dispersion of fine dust over large regions, development of control strategies for non-croplands, geographic information system (GIS) regional applications, assessing sustainable removal of residues, and predicting erosion from military training lands. In addition to the United States, WEPS has been applied worldwide including in Argentina, Burkina Faso, Canada, China, Germany, Mexico, Niger, and Sweden. The model erosion component has been extensively validated in the literature with good agreement between measured and predicted values. A list of WEPS-related peer-reviewed publications is included at the end of this Handbook.

This USDA Agriculture Handbook is a technical reference that provides a complete description of the wind erosion and other science contained within the WEPS model. While the WEPS model is continually being improved and updated, this document is written primarily for WEPS version 1.3.9 (often referred to as “WEPS 1.0” throughout this Handbook). However, much of the science described herein will apply to future versions of the model as well. The WEPS and the companion Single-event Wind Erosion Evaluation Program (SWEEP) models, along with user manuals and other documentation, are available as part of the WEPS download at:
<https://www.ars.usda.gov/services/software/download.htm?softwareid=415>.

WEPS represents a significant body of work by USDA Agricultural Research Service (ARS) scientists and collaborators and it supports an overall ARS goal of increasing

agricultural productivity while reducing the environmental impacts of agriculture. As such, WEPS potentially can make an impact to the sustainable food and fiber supply for U.S. and world populations.

John Tatarko

Soil Scientist

USDA-ARS-Rangeland Resources and Systems Research Unit

Fort Collins, Colorado, USA

Contents

Preface

Table of Contents

Chapter 1: Introduction to the Wind Erosion Prediction System (WEPS)

J. Tatarko and L.E. Wagner

Chapter 2: A History of Wind Erosion Prediction Models in the U. S. Department of Agriculture, Part 1: Prior to the Wind Erosion Prediction System

J. Tatarko, M.A. Sporcic, and E.L. Skidmore

Chapter 3: A History of Wind Erosion Prediction Models in the U.S. Department of Agriculture, Part 2: The Wind Erosion Prediction System (WEPS)

L.E. Wagner

Chapter 4: Weather Generators of WEPS

S.J. van Donk, J. Tatarko, E.L. Skidmore, L.E. Wagner, and F. Fox

Chapter 5: Erosion Submodel of WEPS

L.J. Hagen and F.A. Fox

Chapter 6: Hydrology Submodel of WEPS

F.A. Fox, A.A. Durar, and E.L. Skidmore

Chapter 7: Management Submodel of WEPS

L.E. Wagner and F.A. Fox

Chapter 8: Soil Submodel of WEPS

L.J. Hagen

Chapter 9: Crop Submodel of WEPS

F. Fox and A. Retta

Chapter 10: Residue Decomposition Submodel of WEPS

S.J. van Donk, J.L. Steiner, and H.H. Schomberg

Chapter 11: Inputs and Command Line Arguments for WEPS

L.E. Wagner

Chapter 12: Single Storm Applications of WEPS and the Single-event Wind Erosion Evaluation Program (SWEEP)

J. Tatarko

Chapter 13: Future Work and Uses of WEPS

L.E. Wagner

Appendix A: Contributing Authors and Affiliations

Appendix B: List of WEPS-Related Peer-Reviewed Publications

Introduction to the Wind Erosion Prediction System (WEPS)

Contributors:

J. Tatarko
L.E. Wagner

Abstract

The Wind Erosion Prediction System (WEPS) was developed by a multidisciplinary team of U.S. Department of Agriculture (USDA) scientists in collaboration with other agencies and private cooperators in response to customer requests, primarily those of USDA Natural Resources Conservation Service (NRCS), for improved wind erosion prediction technology. WEPS is designed to provide estimates of soil loss by wind from cultivated, agricultural fields and is intended to replace the predominately empirical Wind Erosion Equation (WEQ) as a prediction tool for those who plan soil conservation systems, conduct environmental planning, or assess offsite impacts of wind erosion. WEPS also has capabilities for other land management situations in which wind-affected soil movement is a problem. WEPS consists of the computer implementation of the WEPS science model with a graphical user interface designed to provide an easy-to-use way to enter inputs into the model and obtain output reports. WEPS is a process-based, daily time-step wind erosion simulation model. As such, it simulates not only basic wind erosion processes but also the processes that modify a soil's susceptibility to wind erosion. The structure of WEPS is modular and consists of a user interface, a science model including six submodels, two weather generators, and five databases. The user interface allows users to create input files with information from user inputs and the databases. WEPS supports an overall USDA Agricultural Research Service (ARS) goal of increasing agricultural productivity while reducing the environmental impacts of agriculture. As such, WEPS potentially can make an impact in the sustainable food and fiber supply for U.S. and world populations.

Introduction

Soil erosion by wind is a serious problem in the United States and the rest of the world. Wind erosion threatens agriculture and Earth's natural resources because it renders soil less productive by removing the most fertile part of the soil, namely, the clays and organic matter. Removal of clays and organic matter also damages soil structure. In addition to the soil, wind erosion can damage plants, primarily through the abrasive action of saltating particles on seedlings and fruits. Eroded soil can be deposited into waterways, degrading water quality and aquatic ecosystems. In addition, soil emitted into the air damages air quality. By affecting these resources, wind erosion can also become a health hazard to humans and animals. The ability to accurately simulate soil loss by wind is essential, among other things, for conservation planning, natural resource inventories, and reducing air and water pollution from windblown sources.

The Wind Erosion Equation (WEQ) was developed by the late W.S. Chepil and others and was published in 1965 by Woodruff and Siddoway (1965). For years, WEQ has represented the most comprehensive and widely used model in the world for estimating soil loss by wind from agricultural fields. The functional form of WEQ is:

$$E = f(I, K, C, L, V) \quad [1]$$

where

E = the average soil loss (tons acre⁻¹ year⁻¹),

I = the soil erodibility,

K = the soil ridge roughness,

C = the climatic factor,

L = the field length along the prevailing wind erosion direction, and

V = the vegetative factor.

WEQ is largely empirical in nature, derived from nearly 20 years of field and laboratory studies by scientists at the ARS Wind Erosion Research Unit in Manhattan, KS (Armbrust et al. 1964; Chepil 1958, 1959, 1960; Chepil and Woodruff 1959; Woodruff and Siddoway 1965; Skidmore 1965; Skidmore et al. 1970). Many improvements were made to WEQ over the next 30 years. Because of the limitations of adapting WEQ to many problems, as well as advancements in wind erosion science and computer technology, NRCS requested that ARS develop a replacement for WEQ (Hagen 1991).

Development of WEPS

Research in the 1980s (Cole et al. 1983, Cole 1984, Lyles et al. 1985) provided the initial attempt to outline a process-based approach to simulating wind erosion that would replace WEQ. Following this initial work, Hagen (1991) developed the modular structure used in the current WEPS, and the experimental research needed to support that structure was outlined. Numerous field and laboratory studies were conducted to develop relationships between surface conditions and erosion. Field and laboratory experimental data were collected to support the simulation of weather (Skidmore and Tatarko 1990; van Donk et al. 2005), hydrology (Durar et al. 1995), crop growth (Retta and Armbrust 1995, Retta et al. 2000), residue decomposition (Schomberg et al. 1995), soil processes (Lyles and Tatarko 1987; Potter 1990; Zobeck and Popham 1990, 1992; Layton et al. 1994), field management (Wagner et al. 1992, Wagner and Ding 1993, Wagner and Nelson 1995), and erosion (Hagen 2004b; Hagen and Armbrust 1992, Hagen et al. 1999, 2010). Experiments were also conducted to validate that the erosion routines were producing accurate and precise erosion estimates (Fryrear et. al. 1991; Feng and Sharratt 2007, 2009; Hagen 2004a).

A multidisciplinary team that included climate modelers, agronomists, agricultural engineers, soil scientists, and crop modelers was assembled to develop WEPS. The WEPS development project had a multi-agency commitment including ARS, NRCS, and USDA-Forest Service, along with the U.S. Environmental Protection Agency (EPA), the U.S. Army Corps of Engineers, and the Bureau of Land Management. In 2005, WEPS was released to NRCS for testing and further development for field office conservation planning. The first official release of WEPS for use by NRCS was in 2010.

User Requirements

Early in the WEPS development process, input was requested from potential users on the needed capabilities of a new wind erosion simulation model. These user requirements were summarized by Hagen (1991) and were the basis of WEPS, which was designed to address the following needs:

1. Providing more accurate and more detailed estimates of soil loss by wind from agricultural fields.

Results for WEQ were an annual average soil loss based essentially on average weather and field conditions. Because erosion is often the result of extreme weather events (e.g., high wind or dry soil), an approach that accounts for such extreme conditions was needed to simulate the extreme soil loss for these events. In addition, WEPS is capable of simulating surface conditions and erosion loss on a relatively fine temporal scale (e.g., daily or even hourly); however, for practical purposes, the default time step for WEPS output is 2 weeks. Such temporal detail, compared with the annual average of WEQ, allows users to observe the periods of excessive erosion and the corresponding wind or surface conditions that caused the soil loss (e.g., low vegetative cover). Consequently, conditions can be addressed by altering management or through other control measures.

2. Developing more cost-effective erosion control methods.

WEPS is a valuable tool for testing various alternate management scenarios or control methods through simulation because of the level of detail it provides in soil loss and field conditions. Users can evaluate each scenario before changing farming practices and observe and adjust surface conditions and management during periods of excessive loss to minimize erosion.

3. Simulating the amount of soil loss by direction.

The capability of WEPS to provide the direction of soil loss is useful because of increasing concern about offsite impacts of wind erosion on soil, water, and air quality. For example, creep and saltation loss to a roadside ditch or waterway will affect water quality, so users can focus attention on scenarios to control loss in that direction. Similarly, WEPS can simulate suspension loss in the direction of highly populated areas and control strategies. Depending on the direction and period of loss, control strategies that take advantage of the directional nature of the loss, such as barriers, trap strips, strip cropping, or directional tillage, can be employed.

4. Separating soil loss into creep + saltation, suspension, and PM10 components.

Each of these erosion components has specific characteristics and effects. Creep + saltation-sized material is typically deposited locally, where the material can affect soil and water quality, bury roads and irrigation ditches, or be deposited as dunes in fences or windbreaks. Suspension-sized material is small enough to be lifted into the air and carried over great distances. As such, it is a detriment to air quality, becomes a respiratory-health hazard, reduces visibility along transportation systems, and can be deposited on snowpack, affecting snow-melt and water quality. PM10 has been determined by the EPA to be a hazard to air quality and a respiratory hazard in particular (U.S. EPA 1996). Estimating soil loss of each of these components can aid in environmental assessments as well as designing strategies for reducing emissions of each component.

Taking all user requirements into consideration, WEPS is designed to be an aid in (1) planning soil conservation systems, (2) environmental assessment and planning, and (3) determining offsite impacts of wind erosion. NRCS is currently using WEPS to (1) assist land managers in developing farming systems to control wind erosion, (2) establish acceptable field-level conservation plans, and (3) determine wind erosion susceptibility as part of the Conservation Reserve Program (CRP) and other national programs.

WEPS Modeling Approach

WEPS is a process-based, daily time-step model that simulates weather, field conditions, and erosion. As such, it simulates not only basic wind erosion processes but also the processes that modify a soil's susceptibility to wind erosion. The WEPS 1.0 model release is designed to provide users with a simple tool for inputting initial field conditions, calculating soil loss, and displaying either simple or detailed outputs for designing erosion control systems.

WEPS 1.0 Geometries

To simplify inputs, WEPS 1.0 is designed to allow users to specify the simulation region or field within specific geometric constraints (Figure 1). The simulation region is limited to a rectangular area, but users can simulate other field shapes such as circles or half-circles by defining a rectangle of the same area and general dimensions of the desired field shape. Users also can rotate the simulation area to orient the field correctly on the landscape to account for the effects of varying wind directions.

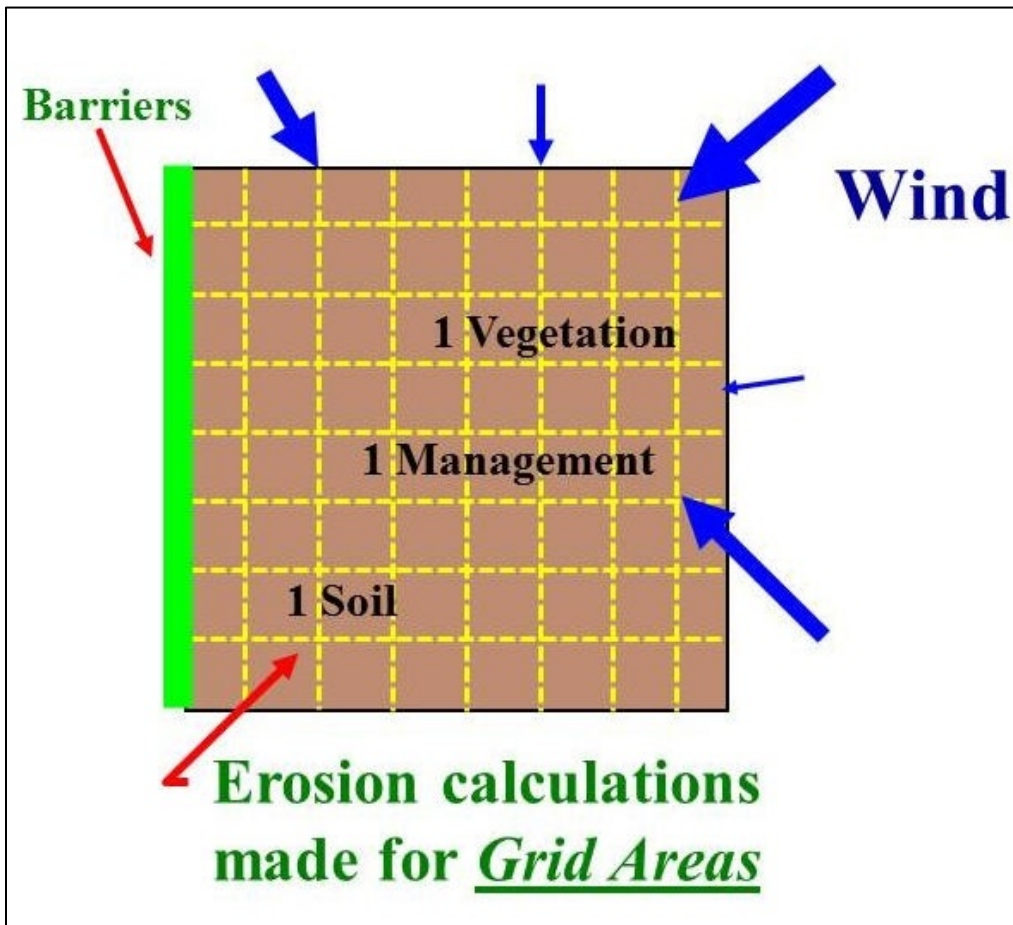


Figure 1. Diagram illustrating WEPS 1.0 simulation region geometries.

The model assumes a uniform simulation region surface in that only one soil type (soil properties), crop type (biomass properties), and management are uniformly distributed over the field. In reality, fields often are not uniform, so users can select the dominant-

critical (i.e., most erodible) soil or crop condition for a simulation. Users also can place barriers on any or all field boundaries. Barriers reduce the wind speed in the sheltered area on both the upwind and downwind sides. The Erosion submodel determines the threshold friction velocity at which erosion can begin for each surface condition. And when wind speeds exceed the threshold, the submodel calculates the loss/deposition over a series of individual grid cells representing the field. The soil/loss deposition is divided into components of creep + saltation and suspension, because each has unique transport modes, as well as offsite effects. The field surface is updated periodically during erosion events to simulate the changes caused by erosion. Surface updating during an erosion event includes changes to aggregate size distribution of the surface as fine particles are removed and smoothing of ridge roughness as ridges are eroded and furrows fill with eroded materials.

WEPS 1.0 Model Implementation

The structure of WEPS 1.0 is modular and consists of (1) the science model, which calculates the surface properties and changes due to management, weather, and erosion, coded in FORTRAN 95; and (2) a graphical user interface, which is coded in JAVA, for ease of entering inputs and observing results. The model also includes five databases, two weather simulation models, and six submodels that calculate surface conditions and soil loss (Figure 2).

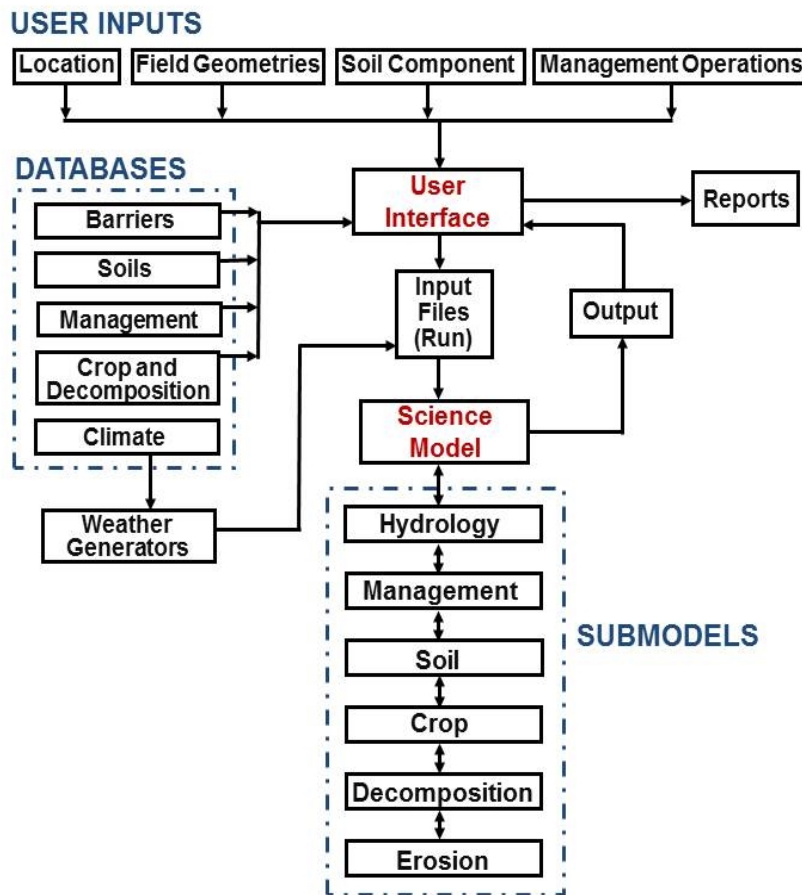


Figure 2. WEPS 1.0 model implementation scheme.

The user interface provides a means for users to enter initial conditions such as field dimensions, orientation, barriers, location, management operations, and soil component for the simulation region. Field dimensions are entered as a length and width, and orientation is entered as an angle deviation from north. Users select the barrier type from a list through the interface. For location, users can either select the State and county or enter a latitude and longitude for simulation. The interface then selects the weather stations for which historical weather parameters are used to simulate weather parameters. The soil component is selected from a list of soils supplied by the NRCS Soil Survey Geographic (SSURGO) database for the Soil Survey Area of the simulation region. Management operations and dates are compiled in the Management Crop Rotation Editor for WEPS (MCREW), a spreadsheet-type table editor.

Depending on the user-supplied inputs for the simulation, the interface accesses five databases that include climate, soils, operations, barriers, and crop growth/residue decomposition. These databases provide needed parameters for user-specified location and conditions. The interface writes the information needed for a WEPS simulation, obtained from the user and the databases, to input files. The interface also calls the weather generator, which produces two weather files containing daily precipitation, maximum and minimum temperatures, solar radiation, and dew-point temperature, as well as a daily wind direction and sub-daily (e.g., hourly) wind speeds. These input files for a given simulation are collectively known in WEPS as a "Run." To reduce computation time, a daily time-step is used in WEPS, except for selected subroutines in the Hydrology and Erosion submodels, which may use hourly or sub-hourly time-steps (e.g., 15 minutes). The science model reads the input run files and calls the Hydrology, Soil, Plant Growth (Crop), and Decomposition submodels, which account for changes in the soil surface erodibility as influenced by Management and Weather. If surface conditions are such that erosion can occur for the maximum wind speed for the day, Erosion submodel routines are called to calculate soil loss and deposition. Soil erosion by wind is initiated when the wind speed exceeds the saltation threshold speed for a given soil and biomass condition. After initiation, the duration and severity of an erosion event depend on the wind speeds and the evolution of surface conditions. During a simulation run, WEPS model outputs are written to various output files that are, in turn, summarized and displayed within the WEPS interface.

WEPS Model Use

WEPS is a comprehensive wind erosion model with many options for inputs and outputs. For basic simulations, however, WEPS 1.0 is simple to operate. Users enter only four types of information on the main screen: (1) description of the simulation region geometry by defining the field dimensions and field orientation, (2) geographic field location to generate simulated weather, (3) soil for the simulation field, and (4) the management operations and sequence. For U.S. simulations, the last three may be selected from lists provided within the WEPS model. New input files will usually be created using previous input files as templates and modified within the user interface. By varying inputs such as field management, users can explore management alternatives to control soil loss by wind. Interpreting the outputs of WEPS is an integral part of using WEPS as a tool to develop conservation plans for controlling wind erosion. WEPS provides options for viewing very detailed outputs by periods (default is 2 weeks), including soil loss as creep + saltation, suspension, and PM10. Period output is also available for weather parameters such as wind energy, as well as surface conditions such as soil erodibility and biomass amounts. Graphical plots of outputs also are available.

Such information is useful in determining which period is resulting in severe erosion and the conditions that are contributing to the loss. WEPS outputs also include amount of loss for each direction, which helps users place barriers, strip cropping, or other directional erosion control methods. WEPS also has a Multiple Run Management View option to allow easy comparisons of run outputs from alternative run scenarios.

WEPS simulation of soil erosion has undergone extensive field and wind tunnel testing and validation. Good agreement (i.e., R^2 s ranging from 0.87 to 0.98) was found in a number of studies between measured and WEPS-simulated erosion (Buschiazzo and Zobeck 2008, Funk et al. 2004, Liu et al. 2014). Soil loss measurements from 46 storm events in 6 States were compared with predictions from the WEPS Erosion submodel by Hagen (2004), who found that the measured and simulated erosion values were in “reasonable agreement” ($R^2 = 0.71$). Pi et al. (2016) validated SWEEP in a desert-oasis ecotone in China and found that the model appeared to adequately simulate total soil loss according to the high index of agreement ($d = 0.76$). Feng and Sharratt (2009) tested the WEPS Erosion submodel and concluded that the model underestimated soil loss by overestimating the threshold friction velocity, but it should be noted that they studied only small-intensity storms. Other researchers have also found WEPS to underestimate the occurrence of small storms (Feng and Sharratt 2007, Funk et al. 2004). Hagen (2004a) found a similar response for small storms, which he attributed to spatial variability of the test sites having small inclusions of higher erodibility than the average surface. The effects of field spatial variability on erodibility parameters and subsequent wind erosion prediction were also cited by van Donk and Skidmore (2003) for WEPS validations in eastern Colorado and Visser et al. (2005b) in Burkina Faso. Good agreement was also found by Hagen et al. (2010) between predicted and measured saltation ($R^2 = 0.92$) and suspension ($R^2 = 0.99$) for nine storms across five sites in the United States.

WEPS has been applied in a variety of research studies, including predicting the dispersion of fine dust over large regions (Diaz et al. 2010, Chung et al. 2013), development of control strategies for non-croplands (Hagen et al. 2009, Li et al. 2014), GIS applications (Gao et al. 2013), assessing sustainable removal of residues (Nelson et al. 2015), and predicting erosion from military training lands (van Donk et al. 2003). WEPS has been applied in Burkina Faso (Visser et al. 2005a, 2005b), Argentina (Buschiazzo and Zobeck 2008), Canada (Coen et al. 2004), China (Chen et al. 2013, Jia et al. 2014), Germany (Funk et al. 2004, Maurer and Gerke 2011), Mexico (Diaz et al. 2010), and Sweden (Qi et al. 2014).

More detailed features of WEPS and information on use of WEPS outside the United States are included in the WEPS User Manual, which is available online from ARS as part of the WEPS download at:
<https://www.ars.usda.gov/services/software/download.htm?softwareid=415>.

Conclusions

The Wind Erosion Prediction System is a process-based, daily time-step model that simulates weather, field conditions, and erosion. WEPS was developed in response to customer requests for improved wind erosion simulation technology, and it is intended to replace the predominately empirical Wind Erosion Equation as a prediction tool for those who plan soil conservation systems, conduct environmental planning, or assess offsite impacts of wind erosion. The WEPS model is improved with periodic updates. WEPS

represents a significant body of work by ARS scientists and supports an overall ARS goal of increasing agricultural productivity while reducing the environmental impacts of agriculture. As such, WEPS potentially can make an impact in the sustainable food and fiber supply for U.S. and world populations.

References

Armbrust, D.V., W.S. Chepil, and F.M. Siddoway. 1964. Effects of ridges on erosion of soil by wind. *Soil Science Society of America Proceedings* 28:557-560.

Buschiazzo, D.E. and T.M. Zobeck. 2008. Validation of WEQ, RWEQ and WEPS wind erosion for different arable land management systems in the Argentinean Pampas. *Earth Surface Processes and Landforms* 33:1839-1850.

Chen, L., H. Zhao, B. Han, and Z. Bai. 2013. Combined use of WEPS and Models-3/CMAQ for simulating wind erosion source emission and its environmental impact. *Science of Total Environment* 466-467, 762-769.

Chepil, W.S. 1958. Soil Conditions That Influence Wind Erosion. Technical Bulletin Number 1185. U.S. Department of Agriculture, Agricultural Research Service, Washington, DC.

Chepil, W.S. 1959. Wind erodibility of farm fields. *Journal of Soil and Water Conservation* 14(5):214-219.

Chepil, W.S. 1960. Conversion of relative field erodibility to annual soil loss by wind. *Soil Science Society of America Proceedings* 24(2):143-145.

Chepil, W.S. and N.P. Woodruff. 1959. Estimations of Wind Erodibility of Farm Fields. USDA, ARS Production Research Report Number 25. U.S. Department of Agriculture, Agricultural Research Service, Washington, DC.

Chung, S.H., F.L. Herron-Thorpe, B.K. Lamb, T.M. VanReken, J.K. Vaughan, J. Gao, L.E. Wagner, and F. Fox. 2013. Application of the wind erosion prediction system in the AIRPACT regional air quality modeling framework. *Transactions of the American Society of Agricultural and Biological Engineers* 56(2):625-641.

Coen, G.M., J. Tatarko, T.C. Martin, K.R. Cannon, T.W. Goddard, and N.J. Sweetland. 2004. A method for using WEPS to map wind erosion risk of Alberta soils. *Environmental Modelling and Software* 19(2):185-189.

Cole, G.W. 1984. A stochastic formulation of soil erosion caused by wind. *Transactions of the American Society of Agricultural Engineers* 27(5):1405-1410.

Cole, G.W., L. Lyles, and L.J. Hagen. 1983. A simulation model of daily wind erosion soil loss. *Transactions of the American Society of Agricultural Engineers* 26:1758-1765.

Diaz, E.N., J. Tatarko, A.D. Jazcilevich, A.R. Garcia, E. Caetano, and L.G. Ruiz-Suarez. 2010. A modeling study of aeolian erosion enhanced by surface wind confluences over Mexico City. *Aeolian Research* 2:143-157.

Durar, A.A., J.L. Steiner, S.R. Evett, and E.L. Skidmore. 1995. Measured and simulated surface soil drying. *Agronomy Journal* 87(2):235-144.

Feng, G. and B.S. Sharratt. 2007. Validation of WEPS for soil and PM10 loss from agricultural fields on the Columbia Plateau of the United States. *Earth Surface Processes*

and Landforms 32:743-753.

Feng, G. and B.S. Sharratt. 2009. Evaluation of the SWEEP model during high winds on the Columbia Plateau. *Earth Surface Processes and Landforms* 34:1461-1468.

Fryrear, D.W., J.E. Stout, L.J. Hagen, and E.D. Vories. 1991. Wind erosion: field measurement and analysis. *Transactions of the American Society of Agricultural Engineers* 34(1):155-160.

Funk, R., E.L. Skidmore, and L.J. Hagen. 2004. Comparison of wind erosion measurements in Germany with simulated soil losses by WEPS. *Environmental Modelling and Software* 19(2):177-183.

Gao, J., L.E. Wagner, F. Fox, S.H. Chung, J.K. Vaughan, and B.K. Lamb. 2013. Spatial application of WEPS for estimating wind erosion in the Pacific Northwest. *Transactions of the American Society of Agricultural and Biological Engineers* 6(2):613-624.

Hagen, L.J. 1991. A Wind Erosion Prediction System to meet user needs. *Journal of Soil and Water Conservation* 6:106-111.

Hagen, L.J. 2004a. Evaluation of the Wind Erosion Prediction System (WEPS) Erosion Submodel on cropland fields. *Environmental Modeling and Software* 19(2):171-176.

Hagen, L.J. 2004b. Fine particulates (PM10 and PM2.5) generated by breakage of mobile aggregates during simulated wind erosion. *Transactions of the American Society of Agricultural and Biological Engineers* 47(1):108-112.

Hagen, L.J. and D.V. Armbrust. 1992. Aerodynamic roughness and saltation trapping efficiency of tillage ridges. *Transactions of the American Society of Agricultural Engineers* 35(4):1179-1184.

Hagen, L.J., L.E. Wagner, and E.L. Skidmore. 1999. Analytical solutions and sensitivity analyses for sediment transport in WEPS. *Transactions of the American Society of Agricultural Engineers* 42(6):1715-1721.

Hagen, L.J., P.R. Schroeder, and L. Thai. 2009. Estimated particle emissions by wind erosion from the Indiana Harbor Combined Disposal Facility. *Practice Periodical of Hazardous, Toxic, and Radioactive Waste Management* 13(1):20-28.

Hagen, L.J., R.S. Van Pelt, and B.S. Sharratt. 2010. Estimating the saltation and suspension components from field wind erosion. *Aeolian Research* 1:147-153.

Jia, Q., N. Al-Ansari, and S. Knutsson. 2014. Modeling of wind erosion of the Aitik Tailings Dam using SWEEP model. *Engineering* 6(7):355-364.

Layton, J.B., E.L. Skidmore, and C.A. Thompson. 1994. Winter-associated changes in dry-soil aggregation as influenced by management. *Soil Science Society of America Journal* 57:1568-1572.

Li, J., G.S. Okin, J. Tatarko, N.P. Webb, and J.E. Herrick. 2014. Consistency of wind erosion assessments across land use and land cover types: a critical analysis. *Aeolian*

Research 15:253-260.

Liu, B., J. Qu, Q. Niu, and Q. Han. 2014. Comparison of measured wind tunnel and SWEEP simulated soil losses. *Geomorphology* 207:23-29.

Lyles, L., G.W. Cole, and L.J. Hagen. 1985. Wind erosion: processes and prediction. *In* R.F. Follett and B.A. Stewart, eds., *Soil Erosion and Crop Productivity*, pp. 163-172. ASA-CSSA-SSSA, 677 South Segoe Road, Madison, WI 5371 1, USA.

Lyles, L. and J. Tatarko. 1987. Precipitation effects on ridges created by grain drills. *Journal of Soil and Water Conservation* 42(4):269-271.

Maurer, T. and H.H. Gerke. 2011. Modelling Aeolian sediment transport during initial soil development on an artificial catchment using WEPS and aerial images. *Soil & Tillage Research* 117:148-162.

Nelson, R., J. Tatarko, and J.C. Ascough II. 2015. Soil erosion and organic matter variations for central Great Plains cropping systems under residue removal. *Transactions of the American Society of Agricultural and Biological Engineers* 58(2):415-427.

Pi, H., B. Sharratt, G. Feng, J. Lei, X. Li, and Z. Zheng. 2016. Validation of SWEEP for creep, saltation, and suspension in a desert–oasis ecotone. *Aeolian Research* 20:157-168.

Potter, K.N. 1990. Estimating wind-erodible materials on newly crusted soils. *Soil Science* 150(5):771-776.

Jia, Q., N. Al-Ansari, and S. Knutsson. 2014. Modeling of wind erosion of the Aitik Tailings Dam using SWEEP Model. *Engineering* 6:355-364.

Retta, A. and D.V. Armbrust. 1995. Estimation of leaf and stem area in the Wind Erosion Prediction System (WEPS). *Agronomy Journal* 87:93-98.

Retta, A., D.V. Armbrust, L.J. Hagen, and E.L. Skidmore. 2000. Leaf and stem area relationships to masses and their height distributions in native grasses. *Agronomy Journal* 92(2):225-230.

Schomberg, H.H., J.L. Steiner, S.R. Evett, and A.P. Moulin. 1995. Climatic influence on residue decomposition prediction in the Wind Erosion Prediction System. *Theoretical and Applied Climatology* 54:5-16.

Skidmore, E.L. 1965. Assessing wind erosion forces: directions and relative magnitudes. *Soil Science Society of America Proceedings* 29(5):587-590.

Skidmore, E.L., P.S. Fisher, and N.P. Woodruff. 1970. Computer equation aids wind erosion control. *Crops and Soils* 22(8):19-20.

Skidmore, E.L. and J. Tatarko. 1990. Stochastic wind simulation for erosion modeling. *Transactions of the American Society of Agricultural Engineers* 33:1893-1899.

Stetler, L.D. and K.E. Saxton. 1996. Wind erosion and PM10 emissions from agricultural fields on the Columbia Plateau. *Earth Surface Processes and Landforms* 21:673-685.

- U.S. EPA. 1996. National ambient air quality standards for particulate matter: proposed decision. 40 CFR Part 50, Vol. 62(138) 3851 (July 18,1997).
- van Donk, S.J., X. Huang, E.L. Skidmore, A.B. Anderson, D.L. Gebhart, V.E. Prehoda, and E.M. Kellogg. 2003. Wind erosion from military training lands in the Mojave Desert, California, USA. *Journal of Arid Environments* 54(4):687-703.
- van Donk, S.J. and E.L. Skidmore. 2003. Measurement and simulation of wind erosion, roughness degradation and residue decomposition on an agricultural field. *Earth Surface Processes and Landforms* 28(11):1243-1258.
- van Donk, S.J., L.E. Wagner, E.L. Skidmore, and J. Tatarko. 2005. Comparison of the Weibull Model with measured wind speed distributions for stochastic wind generation. *Transactions of the American Society of Agricultural Engineers* 48 (2):503-510.
- Visser, S.M., L. Stroosnijder, and W.J. Chardon. 2005a. Nutrient losses by wind and water, measurements and modeling. *CATENA* 63(1):1-22.
- Visser, S.M., G. Sterk, and D. Karssenberg. 2005b. Wind erosion modeling in a Sahelian Environment. *Environmental Modelling and Software* 20(1):69-84.
- Wagner, L.E., N.M. Ambe, and P. Barnes. 1992. Tillage-induced soil aggregate status as influenced by water content. *Transactions of the American Society of Agricultural Engineers* 35(2):499-504.
- Wagner, L.E. and D.J. Ding. 1993. Stochastic modeling of tillage-induced aggregate breakage. *Transactions of the American Society of Agricultural Engineers* 36(4):1087-1092.
- Wagner, L.E. and R.G. Nelson. 1995. Mass reduction of standing and flat residues by selected tillage implements. *Transactions of the American Society of Agricultural Engineers* 38(2):419-427.
- Woodruff, N.P. and F.H. Siddoway. 1965. A wind erosion equation. *Soil Science Society of America Proceedings* 29(5):602-608.
- Zobeck, T.M. and T.W. Popham. 1990. Dry aggregate size distribution of sandy soils influenced by tillage and precipitation. *Soil Science Society of America Journal* 54(1):197-204.
- Zobeck, T.M. and T.W. Popham. 1992. Influence of microrelief, aggregate size, and precipitation on soil crust properties. *Transactions of the American Society of Agricultural Engineers* 35(2):487-492.

A History of Wind Erosion Prediction Models in the U.S. Department of Agriculture, Part 1: Prior to the Wind Erosion Prediction System

Contributors:

J. Tatarko
M.A. Sporcic
E.L. Skidmore

Abstract

The Great Plains experienced an influx of settlers in the late 1850s to 1900. Periodic drought was hard on both settlers and the soil, and severe wind erosion resulted. The period from 1931 to 1939, known as the “Dirty Thirties” or the “Dust Bowl,” produced many severe windstorms. The resulting dusty sky over Washington, DC, helped Hugh Hammond Bennett gain political support for the Soil Conservation Act of 1937, which established the U.S. Department of Agriculture (USDA), Soil Conservation Service (SCS). Austin W. Zingg and William S. Chepil began wind erosion studies at a USDA laboratory at Kansas State University in 1947. Neil P. Woodruff and Francis H. Siddoway published the first widely used model for wind erosion in 1965, called the “Wind Erosion Equation” (WEQ). WEQ was solved using a series of charts and lookup tables. Subsequent improvements to WEQ included monthly magnitudes of the total wind, a computer version of WEQ programmed in FORTRAN, small-grain equivalents for range grasses, tillage systems, effects of residue management, crop row direction, cloddiness, monthly climate factors, and the weather. The SCS and the USDA Natural Resources Conservation Service (NRCS) produced several computer versions of WEQ with the goal of standardizing and simplifying it for field personnel, including a standalone version of WEQ developed in the late 1990s using Microsoft Excel. Although WEQ was a great advancement to the science of prediction and control of wind erosion on cropland, it had many limitations that prevented its use on many lands throughout the United States and other parts of the world. In response to these limitations, the USDA developed a process-based model known as the “Wind Erosion Prediction System” (WEPS). The USDA Agricultural Research Service (ARS) has taken the lead in developing science and technology for wind erosion prediction.

Introduction

Wind erosion has been an agricultural issue in the semi-arid central U.S. Great Plains since settlers first plowed prairie grasslands to produce food and fiber. The years from 1931 to 1939 saw very low rainfall in the U.S High Plains region centered in Texas, New Mexico, Colorado, Oklahoma, and Kansas. The resulting severe wind erosion caused concern over the loss of our soil resources, and a national effort to quantify and control the amount of wind erosion on our Nation’s farmland began. The U.S. Soil Erosion Service, established in 1933, which became the Soil Conservation Service and most recently the Natural Resources Conservation Service—along with the Agricultural Research Service and land-grant universities—has been working for over 75 years to advise growers on the care of wind-erodible land. Throughout this time, research has

been conducted, and many soil loss prediction methods have been developed to better understand and predict soil erosion. This publication summarizes the development of wind erosion prediction models in USDA prior to the development of the current WEPS model in the mid-1980s. The history and development of the WEPS model is described in detail in a separate chapter by Wagner in this volume.

Early Observations of Wind Erosion

Farmers and ranchers settled the U.S. Great Plains region in the late 1800s. From 1850 to 1900, the population of the area increased from 300,000 to 7,000,000 (Anderson and Hill 2004) with a concurrent large increase in the land converted to cropland, most of which was planted to wheat. Mechanization using tractors allowed farmers to cultivate previously unplowed areas of the short grass prairie (Armburst 1999).

Early wind erosion literature focused on the scope of the problem and control measures. The first scientific report of wind erosion on cultivated U.S. land was made by King (1894) in Wisconsin. King recommended strip-cropping, green manure, roughening the surface, and windbreaks to control wind erosion. Udden (1896) published some of the first quantitative estimates of solid, suspended material in dust storms. He reported 160 to 126,000 tons per cubic mile of dust and indicated that an average of 850 million tons of dust was being carried 1,440 miles each year in the Western United States. Free and Westgate (1910) discussed four actions to control soil blowing: (1) increasing the water content of the soil, (2) increasing the amount of humus (organic matter in soil), (3) providing a cover of growing vegetation, and (4) leaving the stubble of the last crop standing on the land until next planting. A comprehensive review of wind erosion science from the perspective of aeolian geology was published by Free (1911) with additional control methods to those mentioned by Free and Westgate (1910), including decreasing summer fallow and planting trees in rows to slow the wind. Free was also one of the earlier writers to describe wind erosion and windblown dust as an agent of soil formation and modification. Several periods of dry conditions from the 1890s as well as the 1910s caused severe wind erosion (Chepil 1957).

The Impacts of the Dust Bowl on Research and Modeling

Probably the most severe period of wind erosion occurred in the 1930s in the U.S. Great Plains. Figure 1 shows the rainfall patterns for southwest Kansas that resulted in the severe erosion of the 1930s. Starting in 1931, rainfall was below average for the subsequent 9 years. Rainfall in 1937 was 208 mm (8 inches) below the average of 478 mm (18.8 inches), which resulted in consecutive years of winter wheat crop failure. At that time, knowledge of wind erosion soil loss was limited. The Great Depression compounded the difficult times brought on by the drought's effects.

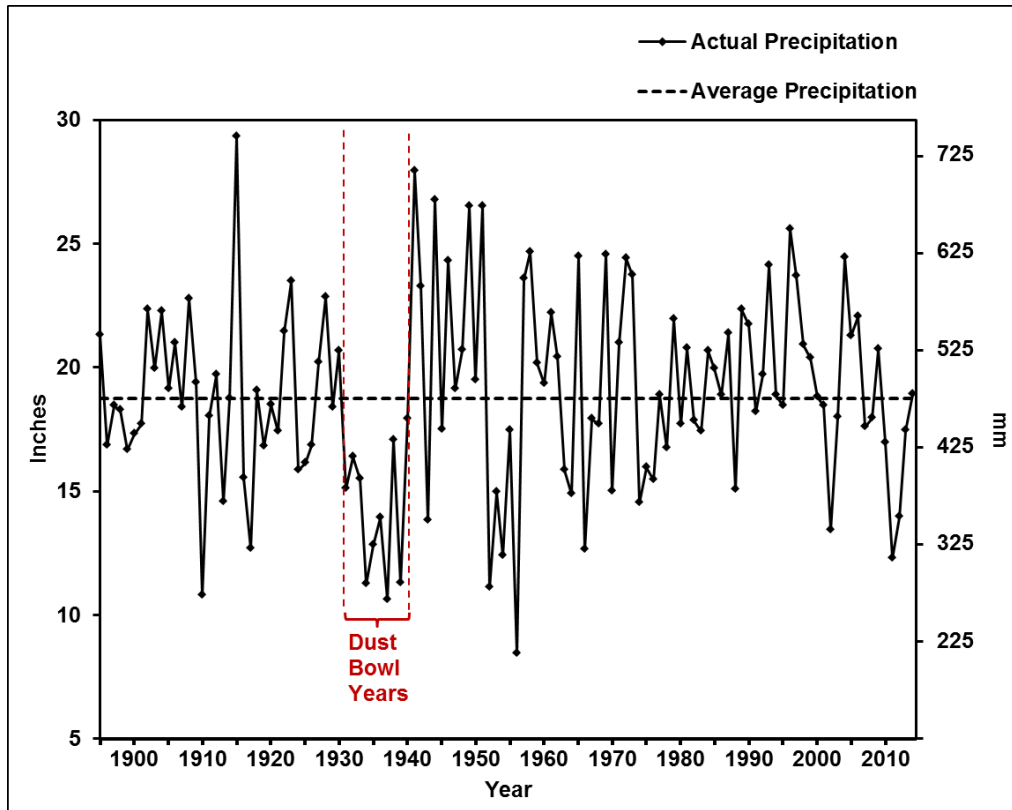


Figure 1. Southwest Kansas rainfall, 1895 to 2014 (data from NOAA 2015). Note the dry years of 1931 to 1940.

The severity of the drought resulted in large amounts of erosion throughout the Great Plains of North America, with the most severe damage occurring in New Mexico, Colorado, Kansas, Oklahoma, and Texas. Figure 2 is a typical photograph of the Dust Bowl era. Even before the Dust Bowl, Hugh Hammond Bennett, a soil scientist at the U.S. Bureau of Chemistry and Soils, thought much more could be done to manage natural resources wisely. Bennett and Chapline (1928) made their case for soil conservation in *Soil Erosion: A National Menace*. Later, in April 1935, Bennett used a big dust storm to persuade Congress to address the problem (Brink 1951, Egan 2006). On a day he was testifying before Congress in support of the Soil Conservation Act, Bennett was able to prolong his presentation long enough for legislators to see a large storm settle dust over the Capitol as the bill came to a vote. The Act that was, in part, intended to reduce the Nation's soil loss also established the Soil Conservation Service and was the first soil conservation act in history (Brink 1951). Bennett served as the first chief of the SCS until his retirement in 1951. Later, the SCS published several regional guides for wind erosion control, including *The Guide for Wind Erosion Control in the Northeastern States* (Hayes 1966) and *The Guide for Wind Erosion Control on Cropland in the Great Plains States* (Craig and Turelle 1964).



Figure 2. Typical dust storm from the 1930s (USDA-NRCS, 2015).

As wind erosion research in the United States was beginning, R.A. Bagnold, Cambridge University, M.A. in engineering, published *The Physics of Blowing Sand and Desert Dunes* (1941). Bagnold (1941, p. xxi) departed from the traditional line of thinking when he said, “The subject of sand movement lies far more in the realm of physics than of geomorphology.” Some have called him the father of saltation. Lyles (1985, p. 209) stated, “Although the ‘what’ of wind erosion might have been known during the 1930s, the ‘how to’ or the ‘how much’ of control principles and practices for the widely diverse soils, crops, and climate of the West were largely unknown.” He went on to say, “The goal of erosion researchers has been the quantification of the need for protection and the means to provide it, given those variables of soils, crops, and climate.”

Early Wind Erosion Research in the USDA

The Flannagan-Hope Bill, officially the Agricultural Marketing Act of 1946 (Public Law 733, 79th Congress), was passed in part “... to provide further research into basic laws and principles relating to agriculture...” and was the source of much of the funding for establishing the Wind Erosion Project in Manhattan, KS, which was administered by the Research Division of SCS. A laboratory was established on the campus of Kansas State Agriculture College in 1947. The management of this laboratory was transferred to ARS in 1953 (Armbrust 1999).

Austin W. Zingg, a mechanical engineer, was the first supervisor of the facility, the High Plains Wind Erosion Laboratory. William S. Chepil, a soil scientist, became project leader in 1953 and remained in the position until his death in 1963. Initial work focused on developing research equipment such as laboratory and portable wind tunnels and procedures to characterize the soil surface response to wind erosion. Developing a

fundamental understanding of the processes of wind erosion and soil properties that affect wind erosion were also primary goals of the project. Chepil's groundbreaking work focused on five key factors that affect wind erosion (Chepil 1960, Chepil and Woodruff 1954, Chepil et al. 1962, Chepil and Woodruff 1963): (1) soil cloddiness, (2) ridge roughness, (3) climate, (4) field length, and (5) vegetative material. The initial attempt by Chepil to model soil loss by wind was based on wind tunnel experiments and consisted of a simple equation relating soil loss to degree of cloddiness, roughness, and vegetation (Chepil and Woodruff 1959, Woodruff and Siddoway 1965). This initial model had the following relationship:

$$X = a (I / (RK))^b \quad [1]$$

where

X = wind tunnel erodibility in tons acre⁻¹,

I = soil erodibility based on percent of soil fraction greater than 0.84 mm in diameter,

R = amount of crop residue in pounds acre⁻¹,

K = ridge roughness equivalence in inches compared to a standard height-spacing ratio of 1:4, and

a and b = constants that depend on past erosional history, type of residue and roughness, and condition of surface crust.

The equation was continually improved as new research and data became available.

The Wind Erosion Equation

The first published comprehensive attempt to model wind erosion on agricultural fields was based largely on the work of Chepil and published by Woodruff and Siddoway in 1965. The Wind Erosion Equation (WEQ) was an empirical model with the following functional form:

$$E = f (I, K, C, L, V) \quad [2]$$

where

E = soil loss (mass area⁻¹ yr⁻¹),

I = soil erodibility,

K = ridge roughness,

C = climatic factor,

L = field length, and

V = vegetative factor.

These factors were developed from wind tunnel and field research and are derived from the interactions of 11 primary parameters. The soil erodibility factor (I) is a measure of the potential soil loss from a wide, bare, smooth, unsheltered, and non-crust surface and can be adjusted to account for the presence of hills, knoll topography, and mechanical stability of soil crust if necessary. Woodruff and Siddoway (1965), however, recommend that crusts be disregarded because of their transience. The ridge roughness factor (K) adjusts soil erodibility for soil surface roughness other than that caused by clods or vegetation and is typically formed by farming implements (e.g., ridges and furrows). The climatic factor (C) includes the effect of wind velocity and soil moisture,

which is proportional to the Thornthwaite P-E Index (Thornthwaite 1931). The field length factor (L) is the distance across the field along the prevailing wind erosion direction. The rate of erosion is zero at the upwind field edge and increases with distance across the field downwind. If the field is long enough, soil movement by wind reaches a maximum for the given wind. If wind barriers are present, L is adjusted to account for the shelter effect of the barriers. The vegetative factor (V) adjusts the soil loss given by the other factors to account for any vegetative material on the soil surface. The V factor accounts for the quantity, kind, and orientation of vegetative cover. The relationships between these factors are complex, and interactions occur among them such that labor-intensive graphical and tabular solutions were required.

Improvements to WEQ

The purpose of WEQ was twofold: (1) to serve as a tool for determining the potential amount of wind erosion for a particular field under existing local conditions, and (2) to serve as a guide for determining the conditions of cloddiness, roughness, vegetative cover, sheltering from wind barriers, or width and orientation of field necessary to control wind erosion (Chepil and Woodruff 1963). Woodruff and Siddoway (1965) cited several shortcomings and limitations of WEQ, stating that variables that influence wind erosion were lacking and the interaction of the combined factors was not well understood. They listed specific details that were missing in WEQ. First, they argued that information was needed on the influence of different implements on soil cloddiness, soil ridge roughness, and vegetative cover. This information was deemed important in prescribing effective methods of tillage to control erosion. Second, prevailing wind direction had been determined only for the Great Plains and needed to be expanded to the rest of the United States. Better information on surface soil moisture related to the climatic factor was also needed. The Thornthwaite Index was considered only a rough estimate of moisture conditions. Third, the climatic factor was needed on a monthly or seasonal basis to permit better evaluation of short-term, highly erosive periods. Fourth, seasonal and annual soil erodibility needed to be determined for various soil types. Fifth, information was needed on the average distance of full and partial protection from wind erosion afforded by barriers of various widths and spacing in various geographic locations and for various soils. Sixth and lastly, the researchers argued that values of the vegetative cover factor and orientation for crops other than those already investigated were also needed. Research continued for the next 20 years and attempted to address these and other deficiencies to improve WEQ.

Lyles and Allison (1975) modified WEQ equations so that the combined effect of stubble and non-erodible aggregates could be considered. The ridge roughness factor was expanded to include an adjustment for random roughness calculated as standard deviation of soil surface elevation (USDA-NRCS 2011). Armbrust et al. (1982) determined the effect of crop type and tillage on the number, size distribution, and stability of soil aggregates. Researchers improved the soil ridge roughness factor by determining how long ridges created by grain drills persist for several soil textures and rainfall regimes (Lyles and Tatarko 1987). The soil erodibility index was also determined for the spring and fall in seven North Central States that could be used to apply the WEQ for critical or other periods of less than 1 year (Lyles and Tatarko 1988). The climatic factor was expanded to include most of the United States (Skidmore 1965, Skidmore and Woodruff 1968), then the arid Southwest (Lyles 1983). Improvements were also made in accounting for wind erosion direction and the preponderance of wind erosion forces (Skidmore 1965, 1987). Methods of computing a monthly wind erosion climatic factor

were devised (Woodruff and Armbrust 1968, Skidmore 1987). Bondy et al. (1980) proposed a method of computing wind erosion by periods (greater or smaller than 1 year) by partitioning wind-energy distributions. Skidmore (1986) developed a physically based climatic factor for long- and short-term and event soil loss estimates that did not require the use of the Thornthwaite P-E Index, which is highly sensitive to low precipitation and underestimates the effects of humid climates in the climatic factor.

Several studies (Hagen and Skidmore 1971; Hagen et al. 1972, 1981; Skidmore and Hagen 1977; Hagen 1976) determined relationships between wind reductions and windbreak porosities, which facilitated better predictions of protection provided by barriers downwind. The effectiveness of annual crops as wind barriers was also considered (Fryrear 1963), and shelter effects were developed over 12 years of testing for 27 tree and shrub species in the Central Great Plains (Woodruff et al. 1976).

Studies were also conducted to improve estimations of the protection for erodible soil particles provided by standing stubble based on the stubble's height, size, spacing, and orientation (Skidmore et al. 1966, Lyles et al. 1973, Lyles and Allison 1975). The vegetative factor was also expanded to include other crops including corn, cotton, grain sorghum, peanuts, and soybean (Lyles and Allison 1981, Armbrust and Lyles 1985, Skidmore and Nelson 1992). Small-grain equivalents were determined for several non-crop vegetation species such as range grasses and shrubs (Lyles and Allison 1980, Hagen and Lyles 1988). Woodruff et al. (1974) derived curves for converting different amounts of surface-applied and incorporated wet manure to flat, small-grain equivalents.

To improve the shortcomings in WEQ's predictions of annual average soil loss, the model was converted from an annual or period to daily prediction (Cole and Lyles 1984, Skidmore and Williams 1991). This work allowed WEQ to be interfaced with the computer program known as the Erosion Productivity Impact Calculator, or EPIC (Williams et al. 1984). Two WEQ factors for this daily prediction in EPIC, soil erodibility and climatic factor, remained constant for each day of the year. The other variables were subject to daily variation as simulated by EPIC.

In addition to the research efforts mentioned above to improve the science behind WEQ, ARS also attempted to make WEQ easier to use. The first attempt to computerize WEQ was known as WEROS (short for Wind EROSION), a Fortran IV computer program that implemented the original WEQ that determined soil loss on an annual basis (Skidmore, et al. 1970, Fisher and Skidmore 1970). With WEROS, the user could replace the cumbersome task of solving WEQ using tables and nomographs with a mainframe computer. WEROS was later modified to generate lookup tables for SCS where, if the user knew the soil erodibility, roughness, climatic factor, the field length along the prevailing wind erosion direction, and the small-grain equivalent of the vegetation, the soil loss could be found easily. Because many SCS field offices were not equipped with computers at that time, a slide rule-type calculator was developed for solving WEQ (Skidmore 1983). The calculator was used extensively by SCS field personnel for estimating wind erosion and designing wind erosion control systems.

SCS/NRCS Improvements to WEQ

From 1965 to 1992, SCS/NRCS used WEQ to predict wind erosion on farmers' land for conservation programs. At first, WEQ was applied on an annual basis, but this approach was quickly replaced by the Critical Period Method, through which erosion was predicted

for the period of the year most susceptible to wind erosion. As ARS was able to determine the average monthly winds, some areas used the Management Period Method, which attempted to predict erosion for specific crop management periods to further pinpoint where the management system needed improved conservation practices. This allowed a conservation planner to offer small changes in tillage or crop rotation to reduce erosion.

SCS/NRCS made several efforts to simplify WEQ for its use. Random roughness photos with associated random roughness values, as well as random roughness associated with various cropland field operations, were developed (USDA-NRCS 2011). Desktop computers came to the SCS field offices in 1988, and the agency began attempting to bundle WEQ into comprehensive software packages. These included a 1988 DOS version, a 1989 Computer Assisted Management Planning System (CAMPS) version, various 1994-1997 Field Office Computing Systems (FOCS) versions, and finally, in 1998, a Microsoft Excel spreadsheet version (Carlson et al. 1999). Sporcic and Nelson (1999) developed a spreadsheet version of WEQ that used lookup tables and calculated potential soil loss under the Management Period Method. The spreadsheet version of WEQ was used nationally from 1998 to 2010 and significantly reduced the amount of input time required to calculate the management period procedure by hand.

Limitations of WEQ

Despite the efforts cited above to improve the science and usability of WEQ, shortcomings of the model persisted and have been recognized by wind erosion researchers. These limitations have been outlined in a number of publications and are summarized below.

Chepil's method of relating short-term (minutes) soil loss data to annual average soil loss and areas that are wide and long compared with a wind tunnel was inherently inaccurate. The measurements in the wind tunnel were of such short duration, due to the limited amount of erodible soil in the sample trays, that the soil flow rate could not be measured. Instead, the mass of soil lost per unit area was measured and used in computing a measure of relative erodibility (Cole et al. 1983).

Relationships among variables were not accounted for in all combinations of field and climatic conditions (Hagen 1991). Difficulties in determining single values for factors such as I, L, K, and V appear to have arisen because of the ambiguous methods suggested for their determination (Cole 1983). Woodruff and Siddoway (1965, p. 606) stated, "The equation actually evaluates the erodibility of a field having certain L, K, and V values in terms of what it would have been during the severe soil blowing time."

Variation of wind and precipitation from the average is not simulated in WEQ (Skidmore 1976). As a result, extreme weather conditions that in reality greatly influence wind erosion are not easily simulated. Seasonal variation of field erodibility was also difficult to account for in the model. For example, Chepil recognized that all of the factors he defined could change with time. To cope with the wind angle fluctuations, for instance, Chepil et al. (1964) defined a single prevailing wind direction angle for the simulation (Cole 1983).

Inherent uncertainties also exist in the empiricism of the equation development. The surface of the wind tunnel used to derive erodibility for WEQ does not represent the total

field surface that is of interest. Thus, because of the small area of the soil sample tested, soil abrasion is lacking, and the time duration of a wind tunnel test is too short, i.e., minutes, compared to hours on a field. A consequence of the small sample was a difference in the measured dependent variable between tunnel and field (Cole 1984a). Speaking of the limitations of WEQ, Hagen (1991, p. 106) said, “The current technology represents a mature technology that is not easily adapted to untested conditions or climates far different than that of the central Great Plains where the WEQ was developed.” Facing the shortcomings of WEQ, researchers began exploring modeling methods that would overcome the shortcomings of WEQ. Such a model should (1) determine the percentage of eroded material that enters suspension, (2) convert from a deterministic to a stochastic model, (3) allow modeling of single windstorms, and (4) adjust the model to apply to large-scale rather than single field sites (Skidmore 1976). In addition, a new model should (5) simultaneously simulate effects of a growing crop as well as residues from previous crops and, most importantly, (6) compute soil losses for 1-day rather than 1-year intervals (Cole and Lyles 1984).

Beyond WEQ

Research devoted to overcoming the shortcomings of WEQ led to an examination of new science and more process-based ways to approach the simulation of soil loss by wind (Cole et al. 1983, Cole 1984a,b). With these new published approaches to wind erosion simulation as well as the advancement of the personal computing power that would allow adoption by most users of the technology, a new process-based wind erosion simulation model was proposed (Hagen 1988, 1991).

Early in 1986, USDA began a 20-plus-year effort to develop this next generation of wind erosion prediction technology. NRCS began using WEPS in its field offices in 2010 to assist land managers in controlling wind erosion, establishing acceptable field level conservation plans, and determining wind erosion susceptibility as part of the Conservation Reserve Program (CRP) and other national conservation program enrollments. The model is a critical component of the USDA strategy to reduce particulate emissions from cultivated agricultural lands. The history and development of the WEPS model and the future of wind erosion modeling are described in detail in a separate chapter by Wagner.

Summary and Conclusions

Wind erosion in the United States was recognized as early as 1807 by Zebulon Pike (1966). The 1930s brought at least 5 years of severe drought that resulted in many dust storms and severe soil damage to the Great Plains of the United States. This hardship was compounded by the Great Depression. The massive wind erosion and dust storms of that period brought attention to the importance of conserving our Nation’s natural resources, and the Soil Erosion Service was established in response to these events.

The United States has had an active research program into wind erosion since 1947, when the Wind Erosion Project was established at Kansas State Agricultural College in Manhattan, KS. Many research tools and study methods were developed, and a fundamental understanding of the causes and control of wind erosion was advanced. As a result of this research, the Wind Erosion Equation (WEQ) was published in 1965 as a tool to predict soil loss by wind and a means to develop control strategies. A considerable

effort followed to improve and expand WEQ. Despite these efforts, it became clear that WEQ should be replaced with newer wind erosion science and technology. In 1985, an effort was started to develop the process-based Wind Erosion Prediction System.

References

- Anderson, T.L. and P.J. Hill. 2004. *The Not So Wild, Wild West: Property Rights on the Frontier*. Stanford, CA: Stanford University Press.
- Armbrust, D.V. 1999. Fifty years of wind erosion research by USDA Agricultural Research Service at Kansas State University. *In* E.L. Skidmore and J. Tatarko, (eds.), *Wind Erosion - An International Symposium/Workshop, June 3-5, 1997, Proceedings* USDA, ARS, Wind Erosion Research Unit, Kansas State University, Manhattan, KS.
- Armbrust, D.V., J.D. Dickerson, E.L. Skidmore, et al. 1982. Dry soil aggregation as influenced by crop and tillage. *Soil Science Society of America Journal*. 46(2):390-393.
- Armbrust, D.V., and L. Lyles. 1985. Equivalent wind erosion protection from selected growing crops. *Agronomy Journal*. 77(5):703-707.
- Bagnold, R.A. 1941. *The Physics of Blown Sand and Desert Dunes*. London, United Kingdom: Methuen Publishing. 265 pp.
- Bennett, H.H., and W.R. Chapline. 1928. *Soil Erosion: A National Menace*. U.S. Department of Agriculture Circular No. 33. Washington, DC: U.S. Government Printing Office.
- Bondy, E., L. Lyles, and W.A. Hayes. 1980. Computing soil erosion by periods using wind energy distribution. *Journal of Soil Water Conservation*. 35(4):173-176.
- Brink, W. 1951. *Big Hugh: The Father of Soil Conservation*. New York, NY: Macmillan. 167 pp.
- Carlson, J.R., S.L. Ekblad, and G.L. Tibke. 1999. Deployment, support, and use of wind erosion equation (WEQ) software for resource analysis and planning. *In* E.L. Skidmore and J. Tatarko, (eds.), *Wind Erosion - An International Symposium/Workshop, June 3-5, 1997, Proceedings* USDA, ARS, Wind Erosion Research Unit, Kansas State University, Manhattan, KS.
- Chepil, W.S. 1957. Dust Bowl: causes and effects. *Journal of Soil and Water Conservation*. 12(3):108-111.
- Chepil, W.S. 1960. Conversion of relative field erodibility to annual soil loss by wind. *Soil Science Society of America Proceedings*. 24(2):143-145.
- Chepil, W.S., and N.P. Woodruff. 1954. Estimations of wind erodibility of field surfaces. *Journal of Soil and Water Conservation*. 9:257-265, 285.
- Chepil, W.S., and N.P. Woodruff. 1959. Estimations of wind erodibility of farm fields. U.S. Department of Agriculture, Production Research Report No. 25.
- Chepil, W.S., and N.P. Woodruff. 1963. The physics of wind erosion and its control. *Advances in Agronomy*. 15:211-302.

- Chepil, W.S., F.H. Siddoway, and D.V. Armbrust. 1962. Climatic factor for estimating wind erodibility of farm fields. *Journal of Soil and Water Conservation*. 17(4):162-165.
- Chepil, W.S., F.H. Siddoway, and D.V. Armbrust. 1964. In the Great Plains prevailing wind erosion direction. *Journal of Soil and Water Conservation*. 19(2):67-70.
- Cole, G.W. 1983. Wind erosion modeling. Proceedings of the 1983 Natural Resources Modeling Symposium, U.S. Department of Agriculture, Agricultural Research Service, Pingree Park, CO, October 16-21, 1983, pp. 59-63.
- Cole, G.W. 1984a. A method for determining field wind erosion rates from wind tunnel-derived functions. *Transactions of the ASAE*. 27(3):110-116.
- Cole, G.W. 1984b. A stochastic formulation of soil erosion caused by wind. *Transactions of the ASAE*. 27(5):1405-1410.
- Cole, G.W., and L. Lyles. 1984. The wind erosion component of EPIC. Prepared for EPIC - Erosion/Productivity Impact Calculator. U.S. Department of Agriculture, Technical Bulletin No. 1768, pp. 139-151.
- Cole, G.W., L. Lyles, and L.J. Hagen. 1983. A simulation model of daily wind erosion soil loss. *Transactions of the ASAE*. 26(6):1758-1765.
- Craig, D.G., and J.W. Turelle. 1964. Guide for Wind Erosion Control on Cropland in the Great Plains States. Washington, DC: U.S. Department of Agriculture, Soil Conservation Service. Out of print.
- Egan, T. 2006. *The Worst Hard Time: The Untold Story of Those Who Survived the Great American Dust Bowl*. New York, NY: Houghton Mifflin Company.
- Fisher, P.S., and E.L. Skidmore. 1970. WEROS: a Fortran IV program to solve the wind erosion equation. USDA, ARS Publication 41-174. 13 pages.
- Free, E.E. 1911. The Movement of Soil Material by the Wind, With a Bibliography of Eolian Geology, by S.C. Stuntz and E.E. Free. U.S. Department of Agriculture, Bureau of Soils, Bulletin No. 68, pp. 1-173.
- Free, E.E., and J.M. Westgaste. 1910. The Control of Blowing Soils. U.S. Department of Agriculture, Farmers' Bulletin No. 421.
- Fryrear, D.W. 1963. Annual crops as wind barriers. *Transactions of the ASAE*. 6(4):340-342, 352 6(4):340-342, 352.
- Hagen, L.J. 1976. Windbreak design for optimum wind erosion control. Proceedings of the Symposium "Shelterbelts on the Great Plains," Great Plains Agricultural Council Publication No. 78, pp. 31-36.
- Hagen, L.J. 1988. New wind erosion model developments in the USDA. Proceedings of the 1988 Wind Erosion Conference, Lubbock, TX, April 11-13, 1988, pp. 104-116.

- Hagen, L.J. 1991. A wind erosion prediction system to meet user needs. *Journal of Soil and Water Conservation*. 46(2):105-111.
- Hagen, L.J., and L. Lyles. 1988. Estimating small grain equivalents of shrub-dominated rangelands for wind erosion control. *Transactions of the ASAE*. 31(3):769-775.
- Hagen, L.J., and E.L. Skidmore. 1971. Windbreak drag as influenced by porosity. *Transactions of the ASAE*. 14(3):464-465.
- Hagen, L.J., E.L. Skidmore, and J.D. Dickerson. 1972. Designing narrow strip barrier systems to control wind erosion. *Journal of Soil and Water Conservation*. 27(6):269-272.
- Hagen, L.J., E.L. Skidmore, P.L. Miller, et al. 1981. Simulation of effect of wind barriers on airflow. *Transactions of the ASAE*. 24(4):1002-1008.
- Hayes, W.A. 1966. Guide for wind erosion control in the northeastern states. Upper Darby, PA: U.S. Department of Agriculture, Soil Conservation Service. Out of print.
- King, F.H. 1894. Destructive effects of winds on sandy soils and light sandy loam with methods of prevention. Wisconsin Agricultural Experiment Station Bulletin No. 42.
- Lyles, L. 1983. Erosive wind energy distributions and climatic factors for the west. *Journal of Soil and Water Conservation*. 38(2):106-109.
- Lyles, L. 1985. Predicting and controlling wind erosion. *Agricultural History*. 59(2):205-214.
- Lyles, L., and B.E. Allison. 1975. Wind erosion: uniformly spacing nonerodible elements eliminates effects of wind-direction variability. *Journal of Soil and Water Conservation*. 30(5):225-226.
- Lyles, L., and B.E. Allison. 1980. Range grasses and their small grain equivalents for wind erosion control. *Journal of Range Management*. 33(2):143-146.
- Lyles, L., and B.E. Allison. 1981. Equivalent wind-erosion protection from selected crop residues. *Transactions of the ASAE*. 24(2):405-408.
- Lyles, L., N.F. Schmeidler, and N.P. Woodruff. 1973. Stubble requirements in field strips to trap windblown soil. Kansas Agriculture Experimental Station Research Publication No. 164.
- Lyles, L., and J. Tatarko. 1987. Precipitation effects on ridges created by grain drills. *Journal of Soil and Water Conservation*. 42(4):269-271.
- Lyles, L., and J. Tatarko. 1988. Soil wind erodibility index in seven north central states. *Transactions of the American Society of Agricultural Engineers*. 31(5):1396-1399.

- NOAA. 2015. Temperature and Precipitation. Asheville, NC: National Oceanic and Atmospheric Administration, National Climatic Data Center. Available at <https://www.ncdc.noaa.gov/cag/> (Accessed August 10, 2020).
- Pike, Z.M. 1966. The Journals of Zebulon Montgomery Pike: With Letters and Related Documents. Donald Jackson, (Ed.), 2 vols. University of Oklahoma Press. Norman, OK.
- Skidmore, E.L. 1965. Assessing wind erosion forces: directions and relative magnitudes. *Soil Science Society of America Proceedings*. 29(5):587-590.
- Skidmore, E.L. 1976. A wind erosion equation: development, application, and limitations. *In ERDA Symposium Series 38, Atmosphere-Surface Exchange of Particulate and Gaseous Pollutants*. (1974), pp. 452-465.
- Skidmore, E.L. 1983. Wind erosion calculator: revision of residue table. *Journal of Soil and Water Conservation*. 28(2):110-112.
- Skidmore, E.L. 1986. Wind erosion climatic erosivity. *Climatic Change*. 9(1-2):195-208.
- Skidmore, E.L. 1987. Wind-erosion direction factors as influenced by field shape and wind preponderance. *Soil Science Society of America Journal*. 51(1):198-202.
- Skidmore, E.L., P.S. Fisher, and N.P. Woodruff. 1970. Wind erosion equation: computer solution and application. *Soil Science Society of America Proceedings*. 34(5):931-935.
- Skidmore, E.L., and L.J. Hagen. 1977. Reducing wind erosion with barriers. *Transactions of the ASAE*. 20(5):911-915.
- Skidmore, E.L., and R.G. Nelson. 1992. Small-grain equivalent of mixed vegetation for wind erosion control and prediction. *Agronomy Journal*. 84(1): 98-101.
- Skidmore, E.L., N.L. Nossaman, and N.P. Woodruff. 1966. Wind erosion as influenced by row spacing, row direction, and grain sorghum population. *Soil Science Society of America Proceedings*. 30(4):505-509.
- Skidmore, E.L., and J.R. Williams. 1991. Modified EPIC wind erosion model. *In J. Hanks and J.T. Ritchie, (eds.), Modeling Plant and Soil Systems, ASA-CSSA-SSSA Monograph No. 31*, pp. 457-469. Madison, WI.
- Skidmore, E.L., and N.P. Woodruff. 1968. *Wind Erosion Forces in the United States and Their Use in Predicting Soil Loss*. U.S. Department of Agriculture, Agriculture Handbook No. 346. 42 pp.
- Sporcic, M.A., and L. Nelson. 1999. Wind Erosion Equation – Use of Microsoft Excel Spreadsheet. Technical Notes – Agronomy 4, NRCS. Washington, DC: U.S. Department of Agriculture, Natural Resources Conservation Service.
- Thornthwaite, C.W. 1931. Climates of North America according to a new classification. *Geographical Review*. 21:633-655.

Udden, J.A. 1896. Dust and sand storms in the West. *Popular Science Monthly*. 49:953-954.

U.S. Department of Agriculture, Natural Resources Conservation Service. 2011. Section 502: Wind erosion. *In* NRCS National Agronomy Manual, Directive No. 190-V-NAM. Available at: https://www.nrcs.usda.gov/Internet/FSE_DOCUMENTS/stelprdb1043210.pdf. (Accessed August 10, 2020).

U.S. Department of Agriculture, Natural Resources Conservation Service. 2015. NRCS Photo Gallery. Available at: <https://www.flickr.com/photos/usdagov/8191524030/> (Accessed August 10, 2020).

Williams, J.R., C.A. Jones, and P.T. Dyke. 1984. A modeling approach to determining the relationship between erosion and soil productivity. *Transactions of the ASAE*. 27:129-144.

Woodruff, N.P., and D.V. Armbrust. 1968. A monthly climatic factor for the Wind Erosion Equation. *Journal of Soil and Water Conservation*. 23(3):103-104.

Woodruff, N.P., and F.H. Siddoway. 1965. A wind erosion equation. *Soil Science Society of America Proceedings*. 29(5):602-608.

Woodruff, N.P., J.D. Dickerson, E.E. Banbury, et al. 1976. Selected trees and shrubs evaluated for single-row windbreaks in the Central Plains. U.S. Department of Agriculture, ARS-NC-37 (1976). 15 pp.

Woodruff, N.P., L. Lyles, J.D. Dickerson, et al. 1974. Using cattle feedlot manure to control wind erosion. *Journal of Soil and Water Conservation*. 29(3):127-129.

A History of Wind Erosion Prediction Models in the U.S. Department of Agriculture, Part 2: The Wind Erosion Prediction System (WEPS)

Contributor:

L.E. Wagner

Abstract

Development of the Wind Erosion Prediction System (WEPS) was officially inaugurated in 1985 by scientists at the U.S. Department of Agriculture (USDA), Agricultural Research Service (ARS) in response to customer requests, particularly those coming from the USDA, Soil Conservation Service (SCS), for improved wind erosion prediction technology. WEPS was conceived to address deficiencies in the then-20-year-old, predominately empirical Wind Erosion Equation (WEQ) widely used by SCS. This effort sparked an endeavor that relied on novel laboratory wind tunnel research as well as extensive field studies to adequately uncover the physical relationships between surface properties and their susceptibility to and influence on wind erosion. The result is that WEPS incorporates many process-based features and other capabilities not available in any other wind erosion simulation model today. The USDA, Natural Resource Conservation Service (NRCS) has now implemented WEPS as a replacement for WEQ within their agency. However, the road to achieve that replacement required years of close interaction between ARS and NRCS. NRCS had to ensure they had suitable national-scale WEPS databases before implementation. User input simplifications were required as well as modifications to the reports. Run-time concerns also arose during the lengthy testing and evaluation process. Many of these were strictly non-wind erosion science issues that had to be addressed before NRCS could officially implement and begin using WEPS within their agency. The history of the development of WEPS, its unique features, and its solutions to selected critical issues encountered by NRCS prior to implementation are presented and discussed.

Introduction

Circa 1985, wind erosion modeling within the U.S. Department of Agriculture (USDA) had reached a ceiling in the level of maturity attainable with the empirical Wind Erosion Equation (WEQ) (Woodruff and Siddoway 1965). The many weaknesses and limitations of the WEQ had already been recognized by wind erosion researchers and had been outlined in a number of publications (Skidmore 1976; Cole 1983, 1984a) despite the numerous enhancements obtained during its 20-year history (by 1985). Tatarko et al. (2013) summarized the WEQ limitations while covering the early history of wind erosion modeling within USDA. This manuscript completes the history of the Wind Erosion Prediction System (WEPS) era of wind erosion modeling within USDA.

Due to the weaknesses of the WEQ, it became clear, at one point, to USDA wind erosion researchers that a new wind erosion model, including a more process-based, modular structure and a more extensive nature, would be needed to improve wind erosion predictions. The development of WEPS was thus initiated within USDA by Agricultural Research Service (ARS) scientists and in response to customer requests; that is, WEPS

was developed principally from the then-USDA Soil Conservation Service (SCS) for an improvement in wind erosion prediction technology. WEPS was conceived to address deficiencies in the predominately empirical WEQ, which had been widely used at the time by the SCS. WEPS incorporates improved models for computing soil losses by wind from agricultural fields as well as for providing many new capabilities such as calculating suspension loss, estimating PM10 (particles with an aerodynamic diameter of 10 microns or less) emissions, and specifying the direction in which soil leaves the field. WEPS was thus intended to be the future prediction tool of choice for those who plan soil conservation systems, who conduct environmental planning, or who assess offsite impacts caused by wind erosion (Hagen 1991a). The official genesis of WEPS occurred in October 1985 at an organizational meeting in Kansas City, MO, attended by ARS and SCS employees as well as by other government agency representatives, to discuss a replacement for the 20-year-old WEQ. Some noteworthy comments and observations were made at the meeting, as personally recorded by E.L. Skidmore. Dick Amerman, ARS National Program Leader, said, “Develop a physically based model to replace WEQ...”; Klaus Flack, SCS Chief Scientist, stated, “We need erosion prediction, conservation planning, a tool to document and justify conservation programs, allocate resources ... put some good science into the effort.”; Rex Johnston, ARS Southern Plains Area Director, commented, “Some of our basic concepts are faulty... let’s put some good science into the effort.”; and the U.S. Environmental Protection Agency (EPA) requested that the capability to predict PM10 be included in the new model.

An initial multidisciplinary core group was soon formed, composed primarily of ARS and SCS scientists, to begin the development of a new Wind Erosion Model (WEM). Soon afterwards, the term Wind Erosion Research Model (WERM) was used to describe the developing research model. The envisioned complete model to be delivered to customers, with national-scale databases and including a user interface, was to be called the Wind Erosion Prediction System (WEPS). Eventually, WERM was also dropped from the vocabulary in the model-related development documents, with WEPS being the sole surviving acronym now used for all aspects of the project, from the developing science model to the fully released model, which includes the interface and the databases. The term WEPS will be used exclusively within this manuscript to describe the project unless explicitly mentioned otherwise within the cited documents.

The primary ARS scientists constituting the original core team were George Cole, Leon Lyles, Dean Armbrust, Larry Hagen, and Ed Skidmore, from the former ARS Wind Erosion Research Unit (WERU) in Manhattan, KS, and Bill Fryrear, J.D. Bilbro, and Ted Zobeck, from the Conservation and Production Systems Research Unit (CPSRU) in Big Spring, TX. The additional ARS core team members later participating during the development of WEPS were Larry Wagner, John Tatarko, D.J. Ding, Jeff Layton, Amare Retta, Abdu Durar, Naser Mirzamostafa, Fred Fox, and Simon van Donk from WERU; John Stout, Ali Saleh, and Scott van Pelt from CPSRU; Paul Unger, Jean Steiner, and Harry Schomberg with the ARS Conservation and Production Research Laboratory (CPRL) in Bushland, TX; Ken Potter from the ARS Grassland, Soil, and Water Research Laboratory (GSWRL) in Temple, TX; and Keith Saxton, Larry Stetler, and David Chandler with the Hydrology and Remote Sensing Laboratory (HRSL) in Pullman, WA. Some prominent SCS, and later NRCS, employees who were involved with WEPS during its development were Klaus Flach, Bob Grossman, Scott Argabright, Ray Sinclair, Lorenz Sutherland, Henry Bogusch, Dave Lightle, Bruce Wight, Dave Schertz, Chuck Landers, Mike Hubbs, Norm Widman, and, especially, NRCS’s appointed liaisons with WERU such as Gary Tibke, Henry Bogusch, Arnold King, and Michael Sporic.

Numerous collaborators outside the principal ARS research units were also involved in the field and laboratory research conducted for the development of WEPS. The collaborators consisted of soil scientists, agricultural engineers, agronomists, and crop scientists from the ARS research field stations (Steve Merrill and Mike Lindstrom), SCS technical centers, and university researchers (John Lamb, Delbert Mokma, and Ronald Yoder) with a variety of backgrounds and expertise. Hence, the WEPS project was a truly multi-agency, multidisciplinary project. Some major milestones and events during the developmental history of WEPS through the implementation of the model by NRCS are listed in Table 1.

Table 1. Important dates and milestones for the WEPS project.

Dates	Milestone event
October, 1985	Organizational meeting in Kansas City, MO (genesis of WEPS)
1985	Initial core team meeting (George Cole selected as WEPS Project Leader)
17 December, 1985	First revision of WEPS User Requirements Specification (draft)
August, 1986	Larry Hagen appointed as WEPS Project Leader
April, 1991	Final revision of WEPS User Requirements (draft)
August 26-29, 1991	WEPS User Requirements meeting in Kansas City, MO
August, 1995	First WEPS Technical Document published (draft)
September, 1999	Larry Wagner appointed as WEPS Project Leader
4 April, 2005	WEPS formally delivered to NRCS for testing and evaluation
2005	NRCS requested “yield calibration” and “fixed yield:biomass” ratio features be added to WEPS
2006	WEPS incorporates WEPP hydrology to meet NRCS runtime constraints
2006	Added irrigation monitoring processes to represent furrow, sprinkler, and drip
26 February, 2008	WEPS formally delivered to NRCS for training and database population
February, 2010	WEPS accepted by NRCS for implementation
1 October, 2010	WEPS installed on 15,000 computers and operational in 2200 NRCS field offices (version 1.1.16)
7 December, 2010	Official “Notice of Implementation” by NRCS of WEPS use for soil erodibility system calculations in the Federal Registry (Federal Register 2010)
11 February, 2011	Updated WEPS databases provided to NRCS field office computers

1 October, 2011	Updated WEPS pushed to NRCS field office computers (version 1.2.9)
5 July, 2012	Updated WEPS databases pushed to NRCS field office computers
30 October, 2013	Updated WEPS released to NRCS for push to field offices (version 1.3.9)
21 December, 2016	Updated WEPS released to NRCS for push to field offices (version 1.5.52)

The early work on WEPS consisted of identifying core team members, assigning research area leadership responsibilities, developing the initial framework for the model, and outlining the extensive field sampling and numerous laboratory studies needed to obtain the necessary data required for WEPS. Critical national funding was also pursued for WEPS in concert with its sister project, the Water Erosion Prediction Program (WEPP) (Lane and Nearing 1989).

George Cole was selected as the original WEPS program leader due to his background in simulation modeling. Larry Hagen was assigned to lead the fundamental laboratory wind tunnel research necessary for the development of the WEPS Erosion submodel. Ed Skidmore led the field research to obtain the range of the temporal soil properties relevant to wind erosion on Kansas soils, and Ted Zobeck coordinated the effort of many field collaborators to obtain similar data over a range of soil types across the United States. Bill Fryrear was charged with obtaining the field site data for validation of the eventual WEPS Erosion submodel (Table 2). J.D. Bilbro and Dean Armbrust were assigned to obtain the necessary physical plant characteristics relevant to wind erosion and to parameterize that data into a process-based plant growth model. Later additions to the core team assumed additional responsibilities: Abdu Durar – Hydrology submodel and development of an approach to adequately simulate the near surface water content at the air-soil interface; Amare Retta – Plant Growth submodel and plant database development; Larry Wagner – Management submodel development and related field data collection; and Jean Steiner and Harry Schomberg – Decomposition submodel and associated field data collection.

Table 2. WEPS field validation sites.

Location (City, State)	Study Period
Fresno, CA	1993-1995
Akron, CO	1988-1990
Eads, CO	1990-1992
Crown Point, IN	1990-1992
Elkhart, KS	1990-1993
Kennett, MO	1992-1994
Havre, MT	1992-1994

Lindsey, MT	1991-1992
Scobey, MT	1988-1990
Sidney, NE	1988-1991
Mabton, WA	1991
Prosser, WA	1991-1994
Big Spring, TX	1989-1997

Additionally, work on the WEPS User Requirements document with the assistance of SCS was initiated. Some core concepts identified in the first draft of that document by George Cole in 1985 covered how WEPS would perform or achieve the following: (a) be used, e.g., as a conservation planning tool as well as for inventory and assessment purposes by user agencies; (b) have a modular design with core submodel components; (c) include a list of required national databases; (d) observe conservation of mass principles, be process-based, climate driven, deterministic, robust, and validated; (e) be easy to use; (f) reflect impacts of applied management practices on wind erosion susceptibility; and (g) apply to all situations presently covered by WEQ. The concept of a user interface for the model was added in later drafts as a requirement under the “ease of use” directive (e).

One interesting requirement within the first draft was that the system would compute the frequency distribution of wind erosion at the rate of one management practice per 10 minutes and no more than 30 minutes of user time (computer time can be longer) per farm, is to be required in the office to prepare and assemble needed information before going to the field. This was the estimated amount of time that it took a knowledgeable SCS field office employee to apply the paper (non-computerized) version of WEQ at that time. Later revisions of the user requirements document included additional constraints on the computational time and even specified particular computer hardware, including the use of a math coprocessor as a requirement, to meet the new runtimes. The final documented requirements for the runtime in the last draft authored by Hagen in 1991 were “should compute ... annual soil loss values ... at the rate of two minutes for each year of the crop rotation” and “no more than 30 minutes of office time should be required to assemble the needed information before operating the program with a typical client.” However, later discussions between WERU and the NRCS National Agronomist, circa 1993, resulted in a much tighter “5 minutes to obtain and select inputs” and “less than 30 seconds per rotation year for a simulation” requirement upon WEPS. The significance of this one requirement had profound implications both during the development of WEPS and on the final delivered model submitted to NRCS years later.

Multiple meetings with SCS were held over the coming years, with multiple updated drafts produced as a result. The WEPS User Requirements document was never officially signed off by SCS, nor formally published, due to a variety of external factors, although Hagen did publish a manuscript that covered a partial list of those user requirements (Hagen 1991a). Regardless, the WEPS User Requirements document contained the blueprints faithfully followed throughout the development of WEPS. The last formal meeting with SCS regarding the user requirements for WEPS was held August 26-29, 1991, in Kansas City, MO.

Many other meetings, workshops, and training sessions were held, first by the core researchers and the field research collaborators and later with much more direct NRCS involvement, during the WEPS user interface and database development. A listing of such meetings held over the years is shown in Table 3. These meetings covered the basic laboratory and field research that had been conducted early on for WEPS during the core team meetings and later during the many Quarterly ARS/NRCS Agreement meetings (2002-2009) covering the specific modeling and user interface issues, NRCS WEPS testing meetings (2005-2006) covering the following states (MO, KS, CO, NE, NM, ND, SC, ID, MT, IA, NV, WA), the development and population of databases, and eventually the NRCS “train the trainer” workshops (2007).

Table 3. WEPS core team, subgroup, NRCS/ARS agreement and NRCS WEPS testing meetings as well as NRCS Train-the-Trainer workshops.

Dates	Location	Purpose
Oct., 1985	Kansas City, MO	Meeting formalizing the WEPS project
Nov. 3-5, 1987	Manhattan, KS	WEPS Core Team meeting
Apr. 13-15, 1988	Big Spring, TX	WEPS Core Team meeting
Oct. 28-30, 1988	Morris, MN	WEPS Core Team meeting
May 21-23, 1989	Ft. Worth, TX	WEPS Core Team meeting
Sep. 19-21, 1989	Lincoln, NE	WEPS Core Team meeting
Apr. 3-5, 1990	Bushland, TX	WEPS Core Team meeting
Apr. 18-21, 1991	Manhattan, KS	WEPS Core Team meeting
Aug. 26-29, 1991	Kansas City, MO	WEPS User Requirements meeting
Nov. 19-21, 1991	Big Spring, TX	WEPS Core Team meeting
Apr. 21-23, 1992	Manhattan, KS	WEPS Core Team meeting
Oct. 28, 2002; Feb. 3, Apr. 24, Jul. 22, 2003; Mar. 2, Jun. 3, Nov. 5, 2004; Apr. 5, Aug. 11, Dec. 13, 2005; May 2, Sep. 6, Nov. 30, 2006; Mar. 13, Jul. 19, Oct. 11, 2007; Oct. 23, 2008; Jul. 28, 2009	Manhattan, KS	ARS/NRCS Agreement meetings
Mar. 29-31, Jun. 1-3, Aug. 23-25, Dec. 29-30, 2005	Various locations	NRCS WEPS Testing meetings
Nov. 6-8, 2006, Jan. 22-24, Feb. 12-14, Mar. 12-14, Apr. 9-11, 2007	Various locations	NRCS WEPS Train-the-Trainer workshops

It took approximately 10 years to conduct the basic research and field studies required for the WEPS erosion routines and its supporting submodels, to develop the core science model, and to validate the erosion code. Then there was a brief 2-year stint during which the WEPS developers were requested to work on a Revised Wind Erosion Equation (RWEQ) but were later asked to return to working on WEPS. The latter 10-year period was primarily focused on developing the interface and expanding the necessary databases for NRCS implementation. This does not mean that there were no ongoing improvements, bug fixes, and enhancements being made to the science model during the latter 10 years. Some specific major changes as identified in Table 1 during that timeframe were the NRCS-requested yield calibration feature and a fixed yield:biomass ratio for determining crop yields. In addition, the WEPP hydrology code was incorporated to meet NRCS runtime constraints. The iterative process during the NRCS testing stages was crucial to the refinement of the WEPS science model, to the maturation of the usability of the interface, and to the ultimate successful conclusion of the implementation of WEPS within NRCS.

Initial completion dates were underestimated at the beginning of the WEPS project. The program interfaces changed rapidly during this time, starting with the text-based menu systems and concluding with the highly graphical, mouse-based windowed systems. The level of support required by NRCS to develop national-level databases was not anticipated.

Model Description

WEPS was constructed to be modular, unlike most models of that era, e.g., the Erosion Productivity Impact Calculator (EPIC) (Sharpley and Williams 1990). Hence, the advantages of constructing a modular program were already evident. WEPS was also built to incorporate the conservation of mass and momentum principles within the derived relationships, where possible, and to have submodels capable of simulating changes in the relevant properties important to wind erosion on a daily basis.

However, the concepts embodied in WEPS were not determined quickly. The previous work by the ARS scientists formed the initial basis for WEPS: the conversion of WEQ to a daily time step model for inclusion into EPIC (Cole 1983, Cole and Lyles 1984); the concepts of outside influences changing the susceptibility of a surface to wind erosion, e.g., crop growth, temporal soil surface properties modified by climate, changes in soil aggregate status due to tillage, etc. (Lyles and Tatarko 1986); the derivations of the mathematical basis for the physical processes required to compare the wind tunnel relationships with the field-scale erosion rates (Cole 1984a); the expressions of the period or interval for erosion loss (Cole 1984b); the introduction of the conservation of mass and momentum principles into the wind erosion processes (Cole 1985); and the investigations of the probability requirements for the erosion outputs (Cole and Higgins 1985).

WEPS now consists of several major components, which will be further referred to collectively as WEPS 1.0: (a) the WEPS science model; (b) the WEPS interface; and (c) the databases of soils, crop growth/residue decomposition, operations, wind barriers, and climate. The science model is the core wind erosion model used to perform the simulation. The WEPS interface obtains the required inputs from the user and then packages them into the necessary science model input files, executes the science model, and presents the output in a more user-friendly format than provided by the science model itself. The science model, through its respective submodels, estimates the

soil/vegetation surface state on a daily basis with respect to the erodibility of the surface. If the wind speed is significant enough during the day to generate a friction velocity that exceeds the static threshold friction velocity of that surface, then the Erosion submodel will simulate the degree of wind erosion that occurs on a sub-daily time step for that day. Figure 1 shows the basic structure of WEPS 1.0, including the interface user inputs, the databases, and the submodels in the science code. The science model is coded in FORTRAN, which was the programming language initially understood by the majority of scientists at that time. The WEPS interface is coded in Java, as it is the only programming language that has cross-platform capability, including the graphical display elements, without requiring any modifications at the source code or binary level. The databases are of three types: the text-based proprietary (unique to the program/database) formatting for the older databases and records (CLIGEN, WINDGEN, soil, management, and wind barriers), the XML-based for the crop and operation records accessed by the WEPS interface, and the GIS shape file-based for the climate record selection.

Science Model

WEPS is unique as a wind erosion model because it seeks to determine the surface state on a daily and sub-daily basis with respect to the surface's susceptibility to wind erosion.

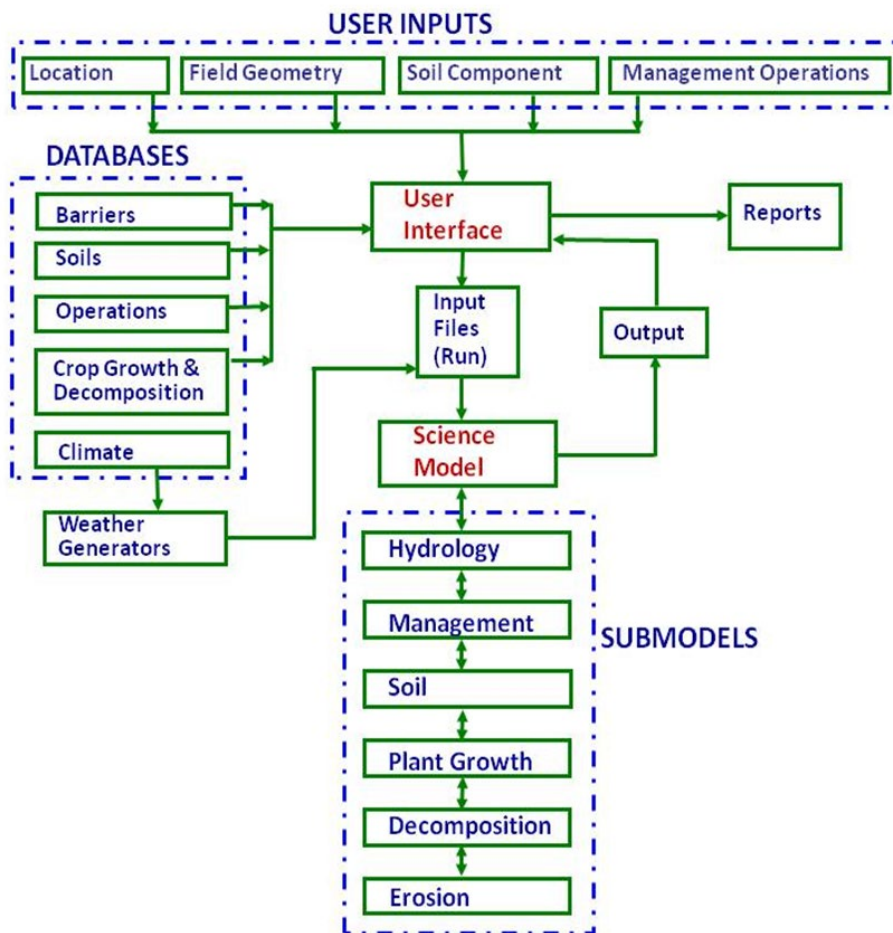


Figure 1. WEPS 1.0 components, submodels, and databases.

No other wind erosion model is capable of this. WEPS simulates many of the physical processes known to occur as a result of wind erosion on cropland. The basic erodibility of the bare soil is determined from the aggregate size distribution on the surface as well as from the density and the dry stability of the aggregates. If the surface is either partially or fully consolidated (e.g., if it is crusted), then the fraction of crusted surface is taken into account along with the crust thickness, its dry stability, and the amount of loose, erodible material on the crust. If the surface consists of non-erodible particles (rocks), then the fraction of the surface that contains rocks discounts the surface's susceptibility to erosion (see Figure 2). The aerodynamic roughness is computed based on both the random roughness and any oriented roughness and its row direction relative to the wind direction. If vegetation exists, then the computed friction velocity is carried down through the plant canopy to the surface (a unique attribute of the WEPS Erosion submodel).

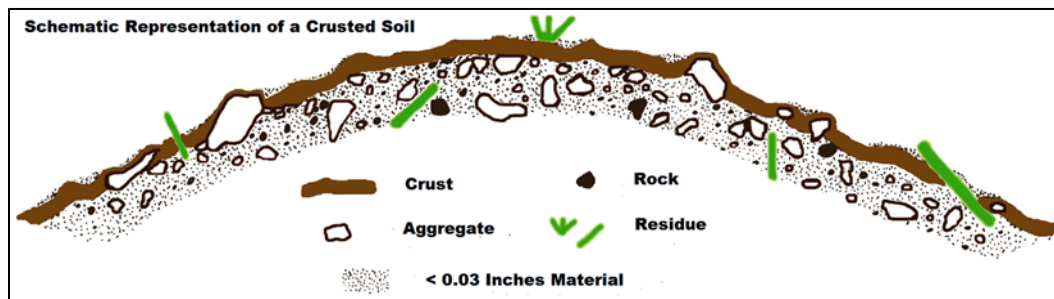


Figure 2. Schematic representation of a crusted soil (Zobeck 1991).

Hydrology

WEPS maintains the current state of the surface on a daily basis, with the modifications to surface wetness maintained on an hourly basis. The user has the option of selecting one of the two hydrology submodels—either (a) the original WEPS Hydrology submodel, which performs a complete one-dimensional Darcy's law simulation of the water movement within the soil profile, including infiltration and evaporation or (b) the WEPP hydrology submodel, which uses Green-Ampt infiltration, a tipping bucket approach to water distribution within the soil profile, and an empirical evaporation withdrawal function (Savabi et al. 1995). Both hydrology submodels also use independently developed routines to simulate the soil freeze/thaw and the snow accumulation/melt. The WEPP hydrology submodel uses a less computationally intensive approach. This submodel is the default hydrology component used by NRCS, although the WEPS hydrology component better simulates the diurnal cycling of the surface moisture and more accurately influences the freeze/thaw and freeze/dry winter processes, all of which impact the surface soil erodibility by wind. The WEPP hydrology submodel was added to meet the NRCS runtime requirements, which WEPS had difficulty attaining at the time (circa 2006) with the computer hardware available then. The Hydrology submodel accounts for 80-90 percent of the total runtime for a typical WEPS simulation. A detailed description of the Hydrology submodel in WEPS is provided in the WEPS Technical documentation (i.e., chapter 6 of this document).

Plant Growth

The Plant Growth submodel (alternatively known as the Crop submodel) simulates the growth of a plant (crops) under applied daily water and temperature stresses. It was originally based on the Erosion Productivity Impact Calculator (EPIC) plant growth model (Sharpley and Williams 1990), but it has been heavily modified to meet the WEPS

requirements for vegetation influences on wind erosion. The leaf mass and the stem mass interact differently with the wind; therefore, the plant biomass accumulation is divided into the stem, leaf, and reproductive components. For better frost damage simulation, the live leaf and dead leaf masses are tracked. To model perennial, winter annual and bi-annual crops, a storage pool accumulates the mass and releases it for regrowth, assuming that all leaf mass is removed. A maximum plant radius prevents one plant from completely covering a large area and is used to divide the stem mass between standing and flat. For crops whose maturity is not purely heat unit driven, the vernalization parameters can also be set. Unlike EPIC, which grows the biomass based on a heat-unit-driven Leaf Area Index (LAI) curve, WEPS grows biomass and divides it into the mass pools and calculates the resulting LAI from the leaf mass. Similarly, the stem biomass is used to calculate a stem area index. Additionally, due to NRCS requests, an individual crop can also be configured such that the after-harvest residue is dependent on the yield, and if need be, this functionality can be disabled for all crops via a command line option to the WEPS science model. A detailed description of the Plant Growth submodel in WEPS is provided in the WEPS Technical documentation (i.e., chapter 9 of this document).

Decomposition

The residue decomposition is driven by temperature, the soil moisture (on the surface for surface residue and within the soil for buried residue), and the decay rate, which is dependent on the parent plant material and the component (Steiner et al. 1994, Schomberg et al. 1996). The stem, leaf, chaff, and root components are tracked separately. Multiple pools of the residue, based on the age, component, and location, are maintained separately within WEPS. The critical residue parameters that impact wind erosion are the leaf area index, the stem area index, the spatial density of the standing stalks (population), and their average diameter and height, as well as the flat residue mass and the cover fraction.

Soil

The Soil submodel simulates the daily changes to the soil and surface that occur due to climatic factors. The ridge and dike height as well as the random roughness are decayed due to cumulative rainfall. The surface crust is formed due to puddling on the surface when the precipitation events exceed the infiltration rate, with the resulting crust stability and thickness as well as the amount of loose erodible material on the crust all determined by the parent soil type. Aggregates consolidate, increasing in size, and aggregate stability increases also occur due to cumulative rainfall. Over time, the bulk density trends to a settled bulk density value that depends on the soil type (Rawls 1983). The aggregate stability and the size are decreased due to freeze/thaw, freeze/dry, and wet/dry cycles. The de-aggregation and re-aggregation processes are reflected in the changes to the size distribution of the aggregates within each soil layer, represented as a modified lognormal distribution (Wagner and Ding 1994).

Management

The Management submodel addresses the variety of land management actions by identifying the primary physical processes involved and by representing each individual management operation as a sequential set of the relevant primary physical processes (Wagner and Fox 2013). Those processes include the following: (1) surface modification (creation or destruction of ridges and/or dikes that form oriented surface roughness, changes in surface random roughness, and destruction of soil crust); (2) soil layer mass

manipulation (changes in aggregate size distribution and soil porosity, mixing of soil and residue among soil layers, and soil layer inversion); (3) biomass manipulation (burying and resurfacing residue, clipping standing residue, flattening standing residue, killing live crop biomass, and biomass removal); and (4) soil amendments (manure and residue additions, planting, and irrigation). A complete list of management operation processes is provided in Table 4.

Table 4. Management operation processes.

Action	Process	Description
Soil surface manipulation	Crust	Process of modifying the soil surface crust characteristics
	Roughen	Process of modifying the random surface roughness
	Ridge/Dike	Process of creating or destroying ridges and/or dikes (oriented surface roughness)
Soil mass manipulation	Crush	Process of applying forces to the soil that modifies the aggregate structure by breaking down soil aggregates
	Loosen	Process of decreasing soil bulk density and increasing porosity (incorporation of air), or the inverse process of increasing the soil bulk density by removing air from the soil (e.g., compaction)
	Mix	Process of blending soil layer properties, including biomass
	Invert	Process of reversing the vertical order of occurrence of the soil layers within the current specified tillage zone
Biomass manipulation	Flatten	Process of converting standing biomass to flat biomass
	Bury	Process of moving surface biomass into the soil
	Re-surface	Process of bringing buried biomass to the surface
	Cut/Remove	Process of cutting standing biomass to a prescribed height and placing the cut material on the surface or, optionally, removing (harvesting) the cut material
	Thin population	Process of reducing number of standing biomass stems by a fraction of the total or to a specified number per unit area and placing thinned material on surface or, optionally, removing (harvesting) it
	Kill/Defoliate	Process of killing or defoliating live (or dead) biomass
	Remove	Process of removing biomass from the system (harvest, grazing, and burning)

	End biomass	Process that completes transfer of killed crop biomass to residue decomposition pools. This WEPS-specific function addresses a deficiency in current model design that does not allow decomposition process to occur automatically within model
Soil amendments	Plant	Process of adding seeds/plants to the soil
	Irrigate	Process of adding water on or into the soil
	Add biomass	Process of adding biomass (residue, manure, wood chips) to the surface and/or into the soil

In accordance with the WEPS design philosophy, the Management submodel simulates these processes via a physical basis if possible, incorporates the conservation of mass concepts, and employs the functional relationships developed from the field and laboratory data, if available, using a minimum of parameters with the readily available and/or attainable values. These processes are assumed to be dependent with respect to each other and are simulated sequentially. Thus, each management operation is represented by an appropriate ordered list of processes. The individual processes and their order of simulation uniquely describe each specific operation effect on the soil, surface, and vegetation present. The typical multi-tool and ganged multi-implement operations also can be easily described in full by repeating the necessary processes for each tool (tillage element), which exist as a component of such operations.

The list of management operations performed for a given management plan (crop rotation/tillage sequence or cyclical list of cultural practices) is specified in a management file. On the dates when operations are to be performed, the Management submodel will execute the specified routines required to simulate the effects of those operations listed in the management file. When the final operation is performed for that particular management/crop rotation cycle, the sequence will then be repeated for the subsequent year(s) until the end of the simulation.

Erosion

WEPS is unique in the detail and completeness that the erosion processes are modeled. Thus, an overview of how erosion is modeled within WEPS is provided here.

In WEPS, the friction velocity was selected to drive erosion, but the meteorological input parameter is the wind speed. However, for any given wind speed, under neutral atmospheric conditions in the surface boundary layer, the friction velocity is proportional to the natural logarithm of the surface aerodynamic roughness. Therefore, to obtain the friction velocity, the aerodynamic roughness term of the log-law wind speed profile must be determined.

For surfaces without standing biomass, the surface aerodynamic roughness is simply controlled by the roughness of both the soil and the flat biomass cover. The controlling (maximum) roughness, e.g., the random, oriented, or flat cover, is calculated, and the

appropriate relationship is selected for use in determining the aerodynamic roughness length.

If standing plant biomass is present, additional calculations are performed to determine the friction velocity at the surface. The effectiveness of leaves is significantly reduced due to their tendency to orient parallel to the wind streamlines (Armbrust and Bilbro 1997). Therefore, an effective biomass drag coefficient is computed, and it discounts the effect of the leaves relative to that of the stems on the wind in determining the aerodynamic roughness length above the canopy surface. The under-canopy aerodynamic roughness length is then calculated (Hagen and Armbrust 1994). Once the aerodynamic roughness length is known, the friction velocity of the surface generated by a given wind speed can then be determined.

To determine the static threshold friction velocity, the potential surface cover must be accounted for and may consist of the following: (a) rocks, (b) crust, and (c) aggregates, with flat and standing biomass above or on those surfaces. The static threshold friction velocities for bare soil surfaces are estimated by equations fitted to wind tunnel data (Hagen 1991b, Chepil and Woodruff 1963). If a flat biomass cover is present, the increase in surface area protected from emission is accounted for (Hagen 1996). Likewise, an increase in the static threshold friction velocity due to surface wetness is also considered (Saleh and Fryrear 1995).

If the computed friction velocity generated by a given wind speed exceeds the computed surface static threshold friction velocity, then erosion will occur and the Erosion submodel will initiate the emission of soil and use a reduced static threshold friction velocity (dynamic threshold friction velocity), which accounts for the fact that saltating particles return additional energy to the stationary aggregates lying on the surface in the saltation/creep transport capacity equations (Bagnold 1943).

The transport of soil during wind erosion occurs in three modes. Creep-size aggregates (0.84-2.0 mm diameter) roll along the surface, saltation-size aggregates (0.10-0.84 mm diameter) hop over the surface, and suspension-size aggregates (< 0.10 mm diameter) move above the surface in the turbulent flow. Obviously, as wind speed increases, turbulence, or sediment loads, change; the diameter of aggregates moving in the various modes also may change slightly. However, in WEPS, these values are assumed constant.

In WEPS, it was assumed that the combined saltation/creep mode of transport has a distinct transport capacity for each surface, based on the surface aerodynamic roughness and wind speed. This assumption generally has been supported by both the field and wind tunnel measurements of the saltation/creep discharge (Greeley and Iversen 1985). Other properties, such as the soil texture, the quantity of loose erodible material on a crusted surface, etc., may limit the supply of saltation/creep-size particles available for emission (transport), especially on short fields. However, these properties do not impact the carrying capacity of the wind (transport capacity) for these particles on a given surface. It was also assumed that the suspension component does not reach a transport capacity on most eroding fields. Thus, separate equations have been developed for saltation/creep, suspension, and PM10 discharge because each responds differently to both the wind forces and the sediment load (Gillette et al. 1998). Separating these erosion components is also useful because they have different potential offsite impacts.

Wind erosion occurs over a wide range of surface conditions. To aid in delineating the erosion rates among the various surfaces, several individual erosion processes were identified in WEPS (Hagen et al. 1999). These processes include (a) the direct entrainment (emission) of loose soil by wind and/or saltation impacts, (b) the abrasion of soil from clods/crust by saltation impacts, and (c) the breakage of saltation/creep-size aggregates into suspension-size particles. These processes were selected for individual simulation because they differ from one another by approximately an order of magnitude in their ability to supply new suspension or saltation/creep-size mass to the airstream in response to a saltation impact (Mirzamostafa et al. 1998). When the saltation/creep discharge exceeds the transport capacity over a region in a local area of the surface, the deposition of saltation/creep occurs. It also was assumed that the coarse fraction of the suspension component begins depositing when moving over areas in the simulation region that are not actively eroding.

For both the saltation/creep and the suspension components, based on the conservation of mass in a control volume, the one-dimensional, quasi-steady state equations for the physical processes were developed (Hagen et al. 1999). They include the following parameters: (a) emission, based on the surface roughness, biomass cover, and aggregate size distribution; (b) abrasion of immobile soil clods and crust by saltation impacts creating additional erodible aggregates (Hagen et al. 1992, Zobeck and Popham 1991; Mirzamostafa et al. 1998); (c) breakage during the transport of saltation-size aggregates into suspension-size aggregates (Mirzamostafa 1996); (d) trapping due to changes in surface conditions that cause a decrease in the threshold friction velocity and capacity; and (e) interception of mobile particles due to the standing biomass.

In WEPS, the simulation region is gridded, with the erosion computed within each uniform-sized rectangular cell. The cell size and shape are both variable, depending on the size and shape of the simulation region. The minimum grid cell X and Y length dimensions are 7 m. Currently, the maximum number of 29×29 (841) cells are used in a typical field size simulation (greater than 200 m by 200 m). The cell size and number were determined based on tradeoffs between the erosion computation accuracy and the runtime considerations for typical U.S. cropland field sizes. The number of cells is more than quadrupled to 59×59 (3,481) cells, if barriers are specified on the simulation region. This was done to properly account for the barrier effects on larger field simulations (that is, to maintain a small enough cell size to properly represent the regions upwind and downwind influenced by the barrier). For each day that erosion occurs, all cells begin with the same initial surface conditions. Likewise, the initial friction velocity for each cell is the same, except within the influence zone of a wind barrier. The friction velocity is then depressed, based on (a) the barrier porosity, (b) the barrier height, and (c) the distance from the barrier for each cell within 15 and 5 times the barrier height downwind and upwind, respectively. As the erosion process proceeds, the surface state is updated dynamically within the Erosion submodel for each cell. The effects of the erosion processes are all simulated within the Erosion submodel of WEPS. These include (a) abrading through the surface crust, (b) deflating the erodible-size surface aggregates and therefore increasing the non-erodible aggregates and rocks on the surface, and (c) smoothing of both the oriented and random roughness due to the trapping and sheltering of eroding particles. The updating of the surface occurs at different time intervals and is dependent on the relative erosive wind energy (level of erosion) occurring at the most erosive grid cell during the previous time step.

Interface

NRCS would not have been able to implement WEPS without an interface or the national databases that made it easy for the field office staff to select necessary inputs and view the simulation results easily. Significant effort was expended on developing the interface, iteratively revising it to better meet their needs and assisting them in populating the necessary databases. Many resources were spent, at least time-wise, on the development and expansion of the interface and databases as were spent on the development of the WEPS science model. However, it is the author's belief that WEPS would never have been implemented within NRCS without these non-science components having been addressed and completed as a part of WEPS 1.0.

The WEPS interface, written in Java to be as cross-platform as possible, obtains the required inputs from the user. When a WEPS run is initiated, the interface creates the necessary science model input files from those previously selected inputs, runs the CLIGEN and WINDGEN generators to generate the climate and wind data files, respectively, if configured to do so, and then executes the science model. Upon completion, the interface presents the output in a more user-friendly format than provided by the science model itself. Figure 3 shows the main WEPS interface screen.

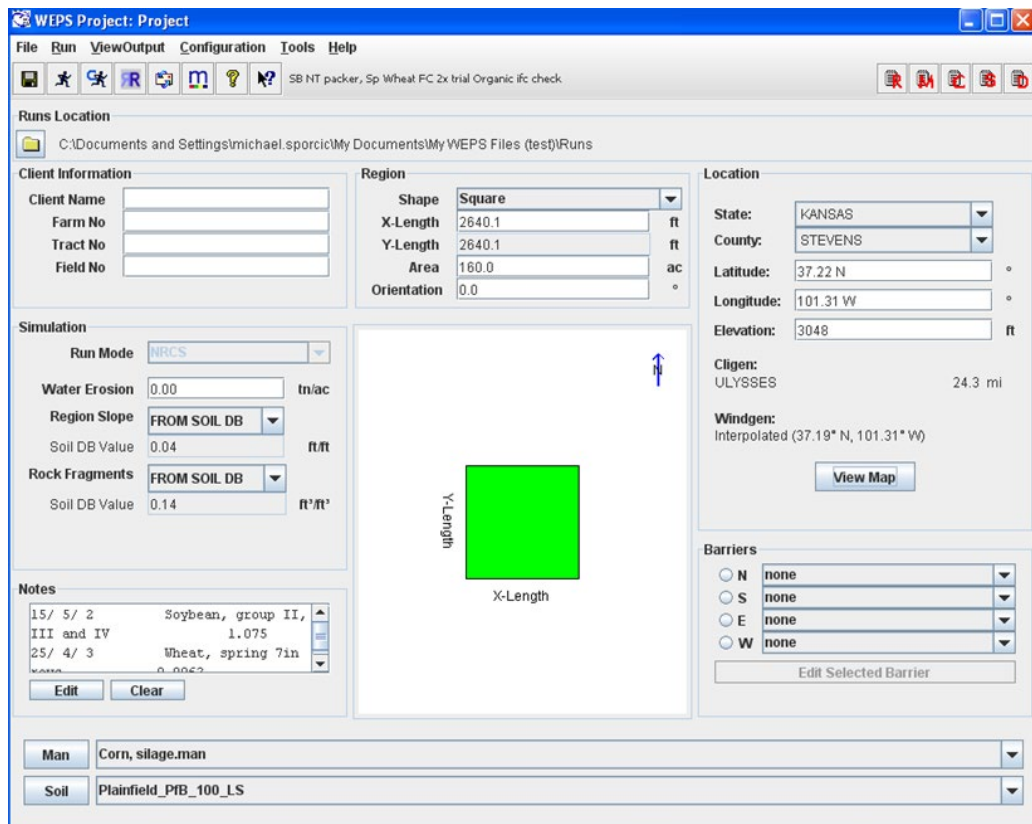


Figure 3. Main screen of WEPS User Interface.

Inputs

Through the interface, there are only four main inputs required by WEPS: (a) location, (b) field geometry, (c) soil component, and (d) management, as shown in Figure 1.

The location can be specified in a variety of ways by the user: (a) latitude/longitude coordinates directly, (b) through a series of political boundary selections (e.g., State/county selections for the United States), or (c) by selecting a location from a map. Once the location has been selected, the user will usually have the representative CLIGEN and WINDGEN stations selected based on the criteria set within the configuration of the user interface. The options include (a) the nearest station to the specified latitude/longitude, (b) the specified station within a defined polygon region, (c) the interpolated station (currently only available for WINDGEN stations), (d) the user selected, and (e) the specified previously generated or historical data in the CLIGEN and/or WINDGEN file formats. NRCS employs several of these methods, depending on the region in which the model is being applied. For non-NRCS WEPS release configurations, the default station selection is still the NRCS option, but the user is free to select any of the other specific options available, e.g., (a) nearest station with sorted by distance choice list override, (b) nearest station only, (c) file (usually historical data) option, or (d) GIS maps for using the polygons. The WINDGEN station selection also contains the additional interpolation option. The user also has the ability to select one of these options as the default as a configuration setting through the configuration menu setup available from the menu bar on the main WEPS screen. The actual WEPS inputs from these two climate files are described in the next section on databases.

The field geometry is currently restricted to rectangular regions oriented relative to north within the WEPS science model. The user can specify the X and Y lengths and the orientation angle of the region directly from a common set of field shapes in which the size (area) of the simulation region is then specified. Non-rectangular shapes, such as circles, half-circles, and quarter-circles, are handled by internally converting the region to a representative rectangle of the same area within the interface. This approach was added to the interface in response to the WEPS testing conducted by NRCS. This testing revealed problems with the representative field size to be used for non-rectangular fields.

The soil component consists of the intrinsic soil layer and the surface properties. The temporal soil layer and surface properties are either initialized by the user manually or, more commonly, are assigned default values based on a few select intrinsic soil property values within the interface. There are 16 surface properties and 30 soil layer properties required for a fully populated WEPS soil input file (Tables 5 and 6). The user has the option to select a soil component in the following ways: (a) by going through a State/County/Series/mapid/component selection process from either a Microsoft Access format NRCS SSURGO database (Soil Survey Staff, n.d.) file or directly over the Internet through a Simple Object Access Protocol (SOAP) interface, now called a Web Map Service (WMS), connection with the NRCS Soil Data Access URL via <https://sdmdataaccess.nrcs.usda.gov/>; (b) by selecting a WEPS-specific text formatted file; or (c) by manually filling in at least seven soil properties for each soil layer, which is the minimum required to estimate the values for all the remaining properties if the user does not know or does not want to manually populate all the properties. The NRCS users connect to the NRCS Soil Data Access website by default.

Table 5. List of intrinsic soil, layer, and surface properties used by WEPS.

Property	Units	Can estimate through interface (Yes/No)
Slope	$m \cdot m^{-1}$	No
Number of soil layers	unitless	No
Organic matter	$kg \cdot kg^{-1}$	No
Sand	$kg \cdot kg^{-1}$	No
Silt	$kg \cdot kg^{-1}$	Yes
Clay	$kg \cdot kg^{-1}$	No
Rock fragments	$m^3 \cdot m^{-3}$	Yes
*Very coarse sand (fraction of < 2 mm portion of the soil)	$kg \cdot kg^{-1}$	Yes
*Coarse sand (fraction of < 2 mm portion of the soil)	$kg \cdot kg^{-1}$	Yes
*Medium sand (fraction of < 2 mm portion of the soil)	$kg \cdot kg^{-1}$	Yes
*Fine sand (fraction of < 2 mm portion of the soil)	$kg \cdot kg^{-1}$	Yes
Very fine sand (fraction of < 2 mm portion of the soil)	$kg \cdot kg^{-1}$	No
CB (power of Cambell's model)	unitless	Yes
Air entry potential	$J \cdot kg^{-1}$	Yes
Saturated hydraulic conductivity	$m \cdot s^{-1}$	Yes
pH	unitless	Yes
CaCO ₃	$kg \cdot kg^{-1}$	No
Cation exchange capacity	$meq \cdot (100 g)^{-1}$	Yes
Linear extensibility percent	$(mm \cdot mm^{-1}) \cdot 100$	Yes

* Indicated sand fraction parameters are not currently used in WEPS but are required in the soil input file.

Table 6. List of temporal surface and soil layer properties initialized and used by WEPS.

Property	Units	Can estimate through interface (Yes/No)
Crust thickness	mm	Yes
Crust density	Mg·m ⁻³	Yes
Crust stability	ln(J·kg ⁻¹)	Yes
Crust fraction	m ² ·m ⁻²	Yes
Loose material on crust (mass)	kg·m ⁻²	Yes
Loose material on crust (cover)	m ² ·m ⁻²	Yes
Random roughness	mm	Yes
Oriented (ridge) roughness direction	degrees	Yes
Ridge height	mm	Yes
Ridge spacing	mm	Yes
Ridge width	mm	Yes
Soil dry albedo	unitless	Yes
Surface rock fragments	m ² ·m ⁻²	Yes
Bedrock depth	mm	Yes
Restriction depth	mm	Yes
Layer thickness	mm	No
Bulk density (wet)	Mg·m ⁻³	No
Geometric mean diameter of aggregates	mm	Yes
Geometric standard deviation of aggregates	mm	Yes
Maximum aggregate size	mm	Yes
Minimum aggregate size	mm	Yes
Aggregate density	Mg·m ⁻³	Yes
Aggregate stability (dry)	ln(J·kg ⁻¹)	Yes
Water content (initial)	mm ³ ·mm ⁻³	Yes
Water content (saturated)	mm ³ ·mm ⁻³	Yes
Water content (field capacity – 1/3 bar)	mm ³ ·mm ⁻³	Yes
Water content (wilting point – 15 bar)	mm ³ ·mm ⁻³	Yes

The management/crop rotation files consist of the list of operations that a land manager has prescribed for a particular simulation. These typically include the planting and harvesting operations as well as the tillage and any optional irrigation applied to the field with their respective dates. The user can select from the following: (a) Crop Management Zone (CMZ) template files originally created by NRCS for use by their field office staff when using the 2nd Revised Universal Soil Loss Equation (RUSLE2), (b) previously constructed management files created and saved locally by the user, or (c) the creation of a management/crop rotation file from scratch by opening up the Management/Crop Rotation Editor (MCREW) within the interface. Of course, any previously selected file can also be modified within MCREW. Figure 4 shows the MCREW panel with a list of selected operations.

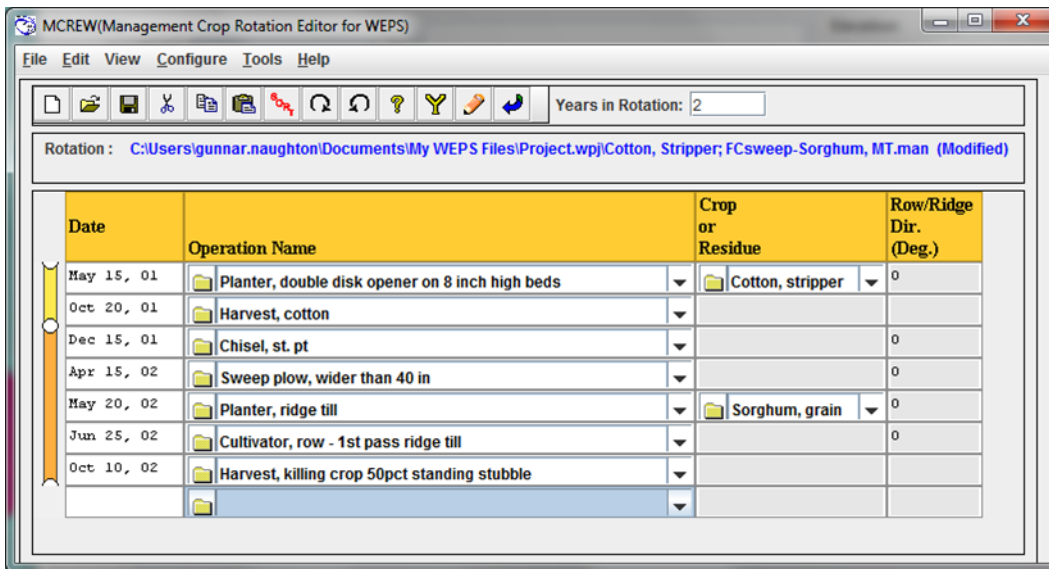


Figure 4. Management/Crop Rotation Editor screens.

Databases

Several national-scale databases were developed by NRCS with assistance from ARS for use with WEPS. The soil database (NASIS) and the CMZ management/crop rotation files mentioned previously were developed by NRCS outside of WEPS. However, due to underpopulated records, required WEPS parameters were originally not available in all soil components to be used with WEPS in the soil database. To address this problem, several directives from the NRCS National Soil Survey Center in Lincoln, NE, were sent out to the State NRCS organizations informing them of the need to complete the necessary data population process prior to WEPS implementation. ARS also developed a conversion process to allow NRCS to transform the original RUSLE2-originated CMZ files into WEPS-compatible CMZ files. This allowed NRCS to have over 25,000 template management files immediately available for use with WEPS during its implementation within their agency. A translation file is provided with WEPS. It describes the specific conversions required between RUSLE2 and WEPS management operation process parameters, automatically handling the majority of differences between the management rotations for the two models.

Additionally, over 300 operations presently exist for simulating tillage, harvesting, grazing, burning, irrigation, and spraying, as well as manure and residue applications, and 235 different crop records were developed to simulate the growing of all major agricultural crops in the United States, including Hawaii and Alaska. NRCS required significant technical assistance in obtaining the necessary parameters for developing operation, crop growth, and decomposition records for WEPS. In addition, “How To” guides were eventually developed and added to the WEPS User Manual to assist a technical user in the process of populating new crop and operation records. Likewise, NRCS (Gary Tibke, Michael Sporcic, Dave Lightle, and Bruce Wight) populated the wind barrier database provided with WEPS 1.0 to include all typical species of plants used for wind barriers listed in the NRCS practice standards.

NRCS runs WEPS exclusively using stochastic weather files generated by the CLIGEN (Nicks et al. 1989) and WINDGEN (van Donk et al. 2005) generators. However, historical weather data can be used if they are in the CLIGEN and WINDGEN generator output file formats for non-NRCS releases of WEPS. The station records were expanded for CLIGEN using the USDA Forest Service’s Rock:Clime Web-based tool (<https://forest.moscowfsl.wsu.edu/cgi-bin/fswepp/rc/rockclim.pl>) to provide additional coverage for selected agricultural cropping regions in the western United States (Elliot et al. 1999). Sixty-eight additional CLIGEN stations were added to the original 2,658 stations that previously existed in the CLIGEN database. Climate parameters provided by CLIGEN used in WEPS are (a) station elevation, which acts as default simulation site elevation unless overridden by user; (b) observed monthly average maximum and minimum temperatures ($^{\circ}\text{C}$), solar radiation ($\text{Langley}\ \text{day}^{-1}$), and precipitation (mm); (c) daily precipitation amount (mm), duration of precipitation event (h), time to peak (h), and precipitation intensity ($\text{mm}\ \text{h}^{-1}$); (d) daily maximum, minimum, and dewpoint temperatures ($^{\circ}\text{C}$); and (e) daily radiation ($\text{Langley}\ \text{day}^{-1}$). Likewise, out of an original 1,051 WINDGEN wind stations, NRCS rejected over 300 stations for various reasons and had ARS assist in the creation of an additional 23 stations for underrepresented regions using the North American Regional Reanalysis (NARR) data (Mesinger et al. 2006) in the western U.S. States. Figures 5 and 6 show the spatial distribution of CLIGEN and WINDGEN stations in the continental United States as currently used by NRCS. WINDGEN-generated parameters used in WEPS are (a) 24-hourly wind speeds ($\text{m}\ \text{s}^{-1}$) and (b) the wind direction (degrees from north) for each day.

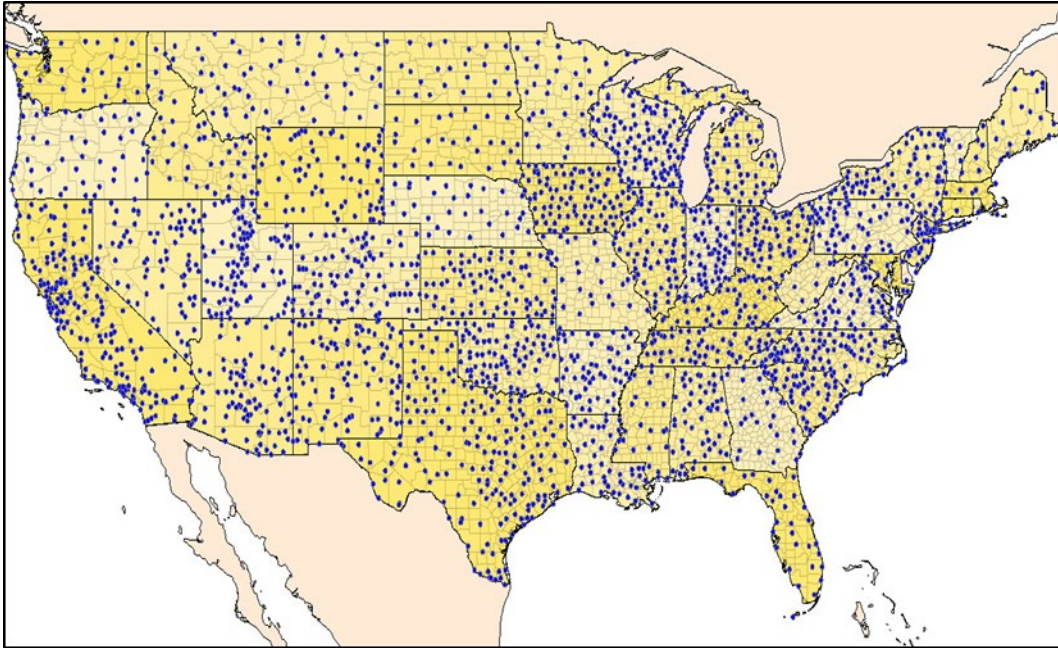


Figure 5. Continental U.S. distribution of CLIGEN stations used by Natural Resources Conservation Service (NRCS).

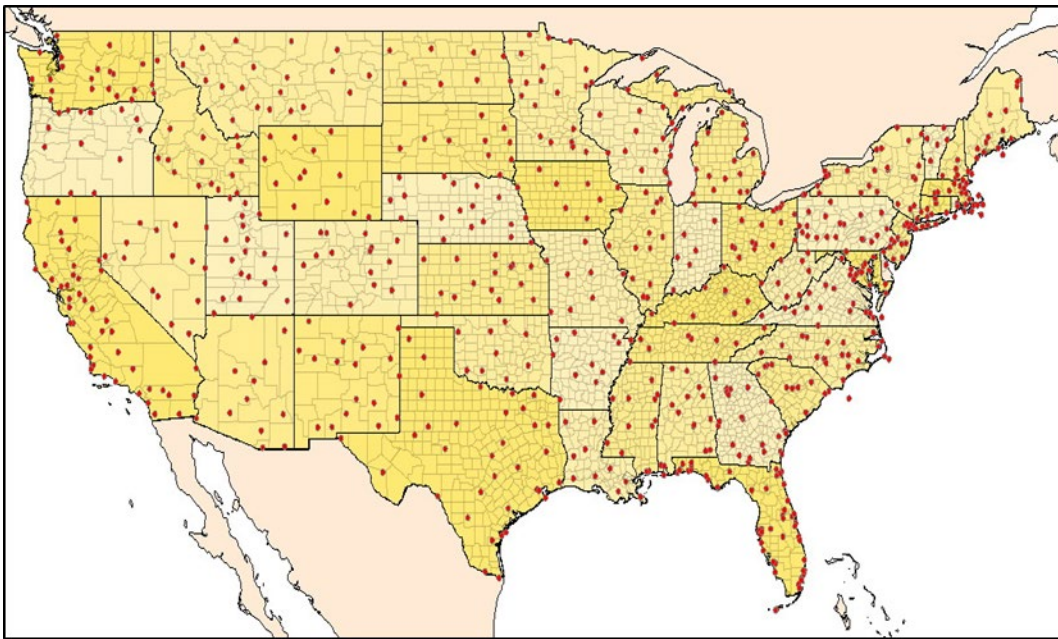


Figure 6. Continental U.S. distribution of WINDGEN stations used by Natural Resources Conservation Service (NRCS).

Originally, the WEPS interface simply selected the nearest station relative to the location selected with an option to manually override that default. However, that approach was deemed unacceptable, especially in the western States, due to the paucity of stations available and the problems associated with selecting a station across a mountain range.

Thus, a polygon approach was developed that provided NRCS with the means to specify a selected station for an identified region within a GIS file. This was performed for both CLIGEN and WINDGEN in regions where this was preferred over the other station selection options. Likewise, due to the spatially limited and highly variable wind stations available, NRCS wanted to use interpolated WINDGEN station records to reduce the sometimes very sharp changes in erosive wind energy among adjacent stations. Thus, an interpolation approach was developed by Fred Fox and was applied to eastern United States (east of the Rocky Mountains) for NRCS use. The granularity of the interpolation was set to the county boundary level such that the same interpolated WINDGEN station would be used for all simulations within a county.

A full GIS-compatible package was also added to the WEPS interface for users to be able to see where the CLIGEN and WINDGEN stations were located, where the polygon regions were assigned, and where the interpolated WINDGEN regions exist. Additional GIS layers are also available for viewing, e.g., CMZ zones and country, and State and county boundaries. Other layers can easily be added for viewing as necessary in the future. Users can also use this Map feature to select their simulation site location.

Outputs

WEPS was principally designed to address NRCS’s needs for wind erosion modeling. Thus, the most common outputs were tailored to NRCS’s needs, and the default Summary Erosion Report was designed primarily based on NRCS input as to what was wanted (see Table 7). Additionally, there are individual Management Rotation, Crop Yield, and Soil Conditioning Index (SCI) reports available. A detailed table report is also available, which displays selected properties, such as the erosion rates, surface conditions, biomass status, etc., on a periodic basis for the entire rotation sequence. However, WEPS provides much more output than what typical NRCS users currently make use of. For example, a confidence interval is available for the long-term annual average erosion estimate; as well as the ability to describe the fractional areas of a simulation region under active deposition and heavy saltation/creep activity, but with little net erosion occurring (saltation/creep threshold reached); and the ability to plot individual parameters on a periodic basis over time.

Table 7. List of output parameters available in the WEPS Run Summary Report.

Report Section	Parameters
General WEPS simulation run information	WEPS Run Date Client Name; Farm No., Tract No., Field No. Management rotation file used in the WEPS simulation Soil file name used in the WEPS simulation Location of the WEPS run on the computer
Simulation site information	X-length, Y-length, Area, Elevation, and Orientation

	Mode of WEPS simulation run (NRCS, Cycle, Dates)
	Soil Loss Tolerance value ($T \text{ ac}^{-1} \text{ yr}^{-1}$)
	Site location (Country, State, County/Parish)
	Site location latitude and longitude coordinates
	CLIGEN and WINDGEN station names
Erosion output	Rotation year, total rotation, and crop interval periods, each providing average annual gross loss, and the net soil loss from the field for average annual, creep+saltation, suspension, and PM10 emissions ($T \text{ ac}^{-1}$ or kg m^{-2})
Management rotation information	Crops grown with the harvest date, above ground residue at harvest (lb ac^{-1} or kg m^{-2}), harvest yield (crop dependent units), and the percent moisture content in which the yield is reported
Soil Conditioning Index summary	SCI, Energy Calculator, average annual STIR value, wind and water erosion soil loss values used in SCI calculations, and the SCI subfactors
Rotation STIR (Soil Tillage Intensity Rating) Energy	The date of operation, operation name, and fuel type used and STIR value computed, as well as the energy used by the operation and the cost per unit area for each operation. In addition, the total rotation's STIR value, energy used, and cost, as well as the total per-unit area energy used and cost.
Crop Interval STIR Energy	The STIR value and per-unit area energy and cost for each crop interval (defined by NRCS as the first operation following the harvest of the previous crop to when the crop itself is harvested)
Notes	Relevant information optionally provided here by WEPS and/or the user

Development Issues

Some development issues have already been mentioned (database population and vetting, desire for crop yields to be related to harvest residue, etc.). Some of these merit additional discussion. The runtime requirements imposed by NRCS were the biggest hurdle WEPS had to overcome. The runtime requirements eventually caused developers to incorporate an alternative Hydrology submodel, which was inferior with respect to some important specific wind erosion-related processes, e.g., the ability to simulate diurnal rewetting of

the surface and to allow upward migration of moisture in the soil profile, further limiting its ability to simulate surface wet/dry cycles. Additionally, the number of rotation cycles simulated was lowered to 15 cycles at one time to meet the runtime requirements. Eventually, the cycle number was extended back to 50 due to improvements in computer hardware and reductions in WEPS runtime due to code modifications. (WEPS inherently gives better long-term average annual erosion results when run for longer time periods due to additional cycles providing a more complete statistical sampling of the combination of the weather and wind conditions generated by CLIGEN and WINDGEN).

Due to the familiarity of NRCS users with the strong relationship between the average yield and the after-harvest residue, NRCS insisted that crop yields be tied to the after-harvest residue produced. Hence, the WEPS Plant Growth submodel was extended to provide that feature for the majority of crops. NRCS also submitted the desire to specify an average yield prior to a WEPS run. This was accommodated by allowing a calibration run mode that would iteratively run WEPS first without generating any user output except the adjustment needed to grow the crops with the desired average yield under the specified location/climate/soil/management conditions, and then running WEPS a final time with the adjustments applied to the plant growth processes to achieve the specified average yield.

Because NRCS uses RUSLE2 for predicting water erosion, they desired commonality between the elements in both WEPS and RUSLE2, where possible. Thus, especially in the representation of effects due to management (tillage) processes, effort was expended to align as many of the simulated processes as possible between the two models. Therefore, each specific physical tillage process simulated in WEPS and RUSLE2 was evaluated, and a common definition and common equations were agreed upon between the model developers to promote commonality. Likewise, the coefficients of those common equations, which were assigned to management operations, were made equal between the two models. It was not possible to make all management processes identical due to differences in the two models, but this process did help NRCS during the WEPS implementation phase.

Additionally, NRCS requested that the Energy Calculator and the Soil Conditioning Index (SCI) be added to the model, even though neither has any direct requirement for simulations of wind erosion. Naturally, further changes to the WEPS interface were requested to de-clutter it and to enhance ease of use. Nearly all of these NRCS requests were addressed during the extended testing and implementation phases held from 2005 to 2010. Figure 7 shows a map of the United States listing the CMZ's WEPS testing/training sessions conducted during that time period.

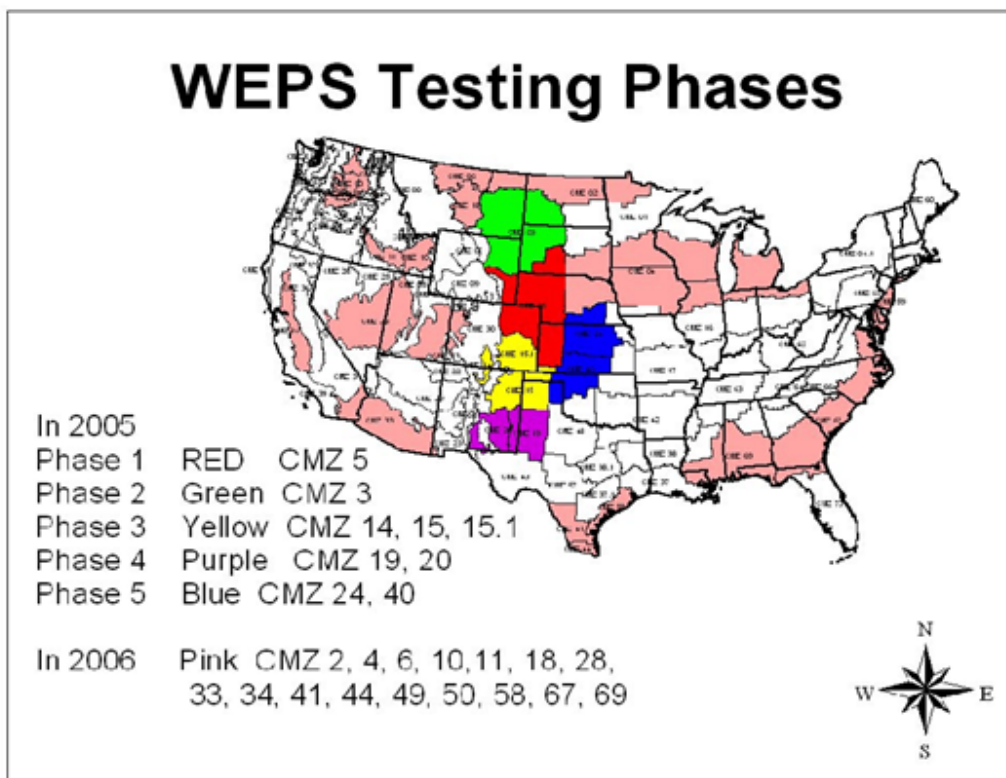


Figure 7. Natural Resources Conservation Service (NRCS) WEPS testing locations by Crop Management Zone (CMZ).

Summary and Conclusions

As a process-based planning tool, WEPS is very good at reflecting the relative effects of various cropland management practices on the susceptibility of a site to wind erosion. WEPS requires only four inputs to make a simulation: (1) the field size, shape, and orientation; (2) the soil type; (3) the management/crop rotation practice applied; and (4) the climate experienced at the site. If these inputs are available, WEPS can make a multiyear simulation run, typically in less than a minute, which will reflect the seasonal and year-to-year variability of the climate. WEPS can also provide estimates of the long-term erosion rate and allow the user to identify when the site is most susceptible to erosion during the crop/rotation cycle. WEPS was a multi-agency, multidiscipline project that took 20 plus years to develop, refine, and ultimately be employed by a user agency for use in determining erosion estimates on agricultural cropland fields. However, WEPS advanced the state of the science in wind erosion modeling during that time.

Acknowledgments

Due to the total length of time necessary to develop WEPS and to implement WEPS by NRCS, the project could have easily been terminated by the ARS leadership. We thank ARS administrators Edward B. Knipling, Jr., and Floyd Horn for supporting WEPS through to completion, as well as ARS national program leaders Dick Amerman, Steve Rawlins, Mark Wertz, and Charlie Walthall, for consistently supporting WEPS during its development and for helping to secure extra funding through ARS management. A thank

you is also extended to the EPA for providing significant extramural funds for the necessary research to develop a PM10 prediction module for WEPS. Special recognition also goes to Will Blackburn, ARS Northern Plains Area Director, for his unwavering support of WEPS and for his special interest in achieving the implementation of WEPS within NRCS. This was exemplified by Will Blackburn's initial assistance in establishing the quarterly meetings with NRCS, specifically focused on addressing their WEPS concerns prior to implementation, and then in attending each of those meetings.

References

- Armbrust, D.V., and J.D. Bilbro. 1997. Relating plant canopy characteristics to soil transport capacity by wind. *Agronomy Journal*. 89:157-162.
- Bagnold, R.A. 1943. *The physics of blown sand and desert dunes*. New York, NY: William Morrow and Co.
- Chepil, W.S., and N.P. Woodruff. 1963. The physics of wind erosion and its control. *Advances in Agronomy*. 15:211-302.
- Cole, G.W. 1983. Wind erosion modeling. Proceedings of the 1983 Natural Resources Modeling Symposium, USDA, ARS, Pingree Park, CO, October 16-21, 1983, pp. 59-63.
- Cole, G.W. 1984a. A method for determining field wind erosion rates from wind tunnel-derived functions. *Transactions of the ASAE*. 27(3):110-116.
- Cole, G.W. 1984b. A stochastic formulation of soil erosion caused by wind. *Transactions of the ASAE*. 27(5):1405-1410.
- Cole, G.W. 1985. Some wind erosion process measures. *Transactions of the ASAE*. 28(4):1108-1114, 1123.
- Cole, G.W., and J.J. Higgins. 1985. A probability criterion for acceptable soil erosion. *Transactions of the ASAE*. 28(6):1921-1926.
- Cole, G.W., and L. Lyles. 1984. The Wind Erosion Component of EPIC. Prepared for EPIC - Erosion/Productivity Impact Calculator. U.S. Department of Agriculture, Technical Bulletin No. 1768, pp. 139-151.
- Cole, G.W., L. Lyles, and L.J. Hagen. 1983. A simulation model of daily wind erosion soil loss. *Transactions of the ASAE*. 26(6):1758-1765.
- Elliot, W.J., D.L. Scheele, and D.E. Hall. 1999. Rock:Climate Rocky Mountain Research Station Stochastic Weather Generator. Available at: <https://forest.moscowfsl.wsu.edu/cgi-bin/fswepp/rc/rockclim.pl> (Accessed August 10, 2020).
- Gillette, D.A., D.W. Fryrear, T.E. Gill, et al. 1998. Relation of vertical flux of particles smaller than 10 microns to total aeolian horizontal mass flux at Owens Lake. *Journal of Geophysical Research*. 34(4):26009-26015.
- Greeley, R., and J.D. Iversen. 1985. *Wind as a Geological Process*. New York, NY: Cambridge University Press.
- Hagen, L.J. 1991a. A wind erosion prediction system to meet user needs. *Journal of Soil and Water Conservation*. 46(2):105-111.
- Hagen, L.J. 1991b. Wind erosion: emission rates and transport capacities on rough surfaces. American Society of Agricultural Engineers paper No. 912082.

- Hagen, L.J. 1996. Crop residue effects on aerodynamic processes and wind erosion. *Theoretical and Applied Climatology*. 54:39-46.
- Hagen, L.J., and D.V. Armbrust. 1994. Plant canopy effects on wind erosion saltation. *Transactions of the ASAE*. 37(2):461-465.
- Hagen, L.J., E.L. Skidmore, and A. Saleh. 1992. Wind erosion: prediction of aggregate abrasion coefficients. *Transactions of the ASAE*. 35(6):1847-1850.
- Hagen, L.J., L.E. Wagner, and E.L. Skidmore. 1999. Analytical solutions and sensitivity analysis for sediment transport in WEPS. *Transactions of the ASAE*. 42(6):1715-1721.
- Lane, L.J., and M.A. Nearing, (eds.), 1989. USDA-Water Erosion Prediction Project: Hillslope Profile Model Documentation. NSERL Report No. 2. U.S. Department of Agriculture, Agricultural Research Service, National Soil Erosion Research Laboratory, West Lafayette, IN.
- Lyles, L., and J. Tatarko. 1986. Wind erosion effects on soil texture and organic matter. *Journal of Soil and Water Conservation*. 41(3):191-93.
- Mesinger, F., G. DiMego, E. Kalnay, et al. 2006. North American Regional Reanalysis. *Bulletin of the American Meteorological Society*. 87(3):343-360.
- Mirzamostafa, N. 1996. Suspension Component of Wind Erosion. Ph.D. dissertation. Manhattan, KS: Kansas State University.
- Mirzamostafa, N., L.J. Hagen, L.R. Stone, et al. 1998. Soil aggregate and texture effects on suspension components from wind erosion. *Soil Science Society of America Journal*. 62(5):1351-61.
- Nicks, A., L.J. Lane, and G.A. Gander. 1989. Weather generator. *In* USDA-Water Erosion Prediction Project: Hillslope Profile Model Documentation. NSERL Report No. 2, section 2.1-2.22. West Lafayette, IN: U.S. Department of Agriculture, Agricultural Research Service, National Soil Erosion Research Laboratory.
- Rawls, W.J. 1983. Estimating soil bulk density from particle size analysis and organic matter content. *Soil Science*. 134(2):123-125.
- Saleh, A., and D.W. Fryrear. 1995. Threshold wind velocities of wet soils as affected by wind blown sand. *Soil Science*. 160(4):304-309.
- Savabi, M.R., R.W. Skaggs, and C.A. Onstad. 1995. Subsurface hydrology. *In* D.C. Flanagan and M.A. Nearing, (eds.), USDA Water Erosion Prediction Project (WEPP) Hillslope Profile and Watershed Model Documentation. s.l.:NSERL Report No. 10, section 6.1-6.14. West Lafayette, IN: U.S. Department of Agriculture, Agricultural Research Service, National Soil Erosion Research Laboratory.
- Schomberg, H.H., J.L. Steiner, S.R. Evett, et al. 1996. Climatic influence on residue decomposition prediction in the Wind Erosion Prediction System. *Theoretical and Applied Climatology*. 54:5-16.

Sharpley, A.N., and J.R. Williams. 1990. EPIC-Erosion/Productivity Impact Calculator: 1. Model Documentation. U.S. Department of Agriculture, Technical Bulletin No. 1768.

Skidmore, E.L. 1976. A wind erosion equation: development, application, and limitations. *In* ERDA Symposium Series 38, Atmosphere-Surface Exchange of Particulate and Gaseous Pollutants. pp. 452-65.

Soil Survey Staff, n.d. Soil Data Access. U.S. Department of Agriculture, Natural Resources Conservation Service, Soil Survey Geographic (SSURGO) Database. Available at <https://sdmdataaccess.nrcs.usda.gov/> (Accessed August, 10, 2020).

Steiner, J.L., H.H. Schomberg, J.C.L. Douglas, et al. 1994. Standing stem persistence in no-tillage small-grain fields. *Agronomy Journal*. 86:76-81.

Tatarko, J., M.A. Sporcic, and E.L. Skidmore. 2013. A history of wind erosion prediction models in the United States Department of Agriculture prior to the Wind Erosion Prediction System. *Aeolian Research*. 10:3-8.

Federal Register, 2010. Notice of implementation of the Wind Erosion Prediction System for soil erodibility system calculations for the Natural Resources Conservation Service. *Federal Register* 75, Number 234 (7 December 2010), 75961-75962. Print.

van Donk, S.J., L.E. Wagner, E.L. Skidmore, et al. 2005. Comparison of the Weibull Model with measured wind speed distributions for stochastic wind generation. *Transactions of the ASABE*. 48(2):503-510.

Wagner, L.E., and F.A. Fox. 2013. The management submodel of the Wind Erosion Prediction System. *Applied Engineering in Agriculture*. 29(3): 361-372.

Wagner, L.E., and D.J. Ding. 1994. Representing aggregate size distributions as modified lognormal distributions. *Transactions of the ASAE*. 37(3):815-821.

Woodruff, N.P., and F.H. Siddoway. 1965. A wind erosion equation. *Soil Science Society of America Proceedings*. 29(5):602-608.

Zobeck, T.M., and T.W. Popham. 1991. Influence of abrader flux and soil properties. *Soil Science Society of America Journal*. 55(4):1091-1097.

Weather Generators of WEPS

Contributors:

S.J. van Donk
J. Tatarko
E.L. Skidmore
L.E. Wagner
F. Fox

Abstract

The Wind Erosion Prediction System (WEPS) requires specific weather data in order to simulate the processes governing soil erosion by wind. The WEPS weather generators simulate the needed weather data through two separate weather models. CLIGEN (CLimate GENerator) is a stochastic generator of climate (weather) data, simulating daily estimates of precipitation (amount, duration, and peak intensity), temperature (maximum, minimum, and dewpoint), wind (direction and speed), and solar radiation. It generates these for a single geographic point, using monthly statistical parameters (means, standard deviations, skewness, etc.) derived from historical measurements. Wind is the principal driver of WEPS simulation of windblown sediment loss from a field. The wind parameters in CLIGEN are not adequate for WEPS, and so the WINDGEN model was created to provide wind parameters needed by the WEPS model. Similar to CLIGEN, WINDGEN is a stochastic wind generator for WEPS that uses monthly parameters derived from historical measurements to generate wind, providing the unique requirements of hourly wind speeds and daily wind direction for each day of simulation. Since WINDGEN bases its generations on historical statistics of wind, it reflects the past wind histories at a given location. Station parameter files (summary statistics) to run both generators are available for several thousand U.S. locations.

Introduction

The Wind Erosion Prediction System (WEPS) requires at least hourly wind speed and daily wind direction data to simulate the process of soil erosion by wind. These and other weather variables (e.g., precipitation, air temperature, and solar radiation) are also needed to drive the simulation of temporal changes in hydrology, soil erodibility, plant growth, and residue decomposition in WEPS. Two separate stochastic weather generators are used with WEPS: WINDGEN for wind data and CLIGEN for all other weather data. Both CLIGEN and WINDGEN are executed under the WEPS user interface, which then generate their respective weather series data that are used by the WEPS science model.

CLIGEN

Purpose and Brief History

WEPS uses CLIGEN (CLimate GENerator) to stochastically generate (simulate) daily weather data. These data are then used to drive other WEPS submodels, such as the Hydrology, Plant Growth (Crop), and Residue Decomposition submodels. CLIGEN is based on weather generators used in the EPIC (Williams et al. 1984) and SWRRB (Williams et al. 1985) models. The weather generation methods used in these models

were modified to include additional requirements for rainfall intensity distributions (Nicks et al. 1995). CLIGEN was originally developed for the Water Erosion Prediction Project (WEPP) family of erosion models (Nicks et al. 1987, 1995). Later on, others such as Meyer (2008) and Rust et al. (2011), addressed various aspects of CLIGEN.

Overview

CLIGEN is a stochastic generator of climate (weather) data simulating daily estimates of precipitation (amount, duration, and peak intensity), temperature (maximum, minimum, and dewpoint), wind (direction and speed), and solar radiation. It generates these for a single geographic point, using monthly parameters (means, standard deviations, skewness, etc.) derived from historic measurements. Station parameter files (summary statistics) to run CLIGEN are available for several thousand U.S. sites.

Unlike other climate generators, CLIGEN estimates parameters for individual storms, including amount of precipitation, storm duration, peak (maximum) precipitation intensity, and the time it takes to reach peak intensity. All these aspects of precipitation are required to run WEPS. The daily wind data generated by CLIGEN are not used in WEPS because WEPS requires hourly wind data for wind erosion prediction. Thus, the WEPS project has developed its own stochastic generator for wind data (WINDGEN) that generates the hourly wind data required.

With the exception of the temperatures (maximum, minimum, and dewpoint), daily estimates for each weather variable are generated independently of one another (no cross-correlation). For example, CLIGEN generates solar radiation and temperatures independently from precipitation, although, in the real world, these variables are not independent, i.e., there is significant cross-correlation. Whether the lack of cross-correlation in CLIGEN is an important issue for WEPS is not well known at this point, although it is likely that it will affect the simulation of wind erosion. For example, if erosive winds occur before precipitation, wind erosion will be higher than if they occur after precipitation.

The random number generator works in such a way that subsequent runs on the same computer, made with identical inputs (seed values), will produce identical results. However, when performing checks on CLIGEN's uniform random number generator and standard normal generator, it was discovered that they were not operating correctly, i.e., not generating truly random values. This problem was addressed by introducing a form of quality control borrowed from industrial engineering (Meyer et al. 2008).

Rust et al. (2011) later improved the quality of input climate datasets, updated them with more current data when available, and attempted to document their source. This improved database is available with the current version of WEPS. Rust et al. (2011) also started converting CLIGEN from FORTRAN to Java to improve code readability and maintainability, and to make it more compatible with the USDA Object Modeling System (OMS) project (David et al. 2002, 2013). As part of this process, they improved the manner in which temporal interpolations are performed to better reflect seasonality. In addition, they addressed issues with the random number generation and errors in how parameters, such as standard deviation parameters, were interpolated (Rust et al. 2011). These improvements, however, are not yet available with the current version of WEPS, since it still uses the FORTRAN version of CLIGEN, not the JAVA version.

Rust et al. (2011) discussed needed improvements, including (1) improving auto-correlation within a weather variable and cross-correlation between weather variables, (2) making the stochastically generated data correspond better to the original observed data (monthly averages and standard deviations calculated from the generated daily values to closely match those calculated from the original data set), (3) changing how random numbers are created and tested, and (4) moving to a histogram-based precipitation model to address issues with the precipitation distribution and intensity parameters currently in CLIGEN. One approach to addressing the cross-correlation issues is to convert to a GEM/WGEN (USDA-NRCS 2014) type approach for ensuring cross-correlation for basic elements such as Tmax, Tmin, Td, and solar radiation.

CLIGEN Data Set

Initially, CLIGEN used a program called “dat2par” (Scheele and Hall 2000) to create the majority of the U.S. stations in the CLIGEN database record or CLIGEN station parameter file (Table 1). Several meteorological and parameter datasets were used to create the CLIGEN database records. For daily precipitation and maximum and minimum temperatures, there were 2,590 stations (2,718 including the later addition of the Forest Service stations) having data spanning 9 to 117 years with 1,100 stations having greater than 44 years of record. (Note that even though this dataset uses essentially the maximum record length available for a location, one could easily generate alternative datasets using fixed record lengths, e.g., 30 years, spanning specific intervals of time, that could potentially be used for evaluating model responses to historically measured climate change in the records.) Solar radiation and half-hour maximum precipitation parameter data are from 142 stations of unknown origin. Time-to-peak distribution data are from 1,548 stations, and dewpoint temperature data are from 273 stations, both also of unknown origin. Finally, 852 wind stations were also used, again of unknown origin, but this wind data are not used by WEPS.

Table 1. Example of a CLIGEN database record (CLIGEN input) for Liberal, KS. From this record, CLIGEN stochastically generates weather data that are then used as input for other WEPS submodels—see Table 3.*

```

1  LIBERAL KS                144695 0
2  LATT= 37.03 LONG=-100.92 YEARS= 54. TYPE= 3
3  ELEVATION = 2840. TP5 = 2.66 TP6= 4.67
4  MEAN P .18 .18 .26 .27 .41 .36 .40 .33 .28 .31 .23 .17
5  S DEV P .20 .29 .36 .35 .65 .45 .51 .44 .41 .52 .30 .19
6  SKEW P 2.30 3.07 2.34 2.59 5.84 2.19 2.26 2.32 3.03 4.67 2.76 2.50
7  P(W/W) .28 .31 .31 .36 .44 .41 .35 .36 .33 .38 .38 .29
8  P(W/D) .07 .09 .13 .14 .21 .21 .20 .18 .15 .10 .09 .08
9  TMAX AV 47.54 52.76 60.72 71.99 80.07 90.22 95.15 93.45 85.66 74.75 58.99 49.59
10 TMIN AV 20.86 24.89 31.03 41.96 51.84 61.74 66.77 65.05 56.51 44.29 31.14 23.39
11 SD TMAX 14.29 14.24 14.27 11.65 10.50 9.06 6.81 7.38 9.97 11.40 12.46 13.02
12 SD TMIN 9.37 8.84 9.07 8.14 7.33 6.22 4.35 4.60 7.86 7.88 8.37 8.63
13 SOL.RAD 252. 322. 426. 523. 560. 636. 628. 556. 491. 366. 339. 236.
14 SD SOL 21.8 30.7 41.0 53.1 72.2 59.5 55.0 119.4 51.1 26.8 23.6 17.9
15 MX .5 P .26 .07 .31 1.24 1.02 1.54 1.59 1.23 .78 .46 .56 .58
16 DEW PT 18.26 22.21 23.68 33.63 46.10 54.62 58.36 57.95 49.94 39.15 27.15 21.21
17 Time Pk .573 .699 .759 .829 .845 .860 .885 .902 .906 .938 .966 1.000
18 % N 7.12 6.47 7.39 6.53 4.85 2.87 2.21 2.44 3.65 5.56 6.49 6.93
19 MEAN 6.40 6.82 7.11 6.99 6.08 5.06 4.91 5.06 5.50 5.57 6.45 6.20
20 STD DEV 3.05 3.35 3.39 3.34 2.80 2.23 2.53 2.49 2.66 2.72 3.15 2.97
21 SKEW .41 .77 .53 .43 .16 .37 .92 1.14 .65 .72 .72 .65
. . . . .
82 CALM 2.14 2.14 1.54 1.57 1.63 1.62 2.05 2.02 2.30 2.57 2.42 2.12
83
84 INTERPOLATED DATA (station & weighting factor)
85

```

```

86 ---Wind Stations---
87 GARDEN CITY KS .424 GAGE OK .337 DALHART TX .239
88 ---Solar Radiation and Max .5 P Stations---
89 DODGE CITY, KANSAS .529 AMARILLO, TEXAS .292 PUEBLO, COLORADO .179
90 ---Dewpoint Stations---
91 KS DODGE CITY .474 NM CLAYTON .265 TX AMARILLO .261
92 ---Time Peak Stations---
93 SUBLETTE KS .357 RANGE OK .324 RIVERSIDE 4 W OK .319

```

Description of items in Table 1

Line 1 Station name, State ID, station ID, code (code is not used in CLIGEN)

Line 2 Latitude, longitude, station years of record, type (integer value 1-4 to set single storm parameters and used to determine the maximum rainfall intensity. The values set in the code: 180.34, 154.94, 307.34, and 330.2 mm/h for Types 1-4, respectively.)

Line 3 Elevation above sea level (feet), TP5: maximum 30-minute precipitation depth (inches) (not used in CLIGEN), TP6: maximum 6-hour precipitation depth (inches)

Line 4 Mean liquid equivalent precipitation depth (inches) for a day precipitation occurs (total precipitation for the month divided by the number of days in which precipitation occurs)

Lines 4-82 Monthly data: first value is for January, last value is for December

Line 5 Standard deviation of daily precipitation value (inches)

Line 6 Skew coefficient of daily precipitation value

Line 7 Probability of a wet day following a wet day

Line 8 Probability of a wet day following a dry day

Line 9 Mean maximum daily air temperature (degrees Fahrenheit)

Line 10 Mean minimum daily air temperature (degrees Fahrenheit)

Line 11 Standard deviation for daily maximum temperature (degrees Fahrenheit)

Line 12 Standard deviation for daily minimum temperature (degrees Fahrenheit)

Line 13 Mean daily solar radiation (Langleys)

Line 14 Standard deviation for daily solar radiation (Langleys)

Line 15 Mean maximum daily 30-minute liquid precipitation intensity (inches/hour)

Line 16 Mean daily dew point temperature (degrees Fahrenheit)

Line 17 These 12 values represent a cumulative distribution of computed time to peak rainfall intensity values based on the National Weather Service 15-minute rainfall data. The 12 values represent the fraction of computed time to peak values, respectively, between 0.0-0.0833, 0.0833-0.1667, 0.1667-0.25, 0.25-0.3333, 0.3333-0.4167, 0.4167-0.5, 0.5-0.5833, 0.5833-0.6667, 0.6667-0.75, 0.75-0.8333, 0.8333-0.9167, and 0.9167-1.0.

Line 18 Percentage of time wind from this direction

Lines 18-21 Wind information for winds coming from the North

Lines 18-81 Information on wind direction and speed for 16 wind directions

Line 19 Average wind velocity (meters/second)

Line 20 Standard deviation of winds (meters/second)

Line 21 Skew coefficient of wind data

Line 82 Percentage of time there are calm conditions

Lines 84-93

Stations from which weather data were interpolated and weighting factor assigned to each station (wind data not used in WEPS)

*More detailed information on the CLIGEN input has been provided by Frankenberger (2008).

As part of the process of conducting a quality check of the CLIGEN station data, Rust et al. (2011) attempted to locate the original data sources. However, as mentioned previously, several are unknown, although most of the actual data were still available. In addition, newer datasets were located that could be used to update the CLIGEN database. The TD3200 dataset (NCDC et al. 1981) consisting of 8,000 stations (NCDC 2009) was used to replace the original daily precipitation/temperature data for the existing CLIGEN stations. The updated database using the TD3200 dataset (through 2008) is included with the current version of WEPS.

The TD3210 dataset consisting of 1,380 stations (NCDC et al. 1987) contains solar radiation data (NCDC 1998) that could be used to eventually replace and extend the original 142 solar radiation stations. In addition, the TD6406 data set with 954 stations containing 1-minute interval precipitation data (NCDC 2006) can be used to obtain time-to-peak distributions, dewpoint temperature, and half-hour maximum precipitation data. The increased number of stations would allow better interpolation of solar radiation and half-hour maximum precipitation. These datasets have not yet been culled based on defined quality controls (minimum years of data, missing/invalid data removed, etc.) and have not been used to update the current CLIGEN database (Rust et al. 2011).

CLIGEN requires specially formatted monthly statistical weather data, which are not readily available in many countries. Data and software to build station files for international sites, as well as CLIGEN station parameter files for several thousand U.S. sites, are available for download from the USDA-ARS website (USDA, 2014). New CLIGEN stations can be created using observed data or existing stations (USDA 2006). In addition, Gete et al. (2009) developed BPCDG (Breakpoint Climate Data Generator), which generates breakpoint climate data using observed standard weather datasets that can then be used as input in downstream models.

The USDA Forest Service (FS) has developed the Rocky Mountain Research Station Stochastic Weather Generator (Rock:Clime), a web-based interface to CLIGEN (Elliot et al. 1999). Rock:Clime has been used to create additional CLIGEN stations for use in high-altitude regions, adjusting temperature variables of existing stations to account for elevation differences. It builds climate files for the FS WEPP interfaces to the WEPP model and includes a database of more than 2,600 weather stations from all 50 States, the Pacific Islands, Puerto Rico, and the Virgin Islands. These stations are included with WEPS.

Stochastic Weather Generator

There are two steps in the stochastic generation of weather data. First, weather statistics are calculated from a historical record of measured data. This step is done only once, and the results are saved as the “CLIGEN database record” (Table 1), which was previously described. WEPS comes with this database as well as with a CLIGEN index file (Table 2) that can be used for obtaining faster access to the desired database record information.


```

6  Observed monthly ave max temperature (C)
7   8.6 11.5 16.0 22.2 26.7 32.3 35.1 34.1 29.8 23.8 15.0  9.8
8  Observed monthly ave min temperature (C)
9  -6.2 -4.0 -0.5  5.5 11.0 16.5 19.3 18.4 13.6  6.8 -0.5 -4.8
10 Observed monthly ave solar radiation (Langleys/day)
11 252.0 322.0 426.0 523.0 560.0 636.0 628.0 556.0 491.0 366.0 339.0 236.0
12 Observed monthly ave precipitation (mm)
13 12.6 14.8 32.5 36.9 88.0 72.0 74.1 57.0 39.0 33.9 22.2 13.6
14 da mo year prcp dur tp ip tmax tmin rad w-vl w-dir tdew
15      (mm) (h)          (C) (C) (l/d) (m/s) (Deg) (C)
16  1  1  1  0.0 0.00 0.00 0.00 -1.4 -9.5 185. 4.7 268. -12.6
17  2  1  1  0.0 0.00 0.00 0.00  0.7 -9.3 286. 3.3  94.  -7.8
18  3  1  1  0.0 0.00 0.00 0.00 12.2 -10.4 230. 5.4 298. -19.3
19  4  1  1  0.0 0.00 0.00 0.00 13.8 -0.5 175. 4.7 250.  0.4
20  5  1  1  0.0 0.00 0.00 0.00 26.9  6.1 162. 5.8 258. 12.1
21  6  1  1  0.0 0.00 0.00 0.00 11.6  1.4 204. 5.6  27. -0.2
22  7  1  1  0.0 0.00 0.00 0.00 17.9 -2.0 294. 3.0 173. -2.5
23  8  1  1  0.0 0.00 0.00 0.00 13.9 -1.1 281. 8.1 360. -9.7
24  9  1  1  0.0 0.00 0.00 0.00  8.8 -8.4 263. 3.3 319. -7.8
25 10  1  1  0.0 0.00 0.00 0.00  6.8 -10.4 269. 0.0  0. -18.4
26 11  1  1  0.0 0.00 0.00 0.00  2.2 -9.6 271. 9.3 339. -8.5
27 12  1  1  0.0 0.00 0.00 0.00  6.8 -2.6 238. 5.1 309. -2.2
28 13  1  1  0.0 0.00 0.00 0.00 -1.7 -8.3 168. 3.3 226. -9.8
29 14  1  1  0.0 0.00 0.00 0.00  0.8 -7.5 194. 7.5 333. -11.3
30 15  1  1  0.0 0.00 0.00 0.00  0.0 -10.1 202. 3.4  44. -16.5
31 16  1  1  0.0 0.00 0.00 0.00  9.8 -4.2 241. 7.6 267. -1.5
32 17  1  1  0.0 0.00 0.00 0.00  3.1 -12.3 215. 5.3 305. -4.7
33 18  1  1  0.0 0.00 0.00 0.00  6.0 -12.7 185. 0.1 178. -15.1
34 19  1  1  0.0 0.00 0.00 0.00 -5.9 -8.9 220. 4.0 283. -11.3
35 20  1  1  0.0 0.00 0.00 0.00  9.5 -11.0 168. 3.0  42. -12.9
36 21  1  1  0.0 0.00 0.00 0.00  9.6 -3.0 172. 0.0  0.  0.6
37 22  1  1  0.0 0.00 0.00 0.00 20.2  2.2 183. 4.6 179.  1.0
38 23  1  1  0.0 0.00 0.00 0.00  6.6 -4.9 295. 5.4 193. -12.9
39 24  1  1  0.0 0.00 0.00 0.00 10.7 -8.4 281. 8.6  32. -13.8
40 25  1  1  0.0 0.00 0.00 0.00 18.7 -1.8 301. 1.0 291. -6.5
41 26  1  1  0.0 0.00 0.00 0.00  5.0 -6.7 265. 10.1 197. -2.7
42 27  1  1  0.0 0.00 0.00 0.00 21.5  0.3 245. 6.2 236. -1.0
43 28  1  1  1.6 1.05 0.08  4.43 28.3 -0.1 324. 8.7 204. -4.3
44 29  1  1  0.0 0.00 0.00 0.00  8.2 -7.9 279. 4.7 166. -5.9
45 30  1  1  0.0 0.00 0.00 0.00 18.6 -7.1 274. 7.1 210. -9.1
46 31  1  1  0.0 0.00 0.00 0.00 -5.4 -9.9 318. 10.3  12. -11.7
47  1  2  1  0.0 0.00 0.00 0.00 21.6  0.8 274. 6.0 230.  2.5
48  2  2  1  0.0 0.00 0.00 0.00  3.7 -11.0 186. 9.6  44. -10.0
49  3  2  1  0.0 0.00 0.00 0.00 16.1 -0.2 225. 4.3 111.  5.0
50  . . . . . . . . . . . . . . . .
51  . . . . . . . . . . . . . . . .
52  . . . . . . . . . . . . . . . .

```

Description of items in Table 3

Line 1 CLIGEN version number

Line 2 The first number specifies the CLIGEN simulation mode where "1" means a continuous storm simulation and a "2" means a single storm simulation.
The second number specifies whether breakpoint data are used, where a "0" means that no breakpoint data are used and a "1" means that breakpoint data are used.
The third number specifies the evapotranspiration equation to use, where a "0" means that wind information exists and to use the Penman ET equation and a "1" means no wind information exists and to use the Priestly-Taylor ET equation.

Line 3 CLIGEN station (Liberal, KS, in this example) used to generate this data file, CLIGEN version number, and command line arguments used during the generation of this file

Line 4 Text header for data on line 5

Line 5	Latitude (degrees, positive is North), longitude (degrees, negative is West), elevation (m), number of years of data used to develop the CLIGEN database record, beginning year used in this daily output file, number of years of daily simulated data, and command line used to generate this CLIGEN output file
Lines 7, 9, 11, 13	Observed average monthly data: first value is for January, last value is for December
Line 7	Maximum temperature (degrees Celsius)
Line 9	Minimum temperature (degrees Celsius)
Line 11	Solar radiation (Langleys/day)
Line 13	Precipitation (millimeters)
Lines 14, 15	Column headings
Lines 16+	Weather data, one line per day
Columns 1, 2, 3	day mo year – day, month, and year of simulation
Column 4	prcp – amount of precipitation (millimeters)
Column 5	dur – duration of precipitation (hours)
Column 6	tp – time it takes to reach peak (maximum) precipitation (minutes), tp=0 if rcp=0
Column 7	ip – intensity of peak precipitation (millimeters/hour), ip=0 if prcp=0
Column 8	tmax – maximum temperature (degrees Celsius)
Column 9	tmin – minimum temperature (degrees Celsius)
Column 10	rad – solar radiation (Langleys)
Column 11	w-vl – average wind speed (meters/second), not used in WEPS
Column 12	w-dir – wind direction (degrees clockwise with North=0, East=90, South=180, and West=270), not used in WEPS
Column 13	tdew – dew point temperature (degrees Celsius)

Table 4. Command line options for CLIGEN version 5.3.

CLIGEN stochastically generates (simulates) daily weather data (Table 3) from summary statistics (Table 1). Simulation is always initiated on the first day of a year and produced in multiples of 1 full calendar year.

usage: cligen -S# -s# -i dbfile -o outfile -b# -y# -f -F -H -r# -t# -I# -v -V -h -? -O
 Make sure there are no spaces between each flag and its parameter. If command line options are omitted, CLIGEN will interactively request the required information.

Option	Description
S#	Valid State ID
s#	Valid station ID
i dbfile	Weather database (input) file
o outfile	Output file
b#	Beginning simulation year
y#	Number of years to simulate (generate)
f	Old WEPS record format
F	Overwrite output file if it exists
H	Omit header output
r#	Random number seed

t#	Simulation type: 4=single storm, 5=multiple years
I#	Interpolation method: 0=none (default), 1=linear, 2=Fourier, 3=interpolation preserving monthly means
v or V	Verbose option: generate additional information
h or ?	Display command line options and exit program
O filename	Use observed data

Example:

Cligen -S14 -s4695 -iupd_US_cligen_stations.par -t5 -I3 -F -b01 -y100 -oliberal.cli

This directs CLIGEN to search in the wind database 'upd_US_cligen_stations.par' for the station with State ID 14 (Kansas), station code 4695 (Liberal), generate 100 years of daily weather data with starting year 1, using the interpolation method that preserves monthly means, and write the generated data to the file 'liberal.cli'.

To determine if precipitation occurs on a given day, two conditional probabilities are used: the probability of a wet day following a wet day (Table 1, line 7) and the probability of a wet day following a dry day (Table 1, line 8). After the occurrence of precipitation on a given day has been determined, the precipitation amount (Table 3, column 4) is generated from the average daily precipitation for a month on days with precipitation (Table 1, line 4), the standard deviation of the daily precipitation (Table 1, line 5), and the coefficient of skew of the daily precipitation (Table 1, line 6).

Both storm duration (Table 3, column 5) and peak storm intensity (Table 3, column 7) are generated stochastically, based on a new random number draw, from the maximum 30-minute precipitation (Table 1, line 15) and the precipitation amount generated for that day (Table 3, column 4). Time from the beginning of the storm to the peak intensity (Table 3, column 6) is calculated from information provided in Table 1, line 17.

Maximum temperature (Tmax) (Table 3, column 8), minimum temperature (Tmin) (Table 3, column 9), and dewpoint temperature (Tdew) (Table 3, column 13) are generated from the monthly mean maximum temperature (Table 1, line 9), the standard deviation of the daily maximum temperature (Table 1, line 11), the monthly mean minimum temperature (Table 1, line 10), the standard deviation of the daily minimum temperature (Table 1, line 12), and the mean dewpoint temperature (Table 1, line 16) using the method from Meyer (2004).

Quoting directly, "The current day's maximum temperature, minimum temperatures, and dew point temperature are assumed to be independent normal distributions. (Common sense tells us they are not independent, but assuming that they are greatly simplifies the mathematics.) When the SD of Tmin is less than that of Tmax, Tmin's daily value is generated by scaling (multiplying) the SN deviate (positive or negative) by the parameter's standard deviation for the current month and adding its monthly mean. Tmax and Tdew are generated from a "difference" distribution. When SD of Tmax is less than that of Tmin, the calculations for Tdew and Tmin are similarly based on Tmax."

With the assumption of a Standard Normal (SN) distribution, the distribution of the difference between Tmax and Tmin is the difference between means and variances for the two distributions. Once Tmin (or alternately Tmax) is found, the difference between Tmin and Tmax is generated and added to Tmin (or alternately Tmax) to get a value for

Tmax (or alternately Tmin). Dewpoint temperature (Table 3, column 13) is generated from the monthly mean dewpoint temperature (Table 1, line 16) and an average of the standard deviation of the daily minimum and maximum temperature using the same difference approach. Note that while mean dewpoint is part of the CLIGEN station database, dewpoint standard deviation is not. The daily average dewpoint temperature is then limited to be less than or equal to 0.99 of the average of the generated Tmax and Tmin values. If the adjusted Tdew is less than -10 degrees C, it is forced to be 1.1 times the generated Tmin value.

Solar radiation (Table 3, column 10) is generated from the mean monthly solar radiation (Table 1, line 13) and a standard estimated to be 0.25 times the maximum of either the maximum possible solar radiation minus the mean monthly solar radiation or the value of the mean monthly solar radiation—not the solar radiation standard deviation in Table 1, line 14 as indicated in Meyer (2004). It is constrained to be less than or equal to 0.9 times the maximum possible solar radiation and greater than or equal to 0.05 times the maximum possible solar radiation, which is computed from the location of the station and the sun angle on the given day.

CLIGEN generates wind speed and wind direction, although these are not used in WEPS; rather, the WINDGEN model is used (see below). In CLIGEN, wind speed (Table 3, column 11) is generated from the average wind speed, the standard deviation of wind speeds (Table 1, line 5), and the coefficient of skew of the wind data (Table 1, lines 19-21). Wind direction (Table 3, column 12) is generated using a histogram of wind directions (Table 1, line 18), including calm (Table 1, line 82).

After the CLIGEN output file (Table 3) has been generated, it is subsequently used by other WEPS submodels. For more information on CLIGEN, please consult the various resources available, e.g., the CLIGEN website (USDA 2014), the WEPP/CLIGEN documentation (Nicks et al. 1995), and Rust et al. (2011).

WINDGEN

Purpose and Brief History

Developed specifically for use with WEPS, WINDGEN stochastically generates hourly wind speed and daily wind direction (van Donk et al. 2005) because the daily wind speed data available in CLIGEN were inadequate for use in WEPS. The first work, presented in Fort Collins, CO, in January 1989 at the Sustainable Agriculture for the Great Plains Symposium (Skidmore and Tatarko 1991), described the underlying fundamental approaches used to develop WINDGEN based on the Wind Energy Resource Information System (WERIS) data (NCDC TD-9793) described in Elliot et al. (1986). An early version of WINDGEN and its database were described by Skidmore and Tatarko (1990). The first functional WINDGEN generator and related database utilities were discussed by Wagner et al. (1992).

Overview

Often, it is not practical to use measured historical wind data with WEPS, since many wind records are not serially complete and have missing data. Also, one may want to simulate wind erosion for a longer period than the length of the measured data record, e.g., 50 years, which is the length of a typical WEPS simulation run for a single-year management rotation. In addition, the measured data require much more computer disk

space than wind summary statistics and may also contain gaps in the record that don't occur with generated data. Therefore, stochastic wind generation is often more appropriate for using with WEPS than for using the measured data directly.

The range of wind speeds that is of interest to wind erosion researchers is unique compared to that of other users of wind data. A stochastic wind generator that is satisfactory for other applications may not be satisfactory for application in wind erosion prediction. For example, the wind power industry is interested in consistent wind speeds, but only up to a certain value, e.g., 8 m s^{-1} , at which a wind turbine generates its maximum power (Justus et al. 1976, Hennessey 1977). Thus, for the wind power industry, it is not critical that a stochastic wind generator exactly reproduces wind speeds greater than 8 m s^{-1} and that their data are possibly biased to areas with known or suspected consistent winds. The construction industry is interested only in the maximum wind speed that a structure may experience during its lifetime (Mayne 1979, Cook 1982). For the prediction of evaporation and transpiration, one is interested in the entire range of wind speeds; but again, exact simulation of high wind speeds is not critical. Requirements for wind erosion modeling are unique in this respect.

Distributions of weather variables are needed by stochastic weather generators to be able to generate data. Wind speed distributions have been described by the two-parameter Weibull model (Takle and Brown 1978, Corotis et al. 1978, Skidmore and Tatarko 1990), the two-parameter gamma model (Nicks and Lane 1989), and the one-parameter Rayleigh model, which is a special case of the Weibull model (Hennessey 1977, Corotis et al. 1978). The Weibull is the most widely used model.

An early version of WINDGEN was used to generate wind speeds from Weibull parameters (Skidmore and Tatarko 1990), but generated wind speeds were suspect in certain locations. Thus, the subject of stochastic wind speed generation was revisited, and WEPS currently no longer uses the Weibull model or any other model (van Donk et al. 2005). Another reason was the availability of an updated, quality-controlled, hourly wind database (NCDC et al. 2002).

WINDGEN Dataset

A quality-controlled hourly wind dataset (TD-6421, version 1.1) (NCDC et al. 2002), including 1,304 stations in the 48 contiguous States, was obtained from NCDC. If the data were not measured at 10 m height, NCDC adjusted them to this height. The dataset includes data up to the year 2000 (1976 for the previous WEPS dataset), providing longer data records and more-recent data. The longest record is 65 years. Stations with less than 5 years of data were excluded, leaving 971 stations for use with a stochastic generator. This provided a denser network than the 673 stations previously used in WEPS. Specifically, for NRCS use, the number of stations was further reduced, to 739, to eliminate duplication of nearby stations, especially in metropolitan areas. To serve underrepresented areas, particularly in the western United States, additional stations were “created” using NARR (North American Regional Reanalysis) (Mesinger et al. 2006) and other datasets. The NARR dataset includes 10 m winds and 2 m temperatures and dewpoints for grid points every 32 km across the United States for 30 years or more. These data were used to build “estimated” climatologies for these modeled points, and from these climatologies, WINDGEN NARR stations were developed for critical and otherwise data-lacking locations. Thus, the total number of U.S. stations for NRCS use is currently 760 and 1,046 for other users.

The dataset contains both Automated Surface Observing System (ASOS) (Lockhart 2000, McKee et al. 2000) data and manually observed wind data collected before ASOS. The ASOS data are 2-minute averages, and the before-ASOS data are 1-minute averages, measured every hour. ASOS replaced manual observations beginning in the late 1980s and early 1990s. More than 800 stations have no ASOS data at all, and none of the stations has more than 8 years of ASOS data. Analysis of 28 stations with the longest ASOS records showed that on average for the ASOS data, the mean wind speed was 3.6 m s^{-1} , the erosive wind power density was 2.9 Wm^{-2} , and the percentage of wind speeds exceeding 10 m s^{-1} was 1.8%. For the before-ASOS data, these figures were 4.0 m s^{-1} , 5.3 Wm^{-2} , and 2.8%, respectively. Despite these differences, all data were utilized in order to have the benefit of the full data record, rather than reducing the record length by excluding either the ASOS data or the before-ASOS data. The longer the record, the better the true distribution is captured. Records are already short since not just one record is used for a location, but 192 records: one record for each month-wind direction combination (12 months times 16 wind directions).

Wind speeds are generated using different parameter sets for each month of the year, and they also have wind direction dependence, since some months and directions have greater wind speeds than others. Monthly wind speed parameters are important because when WEPS simulations are conducted for a given farm field, there can be differences in simulated wind erosion in one month compared to another. For instance, most winter wheat fields in the U.S. Great Plains will be better protected with biomass in May than in February. Wind speed by direction is important for determining distances to non-erodible field boundaries. The longer this distance, the greater wind erosion episode can be expected. Wind direction relative to the direction of tillage operations and row crops is also important for wind erosion. Ridges and rows offer more protection against perpendicular winds than against parallel winds. In addition, the proper placement of wind barriers depends on wind direction.

Stochastic Wind Generator

There are two steps in the stochastic generation of wind data. First, statistics describing the distributions of wind direction and speed are calculated from a historical record of measured data (Table 5). This step is done only once, and the results are saved as the “WINDGEN database record” (Table 6). WEPS comes with this database. Second, wind data are stochastically generated from this database by WINDGEN. This is done every time a WEPS simulation is made.

Table 5. Example of a WINDGEN database record (WINDGEN input) for Sidney, NE. From this record, WINDGEN stochastically generates wind directions and speeds that are then used as input for other WEPS submodels - see Table 6.

```

1      # 725610 US NE SIDNEY
2      41 6 N 102 59 W 1312 19770101 20001231 AUU
3      6.0 7.5 10.1 10.8 9.9 8.4 7.3 7.2 8.9 8.3 7.5 6.6
4      2.0 2.7 3.6 4.2 4.3 4.0 4.2 4.0 4.3 3.3 2.8 2.5
5      1.6 2.0 2.4 3.3 3.8 3.5 3.9 3.9 3.3 2.4 1.6 1.5
6      1.5 1.8 2.4 2.9 3.2 3.7 3.8 3.3 2.9 1.8 1.3 1.2
7      1.9 2.3 3.3 4.0 4.4 6.0 5.7 4.4 3.8 3.0 1.6 1.5
8      1.5 2.0 3.7 3.9 4.6 5.4 5.3 4.7 3.4 2.7 1.4 1.0
9      2.4 3.0 4.7 5.4 6.6 7.4 8.8 7.7 5.4 4.1 2.2 1.5
10     3.9 4.7 6.3 7.2 10.4 10.1 11.5 11.8 9.4 6.3 3.3 2.7
11     5.7 6.4 7.9 7.7 11.9 13.4 13.9 14.7 13.1 8.4 6.1 5.4
12     4.4 4.7 4.2 4.3 4.7 5.3 6.1 6.6 6.3 5.0 5.7 5.2
13     6.6 5.5 4.8 3.9 3.7 4.4 4.4 4.8 5.1 5.4 6.3 7.1

```


- 20-211 Cumulative wind speed distributions for 12 months and 16 wind directions.
 Line 20 is January, winds from the North.
 Line 21 is January, winds from the North-Northeast, etc.
 Line 36 is February, winds from the North.
 Line 37 is February, winds from the North-Northeast, etc.
 The “cut-off” wind speeds are 0.5, 1.5, 2.5, ..., 18.5, 19.5, 20.5, 25.5, 30.5, 35.5, 40.5, and 45.5 m s⁻¹.
 By definition, the fraction of wind speeds ≤ 0.5 m s⁻¹ = 0 (calms are treated separately).
 The first column is the fraction of wind speeds ≤ 1.5 m s⁻¹.
 The second column is the fraction of wind speeds ≤ 2.5 m s⁻¹, etc.
 Blank space on the right-hand side of a line should be interpreted as 1.000.
 The highlighted distribution of line 210 is also shown in Figure 1.
- 212 Average ratio of maximum mean hourly to minimum mean hourly observed wind speeds by month (no longer used in WEPS).
- 213 Average hour of maximum wind speed by month.
-

Table 6. Example of a WINDGEN output file for Sidney, NE. This file is used as input for other WEPS submodels.

```

1 # WIND_GEN4 $Revision: 1.1 $ Hourly values per day output
2 # station: 725610 SIDNEY, NE US
3 # lat: 41deg 6min N lon: 102deg 59min W
4 # period: 19770101-20001231 el:1312m
5 # day mo year dir hr1 hr2 hr3 hr4 hr5 hr6 hr7 hr8 . .
6 # deg m/s m/s m/s m/s m/s m/s m/s m/s . .
7 # -----
8 1 1 1 247.5 1.7 2.1 2.7 3.3 3.6 4.0 4.2 4.5 . .
9 2 1 1 270.0 2.3 3.0 3.7 4.0 4.2 4.6 5.0 5.3 . .
10 3 1 1 45.0 1.6 1.8 2.2 2.9 3.7 4.1 4.7 5.2 . .
11 4 1 1 337.5 2.4 3.6 4.4 5.1 5.9 6.7 7.1 7.7 . .
12 5 1 1 67.5 0.9 1.5 2.0 2.3 2.5 3.1 3.6 4.1 . .
13 6 1 1 292.5 2.1 3.1 3.9 4.2 4.7 5.2 5.7 6.1 . .
14 7 1 1 270.0 2.3 3.0 3.6 3.9 4.2 4.6 4.9 5.3 . .
15 8 1 1 315.0 2.3 3.7 4.0 4.8 5.4 6.0 6.7 7.5 . .
16 9 1 1 315.0 3.0 3.9 4.3 5.0 5.5 6.3 6.9 7.9 . .
17 10 1 1 270.0 2.1 3.0 3.6 3.9 4.2 4.5 4.8 5.3 . .
18 11 1 1 292.5 2.3 3.5 4.0 4.4 4.9 5.4 6.0 6.4 . .
19 12 1 1 292.5 2.3 3.5 4.0 4.3 4.8 5.3 5.9 6.2 . .
20 13 1 1 157.5 1.6 2.5 3.6 4.0 4.3 4.6 5.0 5.8 . .
21 14 1 1 270.0 2.5 3.1 3.7 4.0 4.3 4.6 5.0 5.3 . .
22 15 1 1 337.5 2.2 3.6 4.3 5.0 5.9 6.5 7.1 7.6 . .
23 16 1 1 0.0 2.1 3.1 3.7 4.5 4.9 6.0 6.3 7.0 . .
24 17 1 1 0.0 1.7 2.7 3.6 4.1 4.7 5.5 6.2 6.6 . .
25 18 1 1 292.5 2.2 3.2 3.9 4.3 4.8 5.3 5.7 6.1 . .
26 19 1 1 225.0 1.2 1.8 2.4 3.3 3.8 4.2 4.7 5.1 . .
27 20 1 1 337.5 2.2 3.5 4.2 4.9 5.9 6.5 7.0 7.6 . .
28 21 1 1 292.5 2.2 3.2 4.0 4.3 4.8 5.3 5.8 6.2 . .
29 22 1 1 337.5 2.1 3.1 4.1 4.8 5.6 6.4 6.9 7.3 . .
30 23 1 1 337.5 2.1 3.5 4.2 4.9 5.6 6.4 7.0 7.4 . .
31 24 1 1 45.0 1.6 1.8 2.3 3.1 3.8 4.1 4.7 5.2 . .
32 25 1 1 315.0 2.9 3.9 4.2 4.9 5.5 6.2 6.9 7.8 . .
33 26 1 1 315.0 2.6 3.8 4.2 4.9 5.4 6.1 6.8 7.6 . .
34 27 1 1 225.0 1.5 1.9 2.6 3.4 3.9 4.4 4.8 5.1 . .
35 28 1 1 270.0 2.0 2.9 3.6 3.9 4.2 4.4 4.8 5.2 . .

```

36	29	1	1	292.5	2.9	3.8	4.2	4.6	4.9	5.4	5.8	6.4	.	.
37	30	1	1	0.0	1.9	2.8	3.6	4.2	4.8	5.6	6.2	6.8	.	.
38	31	1	1	0.0	2.0	2.9	3.7	4.2	4.8	5.7	6.2	6.8	.	.
39	1	2	1	67.5	1.4	1.7	2.1	2.4	3.0	3.7	4.1	4.3	.	.
40	2	2	1	270.0	1.7	2.2	3.0	3.7	4.0	4.5	5.0	5.6	.	.
41	3	2	1	292.5	2.4	3.5	3.9	4.3	4.8	5.2	5.6	6.1	.	.
42
43
44

Description of items in Table 6

Line 1	WINDGEN info: generator version and type of output file
Lines 2-4	Repeat of information in Table 5, lines 1 and 2
Lines 5, 6	Column headings
Lines 8+	wind data, one line per day
Columns 1, 2, 3	day mo year – day, month, and year of simulation
Column 4	dir – wind direction for the day. WEPS assumes that the direction is constant for the entire day (degrees clockwise with North=0, East=90, South=180, and West=270).
Columns 5-28	hr1 hr2 . . . - 24 hourly wind speeds (m s^{-1})

1. Calculation of statistics from measured data (only once - results are saved as the “WINDGEN database record”)

Wind direction frequencies are calculated for each of 16 directions for each month (Table 5, lines 3-18). Wind speeds less than or equal to 0.5 m s^{-1} are classified as “calm” (Table 5, line 19). For wind speeds that are not calm, the fraction less than or equal to certain “cut-off” wind speeds is calculated for each month-direction combination ($12 \times 16 = 192$ combinations per station; Table 5, lines 20-211). These cut-off wind speeds are 0.5, 1.5, 2.5, ..., 18.5, 19.5, 20.5, 25.5, 30.5, 35.5, 40.5, and 45.5 m s^{-1} . By definition, the fraction of wind speeds $\leq 0.5 \text{ m s}^{-1} = 0.0$ (the calm winds are treated separately) and the fraction of wind speeds $\leq 45.5 \text{ m s}^{-1} = 1.0$. This implies that the greatest possible wind speed that can be generated is 45.5 m s^{-1} .

2. Stochastic wind generation by WINDGEN (every time a WEPS simulation is made)

Typically, when a WEPS simulation is run, wind data are generated for many years, e.g., 50 years. First, one of the 16 cardinal wind directions (or calm) is selected from Table 5 using a random number generator with the distribution for the current month. The selected wind direction (or calm) is applied for an entire day. Next, if calm was selected, 24 hourly wind speeds of 0 m s^{-1} are prescribed for that day. Otherwise, 24 hourly wind speed values are generated from the cumulative wind speed distribution for the selected direction and month (lines 20-211 in Table 5). From the wind speed distribution for the current month and wind direction (Table 5), a wind speed is stochastically generated from the linearly interpolated distribution using a random number generator (Figure 1).

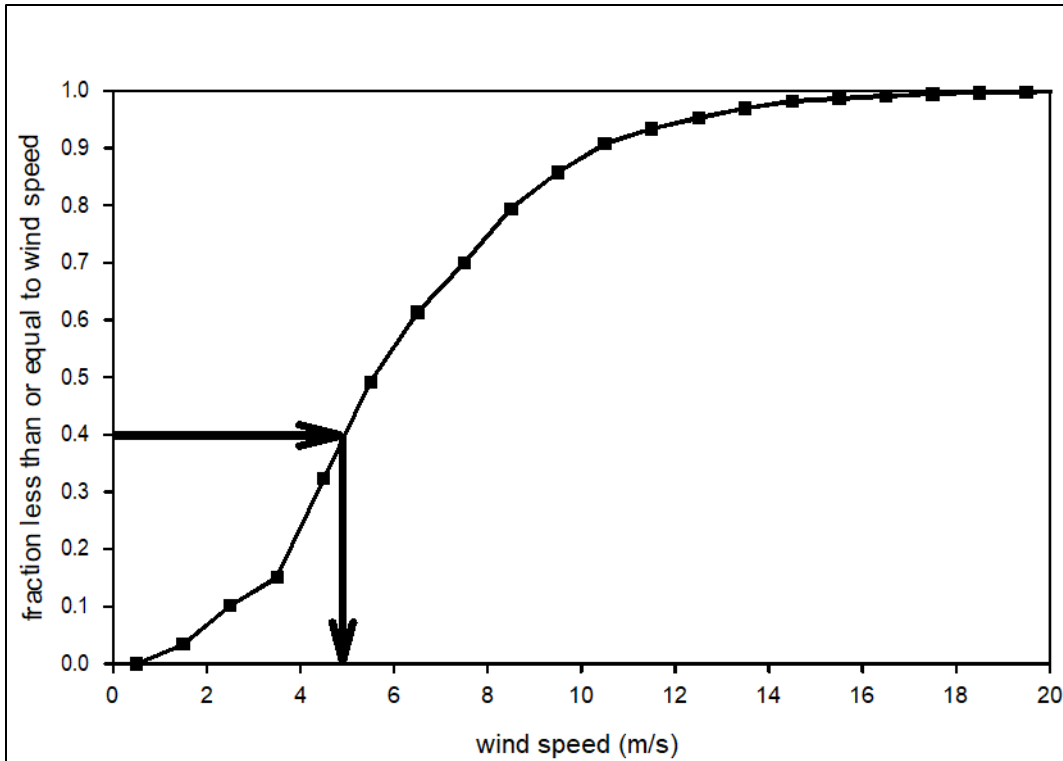


Figure 1. Cumulative distribution of measured wind speed data for Sidney, NE, for December with winds coming from the Northwest (the highlighted wind speed distribution of line 210 in Table 5). In this example, when a random number of 0.40 from a uniform distribution between 0 and 1 is drawn, a wind speed of $\sim 4.8 \text{ m s}^{-1}$ will be generated.

However, using the above procedure by itself would generate a random order of erosive winds, creating erosive windstorms lasting only 1 hour rather than more typical windstorms of a longer duration. The average dust storm in the U.S. Great Plains lasts 6.6 hours (Hagen and Woodruff 1973), but there is no true auto-correlation for the generated hourly wind speeds in WINDGEN. Instead, as a first approximation, the 24 hourly wind speed values for a given day are rearranged to allow for the creation of more realistic windstorms that last longer than 1 hour. No adjustments are currently made to provide hourly wind speed consistency across midnight on succeeding days.

To obtain a sufficient number of high hourly wind speeds to construct reasonable windstorms, multiple pools of randomly generated hourly wind speeds are created for 5 (default value) days, one for each selected wind direction and month. The six (default value) highest wind speeds in the pools for the selected wind direction and month are placed in the first day; the next six highest wind speeds are placed in the second day with the same wind direction and month; and so forth. The remaining lower wind speeds are then randomly distributed throughout the 5 days in each pool.

For each day, the highest hourly wind speed is set to the “hour of maximum wind speed” (a parameter in the wind database record; line 213 in Table 5), and the remaining wind speeds are then placed around that hour such that the next two highest hourly wind speeds occur an hour before, and an hour after, the “hour of maximum wind speed.” The


```

41 19 N 105 40 W 2218 19720101 20001231 A U U 725645 US WY LARAMIE
39 52 N 104 40 W 1656 19740101 20001231 A U U 725650 US CO DENVER INTNL ARPT
41 52 N 103 36 W 1206 19430101 20001231 A U U 725660 US NE SCOTTSBLUFF/HEILIG
42 52 N 100 33 W 792 19480101 20001231 A U U 725670 US NE VALENTINE (AMOS)
42 55 N 106 28 W 1612 19400101 20001231 A U U 725690 US WY CASPER/NATRONA INTL
40 31 N 107 33 W 1915 19770101 20001231 A U U 725700 US CO CRAIG (AMOS)
40 26 N 109 31 W 1608 19730101 20001231 A U U 725705 US UT VERNAL
40 29 N 107 13 W 2012 19730101 20001231 A U U 725715 US CO HAYDEN/YAMPA (AWOS)
39 32 N 107 48 W 1622 19720101 19961231 A U U 725716 US CO RIFLE (AWRS)
40 47 N 111 58 W 1288 19410101 20001231 A U U 725720 US UT SALT LAKE CITY INTL
40 13 N 111 43 W 1369 19800101 20001231 A U U 725724 US UT PROVO MUNI (AWOS)
41 36 N 109 4 W 2056 19720101 19851231 A U U 725740 US WY ROCK SPRINGS
41 48 N 107 12 W 2077 19720101 20001231 A U U 725745 US WY RAWLINS / MUNI APT
41 12 N 112 1 W 1362 19720101 20001231 A U U 725750 US UT OGDEN-HINCKLEY MUNI
41 7 N 111 58 W 1459 19410101 20001231 A U U 725755 US UT HILL AFB/OGDEN
42 49 N 108 44 W 1694 19480101 20001231 A U U 725760 US WY LANDER/HUNT FIELD
43 4 N 108 28 W 1684 19720101 20001231 A U U 725765 US WY RIVERTON REGIONAL
41 17 N 111 2 W 2183 19720101 20001231 A U U 725775 US WY EVANSTON/BURNS FLD
43 36 N 110 44 W 1964 19730101 20001231 A U U 725776 US WY JACKSON HOLE (AWOS)
42 55 N 112 34 W 1365 19430101 20001231 A U U 725780 US ID POCATELLO MUNICIPAL
43 31 N 112 4 W 1445 19720101 20001231 A U U 725785 US ID IDAHO FALLS/FANNING
. . . . .

```

Description of items in the first line in Table 7

Item	Description
41 6 N	Latitude (41° 6' North)
102 59 W	Longitude (102° 59' West)
1312	Elevation (meters)
19770101	Beginning record date (yyyymmdd)
20001231	Ending record date (yyyymmdd)
A U U	Three letters containing record information (no longer used in WEPS)
725610	A unique number (WMO) for the station
US	Country
NE	State
SIDNEY MUNI (AMOS)	Name of the station

Table 8. Command line options for WINDGEN version 4.

WINDGEN stochastically generates (simulates) hourly wind data (Table 6) from summary statistics (Table 5). Wind simulation is always initiated on the first day of a year and produced in multiples of 1 full calendar year. Leap years are accounted for. Only the -s option is required.

usage: wind_gen4 -D -V -v -h -l -f dbfile -o outfile -s # -x # -r # -b # -y # -u # -d # -?

Option	Default value	Description
D		Debug flag: additional output is generated for debugging purposes
V		Display WINDGEN version only and exit program
v		Verbose option: generate additional information. This option would typically be used in situations where a corrupted wind database was suspected because of possibly erroneous output data being observed.

h		Do not generate a heading (title) for the output
l		Generate long (additional) output; currently only generates additional column headings but no data
f dbfile	wind_gen.wdb	Wind database (input) file
o outfile	screen display	Output file; the default output (screen display) is used if this option is not specified
s #		Valid station code (WBAN number); this option is REQUIRED.
x #		Station database index number (an index number for the station code specified with the -s option) to obtain faster access to the desired database record information
r #	54321	Random number seed
b #	1	Beginning simulation year
y #	1	Number of years to simulate (generate)
u #	6	Storm duration length in hours (24 or less)
d #	5	Number of days to build storms from (7 or less)
?		Display command line options and exit program

Examples:

wind_gen4 -s 724515 -o GardenCity.out

This directs WINDGEN to search in the default wind database (wind_gen.wdb) for the station with station code 724515 (Garden City, KS), generate 1 year of daily wind data, and write it to the file 'GardenCity.out'.

wind_gen4 -s 724515 -f ks.wdb -b 1980 -y 30 -o GardenCity.out

This directs WINDGEN to search in the wind database 'ks.wdb' for the station with station code 724515 (Garden City, KS), generate 30 years of daily wind data with a starting year of 1980, and write it to the file 'GardenCity.out'.

Spatial Interpolation of Wind Stations

The stations used for wind simulation are spaced widely enough so that large differences may exist between the wind distributions for adjacent stations. Selecting the nearest wind station can result in large simulated erosion differences between two nearby locations if they use different wind stations. To address this issue, spatial interpolation is used to create an intermediate station from a weighted average of the summary statistics (Table 5) for the nearest stations. Presently, three stations and weights for spatial interpolation are found from the Delaunay triangulation of the WINDGEN station locations by incorporating STRIPACK (Renka 1997). Station weights, which necessarily sum to 1, are found by normalizing the unnormalized barycentric (or areal) coordinates returned by STRIPACK routine TRFIND using the program INTERPOLATE (Table 9). The interpolation program also implements a nearest neighbor approach that will use a designated number of closest stations and create distance-based weights. This method has not been tested with the WEPS interface code and could be easily implemented if desired.

Table 9. Command line options for WINDGEN interpolation routine.

Given a point on the map, the INTERPOLATE routine creates the Delaunay triangulation of the WINDGEN station geographic coordinates, subject to a bounding polygon with added shadow points for the boundary regions and returns three station IDs and associated weights to be used for interpolating the input point.

usage: interpolate -? -h -d -f idxfile -i # -lat # -lon # -n -o outfile -p polyfile -T -v

Option	Default value	Description
?, h		Display help screen
d		Create debugging output files
f idxfile	./wind_gen_his_upper_US.idx	WINDGEN index file name
i #	0	Use inverse distance weighting with
# points		
lat #	1000	Latitude (North is positive)
lon #	1000	Longitude (East is positive)
n		Bounding polygon NOT used
o outfile	./interpolate.txt	Name of output file to contain list of station codes and weights
p polyfile	./boundary.pol	Bounding polygon file name
T		Use Delauney triangulation weighting
v		Create Voronoi output file

Example:

interpolate.exe -f "L:\weps\weps.install\db\windgen\wind_gen_his_upper_US.idx" -p "L:\weps\weps.install\db\windgen\interpolation_boundary.pol" -lat 39.30 -lon -96.74 -o weights.txt

This directs INTERPOLATE to use the stations listed in the .idx file, bounded by the points in the .pol file, to find the station IDs and interpolation weights for the geographic point at 39.30 degrees North, 96.74 degrees West. The result of this command is a list of station codes and weights that is written to the file 'weights.txt'. This output is input for the program INTERP_WDB described in Table 10.

The station codes and station weights are then read by the WEPS interface code that extracts the histogram for each station from the WINGEN database file and writes each one to a file with the station code as the name. Given three station file names and their corresponding weights, each element of the summary statistics (Table 5) record from each station is multiplied by the corresponding station weight and summed to create the intermediate station element using the program INTERP_WDB (Table 10).

Table 10. Command line options for routine creating a new WINDGEN histogram file.

INTERP_WDB uses an input set of n (currently n=3) WINDGEN histogram files and weights to create a weighted average WINDGEN histogram file.

usage: interp_wdb.exe output.wdb histogram _1 station_weight_1 histogram _2
station_weight_2 ... histogram _n station_weight_n

Option	Default value	Description
output.wdb		Output file name
histogram _1		First WINDGEN histogram file
station_weight_1		Weight to be used with first
station		
histogram _2		Second WINDGEN histogram
file		
station_weight_2		Weight to be used with second
station		
histogram _n		nth WINDGEN histogram file
station_weight_n		Weight to be used with nth
station		

Example:

**interp_wdb.exe test.wdb 724555 0.8156743504085082 725515 0.1194967817223571
724580 6.482886786913460E-02**

Creates a weighted average WINDGEN station histogram file named ‘test.wdb’ using station 724555 with a weight of 0.8156743504085082, station 725515 with a weight of 0.1194967817223571, and station 724580 with a weight of 6.482886786913460E-02. The input for this program is the output from the INTERPOLATE program described in Table 9.

During testing, it was noted that incomplete coverage of the stations will result in choosing very distant stations when triangulating stations located near the borders of the United States. To prevent interpolations made near the boundaries from using distant stations, pseudo-stations were created by reflecting station locations near the boundary perpendicularly across the polygon boundary (Figure 2). This serves to limit the triangulations near the boundary to the set of points near the boundary location.

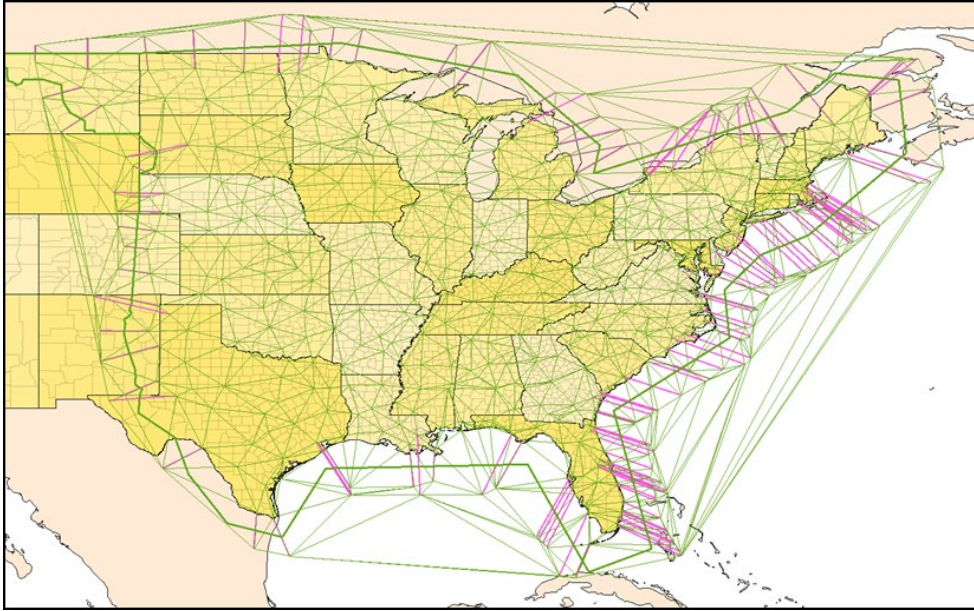


Figure 2. WINDGEN interpolation region triangulation within boundary region with reflected boundary stations.

Due to the magnitude of terrain relief between stations, it was deemed inappropriate to use interpolation in the mountain regions of the Western United States as well as select regions where interpolation was not working acceptably for NRCS. To address this issue, station selection polygons were defined (Figure 3). These selection polygons define areas where NRCS has associated a specific WINDGEN station record to be used for that area.

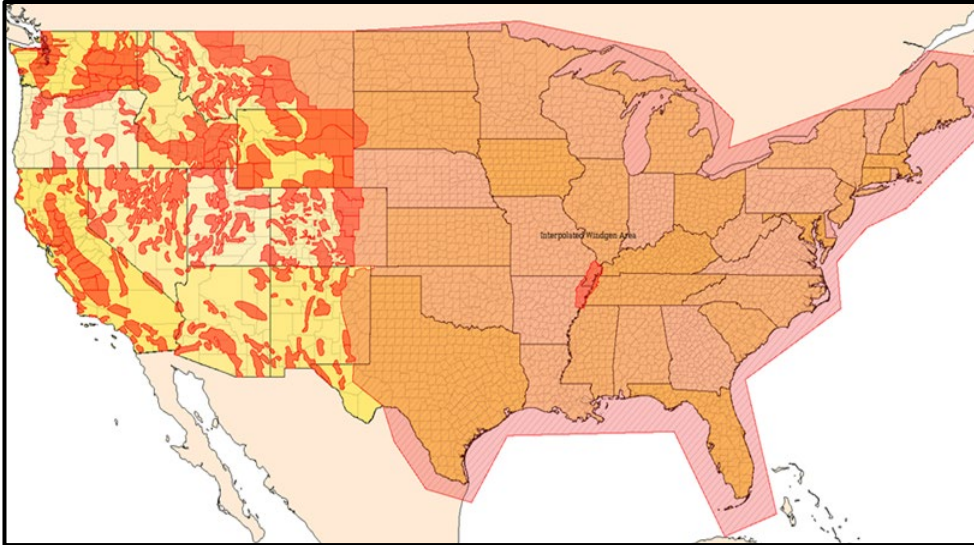


Figure 3. WINDGEN interpolation area polygon and Western region station selection polygons. The red sections are the station selection polygons, the darker regions (overlaid with purple) east of the Rockies are the interpolation region, and the yellow shades west of the Rockies are the sorted station selection regions used by the “NRCS” station selection setting.

In the WEPS interface, for NRCS, the WINDGEN station to be used for stochastic wind generation is found by first looking at the station selection polygon; and if the location is within a station selection polygon, the station record associated with that polygon is used. If the location is not within a station selection polygon, and it is within the interpolation region polygon, interpolation is performed, resulting in a temporary interpolated station record. NRCS use of WEPS focuses on counties as the primary administrative unit, so when WEPS is running in “NRCS mode,” interpolation in the interface snaps to the county centroid, resulting in a single interpolated location for each county (primarily for locations east of the Rockies). Finally, if it is not in either, a list of stations sorted by distance from nearest to most distant is presented to the user for selection.

Also available for non-NRCS users within the interface are (a) a GIS mode, which only uses the station selection polygons and falls back to the sorted station selection mode if the location does not reside in a station selection polygon; (b) an interpolation mode, which ignores the interpolation boundary and reflected points and does not snap to the county centroid; (c) a nearest station selection mode; (d) a sorted-by-distance station selection list mode for manual station selection; and (e) a historical wind data file mode.

Summary

The widespread use of the CLIGEN weather generator in WEPS simulations by NRCS has driven improvements to the CLIGEN databases, changed how stations are assigned and selected for NRCS use, and highlighted the improvements needed in the weather generation infrastructure. The addition of auto-correlation with and cross-correlation between generated variables and better representation of precipitation patterns should be high priorities as the improvement of climate generation is planned for the future. All of the critical issues have been addressed to some degree by others, but no tool has integrated all the improvements in order to make a complete tool. For better simulation of

wind erosion, generation of sub-daily wind speed should be incorporated into any complete climate generation tool in order to account for the cross-correlation of wind with precipitation events. Weather simulation is used in a wide variety of model applications (wind erosion, water erosion, farm management, crop growth, residue decomposition, crop disease, watershed modeling, water quality modeling, wind energy, engineering risk assessment, climate change, etc.), each with a unique focus on the aspect of climate simulation that most affects its application. A future climate generation tool incorporating the improvements made to climate generation across the widest range of disciplines possible would find wide application.

References

- Cook, N.J. 1982. Towards better estimation of extreme winds. *Journal of Wind Engineering and Industrial Aerodynamics*. 5:109-137.
- Corotis, R.B., A.B. Sigl, and J. Klein. 1978. Probability models of wind velocity magnitude and persistence. *Solar Energy*. 20:483-493.
- David, O., J.C. Ascough II, W. Lloyd, et al. 2013. A software engineering perspective on environmental modeling framework design: the Object Modeling System. *Environmental Modelling & Software* 39:201-213, doi: 10.1016/j.envsoft.2012.03.006.
- David, O., S.L. Markstrom, K.W. Rojas, et al. 2002. The Object Modeling System. *In* L.R. Ahuja, L. Ma, and T.A. Howell, eds., *Agricultural System Models in Field Research and Technology Transfer*, pp. 317-330. Boca Raton, FL: Lewis Publishers.
- Elliot, D.L., C.G. Holladay, W.R. Barchet, et al. 1986. Wind Energy Resource Atlas of the United States. DOE/CH 10093-4. Available at: <https://rredc.nrel.gov/wind/pubs/atlas/> (Accessed September 24, 2019).
- Elliot, W.J., D.L. Scheele, and D.E. Hall. 1999. Rock:Clime, Rocky Mountain Research Station Stochastic Weather Generator, Technical Documentation. Available at: <https://forest.moscowfsl.wsu.edu/fswepp/docs/rockclimdoc.html> (Accessed August 10, 2020).
- Frankenberger, J. 2008. Format of CLIGEN weather station statistics input files. Available at: https://www.ars.usda.gov/SP2UserFiles/ad_hoc/36021500WEPP/cligen/cligenparms.pdf (Accessed August 10, 2020).
- Gete, Z., T. Winter, and D. Flanagan. 2009. BPCDG: Breakpoint Climate Data Generator for WEPP Using Observed Standard Weather Data Sets. Available at: https://www.ars.usda.gov/SP2UserFiles/ad_hoc/36021500WEPP/Bpcdg.pdf (Accessed August 10, 2020).
- Hagen, L.J., and N.P. Woodruff. 1973. Air pollution from dust storms in the Great Plains. *Atmospheric Environment*. 7: 323-332.
- Hennessey, J.P. 1977. Some aspects of wind power statistics. *Journal of Applied Meteorology*. 16:119-128.
- Justus, C.G., W.R. Hargraves, and A. Yalcin. 1976. Nationwide assessment of potential output from wind-powered generators. *Journal of Applied Meteorology*. 15:673-678.
- Lockhart, T.J. 2000. A summary of wind climate continuity with ASOS. *In* Proceedings of the 12th AMS Conference on Applied Climatology, pp. 131-133. Boston, MA: American Meteorological Society.
- Mayne, J.R. 1979. The estimation of extreme winds. *Journal of Industrial Aerodynamics*. 5:109-137.

McKee, T.B., N.J. Doesken, C.A. Davey, and R.A. Pielke. 2000. Climate Data Continuity With ASOS. Climatology Report No. 00-3. Colorado Climate Center, Department of Atmospheric Science, Colorado State University, Fort Collins, CO.

Mesinger, F., G. DiMego, E. Kalnay, et al. 2006. North American regional reanalysis. *Bulletin of the American Meteorological Society* 87:343-360, doi: 10.1175/BAMS-87-3-343.

Meyer, C.R. 2004. General description of the CLIGEN model and its history. Available at: https://www.ars.usda.gov/SP2UserFiles/ad_hoc/36021500WEPP/cligen/CLIGENDescription.pdf (Accessed August 10, 2020).

Meyer, C.R., C.S. Renschler, and R.C. Vining. 2008. Implementing quality control on a random number stream to improve a stochastic weather generator. *Hydrological Processes*. 22(8):1069-1079.

National Oceanic and Atmospheric Administration, National Climatic Data Center. 1998. Summary of the Data First Order TD-3210. Available at: https://iridl.ldeo.columbia.edu/SOURCES/.NOAA/.NCDC/.DAILY/.FSOD/.dataset_documentation.html (Accessed August 10, 2020).

National Oceanic and Atmospheric Administration, National Climatic Data Center. 2006. Data Documentation for Data Set 6406 (DSI-6406). Available at: <https://www1.ncdc.noaa.gov/pub/data/documentlibrary/tddoc/td6406.pdf> (Accessed August 10, 2020).

National Oceanic and Atmospheric Administration, National Climatic Data Center. 2009. Data Documentation for Data Set 3200 (DSI-3200). Available at: <https://www1.ncdc.noaa.gov/pub/data/documentlibrary/tddoc/td3200.pdf> (Accessed August 10, 2020).

National Oceanic and Atmospheric Administration, National Climatic Data Center/National Environmental Satellite, Data, and Information Service. 2002. NCDC TD6421 Enhanced Hourly Wind Station Data for the Contiguous United States. Research Data Archive at the National Center for Atmospheric Research, Computational and Information Systems Laboratory. Available at: <https://rda.ucar.edu/datasets/ds471.0/> (Accessed August 10, 2020).

National Oceanic and Atmospheric Administration, National Climatic Data Center/National Environmental Satellite, Data, and Information Service/National Weather Service; and U.S. Department of Transportation, Federal Aviation Agency. 1981, updated monthly. NCDC TD3200 U.S. Cooperative Summary of Day, (1890-1948)-continuing. Research Data Archive at the National Center for Atmospheric Research, Computational and Information Systems Laboratory. Available at: <https://rda.ucar.edu/datasets/ds510.0/> (Accessed August 10, 2020).

National Oceanic and Atmospheric Administration, National Climatic Data Center/National Environmental Satellite, Data, and Information Service/National Weather Service; U.S. Department of Defense, Air Force Weather Agency; and U.S. Department of Transportation, Federal Aviation Agency. 1987, updated monthly. NCDC

- TD3210 U.S. First Order Summary of Day, (1884-1948)-continuing. Research Data Archive at the National Center for Atmospheric Research, Computational and Information Systems Laboratory. Available at: <https://rda.ucar.edu/datasets/ds509.0/> (Accessed August 10, 2020).
- Nicks, A.D., and L.J. Lane. 1989. Weather generator. *In* L.J. Lane and M.A. Nearing, eds., USDA–Water Erosion Prediction Project: Hillslope Profile Model Documentation, NSERL Report No. 2, pp. 2.1-2.19. USDA-ARS National Soil Erosion Research Laboratory, West Lafayette, IN.
- Nicks, A.D., L.J. Lane, and G.A. Gander. 1995. Weather generator. *In* D.C. Flanagan and M.A. Nearing, eds., USDA–Water Erosion Prediction Project: Hillslope Profile and Watershed Model Documentation, NSERL Report No. 10. USDA-ARS National Soil Erosion Research Laboratory, West Lafayette, IN. Available at: https://www.ars.usda.gov/SP2UserFiles/ad_hoc/36021500WEPP/chap2.pdf (Accessed August 10, 2020).
- Nicks, A.D., J.R. Williams, C.W. Richardson, and L.J. Lane. 1987. Generating climatic data for a water erosion prediction model. Paper No. 87-2541, International Winter Meeting of the American Society of Agricultural Engineers, December 15-18, 1987, Chicago, IL.
- Renka, R. 1997. Algorithm 772: STRIPACK, Delaunay Triangulation and Voronoi Diagram on the Surface of a Sphere. *ACM Transactions on Mathematical Software*. 23(3):416-434.
- Rust, W.J., F. Fox, and L.E. Wagner. 2011. CLIGEN: Addressing deficiencies in the generator and its databases. ASABE International Symposium on Erosion and Landscape Evolution, September 18-21, 2011, Anchorage, AK (ASABE Paper No. 11115).
- Scheele, D.L., and D.E. Hall. 2000. Corrections and improvements to the CLIGEN climate database. USDA Forest Service Rocky Mountain Research Station, Moscow Forestry Sciences Laboratory. May 18, 2000. Modified June 2003. Available at: <https://forest.moscowfs.l.wsu.edu/enr/library/Hall/Hall2000l/2000l.html> (Accessed August 10, 2020).
- Skidmore, E.L., and J. Tatarko. 1990. Stochastic wind simulation for erosion modeling. *Transactions of the ASAE*. 33(6):1893-1899.
- Skidmore, E.L., and J. Tatarko. 1991. Wind in the Great Plains: speed and direction distributions by month. *In* J.D. Hanson, M.J. Shaffer, and C.V. Cole, (eds.), *Sustainable Agriculture for the Great Plains*, pp. 195-213. USDA. ARS Publication 89.
- Takle, E.S., and J.M. Brown. 1978. Note on the use of Weibull statistics to characterize wind speed data. *Journal of Applied Meteorology*. 17:556-559.
- U.S. Department of Agriculture, Agricultural Research Service. 2006. Using Climate Data in the WEPP Windows Interface. Available at: https://www.ars.usda.gov/SP2UserFiles/ad_hoc/36021500WEPP/usingclimate.pdf (Accessed August 10, 2020).

U.S. Department of Agriculture, Agricultural Research Service. 2014. CLIGEN. Available at: <https://www.ars.usda.gov/midwest-area/west-lafayette-in/national-soil-erosion-research/docs/wepp/cligen/> (Accessed August 10, 2020).

U.S. Department of Agriculture, Natural Resources Conservation Service. 2014. GEM, Weather Generator Technology, Generation of Weather Elements for Multiple Applications. Available at: <https://www.nrcs.usda.gov/wps/portal/nrcs/detailfull/national/water/manage/hydrology/?cid=stelprdb1043533> (Accessed August 10, 2020).

Van Donk, S.J., L.E. Wagner, E.L. Skidmore, and J. Tatarko. 2005. Comparison of the Weibull model with measured wind speed distributions for stochastic wind generation. *Transactions of the ASAE*. 48(2):503-510.

Visser, S.M., J.K. Leenders, and M. Leeuwis. 2003. Farmers' perceptions of erosion by wind and water in northern Burkina Faso. *Land Degradation and Development*. 14:123-132.

Wagner, L.E., J. Tatarko, and E.L. Skidmore. 1992. WIND-GEN: a statistical database and generator for wind data. Paper No. 92-211, International Summer Meeting of the American Society of Agricultural Engineers, June 21-24, 1992, Charlotte, NC.

Williams, J.R., C.A. Jones, and P.T. Dyke. 1984. A modeling approach to determining the relationship between erosion and soil productivity. *Transactions of the ASAE*. 27(1):129-144.

Williams, J.R., A.D. Nicks, and J.G. Arnold. 1985. Simulator for water resources in rural basins. *American Society of Civil Engineers Hydraulics Journal*. 111(6):970-986.

Erosion Submodel of WEPS

Contributors:

L.J. Hagen

F.A. Fox

Abstract

The Erosion submodel of the Wind Erosion Prediction System (WEPS) calculates the wind energy available at the soil surface to cause erosion and the erosion processes in prediction equations for the saltation+creep and suspension components. Given the wind velocity above the surface, the friction velocity at the soil surface is found accounting for the effects of wind barriers, surface roughness, and cover. The erosion processes begin with calculation of surface threshold friction velocities and end with periodic updates in surface conditions caused by the soil loss and deposition that occur during erosion. Wind erosion equations for a uniform surface during quasi-steady conditions are based on the principle of conservation of mass. The major processes involved in saltation+creep creation and transport are simulated. These processes include direct emission of loose material, entrainment of material abraded from exposed clods and crust, breakage of saltation+creep aggregates into suspension-size. Trapping of saltation+creep when transport capacity is exceeded on micro-relief and interception by plant stalks is also considered. In a second portion of the submodel, the major processes involved in creation and transport of the suspension component of wind erosion are simulated. These processes include emission of loose material, abrasion from exposed clods and crusts, and breakage of the saltation+creep to form suspension-size aggregates. A downward flux to the surface of coarse fractions of the suspension component is also simulated in portions of the simulation region, where saltating aggregates were not present. The Erosion submodel of WEPS provides estimates of onsite and offsite impacts of erosion and also predicts the size components of the moving soil for improved conservation planning and evaluations of associated environmental impacts.

Introduction

The Wind Erosion Prediction System (WEPS) is a continuous, process-based model whose purpose is to estimate wind erosion on croplands (Hagen 1991a, USDA-ARS 2013). WEPS is composed of a user-interface, databases, and a science model composed of several submodels. The submodels include erosion (ESM), crop growth, residue decomposition, hydrology, soil, and management. Ancillary models include the weather and wind generators. The submodels estimate the soil/vegetation surface state on a daily basis with respect to the erodibility of the surface. If the wind speed during the day generates an erosive force that exceeds the erodibility threshold of that surface, then the ESM will simulate the amount of wind erosion that occurs on a sub-daily time step for that day. To aid in estimating onsite and offsite impacts of erosion, the submodel predicts the size components of the moving soil.

In addition to WEPS, a second model has been created that uses ESM. The Single Wind Erosion Event Program (SWEEP) models single day wind events. It simulates a single

day from a WEPS run making possible rapid evaluations of the effect of the surface state on wind erosion potential.

Background

The dire consequences of wind erosion were dramatically demonstrated during the Dustbowl period of the United States Plains region during the 1930's. The combination of high temperatures, drought conditions, and intensive tillage practices led to gigantic clouds of wind-blown soil, some of which reached great cities on the East Coast of the United States. These clouds lead to significant health problems for residents of the Dustbowl regions as well as significantly diminishing the fertility of the soil for agriculture. In response, the federal government established the Wind Erosion Research Unit (WERU) in the Department of Agriculture and charged it with doing the basic research needed to understand the wind erosion process and ways to mitigate the effects of wind erosion on the nation's farms. WEPS is part of WERU's response to that mandate.

The Natural Resources Conservation Service (NRCS) has adopted WEPS as their primary tool for evaluating management effects on wind erosion susceptibility. To facilitate serving their customers, NRCS requested a maximum WEPS run-time of one minute on fields with a crop rotation length of a single year. The stringent run-time requirement influenced many choices in developing ESM as well as other WEPS submodels, while still maintaining the overall goal of developing a physically-based model. To reduce run-time in the ESM, quasi-steady state solutions to differential equations were used to simulate the eroding soil loss and deposition. To initiate erosion, a static threshold friction velocity of 0.23 m s^{-1} or more was selected to skip erosion calculations during minor erosion events. A coarse mesh of rectangular grid cells was imposed upon the simulation region to allow spatial updates of the surface during erosion events, while minimizing the number of calculation cells. To confine the calculations to a single pass in each time step, the order of erosion calculation was always from upwind to downwind cells. Finally, to minimize the number of time steps required, the duration of each time step was made dependent on erosion amounts. These limitations and any methods implemented for overriding them are noted in their specific sections below.

Erosion Processes

Wind erosion is the process of soil particles on the soil surface moving due to wind. Modelling the erosion of soil by wind starts as a classic fluid dynamics problem. The fluid, air, moves across a surface. The moving fluid creates a shear force on the surface. The shear force acts on loose material on the surface, and at some magnitude causes the unattached material to move, either along the surface or up into the air stream.

Undisturbed land with adequate vegetation does not erode due to wind. A lack of vegetation due to natural conditions or land management can allow wind erosion to occur, although simply working the land is not sufficient to cause wind erosion. Sandy and silty soils tend to erode more easily than does clay or rock dominated soils. Wind barriers, growing crops, crop residue, snow and rain modify erodibility. Wind barriers and growing crops reduce the effective surface shear force. Snow changes the soil surface by making it inaccessible. Crop residue, both standing and flat, does both. Moisture from rainfall adheres soil particles to the surface.

Submodel Structure

The ESM uses parameters supplied by other submodels that describe the soil surface, flat biomass cover, standing biomass leaf and stem areas, wind barriers, and weather to: a) determine if wind erosion can occur in a simulation region on a given day, b) simulate the processes of wind erosion, when erosion occurs, and c) update changes in the soil surface during erosion events. Surface updating enables the model to simulate both source limited and wind energy limited erosion events. Both the surface descriptions and the simulated erosion processes were defined so that each can be experimentally measured (Hagen 2001, Mirzamostafa et al. 1998).

Submodel Outputs

The main submodel outputs are daily estimates of both total soil loss from the simulation region as well as components of the soil loss moving across each field boundary. These components are saltation+creep (>0.10 mm diameter) and suspended soil (<0.10 mm diameter). The mass of particles less than 10 microns in aerodynamic diameter (PM₁₀) in the suspended soil are also predicted. Files of time-varying emissions from all simulation region subdivisions for use as source terms in dust diffusion and transport models can also be output. To compare simulation results to measured erosion data, input files with measured weather and measured surface conditions can be used in place of simulated weather and simulated surface conditions.

Operation Overview

The purpose of ESM is to estimate the amount of soil displacement in a defined field with defined surface and soil characteristics and a defined wind profile over a defined time. All of these defined parameters implicitly make assumptions that need to be carefully described.

The field is defined to be rectangular in shape with fixed dimensions and surrounded by a non-erodible border. Initially, the field is assumed to be homogeneous. That is, the soil characteristics are uniform, any plowed ridges are uniform, surface aggregates are uniform, any armoring of the surface is uniform, residues are uniformly distributed, the field is assumed to be uniformly flat and barriers have uniform height and porosity.

The model then overlays the field with a rectangular grid. The purpose of the grid is twofold. First, during an erosive event, surface changes do not occur uniformly throughout the field. Erosion tends to start near the windward edge of the field and progress across the field. Dividing the field into cells allows the assumption of a locally uniform surface to be maintained, i.e. during the event the field becomes non-uniform, but the cell is assumed to remain uniform. Second, the cells are used as an accounting device to track the displacement of soil. Both the soil that leaves the field and the soil that moves from one place in the field to another is accounted for.

Once the grid is in place, the actual simulation begins. ESM is driven by wind data. It assumes that the wind direction is constant for a 24-hour period with hourly wind speed inputs when called from WEPS. When called from SWEEP, the wind speed interval can be varied. The model also calculates its sweep pattern at this time. That is, the model determines the order of calculation for the grid cells. At each time step, the model starts with the most windward cell so that any soil displaced from one cell will be accounted for in an adjoining cell during the current time step.

The model takes the first interval wind speed and converts it to a friction velocity at the field location. Friction velocity is proportional to the momentum transfer of the wind to the surface and is calculated from the wind speed, surface aerodynamic roughness and vegetation silhouette. If the friction velocity is less than the minimum threshold friction velocity of the cells (threshold friction velocity is the minimum friction velocity for erosion to start) then the model immediately proceeds to the next hour's wind speed and notes that no erosion occurred during this hour.

If the friction velocity is greater than any cell's threshold friction velocity, then erosion may occur. At this point, a time step usually less than the wind speed interval, is calculated. The model assumes a quasi-steady state. That is, as the model proceeds through the cells, it calculates fluxes based upon the friction velocity and surface characteristics and integrates the mass change for the cell by multiplying the flux for the cell by the time step. There are three separate fluxes that are calculated and tabulated for different sized particles: saltation+creep, suspension, and PM₁₀.

Once the accounting is done the cell surface characteristics are updated. This includes increasing or decreasing the reservoirs of saltation+creep, suspension, and PM₁₀ particles due to the effects of breakage from saltating aggregates, changing the aerodynamic roughness of the surface due to ridge degradation, etc. There is also a check to determine if there are limiting factors that may require the length of the next time step to be reduced.

Once time steps for the wind speed interval are completed, the next wind speed is used, and the process continues. Once the 24 hours is over, the daily totals are calculated and stored and the routine returns. In WEPS, ESM is called sequentially after the other submodels have completed on a daily time-step. In SWEEP, ESM is called just once. The daily simulation flow is illustrated in Figure 1.

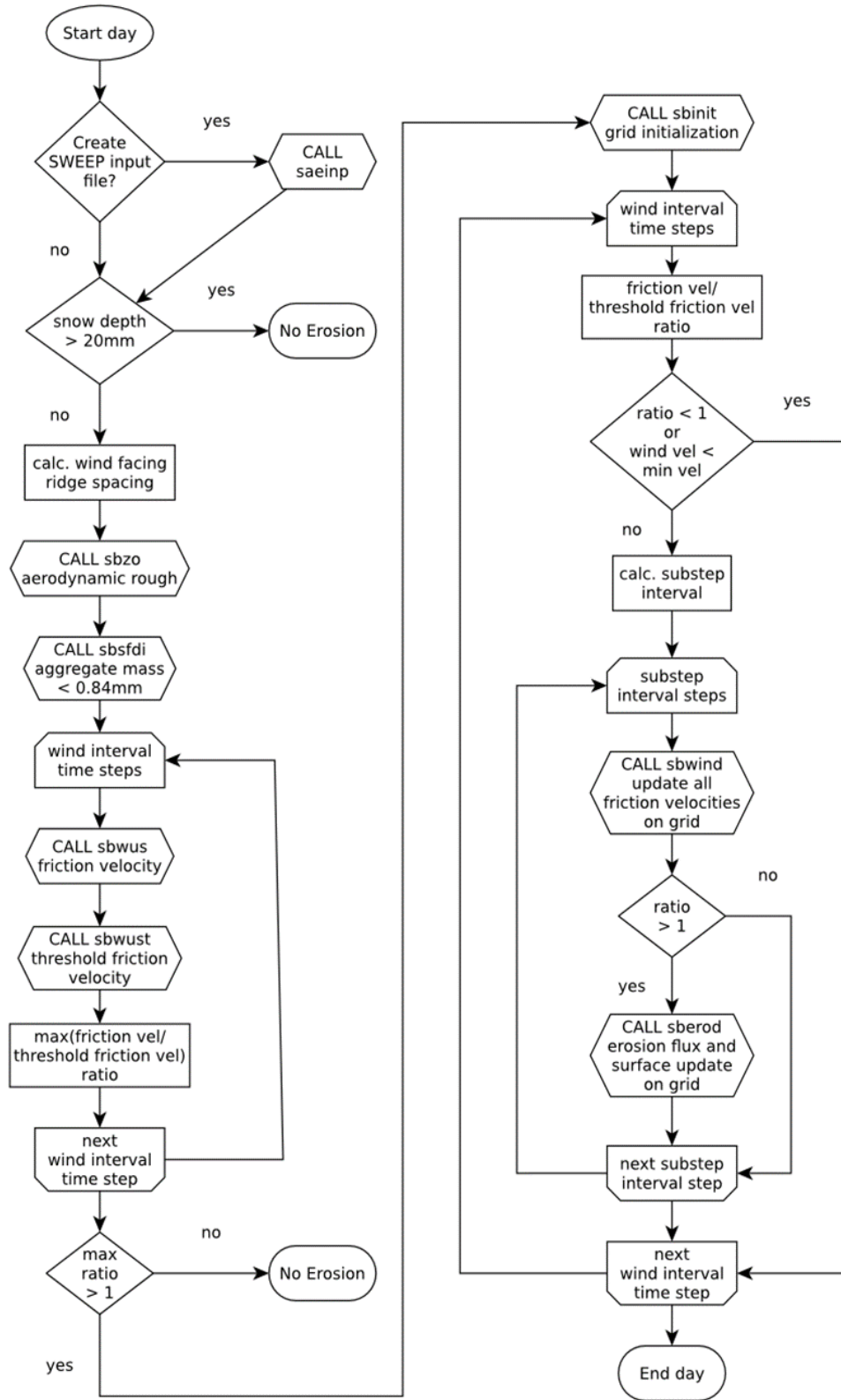


Figure 1. Flowchart of Erosion submodel execution logic.

It is important to note that in WEPS the changes in the surface conditions from the movement of soil by wind are not yet used to update the soil surface for the following day. The homogenous soil surface conditions determined by the other submodels are used to reinitialize the grid cell values to start the next simulation day. This eliminates the need to divide the field into various subregions as the new nonuniform soil surface conditions will affect the simulation of crop growth, hydrology, decomposition, management operations, and climatic effects on soil conditions. Each daily erosion simulation is considered to be an independent trial of the soil and its management, not of the cumulative effect of the erosion events. In addition, field studies have shown that 2-3 days after an erosion event, the reservoirs of suspension sized particles have been observed to return to pre-event levels. Therefore, it seems more appropriate to re-initialize the surface parameters rather than keep the simulated results. Future research may justify retaining the change in surface conditions due to wind erosion events by creating subregions or averaging the changes.

Input Details

There are four basic types of inputs for ESM: field size and orientation, wind speeds and direction, wind barrier(s), and initial soil surface and layer characteristics.

Field (Physical Region)

In ESM, the erodible simulation region is rectangular in shape and surrounded by a boundary that does not allow moving soil in the saltation+creep transport mode to enter the simulation region from upwind, i.e. the erodible area is assumed to be surrounded by a non-erodible boundary (Figure 2). To facilitate calculations and accounting, a rectangular, not necessarily square, grid is generated that overlays the erodible simulation region. Erosion is calculated in individual grid cells using a single pass over all the cells. Using a single pass requires that the sequence of calculations be selected so that they always proceed along the downwind direction.

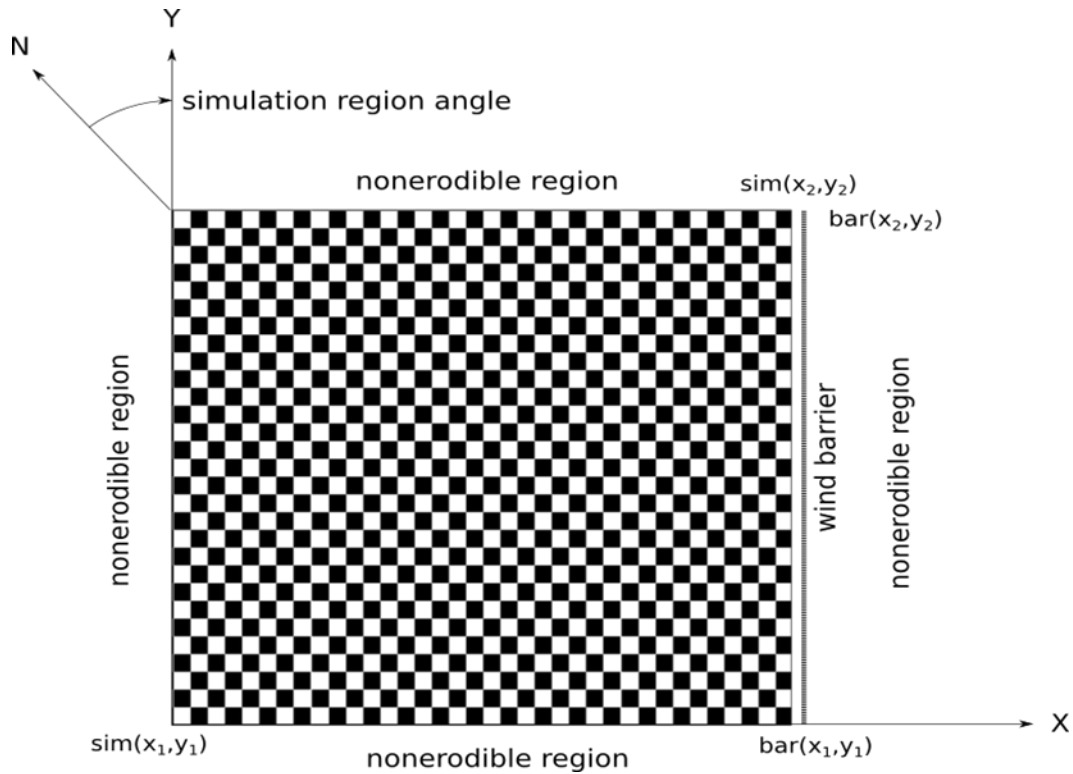


Figure 2. Simulation region geometry in Cartesian coordinate system. The erodible region is a rectangle defined by the Cartesian (x, y) coordinates of the opposite corners. Barriers are defined by the Cartesian coordinates of the end points of the barrier. The simulation region and barriers are then referenced to true North by an angle of rotation. The simulation region is divided into grid cells for erosion calculations.

In WEPS 1.0 the generated grid has a maximum of size of interior 29×29 grid cells with a minimum of 7 m cell length. In narrow strips 3 grid cells are always generated, so the minimum cell length may be less than 7 m. The number of grid cells was restricted to reduce computation time but can easily be modified in the code. When barriers are present, the maximum is increased to 59×59 . The increased number of grid cells is necessary to permit adequate resolution of the barrier reductions in the wind speed for sufficiently large fields. SWEEP allows for overriding the default number of grid cells using command line options.

Input Winds

Simulated, hourly, wind speeds (m s^{-1}) from a weather station representative of the simulation region are normally input to the submodel. The wind speeds generated from the WEPS wind database are at a 10 m height (van Donk et al. 2005). The aerodynamic roughness at the weather stations is assumed to be 25 mm. For WEPS simulations using measured wind data, it needs to be adjusted to these conditions. A simulated daily wind direction is also input to the submodel. ESM is not called unless maximum daily wind speed at 10 m height exceeds 8 m s^{-1} . By doing so, only major erosion events are simulated. Then the maximum daily wind speed is used to determine if erosion can occur in the simulation region. If snow depth exceeds 20 mm, no erosion is simulated. When the Erosion submodel is called, a minimum wind speed is specified, below which no erosion grid calculations are performed in an attempt to reduce erosion calculation

overhead. When called from WEPS, the minimum wind speed is set to 5 m s^{-1} . When using the SWEEP interface to simulate a single erosion event, this value is defaulted to 5 m s^{-1} but may be modified using a command line argument. Also, in SWEEP, measured wind data at the simulation field or from other heights may be used as input to the submodel by setting *wzoflg* to 1 and entering the anemometer height. The aerodynamic roughness of the field will then be used to find the friction velocity.

Wind Barriers

Up to five (limitation of present FORTRAN code) wind barriers can be placed arbitrarily on erodible areas or boundaries of the simulation region (see Figure 2). The submodel inputs required to define each wind barrier include the locations of the barrier ends in simulation region coordinates, $\text{bar}(x_1, y_1)$ and $\text{bar}(x_2, y_2)$. Other inputs needed to define the barrier include the height, optical porosity, and total width of the barrier. The user interface in WEPS 1.0 currently restricts the maximum number of barriers to four and allows them to be placed only on the simulation region boundaries. This restriction is expected to be removed in later interface versions that will allow the user to draw the barriers onto a geographic representation of the field. Barriers in the SWEEP interface are not restricted to the simulation region boundaries.

Input Surface Conditions

The surface conditions considered are combinations of the following:

1. Surface roughness - random and/or oriented measured below the standing biomass canopy but on top of flat residues (Figure 3).
2. Surface covers - flat, random biomass cover; crust with loose, erodible soil on crust; aggregated soil; and rock cover ($>2.0 \text{ mm dia.}$) (Figure 4);
3. Surface soil moisture, crust/consolidated zone parameters (dry stability and thickness), aggregate parameters (dry stability and size distribution); and
4. Standing biomass parameters (leaf area index, stalk silhouette area index, height, row spacing, position on ridge, and orientation) (Figure 5).

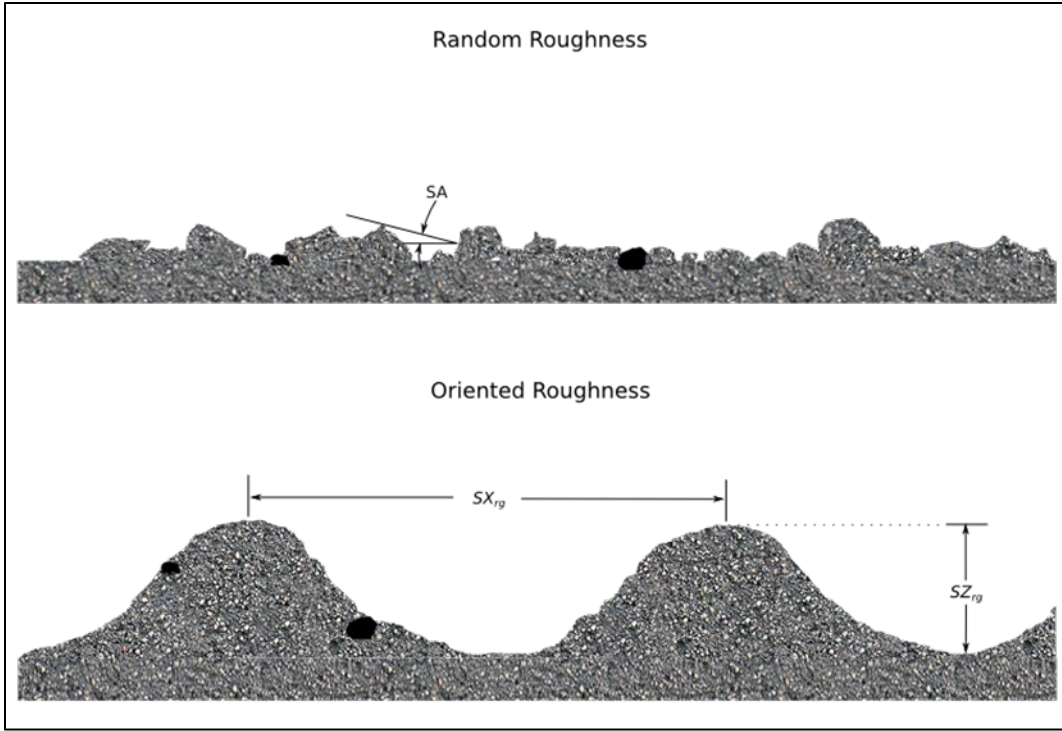


Figure 3. Random roughness shelter angles (SA) and oriented roughness spacing (SX_{rg}) and height (SZ_{rg}) used in ESM.

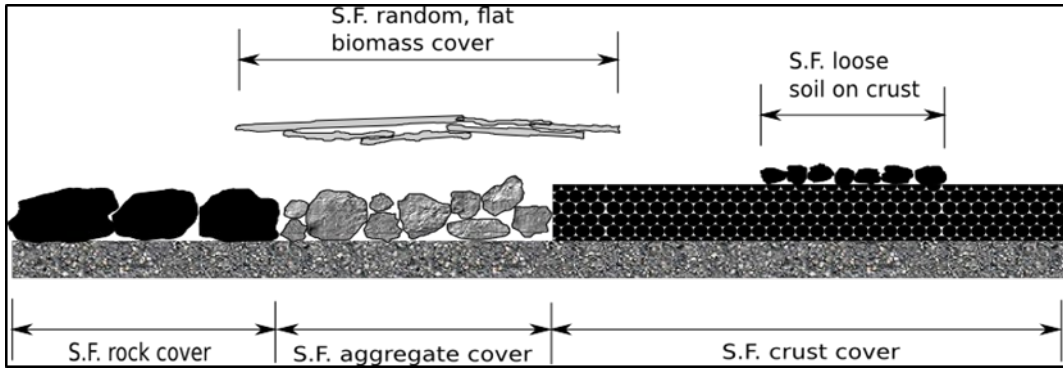


Figure 4. Surface cover fraction (S.F.) descriptions used in ESM.

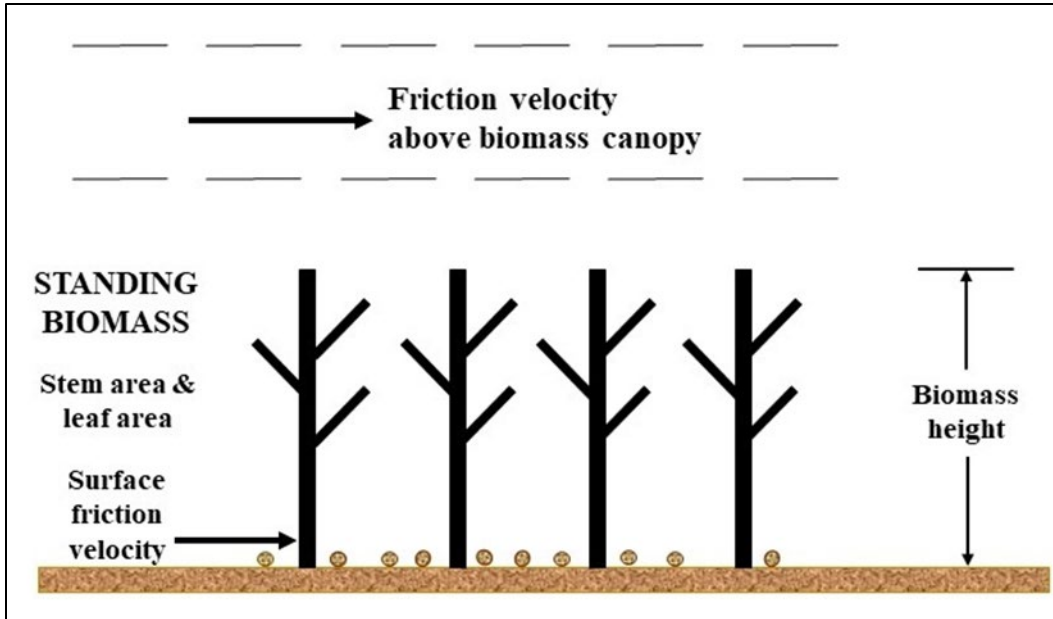


Figure 5. Friction velocity above biomass canopy.

Physical Process Erosion Theory

The atmospheric boundary layer conditions most often encountered with the movement of soil by wind are best described as turbulent with neutral buoyancy. The wind velocity profile can then be described by the equation (Priestley 1959):

$$\frac{U}{U_*} = \frac{1}{K} \ln \left(\frac{Z - Z_d}{Z_0} \right) \quad [1]$$

where

U = wind velocity at height Z (m s^{-1}),

U_* = friction velocity (m s^{-1}),

K = Von Karmen's constant (approximately equal to 0.4),

Z = height above the surface (mm),

Z_d = zero-plane displacement (mm), and

Z_0 = aerodynamic roughness length (mm).

The friction velocity at the soil surface, defined as the square root of surface shear stress divided by the fluid density, is the primary expression of the force of the wind available to cause soil movement.

Processed Based Modeling

Process-based models use formulas derived from observations to calculate the amounts for a given set of input values and a given amount of time. In this model, erosion rates are the critical, observed values. The rate of erosion is assumed to be quasi-steady state. That is, for time periods of interest, the rate of erosion is constant. It is also assumed that there is a reservoir of erodible particles to which the erosion rate is applied. Obviously, this

reservoir can be depleted during an erosive event. Not quite so obviously, there are processes during an erosion event that can replenish these reservoirs. Soil transport during wind erosion occurs in three modes (Chepil and Woodruff 1963): creep-size aggregates (0.84 - 2.0 mm diameter) roll along the surface, saltation-size aggregates (0.10 - 0.84 mm diameter) hop over the surface, and suspension-size aggregates (<0.10 mm diameter) move above the surface in the turbulent flow. Obviously, as wind speeds, turbulence, or sediment loads change, the diameter of aggregates moving in the various modes also may change slightly (Pye 1987).

In ESM, we have assumed that the combined saltation+creep mode of transport has a distinct transport capacity for each surface, based on the surface roughness and wind speed. This assumption is generally supported by both field and wind tunnel measurements of the saltation+creep discharge (Greeley and Iverson 1985). We also assumed that the suspension component does not reach a transport capacity on most eroding fields. Given the different responses to both the wind forces and sediment load (Gillette et al. 1997), separate equations were developed for saltation+creep, suspension, and PM₁₀ (<0.01 mm diameter) discharge. PM₁₀ is a subset of suspension that is of particular interest to EPA, et al., due to the health consequences of breathing high concentrations of PM₁₀. Separating these erosion components also is useful due to their different potential off-site impacts.

Wind erosion occurs over a wide range of surface conditions. To aid in delineating erosion rates among the various surfaces, several individual erosion processes are identified in ESM (Hagen et al. 1995) (Figure 6). These processes include direct entrainment (emission) of loose soil by wind and/or saltation impacts, abrasion of soil from clods/crust by saltation impacts, and breakage of saltation+creep-size aggregates to suspension-size. These processes differ from one another by approximately an order of magnitude in their ability to supply new suspension or saltation+creep-size mass to the airstream in response to a saltation impact (Mirzamostafa et al. 1998) and are simulated individually. When the saltation+creep discharge exceeds transport capacity over cells in a local area of the surface, trapping of saltation+creep occurs. It is also assumed that the coarse fraction of the suspension component begins deposition when moving over cells in the simulation region that have standing residue or no active saltation and sufficient roughness.

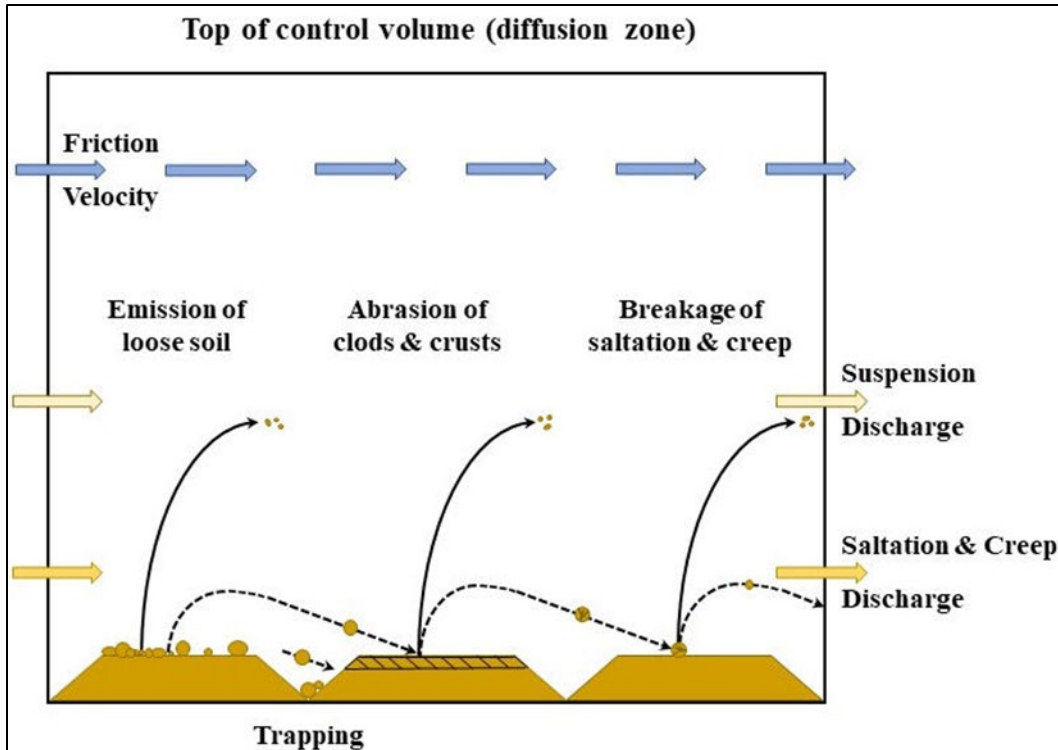


Figure 6. Simulated erosion processes on a bare soil in an individual grid cell.

Field surfaces vary both temporally and spatially. By partitioning complex areas into a series of small, uniform areas by gridding, and periodically updating the surface conditions, one may encompass both the spatial and temporal variations in fields. However, to simplify user inputs, the initial condition of the simulation region is assumed to have uniform soil and management. To meet stringent run-time requirements, the quasi-steady state solutions to mass conservation equations outlined in this section are used to predict wind erosion.

Finally, ESM uses the same grid for both spatial variation in the field and for accounting for soil movement. This allows the model to identify the areas in the field that experience wind erosion as well as total soil loss for the field as a whole.

Flux Equation

The following equations are used to calculate the boundary discharge, for the three components of erosion: saltation+creep, suspension, and PM_{10} . The three are calculated separately since their formation and transport are largely independent processes. Note that there are two, distinct types of erosion flows being discussed: vertical fluxes that are for individual points, and boundary discharges, which integrate the point fluxes into line discharges. Further note that these solutions are applied to grid cells, not to the field as a whole. This implies that grid cells located on the edge of the field, i.e. adjacent to the non-erodible boundary, have no incoming loading when the wind is blowing in from that boundary. This is an important distinction for the saltation+creep component, which has a finite transport capacity but does not affect suspension or PM_{10} particles, where the model assumes an infinite transport capacity.

Saltation+Creep Component

Based on conservation of mass in a control volume (Figure 6), a one-dimensional, quasi-steady state equation for the physical processes involved in saltation+creep is:

$$\frac{dq_{sc}}{dX} = G_{en} + G_{an} - G_{SSbk} - G_{tp} \quad [2]$$

where

q_{sc} = horizontal saltation+creep discharge ($\text{kg m}^{-1} \text{s}^{-1}$),

X = downwind distance from non-erodible boundary (m),

G_{en} = vertical flux from emission of loose aggregates ($\text{kg m}^{-2} \text{s}^{-1}$),

G_{an} = vertical flux from abrasion of surface clods and crust ($\text{kg m}^{-2} \text{s}^{-1}$),

G_{SSbk} = vertical flux of suspension aggregates from breakage of saltation+creep aggregates ($\text{kg m}^{-2} \text{s}^{-1}$), and

G_{tp} = vertical flux from trapping of saltation+creep aggregates ($\text{kg m}^{-2} \text{s}^{-1}$).

Each of the vertical fluxes represents either source or sink terms in the control volume and can be estimated by the equations that follow. The net emission source term for loose aggregates is:

$$G_{en} = (1 - SF_{SS})C_{en}(q_{en} - q_{sc}) \quad [3]$$

where

SF_{SS} = mass fraction of suspension-size (< 0.10 mm) among loose aggregates < 2 mm diameter),

C_{en} = coefficient of emission (m^{-1}), and

q_{en} = transport capacity of the wind ($\text{kg m}^{-1} \text{s}^{-1}$).

Stout (1990) derived the general form of Eq. 3 and applied it to describe total mass flux at a given height from the surface. However, subsequent research (Hagen 1991b) showed that the abrasion flux from immobile clods and crust was controlled by other factors. Hence, as described here, Eq. 3 applies only to the loose, mobile components of the soil. A typical value for C_{en} on a loose, bare field is about 0.06 (m^{-1}), and values for other conditions have been reported (Hagen et al. 1995). Many transport capacity equations for saltation+creep have been reported (Greeley and Iverson 1985). One of the most frequently used was developed by Lettau and Lettau (1978), which is expressed as:

$$q_{en} = C_s(U_*)^2(U_* - U_{*t}) \quad [4]$$

where

C_s = the saltation transport parameter ($\text{kg*s}^2 \text{m}^{-4}$), with a typical value of about 0.3 or a greater value for surfaces armored with stones,

U_* = friction velocity (m s^{-1}), and

U_{*t} = dynamic threshold friction velocity (m s^{-1}).

The suspension-size aggregates are assumed to be mixed intimately with the saltation+creep-size and emitted with them. Although the suspension-size aggregates absorb part of the aerodynamic and impact energy (represented by the emission coefficient) in order to rise from the surface, they do not contribute toward reaching the transport capacity of saltation+creep. Hence, they are subtracted from the total emission

of loose aggregates in Eq. 3. The net source term for entrainment of saltation+creep aggregates abraded from immobile aggregates and crust by impacting saltation+creep is:

$$G_{an} = (1 - SFSS_{an}) \left[\sum_{i=1}^2 (F_{an_i} C_{an_i}) q_{sc} \right] \left(\frac{q_{en} - q_{sc}}{q_{en}} \right) \quad [5]$$

where

$SFSS_{an}$ = mass fraction of suspension-size from abrasion,

F_{an_i} = mass fraction saltation impacting clods and crust,

C_{an_i} = coefficient of abrasion for pool (m^{-1}), and

i = pool index (1 - ag for aggregates, 2 - cr for crust).

An index of two was used in Eq. 5 since, in general, only two targets, exposed clods and crust, must be considered. Other targets, such as residue and rocks, have a C_{an_i} near zero. The first term, $(1 - SFSS_{an})$, is the fraction of abraded mass that is of saltation+creep-size. Values of $SFSS_{an}$ for some Kansas soils have been measured and ranged from 0.14 to 0.27, depending upon soil texture (Mirzamostafa 1996). The middle, bracketed term on the right-hand-side of Eq. 5 represents the total soil abraded from clods and crust, as confirmed by wind tunnel experiments (Hagen 1991b). Values for C_{an_i} have also been measured for a range of soils and related to their crushing energy (Hagen et al. 1992). The final term in Eq. 5 is the mass fraction entrained in the air stream. Note that the entrainment rate of this newly created saltation+creep is assumed to be similar to that of loose, saltation+creep-size aggregates already present on the surface, and that the entrainment approaches zero at transport capacity.

A sink for the saltation+creep discharge occurs when these aggregates are broken into suspension-size (Mirzamostafa et al. 1998). This effect is simulated as:

$$GSS_{bk} = C_{bk}(q_{sc} - q_s) \quad [6]$$

where

C_{bk} = coefficient of breakage (m^{-1}), and

q_s = discharge of primary (non-breakable) sand particles ($kg\ m^{-1}\ s^{-1}$).

The discharge of primary sand particles, q_s , is approximated using:

$$q_s = SF_{san} q_{sc} \quad [7]$$

where

SF_{san} = surface soil fraction sand, resulting in a soil sand fraction term in the calculation of the breakage coefficient.

The saltation+creep aggregates are more stable than the surface clods and crust, so measured abrasion coefficients average about 9 times more than the breakage coefficients on the same soils (Mirzamostafa 1996). The wind tunnel experiments also demonstrated that the breakage coefficient remained constant during breakdown of the aggregates to primary particles. The means and variances of these coefficients are related to soil

texture. Given q_{sc} , values for q_s can be estimated directly from soil sand content as in Eq. 7.

Another sink term is the removal of saltation+creep from the air stream by trapping mechanisms (Hagen and Armbrust 1992). In WEPS, surface trapping and plant interception are simulated as:

$$G_{tp} = C_t \left(1 - \frac{q_{cp}}{q_{en}}\right) q_{sc} + C_i q_{sc}, \quad q_{en} \geq q_{cp} \quad [8]$$

where

C_t = coefficient of surface trapping (m^{-1}),

C_i = coefficient of plant interception (m^{-1}), and

q_{cp} = transport capacity of the surface ($kg\ m^{-1}\ s^{-1}$).

When erosive winds cross rough surfaces, such as tillage ridges, that are highly erodible, large amounts of soil are entrained, but a portion of the entrained saltation+creep is often trapped in succeeding downwind furrows. This phenomenon results in a local rearrangement of the surface and reduces net removal of the entrained soil. Our conventionally-defined transport capacity, q_{en} , is based on the threshold velocity where erosion begins. But, when trapping of saltation+creep occurs on rough surfaces, one may hypothesize that q_{en} has been exceeded, and that the true transport capacity of the surface is some value, q_{cp} , that is less than q_{en} . However, q_{en} still appears to be the appropriate limiting value to drive the emission process, because more soil is emitted than can be transported from the local area. In WEPS, the first term on the right-hand-side of Eq. 8 simulates trapping of saltation+creep by surface roughness. The true transport capacity of the surface, q_{cp} , is based on the threshold friction velocity needed to remove saltation+creep from the furrows. It is calculated using Eq. 4 for a given roughness at the level of clod and crust cover of the surface.

$$q_{cp} = C_s (U_*)^2 (U_* - U_{*tt}) \quad [9]$$

where

U_{*tt} = dynamic threshold friction velocity of bare surface ($m\ s^{-1}$).

The second term of Eq. 8 represents interception of saltation+creep by standing plant stalks or other near-surface plant parts. For a given soil surface friction velocity, more transport occurs without than with stalks. Also, the transport capacity is higher when the wind direction is parallel to crop rows than when the wind direction is perpendicular to rows. For saltation normal to the row direction, interception can reduce transport capacity from 5 to 10 percent (see Eq. 113). Comparisons to measured data have been reported previously (Hagen and Armbrust 1992).

Solution for Saltation+Creep Discharge

When the source and sink terms are collected on the variable q , Eq. 2 for saltation+creep can be written in the form:

$$\frac{dq_{sc}}{dX} = A + Bq_{sc} - C(q_{sc})^2 \quad [10]$$

where

$$A = (1 - SFSS_{en})C_{en}q_{en} \quad [11]$$

$$B = (1 - SFSS_{an}) \left[\sum_{i=1}^2 (F_{ani}C_{ani}) \right] - (1 - SFSS_{en})C_{en} - C_{bk} - C_t \left(1 - \frac{q_{cp}}{q_{en}} \right) - C_i \quad [12]$$

$$C = (1 - SFSS_{an}) \left[\sum_{i=1}^2 (F_{ani}C_{ani}) \right] \left(\frac{1}{q_{en}} \right) \quad [13]$$

Integrating Eq. 10 along the wind direction, from X_1 to X_2 and q_{sc1} to q_{sc2} , gives the solution:

$$q_{sc2} = \frac{S}{2C} \left(-\tanh(t_1) + \frac{B}{S} \right) \quad [14]$$

where

$$t_1 = \begin{cases} \frac{S}{2}(-\Delta X) + 0.5 \ln \left(\frac{1+p}{1-p} \right), & -1 < p < 1 \\ -20, & p \leq -1 \\ 20, & p \geq 1 \end{cases} \quad [15]$$

$$S = \sqrt{4AC + B^2} \quad [16]$$

$$p = \frac{-2Cq_{sc1} + B}{S} \quad [17]$$

$$\Delta X = (X_2 - X_1) \quad [18]$$

The distance that the wind travels across a grid cell, ΔX is calculated from the uniform grid cell spacing and wind direction. It is adjusted to an effective distance to account for the effects of moving diagonally across a rectangular cell as:

$$\Delta X = ld \times \left(1 - 0.292893 \frac{la \times lb}{ix \times jy} \right) \quad [19]$$

$$\left\{ \begin{array}{l} la = jy \\ lb = |\tan(awa) \times jy| \\ ld = \left| \frac{jy}{\cos(awa)} \right| \end{array} \right\}, \quad |\tan(awa)| \leq \frac{ix}{jy} \quad [20]$$

$$\left\{ \begin{array}{l} la = \sqrt{ld^2 - lb^2} \\ lb = ix \\ ld = \left| \frac{ix}{\sin(awa)} \right| \end{array} \right\}, \quad |\tan(awa)| > \frac{ix}{jy}$$

$$awa = WA_{dir} - amasim \quad [21]$$

where

ΔX = effective distance wind travels across grid cell (m),

ix = grid cell spacing in the x direction (m),

iy = grid cell spacing in the y direction (m),

awa = wind direction relative to the simulation region y-axis (degrees).

$amasim$ = angle of the simulation region y-axis relative to geographic north (degrees),
and

$WAdir$ = wind direction relative to geographic north (degrees).

Suspension Component

Based on conservation of mass in a control volume that extends to the top of the dust cloud, a one-dimensional, quasi-steady state equation for the physical processes generating the suspension component is:

$$\frac{dq_{ss}}{dX} = (GSS_{en} + GSS_{an} + GSS_{bk})(1 - CSS_i), \quad U_* > U_{*t} \quad [22]$$

or

$$\frac{dq_{ss}}{dX} = -GSS_{dp}, \quad U_* < U_{*t} \quad [23]$$

where

q_{ss} = horizontal suspension component discharge ($\text{kg m}^{-1} \text{s}^{-1}$),

GSS_{en} = vertical emission flux of loose, suspension-size aggregates ($\text{kg m}^{-2} \text{s}^{-1}$),

GSS_{an} = vertical flux of suspension-size aggregates created by abrasion of clods and crust ($\text{kg m}^{-2} \text{s}^{-1}$),

GSS_{bk} = vertical flux of suspension-size aggregates created by breakage of saltation+creep-size aggregates ($\text{kg m}^{-2} \text{s}^{-1}$),

CSS_i = fraction of suspension-size aggregate flux intercepted by standing biomass, and

GSS_{dp} = vertical flux (deposition) of suspension-size aggregates above a non-eroding surface ($\text{kg m}^{-2} \text{s}^{-1}$).

The source and sink terms for the suspension component are simulated by the equations that follow. For direct emission of loose, suspension-size material by 'splash' impacts and aerodynamic forces:

$$GSS_{en} = SFSS_{en} C_{en} (q_{en} - q_{sc}) + C_m q_{sc} \quad [24]$$

where

C_m = a coefficient of mixing, value about $(0.0001 SFSS_{en}) (\text{m}^{-1})$.

Below transport capacity, the driving force causing the emission flux of suspension-size soil is assumed to be similar to that in Eq. 3 causing the saltation+creep emission flux.

This assumption is supported by wind tunnel measurements that show a mixture of suspension-size aggregates and a mixture of saltation-size have about the same threshold velocities (Chepil 1951). However, two additional assumptions are inherent in Eq. 24.

The first is that the loose components of saltation+creep and suspension-size aggregates

occur as a uniform mixture in the field. As a consequence, during simple net emission, the suspension fraction emitted with the saltation+creep remains the same as it was in the soil. Hence, the suspension fraction can be estimated as:

$$SF_{SS_{en}} = \frac{SF_{SS}}{SF_{er}} \quad [25]$$

where

SF_{SS} = soil mass fraction of loose, suspension-size, less than about 0.1 mm, and

SF_{er} = soil mass fraction of loose, erodible-size, less than about 2.0 mm.

The second assumption in Eq. 24 is that an additional small amount of suspension-size aggregates that are disturbed by the saltation impacts also are entrained, because transport capacity for the suspension component generally is not limiting. The result of this process is gradual depletion of the loose, suspension-size aggregates at the surface. However, when net emission of suspension-size exceeds net emission of saltation+creep-size aggregates, the latter soon dominate the surface area and absorb the impacts, so the process tends to be self-limiting.

For suspension flux created by abrasion of clods and crust:

$$G_{SS_{an}} = SF_{SS_{an}} \left[\sum_{i=1}^2 (F_{an_i} C_{an_i}) \right] q_{sc} \quad [26]$$

Additional discussion and measurements of this source term were reported by Mirzamostafa et al. (1998). For the source of suspension flux created by breakage of saltation+creep aggregates, the term is the same as the sink term in the saltation+creep equation and simulated as:

$$G_{SS_{bk}} = C_{bk}(q_{sc} - q_s) \quad [27]$$

Breakage from impact on immovable targets is assumed to come only from the impacting saltation+creep alone. Breakage coefficients for saltation-size aggregates have been measured in the wind tunnel (Mirzamostafa et al. 1998). But the breakage component from impacts on other saltation+creep is assumed to come from both the impacting and target aggregates. Breakage from impact on a mobile target is less likely than breakage from impact on immobile targets. However, these assumptions need further experimental verification.

Finally, the sink term for trapping of suspension flux occurs when the suspension discharge passes over grid cells without active saltation to maintain the suspension flux from the surface. Typically, this implies the presence of a vegetated, wet, or rough armored surface. The largest suspension particles, 0.05 to 0.10 mm, comprise roughly half the mass of the suspension discharge (Chepil 1951, Zobeck and Fryrear 1986). Through diffusion and settling, they move rapidly toward non-eroding surfaces in the simulation region, which serve as sinks. The process is simulated as:

$$G_{SS_{dp}} = -C_{dp}q_{ss}, \quad q_{ss} > 0.5q_{ss0} \quad [28]$$

where

q_{ss0} = maximum value of q_{ss} entering deposition region ($\text{kg m}^{-1} \text{s}^{-1}$), and
 C_{dp} = coefficient of deposition of suspension-size (m^{-1}).

The maximum value of C_{dp} is about 0.005, but less for smooth surfaces or large upwind areas that produce high dust clouds thus, moving a large portion of the soil away from the deposition surface.

Solution for Suspension Discharge

When the source terms are collected, Eq. 22 can be written in the form:

$$\frac{dq_{ss}}{dX} = F + G q_{sc} \quad [29]$$

$$F = (SFSS_{en}C_{en})(1 - CSS_i)q_{en}GSS_{dp} = -C_{dp}q_{ss}, \quad q_{ss} > 0.5q_{ss0} \quad [30]$$

$$G = \left(-SFSS_{en}C_{en} + SFSS_{an} \left[\sum_{i=1}^2 (F_{an_i}C_{an_i}) \right] + C_{bk} + C_m \right) (1 - CSS_i) \quad [31]$$

Substituting the general solution of Eq. 2, $q(X)$, into Eq. 29 and integrating along the wind direction from X_1 to X_2 and q_{ss1} to q_{ss2} gives the following equation for suspension discharge:

$$q_{ss2} = q_{ss1} + \frac{1}{2C} ((-G \cdot S + G \cdot B + 2F \cdot C)(\Delta X) + 2G (-\ln(2) + \ln(\exp(S(\Delta X))(1 - P) + P + 1))) \quad [32]$$

In regions of deposition of suspension component, integration of Eq. 29 from location X_1 , with discharge q_{ss1} , gives the following for suspension discharge, q_{ss2} , at downwind location X_2 :

$$q_{ss2} = q_{ss1} \exp(-C_{dp}(\Delta X)) \quad [33]$$

A value of $C_{dp} = 0.005$ in Eq. 33 matches the deposition measured at about 100 meters downwind of the eroding field at Big Spring; it under-predicts deposition closer to the boundary. However, the stable downwind area had considerable standing vegetation that made it a more effective sink than a smoother downwind surface (Hagen et al. 2007). For a typical size distribution of suspended dust, only about 50 percent will likely be deposited near an eroding source field, thus the limitation in Eq. 28. In the future, C_{dp} should be a function of downwind aerodynamic roughness and perhaps a more complicated deposition equation.

PM₁₀ Component

Simulation equations for particles with aerodynamic diameters less than 10 μm (PM₁₀ component) of the suspended soil also were developed by Hagen et al. (1996). Three different sources of PM₁₀ were identified to contribute different fractions of PM₁₀ from the suspension generated from each source. This results in the parameterized equation:

$$\frac{dq_{10}}{dX} = SF10_{en}G_{SS_{en}} + SF10_{an}G_{SS_{an}} + SF10_{bk}G_{SS_{bk}} \quad [34]$$

where

$SF10_{en}$ = soil fraction of PM_{10} in suspension-size surface soil,

$SF10_{an}$ = soil fraction of PM_{10} in suspension-size aggregates created during abrasion of clods and crust, and

$SF10_{bk}$ = soil fraction of PM_{10} in suspension-size aggregates broken from saltation and creep-size aggregates.

Solution for PM_{10} Discharge

When the source terms are collected, Eq. 34 can be written in the form:

$$\frac{dq_{10}}{dX} = H + K q_{sc} \quad [35]$$

where

$$H = SF10_{en}F \quad [36]$$

and

$$K = SF10_{en}(C_m - SF_{SS_{en}}C_{en}) + SF10_{an}SF_{SS_{an}} \left[\sum_{i=1}^2 (F_{an_i}C_{an_i}) \right] + SF10_{bk}C_{bk} \quad [37]$$

Substituting the general solution of Equation 2, $q(x)$, into Eq. 34 and integrating along the wind direction from X_1 to X_2 and q_{10_1} to q_{10_2} gives the following equation for PM_{10} discharge.

$$q_{10_2} = q_{10_1} + \frac{1}{2C} ((-K \cdot S + K \cdot B + 2H \cdot C)(\Delta X) + 2K (-\ln(2) + \ln(\exp(S(\Delta X))(1 - P) + P + 1))) \quad [38]$$

Cell Parameters

The analytic solutions presented in the prior sections for erosion fluxes in each cell require a number of parameters. These parameters were derived from a wide range of experimental data. Parameters are summarized in the following sections for: a) aerodynamic roughness, b) friction velocity, c) wind barriers, d) threshold friction velocity, e) emission parameters, f) abrasion parameters, g) breakage parameters, and h) trapping and interception parameters.

Aerodynamic Roughness

In WEPS, friction velocity drives erosion, but the meteorological input parameter is wind speed. For any given wind speed under neutral atmospheric conditions in the surface boundary layer, friction velocity is proportional to the natural logarithm of the surface aerodynamic roughness (Panofsky and Dutton 1984). To determine friction velocity, the aerodynamic roughness term of the log-law wind speed profile must be determined. For surfaces without standing biomass, the surface aerodynamic roughness is controlled by roughness of both the soil and flat biomass cover. In ESM, tillage ridges are characterized by their height, spacing, orientation, top bed width, and the spacing of furrow dikes. The

dike height is not used in this calculation but is always by definition less than the ridge height. For ridge heights greater than 5 mm, the normalized aerodynamic roughness for ridges was found by Hagen and Armbrust (1992) as seen in Figure 7, to be:

$$\frac{Z0_{rg}}{SZ_{rg}} = \begin{cases} \frac{1}{-64.1 + 135.5hl + \frac{20.84}{\sqrt{hl}}}, & SZ_{rg} > 5 \\ 0 & SZ_{rg} \leq 5 \end{cases} \quad [39]$$

where

$Z0_{rg}$ = aerodynamic roughness of the ridges (mm), and

hl = ridge height divided by ridge spacing.

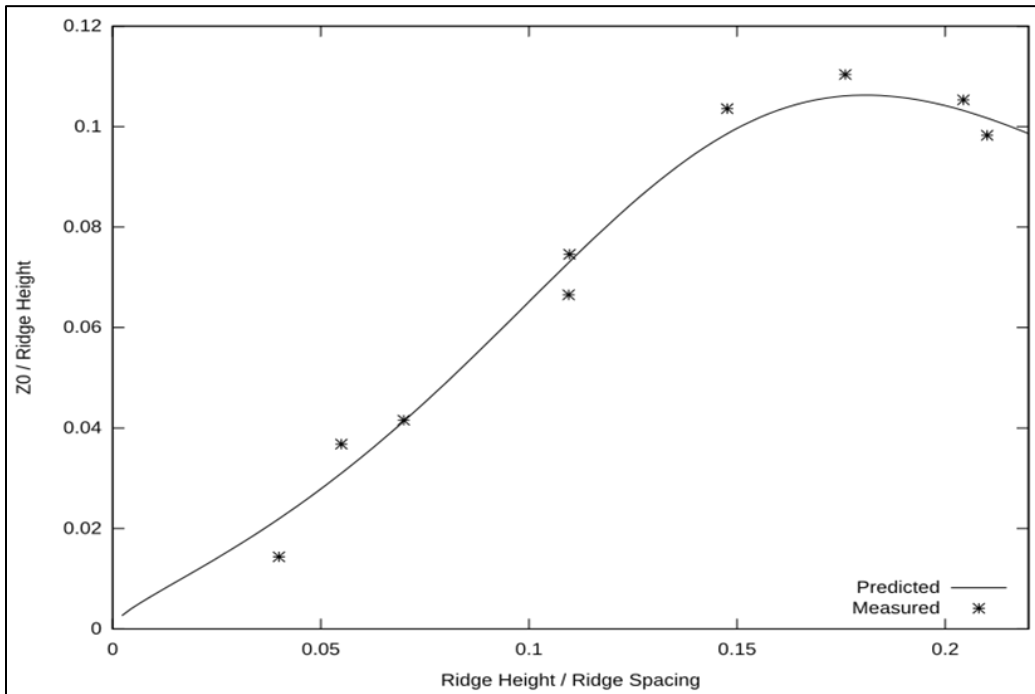


Figure 7. Ratio of aerodynamic roughness to ridge height as a function of the ridge height to spacing ratio where predicted is Eq. 39 and measured is from Hagen and Armbrust (1992).

The ratio of ridge height to ridge spacing is limited to a maximum of 0.2, an estimate of the limitations of soil and the formation of ridges by tillage.

$$hl = \min\left(0.2, \frac{SZ_{rg}}{SXP_{rg}}\right) \quad [40]$$

where

SZ_{rg} = ridge height (mm), and

SXP_{rg} = ridge spacing parallel to the wind direction (mm).

When the wind direction is not perpendicular to the ridges, the effective ridge spacing is increased. When furrow dikes are present, and the wind is more parallel to the furrows, the effective ridge spacing is limited to the dike spacing. Additionally, with the effect of turbulence, the aerodynamic roughness of ridges never completely disappears when the wind is completely parallel to the ridges. This is approximated by limiting the sine of the angle to ≥ 0.1 . The effective ridge spacing parallel to the wind direction is found by:

$$SX_{P_{rg}} = \begin{cases} \min\left(SX_{dk}, \frac{SX_{rg}}{\max(0.1, |\sin(|WA_{dir} - SA_{rg}|)|)}\right), & SX_{dk} > \frac{SX_{rg}}{3} \\ \frac{SX_{rg}}{\max(0.1, |\sin(|WA_{dir} - SA_{rg}|)|)}, & SX_{dk} \leq \frac{SX_{rg}}{3} \end{cases} \quad [41]$$

where

SX_{rg} = ridge spacing (mm),

SX_{dk} = furrow dike spacing (mm),

WA_{dir} = wind direction (degrees), and

SA_{rg} = ridge orientation, clockwise from north and parallel to the ridge (degrees).

The resulting relationship for aerodynamic roughness as a function of all these limits is shown in Figure 8.

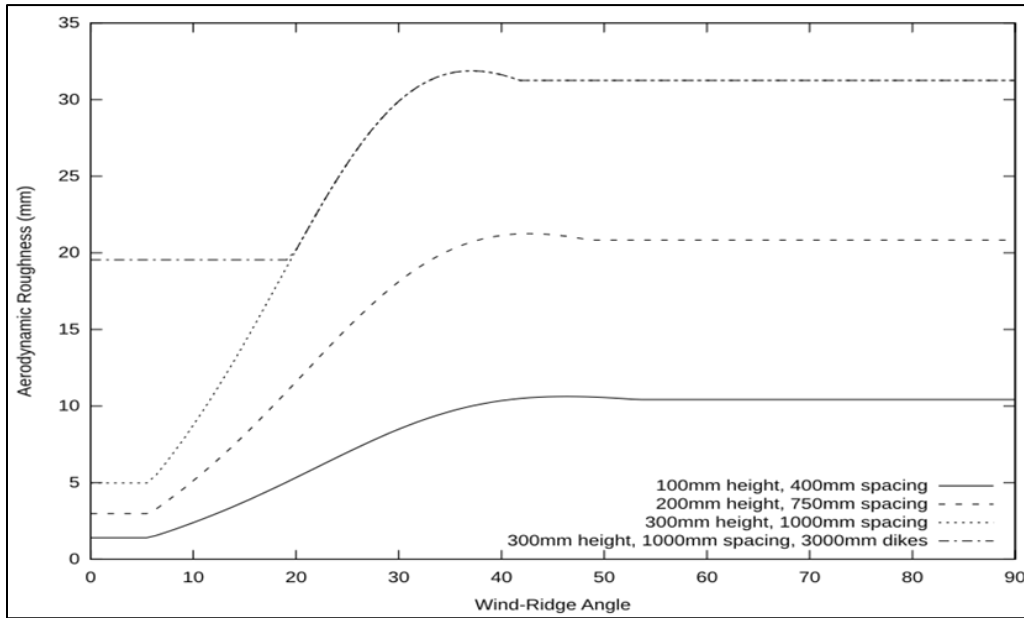


Figure 8. Aerodynamic roughness as a function of the angle between the wind direction and ridge direction for several sample ridge heights, ridge spacings and dike spacings.

Random roughness without standing biomass is limited to the range 1.67 to 100 mm, i.e. 0.5 to 30 mm equivalent aerodynamic roughness. Aerodynamic roughness is found from random roughness using:

$$Z_{0rr} = \min(30, \max(0.5, 0.3 SZ_{rr})) \quad [42]$$

where

Z_{0rr} = aerodynamic roughness of random roughness including any flat biomass cover (mm), and

SZ_{rr} = random roughness (mm).

The aerodynamic roughness for the soil surface, Z_0 , calculated as the maximum of the ridge and random aerodynamic roughness is expressed as:

$$Z_0 = \max(Z_{0rg}, Z_{0rr}) \quad [43]$$

If standing plant biomass is present, the aerodynamic roughness for length of the canopy is calculated from a biomass drag coefficient. Some crops are planted in a ridged field in the bottom of the furrow, resulting in a reduction of biomass drag. The biomass drag is also reduced when rows are spaced more than 5 times the biomass height. The standing biomass is considered composed of two parts, the current growing crop, and all other decomposing biomass. First, effective leaf and stem area indexes are calculated for all standing biomass as:

$$BR_{lai} = R_{crow} R_{rg} C_{lai} + BD_{lai} \quad [44]$$

and

$$BR_{sai} = R_{rg} C_{sai} + BD_{sai} \quad [45]$$

where

BR_{lai} = biomass effective leaf area index ($m^2 m^{-2}$),

BR_{sai} = biomass effective stem area index ($m^2 m^{-2}$),

BD_{lai} = decomposing biomass leaf area index ($m^2 m^{-2}$),

BD_{sai} = decomposing biomass stem area index ($m^2 m^{-2}$),

C_{lai} = growing crop leaf area index ($m^2 m^{-2}$),

C_{sai} = growing crop stem area index ($m^2 m^{-2}$),

R_{crow} = reduction of effective leaf area due to crop row spacing (generally no effect until spacing is > 5 crop heights), and

R_{rg} = reduction of effective leaf and stem area when crop partly sheltered in furrow.

Empirical estimates of the reduction factors are:

$$R_{crow} = \begin{cases} \min \left[1, \frac{1}{0.92 + \frac{0.021 C X_{row}}{CZ - 0.5 S Z_{rg}}} \right], & CZ > 0.5 S Z_{rg} \\ 0, & CZ \leq 0.5 S Z_{rg} \end{cases} \quad [46]$$

and

$$R_{rg} = \begin{cases} 1.0 - \frac{0.5SZ_{rg}}{CZ}, & CZ > 0.5SZ_{rg} \\ 0, & CZ \leq 0.5SZ_{rg} \end{cases} \quad [47]$$

where

CZ = growing crop height (m),
 CX_{row} = growing crop row spacing (m), and
 SZ_{rg} = ridge height (m).

Leaves tend to orient parallel to the wind streamlines (Armbrust and Bilbro 1997) and the effective biomass drag coefficient as a function of leaf and stem area indexes is adjusted to reflect this as:

$$BR_{cd} = 0.2BR_{lai}(1.0 - \exp(-BR_{lai})) + BR_{sai} \quad [48]$$

where

BR_{cd} = effective biomass drag coefficient.

The standing biomass aerodynamic roughness as a function of the effective biomass drag coefficient is taken from Hagen (1994) and calculated for an average stem diameter of 20 mm. While aerodynamic roughness may decrease slightly with decreased stem diameter, the effect of varying stem diameter is considered small enough to be neglected. For low values of the effective biomass drag coefficient, the roughness of the underlying surface will influence the canopy aerodynamic roughness as well, with the aerodynamic roughness with a canopy present never being less than the aerodynamic roughness of the underlying soil surface.

This assumption needs to be revisited. For dense biomass cover, the underlying surface is probably irrelevant. This may affect a multi-subregion simulation if a very rough soil surface is well vegetated as a subregion upwind of an erodible surface. The transition to the erodible surface could be significantly different.

For $BR_{cd} > 0.1$, the aerodynamic roughness of standing biomass is found using Hagen and Armbrust (1994) and assuming an average stem diameter of 20 mm:

$$Z0_v = \frac{BZ}{17.27 - \frac{1.254 \ln(BR_{cd})}{BR_{cd}} - \frac{3.714}{BR_{cd}}} \quad [49]$$

where

BZ = biomass height (mm).

This relationship and the data from which it was derived are shown in Figure 9. When $BR_{cd} \leq 0.1$, the relationship is affected by the vegetation height becoming:

$$Z_{0v} = \begin{cases} BZ \left(\frac{Z_0}{BZ} + \frac{0.11 - \frac{Z_0}{BZ}}{4.60517} \ln \left(\frac{BR_{cd}}{0.001} \right) \right) & BZ > 5 \text{ and } BR_{cd} > 0.001 \\ 0 & BZ \leq 5 \text{ or } BR_{cd} \leq 0.001 \end{cases} \quad [50]$$

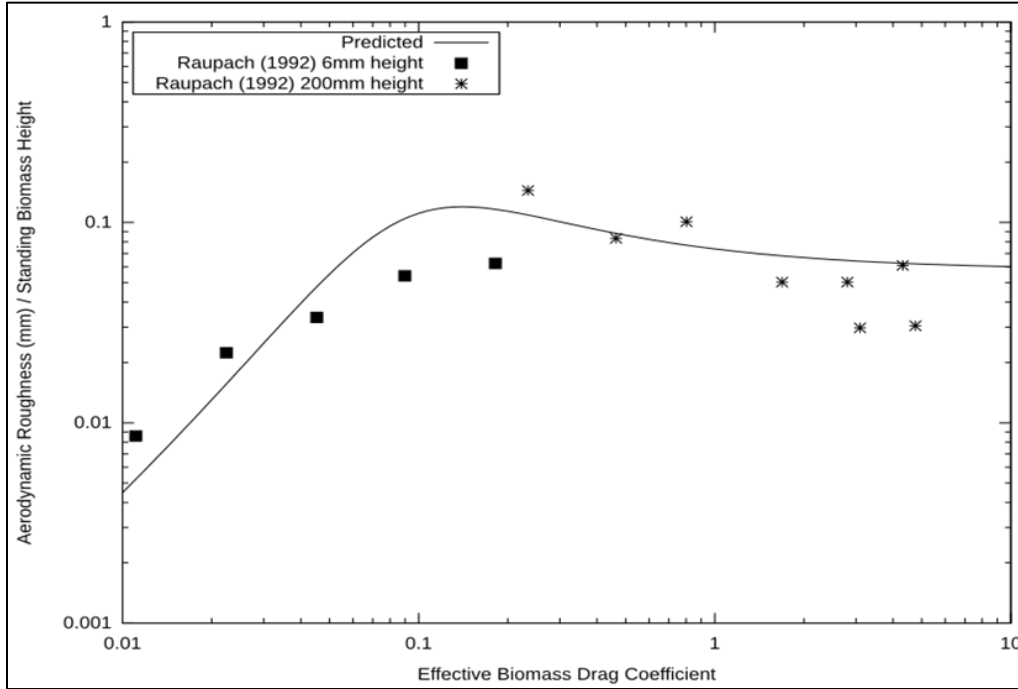


Figure 9. The aerodynamic roughness / vegetation height ratio from Eq. 49 and the data from Raupach (1992), drag elements with both 6 mm and 200 mm heights mounted on a smooth substrate.

Finally, the aerodynamic roughness cannot be less than the roughness of the underlying surface becoming:

$$Z_{0v} = \max(Z_{0v}, Z_0) \quad [51]$$

The interactive effect of stem height and the underlying aerodynamic roughness on the aerodynamic roughness is illustrated in Figure 10.

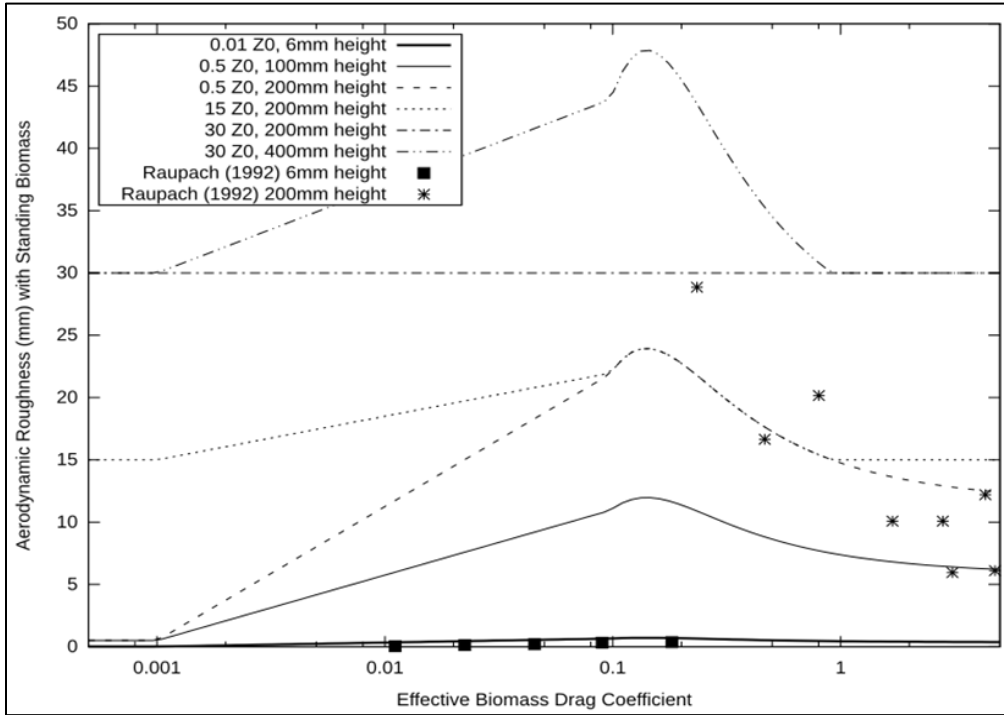


Figure 10. Aerodynamic roughness with standing biomass as a function of effective biomass drag coefficient with various levels of Z_0 , the aerodynamic roughness of the underlying surface. Predicted is Eq. 49, 50, and 51 and data is from Raupach (1992) are rods used to simulate standing stems.

Friction Velocity

Friction velocity at the simulation region is calculated in two steps. First, the friction velocity at the weather station, where wind speeds are measured, is calculated for strong winds with neutral stability using the log-law profile (Panofsky and Dutton (1984):

$$U_{*st} = \frac{0.4U_{st}}{\ln\left(\frac{Z_{st}}{Z_{0st}}\right)} \quad [52]$$

where

U_{*st} = friction velocity at the weather station (m s^{-1}),

U_{st} = wind speed at weather station (m s^{-1}),

Z_{st} = anemometer height at the weather station (mm); (wind speeds were adjusted to 10 m height in WEPS data base), and

Z_{0st} = aerodynamic roughness at weather station, assumed to be 25 mm in WEPS.

Second, the friction velocity at the simulation region is calculated based on the ratio of aerodynamic roughness at the simulation region to that at the wind speed measurement station. This equation approximates a procedure suggested by Lettau (Panofsky and Dutton 1984).

$$U_{*v} = U_{*st} \left(\frac{Z0_v}{Z0} \right)^{0.067} \quad [53]$$

where

U_{*v} = friction velocity above the surface including any standing biomass (m s^{-1}), and
 $Z0_v$ = as defined by Eqs. 49, 50, and 51.

If there is sufficient standing biomass, the friction velocity at the soil surface is calculated (Figure 11) (Hagen and Armbrust 1992) as:

$$U_* = \min \left(1, U_{*v} \left(0.86 \exp \left(\frac{-BR_{cd}}{0.0298} \right) + 0.25 \exp \left(\frac{-BR_{cd}}{0.356} \right) \right) \right) \quad [54]$$

where

U_* = friction velocity at soil surface below standing biomass (m s^{-1}).

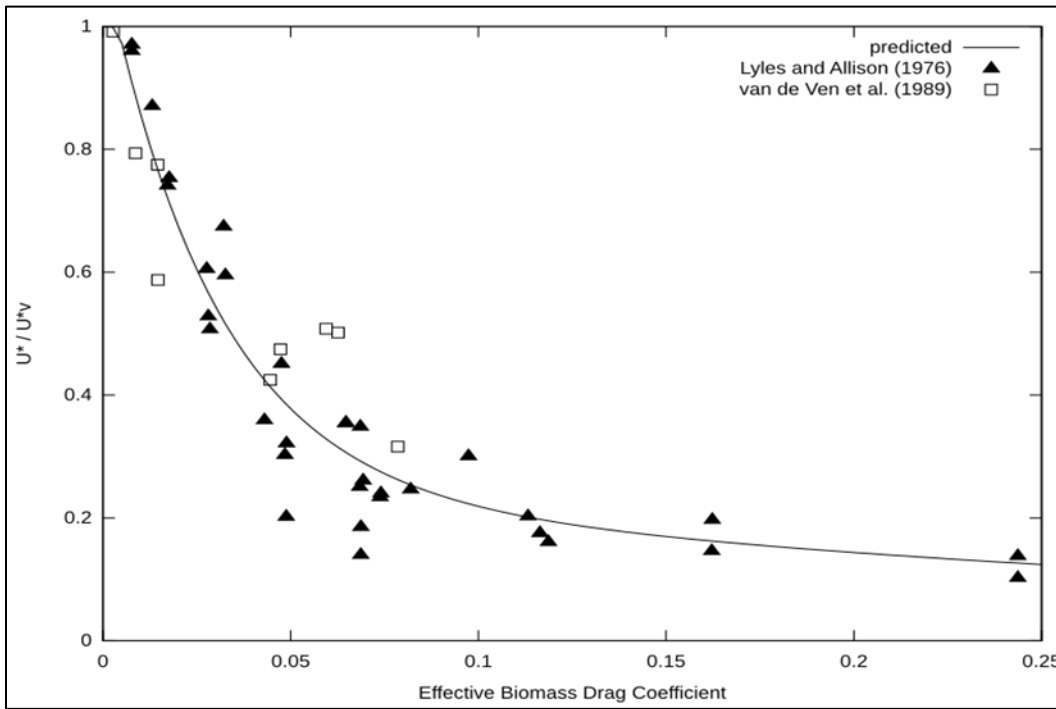


Figure 11. Reduction in friction velocity through biomass canopy as a function of biomass drag coefficient where predicted is Eq. 54 and data are Lyles and Allison (1975) and van de Ven et al. (1989).

At this point in the calculations, the influence of barriers or hills on friction velocity are still neglected.

Wind Barrier Parameters

Wind barriers (e.g. trees, hedgerows, trap strips, snow fences, etc.) create upwind and downwind sheltered areas. ESM treats barriers as overlays on the grid as opposed to creating non-erodible cells in the grid.

The barrier effects are simulated by calculating the fraction of open field friction velocity that occurs in the portion of the simulation region that is sheltered by barriers. When two barriers shelter the same area, the lowest fraction of open field friction velocity created by a single barrier is selected for the grid cell for each wind direction. An analysis of field windbreak systems using this procedure was reported by Vigiak et al. (2003).

The rectangular simulation region has a y-axis positioned within ± 45 degrees from north. Wind directions relative to the y-axis are calculated for 8 cardinal wind directions as:

$$awark = 45(k - 1) - amasim \quad [55]$$

where

k = index of cardinal wind directions in clockwise direction ($k = 1$ is north),
 $awark$ = cardinal wind direction k relative to the simulation region y-axis (degrees), and
 $amasim$ = angle of the simulation region y-axis relative to geographic north (degrees).

Only 8 cardinal directions were selected for computational efficiency, being a precalculation done only once per simulation. Wind direction from WINDGEN is provided for the 16 cardinal directions and measured wind data can be at much higher resolution. It should be possible to use the provided wind direction for the calculation on a daily basis with little increase in computational effort. For each grid cell in the simulation region, calculations are used to determine the influence of each barrier in succession. The accuracy of the calculations could be increased by decreasing the grid cell size relative to the barrier height, but this can significantly increase computational effort.

A series of calculations were needed to determine the distance along the wind direction from the barrier to a grid cell, and their geometry is illustrated in Figure 12. First, the coordinates (x_i, y_j) of the center of each cell are calculated. Next, distances (a and c) from the grid cell to the barrier ends and the barrier length (b) are determined. If a grid cell is on the barrier, i.e., $a + c = b$, then the fraction reduction in friction velocity is calculated directly.

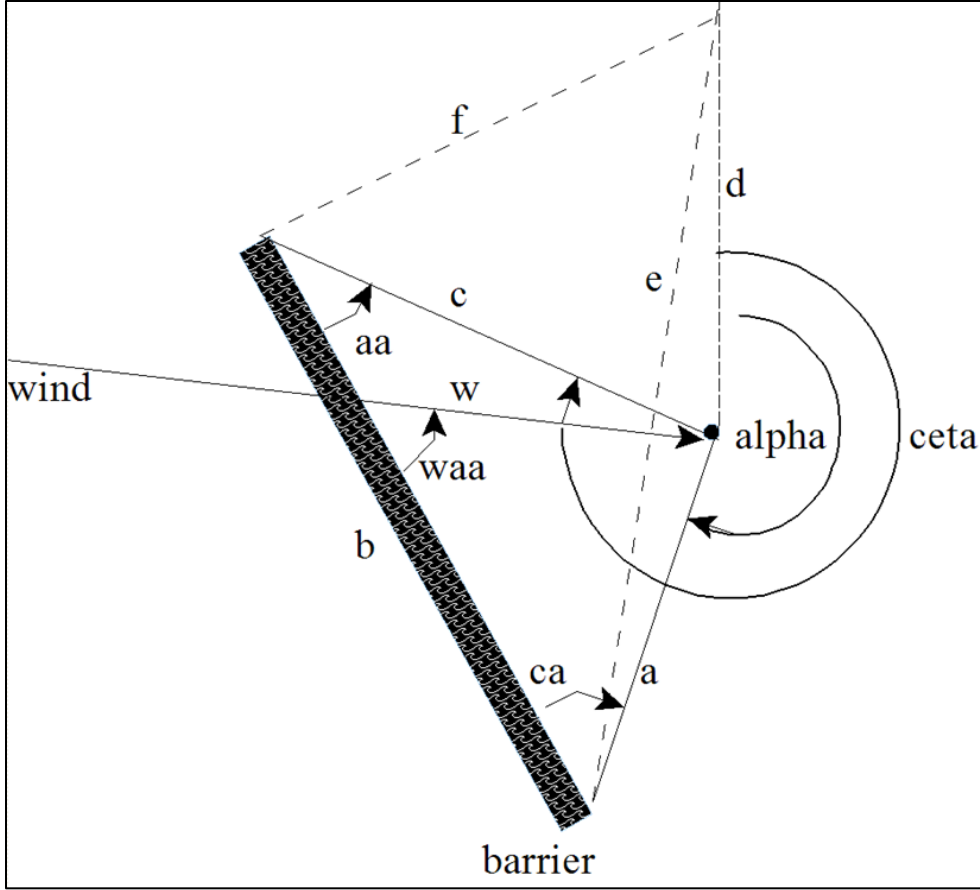


Figure 12. Geometry of barrier effect calculations.

For cells not on the barrier, angles at the barrier ends (aa and ca) are calculated. For example,

$$aa = \cos^{-1} \frac{(b^2 + c^2 - a^2)}{2bc} \quad [56]$$

$$ca = \cos^{-1} \frac{(a^2 + b^2 - c^2)}{2ab} \quad [57]$$

If the angles aa or ca are greater than 90 degrees, then the minimum distance between the cell center and the barrier (d_{min}) is the minimum of the lengths a or c . Otherwise d_{min} is calculated as in Figure 12:

$$d_{min} = \frac{b * \sin(aa) * \sin(ca)}{\sin(aa + ca)} \quad [58]$$

If d_{min} is less than 35 times the barrier height, additional calculations are used to determine the range of wind angles for which the barrier is upwind from the cell. To accomplish this task, two angles ($alpha$ and $ceta$, degrees from the line passing through the cell coordinates toward the positive y axis direction and lines a and c) were

calculated. Next, for each relative wind direction that is between the angles α and β , i.e., the barrier is upwind of the grid cell, the distance between the barrier and the grid cell along the wind direction vector (w) is calculated by the sine rule as:

$$w = \frac{a * \sin(\beta)}{\sin(\alpha)} \quad [59]$$

where

α = the angle between the barrier and the wind direction.

The leeward distance w is converted to units of barrier heights, wz , and used in empirical equations developed using the data of Hagen et al. (1981), Eimern et al. (1964), Raine and Stevenson (1977), and Hiesler and DeWalle (1988) to estimate the fraction of open field friction velocity (f_{u*}) in the sheltered area (Figure 13). Note that an effective optical porosity of 1.0 can be used to give some barrier effect for minor or intermittent barriers. It should not be used when no barrier is present. The maximum porosity used in the development of the equations is 0.8, which should be considered the limit for equation validity. Also, in many areas, very porous barriers, such as barbed wire fencing, have the effect of capturing wind-blown material (typically tumbleweeds), which greatly decreases their porosity.

$$f_{u*} = 1 - \exp(-m * wz^2) + n * \exp(-0.003(wz + s)^t) \quad [60]$$

where

f_{u*} = fraction of open field friction velocity, and
 m, n, s, t = equation coefficients.

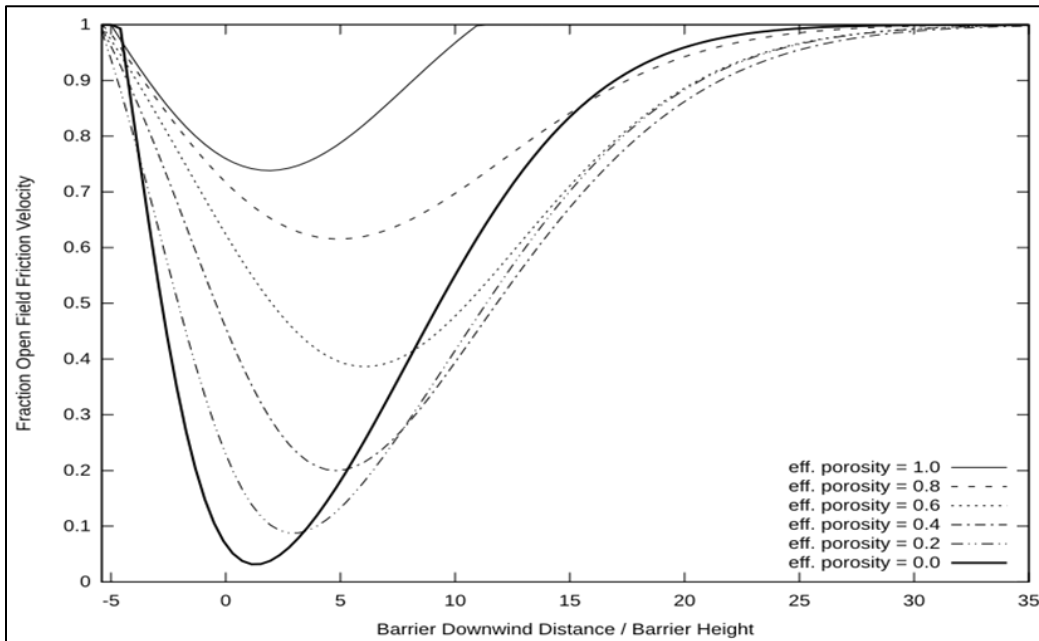


Figure 13. Fraction of open field friction velocity as a function of distance downwind of barrier (negative distance is upwind of barrier) shown for different values of effective porosity.

The equation coefficients m, n, s, t are given by:

$$m = 0.008 - 0.17pb + 0.17pb^{1.05} \quad [61]$$

$$n = 1.35 \exp(-0.5pb^{0.2}) \quad [62]$$

$$s = 10(1 - 0.5pb) \quad [63]$$

$$t = 3 - pb \quad [64]$$

where

pb = effective barrier porosity.

Effective barrier porosity is found by adjusting optical barrier porosity as a function of barrier width (Figure 14) using:

$$pb = pbr + (1 - \exp(-0.5xbr))^{0.3}(1 - pbr) \quad [65]$$

where

pbr = optical barrier porosity, and

xbr = normalized barrier width (barrier width divided by barrier height).

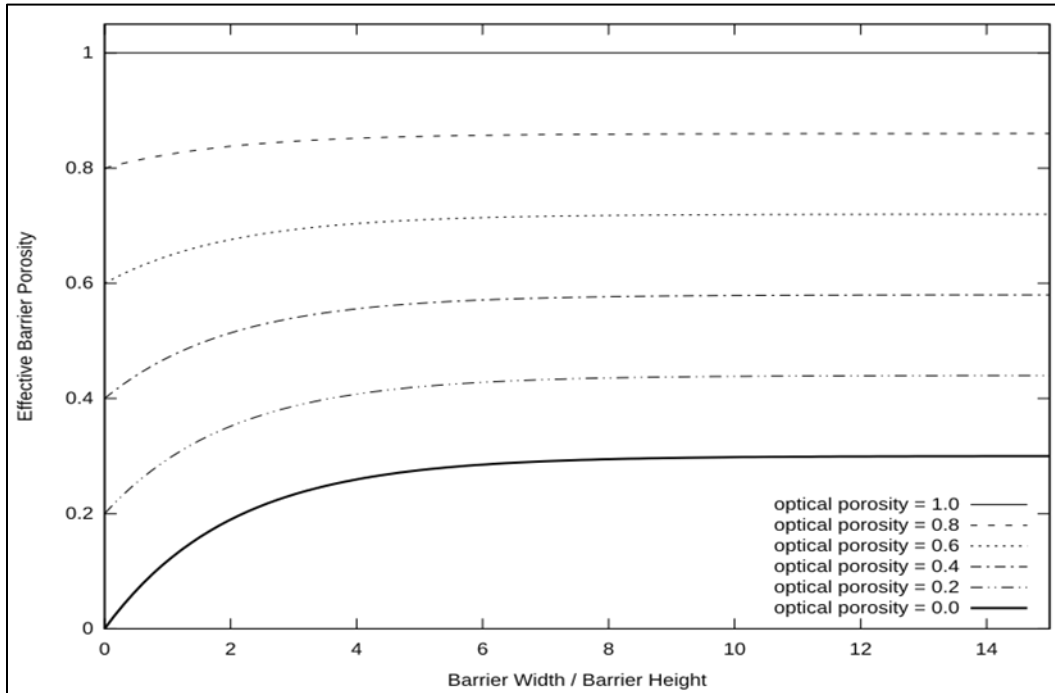


Figure 14. Effective barrier porosity as a function of normalized barrier width.

For all other grid cells, which are not in the lee shelter region, but within 5 barrier heights from the barrier, a barrier influence was calculated using the minimum distance, wz , as a negative number in Eq. 60. When two or more barriers shelter the same area, the lowest fraction calculated for an individual barrier shelter is selected by the submodel.

Knowing the influence of the barriers on each individual grid cell for the eight cardinal wind directions, when given a wind direction k , the friction velocity for each grid cell is found using:

$$U_*^{i,j} = U_* f u_*^{i,j,k} \quad [66]$$

where

$U_*^{i,j}$ = the adjusted friction velocity for cell i,j with wind from direction k , and

$f u_*^{i,j,k}$ = the reduction in wind velocity due to barriers for cell i,j from wind direction k .

Hills

Hills are not simulated in the current release of WEPS. However, it is anticipated that a speed up or slow down factor will be assigned to each cell based upon the wind direction as influenced by topography. Whether the necessary topographical data for each cell is provided externally, in an individual file, or natively as part of the field description has not been decided. Since the WINDGEN generator simulates a single wind direction for each day, only one set of factors would be used for each day with erosion at this time.

Threshold Friction Velocity

The velocity at which soil aggregates begin to saltate is defined as the static threshold friction velocity. Static threshold friction velocity is calculated in each grid cell as influenced by aggregate size and density, clod/crust cover, surface roughness, flat biomass cover, and surface soil wetness at noon.

As noted earlier, the fractional values of aggregated and crusted surface sum to one. However, to calculate the true fraction of bare, immobile surface, one must correct for both small aggregates and rock fraction, if present. Hence, the fraction of bare surface with immobile cover is:

$$SF_{cv} = [(1 - SF_{cr})(1 - SF_{84}) + SF_{cr} - SF_{cr}SF_{los}](1 - SV_{roc}) + SV_{roc} \quad [67]$$

where

SF_{cv} = soil fraction covered by clod, crust, and rock so it does not emit,

SF_{cr} = soil fraction covered by crust, but excluding the fraction of rock-covered area,

SF_{los} = soil fraction covered with loose, erodible soil on the crusted area,

SV_{roc} = soil volume rock >2.0 mm ($m^3 m^{-3}$), and

SF_{84} = soil fraction covered with aggregates <0.84 mm in diameter on the non-crusted area but excluding the fraction of rock-covered area.

The value of SF_{84} is calculated from the modified lognormal aggregate size distribution (Wagner and Ding 1994) input to ESM from other submodels as:

$$SF_{84} = \begin{cases} 0.5 \left(1 + \operatorname{erf} \left(\frac{\ln(SLT)}{\sqrt{2} \ln(SO_{ags})} \right) \right), & SL_{agx} > 0.84 \\ & \text{and } SL_{agn} < 0.84 \\ 1, & SL_{agx} \leq 0.84 \\ 0, & SL_{agn} \geq 0.84 \end{cases} \quad [68]$$

$$SLT = \frac{(0.84 - SL_{agn})(SL_{agx} - SL_{agn})}{(SL_{agx} - 0.84)SL_{agm}} \quad [69]$$

where

SL_{agn} = lower limit of size distribution (mm),

SL_{agx} = upper limit of size distribution (mm),

SL_{agm} = geometric mean of size distribution (mm), and

SO_{ags} = geometric standard deviation of size distribution.

To determine threshold friction velocities for bare soil surfaces, estimating equations were fitted to wind tunnel data (Hagen 1991c, Chepil and Woodruff 1963) to give (Figure 15):

$$UB_{*ts} = 1.7 - 1.35 \exp(-b1 - b2(SF_{cv})^2) \quad [70]$$

$$b1 = -0.179 + 0.225(\ln(1 + Z0))^{0.891} \quad [71]$$

$$b2 = 0.3 + 0.06Z0^{1.2} \quad [72]$$

where

UB_{*ts} = static threshold friction velocity of bare surface (m s^{-1}),

$Z0$ = aerodynamic surface roughness (mm), and

$b1, b2$ = coefficients used in Eq. 70.

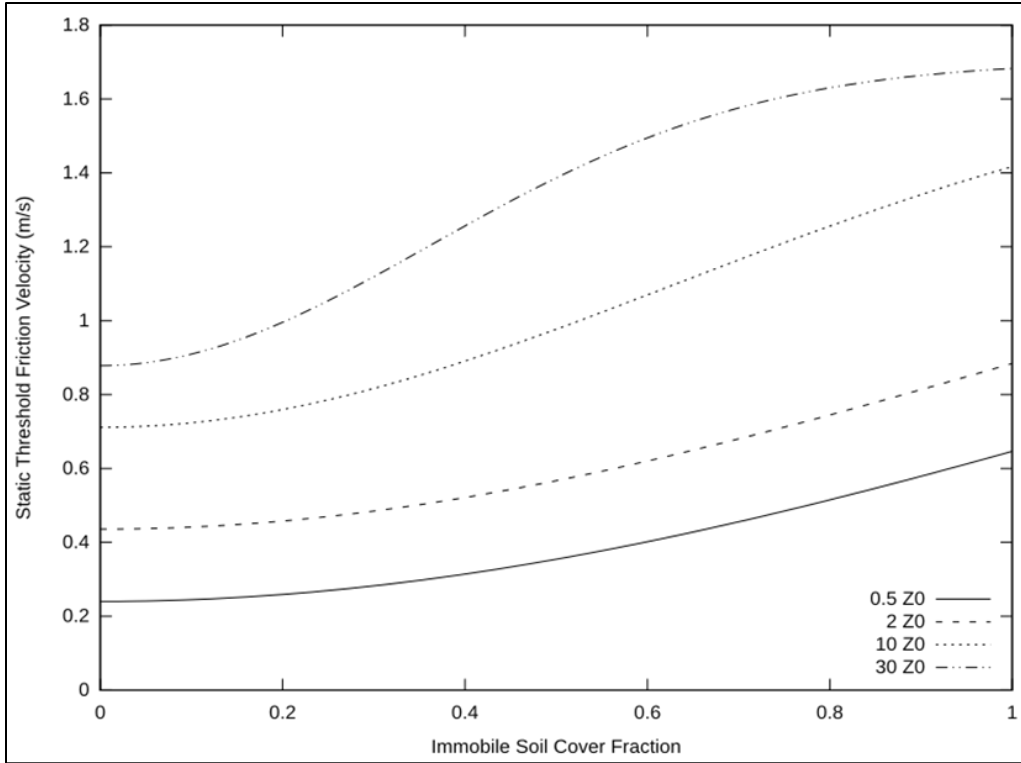


Figure 15. Static threshold friction velocities for various levels of aerodynamic roughness and surface cover as predicted by Eq. 70.

Increased roughness increases form drag at the surface driving the increase in static threshold velocity. The dynamic threshold velocity is increased toward static threshold linearly in proportion to shelter area (SFA_{12}) (Eq. 82).

If random flat biomass cover is present, the increase in static threshold friction velocity is (Figure 16) (Hagen 1996):

$$UC_{*ts} = (1 - \exp(-1.2BFF_{cv}))\exp(-0.3SF_{cv}) \quad [73]$$

where

UC_{*ts} = change in static threshold friction velocity caused by flat biomass cover ($m s^{-1}$),

and

BFF_{cv} = biomass fraction of flat cover.

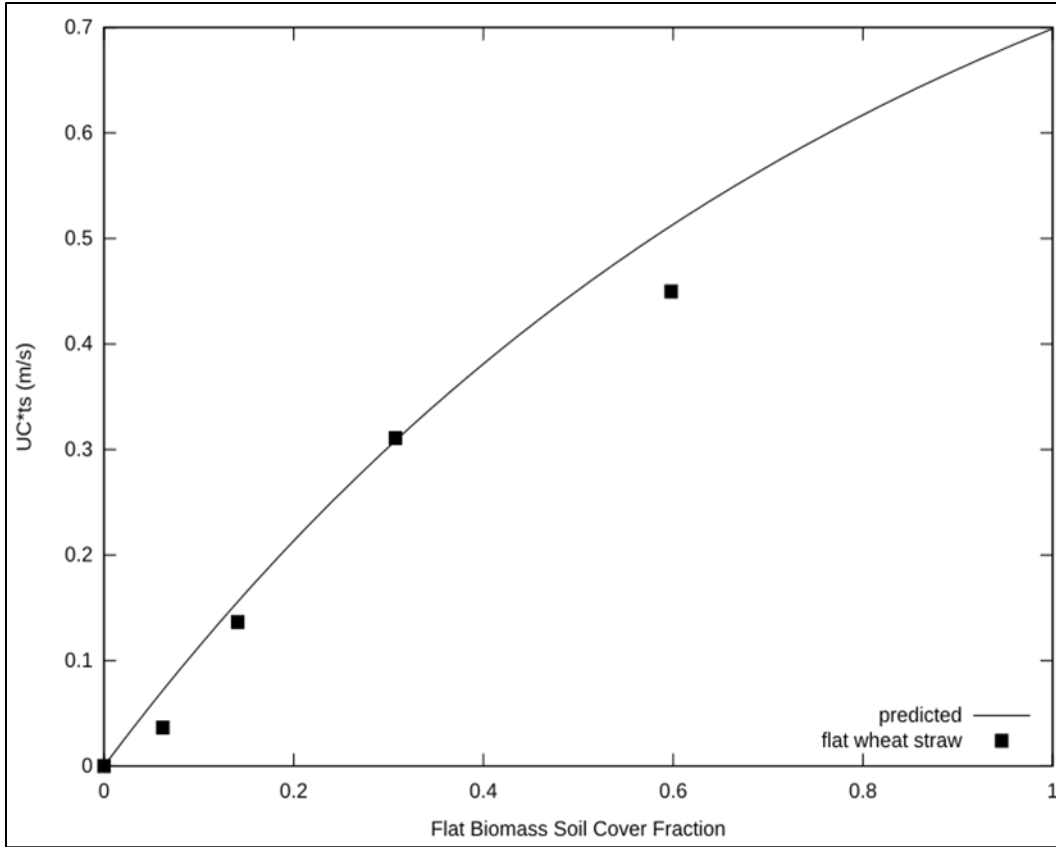


Figure 16. Increase in static threshold friction velocity of erodible sand (0.29-0.42 mm) where flat wheat straw cover data is from (Hagen 1996); Predicted is Eq. 73.

If the surface is wet, threshold velocity increases with the ratio of surface water content to the 15 MPa water content (Figure 17) (Saleh and Fryrear 1995) and is represented by:

$$UW_{*ts} = 0.58 \left(\exp \left(\frac{HRO_{wc}}{HR15_{wc}} \right) - 1 - 0.7 \left(\frac{HRO_{wc}}{HR15_{wc}} \right)^2 \right) \quad [74]$$

where

UW_{*ts} = increase in static threshold friction velocity from surface wetness ($m s^{-1}$),

HRO_{wc} = surface soil water content ($kg kg^{-1}$), and

$HR15_{wc}$ = surface soil water content at 1.5 Mpa ($kg kg^{-1}$).

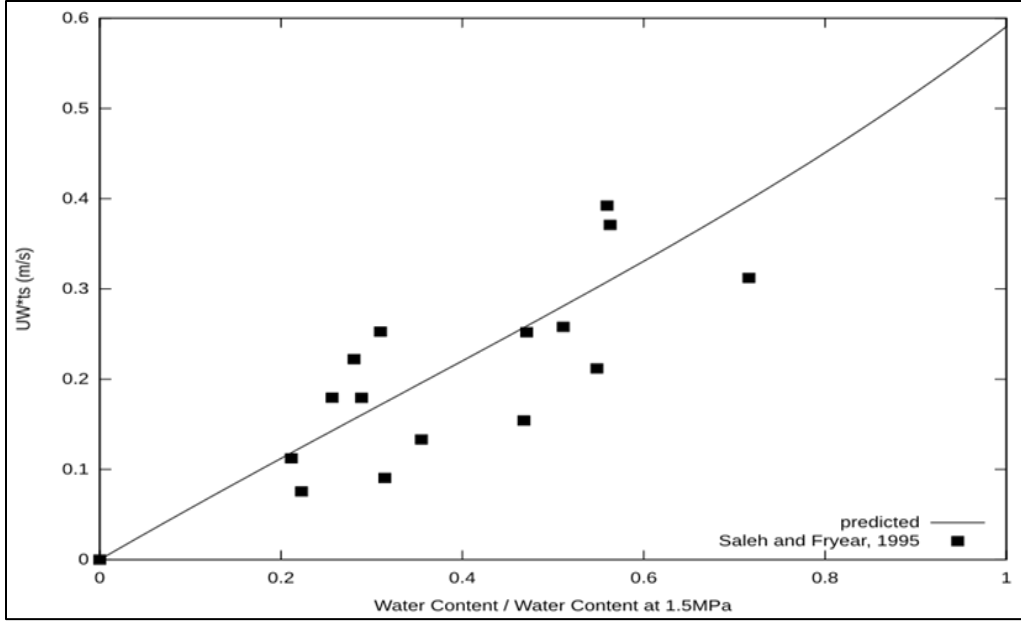


Figure 17. Static threshold velocity change with water content relative to 1.5 Mpa water content, where predicted slope is from Eq. 74 (Saleh and Fryrear 1995).

The equations for static threshold friction velocity were developed from wind tunnel studies where the erodible particles were quartz sand particles with a density of 2.65 Mg m^{-3} . An adjustment for erodible soil, where the erodible particles are more likely to be aggregates, is made. In WEPS, the aggregate density is set to 1.8 Mg m^{-3} while in SWEEP, the value can be specified. The adjustment equation is:

$$UD_{*ts} = 0.3 \left(\sqrt{\frac{SD_{agd}}{2.65}} - 1 \right) \quad [75]$$

where

UD_{*ts} = change in static threshold friction velocity from variable aggregate density (m s^{-1}), and

SD_{agd} = aggregate density (Mg m^{-3}).

Finally, static threshold friction velocity adjusted for the non-erodible soil fraction, flat biomass, surface wetness, and aggregate density is:

$$U_{*ts} = UB_{*ts} + UC_{*ts} + UW_{*ts} + UD_{*ts} \quad [76]$$

where

U_{*ts} = adjusted surface static threshold friction velocity (m s^{-1}).

The static threshold friction velocity used in calculations of trapping and saltation+creep transport capacity equations (Bagnold 1943) is estimated by setting the surface cover

fraction in Eq. 70 to a value of 0.4 and adding all the adjustments for flat biomass cover, surface wetness and aggregate density:

$$U_{*tp} = 1.7 - 1.35 \exp(-b1 - b2(0.4)^2) + UC_{*ts} + UW_{*ts} + UD_{*ts} \quad [77]$$

where

U_{*tp} = static threshold friction velocity for trapping and transport capacity (m s^{-1}).

Eq. 70 is also used to calculate a threshold friction velocity assuming dry conditions, no flat biomass cover, and the minimum aerodynamic roughness of 0.5 mm, which is used in the calculation of the maximum mobile soil fraction available for transport.

$$U_{*to} = 1.7 - 1.35 \exp(-b1^{ic} - b2^{ic} (SF_{cv}^{ic})^2) \quad [78]$$

$$SF_{cv}^{ic} = (1 - SF_{84}^{ic})(1 - SV_{roc}) + SV_{roc} \quad [79]$$

$$b1^{ic} = -0.179 + 0.225(\ln(1 + 0.5))^{0.891} \quad [80]$$

$$b2^{ic} = 0.3 + 0.06(0.5)^{1.2} \quad [81]$$

where

U_{*to} = threshold friction velocity of a bare smooth surface with the erodible fraction of the surface before erosion occurs (m s^{-1}),

SF_{cv}^{ic} = bare surface cover fraction before erosion occurs ($SF_{84}^{ic} = SF_{84}$ before erosion begins),

$b1^{ic}$ = coefficient for smooth surface (aerodynamic roughness equals 0.5 mm), and

$b2^{ic}$ = coefficient for smooth surface (aerodynamic roughness equals 0.5 mm).

When the friction velocity exceeds the static threshold friction velocity and particles are in motion, the dynamic threshold friction velocity, or the friction velocity below which particle movement ceases, is found by applying an adjustment dependent upon the fraction of the surface, which is sheltered by random roughness elements.

$$U_{*t} = U_{*ts} - 0.05(1 - SFA_{12}) \quad [82]$$

where

SFA_{12} = total fraction of area sheltered with shelter angles > 12 degrees.

Likewise, the dynamic threshold for trapping and transport capacity is found using the same adjustment:

$$U_{*tt} = U_{*tp} - 0.05(1 - SFA_{12}) \quad [83]$$

Emission Parameters

As outlined in the theory section, the erosion process is modeled as the quasi-steady state conservation of mass using linked partial differential equations for three size classes of eroding soil. These are saltation+creep size (0.1 to 2.0 mm), suspension size (<0.1 mm), and PM₁₀ size (<0.01 mm).

When the wind transport capacity exceeds the saltation+creep discharge, the net entrainment rate of loose surface soil into the airstream is directly proportional to the coefficient of emission, C_{en} (m⁻¹). A fraction of the emitted soil, SF_{SSen} , becomes part of the suspension discharge, and a fraction of the suspended soil from the emission, SF_{10en} , is PM₁₀. Estimations for the preceding three parameters are presented in this section.

For the complex surfaces simulated in ESM, auxiliary equations were developed to estimate C_{en} . The emission coefficient is calculated as a function of surface complexity as:

$$C_{en} = C_{eno}R_{enb}R_{env} \quad [84]$$

where

C_{eno} = coefficient of emission for a bare, smooth, loose, erodible soil. A typical field value is about 0.06 (m⁻¹),

R_{env} = emission ratio accounting for flat, random vegetation, and

R_{enb} = emission ratio accounting for immobile cover and surface roughness.

The fractional emission factor to account for flat biomass cover is (Hagen 1996) (Figure 18):

$$R_{env} = 0.075 + 0.934\exp\left(-\frac{BF_{cv}}{0.149}\right) \quad [85]$$

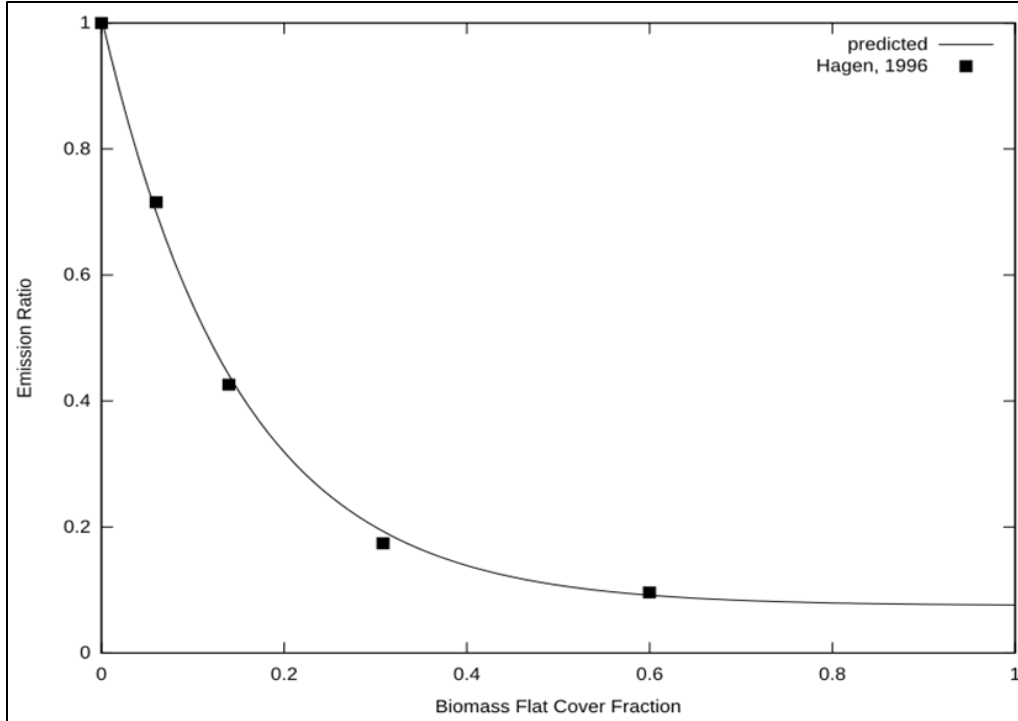


Figure 18. Fractional emission factor of loose soil as function of increasing biomass flat cover where predicted is from Eq. 85 (Hagen 1996).

On rough surfaces, increasing the fraction of surface sheltered from direct saltation impacts by macro-roughness also reduces emission rates. A shelter angle at a point is defined as the largest angle above horizontal to the top of any upwind point. To predict the fraction of surface sheltered from saltation impacts, the random and ridge roughness can be used to estimate the sheltered area. The shelter angle distribution is described by a two parameter Weibull distribution; the two parameters are a scale factor and a shape factor (Potter, Zobeck, and Hagen 1990). The average shape factor measured over a range of roughness was about 0.77 (Potter and Zobeck 1990). The scale factor was related to the random roughness as:

$$SAC_{rr} = 2.3\sqrt{SZ_{rr}} \quad [86]$$

where

SAC_{rr} = Weibull scale factor for random roughness, (degrees), and

SZ_{rr} = random roughness (mm) (Allmaras et al. 1966).

The fraction horizontal area with shelter angles greater than 12 degrees caused by random roughness, SFA_{12rr} , is:

$$SFA_{12rr} = \exp\left(-\left(\frac{12}{SAC_{rr}}\right)^{0.77}\right) \quad [87]$$

Similarly, the fraction of horizontal area sheltered by ridges, SFA_{12rg} , can be calculated as (Potter and Zobeck 1990):

$$SAC_{rg} = \begin{cases} 65.4 \left(\frac{SZ_{rg}}{SXP_{rg}} \right)^{0.65} & , \quad SZ_{rg} > 1 \text{ and } SXP_{rg} > 10 \\ 0 & \text{otherwise} \end{cases} \quad [88]$$

$$SFA_{12rg} = \begin{cases} \exp \left(- \left(\frac{12}{SAC_{rg}} \right)^{0.77} \right) & , \quad SZ_{rg} > 1 \text{ and } SXP_{rg} > 10 \\ 0 & \text{otherwise} \end{cases} \quad [89]$$

where

SAC_{rg} = Weibull scale factor for ridge shelter (degrees),

SZ_{rg} = ridge height (mm),

SXP_{rg} = ridge spacing parallel the wind direction (mm), and

SFA_{12rg} = surface fraction of area with shelter angles >12 degrees for ridges.

The area sheltered by ridges overlaps with the area sheltered by random roughness, so the resulting total fraction of area sheltered with shelter angles >12 degrees, SFA_{12} , (see Figure 19) is estimated as:

$$SFA_{12} = (1 - SFA_{12rg})SFA_{12rr} + SFA_{12rg} \quad [90]$$

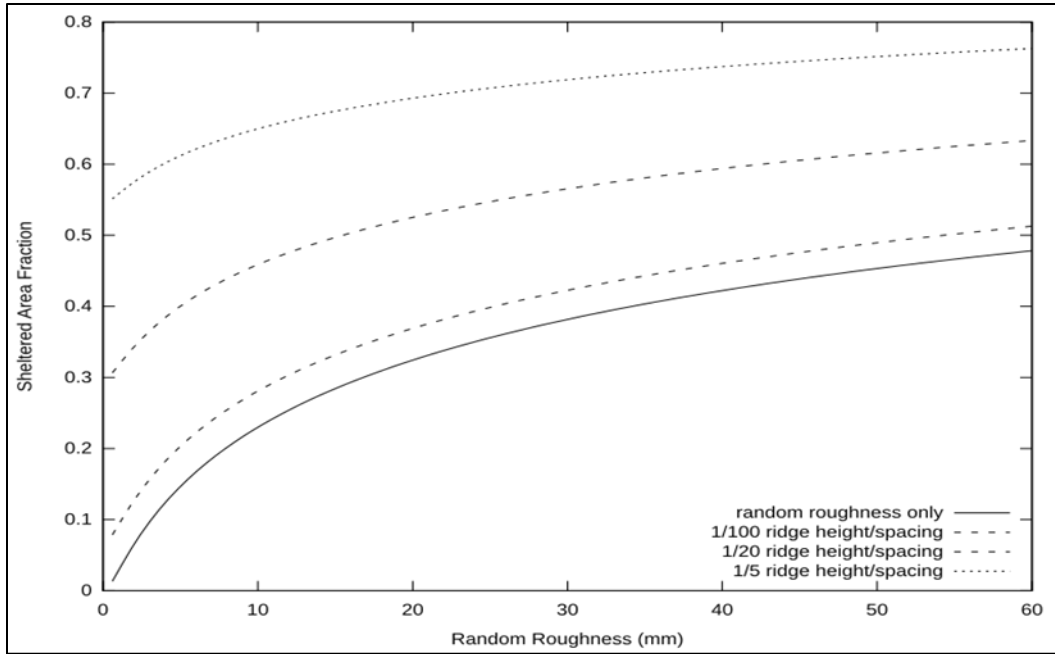


Figure 19. Fraction of horizontal area with shelter angles >12 degrees as a function of random roughness and several ridge height spacing ratios as estimated by Eq. 90.

On horizontal surfaces, immobile individual aggregates, rocks or pieces of crust tend to protrude slightly above the mobile surface and protect about 3 times their own horizontal area from emissions. However, these small protrusions are usually part of the surface micro-roughness and not easily measured by conventional (pin) roughness meters. For comparison, sparse, flat, random biomass protects about 4 times its horizontal cover area from emissions as illustrated in Figure 18. Similar to flat biomass, the areas protected by micro-roughness will begin to overlap as the cover of immobile aggregates, rock, and crust increases. Thus, the area not sheltered by either the micro-roughness or by the macro-roughness, as measured by roughness meters, i.e. Eq. 67, is also used to estimate the emission ratio for bare soil. The emission from the surface is limited by the ability of the friction velocity to move soil particles. The mass of mobile soil particles, SM_{aglos} , is used to find the minimum mass of mobile soil particles at which emission will occur at the current friction velocity. The values are referenced to the bare smooth surface value at a friction velocity of 0.75 m s^{-1} , $SM_{aglosmx}$. The limited surface cover equation becomes:

$$SF_{cv}^{lim} = \begin{cases} [1 - SF_{cr}SF_{los}](1 - SV_{roc}) + SV_{roc}, & SF_{84} \leq SF_{84mn} \\ SF_{cv}, & SF_{84} > SF_{84mn} \end{cases} SFA_{12} \quad [91]$$

where the minimum mobile soil fraction for emission, SF_{84mn} , is found using the following:

$$SF_{84mn} = \max\left(0, \left(\frac{SM_{aglosmx} - SM_{aglos}}{SM_{aglosmx}SF_{84ic}(1.001 - SV_{roc})}\right)\right) \quad [92]$$

$$SM_{aglosmx} = \exp(2.708 - 7.603((1 - SF_{84ic})(1 - SV_{roc})) + SV_{roc}) \quad [93]$$

$$SM_{aglos} = \max\left(0, SM_{aglosmx} \left(\frac{U_*^{i,j} - U_{*ts}}{0.75 - \min(U_{*to}, U_{*ts})}\right)\right) \quad [94]$$

The bare soil emission ratio, R_{enb} , then is (Figure 20):

$$R_{enb} = \left[-0.051 + 1.051 \exp\left(\frac{SF_{cv}^{lim}}{0.33050512}\right)\right] (1 - SFA_{12}) \quad [95]$$

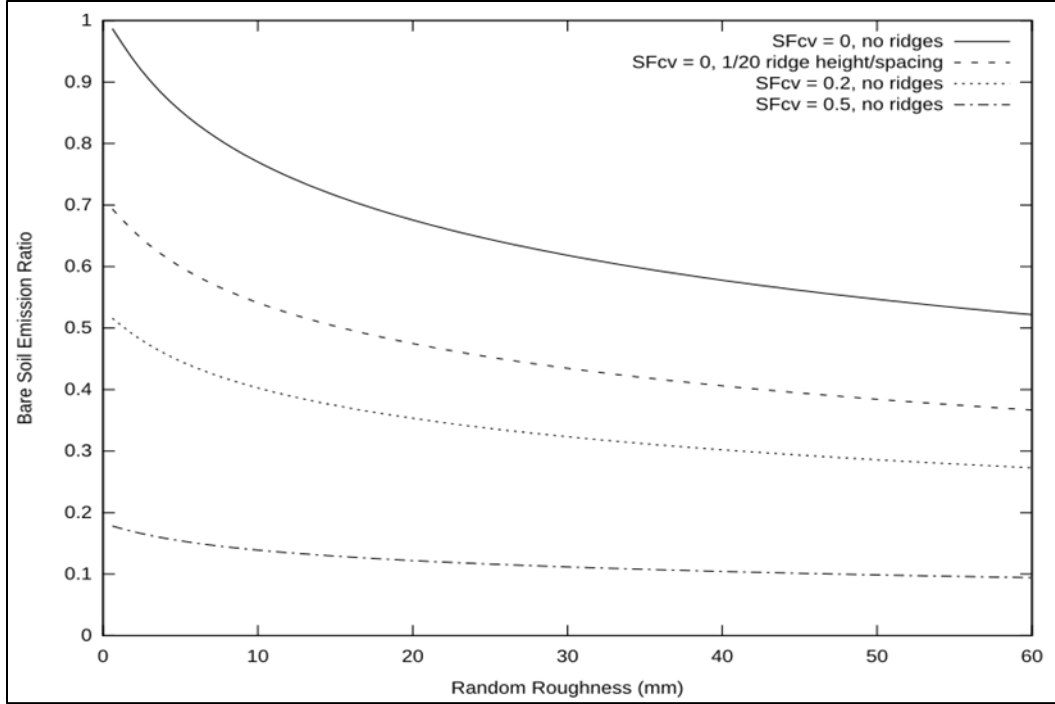


Figure 20. Bare soil emission ratios predicted by Eq. 95 for ranges of immobile soil cover, a sample ridge, and random roughness.

The soil fraction of suspension size in the emitted soil is estimated from the aggregate size distribution and the fraction of the surface that is crusted. As shown, the suspension portion is lower for the loose material on the crust.

$$SF_{ssen} = \left(\frac{SF_{10}}{SF_{200} + 0.001} \right) (1 - 0.8SF_{cr}) \quad [96]$$

where

SF_{10} = soil fraction less than 0.10 mm diameter, and

SF_{200} = soil fraction less than 2.0 mm diameter.

Fraction of PM_{10} in the emitted suspension-size aggregates is estimated as (Hagen, unpublished data):

$$SF_{10en} = 0.0067 + 0.0000487 \left[\min \left(300, \frac{SF_{sil}}{(SF_{cla} + 0.0001)^2} \right) \right] - 0.0000044WZ_{ypt} \quad [97]$$

where

SF_{sil} = surface soil fraction silt,

SF_{cla} = surface soil fraction clay, and

WZ_{ypt} = average annual precipitation (mm).

Abrasion Parameters

The abrasion of immobile soil clods and crust by saltation+creep impacts creates additional erodible aggregates. The rate of creation of additional erodible aggregates depends upon the saltation+creep discharge, q_{sc} ($\text{kg m}^{-1} \text{s}^{-1}$), the fractions of saltation+creep discharge impacting the clods and crust, F_{ani} , and the abrasion coefficients of the target clods and crust, C_{ani} (m^{-1}). A fraction, SF_{ssan} , of the erodible aggregates created by abrasion contribute to the suspension discharge, and a fraction, SF_{10an} , of the suspension-size aggregates created by abrasion are PM_{10} . Estimating equations for these parameters - F_{ani} , C_{ani} , SF_{ssan} , and SF_{10an} - are presented in this section.

The fraction of saltation+creep impact on both clods and crust that are not sheltered by either flat biomass or rock cover, F_{an} , is estimated as:

$$F_{an} = \exp(-4BFF_{cv})\exp(-3SV_{roc}) \quad [98]$$

where

BFF_{cv} = biomass fraction flat cover, and

SV_{roc} = soil volume of rock in surface layer ($\text{m}^3 \text{m}^{-3}$).

The preceding equation assumes that both rock and flat biomass cover protrude slightly above the surrounding surface soil. The fraction of saltation+creep impacting on immobile aggregates, F_{anag} , is estimated as:

$$F_{anag} = (1 - SF_{84})(1 - SF_{cr})F_{an}SF_{ssen} = \left(\frac{SF_{10}}{SF_{200} + 0.001} \right) (1 - 0.8SF_{cr}) \quad [99]$$

where

SF_{84} = soil mass fraction of aggregates <0.84 mm diameter on aggregated surface, and

SF_{cr} = soil fraction of crust cover.

The fraction of saltation+creep impacting on unprotected surface crust, F_{ancr} , is estimated as:

$$F_{ancr} = SF_{cr}(1 - SF_{los})F_{an} \quad [100]$$

where

SF_{los} = fraction of crust covered with loose, erodible soil.

The abrasion coefficients for aggregates and crust are a function of their dry stabilities, and these were related in wind tunnel abrasion experiments (Figure 21) (Hagen et al. 1992) and curve fit to be:

$$C_{anag} = \exp\left(-2.07 - 0.077(SE_{ags})^{2.5} - 0.119\ln(SE_{ags})\right) \quad [101]$$

where

C_{anag} = abrasion coefficient for aggregates (m^{-1}), and
 SE_{ags} = dry stability of immobile aggregates ($\ln(J\ kg^{-1})$), and

$$C_{ancr} = \exp\left(-2.07 - 0.077(SE_{crs})^{2.5} - 0.119\ln(SE_{crs})\right) \quad [102]$$

where

C_{ancr} = abrasion coefficient for crust (m^{-1}), and
 SE_{crs} = dry stability of crust ($\ln(J\ kg^{-1})$).

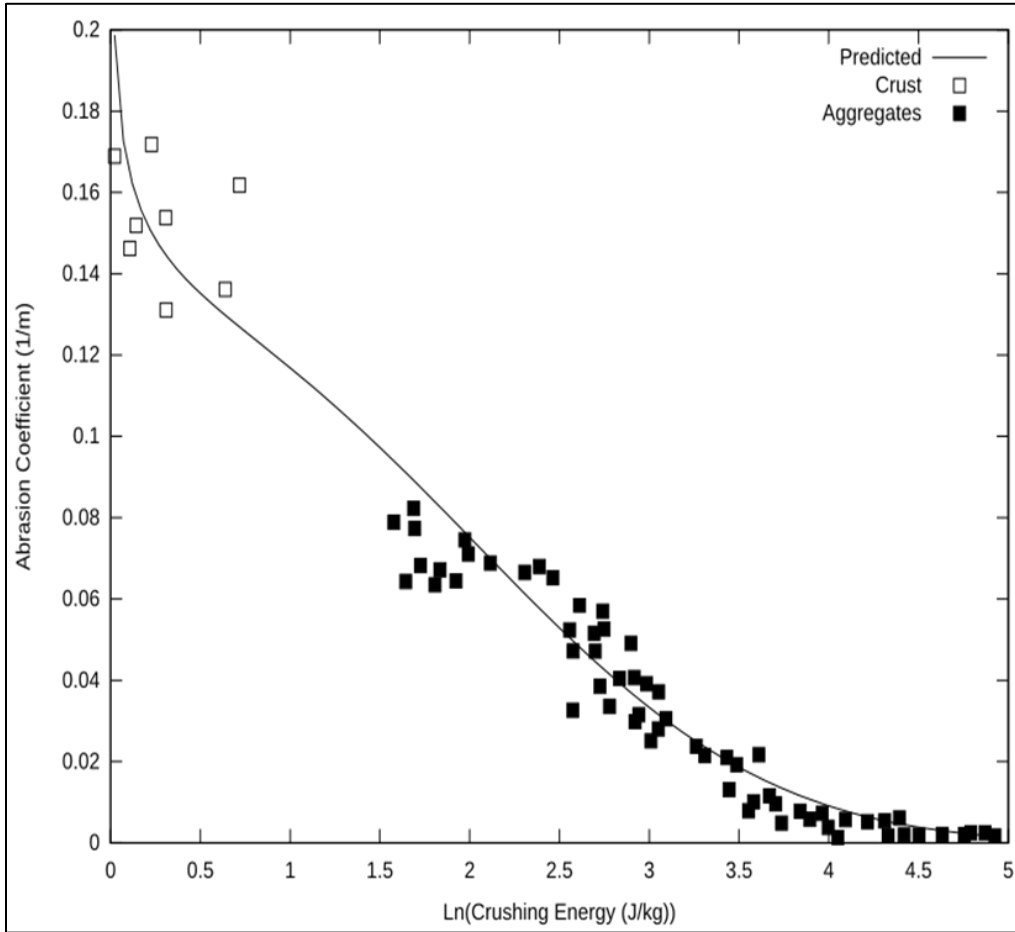


Figure 21. Abrasion coefficients as a function of crushing energy where predicted is Eq. 101 and 102 and data for soil crust and aggregates is from (Hagen et al. 1992).

An approximate estimate for crust abrasion coefficient used in ESM is to set it equal to the aggregated abrasion coefficient (Zobeck and Popham 1991):

$$C_{ancr} = C_{anag} \quad [103]$$

The soil fraction abraded from clods and crust that is of suspension size was determined experimentally (Mirzamostafa et al. 1998) and estimated as (Figure 22):

$$SF_{ssan} = \min \left(1 - (SF_{san} - SF_{vfs}), 0.4 - 4.83SF_{cla} + 27.18(SF_{cla})^2 - 53.7(SF_{cla})^3 + 42.25(SF_{cla})^4 - 10.7(SF_{cla})^5 \right) \quad [104]$$

where

SF_{cla} = surface soil fraction clay,

SF_{san} = surface soil fraction sand, and

SF_{vfs} = surface soil fraction very fine sand.

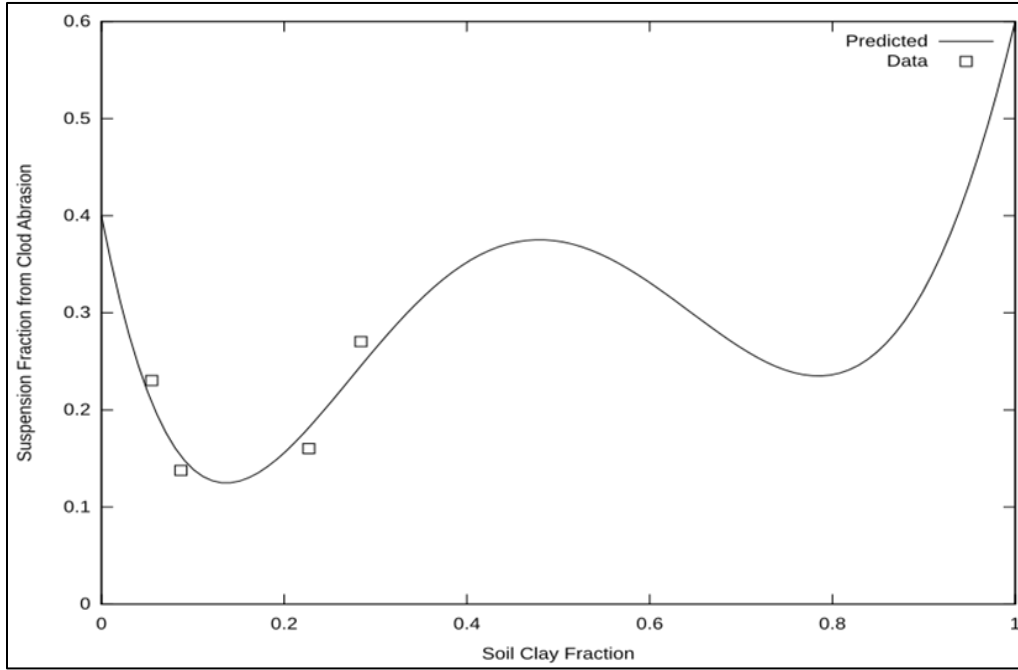


Figure 22. Estimated soil fraction suspension-size in abraded soil as a function of clay content where predicted is Eq. 104 and data is from (Mirzamostafa et al. 1998).

The fraction of PM_{10} in the abraded suspended soil is estimated as (Hagen, unpublished data):

$$SF_{10an} = 0.0116 + \frac{0.00025}{C_{anag} + 0.001} \quad [105]$$

Breakage Parameters

As saltation+creep-size aggregates are transported, they undergo multiple impacts and partial breakdown into suspension-size aggregates. Continuous movement of a single aggregate causes it to breakdown into primary particles, which may be a sand grain at its core. However, individual moving saltation+creep aggregates are frequently interchanged with similar aggregates on the surface, so the rate of breakdown can be estimated by a constant coefficient, C_{bk} (m^{-1}), as (Mirzamostafa 1996):

$$C_{bk} = 0.11C_{anag} \left(1 - (SF_{san} - SF_{vfs}) \right) \quad [106]$$

A fraction, $SF10_{bk}$, of the soil broken to suspension-size is PM_{10} and is estimated as (Hagen 2004):

$$SF10_{bk} = 0.201 - 0.52\ln(SF_{cla}) + 0.422(\ln(SF_{cla}))^2 - 0.1395(\ln(SF_{cla}))^3 + 0.0156(\ln(SF_{cla}))^4 + 0.131\exp\left(\frac{-WZ_{ypt}}{175.6}\right) \quad [107]$$

where

$100 < WZ_{ypt} < 800$ annual precipitation (mm), and
 $0.017 < SF_{cla} < 0.42$ surface soil fraction clay.

Trapping and Interception Parameters

There are three different cases of trapping and two of interception simulated in ESM. Examples of the first two cases can occur when a soil discharge approaches a wind barrier.

In the first case, the grid cell transport capacity, q_{en} , is zero, but the incoming saltation+creep, q_1 , is greater than zero. In this case, saltation+creep leaving the grid cell is set equal to zero and q_1 is the deposition rate for saltation+creep in the grid cell. In addition, the deposition of both the suspension and PM_{10} are simulated by simple exponential decay equations as:

$$q_{ss} = q_{ss_1} \exp(-C_{dp}(\Delta X)) \quad [108]$$

$$q_{10} = q_{10_1} \exp(-C_{10dp}(\Delta X)) \quad [109]$$

where

1 = subscript denoting values at upwind grid cell boundary,
 q_{ss} = suspension discharge ($kg\ m^{-1}\ s^{-1}$) = PM_{10} discharge ($kg\ m^{-1}\ s^{-1}$),
 C_{dp} = coefficient of deposition for suspension, estimated as $0.02\ (m^{-1})$, and
 C_{10dp} = coefficient of deposition for PM_{10} , estimated as $0.001\ (m^{-1})$.

In the second case, the incoming saltation+creep discharge, q_1 , is greater than the transport capacity, q_{en} , in a grid cell. In this case, the saltation+creep discharge for the cell is set to q_{en} , while suspension and PM_{10} discharge are calculated using their usual estimating equations. The difference between q_1 and q_{en} is assigned as the deposition rate for saltation+creep in the grid cell.

In the third case, non-uniform surfaces, such as highly erodible tillage ridges, often emit more erodible saltation+creep than the wind can transport, and the excess emission is trapped in downwind furrows. Trapping is simulated when the surface is rough, i.e., ridge roughness >50 mm or random roughness >10 mm. The rate of trapping of the saltation+creep discharge depends on both the surface conditions and a trapping coefficient, $C_t\ (m^{-1})$. The trapping leads to the commonly-observed flattening of ridges and filling of furrows during erosion events.

An estimate for C_t , can be derived as follows: At sufficient distance downwind the saltation+creep discharge should approach the surface transport capacity. In this

condition the emission flux, G_{en} , must equal the trapping flux, G_{tp} . Expanding and equating these values gives:

$$(1 - SFSS_{en})C_{en}(q_{en} - q) = C_t(q_{en} - q_{cp})\frac{q}{q_{en}}, \quad q_{en} \geq q_{cp} \quad [110]$$

Letting q approach q_{cp} and solving for C_t gives:

$$C_t = (1 - SFSS_{en})C_{en}\frac{q_{en}}{q_{cp}}, \quad q_{en} \geq q_{cp} \quad [111]$$

However, when $q_{en} \gg q_{cp}$, the transport capacity will be between them. Hence, a coefficient was substituted in the prior equation to give (with additional constraints specified):

$$C_t = \begin{cases} C_{tf}(1 - SFSS_{en})C_{en}, & q_{en} \geq q_{cp} \text{ and } (SZ_{rr} > 10 \text{ or } SZ_{rg} > 50) \\ 0, & q_{en} < q_{cp} \text{ or } (SZ_{rr} \leq 10 \text{ and } SZ_{rg} \leq 50) \end{cases} \quad [112]$$

where

C_{tf} = empirical coefficient, with value about 1.2

Plant interception by standing biomass also decreases the discharge of saltation+creep. The deflection of saltation+creep by stems reduces their saltation jump along the wind direction and surface impact kinetic energy. These effects are estimated by an empirical coefficient of interception, C_i (m^{-1}), which is a function of biomass stem area, row orientation, and biomass height. The coefficient of interception is estimated as:

$$C_i = \begin{cases} 0, & BZ < 0.001 \\ \left\{ \begin{array}{l} 0.005 \left(1 - \exp\left(-\frac{0.5SAI}{BZ}\right) \right) \\ \sqrt{\frac{SX_{rg}}{SXPr_g}} (1 - \exp(-50BZ)) \end{array} \right\}, & \begin{array}{l} BZ \geq 0.001 \\ SX_{rg} > 10 \end{array} \\ \left\{ \begin{array}{l} 0.005 \left(1 - \exp\left(-\frac{0.5SAI}{BZ}\right) \right) \\ (1 - \exp(-50BZ)) \end{array} \right\}, & \begin{array}{l} BZ \geq 0.001 \\ SX_{rg} \leq 10 \end{array} \end{cases} \quad [113]$$

where

SAI = stem silhouette area index,

BZ = biomass height (m),

SX_{rg} = ridge spacing (mm), and

$SXPr_g$ = ridge spacing parallel the wind direction.

Standing biomass leaves and stems also intercept a portion of the suspension-size aggregates. In this case, we assumed the suspended soil from upwind was moving above the biomass so only part of the suspension-size soil moving from below to above the

biomass in a grid cell was intercepted. The fraction of the vertical suspension flux intercepted (CSS_i) is estimated as:

$$CSS_i = 0.1SAI \quad [114]$$

Update of Surface Conditions During Wind Erosion

Changes to the soil surface in response to loss or deposition at various downwind field locations are rarely considered in wind erosion models. However, it appears necessary to update surface conditions during significant erosion events to account for depletion of the reservoir of mobile soil on short fields, and to simulate the increased erodibility typically observed on downwind regions in long fields. In general, few measurements are available to validate the simulated response of field surfaces to erosion. Hence, simple equations based on mass balance in the surface layer were developed to simulate changes in the area represented by each grid cell.

Surface Update Intervals (time steps)

In WEPS 1.0, hourly simulated or measured wind speeds are used as model inputs. Other intervals for measured wind speeds can be used as inputs to both WEPS and SWEEP. Accounting routines assume that the intervals used evenly divide one hour and that the same interval is used for the entire simulation.

To minimize model run time, a variable update time interval was implemented. The needed surface update interval depends on the erosion rate, but that is unknown before a simulation is made. Hence, when each new wind speed is input, a relative erosive wind energy (ENG_e , $m^3 m^{-3}$) is calculated for the most erosive grid cell during the previous time step as:

$$ENG_e = (U_{*e})^2(U_{*e} - U_{*te}) \quad [115]$$

where

U_{*e} = estimated friction velocity found to be 0.06 of the 10 meter wind velocity for this time period,

U_{*te} = estimated threshold friction velocity found to be $\frac{U_{*e}}{rut}$, and

rut = ratio of friction velocity for this time period to daily initial threshold friction velocity.

The number of surface updates for each of the wind speeds input during a 24 hour period is:

$$N_t = \max\left(1, \frac{96}{N_{tstep}}\right) \quad [116]$$

$$N = \max(1, (0.5 + 4.6ENG_e)N_t) \quad [117]$$

where

N_{tstep} = number of wind speed intervals input in 24-hour time period,
 N_t = minimum number of time steps required for surface updating for each wind speed interval, and
 N = number of time steps for surface updating for each wind speed interval.

Surface update intervals as a function of relative erosive wind energy then become:

$$\Delta t = \frac{86,400}{N * N_{tstep}} \quad [118]$$

which is illustrated in Figure 23 where
 Δt = surface update time interval (s).

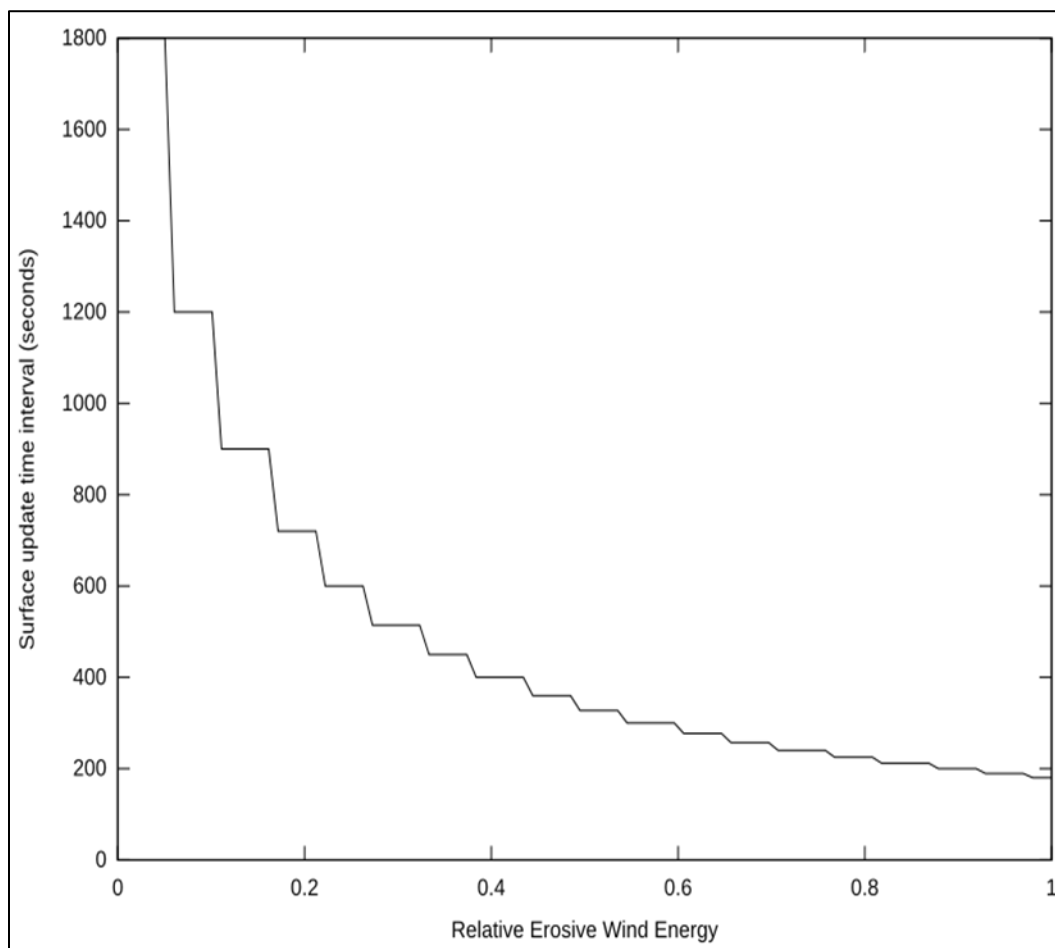


Figure 23. Surface update time interval based on relative erosive wind energy.

Change in Mobile Surface Soil

Two reservoirs of mobile soil may be present at the soil surface. These include mobile soil on a consolidated surface, hereafter called crusted, and mobile soil among the rock and immobile aggregates. Because these reservoirs differ in their response to erosion,

they are updated separately. Written in general form, the equation for the net addition (+) or loss (-) of mobile aggregates during a time interval (Δt) over a field length segment ($x_2 - x_1$) from a reservoir is estimated as:

$$dmt_{los} = dmt + \left[\sum_{i=1}^2 (F_{an_i} C_{an_i}) \right] q_1 \Delta t \quad [119]$$

$$dmt = \left(\frac{-(q_2 - q_1) - (q_{ss_2} - q_{ss_1})}{x_2 - x_1} \right) \Delta t \quad [120]$$

where

dmt_{los} = net change in mobile soil surface aggregates during time interval Δt (kg m^{-2}),

and

dmt = net gain (+) or loss (-) of soil from grid in time interval Δt (kg m^{-2}).

The first term in Eq. 119 represents loss or gain by erosion and the second term represents creation of new mobile aggregates by the abrasion process.

Update of Crusted Surface

Undisturbed, crusted soil surfaces have high threshold wind speeds and are generally stable, unless abraded by mobile soil aggregates. In WEPS, the crust is simulated as a triangular shape (Figure 24). Uniform abrasion of this crust shape continually exposes an increasing area of aggregated soil at the surface. The simple triangular shape was selected because there are spatial variations in crust thickness and resistance to abrasion interacting with preferential zones for abraded impact caused by the surface microtopography within each grid cell that is, nevertheless, assumed to be homogeneous.

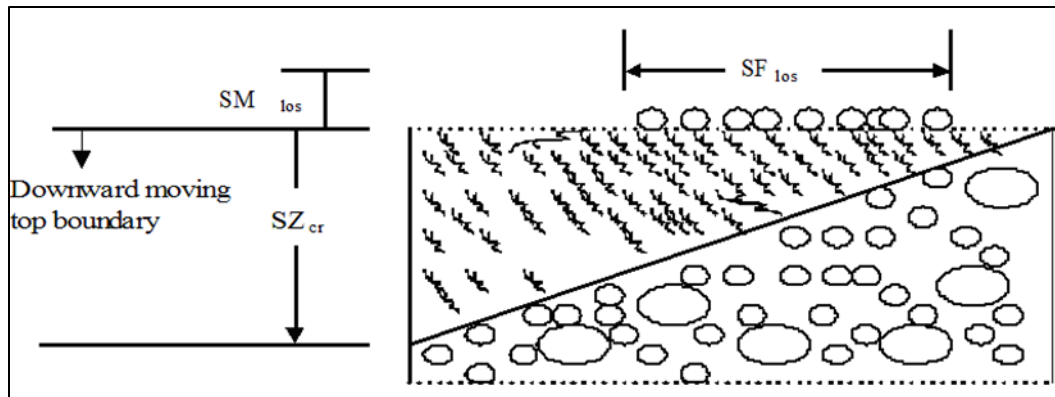


Figure 24. Schematic of triangular-shaped crust on soil surface layer subject to soil loss by wind erosion.

The deflatable mass of mobile soil on the crusted surface, SM_{los0} , is not dependent on the magnitude of the friction velocity above threshold. All of the reservoir is available. If the reservoir of mobile soil on the crust cannot fully supply the simulated soil loss

($-dmt_{los} > SM_{los0}$), the additional soil loss, fdm , is removed from the remaining reservoir of mobile soil among rocks and immobile aggregates.

$$\left\{ \begin{array}{l} SM_{los} = SM_{los0} + dmt_{los} \\ fdm = 0 \end{array} \right\}, \quad -dmt_{los} \leq SM_{los0}$$

$$\left\{ \begin{array}{l} SM_{los} = 0 \\ fdm = (SM_{los0} + dmt_{los}) \frac{SF_{cr}}{1.0001 - SF_{cr}} \end{array} \right\}, \quad -dmt_{los} > SM_{los0} \quad [121]$$

where

SM_{los} = mobile soil aggregates per unit area of the crusted surface (kg m^{-2}),

SM_{los0} = value of SM_{los} at prior time step (kg m^{-2}), and

fdm = additional net change in mobile soil surface aggregates for aggregated surface during time interval Δt (kg m^{-2}).

Updated values of the mobile aggregate mass on the crusted surface are used to update the fraction of mobile crust cover. The layer thickness of mobile aggregate deposits tends to increase with surface roughness. Hence, the coefficient CR_{los} reduces mobile cover as surface roughness increases.

$$SF_{los} = (1 - \exp(3.5 SM_{los}^{1.5})) CR_{los} \quad [122]$$

$$CR_{los} = \exp(-0.8\sqrt{SZ}) \quad [123]$$

$$SZ = \max(SZ_{rg}, 4 SZ_{rr}) \quad [124]$$

where

CR_{los} = roughness dependent fraction of mobile crust cover reduction coefficient,

SZ_{rg} = ridge height (mm), and

SZ_{rr} = random roughness (mm).

Mobile aggregate cover on a crusted surface as a function of mobile mass with various ridge height levels is illustrated in Figure 25.

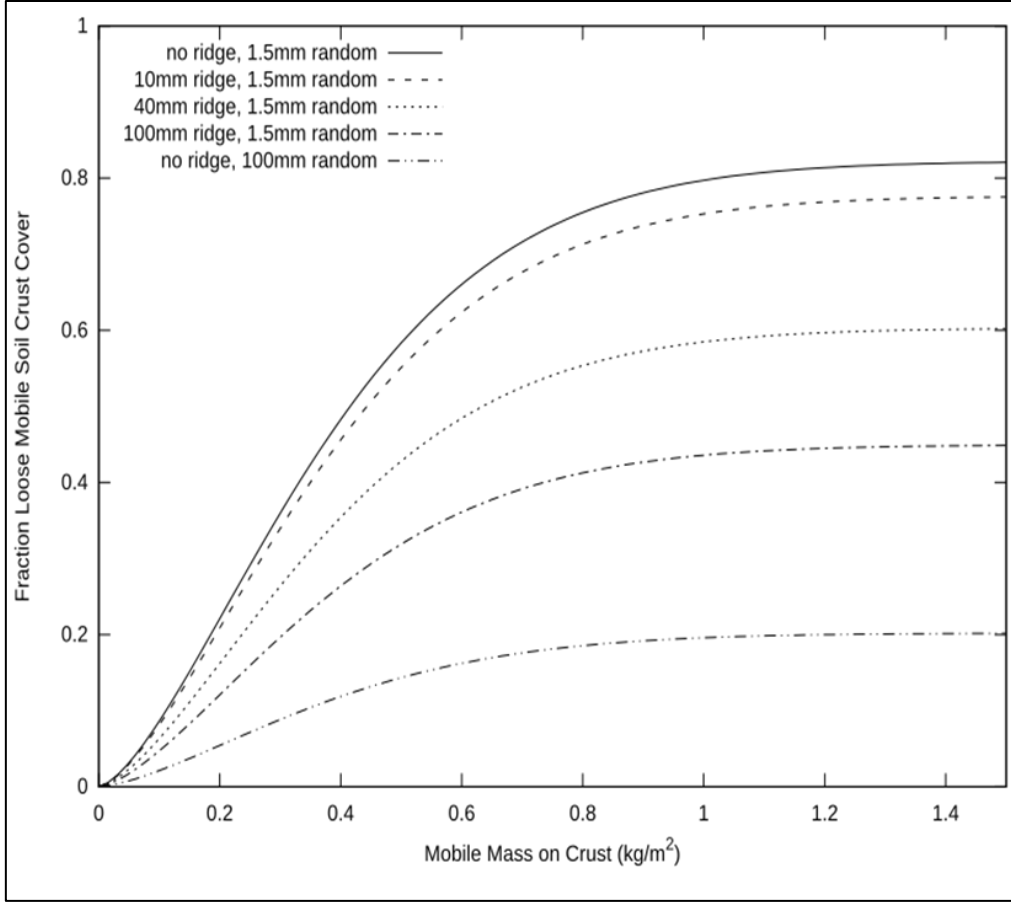


Figure 25. Loose, mobile cover of aggregates on crust as a function of mobile mass for a range of ridge heights.

If fraction crust cover is >0.01 , crust thickness is reduced by abrasion on the crust and is simulated as:

$$SZ_{cr} = SZ_{cr0} - \frac{F_{ancr} C_{ancr} q_1}{1.4 SF_{cr}} \Delta t \quad [125]$$

where

SZ_{cr} = crust thickness (mm),

SZ_{cr0} = crust thickness at prior time step (mm), and

F_{ancr} = updated value from Eq. 100 using updated SF_{los} .

Finally, crust cover is updated in proportion to crust thickness as:

$$SF_{cr} = SF_{cr0} \frac{SZ_{cr}}{SZ_{cr0}} \quad [126]$$

where

SF_{cr0} = is crust cover fraction at prior time step.

Update of Aggregated Surface

On aggregated surfaces some of the mobile material is typically sheltered by micro-roughness of the immobile aggregates. Hence the reservoir of mobile material available for deflation varies with friction velocity. The maximum mass of mobile soil that could be removed under a high friction velocity is $SMag_{mx}$, while removable soil under a lowered friction velocity is $SMag_{los}$ as illustrated in Figure 26. The mobile aggregate cover fraction on the aggregated surface is $SF84$. The aggregate mixture is assumed to be uniform with depth. Hence, as abrasion lowers the soil surface, the top and bottom boundaries move downward so that $SMag_{mx}$ remains constant. The net mass of mobile soil removed (-) or added (+) to the reservoir is dm_{los} .

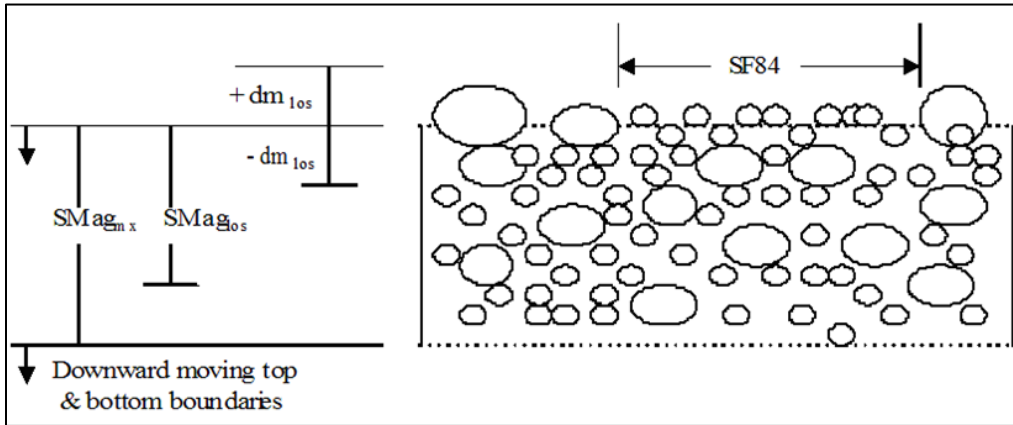


Figure 26. Schematic of aggregated soil surface layer subject to soil loss by wind erosion.

To simulate the aggregated surface, the cumulative change of mass of mobile material is updated as:

$$dm_{los} = dm_{los0} + dmt_{los} + f dm \quad [127]$$

where

dm_{los} = cumulative mobile soil loss or gain on aggregated surface (kg m^{-2}), and
 dm_{los0} = value of dm_{los} at prior time step (kg m^{-2}).

When $dm_{los} < 0$, mobile soil is removed from the initial reservoir among the immobile aggregates. Based on limited wind tunnel measurements, empirical relationships were developed to estimate the mass of mobile aggregates that could be removed from a flat, bare, aggregated surface for a range of friction velocities as illustrated in Figure 27.

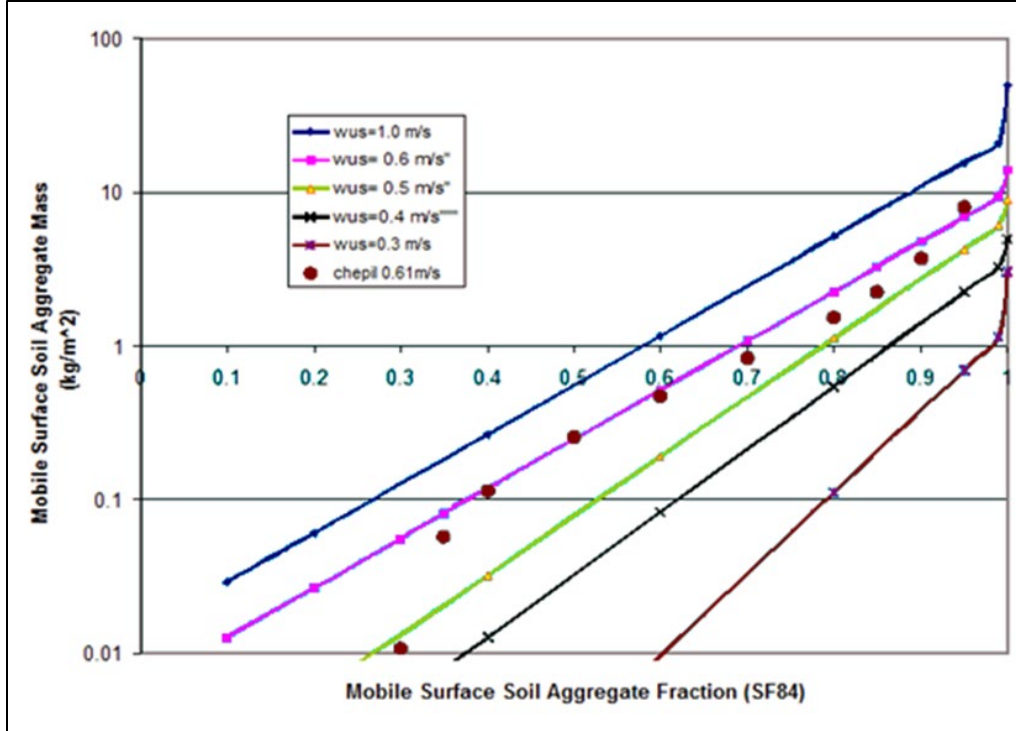


Figure 27. Mass of mobile aggregates that can be removed from flat, bare aggregated surface with various initial mass fractions of mobile aggregates (SF84) for a range of friction velocities without abrasion. Data is from Chepil (1951).

The maximum removable mass in the mobile reservoir was estimated at a friction velocity (U_*) of 0.75 m s^{-1} for a bare, smooth, aggregated surface as:

$$SM_{aglosmx} = \exp(2.708 - 7.603((1 - SF84_{ic})(1 - SVroc_{ic}) + SVroc_{ic})) \quad [128]$$

The total soil mass in the reservoir is then estimated as:

$$SM_{tot} = \frac{SM_{aglosmx}}{SF84_{ic}(1.001 - SVroc_{ic})} \quad [129]$$

The maximum reservoir is reduced by roughness, residue cover, and wetness to estimate the available reservoir at the current friction velocity as:

$$SM_{aglos} = \max\left(0, SM_{aglosmx} \frac{U_* - U_{*t}}{0.75 - U_{*to}}\right) \quad [130]$$

where

U_{*to} = threshold friction velocity for bare, aggregated, smooth soil (m s^{-1}).

When the soil removal from the reservoir with the current friction velocity equals SM_{aglos} , erosion is stopped, and the mobile soil fraction (SF_{84mn}) still remaining in the maximum mobile soil reservoir is:

$$SF_{84mn} = \frac{SM_{aglostm} - SM_{aglos}}{SM_{tot}} \quad [131]$$

When there is net soil mass deposition ($dm_{los} \geq 0$), the immobile surface aggregates can become slowly buried by the addition of mobile soil to the initial reservoir. In this case, the surface fraction of mobile aggregates is adjusted upward. For both loss and deposition, SF_{84} is updated as:

$$SF_{84} = \begin{cases} \frac{SM_{aglostm} + dm_{los}}{SM_{tot}}, & dm_{los} < 0 \\ \frac{SM_{aglostm} + dm_{los}}{SM_{tot} + dm_{los}}, & dm_{los} \geq 0 \end{cases} \quad [132]$$

Update of Soil Fraction <2.0 mm Diameter

The soil fraction <2.0 mm diameter (SF_{200}) is estimated from the values of the soil fraction <0.84 mm diameter (SF_{84}) as:

$$SF_{200} = (2 - SF_{84}) SF_{84} \quad [133]$$

Update of Soil Fraction <0.10 mm Diameter

When soil loss is occurring ($dm_{los} < 0$), SF_{10} is updated in proportion to the changes in SF_{84} . When there is mobile soil gain at the soil surface ($dm_{los} \geq 0$), the suspension-size aggregates less than 0.10 mm diameter (SF_{10}) tend to be sorted out of the depositing soil. Hence, the estimate is:

$$SF_{10} = \begin{cases} SF_{10ic} \frac{SF_{84}}{SF_{84ic}}, & dm_{los} < 0 \\ \frac{SF_{10ic} SM_{tot}}{SM_{tot} + dm_{los}}, & dm_{los} \geq 0 \end{cases} \quad [134]$$

where

SF_{10ic} = is the SF_{10} initial condition at the beginning of the erosion event, and

SF_{84ic} = is the SF_{84} initial condition at the beginning of the erosion event.

Update of Surface Rock Volume

The rocks (>2.0 mm diameter) are assumed to be mixed with the soil and have a uniform vertical distribution. If an initial desert pavement is present, the surface is generally assumed to be stable. Surface rock volume increases or decreases in proportion to the deflation or deposition from the surface area that is not covered by rock and is estimated to slowly change by the equation:

$$SV_{roc} = \min \left\{ 1, \max \left\{ 0, SV_{roc0} - \left(\frac{1 - SV_{roc0}}{1 - SV_{rocic}} \right) \left(\frac{7.5 dmt}{1200(1.001 - SV_{rocic})} \right) \right\} \right\} \quad [135]$$

where

SV_{roc} = soil rock volume ($m^3 m^{-3}$),

SV_{roc0} = soil rock volume at prior time-step ($m^3 m^{-3}$), and

SV_{roci} = soil rock volume at beginning of erosion event ($m^3 m^{-3}$).

Update Surface Roughness

Roughness elements consist of random roughness and, if present, oriented roughness such as tillage ridges. The first step in updating roughness is estimating the effects of changes in loose soil depth generated by the various erosion processes. Trial relationships were developed based on qualitative criterion for testing. When the soil surface has roughness elements that actively trap saltation-size aggregates ($C_t > 0$) and net deposition of mobile soil in sheltered areas ($dmt_{los} > 0$), roughness height decreases. When saltation trapping occurs ($C_t > 0$), but with a net loss from both sheltered and unsheltered areas ($dmt_{los} \leq 0$), roughness height decreases, but more slowly. When no saltation trapping is occurring ($C_t = 0$), i.e the soil surface is relatively smooth, a net deposition increase over much of the area ($dmt_{los} > 0$) decreases roughness height. Finally, when no saltation trapping is occurring ($C_t = 0$), the net loss of loose surface material ($dmt_{los} \leq 0$) increases roughness. Quantitative research is needed to refine these relationships.

$$SZ_v = \begin{cases} \frac{-2.0dmt_{los}}{1.2}, & C_t > 0 \text{ and } dmt_{los} > 0 \\ \frac{dmt_{los}}{1.2}, & C_t > 0 \text{ and } dmt_{los} \leq 0 \\ \frac{-dmt_{los}}{1.2}, & C_t = 0 \text{ and } dmt_{los} > 0 \\ \frac{0.5dmt_{los}}{1.2}, & C_t = 0 \text{ and } dmt_{los} \leq 0 \end{cases} \quad [136]$$

where

SZ_v = change is roughness height caused by deposition or emission for time step Δt (mm).

The change in roughness height caused by abrasion of immobile clods and crust is:

$$SZ_{an} = \frac{-2.0[\sum_{i=1}^2 (F_{an_i} C_{an_i})]q_1 \Delta t}{1.4} \quad [137]$$

where

SZ_{an} = change is roughness height caused by abrasion for time step Δt (mm).

Total roughness height change is then expressed as, SZ_t (mm) is:

$$SZ_t = SZ_v + SZ_{an} \quad [138]$$

where

SZ_t = total change is roughness height for time step Δt (mm).

Ridge height is updated as:

$$SZ_{rg} = \max\{0, SZ_{rg0} + SZ_t\} \quad [139]$$

where

SZ_{rg} = ridge height (mm), and

SZ_{rg0} = ridge height at prior time-step (mm).

Random roughness is updated as:

$$SZ_{rr} = \max\left\{1.5, SZ_{rr0} \frac{SZ_t}{4.0}\right\} \quad [140]$$

where

SZ_{rr} = random roughness (mm), and

SZ_{rr0} = random roughness at prior time-step (mm).

Output from Erosion to Files

The submodel outputs include estimates of both total soil loss from the simulation region as well as components of the soil loss moving across each field boundary. These components are saltation+creep (>0.10 mm diameter) and suspended soil (<0.10 mm diameter). The mass of particles less than 10 microns in aerodynamic diameter (PM₁₀) in the suspended soil also is predicted. Files of time-varying emissions for use as source terms in dust diffusion and transport models can also be output. To compare simulation results to measured erosion data, input files of measured weather can be used in place of the simulated weather.

When called from the full WEPS model, the summary results of total erosion, creep+saltation, suspension, and PM₁₀ from each erosion day are provided to routines, which summarize erosion results by period, over all years and by year. In addition, the daily erosion mass across the four field side boundaries are also provided for summarization.

When called from the SWEEP model, output files are created for daily total erosion amounts for all components (*.erod) (Figure 28); hourly total erosion amounts for all components (*.emit) (Figure 29); field grid cell boundary total erosion amounts and field grid cell total erosion amounts for all components (*.egrd) (Figure 30); and detailed conditions and erosion amounts for each grid cell by time step (*.sgrd) (Figure 31).

7.977219	1.903312	6.073907	0.232969	test.in
----------	----------	----------	----------	---------

Figure 28. Example *.erod file showing total erosion results. Values are total erosion, creep+saltation, suspension, and the PM₁₀portion of suspension for a single day erosion event in kg m².

```

SBEMIT output
Date of run: Feb 08, 2010 15:02:31

```

yr	mo	day	hr	ws	emission (kg m-2 s-1)		susp	PM10
					total	salt/creep		
1	1	1	1.000	1.60	0.00000000	0.00000000	0.00000000	0.00000000
1	1	1	2.000	0.00	0.00000000	0.00000000	0.00000000	0.00000000
1	1	1	3.000	0.00	0.00000000	0.00000000	0.00000000	0.00000000
1	1	1	4.000	0.00	0.00000000	0.00000000	0.00000000	0.00000000
1	1	1	5.000	0.00	0.00000000	0.00000000	0.00000000	0.00000000
1	1	1	6.000	1.00	0.00000000	0.00000000	0.00000000	0.00000000
1	1	1	7.000	2.10	0.00000000	0.00000000	0.00000000	0.00000000
1	1	1	8.000	2.80	0.00000000	0.00000000	0.00000000	0.00000000
1	1	1	9.000	3.30	0.00000000	0.00000000	0.00000000	0.00000000
1	1	1	10.000	4.00	0.00000000	0.00000000	0.00000000	0.00000000
1	1	1	11.000	5.60	0.00000000	0.00000000	0.00000000	0.00000000
1	1	1	12.000	6.60	0.00000000	0.00000000	0.00000000	0.00000000
1	1	1	13.000	12.70	0.00000000	0.00000000	0.00000000	0.00000000
1	1	1	14.000	14.50	0.00000000	0.00000000	0.00000000	0.00000000
1	1	1	15.000	19.40	0.00000000	0.00000000	0.00000000	0.00000000
1	1	1	16.000	27.80	0.00221589	0.00052870	0.00168720	0.00006471
1	1	1	17.000	14.80	0.00000000	0.00000000	0.00000000	0.00000000
1	1	1	18.000	14.30	0.00000000	0.00000000	0.00000000	0.00000000
1	1	1	19.000	7.90	0.00000000	0.00000000	0.00000000	0.00000000
1	1	1	20.000	5.90	0.00000000	0.00000000	0.00000000	0.00000000
1	1	1	21.000	4.50	0.00000000	0.00000000	0.00000000	0.00000000
1	1	1	22.000	3.60	0.00000000	0.00000000	0.00000000	0.00000000
1	1	1	23.000	3.00	0.00000000	0.00000000	0.00000000	0.00000000
1	1	1	24.000	2.40	0.00000000	0.00000000	0.00000000	0.00000000

Figure 29. Example *.emit file listing showing hourly wind speed (ws), and emissions for each hour.

```

OUTPUT FROM ERODOUT.FOR

Date of run: Feb 08, 2010 15:02:31

<field dimensions>
  0.00      0.00      0.00      705.61      705.61
</field dimensions>

Total grid size: ( 31 , 31 )   Inner grid size: ( 29 , 29 )

Passing Border Grid Cells - Total      egt+egsss(kg/m)
top(i=1,imax-1,j=jmax) bottom(i=1,imax-1,j=0) right(i=imax,j=1,jmax-1) left(i=0, j=1,jmax-1)
73.9373      308.7460      . . .      4701.3433      4795.3286
0.0000      0.0000      . . .      0.0000      0.0000
73.9308      308.7312      . . .      4701.3125      4795.3008
0.0000      0.0000      . . .      0.0000      0.0000

Passing Border Grid Cells - Salt/Creep      egt(kg/m)
top(i=1,imax-1,j=jmax) bottom(i=1,imax-1,j=0) right(i=imax,j=1,jmax-1) left(i=0, j=1,jmax-1)
55.4283      213.7831      . . .      736.4492      736.4492
0.0000      0.0000      . . .      0.0000      0.0000
55.4235      213.7734      . . .      736.4448      736.4448
0.0000      0.0000      . . .      0.0000      0.0000

Passing Border Grid Cells - Suspension      egtss(kg/m)
top(i=1,imax-1,j=jmax) bottom(i=1,imax-1,j=0) right(i=imax,j=1,jmax-1) left(i=0, j=1,jmax-1)
18.5090      94.9629      . . .      3964.8940      4058.8796
0.0000      0.0000      . . .      0.0000      0.0000
18.5072      94.9578      . . .      3964.8679      4058.8560
0.0000      0.0000      . . .      0.0000      0.0000

Passing Border Grid Cells - PM10      egt10(kg/m)
top(i=1,imax-1,j=jmax) bottom(i=1,imax-1,j=0) right(i=imax,j=1,jmax-1) left(i=0,j=1,jmax-1)
0.492453      2.614820      . . .      154.967459      158.734940
0.000000      0.000000      . . .      0.000000      0.000000
0.492406      2.614674      . . .      154.966527      158.734009
0.000000      0.000000      . . .      0.000000      0.000000

<grid data> | (Total Soil Loss|soil loss|(kg/m^2)
-3.4172      -10.5349      . . .      -7.7256      -7.7256
-2.9982      -9.9498      . . .      -7.7256      -7.7256
. . . . .
-0.2785      -0.4988      . . .      -9.9495      -10.5346
-0.2074      -0.2785      . . .      -2.9980      -3.4170
</grid data>

<grid data> | (Saltation/Creep Soil Loss|salt/creep soil loss|(kg/m^2)
-2.5594      -7.1146      . . .      0.0000      0.0000
-2.2505      -6.7302      . . .      0.0000      0.0000
. . . . .
-0.2146      -0.3720      . . .      -6.7301      -7.1144
-0.1643      -0.2146      . . .      -2.2503      -2.5594
</grid data>

<grid data> | (Suspension Soil Loss|suspension soil loss|(kg/m^2)
-0.8577      -3.4203      . . .      -7.7256      -7.7256
-0.7478      -3.2195      . . .      -7.7256      -7.7256
. . . . .
-0.0639      -0.1268      . . .      -3.2194      -3.4202
-0.0432      -0.0639      . . .      -0.7477      -0.8576
</grid data>

<grid data> | (PM10 Soil Loss|PM10 soil loss|(kg/m^2)
-0.022817      -0.095288      . . .      -0.309679      -0.309679
-0.019896      -0.089171      . . .      -0.309679      -0.309679
. . . . .
-0.001336      -0.003222      . . .      -0.089169      -0.095284
-0.000662      -0.001336      . . .      -0.019894      -0.022815
</grid data>

**Averages - Field
  Total      salt/creep      susp      PM10
  egt      kg/m^2      egtss      egt10
-----
-7.9772      -1.9023      -6.0739      -0.232969

**Averages - Crossing Boundaries
Location      Total Salt/Creep      Susp      PM10
kg/m-----
top      2814.42      671.50      2142.92      82.19
bottom      0.00      0.00      0.00      0.00
right      2814.39      671.50      2142.89      82.19
left      0.00      0.00      0.00      0.00

  Comparison of interior & boundary loss
  interior      boundary      int/bnd ratio
-3971741.0000      3971743.2500      -1.0000

repeat of total, salt/creep, susp, PM10:      7.9772      1.9023      6.0739      0.232969

```

Figure 30. Example portion of *.egrd file showing, grid parameters, daily total boundary grid emissions and daily total soil loss for each for each grid cell and by component. Grid cells were omitted for brevity and are indicated by “...” in both horizontal and vertical directions. Note the use of tags to delineate beginning and end of grid data.

```

Date of run: Feb 08, 2010 15:02:31
anesht = 10.00 m   waoflg = 0
wind direction = 225.00 deg
wind direction relative to field orientation = 225.00 deg
wind quadrants = 6
orientation and dimensions of sim region
anasin(deg)  amxsim - (x1,y1) (x2,y2)
              0.00  0.00  0.00  705.61  705.61
Surface properties
Ridge spacing parallel to wind direction 323.29 (mm)
Crop row spacing 0.20 (mm)
Crop seeding location relative to ridge 0 (0 - furrow, 1 - ridge)
Composite weighted average biomass height 0.76 (m)
Biomass leaf area index 0.00 (m^2/m^2)
Biomass stem area index 0.00 (m^2/m^2)
Biomass flat cover 0.08 (m^2/m^2)
Average yearly total precipitation 300.00 (mm)
</field dimensions>
0.00  0.00  0.00  705.61  705.61
</field dimensions>
yr mon day hr upd_pd jj nn(subpd) rpd (sbout 1) 1 1 1 15.000 1 1 27 648
pd wind speed, dir and dir rel to field 27.80 225.00 225.00
Surface layer properties
Surface course fragments 0.00 (m^3/m^3)
Initial soil mass fraction in surface layer < 0.10 mm 0.15 (kg/kg)
Initial soil mass fraction in surface layer < 0.84 mm 0.48 (kg/kg)
PM10 emission properties
Soil fraction PM10 in abraded suspension 0.02
Soil fraction PM10 in emitted suspension 0.01
Soil fraction PM10 in saltation breakage suspension 0.05
Coefficient of abrasion of aggregates 0.07
Coefficient of abrasion of crust 0.07
<grid data> | 1 1 1 15.000|Surface Friction Velocity|friction velocity|(m/s)
<grid data> | 1 1 1 15.000|Threshold Surface Friction Velocity|threshold friction velocity|(m/s)
<grid data> | 1 1 1 15.000|Transport Threshold Surface Friction Velocity|transport threshold friction velocity|(m/s)
<grid data> | 1 1 1 15.000|Surface Random Roughness|random roughness|(mm)
<grid data> | 1 1 1 15.000|Surface Oriented Roughness|ridge height|(mm)
<grid data> | 1 1 1 15.000|Surface Rock|surface volume rock fraction|(m^3/m^3)
<grid data> | 1 1 1 15.000|Soil Agg. Size<0.01|mass fraction < 0.01 mm size|(fract.)
<grid data> | 1 1 1 15.000|Soil Agg. Size<0.1|mass fraction < 0.1 mm size|(fract.)
<grid data> | 1 1 1 15.000|Soil Agg. Size<0.84|mass fraction < 0.84 mm size|(fract.)
<grid data> | 1 1 1 15.000|Soil Agg. Size<2.0|mass fraction < 2.0 mm size|(fract.)
<grid data> | 1 1 1 15.000|Soil Agg. Size for u* to be the thresh. friction velocity|"effective" mass fraction < 0.84 mm size|(fract.)
<grid data> | 1 1 1 15.000|Mobile soil removable from aggregated surface|mass removable|(kg/m^2)
<grid data> | 1 1 1 15.000|Change in mobile soil on aggregated surface|net mass change|(kg/m^2)
<grid data> | 1 1 1 15.000|Consolidated crust thickness|crust thickness|(mm)
<grid data> | 1 1 1 15.000|Fraction of Surface covered with Crust|crust cover|(fract.)
<grid data> | 1 1 1 15.000|Fraction of Crusted Surface covered with Loose Erodible Soil |loose erodible material|(fract.)
<grid data> | 1 1 1 15.000|Mass of Loose Erodible Soil on Crusted Surface|loose erodible material|(kg/m^2)
yr mon day hr upd_pd jj nn(subpd) rpd (sbout 2) 1 1 1 15.027 1 1 27 648
<grid data> | 1 1 1 15.027|Cumulative Total Soil Loss|soil loss|(kg/m^2)
<grid data> | 1 1 1 15.027|Cumulative Saltation/Creep Soil Loss|salt/creep soil loss|(kg/m^2)
<grid data> | 1 1 1 15.027|Cumulative Suspension Soil Loss|suspension soil loss|(kg/m^2)
<grid data> | 1 1 1 15.027|Cumulative PM10 Soil Loss|PM10 soil loss|(kg/m^2)
<grid data> | 1 1 1 15.027|Surface Random Roughness (after)|random roughness|(mm)
<grid data> | 1 1 1 15.027|Surface Oriented Roughness (after)|ridge height|(mm)
<grid data> | 1 1 1 15.027|Surface Rock (after)|surface volume rock fraction|(m^3/m^3)
<grid data> | 1 1 1 15.027|Soil Agg. Size < 0.01|mass fraction < 0.01 mm size|(fract.)
<grid data> | 1 1 1 15.027|Soil Agg. Size < 0.1|mass fraction < 0.1 mm size|(fract.)
<grid data> | 1 1 1 15.027|Soil Agg. Size < 0.84|mass fraction < 0.84 mm size|(fract.)
<grid data> | 1 1 1 15.027|Soil Agg. Size < 2.0|mass fraction < 2.0 mm size|(fract.)
<grid data> | 1 1 1 15.027|Soil Agg. Size for u* to be the thresh. friction velocity (af)|"effective" mass fraction < 0.84 mm size|(fract.)
<grid data> | 1 1 1 15.027|Mobile soil removable from aggregated surface (after)|mass removable|(kg/m^2)
<grid data> | 1 1 1 15.027|Change in mobile soil on aggregated surface (after)|net mass change|(kg/m^2)
<grid data> | 1 1 1 15.027|Consolidated crust thickness (after)|crust thickness|(mm)
<grid data> | 1 1 1 15.027|Fraction of Surface covered with Crust (after)|crust cover|(fract.)
<grid data> | 1 1 1 15.027|Fraction of Crusted Surface covered with Loose Erodible Soil (a)|loose erodible material|(fract.)
<grid data> | 1 1 1 15.027|Mass of Loose Erodible Soil on Crusted Surface (after)|loose erodible material|(kg/m^2)
egavg = -0.26 -0.36 -0.41 -0.42 -0.42 -0.42 -0.42 -0.42 -0.42 -0.41 -0.41 -0.41 -0.41 -0.41 -0.41 -0.41 -0.41 -0.41 -0.41
egavg = -0.41 -0.41 -0.41 -0.41 -0.41 -0.41 -0.41 -0.41 -0.41 -0.41 -0.41 -0.41 -0.41 -0.41 -0.41 -0.41 -0.41 -0.41 -0.41
-----
yr mon day hr upd_pd jj nn(subpd) rpd (sbout 1) 1 1 1 15.027 2 2 27 648
pd wind speed, dir and dir rel to field 27.80 225.00 225.00
Surface layer properties
. . .
. . .
. . .
<grid data> | 1 1 1 16.000|Mass of Loose Erodible Soil on Crusted Surface (after)|loose erodible material|(kg/m^2)
</grid data>
egavg = -1.15 -2.66 -4.21 -5.62 -6.48 -6.98 -7.25 -7.42 -7.51 -7.58 -7.62 -7.67 -7.70 -7.72 -7.75 -7.77 -7.79 -7.81 -7.82 -7.85
egavg = -7.87 -7.88 -7.90 -7.91 -7.92 -7.94 -7.95 -7.96 -7.98
-----
**Averages - Field
Total salt/creep susp PM10
egs egtss egt10
-----kg/m^2-----
-7.9772 -1.9032 -6.0739 -0.282969
-----
**Averages - Crossing Boundaries
Location Total Salt/Creep Susp PM10
-----kg/m-----
top 2814.42 671.50 2142.92 82.19
bottom 0.00 0.00 0.00 0.00
right 2814.59 671.50 2142.89 82.19
left 0.00 0.00 0.00 0.00
-----
Comparison of interior & boundary loss
interior boundary int/bnd ratio
-8971741.0000 8971742.2500 -1.0000

```

Figure 31. Example portion of *.sgrd file showing values presented for each simulation time step. Data values and successive time steps are omitted for brevity. Missing data are indicated by “...” in both horizontal and vertical directions. Conditions are given at the beginning of the time step and emissions and conditions upon completion of the time step follow.

References

- Allmaras, R.R., R.E. Burwell, W.E. Larson, and R.F. Holt. 1966. Total Porosity and Random Roughness of the Interrow Zone as Influenced by Tillage” USDA Conservation Research Report 7.
- Armbrust, D.V., and J.D. Bilbro Jr. 1997. Relating Plant Canopy Characteristics to Soil Transport Capacity by Wind. *Agronomy Journal*. 89: 157–162.
- Bagnold, R.A. 1943. *The Physics of Blown Sand and Desert Dunes*. Methuen, London, England.
- Chepil, W.S. 1951. Properties of Soil Which Influence Wind Erosion. IV. State of Dry Aggregate Structure. *Soil Science*. 72 (5): 387–401.
- Chepil, W.S., and N.P. Woodruff. 1963. *The Physics of Wind Erosion and Its Control*. *Advances in Agronomy*. 15: 211–302.
- Eimern, J. van, R. Karschon, L.A. Razumova, and G.W. Roberston. 1964. Windbreaks and Shelterbelts. *World Meteorology. Organ. Tech. Notes* 59.
- Gillette, D.A., D.W. Fryrear, T.E. Gill, T. Ley, T.A. Cahill, and E.A. Gearhart. 1997. Relation of Vertical Flux of Particles Smaller Than 10 Microns to Total Aeolian Horizontal Mass Flux at Owens Lake. *J. Geophysical Research*. 102 (D22): 26009–26015.
- Greeley, R., and J.D. Iverson. 1985. *Wind as a Geological Process*. Cambridge Univ. Press, Cambridge England.
- Hagen, L.J. 1991a. A Wind Erosion Prediction System to Meet User Needs” *Journal of Soil and Water Conservation*. 46: 106–111.
- Hagen, L.J. 1991b. Wind Erosion Mechanics: Abrasion of Aggregated Soil. *Trans. ASAE (Corrected)* 34 (4): 831–837.
- Hagen, L.J. 1991c. Wind Erosion: Emission Rates and Transport Capacities on Rough Surfaces. *American Society of Agricultural Engineers Paper Number 912082*. St. Joseph, MI.
- Hagen, L.J. 1994. Plant Canopy Effects on Wind Erosion Saltation. *Transactions of the American Society of Agricultural Engineers*. 37 (2): 461–465.
- Hagen, L.J. 1996. Crop Residue Effects on Aerodynamic Processes and Wind Erosion. *Theoretical and Applied Climatology*. 54: 39–46.
- Hagen, L.J. 2001. Validation of the Wind Erosion Prediction System (WEPS) Erosion Submodel on Small Cropland Fields. *In Proc. of International Symposium on Soil Erosion Research for the 21st Century, Jan 3-5, 2001, American Society of Agricultural Engineers, Honolulu, HI*.

- Hagen, L.J. 2004. Fine Particulates (PM₁₀ and PM_{2.5}) Generated by Breakage of Mobile Aggregates During Simulated Wind Erosion. *Transactions of the American Society of Agricultural Engineers*. 47 (1): 107–112.
- Hagen, L.J., and D.V. Armbrust. 1992. Aerodynamic Roughness and Saltation Trapping Efficiency of Tillage Ridges. *Transactions of the American Society of Agricultural Engineers*. 35 (4): 1179–1184.
- Hagen, L.J. and D.V. Armbrust. 1994. Plant Canopy Effects on Wind Erosion Saltation. *Trans of the American Society of Agricultural Engineers*. 37(2): 461-465.
- Hagen, L.J., N. Mirzamostafa, and A. Hawkins. 1996. PM-10 Generation by Wind Erosion. *International Conference on Air Pollution from Agricultural Operations*. MidWest Plan Service. Kansas City, MO.
- Hagen, L.J., S. van Pelt, T.M. Zobeck, and A. Retta. 2007. Dust Deposition Near an Eroding Source Field. *Earth Surface Processes and Landforms*. 32 (2): 281–289.
- Hagen, L.J., E.L. Skidmore, and A. Saleh. 1992. Prediction of Aggregate Abrasion Coefficients. *Transactions of the American Society of Agricultural Engineers*. 35 (6): 1847–1850.
- Hagen, L.J., E.L. Skidmore, P.L. Miller, and J.E. Kipp. 1981. Simulation of the Effect of Wind Barriers on Airflow. *Transactions of the American Society of Agricultural Engineers*. 24 (4): 1002–1008.
- Hagen, L.J., L.E. Wagner, J. Tatarko, E.L. Skidmore, A.A. Durar, J.L. Steiner, H.H. Schomberg, et al. 1995. USDA Wind Erosion Prediction System: Technical Description. *In Proc. of WEPP/WEPS Symposium, August 9-11, Des Moines, IA*. Ankeny, IA: Soil and Water Conservation Society.
- Hiesler, G.M., and D.R. DeWalle. 1988. Effects of Windbreak Structure on Wind Flow. *Agriculture, Ecosystems and Environment*. 22: 41–69.
- Lettau, H.H., and K. Lettau. 1978. Experimental and Micro-Meteorological Studies of Dune Migration. *In Exploring the World's Driest Climate*, H.H. Lettau and K. Lettau, (eds.), 110–147. Madison, Wisconsin: Institute of Environmental Studies, University of Wisconsin.
- Lyles, L., and B.E. Allison. 1975. Wind erosion: Uniformly spacing nonerodible elements eliminates effects of wind-direction variability. *Journal of Soil and Water Conservation*. 30(5):225-22.
- Mirzamostafa, N. 1996. Suspension Component of Wind Erosion. PhD thesis, Manhattan, KS, Kansas State University.
- Mirzamostafa, N., L.J. Hagen, L.R. Stone, and E.L. Skidmore. 1998. Soil Aggregate and Texture Effects on Suspension Components from Wind Erosion. *Soil Science Society of America Journal*. 62 (5): 1351–1361.

- Panofsky, H.A., and J.A. Dutton. 1984. *Atmospheric Turbulence*. John Wiley & Sons, New York.
- Potter, K.N., and T.M. Zobeck. 1990. Estimation of Soil Microrelief. *Transactions of the American Society of Agricultural Engineers*. 33 (1): 156–161.
- Potter, K.N., T.M. Zobeck, and L.J. Hagen. 1990. A Microrelief Index to Estimate Soil Erodibility by Wind. *Transactions of the American Society of Agricultural Engineers*. 33 (1): 151–155.
- Priestley, C.H.B. 1959. *Turbulent Transfer in the Lower Atmosphere*. The University of Chicago Press. Chicago.
- Pye, K. 1987. *Aeolian Dust and Dust Deposits*. Academic Press, London, England.
- Raine, J.K., and D.C. Stevenson. 1977. Wind Protection by Model Fences in a Simulated Atmospheric Boundary Layer. *Journal of Industrial Aerodynamics*. 2: 159–180.
- Raupach, M.R. 1992. Drag and Drag Partition on Rough Surfaces. *Boundary Layer Meteorology*. 60: 375–395.
- Saleh, A., and D. W. Fryrear. 1995. Threshold Wind Velocities of Wet Soils as Affected by Wind Blown Sand. *Soil Science*. 160 (4): 304–309.
- Stout, J. 1990. Wind Erosion within a Simple Field. *Transactions of the American Society of Agricultural Engineers*. 33 (5): 1597–1600.
- USDA-ARS. 2016. WEPS - Researcher, Developer, Public Release (1.5.52). Available at: <https://www.ars.usda.gov/services/software/download.htm?softwareid=415>. (Accessed August 10, 2020).
- van Donk, S.J., L.E. Wagner, E.L. Skidmore, and J. Tatarko. 2005. Comparison of the Weibull Model with Measured Wind Speed Distributions for Stochastic Wind Generation. *Transactions of the American Society of Agricultural Engineers*. 48 (2): 503–510.
- van de Ven, T.A. M., D. W. Fryrear, and W.P. Spaan. 1989. Vegetation characteristics and soil loss by wind. *Journal of Soil and Water Conservation*. 44:347–349.
- Vigiak, O. , G. Sterk, A. Warren, L. J. Hagen. 2003. Spatial modeling of wind speed around windbreaks. *Catena* 52(273-288).
- Wagner, L.E., and D. Ding. 1994. Representing Aggregate Size Distribution as Modified Lognormal Distributions. *Transactions of the American Society of Agricultural Engineers*. 37 (3): 815–821.
- Zobeck, T.M., and D.W. Fryrear. 1986. Chemical and Physical Characteristics of Windblown Sediment, I. Quantities and Physical Characteristics. *Transactions of the American Society of Agricultural Engineers*. 29 (4): 1032–1036.

Zobeck, T.M., and T.W. Popham. 1991. Influence of Abrader Flux and Soil Properties. *Soil Science Society of America Journal*. 55 (4): 1091–1097.

Table 1. List of symbols for the Erosion submodel of WEPS.

Symbol	Definition	Unit	Variable Name *
a, c	distances from the grid cell to the barrier end	m	a, c
aa, ca	angles at the barrier ends	degrees	aa, ca
$alpha, ceta$	angles from a line passing through the cell coordinates toward the positive y axis direction and lines a and c	degrees	alpha, ceta
awa	wind direction relative to the simulation region y-axis	degrees	awa
$awark$	cardinal wind direction k relative to the simulation region y-axis	degrees	awar(k)
$amasim$	angle of the simulation region y-axis relative to geographic north	degrees	amasim
b	barrier length	m	b
$b1, b2$	coefficients used in Eq. 70	unitless	b1, b2
$b1^{ic}, b2^{ic}$	coefficients for smooth surface (aerodynamic roughness equals 0.5 mm)	unitless	b1, b2
BD_{lai}	decomposing biomass leaf area index	$m^2 m^{-2}$	bdrlai
BD_{sai}	decomposing biomass stem area index	$m^2 m^{-2}$	bdrsai
BFF_{cv}	biomass fraction of flat cover	unitless	bffcvcv
BR_{cd}	effective biomass drag coefficient	unitless	brcd
BR_{lai}	biomass effective leaf area index	$m^2 m^{-2}$	bbrlai
BR_{sai}	biomass effective stem area index	$m^2 m^{-2}$	bbrsai
BZ	biomass height	mm or m	abzht
$C10_{dp}$	coefficient of deposition for PM10, estimated as 0.001	m^{-1}	c10dp
C_{ani}	coefficient of abrasion for aggregates and crust ($Can1=Canag$, $Can2=Cancr$)	m^{-1}	-

C_{anag}	abrasion coefficient for aggregates	m^{-1}	canag
C_{ancr}	abrasion coefficient for crust	m^{-1}	cancr
C_{bk}	coefficient of breakage	m^{-1}	cbk
C_{dp}	coefficient of deposition of suspension-size	m^{-1}	cdp
C_{en}	coefficient of emission	m^{-1}	cen
C_{eno}	coefficient of emission for a bare, smooth, loose, erodible soil. A typical field value is about 0.06	m^{-1}	ceno
C_i	coefficient of plant interception	m^{-1}	ci
C_{lai}	growing crop leaf area index	$m^2 m^{-2}$	bclai
C_m	a coefficient of mixing, value about 0.0001 SF _{ssen}	m^{-1}	cm
CR_{los}	roughness dependent fraction of mobile crust cover reduction coefficient	unitless	crlos
C_s	the saltation transport parameter, with a typical value of about 0.3 or for surfaces armored with stones a greater value	$kg s^2 m^{-4}$	cs
C_{sai}	growing crop stem area index	$m^2 m^{-2}$	bcrsai
C_{ssi}	fraction of suspension-size aggregate flux intercepted by standing biomass	-	-
C_t	coefficient of surface trapping	m^{-1}	ct
C_{tf}	empirical coefficient, with value about 1.2	unitless	ctf
CX_{row}	growing crop row spacing	m	bexrow
CZ	growing crop height	m	bczht
D_{min}	minimum distance between the cell center and the barrier	m	dmin
Δt	surface update time interval	s	time
ΔX	effective distance wind travels across grid cell	m	lx

dm_{los}	cumulative mobile soil loss or gain on an aggregated surface	kg m ⁻²	dmlos
dm_{los0}	value of dm_{los} at prior time step	kg m ⁻²	-
dmt	net gain (+) or loss (-) of soil from grid in time interval Δt	kg m ⁻²	dmt
dmt_{los}	net change in mobile soil surface aggregates during time interval Δt	kg m ⁻²	dmtlos
ENG_e	relative erosive wind energy	m ³ s ⁻³	enge
F_{an1}	mass fraction saltation impacting immobile aggregates and unprotected surface crust ($F_{an1}=F_{anag}$, $F_{an2}=F_{ancr}$)	unitless	-
F_{anag}	fraction of saltation+creep impacting immobile aggregates	unitless	fanag
F_{ancr}	fraction of saltation+creep impacting on unprotected surface crust	unitless	fancr
fdm	additional net change in mobile soil surface aggregates for aggregated surface during time interval Δt	kg m ⁻²	fdm
fu^*	fraction of open field friction velocity	unitless	fu
$fu^{*i,j,k}$	the reduction in wind velocity due to barriers for cell i, j from the wind	unitless	w0br(i,j,k)
G_{an}	vertical flux from abrasion of surface clods and crust	kg m ⁻² s ⁻¹	-
G_{en}	vertical flux from emission of loose aggregates	kg m ⁻² s ⁻¹	-
GSS_{an}	vertical flux of suspension-size aggregates created by abrasion of clods and crust	kg m ⁻² s ⁻¹	-
GSS_{bk}	vertical flux of suspension-size aggregates created by breakage of saltation+creep-size aggregates	kg m ⁻² s ⁻¹	-
GSS_{dp}	vertical flux (deposition) of suspension-size aggregates above a non-eroding surface	kg m ⁻² s ⁻¹	-
GSS_{en}	vertical emission flux of loose, suspension-size aggregates	kg m ⁻² s ⁻¹	-

G_{ip}	vertical flux from trapping of saltation+creep aggregates	$\text{kg m}^{-2}\text{s}^{-1}$	-
hl	ridge height divided by ridge spacing	unitless	hl
$HR0_{wc}$	surface soil water content	kg kg^{-1}	hrwc0
$HR15_{wc}$	surface soil water content at 1.5 MPa	kg kg^{-1}	hrwcw
ix	grid cell spacing in the x direction	m	ix
jy	grid cell spacing in the y direction	m	jy
k	index of cardinal wind directions in clockwise direction ($k=1$ is north)	unitless	-
K	Von Karmen's constant (approximately equal to 0.4)	unitless	-
m, n, s, t	barrier friction velocity reduction equation coefficients	unitless	m,n,s,t
N	number of time steps for surface updating for each wind speed interval	unitless	n
N_t	minimum number of time steps required for surface updating for each wind speed interval	unitless	nt
$N_{t_{step}}$	number of wind speed intervals input in 24 hour time period	unitless	nt step
pb	effective barrier porosity	unitless	pb
pbr	optical barrier porosity	unitless	pbr
q_{10i}	grid cell incoming PM_{10}	$\text{kg m}^{-1} \text{s}^{-1}$	q10i
q_i	grid cell incoming saltation+creep	$\text{kg m}^{-1} \text{s}^{-1}$	qi
q_{cp}	transport capacity of the surface	$\text{kg m}^{-1} \text{s}^{-1}$	qcp
q_{en}	transport capacity	$\text{kg m}^{-1} \text{s}^{-1}$	qen
q_s	discharge of primary (non-breakable) sand particles	$\text{kg m}^{-1} \text{s}^{-1}$	-
q_{sc}	horizontal saltation+creep discharge	$\text{kg m}^{-1} \text{s}^{-1}$	qo
q_{ss}	horizontal suspension component discharge	$\text{kg m}^{-1} \text{s}^{-1}$	-
q_{SSo}	maximum value of q_{ss} entering deposition region	$\text{kg m}^{-1} \text{s}^{-1}$	-

q_{ss1}	grid cell incoming suspension	$\text{kg m}^{-1} \text{s}^{-1}$	qssi
q_{ss2}	suspension discharge at downwind location X_2	$\text{kg m}^{-1} \text{s}^{-1}$	qsso
R_{crow}	reduction of effective leaf area when crop rows spaced >5 crop heights	unitless	red_fac
R_{enb}	bare soil emission ratio accounting for immobile cover and surface roughness	unitless	renb
R_{env}	emission ratio accounting for flat, random vegetation	unitless	renv
R_{rg}	reduction of effective leaf and stem area when crop partly sheltered in furrow	unitless	red_fac
rut	ratio of friction velocity for this time period to daily initial threshold friction velocity	unitless	rut
SAC_{rg}	Weibull scale factor for ridge shelter	degrees	sarg
SAC_{rr}	Weibull scale factor for random roughness	degrees	sarrc
SAI	stem silhouette area index		bcrsai
SA_{rg}	ridge orientation, clockwise from north and parallel to the ridge	degrees	asargo
SD_{agd}	aggregate density	Mg m^{-3}	sdagd
SE_{ags}	dry stability of immobile aggregates	$\ln (\text{J kg}^{-1})$	seags
SE_{crs}	dry stability of crust	$\ln (\text{J kg}^{-1})$	secr
$SF10_{an}$	soil fraction of PM_{10} in suspension-size aggregates created during abrasion of clods and crust	unitless	sf10an
$SF10_{bk}$	soil fraction of PM_{10} in suspension-size aggregates broken from saltation and creep-size aggregates	unitless	sf10bk
$SF10_{en}$	soil fraction of PM_{10} in suspension-size surface soil	unitless	sf10en
SF_{10}	soil fraction less than 0.10 mm diameter	unitless	sf10
SF_{10ic}	is the SF_{10} initial condition at the beginning of the erosion event	unitless	sf10ic

SF_{200}	soil fraction less than 2.0 mm diameter	unitless	sf200
SF_{84}	soil fraction covered with aggregates <0.84 mm in diameter on the non-crusted area, excluding the fraction of rock-covered area	unitless	sf84
SF_{84ic}	is the SF_{84} initial condition at the beginning of the erosion event	unitless	sf84ic
SF_{84mn}	minimum mobile soil fraction for emission	unitless	sf84mn
SFA_{12}	total fraction of area sheltered with shelter angles > 12 degrees	unitless	sfa12
SFA_{12rg}	surface fraction of area with shelter angles > 12 degrees for ridges	unitless	-
SFA_{12rr}	surface fraction of area with shelter angles > 12 degrees for random roughness	unitless	-
SF_{cla}	surface soil fraction clay	unitless	sfcla
SF_{cr}	soil fraction covered by crust, excluding the fraction of rock-covered area	unitless	sfer
SF_{cr0}	crust cover fraction at prior time step	unitless	-
SF_{cv}	soil fraction covered by clod, crust, and rock so it does emit	unitless	sfcv
SF_{cv}^{ic}	bare surface cover fraction before erosion occurs ($SF = SF_{84}$ before erosion begins)	unitless	-
SF_{cv}^{lim}	soil fraction limited by ability of friction velocity to move soil particles	unitless	-
SF_{er}	soil mass fraction of loose, erodible-size, less than about 2.0 mm	unitless	-
SF_{tos}	soil fraction covered with loose, erodible soil on the crusted area	unitless	sflos
SF_{san}	surface soil fraction sand	unitless	sfsan
SF_{sil}	surface soil fraction silt	unitless	sfzil
SF_{ss}	soil mass fraction of loose, suspension-size less than 0.1 mm	unitless	-

SF_{ssan}	mass fraction of suspension-size from abrasion	unitless	sfssan
SF_{ssen}	mass fraction of suspension-size (< 0.10 mm) among loose aggregates (< 2.0 mm diameter)	unitless	sfssen
SF_{vfs}	surface soil fraction very fine sand	unitless	sfvfs
SL_{agn}	lower limit of size distribution	mm	slagn
SL_{agx}	upper limit of size distribution	mm	slagx
SL_{agm}	geometric mean of size distribution	mm	slagm
SM_{aglos}	mass of mobile soil particles	kg m ⁻²	smaglos
$SM_{aglosmx}$	mass of mobile soil particles for a bare, smooth surface at a friction velocity of 0.75 m s ⁻¹	kg m ⁻²	smaglosmx
SM_{los}	mobile soil aggregates per unit area of the crusted surface	kg m ⁻²	smlos
SM_{los0}	value of SM_{los} at prior time step		-
SO_{ags}	geometric standard deviation of size distribution	mm	s0ags
SV_{roc}	soil volume rock >2.0 mm	m ³ m ⁻³	svroc
SV_{roc0}	soil rock volume at prior time-step	m ³ m ⁻³	-
SV_{roci}	soil rock volume at beginning of erosion event	m ³ m ⁻³	-
SX_{dk}	furrow dike spacing	mm	asxdks
SX_{rg}	ridge spacing	mm	asxrgs
SXP_{rg}	ridge spacing parallel the wind direction	mm	sxp _{rg}
SZ_{an}	change in roughness height caused by abrasion for time step Δt	mm	-
SZ_{cr}	crust thickness	mm	szcr
SZ_{cr0}	crust thickness at prior time step	mm	-
SZ_{rg}	ridge height	mm	szrgh
SZ_{rg0}	ridge height at prior time-step	mm	-

SZ_{rr}	random roughness	mm	slrr
SZ_{rr0}	random roughness at prior time-step	mm	-
SZ_t	total change in roughness height for time-step Δt	mm	-
SZ_v	change in roughness height caused by deposition or emission for time step Δt	mm	szv
U	wind velocity at height Z	$m s^{-1}$	-
U_{st}	wind speed at weather station	$m s^{-1}$	awu
U^*	friction velocity at soil surface below standing biomass when present	$m s^{-1}$	wus
$U_*^{I,j}$	the adjusted friction velocity for cell i , j with wind from direction k	$m s^{-1}$	wus(i,j)
U^*_e	estimated friction velocity found to be 0.06 of the 10 meter wind velocity for this time period	$m s^{-1}$	wuse
U^*_{st}	friction velocity at the weather station	$m s^{-1}$	wusst
U^*_t	dynamic threshold friction velocity	$m s^{-1}$	-
U^*_{te}	estimated threshold friction velocity found to be U^*_e / rut	$m s^{-1}$	wuste
U^*_{to}	threshold friction velocity of a bare, smooth surface with the erodible fraction of the surface before erosion occurs	$m s^{-1}$	wusto
U^*_{tp}	static threshold friction velocity for trapping and transport capacity	$m s^{-1}$	wusp
U^*_{ts}	adjusted surface static threshold friction	$m s^{-1}$	wust
U^*_{tt}	dynamic threshold friction velocity of bare surface	$m s^{-1}$	-
U^*_v	friction velocity above the surface including any standing biomass	$m s^{-1}$	wusv
UB^*_{ts}	static threshold friction velocity of bare surface	$m s^{-1}$	wubsts
UC^*_{ts}	change in static threshold friction velocity caused by flat biomass cover	$m s^{-1}$	wucsts

UD_{*ts}	change in static threshold friction velocity from variable aggregate density	$m s^{-1}$	wucdts
UW_{*ts}	increase in static threshold friction velocity from surface wetness	$m s^{-1}$	wucwts
w	distance between the barrier and the grid cell along the wind direction vector	m	w
waa	angle between the barrier and the wind direction	degrees	waa
$WAdir$	wind direction relative to geographic north	degrees	<i>awadir</i>
wz	distance from barrier w converted to units of barrier heights	unitless	x
WZ_{ypt}	average annual precipitation	mm	awzypt
X	downwind distance from non-erodible	m	-
$x_{i,yj}$	coordinates of the center of each cell	m	lx, ly
xbr	normalized barrier width (barrier width divided by barrier height)	unitless	xw
Z_0	aerodynamic roughness length	mm	sbz0
Z_{0rg}	aerodynamic roughness of the ridges	mm	wzorg
Z_{0rr}	aerodynamic roughness of random roughness including any flat biomass cover	mm	wzorr
Z_{0st}	aerodynamic roughness at weather station, assumed to be 25 mm in WEPS	mm	awzzo
Z	height above the surface	mm	-
Z_d	zero-plane displacement	mm	-
Z_{st}	anemometer height at the weather station; (wind speeds were adjusted to 10 m height in the WEPS data base)	mm	anemht
Z_{0v}	as defined by Eq. 49, 50, and 51	mm	wzzov

*a dash (-) in this column indicates there is no variable name.

Hydrology Submodel of WEPS

Contributors:

F.A. Fox
A.A. Durar
E.L. Skidmore

Abstract

The Hydrology submodel of the Wind Erosion Prediction System (WEPS) models the movement of water within the atmospheric boundary layer and vadose zone. Inputs generated by weather generators as well as the crop growth, soil, management, and residue decomposition submodels provide inputs to the Hydrology submodel. The Hydrology submodel tracks the soil water content and temperature, with special emphasis on the water content at the soil-atmosphere interface, which is a significant factor in the wind erosion threshold friction velocity. The soil water content affects crop growth and residue decomposition. Changes in soil water content and temperature influence changes in the soil aggregate size distribution and soil aggregate stability, which are also significant factors in the erodibility of soil by wind. The Hydrology submodel of WEPS maintains a continuous, daily, soil water mass and energy balance including a surface snow layer. Evapo-transpiration is partitioned into evaporation at the soil/snow atmospheric interface and crop transpiration, accounting for standing and flat crop residue evaporation suppression effects. Water flows modeled include rainfall, runoff, surface and subsurface irrigation applications, and drainage. Soil texture and bulk density are used to estimate soil hydraulic properties. Two methods of solving the soil water balance are implemented. In the first, the one-dimensional Darcy equation is applied to a thinly layered soil profile and solved as a system of ordinary differential equations. The soil water content at the soil-atmosphere interface is then estimated using the functional relationship between surface-soil wetness and the evaporation ratio. The second, faster, method uses the Water Erosion Prediction Project (WEPP) hydrology model adapted to the WEPS modeling system. For this, the soil water content at the soil-atmosphere interface is estimated using the water content of a very thin surface layer. Using data from two field studies, the Hydrology submodel of WEPS shows good results in estimating the susceptibility of the soil to wind erosion from a dry surface when configured to use the evaporation ratio with the one-dimensional Darcy equation method or when using the WEPP hydrology component. The one-dimensional Darcy equation method over-predicted the cumulative evaporation from the soil profile, limiting its usefulness for predicting crop available water after fallow periods. Use of the WEPP hydrology component for this purpose would give better results, although it under predicts the loss of water to evaporation during long periods without rainfall. Additional validation is recommended.

Introduction

An unpublished draft of the technical documentation of the Hydrology submodel of the Wind Erosion Prediction System (WEPS) was created by Durar and Skidmore in 1995 to reflect the current status of the Hydrology submodel code in the early stages of its development, 19 years ago as of this writing. That document was primarily comprised

from Durar (1991) and Durar et al. (1995). This present document is a modification of that original document specifically reflecting the changes made to the Hydrology submodel code since that time by the first author.

Simulation runs made with WEPS during further development and during testing by Natural Resource Conservation Service (NRCS) personnel revealed elements that did not perform across a wide range of soil types, climatic conditions, and management scenarios. The section, “Precipitation, Snow, Snow Melt, and Soil Temperature”, reflects the addition of a daily mass and energy balance to correct a problem with model runs in the Northern Great Plains, where modeled snow cover would remain throughout the summer. Revisions in the section, “Daily Potential Evapotranspiration” are limited to the addition of Eq. 55. The section, “Potential Soil Evaporation and Plant Transpiration”, reflects the modification of evapo-transpiration partitioning and the modification of residue evaporation suppression to account for standing and flat residue. In the section, “Actual Transpiration and Water Stress Factor”, Eq. 64 and the preceding paragraph indicate changes made to better model plant transpiration in extremely sandy soils. In the section, “Infiltration, Surface Runoff, Evaporation, and Deep Percolation”, changes made were to convert the solution of the one-dimensional Darcy equation from a simplified forward finite difference technique to the solution of a system of ordinary differential equations, to modify the partitioning of infiltration and runoff, to incorporate surface and subsurface irrigation, to add new soil surface evaporation methods, and to modify rainfall, irrigation, and evaporation disaggregation methods. This was mainly in response to observed instability in the soil water redistribution routines, availability of additional research in the literature, and the need for better irrigation water application integration. The section, “Infiltration, Surface Runoff, Evaporation, and Deep Percolation”, describes the addition of an alternate fast stable hydrology method in response to NRCS field office needs for faster simulation times. The section, “Estimating Soil Hydraulic Properties”, describes the addition of new routines to estimate soil hydraulic properties across a wider range of soil types and under conditions of changing bulk density. The sections, “Soil Wetness at the Soil-Atmosphere Interface” and “Simulation of Diurnal Soil Temperature”, essentially remain unchanged. For the section, “Submodel Testing and Evaluation”, results from the current version of model were incorporated into the validation scenarios and the discussion modified to reflect the new results.

The Hydrology submodel uses inputs generated by other WEPS weather generators (i.e., Weather) and submodels such as Crop, Soil, Management, and Decomposition to predict water content in the various layers of the soil profile and at the soil-atmosphere interface throughout the simulation period. Accurate simulation by the other WEPS submodels requires prediction of the daily changes in soil water profiles. However, estimating soil wetness at the soil-atmosphere interface is emphasized, because it significantly influences the susceptibility of the soil to wind erosion.

The Hydrology submodel of WEPS maintains a continuous, daily, soil water balance using the equation:

$$swc = swci + (prcp - snow + dirg) + snmlt - runoff - eta - dprc \quad [1]$$

where

swc = the amount of water on the soil profile in any given day (mm),

$swci$ = the initial amount of water in the soil profile (mm),

prcp = the amount of daily precipitation (mm),
dirg = the amount of daily irrigation (mm),
snow = the amount of daily precipitation that falls as snow,
snmelt = the daily snow melt (mm),
runoff = the amount of daily surface runoff (mm),
eta = the amount of daily actual evapotranspiration (mm), and
dprc = the amount of daily deep percolation (mm).

The amount of daily precipitation (*prcp*) is partitioned between rainfall and snowfall on the basis of the average daily air temperature. Melted snow (*snmelt*) and, if applied above ground, daily irrigation (*dirg*) are added to the precipitation term in Eq.1 when accounting for daily runoff and infiltration.

Simulation of soil-water dynamics on a daily basis by the Hydrology submodel was first implemented using the one-dimensional application of Darcy's law as a system of ordinary differential equations (Hillel 1977), which was translated from CSMP into FORTRAN 77 except for the integration method. Infiltration was found using the SCS runoff curve number approach (USDA Soil Conservation Service 1972) and was considered instantaneous. The redistribution of water within the soil was then solved using an explicit finite difference method with rectangular integration and one hour time steps (Durar et al. 1995, Durar 1991). While adequate for some conditions, the method exhibited numerical instability and was later modified to use integration routines of LSODA (Hindmarsh 1983), allowing for the dynamic simulation of infiltration, runoff, and evapotranspiration, with some penalty in computation time. For use with NRCS, the time required to complete a simulation was longer than acceptable for the computer systems available to them at the time and a faster method was required. For that reason, the Water Erosion Prediction Project (WEPP) Hydrology submodel (Flanagan and Nearing 1995) was integrated into the WEPS Hydrology submodel. The WEPP Hydrology submodel is faster, and provides stable solutions to the soil water balance, but does not physically model the water content of the soil surface, especially diurnal water content fluctuations near the soil surface, requiring the use of estimation techniques. Both the Darcian-based method and the WEPP method are implemented in WEPS and either can be selected for a simulation run. In this Hydrology submodel chapter the common elements are described, the Darcian-based equations are described in detail, and the modifications required for using the WEPP method are enumerated. Comparisons between the two methods are given in two surface drying validation cases.

The Hydrology submodel estimates surface runoff and infiltration for each simulation day that has precipitation, irrigation, or snowmelt. Both the Darcian-based method and the WEPP method require a time-intensity curve for all water sources, which are either directly input to the simulation or estimated. Both methods then distribute the infiltration water into the soil, determine the runoff amount, and indicate any deep percolation amounts. Potential evapotranspiration is calculated using a revised version of Penman's combination method (Van Bavel 1966). The total daily rate of potential evapotranspiration is then partitioned on the basis of the plant leaf area index into potential soil evaporation and potential plant transpiration. The potential rate of soil evaporation is adjusted to account for the effect of plant residues in the simulation region. Furthermore, the daily potential rates of soil evaporation and plant transpiration are adjusted to actual rates on the basis of water availability in the soil profile.

Knowledge of the relationship between unsaturated hydraulic conductivity and soil water content is required for solving the governing transport equations of water movement through the soil. The Darcian-based method uses Campbell's (1974) method to calculate the unsaturated hydraulic conductivity of the soil from the more readily available soil water characteristic curve and saturated hydraulic conductivity data. Soil water characteristic curve data for soils are not always available, and estimation methods based on basic physical properties are implemented.

The Darcian-based method estimates hourly soil wetness at the soil-atmosphere interface with the functional relationship between surface-soil wetness and the evaporation ratio. The WEPP method uses the top layer surface water content.

Submodel Development and Description

As stated by Durar et al. (1995), some of the algorithms used in the Hydrology submodel are similar to those used in well-established models such as the Soil-Plant-Atmosphere-Water model (SPA) (Saxton and Bluhm 1982, Saxton et al, 1974, 1984, Sudar et al. 1981), the field scale model for Chemicals, Runoff, and Erosion from Agricultural Management Systems (CREAMS) (Smith and Williams 1980), and the Erosion Productivity Impact Calculator model (EPIC) (Williams et al. 1984, 1990). Significant modifications were made by Durar (1991), with later modifications by the first author, and new algorithms were added to meet the unique requirements of WEPS for faster simulation of the diurnal changes in soil water content, particularly at the soil-atmosphere interface.

Precipitation, Snow, Snow Melt, and Soil Temperature

In order to better model winter conditions in northern latitudes, a daily mass and energy balance was applied to the layered soil system and an additional surface snow layer. Campbell (1985) gives a finite difference energy balance equation, but does not include freezing, thawing, or mass fluxes in his development. Using that equation as a starting point, a daily mass and energy balance was developed by the first author to include freezing, thawing, and snow cover mass fluxes.

Daily precipitation can occur as either rain or snow. No consideration is given to wintery mix, sleet, or hail. Precipitation is considered to be snow if the daily average temperature is 0 °C or below. Irrigation can also provide an above ground water source, and for our purposes, it is considered to be liquid when it reaches the surface. If there is an existing snow layer when either precipitation or irrigation above the snow layer occurs, a mass and energy balance of the snow layer is calculated. Irrigation and precipitation are applied to the snow layer separately, and any drainage amount from the snow layer is tracked separately as well to allow different durations for the two water sources in the infiltration calculations. The mass of any added water, either snow, rain, or irrigation, is found using:

$$M_{adv} = x_{adv}\rho_w \quad [2]$$

where

M_{adv} = the mass of added water (kg m⁻²),
 x_{adv} = the depth of added water (m), and
 ρ_w = the density of water (kg m⁻³).

The energy of the added water depends on its temperature and state and is found using:

$$Q_{adw} = \begin{cases} M_{adw}(T_{dav}c_{ice} - H_{fus}), & T_{dav} \leq 0, \text{ snow} \\ M_{adw}T_{dav}c_{wat}, & T_{dav} > 0, \text{ rain, irrigation} \end{cases} \quad [3]$$

where

Q_{adw} = the energy content of the added water (J m^{-2}),

T_{dav} = the daily average air temperature and considered to be the water temperature as well ($^{\circ}\text{C}$),

H_{fus} = the latent heat of fusion of water (J kg^{-1}),

c_{ice} = the specific heat capacity of ice ($\text{J kg}^{-1} \text{ } ^{\circ}\text{C}^{-1}$), and

c_{wat} = the specific heat capacity of liquid water ($\text{J kg}^{-1} \text{ } ^{\circ}\text{C}^{-1}$).

Water added to the snow layer as a liquid does not augment the snow layer depth but is assumed to enter the pore spaces. When the water is added to the snow layer as snow, its thickness also needs to be added. For new snow, the thickness added is found using the new snow density, adapted from Anderson (1976):

$$\rho_{asn} = \begin{cases} 50, & T_{wb} \leq -14.99 \\ 50 + 1.723(T_{wb} + 14.99)^{1.5}, & -14.99 < T_{wb} < 0 \\ 150, & T_{wb} \geq 0 \end{cases} \quad [4]$$

where

ρ_{asn} = the density of new snow (kg m^{-3}) and

T_{wb} = the wet bulb temperature ($^{\circ}\text{C}$).

The thickness to be added to the snow layer for this precipitation event becomes:

$$x_{asn} = \begin{cases} \frac{M_{adw}}{\rho_{asn}}, & T_{dav} \leq 0, \text{ snow} \\ 0, & T_{dav} > 0, \text{ rain, irrigation} \end{cases} \quad [5]$$

where

x_{asn} = the thickness to be added to the existing snow layer (m).

Using the new mass, depth, and energy being added to the snow layer, the average properties of the layer can be found and drainage from the snow layer determined. The total energy of the previously existing snow layer is:

$$Q_{sno} = M_{sno}(F_{ice}(T_{sno}c_{ice} - H_{fus}) + (1 - F_{ice})T_{sno}c_{wat}) \quad [6]$$

where

Q_{sno} = the relative total energy of the existing snow layer (J m^{-2}),

M_{sno} = the total mass of the existing snow layer (kg m^{-2}),

F_{ice} = the mass fraction of water in the existing snow layer that is frozen, and

T_{sno} = the temperature of the existing snow layer ($^{\circ}\text{C}$).

For the amended snow layer, the mass becomes:

$$\begin{aligned} M'_{sno} &= M_{sno} + M_{adw} \\ x'_{snw} &= \frac{M'_{sno}}{\rho_w} \end{aligned} \quad [7]$$

where

M'_{sno} = the mass of the amended snow layer (kg m⁻²) and

x'_{snw} = the depth of water in the amended snow layer in liquid water equivalent (m).

The total energy becomes:

$$Q'_{sno} = Q_{sno} + Q_{adw} \quad [8]$$

where

Q'_{sno} = the relative total energy of the amended snow layer (J m⁻²).

The modified depth becomes:

$$x'_{sno} = x_{sno} + x_{asn} \quad [9]$$

where

x'_{sno} = the depth of the amended snow layer (m).

The average state of the amended snow layer is found from the mass, energy, and density. Where liquid water has been added to the snow layer, drainage may occur. If the layer were totally frozen at 0° C, the total energy of the layer would be:

$$Q'_{frz} = -H_{fus}M'_{sno} \quad [10]$$

where

Q'_{frz} = the relative total layer energy if fully frozen at 0° C (J m⁻²).

The temperature, frozen fraction of the layer, depth, and water content adjustments can now be determined. When the frozen fraction goes to zero, all of the snow water content will be liquid, the snow layer will be set to zero, and the water will be made available for infiltration and/or runoff as either precipitation that passed through the snow layer or irrigation that passed through the snow layer.

$$Q'_{sno} \leq Q'_{frz} \left\{ \begin{aligned} T'_{sno} &= \frac{\left(\frac{Q'_{sno}}{M'_{sno}} + H_{fus} \right)}{c_{ice}} \\ F'_{ice} &= 1.0 \\ x_{mlt} &= 0 \end{aligned} \right. \quad [11]$$

$$\begin{aligned}
& Q'_{frz} < Q'_{sno} \\
& T'_{sno} = 0 \\
& F'_{ice} = \frac{-Q'_{sno}}{M'_{sno} H_{fus}} \\
& x''_{sno} = x'_{sno} \left(\frac{F'_{ice} M'_{sno}}{F_{ice} M_{sno}} \right) \\
& \rho''_{sno} = \frac{M'_{sno}}{x''_{sno}} \\
& \left. \begin{array}{l} < 0, \\ \rho''_{sno} > 350, \end{array} \right\} \begin{cases} F''_{ice} = \min \left(1, F'_{ice} \frac{\rho''_{sno}}{350} \right) \\ x_{melt} = x'_{snw} \left((1 - F'_{ice}) - (1 - F''_{ice}) \frac{F'_{ice}}{F''_{ice}} \right) \\ x''_{snw} = x'_{snw} - x_{melt} \\ \rho''_{sno} \leq 350, \{ x_{melt} = 0 \end{cases} \\
& Q'_{sno} \geq 0, \left\{ \begin{array}{l} T'_{sno} = 0 \\ F'_{ice} = 0 \\ x''_{sno} = 0 \\ x''_{snw} = 0 \\ x_{melt} = x'_{snw} \end{array} \right.
\end{aligned}$$

where

T'_{sno} = the temperature of the amended snow layer (°C),

F'_{ice} = the fraction of frozen water in the amended snow layer,

F''_{ice} = the fraction of frozen water in the amended snow layer accounting for the change in snow density,

x''_{sno} = the depth of the snow layer adjusted for the change in frozen water fraction,

ρ''_{sno} = the density of the snow layer adjusted for the change in frozen water fraction (kg m⁻³),

x_{melt} = the liquid water that drains from the snow layer (m), and

x''_{snw} = the depth of water in the snow layer after drainage in liquid water equivalent (m).

The depth of precipitation and/or above ground irrigation captured by the snow layer and the snow melt are then:

$$\begin{aligned}
snow &= x''_{snw} \\
snmelt &= x_{melt}
\end{aligned} \tag{12}$$

The snow melt component of the Hydrology submodel of WEPS is based on a daily single snow layer energy balance combined with the energy balance of the soil layers. To simplify the calculations, the daily average temperature of each layer, either snow or soil, is found using a daily energy balance independent of the soil water dynamic calculations. The change in the heat energy content of a layer is written as:

$$q = R_{rn} + h_a(T_a - T_l) - h_b(T_l - T_b) \quad [13]$$

where

q = the change in heat energy content of the layer ($\text{J m}^{-2} \text{s}^{-1}$),

R_{rn} = the net radiation gain to the upper surface of the layer ($\text{J m}^{-2} \text{s}^{-1}$),

h_a = the heat transfer coefficient between this layer and the layer above ($\text{J m}^{-2} \text{s}^{-1} \text{ } ^\circ\text{C}^{-1}$),

h_b = the heat transfer coefficient between this layer and the layer below ($\text{J m}^{-2} \text{s}^{-1} \text{ } ^\circ\text{C}^{-1}$),

T_a = the temperature of the layer above ($^\circ\text{C}$),

T_l = the temperature of the layer ($^\circ\text{C}$), and

T_b = the temperature of the layer below ($^\circ\text{C}$).

For all soil layers, the net radiation is considered to be zero, including the surface layer where the net surface radiation is accounted for by the surface energy balance used to find latent heat transfer.

For the snow layer, the net radiation is found using Wright's modified version of Penman's general relationship (Wright 1982) outlined by Allen et al. (1989) with the albedo of the snow surface. If a snow cover exists with 5 mm or greater water content, the value of albedo is set to 0.6. If the snow cover is less than 5 mm and no crop is growing, the soil albedo is used.

Using the method of Campbell (1985), the heat transfer coefficient, h_a , between the layer above and the current layer uses the geometric means of the thermal conductivity divided by half the layer thickness, written as:

$$h_a = \frac{2k_a k_l}{x_a k_a + x_l k_l} \quad [14]$$

where

k_a = the thermal conductivity of the layer above ($\text{J s}^{-1} \text{ m}^{-1} \text{ } ^\circ\text{C}^{-1}$),

k_l = the thermal conductivity of this layer ($\text{J s}^{-1} \text{ m}^{-1} \text{ } ^\circ\text{C}^{-1}$),

x_a = the thickness of the layer above (m), and

x_l = the thickness of this layer (m).

The thermal transfer coefficient between this layer and the layer below is found similarly. Thermal conductivity for a soil layer is found using the volumetrically weighted method attributed to Johansen in Peters-Lidard et al. (1998), given as:

$$k_l = N_{ker}(k_{ss} - k_{sd}) + k_{sd} \quad [15]$$

where

N_{ker} = the Kersten number,

k_{ss} = the thermal conductivity of saturated soil ($\text{J s}^{-1} \text{ m}^{-1} \text{ } ^\circ\text{C}^{-1}$), and

k_{sd} = the thermal conductivity of dry soil ($\text{J s}^{-1} \text{ m}^{-1} \text{ } ^\circ\text{C}^{-1}$).

The Kersten number is found using:

$$N_{ker} = \begin{cases} 0, & S_w \leq 10^{\left(\frac{-1}{1-0.3F_{san}}\right)} \\ (1 - 0.3F_{san})\log_{10}(S_w) + 1, & S_w > 10^{\left(\frac{-1}{1-0.3F_{san}}\right)} \end{cases} \quad [16]$$

where

F_{san} = the mass fraction of sand in the mineral portion of the soil and

S_w = the degree of saturation found from the ratio of volumetric water content to saturated volumetric water content.

The thermal conductivity of dry soil is given as:

$$k_{sd} = \frac{135\rho_b + 64.7}{2700 - 947\rho_b} \quad [17]$$

where

k_{sd} = the dry soil thermal conductivity ($J s^{-1} m^{-1} ^\circ C^{-1}$) and

ρ_b = the bulk density of the soil ($Mg m^{-3}$).

The thermal conductivity of saturated soil is found using:

$$k_{ss} = (k_{sm})^{(1-\theta_s)}(k_{ice})^{(\theta_s-f_{wat})}(k_{wat})^{(f_{wat})} \quad [18]$$

where

k_{ss} = the thermal conductivity of saturated soil ($J s^{-1} m^{-1} ^\circ C^{-1}$),

k_{sm} = the thermal conductivity of solid soil matrix consisting of mineral and organic material elements ($J s^{-1} m^{-1} ^\circ C^{-1}$),

k_{ice} = the thermal conductivity of ice ($J s^{-1} m^{-1} ^\circ C^{-1}$),

k_{wat} = the thermal conductivity of water ($J s^{-1} m^{-1} ^\circ C^{-1}$),

θ_s = the soil water content at saturation (m^3 water m^{-3} bulk soil), and

f_{wat} = the volume fraction of the soil water that is liquid water.

The thermal conductivity of the solid soil matrix is found using:

$$k_{sm} = (k_{qtz})^{(f_{qtz})}(k_{min})^{(1-f_{qtz}-f_{om})}(k_{om})^{(f_{om})} \quad [19]$$

where

k_{sm} = the thermal conductivity of the solid soil matrix ($J s^{-1} m^{-1} ^\circ C^{-1}$),

k_{qtz} = the thermal conductivity of quartz ($J s^{-1} m^{-1} ^\circ C^{-1}$),

k_{min} = the thermal conductivity of the non-quartz mineral portion of the soil ($J s^{-1} m^{-1} ^\circ C^{-1}$),

k_{om} = the thermal conductivity of the organic matter portion of the soil ($J s^{-1} m^{-1} ^\circ C^{-1}$),

f_{qtz} = the volumetric fraction of soil that is quartz, and

f_{om} = the volumetric fraction that is organic matter.

Using values from Bristow (2002), $k_{qtz} = 8.8$, $k_{min} = 2.9$, $k_{om} = 0.25$, $k_{ice} = 2.18$, and k_{wat} uses the relationship:

$$k_{wat} = 0.552 + 0.00234T_{wat} - 1.1 * 10^{-5}(T_{wat})^2 \quad [20]$$

where

T_{wat} = the temperature of the water ($^{\circ}\text{C}$).

The volume fraction of water in the soil is found using:

$$f_{wat} = \frac{\theta_s \rho_{ice} (1 - F_{ice})}{\rho_{ice} (1 - F_{ice}) + F_{ice}} \quad [21]$$

where

ρ_{ice} = the density of ice (Mg m^{-3}) and

F_{ice} = the mass fraction of water in the soil that is frozen.

The volume fraction of quartz in the soil is calculated by:

$$f_{qtz} = \frac{F_{san} (1 - F_{om})}{1 + F_{om} \left(\frac{\rho_{qtz}}{\rho_{om}} - 1 \right)} \quad [22]$$

where

F_{san} = the mass fraction of sand in the mineral portion of the soil,

F_{om} = the mass fraction of organic matter in the solid mass portion of the soil,

ρ_{qtz} = the density of quartz (Mg m^{-3}), and

ρ_{om} = the density of the organic matter (Mg m^{-3}).

Similarly, the volume fraction of organic matter in the soil is found using:

$$f_{om} = \frac{F_{om} (1 - F_{san})}{(1 - F_{om}) \frac{\rho_{om}}{\rho_{qtz}} - F_{om}} \quad [23]$$

The density of soil organic matter varies, with values given of 1.37 Mg m^{-3} in Baver et al. (1972) and 1.1 Mg m^{-3} in Marshall and Holmes (1979). An “average” value of 1.23 Mg m^{-3} is used here. The common value for the density of quartz is 2.65 Mg m^{-3} .

When the surface layer is a snow layer, the conductive thermal transfer coefficient to the atmosphere, h_a , is the conductivity of the layer divided by one half the layer thickness, written as:

$$h_a = 2.0 \frac{k_{sno}}{x_{sno}} \quad [24]$$

where

k_{sno} = the thermal conductivity ($\text{J s}^{-1} \text{ m}^{-1} \text{ }^{\circ}\text{C}^{-1}$) and

x_{sno} = the thickness of the snow layer (m).

The thermal conductivity is a function of snow density and uses the relationship originally developed by DeVries, used in SHAW, and given in Anderson (1976) as:

$$k_{sno} = 0.021 + 2.51 \left(\frac{\rho_{sno}}{1000} \right)^2 \quad [25]$$

where

ρ_{sno} = the snow density (kg m⁻³).

When there is no snow layer, the thermal conductivity and thickness of the residue layer are used to find an effective thermal conductivity for heat transfer to the atmosphere as described in van Donk and Tollner (2000). As a first approximation, the wind velocity function is ignored, and the heat capacity of the residue layer is also assumed to be zero. This is written as:

$$k_a = \frac{1}{\left(\frac{0.5 \frac{x_l}{k_l} + \frac{x_{res}}{k_{res}}}{0.5x_l + x_{res}} \right)} \quad [26]$$

where

k_{res} = the thermal conductivity of the residue layer, estimated at 0.22 (J (s⁻¹ m⁻¹ °C⁻¹)) and

x_{res} = the thickness of the residue layer (m).

The thickness of the residue layer is estimated using:

$$x_{res} = \frac{M_{res}}{\rho_{res}} \quad [27]$$

where

M_{res} = the mass of residue flat on the soil surface (kg m⁻²) and

ρ_{res} = the residue density, estimated to be 13 kg m⁻³.

The heat transfer coefficient for the bottom layer is found using the thermal conductivity of the bottom layer and the distance from the center of the layer to the depth where the temperature is assumed to be constant at the average annual temperature, in this case 5 m.

To find the new temperature for a layer, the energy balance is written as:

$$T'_l = \frac{\left(T_l + \frac{\Delta t q}{C_{vl} x_l} \right)}{\left(1 + \frac{\Delta t (h_a + h_b)}{C_{vl} x_l} \right)} \quad [28]$$

where

T'_l = the new layer temperature at the end of the time step (°C),

T_l = the temperature of the layer at the beginning of the time step (°C),

Δt = the time step (s), and

C_{vl} = the volumetric heat capacity of the layer (J m⁻³ °C⁻¹).

For any layer, the mass fraction weighted volumetric heat capacity, based on the method by De Vries and defined in Kluitenberg (2002), is written as:

$$C_{vl} = 1000\rho_b \left[\begin{array}{l} F_{san}c_{san}(1 - F_{om}) + F_{sil}c_{sil}(1 - F_{om}) \\ + F_{cla}c_{cla}(1 - F_{om}) + F_{om}c_{om} \\ + w c_{wat}(1 - F_{ice}) + w F_{ice}c_{ice} \end{array} \right] \quad [29]$$

where

ρ_b = the bulk density of the layer (Mg m^{-3}),

w = the gravimetric water content (Mg m^{-3}),

c = the specific heat capacity of each layer component as designated by the subscript ($\text{J kg}^{-1} \text{ } ^\circ\text{C}^{-1}$), and

F = the mass fraction of each component represented in the layer as designated by the subscript with subscripts *san* for sand, *sil* for silt, *cla* for clay, *om* for organic matter, *wat* for water and *ice* for ice.

Note that F_{san} , F_{sil} , and F_{cla} sum to one so that $(1 - F_{om})$ gives the ratio mass of mineral soil to total mass of dry soil and F_{ice} is the mass fraction of the layer water content that is ice. To find the volumetric heat capacity of the snow layer, the bulk density is set to one, the gravimetric water content is set to one, and all soil fractions set to zero.

As the temperature reaches the freezing/thawing point, the temperature will remain constant while the water changes phase. If the calculation of the new temperature in Eq. 28 crosses 0°C , the latent heat of fusion must be considered. To find the time at which 0°C is reached, T_l in Eq. 28 is set to zero and the equation rearranged giving:

$$\Delta t_{b1} = \frac{-T_l c_{vl} x_l}{q} \quad [30]$$

where

Δt_{b1} = the time required for the layer to reach 0°C (s).

If the starting layer temperature is 0°C , the fraction of the water which is ice could be any value between zero and one inclusive and Δt_{b1} is set to zero. Relative to the beginning of the time step, the time at which the water in the layer is completely thawed, if it is warming, is found using:

$$\Delta t_{b2} = \Delta t_{b1} + \frac{F_{ice} \theta_l H_{fus} x_l \rho_w}{q} \quad [31]$$

where

Δt_{b2} = the time from the beginning of the time step when the layer is completely thawed (s),

θ_l = the volumetric water content of the layer (m^3 water per m^3 layer volume), and

H_{fus} = the latent heat of fusion of water (J kg^{-1}), and

ρ_w = the density of water (kg m^{-3}).

If the layer is cooling, the time at which the layer is completely frozen is found using:

$$\Delta t_{b2} = \Delta t_{b1} + \frac{(F_{ice} - 1)\theta_l H_{fus} x_l \rho_w}{q} \quad [32]$$

If this time Δt_{b2} in either Eq. 31 or 32 is greater than the time step, then the layer temperature remains at 0° C and the new fraction of ice in the layer is found using:

$$F'_{ice} = F_{ice} - \frac{q(\Delta t - \Delta t_{b1})}{\theta_l H_{fus} x_l \rho_w} \quad [33]$$

where

F'_{ice} = the fraction of layer water that is frozen at the end of the time step.

If the layer temperature at the beginning of the time step is 0° C, then the start time for freezing or thawing, Δt_{b1} , is zero.

If this time Δt_{b2} in either Eq. 31 or 32 is less than the time step, then the layer either completely freezes or thaws, and the layer continues warming or cooling for the remainder of the time step ($\Delta t - \Delta t_{b2}$). Substituting this shorter time interval with a starting temperature of 0 °C into Eq. 28 gives the temperature at the end of the time step. Note that the latent heat of evaporation is accounted for in the soil water dynamics calculations and is not considered here.

Having estimated the daily average temperature for each of the layers, the depth of the snow layer is adjusted, the depth of water leaving the snow layer is estimated, and the daily maximum and minimum temperatures for each soil layer are estimated based on the daily maximum and minimum air temperatures.

The depth of the snow layer will change in response to a change in frozen fraction (melting) and compact and settle as a function of snow density and temperature as described in Anderson (1976). First, when the energy balance calculations find the new frozen fraction, the depth of the snow is adjusted using:

$$x'_{sno} = \begin{cases} x_{sno} \frac{F'_{sno}}{F_{sno}}, & F'_{sno} < F_{sno} \\ x_{sno}, & F'_{sno} \geq F_{sno} \end{cases} \quad [34]$$

where

x'_{sno} = the new snow depth due to a change in frozen fraction (m).

Then, changes in the snow depth due to compaction and settling use snow density calculations as follows:

$$\rho'_{sno} = \frac{x_{snw} \rho_{wat}}{x'_{sno}} \quad [35]$$

where

ρ'_{sno} = the average density of the snow layer after adjusting for frozen fraction (kg m⁻³)
and

x_{snw} = the total water content of the snow layer (m of liquid water).

Without the use of multiple snow layers, the increase in density due to compaction is estimated using part of the snow layer water content as overburden using the equation:

$$\rho''_{sno} = \rho'_{sno} \left[1 + 80x_{snw} e^{\left(0.08T'_{sno} - 21\frac{\rho'_{sno}}{1000}\right)} \right] \quad [36]$$

where

ρ''_{sno} = the snow density adjusted for compaction (kg m^{-3}).

The increase in density from settling is estimated using the equation:

$$\rho'''_{sno} = \begin{cases} \rho''_{sno} \left(1 + 0.24e^{(0.4T'_{sno})}\right), & \rho''_{sno} \leq 150 \\ \rho''_{sno} \left(1 + 0.24e^{(0.4T'_{sno})} e^{(-46(\rho''_{sno}-150))}\right), & \rho''_{sno} > 150 \end{cases} \quad [37]$$

where

ρ'''_{sno} = the snow density adjusted for settling (kg m^{-3}) and

T'_{sno} = the daily average temperature of the snow layer ($^{\circ}\text{C}$).

To compensate for using only daily average temperatures, whereas the actual process is affected by the daily maximum temperature, an additional adjustment to the density is applied:

$$\rho''''_{sno} = \begin{cases} \rho'''_{sno}, & T_{dmx} \leq 0 \\ \rho'''_{sno} \left(1 + \frac{T_{dmx}}{25}\right), & T_{dmx} > 0 \end{cases} \quad [38]$$

where

ρ''''_{sno} = the snow density adjusted for the daily maximum air temperature (kg m^{-3}) and

T_{dmx} = the daily maximum air temperature ($^{\circ}\text{C}$).

Once the state of the snow layer has been adjusted, if the frozen fraction is less than one, Eq. 11 is used to determine the amount of water that may drain from the snow layer.

Evapotranspiration

The amount of daily actual evapotranspiration is found:

$$eta = E_a + \mathcal{T}_a \quad [39]$$

where

E_a = the daily actual evaporation (mm day^{-1}) and

\mathcal{T}_a = the daily actual plant transpiration (mm day^{-1}).

Daily potential evapotranspiration is partitioned into daily potential evaporation and daily potential transpiration, each of which may then be limited by available water and physical reduction factors. The daily potential evapotranspiration comes mainly from Durar (1991).

Daily Potential Evapotranspiration

Daily potential evapotranspiration is calculated using the revised combination method of Van Bavel (1966), which combines a surface energy balance equation and an approximate expression of water vapor and sensible heat transfer, as influenced by surface roughness and ambient air properties. Van Bavel considered his method an improvement over the original version of the combination equation (Penman 1948), because it contains no empirical constants or functions.

Van Bavel (1966) conducted an extensive validation of his method in Phoenix, Arizona, concluding that the method provides an excellent estimation of potential evapotranspiration on an hourly and daily basis under a wide variety of test conditions. Further evaluation of the combination method of Van Bavel in Kansas (Skidmore et al. 1969) and Texas (Wendt 1970) showed that it can provide reasonably good estimates of potential evapotranspiration, particularly in areas with large amounts of advection. Furthermore, Jensen (1974) evaluated 16 different methods to estimate potential evapotranspiration at 10 different locations throughout the world. The elevations of these sites ranged from 30 m below sea level to 2774 m above sea level, and the latitudes ranged from 38°S at Victoria, Australia to 56°N at Copenhagen, Denmark. He then ranked Van Bavel's method as one of the best methods to estimate potential evapotranspiration, especially in the inland semi-arid to arid regions.

For use on a daily basis, the Van Bavel equation is expressed as:

$$E\mathcal{T}_p = \frac{\left(\frac{\Delta}{\gamma}\right) \left(\frac{R_n - G}{\lambda}\right) + C_{tt}(e_z^o - e_z)}{\left(\frac{\Delta}{\gamma}\right) + 1} \quad [40]$$

where

$E\mathcal{T}_p$ = the potential evapotranspiration (mm day⁻¹),

$\left(\frac{\Delta}{\gamma}\right)$ = the adjusted ratio of the slope of the saturation vapor pressure curve taken at mean air temperature to the psychrometric constant,

$(R_n - G)$ = the sum of surface energy inputs (MJ m⁻² day⁻¹),

R_n = the net radiation (MJ m⁻² day⁻¹),

G = the soil heat flux (MJ m⁻² day⁻¹),

λ = the latent heat of vaporization (MJ kg⁻¹),

C_{tt} = the turbulent transfer coefficient for water vapor (kg m⁻² kPa⁻¹ day⁻¹),

$(e_z^o - e_z)$ = the saturation vapor pressure deficit of air (kPa),

e_z^o = the daily saturation vapor pressure of the air (kPa), and

e_z = the daily vapor pressure of the air (kPa).

Because the psychrometric constant is proportional to the ambient barometric pressure, the adjusted ratio of the slope of the saturation vapor pressure curve to the psychrometric constant is estimated with the equation:

$$\left(\frac{\Delta}{\gamma}\right) = \frac{101.325}{P_B} \left(\frac{\Delta}{\gamma}\right)_o \quad [41]$$

where

$\left(\frac{\Delta}{\gamma}\right)_o$ = the unadjusted ratio of the slope of the saturation vapor pressure curve taken at mean air temperature to the psychrometric constant and

P_B = the ambient barometric pressure (kPa).

The $(\Delta \gamma^{-1})_0$ term in Eq. 39 is a dimensionless number dependent on air temperature. The tabulated values of the term are listed versus air temperature in Table 5 of Van Bavel (1966). However, to simplify the computation of the term in our computer coding, the data of the table were regressed, and the following expression of $(\Delta \gamma^{-1})_0$ as a function of temperature was obtained:

$$\left(\frac{\Delta}{\gamma}\right)_0 = 67.5242e^{\left(\frac{T_{daj}-149.531}{-4859.0655}\right)} \quad [42]$$

where

T_{daj} = the adjusted mean daily air temperature (°C).

The coefficient of determination (r^2) for Eq. 42 is 1.00. Where the weather data is obtained under conditions of evapotranspiration less than the potential value, the temperatures need to be adjusted to reflect what they would be if potential evapotranspiration were occurring as described in Allen (1996). T_{daj} is found using:

$$\begin{aligned} \Delta T &= T_{dmn} - T_{dew} - 2 \\ T_{mnj} &= \begin{cases} T_{dmn} - 0.5\Delta T, & \Delta T > 0 \\ T_{dmn}, & \Delta T \leq 0 \end{cases} \\ T_{mxj} &= \begin{cases} T_{dmx} - 0.5\Delta T, & \Delta T > 0 \\ T_{dmx}, & \Delta T \leq 0 \end{cases} \\ T_{daj} &= 0.5(T_{mxj} + T_{mnj}) \\ T_{dwj} &= \begin{cases} T_{dew} + 0.5\Delta T, & \Delta T > 0 \\ T_{dew}, & \Delta T \leq 0 \end{cases} \end{aligned} \quad [43]$$

where

T_{dmn} = the daily minimum air temperature (°C),

T_{dew} = the measured dew point temperature (°C),

T_{mnj} = the adjusted daily minimum air temperature (°C),

T_{mxj} = the adjusted daily maximum air temperature (°C), and

T_{dwj} = the adjusted dew point temperature (°C).

The U.S. Standard Atmosphere, 1976 (NOAA et al. 1976), which is an idealized, steady-state representation of the earth's atmosphere, provides an approximation of atmospheric pressure that is sufficiently accurate for estimating potential evapotranspiration. The tabulated data of that report were regressed, and the following expression of atmospheric pressure as a function of elevation was obtained:

$$P_B = 824.4996e^{\left(\frac{(x_{elv}+35702.8022)^2}{-607945000}\right)} \quad [44]$$

where

P_B = the barometric pressure (kPa) and

x_{elv} = the elevation of the site (m).

The coefficient of determination (r^2) for Eq. 44 is 1.00. The range of elevations used in the regression analysis was between -500 m and 30,000 m.

Soil heat flux (G) data, are not always readily available, and the soil heat flux is often negligible on a daily basis. Therefore, the soil heat flux component of the daily surface energy balance is ignored, and the daily sum of surface energy inputs is assumed to equal the daily net radiation.

Daily net radiation is estimated from solar radiation, air temperature, and vapor pressure using Wright's modified version of Penman's general relationship outlined by Allen et al. (1989) as:

$$R_n = (1 - \alpha)R_s - \left(a \frac{R_s}{R_{so}} + b\right) \left(a_1 + b_1 \sqrt{e_d^o}\right) \sigma \frac{T_{mxk}^4 + T_{mnk}^4}{2} \quad [45]$$

where

α = the albedo (reflectance) of the surface,

R_s = the measured short wave (global) solar radiation ($\text{MJ m}^{-2} \text{ day}^{-1}$),

σ = the Stephan-Boltzman constant ($4.903 \times 10^{-9} \text{ MJ m}^{-2} \text{ day}^{-1} \text{ K}^{-4}$),

T_{mxk} = the maximum daily air temperature (K),

T_{mnk} = the minimum daily air temperature (K),

e_d^o = the saturation vapor pressure at the dew-point temperature (kPa),

R_{so} = the clear sky short wave radiation ($\text{MJ m}^{-2} \text{ day}^{-1}$), and

a, b, a_1, b_1 = empirical coefficients.

The empirical coefficients in Eq. 45 were estimated by Wright (1982) as:

$$\begin{aligned} & \left. \begin{aligned} a &= 1.126 \\ b &= -0.07 \end{aligned} \right\} \frac{R_s}{R_{so}} > 0.7, \text{ few clouds} \\ & \left. \begin{aligned} a &= 1.017 \\ b &= -0.06 \end{aligned} \right\} \frac{R_s}{R_{so}} \geq 0.7, \text{ prevalent clouds} \\ & a_1 = 0.26 + 0.1e^{-(0.0154(d_{oy}-180))^2}, \text{ northern latitudes} \\ & a_1 = 0.26 + 0.1e^{-(0.0154(d_{oy}))^2}, d_{oy} \leq 180, \text{ southern latitudes} \\ & a_1 = 0.26 + 0.1e^{-(0.0154(d_{oy}-366))^2}, d_{oy} > 180, \text{ southern latitudes} \\ & b_1 = -0.139 \end{aligned} \quad [46]$$

where

d_{oy} = the day of year (1 to 366).

R_{so} , the clear sky radiation, was estimated (Jensen et al. 1990) as:

$$R_{so} = 0.75R_a \quad [47]$$

where

R_a = extraterrestrial radiation ($\text{MJ m}^{-2} \text{ day}^{-1}$).

R_a is estimated using the following equation by Duffie and Beckman (1980):

$$R_a = \frac{G_{sc}}{\pi} d_r [(\omega_s) \sin \phi \sin \delta + \cos \phi \cos \delta \sin \omega_s] \quad [48]$$

where

G_{sc} = the solar constant, equal to 118.1088 (MJ m⁻² day⁻¹) (London and Frohlich 1982),

d_r = the relative distance of the earth from the sun,

ω_s = the sunset hour angle,

ϕ = the latitude, and

δ = the declination of the sun.

The estimating equations for d_r , ω_s , and δ in Eq. 48 are:

$$d_r = 1 + 0.033 \cos \left(\frac{2\pi d_{oy}}{365} \right) \quad [49]$$

$$\omega_s = \cos^{-1} \left(\frac{\cos r_a}{\cos \phi \cos \delta} - \tan \phi \tan \delta \right) \quad [50]$$

$$\delta = 0.4093 \sin \left(\frac{2\pi(d_{oy} - 81.25)}{365} \right) \quad [51]$$

where

r_a = the solar zenith angle at sunset which can be localized due to topography and adjusted to account for atmospheric refraction effects.

For normal conditions an r_a of 90.833 degrees is used (NOAA 2002).

The latent heat of vaporization (λ) varies with temperature. A regression analysis was performed on the tabulated temperature-latent heat data in Table 2.1 of Hillel (1971), and the following expression of latent heat as a function of temperature was derived:

$$\lambda = 2.500277 - 0.002364T_{daj} \quad [52]$$

where

λ = the latent heat of vaporization (MJ kg⁻¹) and

T_{daj} = the adjusted mean daily air temperature (°C).

The coefficient of determination (r^2) for Eq. 52 is 1.00. The range of temperatures used in the regression analysis was between -10 °C and 50 °C.

The daily saturation vapor pressure is calculated as the average of the saturation vapor pressure at minimum and maximum adjusted daily air temperatures, T_{mnj} and T_{mxj} . The actual daily vapor pressure of the air is estimated as the saturation vapor pressure at the adjusted dew-point temperature, T_{dvwj} . The saturation vapor pressure over water as a function of temperature is estimated using the equation from Murray (1967):

$$e^o = 0.611e^{\left(\frac{17.27T}{T+237.3}\right)} \quad [53]$$

where

T = the temperature (°C) and

e on the right hand side represents the exponential function.

The turbulent transfer coefficient for water vapor is estimated with the equation:

$$C_{tt} = \frac{0.622\rho_{air}k_{vk}^2}{P_B} \frac{U_z * 86400}{\left(\ln\left(\frac{z_a - z_d}{z_{ov}}\right)\right)^2} \quad [54]$$

where

ρ_{air} = the density of air (kg m⁻³),

0.622 = the water-air molecular weight ratio,

k_{vk} = the Von Karman's constant,

P_B = the barometric pressure (kPa),

U_z = the mean daily wind speed at height z_a (m s⁻¹),

z_a = the height of measurement of meteorological sensors for temperature, humidity, and radiation (m),

z_d = the zero plane displacement (m), and

z_{ov} = the roughness length for vapor transfer adjusted as noted by Jensen et al. (1990) (m).

The Von Karman's constant (k_{vk}) is usually used as a universal, dimensionless constant in turbulent flow. Its value has been determined to be near 0.4, with a range of 0.36 to 0.43. However, for Eq. 54 calculations, the value is assumed to be equal to 0.41.

The roughness length (z_{ov}), is related directly to the maximum height of surface protuberances. When the wind blows across a bare soil surface, it is usually slowed down by any surface protuberance (i.e., surface ripples, clods, or individual soil grains) that cause its velocity to decrease to zero. Jensen et al. (1990) notes that the roughness length for vapor transfer is much less than the roughness length for momentum transfer, which in WEPS is termed aerodynamic roughness as described in the Erosion submodel. Based on Jensen's review of Van Bavel's method, the roughness length for vapor transfer (z_{ov}) is set to be one tenth of the aerodynamic roughness. Zero plane displacement (Z_d) is calculated as described in Raupach (1994) as:

$$Z_d = \begin{cases} BZ * \left(1.0 - \frac{1.0 - \exp(-(15.0 * C_{bd})^{0.5})}{(15.0 * C_{bd})^{0.5}}\right), & C_{bd} > 1.0e^{-10} \\ 0, & C_{bd} \leq 1.0e^{-10} \end{cases} \quad [55]$$

where

BZ = biomass height (m),

C_{bd} = the standing biomass drag coefficient as defined in the Erosion submodel.

The wind velocity is adjusted to the local field and meteorological height using the log law relationships described in the Erosion submodel documentation. The height of the

meteorological measurements (z_a) is adjusted for the difference in zero plane displacement between the weather station and the local field per Ahuja et al. (2000):

$$z_a = z_{aw} + z_d - z_{dw} \quad [56]$$

where

z_{aw} = the standard meteorological height at the weather station (normally 2 meters) and
 z_{dw} = the zero plane displacement at the location of the meteorological measurements (m).

The air density (ρ_{air}) is directly proportional to ambient pressure and inversely proportional to temperature. It is estimated by the equation:

$$\rho_{air} = 1000 \left(\frac{P_B}{101.325} \right) \left(\frac{0.001293}{1 + 0.00367T_{daj}} \right) \quad [57]$$

where

ρ_{air} = the density of air (kg m^{-3}),
 P_B = the ambient pressure (kPa), and
 T_{daj} = the adjusted mean daily air temperature ($^{\circ}\text{C}$).

Eq. 57 is a revised version of the density of dry air equation listed in the CRC Handbook of Chemistry and Physics (Weast et al. 1983).

Furthermore, Skidmore et al. (1969) proposed that Van Bavel's (1966) combination equation can be separated into two terms to get estimates of the potential evapotranspiration by radiation and wind which were used in model testing. Accordingly, Eq. 40 can be rewritten as follows:

$$E\mathcal{T}_{pr} = \frac{\left(\frac{\Delta}{\gamma}\right) \left(\frac{R_n - G}{\lambda}\right)}{\left(\frac{\Delta}{\gamma}\right) + 1} \quad [58]$$

$$E\mathcal{T}_{pw} = \frac{C_{tt}(e_z^o - e_z)}{\left(\frac{\Delta}{\gamma}\right) + 1} \quad [59]$$

where

$E\mathcal{T}_{pr}$ = the potential evapotranspiration by radiation (mm day^{-1}) and
 $E\mathcal{T}_{pw}$ = the potential evapotranspiration by wind (mm day^{-1}).

Potential Soil Evaporation and Plant Transpiration

The total daily potential evapotranspiration (ET_p) as computed with Eq. 40 is then partitioned into potential soil evaporation (E_p) and potential plant transpiration (T_p). Potential transpiration is a function of the live leaf area of the plant and described using the transpiration effective leaf area index which is defined as the area of living plant leaves relative to the land area. This is estimated on a daily basis by the Crop submodel of WEPS. Richardson and Ritchie (1973) proposed a function for daily potential transpiration based on leaf area index alone. This was modified to consider live leaf area and to more closely match the partitioning described by Sharpley and Williams (1990),

which partitioned all evapotranspiration to transpiration for leaf area index values greater than 3:

$$\mathcal{T}_p = E\mathcal{T}_p \begin{cases} 1 - e^{(-0.398LAI_{eff})}, & LAI_{eff} \leq 0.144 \\ -0.21 + 0.7\sqrt{LAI_{eff}}, & 0.144 < LAI_{eff} < 3 \\ 1, & LAI_{eff} \geq 3 \end{cases} \quad [60]$$

where

\mathcal{T}_p = the potential daily plant transpiration,
 $E\mathcal{T}_p$ = the potential evapotranspiration (mm day⁻¹), and
 LAI_{eff} = the plant live leaf area index.

The potential soil evaporation is then is estimated by subtraction:

$$E_p = E\mathcal{T}_p - \mathcal{T}_p \quad [61]$$

where

E_p = the potential soil evaporation (mm day⁻¹).

However, if there is any remaining snow cover, evaporation is considered to come first from the snow and then from the soil. Furthermore, the potential soil evaporation is reduced with increased plant residues. The reduction from standing residue is estimated from McMaster et al. (2000) to be:

$$E'_p = E_p e^{(-1.7(C_{bd})^{0.4})} \quad [62]$$

where

E'_p = the potential surface evaporation adjusted for standing biomass (mm day⁻¹) and
 C_{bd} = the standing biomass coefficient of drag as defined in the Erosion submodel.

Flat residue also suppresses the potential surface evaporation. Based on the work of Steiner (1989), the general expression used is:

$$E''_p = E'_p e^{(f_a(M_{rf})^{f_b})} \quad [63]$$

where

E''_p = the potential surface evaporation adjusted for standing and flat residue,
 f_a and f_b = evaporation reduction factors associated with each crop or residue type, and
 M_{rf} = the effective mass of flat residue for evaporation reduction (kg m⁻²).

When multiple types of crop residues exist, the evaporation reduction factors for older residue are used along with the evaporation reduction factors for the next newer residue to find the amount of newer residue that results in the same evaporation reduction as the older residue. This is then added to the newer residue amount. Applying the process recursively, from old to new residue, results in the effective mass of flat residue for evaporation reduction. Table 1 shows values used for crops representative of different residue types.

Table 1. Evaporation reduction factors for flat residue for several representative crop types.

Crop	fa	fb
Wheat	-2.08165	0.548606
Sorghum	-1.20379	0.604887
Cotton	-0.604267	0.711259

Actual Transpiration and Water Stress Factor

As described in Durar (1991), the Hydrology submodel estimates actual plant water uptake (transpiration) and the plant growth water stress factor using an approach similar to that of the EPIC (Williams 1989, Williams et al. 1984, 1990) and WEPP (Savabi et al. 1989) models. For any soil layer, the water uptake from that layer is written:

$$f_{up} = \frac{1 - e\left(-w_{ud}\left(\frac{d_l}{d_{rz}}\right)\right)}{1 - e^{-w_{ud}}} \quad [64]$$

$$W_{up} = T_p(f_{up} - (1 - w_{uc})f_{up}^a) - w_{uc}W_{at}$$

where

f_{up} = the factor for water use distribution by depth,

f_{up}^a = the same factor for the layer above the current layer,

w_{ud} = the water use distribution by depth parameter,

d_l = the depth to the bottom of the soil layer from the soil surface (m),

d_{rz} = the plant root zone depth (m),

W_{up} = the potential plant water-uptake from the soil layer (mm day⁻¹),

T_p = the potential plant transpiration (mm day⁻¹),

w_{uc} = the water use compensation parameter, and

W_{at} = the accumulated actual water use from the soil layers above the layer (mm).

The water use distribution parameter (w_{ud}) is set to 3.065 based on the assumption that about 30% of the total water use comes from the top 10% of the soil root zone. Williams and Hann (1978) described in more detail how to evaluate the water use distribution parameter. The water use compensation parameter (w_{uc}) determines how much additional water plant roots can withdraw from the soil layer if plant root withdrawal from upper layers was less than the maximum amount. A w_{uc} value of zero would allow no additional water to be withdrawn while a value of one would allow as much water as was needed to be withdrawn from the layer. EPIC (Sharpley and Williams 1990) sets the water use compensation parameter for each layer based on the accumulation of root growth stress factors for the layer and all layers above. This was not implemented in WEPS, so the parameter value is set to 0.8 for all layers.

Durar (1991) did not account for extremely sandy soils, so the equations below were added. The potential water use in each soil layer is modified on the basis of soil water availability, soil water conductivity, and texture to obtain the actual water use in each soil layer. If the unsaturated hydraulic conductivity of the soil layer falls below a critical threshold of 1.0e-12 m s⁻¹ (Gardner et al. 1999), or if the volumetric water content θ (m³ m⁻³) is less than or equal to one fourth the saturated volumetric water content θ_s (m³ m⁻³)

(Bristow et al. 1984), then W_{up} the potential plant water-uptake from the soil layer is set to zero. Actual water use for the soil layer is then found from Jensen et al. (1971) to be:

$$W_{ua} = W_{up} \frac{\log_{10}(101 - 100(1 - r_{awc}))}{\log_{10}(101)} \quad [65]$$

where

W_{ua} = the actual plant water-uptake from the soil layer (mm day⁻¹) and
 r_{awc} = the relative amount of available water content for the soil layer (fraction from zero to one) which can be computed using the equation:

$$r_{awc} = \begin{cases} 1, & \theta \geq \theta_f \\ \frac{\theta - \theta_w}{\theta_f - \theta_w}, & \theta_w < \theta < \theta_f \\ 0, & \theta \leq \theta_w \end{cases} \quad [66]$$

where

θ = the volumetric water content (m³ m⁻³),
 θ_f = the soil water content at field capacity (m³ m⁻³), and
 θ_w = the soil water content at wilting point (m³ m⁻³).

This approach represents a compromise among the various models that have been proposed in the literature to describe the relationship between actual and potential transpiration, as influenced by soil water availability (Denmead and Shaw 1962, Holmes and Robertson 1963). Finally, summing the actual water use for all the soil layers in the plant root zone, the water stress factor is computed as:

$$f_{ws} = \frac{\sum_1^{n_{rz}} W_{ua}}{\mathcal{T}_p} \quad [67]$$

where

f_{ws} = the water stress factor (fraction from zero to one),
 \mathcal{T}_p = the potential plant transpiration (mm day⁻¹), and
the summation is over soil layers 1 to n_{rz} where n_{rz} is the total number of soil layers in the plant root zone.

The actual transpiration is then found using:

$$\mathcal{T}_a = f_{ws} \mathcal{T}_p \quad [68]$$

Infiltration, Surface Runoff, Evaporation, and Deep Percolation

The Hydrology submodel estimates runoff for each simulation day that has precipitation, irrigation, or snow melt. The rate and duration of water arrival at the surface, the rate of infiltration, and the surface storage capacity are all factors in estimating the volume of surface runoff. Runoff occurs when the rate of water arrival at the surface exceeds the rate of infiltration, water ponds on the surface, and any surface storage capacity is filled. Deep percolation (drainage) occurs during redistribution when the soil profile is filled and water continues to move downward beyond the defined soil control volume. Two

methods are available. One, based on WEPP (Flanagan and Nearing 1995), finds infiltration using a modification of the Green and Ampt equation, redistributes water based on the concept of field capacity, and uses an empirical approach to predict soil evaporation. The other, a Darcian-based method, implements a one-dimensional formulation of Darcy's law as described by Hillel (1977) to describe infiltration, water redistribution, and evaporation.

All inputs of water into the model are described by application rates and durations. Precipitation data provided to the model is described by the daily precipitation depth (mm), the duration of precipitation (hours), and the time to peak precipitation rate (fraction between 0 and 1). Snow melt is added to the precipitation, and the duration of the combined amount is set to the greater of the duration of precipitation or six hours. Irrigation rates and duration are specified by the irrigation operations themselves, and since the rates are normally constant, surface irrigations are concatenated with precipitation and snow melt to preserve their time and duration characteristics. Subsurface irrigation is directly added into the soil layers where it is located.

Darcy's Law Infiltration, Runoff, Redistribution, and Evaporation

Soil water is continually moving, mainly in response to gradients of soil water potential. Soil conductive properties also control soil water flow between the different layers of the soil profile. This movement of soil water plays a significant role in the various components of the soil water balance, from infiltration and runoff to soil evaporation, deep percolation, and water uptake by plants. Therefore, an accurate evaluation of soil water movement is essential for WEPS.

The governing principles that describe water flow in soils are Darcy's law and the equation of continuity. Darcy's law states that the flow of water is proportional to the driving force of the soil hydraulic gradient. The continuity equation states that the time rate of change in water content is proportional to the divergence of water flux. Richards (1931) derived a water flow equation by combining Darcy's law with the continuity equation. The water flow equations based on Darcy's law start with those used by Hillel (1977) and are similar to those in the SPAW model (Saxton et al. 1984). Modifications based on the work of ten Berge (1990) were made to better fit the intended purpose.

From Hillel (1977) and ten Berge (1990), the flux equation and continuity equation are combined to give:

$$\frac{\partial \theta}{\partial t} = \frac{\partial}{\partial z} \left(K \frac{\partial \psi}{\partial z} \right) - \frac{\partial K}{\partial z} - \frac{\partial}{\partial z} \left(\frac{D_{va}}{\rho_w} \frac{\partial \rho_v}{\partial z} \right) + S \quad [69]$$

where

θ = the volumetric soil water content ($\text{m}^3 \text{m}^{-3}$),

t = time (s),

z = distance below the soil surface (m),

K = the hydraulic conductivity (m s^{-1}),

ψ = the matric potential (m),

D_{va} = the diffusivity of water vapor in air ($\text{m}^2 \text{s}^{-1}$),

ρ_w = the density of water (kg m^{-3}),

ρ_v = the soil air vapor density (kg m^{-3}), and

S = any within layer water source ($\text{m}^3 \text{m}^{-3} \text{s}^{-1}$), such as buried drip irrigation.

The differential equations are cast as algebraic expressions for each soil layer as a system of discrete points in space (depth) and time.

With the division of the soil in layers, the method can also be described as solving a system of ordinary differential equations (ODE). The ODE solver package SLSODA was selected (Hindmarsh 1983, Petzold, 1983), which is publicly available from Lawrence Livermore National Labs (Hindmarsh 2001), and the April 25, 2001 version was used. The user supplies the program with a subroutine that, given the current state of the system, calculates the rate of change of that state, or flux, which SLSODA uses to integrate forward. Multiple integration methods are implemented in SLSODA and it was configured to allow the automatic selection of the appropriate method based on whether it perceived the ODE system to be stiff or non-stiff.

To simulate the soil water system, including infiltration and runoff, the system state variables are the soil water content of each of the layers and the accumulated amounts for the boundary conditions, specifically, surface water supply, runoff, evaporation, infiltration, ponding, and drainage. Other submodels such as management can change the state of the soil water system. SLSODA initialization is therefore performed at the beginning of each simulation day. The soil water system state is returned for each hour of the day, with the integration routines automatically selecting the number of time steps required to return these hourly values. As mentioned by Hillel (1977), the soil hydraulic conductivity and matric potential are both related to the soil water content. Those functions are defined later. No attempt is made to account for hysteresis.

The state variables and net flux equations for each are indexed as shown in Table 2.

Table 2. Index values for state variables and net flux equations for solving the Darcian-based hydrology ODE equations using SLSODA.

State Variable	Index
Surface water supply	1
Runoff	2
Evaporation	3
Infiltration	4
Ponded depth	5
Top soil layer	6 (soil layer 1)
Intermediate soil layers	...
Bottom soil layer	5+ <i>nsl</i> (soil layer <i>nsl</i>)
Drainage	<i>neq</i> (total number of variables, equations, 6+ <i>nsl</i>)

The flux between layers is indexed to the deeper of the two soil layers, or layer *i*. Using this convention, the equation for the water flux between two soil layers is written:

$$q_w^i = \frac{(\phi^{i-1} - \phi^i)K^i}{\Delta z^i} \quad [70]$$

where

q_w^i = the liquid water flux between soil layers *i* and *i-1* (m s⁻¹),

ϕ^i = the hydraulic potential of the soil layer i (m),
 K^i = the hydraulic conductivity between soil layers i and $i-1$ (m s⁻¹), and
 Δz^i = the distance between soil layers i and $i-1$ (m).

The corresponding vapor flux is written:

$$q_v^i = \frac{(\rho_v^{i-1} - \rho_v^i) D_{va}^i}{\rho_w \Delta z^i} \quad [71]$$

where

q_v^i = the water vapor flux between soil layers i and $i-1$ (m s⁻¹),
 ρ_v^i = the water vapor density in the air of the soil layer i (kg m⁻³),
 D_{va}^i = diffusivity of water vapor in air between soil layers i and $i-1$ (m² s⁻¹),
 ρ_w = the density of water (kg m⁻³), and
 Δz^i = the distance between soil layers i and $i-1$ (m).

Combining the two, we get the resultant water flux between soil layers i and $i-1$:

$$q_r^i = q_w^i + q_v^i \quad [72]$$

From these we can find the net flux in each soil layer from:

$$q_n^i = q_r^i - q_r^{i+1} + q_{src}^i \quad [73]$$

where

q_{src}^i = the water flux from any in-layer source such as drip irrigation (m s⁻¹).

For the surface layer and the bottom soil layer, boundary conditions define q_r . In-layer sources are assumed to be at a constant rate for any single day so they are simply quantified by:

$$q_{src}^i = \begin{cases} \frac{x_{scr}}{t_{se} - t_{ss}}, & t_{ss} \leq t_{dy} \leq t_{se} \\ 0, & t_{dy} < t_{ss}, t_{dy} > t_{se} \end{cases} \quad [74]$$

where

x_{scr} = the depth of in-layer source water applied (m),
 t_{dy} = the time of day (s),
 t_{ss} = the source start time (s), and
 t_{se} = the source end time (s).

The flow distance between soil layers i and $i-1$ is calculated using the equation:

$$\Delta z^i = \frac{x_l^{i-1} + x_l^i}{2} \quad [75]$$

where

x_l^i = the thickness of soil layer i (m).

The hydraulic potential of the soil layer i is obtained by summing the soil water matric potential and the gravitational potential (i.e. the negative value of the distance from the soil surface into the subsoil layers):

$$\phi^i = \psi^i - z_l^i \quad [76]$$

where

z_l^i = the depth to the midpoint of soil layer i from the soil's surface (m).

The average hydraulic conductivity for flow between adjoining soil layers i and $i-1$ (intermodal conductivity) uses the arithmetic mean of the two values. Many additional methods are discussed in the literature and Szymkiewicz (2009) provides an excellent summary. All claim better estimates of soil water flow using larger finite difference intervals which reduces the time required to solve the equations. Preliminary testing of the layer thickness weighted mean (Hillel 1977), geometric mean, a new integrated mean (Szymkiewicz 2009, Szymkiewicz and Helmig 2010), and Darcian mean (Gasto et al. 2002) showed only small differences in estimates of soil surface water content over the arithmetic mean for larger difference intervals with no improvement in runtime.

The average vapor diffusivity between soil layers is weighted using the layer thickness as:

$$D_{va}^i = \frac{D_v^{i-1} x_l^{i-1} + D_v^i x_l^i}{2\Delta z^i} \quad [77]$$

where

D_v^i = the vapor diffusivity of soil layer i ($\text{m}^2 \text{s}^{-1}$).

The flux of water out the lower side of the bottom soil layer is equal to the conductivity of the bottom soil layer:

$$q_r^{5+n_{sl}+1} = K^{5+n_{sl}} \quad [78]$$

where

n_{sl} = the number of soil layers.

This is equivalent to a free drainage condition. The vapor flux is considered to be zero. For drainage then, the net flux is found to be:

$$q_n^{5+n_{sl}+1} = q_r^{5+n_{sl}+1} \quad [79]$$

For the surface soil layer, the flux into the upper side is the infiltration minus the evaporation. This is written:

$$q_r^6 = q_n^4 - e_a(1 - f_{pnd}) \quad [80]$$

where

q_n^4 = the net infiltration flux (m s^{-1}),

e_a = the evaporation rate of water from the soil surface (m s^{-1}), and
 f_{pnd} = the fraction of the surface covered by ponded water.

The net infiltration flux is found using:

$$q_n^4 = i_{mx} f_{pnd} + \min(q_n^1, i_{mx})(1 - f_{pnd}) \quad [81]$$

where

i_{mx} = the maximum soil infiltration rate (m s^{-1}) and
 q_n^1 = the rate of surface water supply (m s^{-1}).

The evaporation rate of water from the soil surface is the sum of the rate of capillary rise to the soil surface and the rate of vapor diffusion from the soil surface written as:

$$e_a = \max\left(-e_{mx}, \min\left(e_{mx}, \frac{K^6(\phi^6 - \phi^{air})}{2z^6} + \frac{D_v^6(\rho_v^i - \rho_v^{air})}{\rho_w z^6}\right)\right) \quad [82]$$

where

e_{mx} = the maximum evaporation rate (m s^{-1}),
 ϕ = an index referring to the soil surface layer, and
 air = an index referring to the air above the soil surface layer.

The maximum evaporation rate is defined by the disaggregated daily potential soil evaporation found using:

$$e_{mx} = \begin{cases} 0.1 \frac{1}{t_{dl}} \left(\frac{E_p''}{1000}\right) + 0.9 \frac{\pi}{2} \left(\frac{E_p''}{1000}\right) \sin\left(\frac{\pi}{t_{dl}}(t_{dy} - t_{rise})\right), & t_{rise} < t_{dy} < t_{set} \\ 0.1 \frac{1}{t_{dl}} \left(\frac{E_p''}{1000}\right), & t_{dy} \leq t_{rise}, \quad t_{dy} \geq t_{set} \end{cases} \quad [83]$$

where

t_{dl} = the day length (86400 s),
 t_{rise} = the time of sunrise(s),
 t_{dy} = the time of day (s), and
 t_{set} = the time of sunset (s).

As disaggregated, ninety percent of the potential evaporation occurs during daylight hours and ten percent during night-time hours. Time is referenced to the initialization of the solver routines, which is done every day at midnight in order to account for the effect of other submodels changing the state of the soil. Sunrise and sunset times are found from:

$$\begin{aligned} t_{rise} &= t_{sn} - 3600 \frac{\omega_s}{15} \\ t_{set} &= t_{sn} + 3600 \frac{\omega_s}{15} \end{aligned} \quad [84]$$

where

t_{sn} = the time of solar noon with respect to the standard meridian time zone (s).

This is found using:

$$t_{sn} = 43200 - \Delta t_{eot} - 240(\lambda_{st} - \lambda_{loc}) \quad [85]$$

where

Δt_{eot} = the equation of time (s),

λ_{st} = the standard time zone meridian (degrees from Greenwich meridian going west is positive), and

λ_{loc} = the local meridian (degrees from Greenwich meridian going west is positive).

The local meridian is simply the negative of the longitude. The standard time zone meridian is found using:

$$\lambda_{st} = 15 \text{ nint} \left(\frac{\lambda_{loc}}{15} \right) \quad [86]$$

where

nint = the nearest integer function.

This differs from the politically defined time zones, which are not implemented here. The equation of time is estimated using:

$$\begin{aligned} \Delta t_{eot} &= 9.87 \sin(2b) - 7.53 \cos(b) - 1.5 \sin(b) \\ b &= 2\pi \left(\frac{d_{oy} - 81.25}{365} \right) \end{aligned} \quad [87]$$

The hydraulic potential of the air in reference to the soil is found using the method of ten Berge (1990) to be:

$$\phi^{air} = \frac{C_{ug}}{M_w g} (T_{air} + 273.16) \ln \left(\frac{e_{air}}{e_z^o} \right) \quad [88]$$

where

C_{ug} = the universal gas constant (J mole⁻¹ K⁻¹),

M_w = the molecular weight of water (kg mole⁻¹),

g = the gravitational constant (m s⁻²),

T_{air} = the air temperature at that time of day, and

e_{air} = the vapor pressure of the air at T_{air} (kPa).

The air and the top soil layer are assumed to be at the same gravitational potential. The instantaneous air temperature is estimated from:

$$T_{air} = \begin{cases} \frac{T_{dmx}^p + T_{dmn}}{2} + \left(\frac{T_{dmx}^p - T_{dmn}}{2} \right) \sin \left(\pi \left(\frac{t_{dy}}{t_{hd}} + 1 \right) \right), & t_{dy} < t_{qd} \\ \frac{T_{dmx} + T_{dmn}}{2} + \left(\frac{T_{dmx} - T_{dmn}}{2} \right) \sin \left(\pi \left(\frac{t_{dy}}{t_{hd}} + 1 \right) \right), & t_{dy} < t_{3qd} \\ \frac{T_{dmx} + T_{dmn}^n}{2} + \left(\frac{T_{dmx} - T_{dmn}^n}{2} \right) \sin \left(\pi \left(\frac{t_{dy}}{t_{hd}} + 1 \right) \right), & t_{dy} \geq t_{3qd} \end{cases} \quad [89]$$

where

T_{dmx}^p = the daily maximum air temperature from the previous day (°C),

T_{dmn}^n = the daily minimum air temperature for the next day (°C),

t_{hd} = the half day length (s),

t_{qd} = the one quarter day length (s), and

t_{3qd} = the three quarter day length (s).

The vapor density of the air using the instantaneous air temperature and the PV=nRT relationship is found to be:

$$\rho_v^{air} = 2.166 \frac{e_{air}}{T_{air} + 273.15} \quad [90]$$

The fraction of the surface covered by ponded water is found from the depth of the ponded water using:

$$f_{pnd} = \min \left(1, \sqrt{\frac{z_{pnd}}{z_{pmx}}} \right) \quad [91]$$

where

z_{pnd} = the depth of ponded water(m) and

z_{pmx} = the maximum depth of ponded water where the surface is completely covered (m).

The maximum depth is found using the equation from WEPP (Flanagan and Nearing 1995):

$$z_{pmx} = \max \left(z_{olt}, r_{ran} (0.112 + 3.1r_{ran} - 1.2f_{slp}) \right) \quad [92]$$

where

z_{olt} = the height of any field outlet structure above the surface of the soil (m),

r_{ran} = the random roughness of the soil surface (m), and

f_{slp} = the slope of the soil surface (m m⁻¹).

The maximum soil infiltration rate is the written as:

$$i_{mx} = (\phi_{ae}^6 - \phi^6) \frac{K_{sat}^6 + K^6}{2Z^6} \quad [93]$$

where

ϕ_{ae}^6 = the air entry potential of the soil surface layer (m),
 K_{sat}^6 = the saturated hydraulic conductivity of the soil surface layer (m s⁻¹),
 K^6 = the hydraulic conductivity of the soil surface layer (m s⁻¹), and
 z^6 = the distance from the soil surface to the midpoint of the surface layer (m).

If hysteresis was accounted for, then the hydraulic potential of the soil surface would be zero (air entry potential would go to zero), as is expected. However, without accounting for hysteresis, the hydraulic potential cannot be set to zero and using the air entry potential prevents exceeding saturation.

The net surface water input flux is the sum of rain (plus snowmelt) and irrigation inputs, disaggregated in time:

$$q_n^1 = q_{rain} + q_{sir} \quad [94]$$

where

q_{rain} = the rainfall (plus snowmelt) rate (m s⁻¹) and
 q_{sir} = the surface irrigation application rate (m s⁻¹).

The rainfall (plus snowmelt) rate is found from:

$$q_{rain} = \begin{cases} q_{rp} \frac{t_{dy} - t_{rs}}{t_{rm} - t_{rs}}, & t_{dy} < t_{rm} \\ q_{rp} \frac{t_{dy} - t_{re}}{t_{rm} - t_{re}}, & t_{dy} > t_{rm} \\ q_{rp}, & t_{dy} = t_{rm} \end{cases} \quad [95]$$

where

q_{rp} = the representative peak intensity (m s⁻¹),
 t_{dy} = the time of day (s),
 t_{rs} = the time when rain starts (s),
 t_{re} = the time when the rain ends (s), and
 t_{rm} = the “midpoint” of the rainfall event or when the peak intensity occurs (s).

The representative peak intensity is estimated from:

$$q_{rp} = \frac{2x_{rps}}{t_{re} - t_{rs}} \quad [96]$$

where

x_{rps} = the total depth of rainfall (plus snowmelt) for the event (m).

When snowmelt occurs concurrently with precipitation and the duration of the rainfall event is less than six hours, the duration of the rainfall event is extended to six hours. Similarly, the surface irrigation application rate is found:

$$q_{sir} = \begin{cases} \frac{x_{sir}}{t_{ie} - t_{is}}, & t_{is} \leq t_{dy} \leq t_{ie} \\ 0, & t_{dy} < t_{is} \text{ or } t_{dy} > t_{ie} \end{cases} \quad [97]$$

where

x_{sir} = the depth of irrigation applied (m),

t_{is} = the irrigation start time (s), and

t_{ie} = the irrigation end time (s).

The net ponding flux or the rate of change in ponded depth is found from:

$$q_n^5 = (q_n^1 - i_{mx} - e_{mx})f_{pnd} - q_n^2 \quad [98]$$

where

q_n^2 = the net runoff flux (m s^{-1}), which is found using the following:

$$q_n^2 = \frac{(z_{pnd} - z_{pmx})^{1.5}}{x_{slp}} \sqrt{\frac{8gf_{slp}}{f_{dw}}} \quad [99]$$

where

x_{slp} = the slope length (m) and

f_{dw} = the Darcy Weisbach friction factor, found using equations adapted from WEPP (Flanagan and Nearing 1995):

$$f_{dw} = \frac{12N_{stm}}{220} + 14.5(f_{fcv})^{1.55} + 0.5 \left(e^{(3.02 - 5.04e^{(-161r_{ref})})} \right)^{1.13} e^{\left(-3.09 \left(1 - \frac{\min(r_{ran}, r_{ref})}{r_{ref}} \right) \right)} \quad [100]$$

where

N_{stm} = the number of stems standing on the soil surface ($\# \text{ m}^{-2}$),

f_{fcv} = the fraction of the surface covered by flat biomass, and

r_{ref} = a reference random roughness taken as the random roughness created by the last tillage operation (m).

The daily runoff is the integration of the net runoff flux for the day:

$$runoff = \int_{t=0}^{t_{dl}} q_n^2(t) \quad [101]$$

The net evaporation flux is found as the sum of soil and ponded water evaporation:

$$q_n^3 = e_a(1 - f_{pnd}) + e_{mx}f_{pnd} \quad [102]$$

The daily actual evaporation is the integration of the net evaporation flux for the day:

$$E_a = \int_{t=0}^{t_{dl}} q_n^3(t) \quad [103]$$

Deep percolation is the integration of the net drainage flux for the day:

$$dprc = \int_{t=0}^{t_{dl}} q_n^{neq}(t) \quad [104]$$

The depth of water in the soil control volume can then be expressed as:

$$swc = \sum_{i=6}^{n_{eq}} \theta_i^i x_i^i \quad [105]$$

where

$swci$ would be summed at the beginning of the day ($t=0$) and swc would be summed at the end of the day ($t=t_{dl}$).

WEPP Infiltration, Runoff, Redistribution, and Evaporation

Integration of the WEPP (Flanagan and Nearing 1995) hydrology component required the mapping of data available in WEPS into the proper units and variables for the WEPP code. In some cases, the variables, which were thought to be the same were not, and the proper definition from WEPP had to be integrated as well. Most disruptive was that soil layer thickness in WEPP was fixed. Substitute methods were created for routines that were very dependent on the thickness of the surface layers allowing WEPS layering to be used. The WEPP hydrology component provides a daily soil water balance. An estimation method was created to provide hourly values of surface wetness to WEPS.

The soil layer properties used in WEPP include the layer thickness, current available soil water content, upper limit soil water content, and field capacity water content. These values may change from day to day outside of hydrology, as the soil bulk density and texture change in response to management operations and climate influences. For each layer the values assigned are:

$$\theta = (\theta - \theta_w)x_l \quad [106]$$

where

θ = the WEPP soil layer water content (m),
 θ = the WEPS soil layer water content ($m^3 m^{-3}$),
 θ_w = the WEPS soil layer wilting point water content ($m^3 m^{-3}$), and
 x_l = the thickness of the soil layer (m);

$$\theta_{ul} = (\theta_{es} - \theta_w)x_l \quad [107]$$

where

θ_{ul} = the WEPP soil layer upper limit water content (m) and
 θ_{es} = the WEPS soil layer entrapped air reduced saturation water content ($m^3 m^{-3}$); and

$$\theta_{fc} = (\theta_f - \theta_w)x_l \quad [108]$$

where

θ_{fc} = the WEPP soil layer field capacity water content (m) and
 θ_f = the WEPS soil layer field capacity water content ($m^3 m^{-3}$).

It was also necessary to check that the water content of the layer does not exceed the upper limit. This can occur if the layer water content is close to the upper limit and the layer thickness is reduced due to an increase in soil bulk density within the WEPS Soil submodel. If soil layer water content is greater than the upper limit, the excess is cascaded to lower soil layers until all the soil layers are at or below the soil layer upper limit water content.

Any surface water supply is input into WEPP as breakpoint data. Precipitation data are input into WEPP disaggregation routines directly; however it was necessary to create a method for adding surface irrigation water to the WEPP breakpoint array. It simply adds the irrigation rate to the rainfall rate where their times overlap and adds additional breakpoint elements when irrigation occurs during a time when there is no rainfall.

WEPP uses the soil properties of the top 0.2 meters of the soil for infiltration calculations. Soil properties from the WEPS layers in this range are averaged over the "WEPP surface layer." These include the sand fraction, clay fraction, soil water content, bulk density, porosity (using the volumetric saturated water content in WEPS), and rock volume. Upon completion of WEPP infiltration calculations and insertion of that water into the soil layers, the WEPP soil water redistribution routines are applied.

Evaporation from the soil surface uses the method from Allen et al. (1998) modified to distribute the evaporation amount within the WEPS soil layer structure rather than uniformly over the entire evaporation affected depth. For each soil layer, the total evaporable water is:

$$\theta_{te} = (\theta_f - 0.2\theta_w)x_l \quad [109]$$

where

θ_{te} = the soil layer total evaporable water content (m).

Allen et al. (1998) use one half of the permanent wilting point water content as the lower limit of soil water evaporation. Two tenths of the permanent wilting point water content is used here since WEPS data on soil surface water content suppression of erosion shows an effect for less than one half of permanent wilting point water content. Readily evaporable water is:

$$\theta_{re} = (0.057856(\theta_f - \theta_w) + 0.00028) \frac{x_l}{z_{epd}} \quad [110]$$

where

θ_{re} = the soil layer readily evaporable water content (m) and
 z_{epd} = the evaporation depth or depth to which evaporation occurs (m), which is found by:

$$z_{epd} = 0.09 - 0.077f_{c20} + 0.0006f_{s20} \quad [111]$$

where

f_{c20} = the fraction of clay in the top 20cm of soil and
 f_{s20} = the fraction of sand in the top 20 cm of soil.

The water available for evaporation in each layer is found from:

$$\theta_{wfe} = \theta + 0.8\theta_w x_l \quad [112]$$

For a soil layer that crosses the evaporable depth boundary, the part of the layer within the evaporation depth is used in the calculations. The totals in the evaporation depth for total and readily evaporable water are the sum of the layer values. The amount of water that evaporates from the soil surface any given day is found using:

$$E_a = \begin{cases} E_p, (\theta_{te}^T - \theta_{wfe}^T + E_p) \leq \theta_{re}^T \\ E_{s1} + E_{s2}, (\theta_{te}^T - \theta_{wfe}^T) \leq \theta_{re}^T \\ E_{s1} = \theta_{re}^T - (\theta_{te}^T - \theta_{wfe}^T) \\ E_{s2} = (E_p - E_{s1}) \left(\frac{E_{wfe}^T - E_{s1} - \frac{E_p - E_{s1}}{2}}{E_{te}^T - E_{re}^T} \right)^2 \\ E_p \left(\frac{E_{wfe}^T - \frac{E_p}{2}}{E_{te}^T - E_{re}^T} \right)^2, (\theta_{te}^T - \theta_{wfe}^T) > \theta_{re}^T \end{cases} \quad [113]$$

where

T superscript = a value summed over the entire evaporation depth and
 E_{s1} and E_{s2} = intermediate calculations for simplification.

The distribution of the actual evaporation over the soil layers is done by cascading the amount down through the layers in the evaporation depth. The amount of evaporation removed from each layer is found using:

$$E_l = \min(E_r, 0.3f_{ed}\theta_{wfe}) \quad [114]$$

$$f_{ed} = 1 - \frac{z_l}{z_{epd}}$$

where

E_l = the evaporation removed from the layer (m),
 E_r = the remaining evaporation to be distributed in the soil layers (m), and
 z_l = the distance from the soil surface to the bottom of the soil layer (m).

Starting with the surface layer, the evaporation for the layer is removed from the layer and the remaining evaporation to be distributed is reduced and applied to the next soil layer until all evaporation has been distributed.

Hourly surface layer water content is found by linearly interpolating from either the previous day water content to the present end of day water content, or if there was surface ponding, from a saturated surface water content at the time of the end of ponding to the present end of day water content.

Fundamental soil properties, such as texture and cation exchange capacity, and management actions are passed from the main WEPS routines into the incorporated WEPP routines. The effective saturated hydraulic conductivity used in infiltration is found from these values. The saturated hydraulic conductivity as defined in WEPS is used for all other WEPP water balance/redistribution routines. The matric potential relationships as defined in WEPS are used throughout all included WEPP routines.

Estimating Soil Hydraulic Properties

Knowledge of the relationship between unsaturated hydraulic conductivity and soil water content is required for solving the governing transport equations of water movement through the soil. However, reliable estimates of unsaturated hydraulic conductivity as a function of soil water content are extremely difficult to obtain, not only because of the extensive spatial variability of the parameter in the field but also because its determination in the field and/or laboratory is very difficult and labor intensive (i.e. expensive). To overcome this problem, many methods have been proposed to predict the unsaturated hydraulic conductivity from more easily determined soil parameters. Most of these methods calculate the unsaturated hydraulic conductivity of the soil from the relatively more easily and routinely obtainable soil water characteristic curve and saturated hydraulic conductivity (Millington and Quirk 1959, Brooks and Corey 1964, 1966, Campbell 1974, Mualem 1976, and Van Genuchten 1978, 1980, Rawls and Brakensiek 1989, Rawls et al. 1998).

The Hydrology submodel of WEPS uses Rawls and Brakensiek (1989) and Rawls et al. (1998) methods to estimate the saturated hydraulic conductivity and soil water characteristic curve parameters (Brooks and Corey 1964) so that hydraulic conductivity and soil matric potential can be expressed as a function of volumetric soil water content and bulk density. When the soil is very dry, the relationships based on clay isotherms from ten Berge (1990) are used. The soil water characteristic curve is represented by the equation:

$$\psi = \begin{cases} \psi_{ae}, & \theta \geq \theta_s \\ \psi_{ae} \left(\frac{\theta - \theta_r}{\theta_s - \theta_r} \right)^{\left(\frac{-1}{\lambda_{bc}} \right)}, & \theta_w \leq \theta < \theta_s \\ \frac{C_{ug}}{M_w g} (T_{soil} + 273.16) \ln(\Phi_{sa}), & \theta < \theta_w \end{cases} \quad [115]$$

where

ψ_{ae} = the Brooks and Corey air entry potential (m),

θ_r = the residual soil water content where hydraulic conductivity becomes zero ($\text{m}^3 \text{m}^{-3}$),

λ_{bc} = the Brooks and Corey pore size interaction parameter,

T_{soil} = the temperature of the soil ($^{\circ}\text{C}$), and

Φ_{sa} = the relative humidity of the air in the soil.

From ten Berge (1990), the relative humidity in the soil as a function of water content is:

$$\Phi_{sa} = \begin{cases} \frac{0.8(10)^{-37}}{\theta_{rh80}}, & \theta < 1.0(10)^{-37} \\ \frac{0.8\theta}{\theta_{rh80}}, & 1.0(10)^{-37} \leq \theta < \theta_{rh80} \\ 0.8 + (\Phi_w - 0.8) \left(\frac{\theta - \theta_{rh80}}{\theta_w - \theta_{rh80}} \right), & \theta_{rh80} \leq \theta \leq \theta_w \end{cases} \quad [116]$$

where

θ_{rh80} = the water content of the soil when the soil air is at 80 % relative humidity ($\text{m}^3 \text{m}^{-3}$)
and

Φ_w = the soil relative humidity at the permanent wilting point matric potential, which is found using:

$$\Phi_w = e^{\left(\frac{\psi_w M_w g}{C_{ug}(T_{soil} + 273.16)} \right)} \quad [117]$$

where

ψ_w = the permanent wilting point matric potential (m).

This same equation is used where the soil air relative humidity is required for matric potentials greater than permanent wilting point. The soil water content at a soil relative humidity of 80% is found using:

$$\theta_{rh80} = \left(\frac{\rho_b}{\rho_w} \right) (F_{cl}(1 - F_{om})g_{cl80} + F_{om}g_{om80}) \quad [118]$$

where

F_{om} = the gravimetric fraction of the soil that is organic matter,

g_{cl80} = the gravimetric water content of clay minerals at 80 percent relative humidity (kg water per kg dry mineral), and

g_{om80} = the gravimetric water content of soil organic matter at 80 % relative humidity (kg water per kg dry organic matter).

From Rutherford and Chlou (1992), g_{om80} is set to 0.27 and from ten Berge (1990), g_{cl80} is set to 0.3 assuming a predominance of montmorillonite.

Both air-entry potential and the pore size distribution are considered characteristic hydraulic parameters of the soil. The air-entry potential, which is usually referred to as the bubbling pressure, is related to the maximum pore size forming a continuous network of flow channels within the soil. The air entry potential is defined as the minimum capillary pressure in the drainage cycle at which a continuous no wetting condition exists in the soil, i.e., the potential at which the largest water-filled pores start to drain and, hence, gas flow can be observed. The pore size distribution parameter is a function not only of the size of soil pores but also of the interfacial forces, contact angles, shape of soil pores, etc.

The air entry potential, as implemented from Rawls and Brakensiek (1989) is:

$$\begin{aligned} \psi_{ae} &= -0.01e^{(C_{ae})} \\ C_{ae} &= 5.3396738 + 0.1845038\Gamma_{cl} - 2.48394546f_{por} \\ &\quad - 0.00213853\Gamma_{cl}\Gamma_{cl} - 0.04356349\Gamma_{sa}f_{por} \\ &\quad - 0.61745089\Gamma_{cl}f_{por} + 0.00143598\Gamma_{sa}\Gamma_{sa}f_{por}f_{por} \\ &\quad - 0.00855375\Gamma_{cl}\Gamma_{cl}f_{por}f_{por} - 0.00001282\Gamma_{sa}\Gamma_{sa}\Gamma_{cl} \\ &\quad + 0.00895359\Gamma_{cl}\Gamma_{cl}f_{por} - 0.00072472\Gamma_{sa}\Gamma_{sa}f_{por} \\ &\quad + 0.00000540\Gamma_{cl}\Gamma_{cl}\Gamma_{sa} + 0.50028060\Gamma_{cl}f_{por}f_{por} \end{aligned} \quad [119]$$

where

Γ_{cl} = the percent clay in the soil,

Γ_{sa} = the percent sand in the soil, and

f_{por} = the soil porosity, found from:

$$f_{por} = 1 - \frac{\rho_b}{\rho_p} \quad [120]$$

where

ρ_b = the soil bulk density (Mg m^{-3}) and

ρ_p = the soil particle density (Mg m^{-3}).

No adjustment is made for entrapped air. Soil particle density is adjusted for organic matter content using:

$$\rho_p = \frac{1}{\frac{f_{om}}{\rho_{om}} + \frac{1 - f_{om}}{\rho_{qtz}}} \quad [121]$$

The pore size distribution is:

$$\begin{aligned} \lambda_{bc} &= e^{(C_{ps})} \\ C_{ps} &= -0.7842831 + 0.0177544\Gamma_{sa} - 1.062498f_{por} \\ &\quad - 0.00005304\Gamma_{sa}\Gamma_{sa} - 0.00273493\Gamma_{cl}\Gamma_{cl} \\ &\quad + 1.11134946f_{por}f_{por} - 0.03088295\Gamma_{sa}f_{por} \\ &\quad + 0.00026587\Gamma_{sa}\Gamma_{sa}f_{por}f_{por} \\ &\quad - 0.00610522\Gamma_{cl}\Gamma_{cl}f_{por}f_{por} - 0.00000235\Gamma_{sa}\Gamma_{sa}\Gamma_{cl} \\ &\quad + 0.00798746\Gamma_{cl}\Gamma_{cl}f_{por} - 0.00674491\Gamma_{cl}f_{por}f_{por} \end{aligned} \quad [122]$$

The residual volumetric soil water content is:

$$\begin{aligned} \theta_r &= -0.0182482 + 0.00087269\Gamma_{sa} + 0.00513488\Gamma_{cl} \\ &\quad + 0.02939286f_{por} - 0.00015395\Gamma_{cl}\Gamma_{cl} \\ &\quad - 0.0010827\Gamma_{sa}f_{por} - 0.00018233\Gamma_{cl}\Gamma_{cl}f_{por}f_{por} \\ &\quad + 0.00030703\Gamma_{cl}\Gamma_{cl}f_{por} - 0.0023584\Gamma_{cl}f_{por}f_{por} \end{aligned} \quad [123]$$

The saturated volumetric soil water content is found using the porosity:

$$\theta_s = f_{por} \quad [124]$$

For finding volumetric soil water content from matric potential between saturation and wilting point, part of Eq. 115 is rearranged giving:

$$\theta = \theta_r + (\theta_s - \theta_r) \left(\frac{\psi_{ae}}{\psi} \right)^{\lambda_{bc}} \quad [125]$$

Eq. 125 is used to find the field capacity volumetric soil water content (matric potential is set to one third bar or -3.3989 meters of water at maximum density) and the permanent wilting point volumetric water content (matric potential is set to fifteen bar or -152.95 meters of water at maximum density).

The saturated hydraulic conductivity uses the method from Rawls et al. (1998), which with unit conversions is:

$$K_s = \left(\frac{0.001}{3600} \right) 1930.0 (f_{por} - \theta_f)^{(3-\lambda_{bc})} \quad [126]$$

where the first fraction converts from mm hr⁻¹ to m s⁻¹.

The limits mentioned for the regression equations in Rawls and Brakensiek (1989) are not enforced to allow estimation of the full range of soil textures. Specifically, soils in wind erosion prone regions tend to have higher sand content, notably in the surface layers. Using the estimation equations trends the values in the correct direction but may not capture the full magnitude of the changes. Further research is necessary to evaluate alternative estimation methods.

The unsaturated hydraulic conductivity for a layer is:

$$K_u^i = K_s^i \left(\frac{\theta^i - \theta_r^i}{\theta_s^i - \theta_r^i} \right)^{\left(2.5 + \frac{2}{\lambda^i} \right)} \quad [127]$$

where

the superscript indicates layer *i*,

K_u^i = the unsaturated hydraulic conductivity (m s⁻¹),

K_s^i = the saturated hydraulic conductivity (m s⁻¹),

θ^i = the volumetric soil water content (m³ m⁻³),

θ_r^i = the residual volumetric soil water content (m³ m⁻³),

θ_s^i = the saturated volumetric soil water content (m³ m⁻³), and

λ^i = the Brooks and Corey (1966) pore size interaction term.

Using the method from Campbell (1985), the diffusivity of water vapor in the soil air is found:

$$D_v = 0.66D_{adj}(f_{por} - \theta)$$

$$D_{adj} = D_{stp} \left(\frac{101.3}{P_B} \right) \left(\frac{T_l + 273.16}{273.16} \right)^2 \quad [128]$$

where

D_{adj} = the diffusivity of water vapor in air adjusted for temperature and pressure ($\text{m}^2 \text{s}^{-1}$)

and

D_{stp} = the binary diffusion coefficient for water vapor in air ($2.12\text{E-}5 \text{ m}^2 \text{ s}^{-1}$).

Soil Wetness at the Soil-Atmosphere Interface

This section comes from Durar (1991) and Durar et al. (1995). The water redistribution section of the Hydrology submodel of WEPS accounts for water and vapor flux isothermally. However, a dry soil surface experiences a strong diurnal temperature change. Numerical solutions to the difference equations is also computationally expensive. Configurations to obtain a faster time to solution can result in less accurate representations of the soil surface water content. However, a complete simulation that accounts for linked fluxes of liquid, vapor, and heat is probably too complex, long, and slow to meet the unique requirements of WEPS for fast simulation of the diurnal changes in soil water content at the soil-atmosphere interface. Therefore, the relationship between actual and potential evaporation is used as an estimator of soil surface wetness. Water usually evaporates from the soil surface at the potential rate only when the soil is adequately wet. However, when the soil begins to dry and water is not conducted to the soil-atmosphere interface fast enough to meet the atmospheric evaporation demand, actual evaporation falls behind the potential rate. Holmes and Robertson (1963) verified the unique relationship between soil wetness and the ratio of actual to potential evaporation in a growth chamber experiment conducted with samples from three soil materials (North Gower clay, Matilda silt loam, and 26-mesh quartz sand). In order to make the relationship between the evaporation ratio and soil wetness useful in predicting surface soil wetness as needed by WEPS, the functional relationship between equivalent water content and the ratio of actual to potential evaporation has to be determined first. Jackson's (1973) original soil water and meteorological data from a 1971 bare soil evaporation experiment conducted on an Avondale loam (fine-loamy, mixed (calcareous), hyperthermic Typic Torrifluent) (A.K.A. Adelanto Loam) at the U.S. Water Conservation Laboratory, Phoenix, Arizona was used to derive the relationship between equivalent water content and the evaporation ratio. The hourly meteorological data to calculate the hourly potential evaporation using Van Bavel's (1966) combination equation was also used.

The functional relationship between equivalent water content of the soil surface and hourly evaporation ratios is described with the equation:

$$\theta_e = 0.24308 + \frac{1.37918}{1 + e^{\left(\frac{-(r_e - 0.44882)}{0.081} \right)}} \quad [129]$$

$$r_e = \frac{e_a}{e_{mx}}$$

where

θ_e = the equivalent water content, defined as the ratio of volumetric soil-water content ($\text{m}^3 \text{m}^{-3}$) to volumetric soil-water content for the same soil at -1.5 kJ kg^{-1} soil matric potential and

r_e = the ratio of the actual evaporation rate (e_a) to the potential evaporation rate (e_{mx}).

The surface soil water content is found from the relationship between the evaporation ratio and equivalent surface soil water content using the equation:

$$\theta^s = \theta_e * \theta_w^6 \quad [130]$$

where

θ^s = the surface soil water content ($\text{m}^3 \text{m}^{-3}$) and

θ_w^6 = the permanent wilting point water content of the soil surface layer ($\text{m}^3 \text{m}^{-3}$).

When using thicker layers for a faster finite difference solution of the soil water equations, the surface is drier than the average layer water content. This method is then used along with the surface evaporation ratio derived from the equations of Ritchie as described in Flanagan and Nearing (1995) to estimate the surface water content. This evaporation ratio is calculated separately from the evaporation used in the soil water balance.

Simulation of Diurnal Soil Temperature

Soil properties are affected by freezing and thawing actions. The daily average soil temperatures do not capture the diurnal nature of freezing and thawing. The method of Campbell (1985) is used to estimate daily minimum and maximum soil temperatures at the center of each simulation layer. The basic assumption is that diurnal air temperature variation is a sine function, which drives the diurnal soil temperature variation. The daily minimum and maximum soil temperatures for each layer are found using:

$$T_{dmn}^i = \begin{cases} T_l^i - T_{amp} \left(1 - \frac{z_l^i}{z_{damp}} \right), & z_l^i < z_{damp} \\ T_{avg}^i, & z_l^i \geq z_{damp} \end{cases} \quad [131]$$

$$T_{dmx}^i = \begin{cases} T_l^i + T_{amp} \left(1 - \frac{z_l^i}{z_{damp}} \right), & z_l^i < z_{damp} \\ T_{avg}^i, & z_l^i \geq z_{damp} \end{cases} \quad [132]$$

$$T_{amp} = T_{dmx}^{air} - T_{dav}^{air} \quad [133]$$

$$z_{damp} = \sqrt{\left(\frac{86400}{\pi} \right) \left(\frac{\sum_{i=0}^n k_l^i \frac{x_l^i}{z_l^n}}{\sum_{i=0}^n C_{vl}^i \frac{x_l^i}{z_l^n}} \right)} \quad [134]$$

where

T_{dmn}^i and T_{dmx}^i = the daily minimum and maximum soil temperatures for layer i ($^{\circ}\text{C}$),
 T_{amp} = the amplitude of the daily air temperature variation around the daily average air temperature ($^{\circ}\text{C}$),

z_{damp} = the damping depth, or depth in the soil to which the temperature variation penetrates (m), and

n = the total number of soil layers.

Submodel Testing and Evaluation

For wind erosion modeling, the Hydrology submodel of WEPS needs to do a good job of estimating the dryness of the soil surface (this affects the threshold friction velocity) and the evaporative loss of soil water (this affects fallow efficiency). This has been tested using data sets from two soils.

In the first soil, submodel performance was evaluated by comparing its predictions with the measured soil water content and evaporation data from a 14-d field experiment conducted during March 1971 (Jackson, 1973; Jackson et al., 1973) on an Avondale loam (fine-loamy, mixed (calcareous), hyperthermic Typic Torrifluent). An input soil file was created using the texture of the soil and WEPS estimation equations. The properties found and those published by Jackson (1973) are shown in Figure 1. Weather data for that location was generated using CLIGEN and WINDGEN, and daily data for the 14 days were then inserted into the files. A management file was created containing the tillage operation and the irrigation event. Four simulations were performed using different configurations of WEPS. The “WEPS-full” simulation used the Darcian-based hydrodynamic method with simulation layer thickness consisting of a 2mm surface layer with each successive layer 50 percent thicker and reporting the water content of the 0-2mm layer as the surface water content. The “WEPS-eratio” simulation was identical except it reports the surface water content from the “Evaporation Ratio” method. The “WEPS-WEPP” simulation used the layer configuration of “WEPS-full” with WEPP hydrology which reports the water content of the 0-2mm layer as the surface water content. Figures 2, 3, and 4 summarize the results. The Darcian-based (WEPS-full) method, results in overestimation of capillary rise during drying events and a delay in drying of the soil surface. The Brooks and Corey soil water release curve significantly deviates from the measured curve for this soil. Other models compensate for this by including multiple formulations of the soil water release curve. Jansson and Moon (2001) proposed a linearization of the soil water release curve in the saturated range to better simulate the soil water dynamics. Other authors have proposed new curves. Fredlund and Xing (1994) discuss the different formulations of the soil water release curve and propose yet another. Selecting alternative soil water release curve forms could improve the results if a corresponding unsaturated hydraulic conductivity curve was available. A method for estimating parameters for a wide range of soils would also need to be available. At this time, Rawls and Brakensiek (1989) provide the most complete method for estimating soil hydraulic properties from fundamental physical properties and the parameters for other soil water release curves would need to be derived from their data. Presently, no alternative formulations have been implemented for testing in WEPS. In comparing the present model against the Jackson (1973) data, implementation of a table lookup, as is done in Hillel (1977), should determine if the differences between simulation results and the data are due the difference between the soil water release curve used in the simulation and the measured soil water release curve.

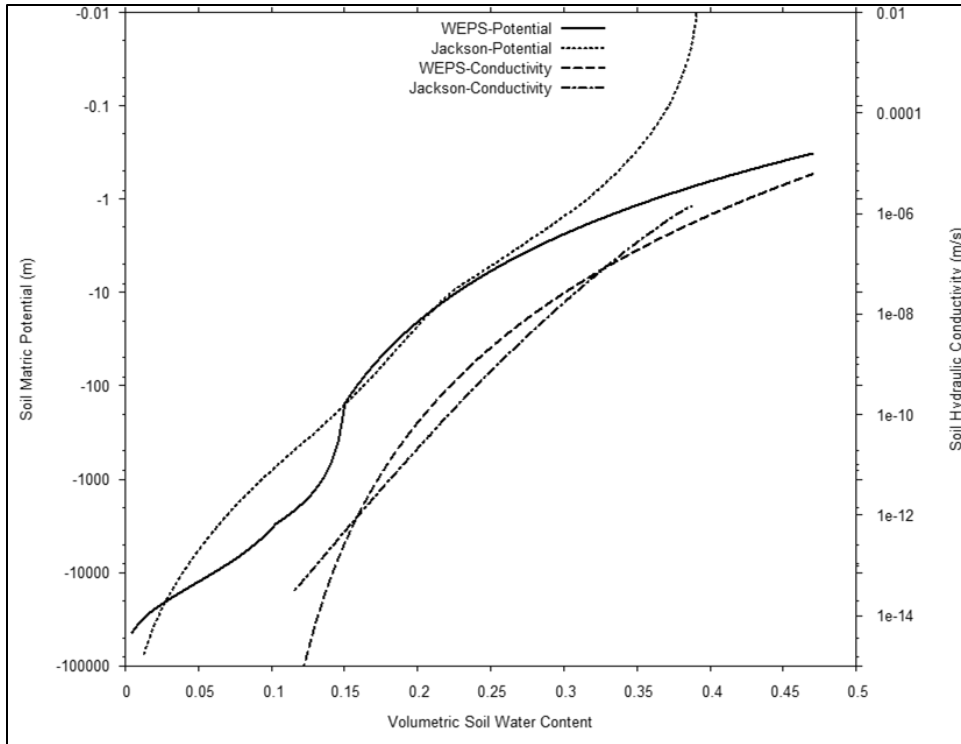


Figure 1. Comparison of Adelanto loam soil hydraulic properties as estimated by WEPS and reported by Jackson (1973). Jackson matric potential is measured and hydraulic conductivity estimated.

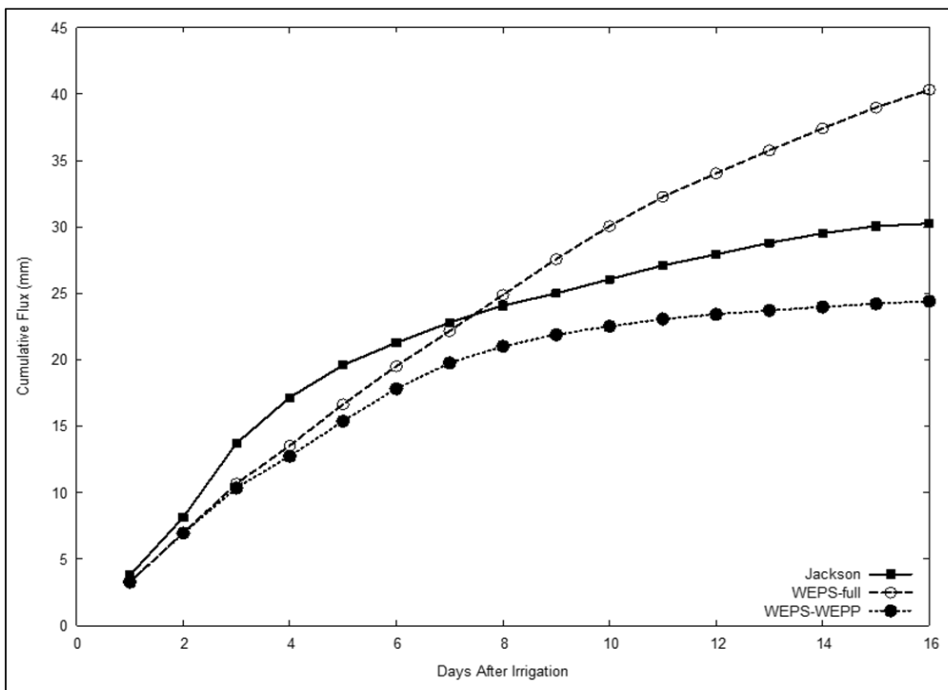


Figure 2. Comparison of cumulative evaporation as measured by Jackson (1973) and simulated by WEPS using Darcian-based hydrodynamic simulation (WEPS-full) and WEPP hydrology (WEPS-WEPP).

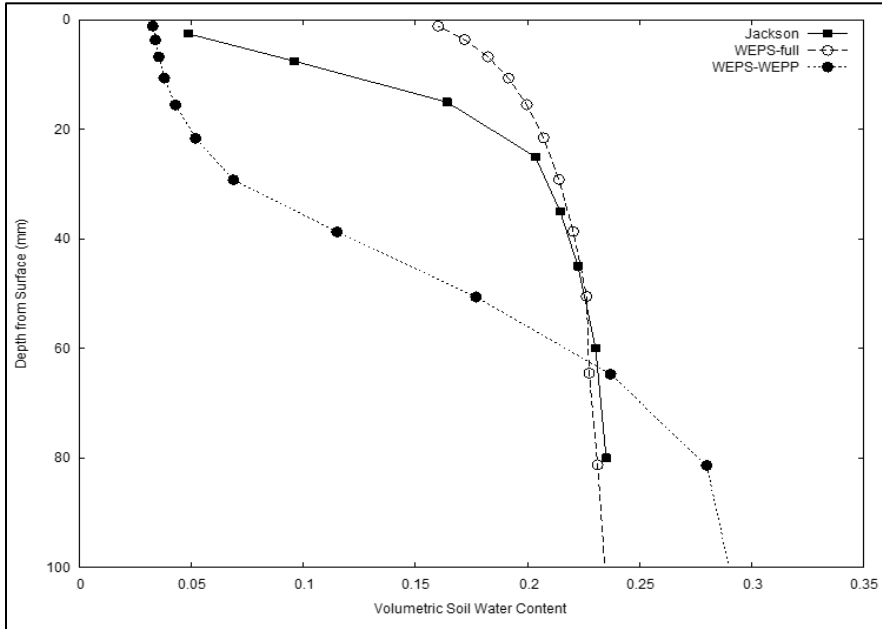


Figure 3. Comparison of surface water content as measured by Jackson (obtained by Durar from author) and simulated by WEPS. PWP indicates permanent wilting point water content where erosion threshold friction velocity is increased by 1 meter per second.

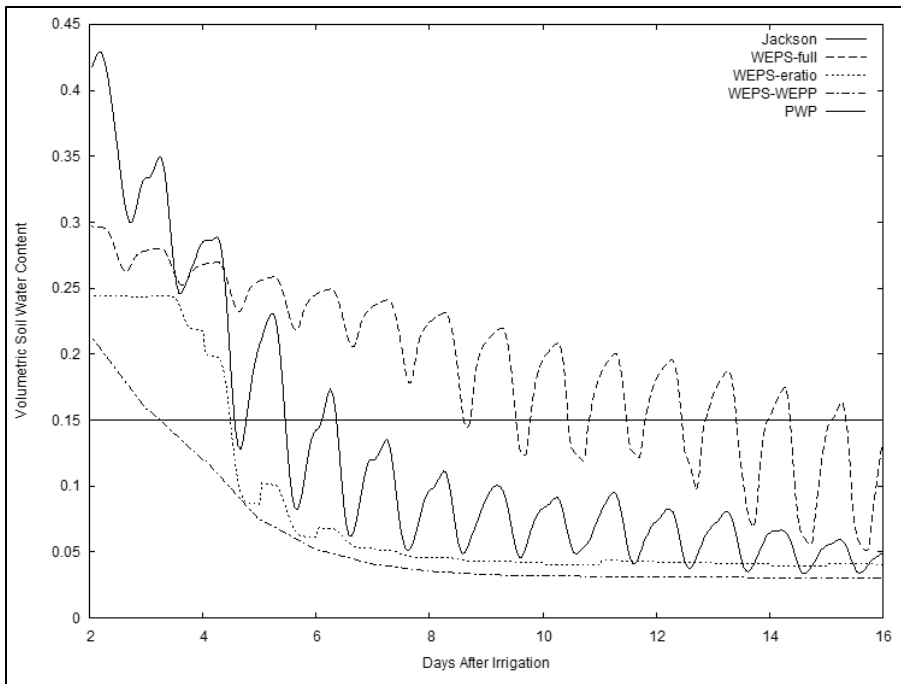


Figure 4. Comparison between Jackson (1973) measured data and simulated values of near surface soil water content profile on day 8 after irrigation at 1800 hours. The value for WEPP is at the end of the day.

Another study was conducted to independently evaluate the performance of a stand-alone version of the Hydrology submodel of WEPS in predicting surface soil drying with different soil and climatic conditions (Durar et al. 1995). A simulation with the Hydrology submodel of WEPS was run for one year. CLIGEN and WINDGEN were used to generate one year of climate data and the daily weather data from the experimental site on the days of the measurements was inserted into the file. The solar radiation values were adjusted until the simulated net radiation matched that reported by Durar et al. (1995). The 24 hourly wind velocities were also adjusted until the daily average wind at the meteorological height matched the measured values. The Pullman clay loam soil was selected from the NRCS NASIS database from the county soil survey of the study location. A management file was created containing the plowing and disking operations prior to the measurement period (dates estimated) and the irrigation application. The same configurations of WEPS as previously described were used. Figures 5, 6, and 7 summarize the comparisons.

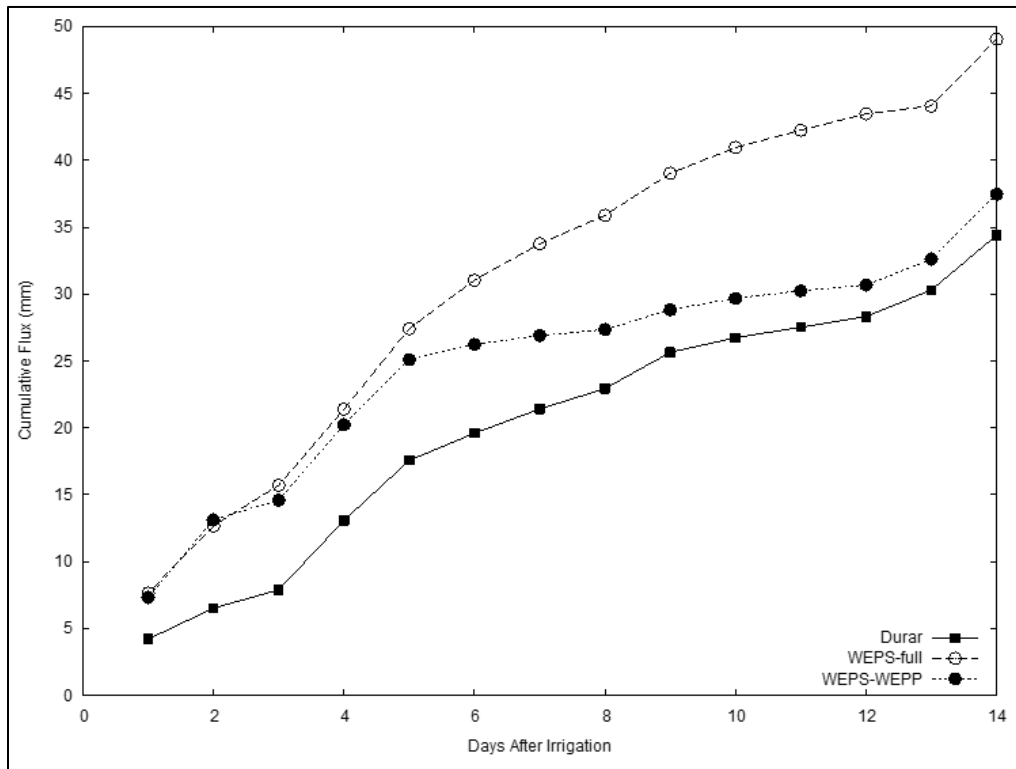


Figure 5. Comparison of cumulative evaporation as measured by Durar et al. (1995) and simulated by WEPS using Darcian-based hydrodynamic simulation (WEPS-full) and WEPP hydrology (WEPS-WEPP).

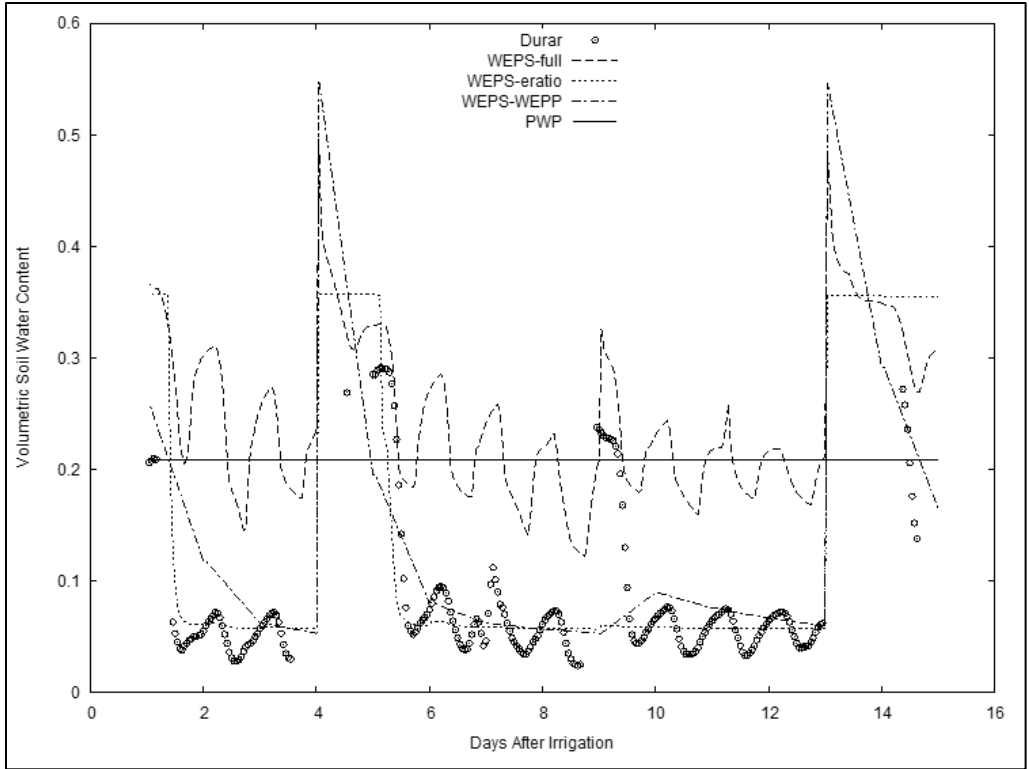


Figure 6. Comparison of surface water content as measured by Durar et al. (1995) and simulated by WEPS. PWP indicates permanent wilting point water content where erosion threshold friction velocity is increased by 1 meter per second.

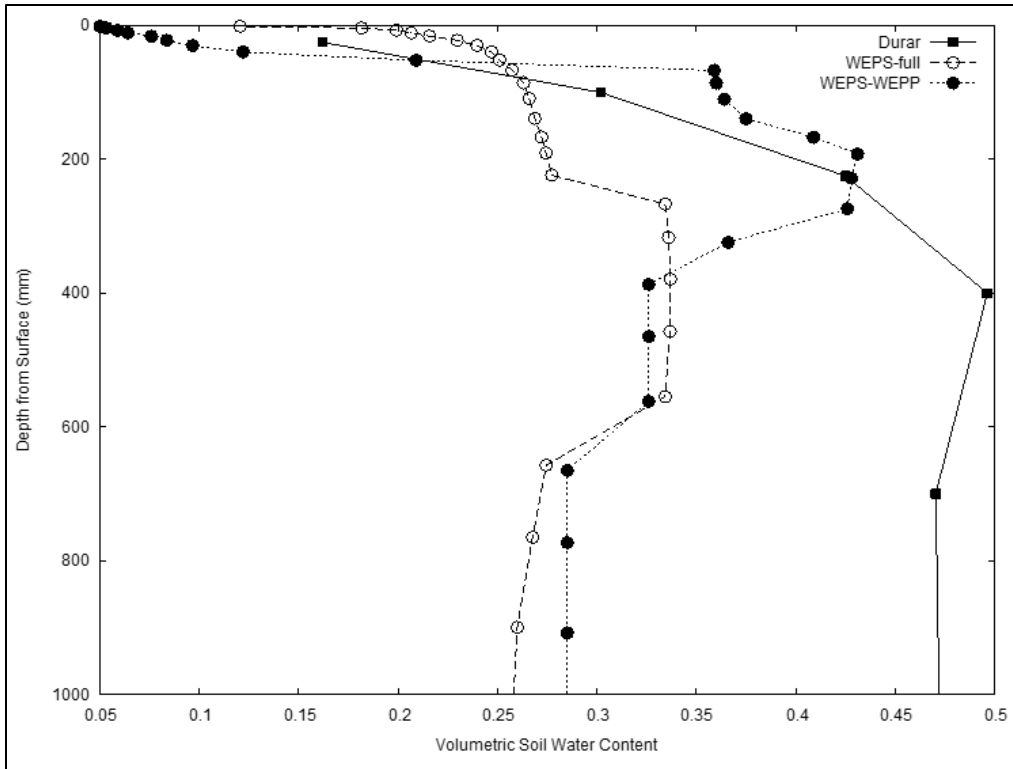


Figure 7. Comparison between Durar et al. (1995) measured data and simulated values of the soil water content profile to 1 meter on day 8 after irrigation at 1800 hours. The value for WEPS-WEPP is at the end of the day.

The submodel accurately predicted that no deep percolation occurred throughout the simulation period. Similar to the previous comparison, Figure 5 shows that the WEPS-full simulation over-predicts the capillary rise of moisture to the surface. The WEPS-WEPP simulation also over-predicts in the early days, but as its defined soil reservoir for evaporation is emptied, it evaporates at a rate less than measured and approaches the same accumulation. Figure 6 also shows a similar pattern to the previous comparison. Both WEPS-WEPP and WEPS-eratio predict a dry soil surface, only without the diurnal variation demonstrated by the measured data. The WEPS-full surface water content shows diurnal variation but remains wetter from too much capillary rise. In Figure 7, it is clear that the Pullman Clay Loam record obtained from the soil survey is much less uniform than the soil at the experimental site. Nevertheless, it also confirms the excessive capillary rise of the WEPS-full simulation and illustrates the limitation of the WEPS-WEPP simulation to accurately predict the shape of the soil water content profile.

Based on our limited testing, the Hydrology submodel of WEPS shows good results in estimating the susceptibility of the soil to wind erosion from a dry surface when configured to use the evaporation ratio with the full hydrodynamic simulation or when using the WEPP hydrology component. Unfortunately, for these soils, the full hydrodynamic simulation over-predicts the cumulative evaporation from the soil profile, limiting its usefulness for predicting crop available water after fallow periods. Use of the WEPP hydrology component for this purpose would give better results, although it under-predicts the loss of water to evaporation during long periods without rainfall. The review of these test cases highlights the need for further examination of the methods used

in the full hydrodynamic simulation and possible improvements to the evaporation methods in the WEPP component. Additionally, the focus in these studies was only on the soil surface dryness and evaporation performance. Other components of the hydrology simulation will affect the crop growth, soil properties, and residue decomposition submodels. Therefore, the following should be considered:

1. Implement routines to use measured soil water data as a means to examine the implementation of the full hydrodynamic method for errors. Implementation and testing of other soil water property functions would also be useful;
2. Broaden the validation efforts to include a wider range of soils, hydrologic, surface, and cover conditions. Obtaining data sets from the literature and from field experimentation should be considered;
3. Analyze the sensitivity of the submodel by evaluating the changes in the prediction of soil wetness by the submodel as influenced by the changes in the values of the input variables that are needed to run the submodel; and
4. Further testing is necessary to validate other elements of WEPS Hydrology submodel, such as rainfall/runoff relationships, snow and snowmelt mechanisms, soil temperature estimations, and plant water stress estimates.

During the development of the WEPS Hydrology submodel, model runtime was a major concern for NRCS use. As a result, efforts to resolve the issues noted in WEPS hydrology were deferred in order to concentrate resources on the integration of the WEPP infiltration and redistribution code. The improved runtime allowed implementation of WEPS for NRCS to occur and currently, NRCS use of WEPS uses the WEPP infiltration and redistribution code for all official model runs.

References

- Ahuja, L.R., K.W. Rojas, J.D. Hanson, et al. 2000. Root zone water quality model, modeling management effects on water quality and crop production. Water Resources Publications, LLC.
- Allen, R.G. 1996. Assessing integrity of weather data for reference evapotranspiration estimation. *Journal of Irrigation and Drainage Engineering*, 122(2):97-106.
- Allen, R.G., M.E. Jensen, J.L. Wright, et al. 1989. Operational estimates of reference evapotranspiration. *Agronomy Journal*. 81(4):650-662.
- Allen, R.G., L.S. Pereira, D. Raes, et al. 1998. Crop evapotranspiration - guidelines for computing crop water requirements - FAO Irrigation and drainage paper 56. FAO - Food and Agriculture Organization of the United Nations Rome.
- Anderson, E.A. 1976. A point energy and mass balance model of snow cover. NOAA Technical Report NWS 19, Office of Hydrology, National Weather Service, Silver Spring, MD.
- Baver, L.D., W.H. Gardner, and W.R. Gardner. 1972. Soil physics Wiley, New York, pg. 44.
- Bristow, K.I. 2002. Thermal conductivity. *In* Dane, J.H. and Topp, G.C. (eds.). Methods of soil analysis, part 4, physical methods. Soil Science Society of America, Inc. Madison, Wisconsin, USA.
- Bristow, K.L., G.S. Campbell, and C. Calissendorff. 1984. The effects of texture on the resistance to water movement within the rhizosphere. *Soil Science Society of America Journal*. 48:266-270.
- Brooks, R.H. and A.T. Corey. 1964. Hydraulic properties of porous media. Hydrology Papers No. 3, Civil Engineering Dep., Colorado State Univ., Fort Collins, CO.
- Brooks, R.H. and A.T. Corey. 1966. Properties of porous media affecting fluid flow. *Journal of Irrigation Drainage Division, American Society of Civil Engineers*. 92(IR 2):61-88.
- Campbell, G.S. 1974. A simple method for determining unsaturated conductivity from moisture retention data. *Soil Science*. 117(6):311-314.
- Campbell, G.S. 1985. Soil physics with BASIC: transport models for soil-plant systems. Elsevier Science Publishers B.V. Amsterdam, The Netherlands.
- Denmead, O.T. and R.H. Shaw. 1962. Availability of soil water to plants as affected by soil moisture content and meteorological conditions. *Agronomy Journal*. 45:385-390.
- Duffie, J.R. and W.A. Beckman. 1980. Solar engineering of thermal processes. John Wiley and Sons, New York.

- Durar, A.A. 1991. Simulation of soil-water dynamics for wind erosion modeling. Ph.D. diss. Kansas State Univ., Manhattan (Diss. Abstr. 91-28491).
- Durar, A.A., J.L. Steiner, S.R. Evett, et al. 1995. Measured and simulated surface soil drying. *Agronomy Journal*. 87(2):235-244.
- Flanagan, D.C. and M.A. Nearing (eds.). 1995. USDA-water erosion prediction project (WEPP) hillslope profile and watershed model documentation. NSERL Report No. 10, National Soil Erosion Research Laboratory, USDA-Agricultural Research Service, West Lafayette, Indiana.
- Fredlund, D.G. and A. Xing. 1994. Equations for the soil-water characteristic curve. *Canadian Geotechnical Journal*. 31(3):521-532.
- Gardner, C.M.K., K.B. Laryea, and P.W. Unger. 1999. Soil physical constraints to plant growth and crop production. AGL/MISC/24/99, Land and Water Development Division, Food and Agriculture Organization of the United Nations, Rome, page 24.
- Gastó, J.M., J. Grifoll, and Y. Cohen. 2002. Estimation of internodal permeabilities for numerical simulation of unsaturated flows. *Water Resources Research*, 38(12):62-1-62-10.
- Hillel, D. 1971. *Soil and water: physical principles and processes*. Academic Press, New York, NY.
- Hillel, D. 1977. *Computer simulation of soil-water dynamics: a compendium of recent work*. International Development Research Centre, Ottawa, Canada.
- Hindmarsh, A.C. 1983. ODEPACK, a systematized collection of ODE solvers. In: *Scientific Computing*, R. S. Stepleman, M. Carver, R. Peskin, W. F. Ames, and W. F. Vichnevetsky (eds.), North-Holland, Amsterdam, 1983 (vol. 1 of IMACS Transactions on Scientific Computation), pp. 55-64.
- Hindmarsh, A.C. 2001. *Serial Fortran Solvers for ODE Initial Value Problems*. Center for Applied Scientific Computing, Lawrence Livermore National Laboratory, Livermore, CA Available at: https://computation.llnl.gov/casc/odepack/odepack_home.html. (Accessed August 10, 2020).
- Holmes, R.M. and G.W. Robertson. 1963. Application of the relationship between actual and potential evapotranspiration in dry land agriculture. *Transactions of the American Society of Agricultural Engineers*. 6(1):65-67.
- Jackson, R.D. 1973. Diurnal changes in soil-water content during drying. p. 37-55. In: R. R. Bruce, K. W. Flach and H. W. Taylor (eds.). *Field soil water regime*. Special Publication 5. Soil Science Society of America, Madison, WI.
- Jackson, R.D., B.A. Kimball, R.J. Reginato, et al. 1973. Diurnal soil water evaporation: time-depth-flux patterns. *Soil Science Society of America Proceedings*. 37(4):505-509.

- Jansson, P. and D.S. Moon. 2001. A coupled model of water, heat and mass transfer using object orientation to improve flexibility and functionality. *Environmental Modeling & Software*. 16(1):37-46.
- Jensen, M.E. (ed.). 1974. Consumptive use of water and irrigation water requirements. A report prepared by the Technical Committee on Irrigation. Water Requirements, Irrigation, and Drainage Division, American Society of Civil Engineers. New York, NY.
- Jensen, M.E., R.D. Burman and R.G. Allen (eds.). 1990. Evapotranspiration and irrigation water requirements, ASCE Manuals and reports on engineering practice; no.70. Am. Soc. Civ. Eng.
- Jensen, M.E., J.L. Wright, and B.J. Pratt. 1971. Estimating soil moisture depletion from climate, crop and soil data. *Transactions of the American Society of Agricultural Engineers*. 14(5):954-959.
- Jumikis, A. R. 1966. Thermal soil mechanics. Rutgers University Press. New Brunswick, NJ.
- Kluitenberg, G.J. 2002. Heat capacity and specific heat. *In* Dane, J.H. and Topp, G.C. (eds.). *Methods of soil analysis, Part 4, physical methods*. Soil Science Society of America, Inc. Madison, Wisconsin, USA.
- London, J. and C. Frohlich. 1982. Extended abstracts presented at the symposium on the solar constant and the spectral distribution of solar irradiance, Int. Assoc. of Meteorology and Atmospheric Physics Third Scientific Assembly, Hamburg, Federal Rep. Germany. 17-28 Aug. 1981. IAMAP, Innsbruck, Austria.
- Marshall, T.J. and J.W. Holmes. 1979. *Soil physics*. Cambridge University Press, Cambridge; New York. Pg. 277.
- McMaster, G.S., R.M. Aiken, and D.C. Nielsen. 2000. Optimizing wheat harvest cutting height for harvest efficiency and soil and water conservation. *Agronomy Journal*. 92(6):1104-1108.
- Millington, R.J. and J.P. Quirk. 1959. Permeability of porous media. *Nature*. 183:387-388.
- Mualem, Y. 1976. A new model for predicting the hydraulic conductivity of unsaturated porous media. *Water Resources Research*. 12(3):513-522.
- Murray, F.W. 1967. On the computation of saturation vapor pressure. *Journal of Applied Meteorology*. 6:203-204.
- NOAA, NASA, and USAF. 1976. U.S. standard atmosphere, 1976. U.S. Government Printing Office, Washington, DC.
- NOAA. 2002. Solar Calculation Details. Available at: <https://www.esrl.noaa.gov/gmd/grad/solcalc/calcdetails.html>. (Accessed Aug 7, 2020).

- Penman, H.L. 1948. Natural evaporation from open water, bare soil, and grass. *Proceedings of the Royal Society (London), Series A* 193:120-146.
- Peters-Lidard, C.D., E. Blackburn, X. Liang, et al. 1998. The effect of soil thermal conductivity parameterization on surface energy fluxes and temperatures. *Journal of the Atmospheric Sciences*. 55:1209-1224
- Petzold, L.R. 1983. Automatic selection of methods for solving stiff and nonstiff systems of ordinary differential equations, *Siam Journal of Scientific Statistical Computing*. 4:136-148.
- Raupach, M.R. 1994. Simplified Expressions for Vegetation Roughness Length and Zero-Plane Displacement as functions of Canopy Height and Area index. *Boundary Layer Meteorology* 71:211-216.
- Rawls, W.J. and D.L. Brakensiek. 1989. Estimation of soil water retention and hydraulic properties. *In* H. J. Morel-Seytoux (ed.). *Unsaturated flow in hydraulic modeling theory and practice*. NATO ASI Series. Series C: Mathematical and Physical Science. 275:275-300.
- Rawls, W.J., D. Gimenez, and R. Grossman. 1998. Use of soil texture, bulk density and slope of the water retention curve to predict saturated hydraulic conductivity. *Transactions of the American Society of Agricultural Engineers*. 41(4):983-988.
- Richards, L.A. 1931. Capillary conduction of liquids through porous mediums. *Physics*. 1:318-324.
- Richardson, C.W. and J.T. Ritchie. 1973. Soil water balance for small watersheds. *Transactions of the American Society of Agricultural Engineers*. 16(1):72-77.
- Rutherford, D.W. and C.T. Chlou. 1992. Effect of water saturation in soil organic matter on the partition of organic compounds. *Environmental Science and Technology*. 26(5):965-970.
- Savabi, M.R., A.D. Nicks, J.R. Williams, et al. 1989. Chapter 7, Water balance and percolation. *In* L. J. Lane and M. A. Nearing (ed.) *USDA-water erosion prediction project: hillslope profile model documentation*. NSERL Report No. 2. USDA-ARS National Soil Erosion Research Laboratory, West Lafayette, IN.
- Saxton, K.E. and G.C. Bluhm. 1982. Regional prediction of crop water stress by soil water budgets and climatic demand. *Transactions of the American Society of Agricultural Engineers*. 25(1):105-110 & 115.
- Saxton, K.E., H.P. Johnson, and R.H. Shaw. 1974. Modeling evapotranspiration and soil moisture. *Transactions of the American Society of Agricultural Engineers*. 17(4):673-677.
- Saxton, K.E., P.F. Brooks, R. Richmond et al. 1984. User's manual for SPAW--a soil-plant-air-water model. Revision No.3 (8/6/84). USDA-ARS in cooperation with Washington State Univ., Pullman, WA.

Sharpley, A.N. and J.R. Williams (eds.). 1990. EPIC—erosion/productivity impact calculator: 1. model documentation. U.S. Department of Agriculture Technical Bulletin Number 1768.

Skidmore, E.L., H.S. Jacobs, and W.L. Powers. 1969. Potential evapotranspiration as influenced by wind. *Agronomy Journal*. 61(4):543-546.

Smith, R.E. and J.R. Williams. 1980. Simulation of the surface water hydrology. p. 13-35. *In* W. G. Knisel (ed.) CREAMS: a field scale model for chemicals, runoff, and erosion from agricultural management systems. USDA Conservation Research Report No. 26, U.S. Dept. of Agric., Washington DC.

Steiner, J.L. 1989. Tillage and surface residue effects on evaporation from soils. *Soil Science Society of America Proceedings*. 53(3):911-916.

Sudar, R.A., K.E. Saxton, and R.G. Spomer. 1981. A predictive model of water stress in corn and soybeans. *Transactions of the American Society of Agricultural Engineers*. 24(1):97-102.

Szymkiewicz, A. 2009. Approximation of intermodal conductivities in numerical simulation of one-dimensional infiltration, drainage, and capillary rise in unsaturated soils. *Water Resources Research* Volume 45, W10403, doi: 10.1029/2008WR007654

Szymkiewicz, A. and R. Helmig. 2010. Comparison of conductivity averaging methods for one-dimensional unsaturated flow in layered soils. Preprint Series, Stuttgart Research Centre for Simulation Technology, Stuttgart, Germany.

ten Berge, H.F.M. 1990. Heat and water transfer in bare topsoil and the lower atmosphere. Pudoc Wageningen.

USDA Soil Conservation Service. 1972. SCS national engineering handbook, section 4, hydrology. NEH-Notice 4-102. Soil Conservation Service, U.S. Department of Agriculture, Washington DC.

Van Bavel, C.H.M. 1966. Potential evaporation: the combination concept and its experimental verification. *Water Resources Research*. 2(3):455-467.

van Donk, S.J. and E.W. Tollner. 2000. Apparent thermal conductivity of mulch materials exposed to forced convection. *Transactions of the American Society of Agricultural Engineers*. 43(5):1117-1127.

Van Genuchten R. 1978. Calculating the unsaturated hydraulic conductivity with a new closed-form analytical model. Research Report 78-WR-08, Water Resources Program, Department of Civil Engineering, Princeton Univ., Princeton, NJ.

Van Genuchten M. Th. 1980. A closed-form equation for predicting the hydraulic conductivity of unsaturated soils. *Soil Science Society of America Journal*. 44(5):892-898.

Weast, R.C., M.J. Astle, and W.H. Beyer. 1983. CRC handbook of chemistry and physics. 64th ed. (1983-1984), Chemical Rubber Company Press, Inc., Boca Raton, Fl.

Wendt, C.W. 1970. Water transfer from soil to the atmosphere as related to climate and soil properties. Tech. Rep. 24. Water Resources Institute. Texas A&M Univ., College Station, TX.

Williams, J.R. 1989. EPIC: the erosion-productivity impact calculator. p. 676-681. *In* Proc. 1989 Summer Computer Simulation Conference, Austin, TX. July 24-27, 1989. The Society for Computer Simulation, San Diego, CA.

Williams, J.R. and R.W. Hann, Jr. 1978. Optimal operation of large agricultural watersheds with water quality constraints. Tech. Rep. 96. Texas Water Resour. Inst. Texas A&M Univ., College Station, TX.

Williams, J.R., C.A. Jones, and P.T. Dyke. 1984. A modeling approach to determining the relationship between erosion and soil productivity. *Transactions of the American Society of Agricultural Engineers*. 27(1):129-144.

Williams, J.R., C.A. Jones, and P.T. Dyke. 1990. The EPIC model. p. 3-92. *In* A.N. Sharpley and J.R. Williams. (ed.) EPIC--erosion/productivity impact calculator: 1. model documentation. USDA Technical Bulletin Number 1768, U.S. Department of Agriculture, Washington DC.

Wright, J.L. 1982. New evapotranspiration crop coefficients. *Journal of Irrigation and Drainage Division, American Society of Civil Engineers*. 108(2):57-74.

Table 3. List of symbols for the Hydrology submodel of WEPS.

Symbol	Definition	Units	Variable Name *
a	empirical coefficient in net radiation equation	unitless	a
a_l	empirical coefficient in net radiation equation	unitless	a1
b	empirical coefficient in net radiation equation	unitless	b
b_l	empirical coefficient in net radiation equation	unitless	-
c	specific heat capacity of each layer component as	$\text{J kg}^{-1} \text{ }^\circ\text{C}^{-1}$	designated by the subscript
C_{bd}	standing biomass coefficient of drag as defined in the Erosion submodel	unitless	brcd
c_{cla}	specific heat capacity of clay	$\text{J kg}^{-1} \text{ }^\circ\text{C}^{-1}$	clayheatcap
c_{ice}	specific heat capacity of ice	$\text{J kg}^{-1} \text{ }^\circ\text{C}^{-1}$	iceheatcap
c_{om}	specific heat capacity of organic matter	$\text{J kg}^{-1} \text{ }^\circ\text{C}^{-1}$	organheatcap
c_{san}	specific heat capacity of sand	$\text{J kg}^{-1} \text{ }^\circ\text{C}^{-1}$	sandheatcap
c_{sil}	specific heat capacity of silt	$\text{J kg}^{-1} \text{ }^\circ\text{C}^{-1}$	silheatcap
C_{tt}	turbulent transfer coefficient for water vapor	$\text{kg m}^{-2} \text{ kPa}^{-1} \text{ day}^{-1}$	ttc
C_{ug}	universal gas constant	$\text{J mole}^{-1} \text{ }^\circ\text{K}^{-1}$	rgas
C_{vl}	volumetric heat capacity of the layer	$\text{J m}^{-3} \text{ }^\circ\text{C}^{-1}$	heat_cap_0
c_{wat}	specific heat capacity of liquid water	$\text{J kg}^{-1} \text{ }^\circ\text{C}^{-1}$	waterheatcap
D_{adj}	diffusivity of water vapor in air adjusted for temperature and pressure	$\text{m}^2 \text{ s}^{-1}$	diffutp
$dirg$	amount of daily irrigation	mm	bhzirr
D_v^i	vapor diffusivity of soil layer i	$\text{m}^2 \text{ s}^{-1}$	soildiffu(lrx)
D_{va}^i	diffusivity of water vapor in air between soil layers i and $i-1$	$\text{m}^2 \text{ s}^{-1}$	diffua(lrx)

d_l	depth to the bottom of the soil layer from the soil surface	m	mmtom*bszlyd(k)
d_{oy}	day of year	unitless	idoym
d_{prc}	amount of daily deep percolation	mm	bhzper
d_r	relative distance of the earth from the sun	unitless	dr
d_{rz}	plant root zone depth	m	mmtom*rootd
D_{stp}	binary diffusion coefficient for water vapor in air	$m^2 s^{-1}$	diffuntp
D_{va}	diffusivity of water vapor in air	$m^2 s^{-1}$	soildiffu
E'_p	adjusted potential surface evaporation for standing biomass	$mm day^{-1}$	ahzep
E''_p	adjusted potential surface evaporation for standing and flat residue	$mm day^{-1}$	ahzep, evapdaypot
e_a	evaporation rate of water from the soil surface	$m^2 s^{-1}$	soil_evap_rate
E_a	actual daily soil evaporation	$mm day^{-1}$	ahzea
e_{air}	vapor pressure of the air at T_{air}	kPa	vpa
E_l	evaporation removed from the layer	m	evaplay
emx	maximum evaporation rate	$m^2 s^{-1}$	max_evap_rate
e^o_d	saturation vapor pressure at the dew-point temperature	kPa	e
e^o_z	daily saturation vapor pressure of the air	kPa	vps
$e^o_z - e_z$	saturation vapor pressure deficit of air	kPa	vpd
E_p	potential daily soil evaporation	$mm day^{-1}$	ahzep
E_r	remaining evaporation to be distributed in the soil layers	m	evaprem
eta	amount of daily actual evapotranspiration	$mm day^{-1}$	ahzeta
$E\mathcal{T}p$	potential evapotranspiration	$mm day^{-1}$	ahzeta
$E\mathcal{T}pr$	potential evapotranspiration by radiation	$mm day^{-1}$	etpr

$E\mathcal{J}p_w$	potential evapotranspiration by wind	mm day ⁻¹	etpw
e_z	daily vapor pressure of the air	kPa	vpa
f_{up}^a	same factor for the layer above the current layer	unitless	wup_fac(k-1)
F_{ice}	mass fraction of water in the existing snow or soil layer that is frozen	unitless	bhfsnfrz
F'_{ice}	fraction of layer water that is frozen at the end of the time step	unitless	bhfsnfrz, froz_end
F'_{ice}	fraction of frozen water in the amended snow layer	unitless	bhfsnfrz
F''_{ice}	fraction of frozen water in the amended snow layer accounting for the change in snow density	unitless	bhfsnfrz
f_a and f_b	evaporation reduction factors associated with each crop or residue type	unitless	coeff_a, coeff_b
fc_{20}	fraction of clay in the top 20 cm of soil	unitless	clay
F_{cla}	mass fraction for clay	unitless	bsfcla, clayfrac
f_{dw}	Darcy Weisbach friction factor	unitless	dw_friction
f_{fcv}	fraction of the surface covered by flat biomass	unitless	f_flat
F_{ice}	mass fraction of the layer water content that is ice	unitless	bhface, froz_beg
f_{om}	volumetric fraction that is organic matter	unitless	volf_organic
F_{om}	mass fraction of organic matter in the solid mass portion of the soil	unitless	bsfom, orgfrac
f_{pnd}	fraction of the surface covered by ponded water	unitless	frac_pond_area
f_{por}	soil porosity	unitless	porosity
f_{qtz}	volumetric fraction of soil that is quartz	unitless	volf_quartz
f_{s20}	fraction of sand in the top 20 cm of soil	unitless	sand

F_{san}	mass fraction of sand in the mineral portion of the soil	unitless	bsfsan
F_{sil}	mass fraction of silt in the mineral portion of the soil	unitless	bsfsil
f_{slp}	slope of the soil surface	$m\ m^{-1}$	soilslope
f_{up}	factor for water use distribution by depth	unitless	wup_fac(k)
f_{wat}	volume fraction of the soil water that is liquid water	unitless	volf_liq_water
f_{ws}	water stress factor	unitless	wsf
G	soil heat flux	$MJ\ m^{-2}\ day^{-1}$	g_soil
g	gravitational constant	$m\ s^{-2}$	gravconst
g_{cl80}	gravimetric water content of clay minerals at 80% relative humidity	$kg\ kg^{-1}$	claygrav80rh
g_{om80}	gravimetric water content of soil organic matter at 80% relative humidity	$kg\ kg^{-1}$	orggrav80rh
G_{sc}	solar constant	$MJ\ m^{-2}\ day^{-1}$	gsc
h_a	heat transfer coefficient between this layer and the layer above	$J\ m^{-2}\ s^{-1}\ ^\circ C^{-1}$	thermt_up
h_b	heat transfer coefficient between this layer and the layer below	$J\ m^{-2}\ s^{-1}\ ^\circ C^{-1}$	thermt_dn
H_{fus}	latent heat of fusion of water	$J\ kg^{-1}$	heat_fusion
i_{mx}	maximum soil infiltration rate	$m\ s^{-1}$	max_infil_rate
K	hydraulic conductivity	$m\ s^{-1}$	cond
K^6	hydraulic conductivity of the soil surface layer	$m\ s^{-1}$	cond(1)
K^6_{sat}	saturated hydraulic conductivity of the soil surface layer	$m\ s^{-1}$	ksat(1)
k_a	thermal conductivity of the layer above	$J\ s^{-1}\ m^{-1}\ ^\circ C^{-1}$	thermk_up
K^i	hydraulic conductivity between soil layers i and $i-1$	$m\ s^{-1}$	conda(lrx)
k_{ice}	thermal conductivity of ice	$J\ s^{-1}\ m^{-1}\ ^\circ C^{-1}$	iceheatcond
K^i_s	saturated hydraulic conductivity	$m\ s^{-1}$	ksat(lrx)
K^i_u	unsaturated hydraulic conductivity	$m\ s^{-1}$	cond(lrx)

k_l	thermal conductivity of this layer	$\text{J s}^{-1} \text{m}^{-1} \text{°C}^{-1}$	thermk_dn
k_{min}	thermal conductivity of the non-quartz mineral portion of the soil	$\text{J s}^{-1} \text{m}^{-1} \text{°C}^{-1}$	mineralheatcond
k_{om}	thermal conductivity of the organic matter part of the soil	$\text{J s}^{-1} \text{m}^{-1} \text{°C}^{-1}$	organicheatcond
k_{qtz}	thermal conductivity of quartz	$\text{J s}^{-1} \text{m}^{-1} \text{°C}^{-1}$	quartzheatcond
k_{res}	thermal conductivity of the residue layer	$\text{J s}^{-1} \text{m}^{-1} \text{°C}^{-1}$	res_cond
k_{sd}	thermal conductivity of dry soil	$\text{J s}^{-1} \text{m}^{-1} \text{°C}^{-1}$	cond_dry
k_{sm}	thermal conductivity of the solid soil matrix	$\text{J s}^{-1} \text{m}^{-1} \text{°C}^{-1}$	cond_soil
k_{sno}	thermal conductivity of the snow layer	$\text{J s}^{-1} \text{m}^{-1} \text{°C}^{-1}$	snowcond
k_{ss}	thermal conductivity of saturated soil	$\text{J s}^{-1} \text{m}^{-1} \text{°C}^{-1}$	cond_sat
k_{vk}	Von Karman's constant	unitless	vk
k_{wat}	thermal conductivity of water	$\text{J s}^{-1} \text{m}^{-1} \text{°C}^{-1}$	cond_water
LAI_{eff}	plant live leaf area index	unitless	eff_lai
M'_{sno}	mass of the amended snow layer	kg m^{-2}	tot_mass
M_{adw}	mass of added water	kg m^{-2}	new_mass
M_{res}	mass of residue flat on the soil surface	kg m^{-2}	bdmres
M_{rf}	effective mass of flat residue for evaporation reduction	kg m^{-2}	pseudo_mass
M_{sno}	total mass of the existing snow layer	kg m^{-2}	old_mass
M_w	molecular weight of water	kg mole^{-1}	molewater
n	total number of soil layers	unitless	layrsn
N_{ker}	Kersten number	unitless	kersten
n_{rz}	total number of soil layers in the plant root zone	unitless	-
n_{sl}	number of soil layers	unitless	layrsn
N_{stm}	number of stems standing on the soil surface	$\# \text{m}^{-2}$	tot_stems
p'''_{sno}	snow density adjusted for settling	kg m^{-3}	-

p''_{sno}	snow density adjusted for compaction	kg m ⁻³	-
P_B	barometric pressure	kPa	bp
$prcp$	amount of daily precipitation	mm	bwzdpt
q	change in heat energy content of the layer	J m ⁻² s ⁻¹	diff_heat_0
Q'_{frz}	relative total layer energy if fully frozen at zero degrees	J m ⁻²	fz_energy
Q'_{sno}	relative total energy of the amended snow layer	J m ⁻²	tot_energy
q^1_n	rate of surface water supply	m s ⁻¹	wfluxn(1)
q^2_n	net runoff flux	m s	wfluxn(2)
q^3_n	net evaporation flux	m s	wfluxn(3)
q^4_n	net infiltration flux	m s ⁻¹	wfluxn(4)
q^5_n	rate of change in ponded depth	m s ⁻¹	wfluxn(5)
Q_{adw}	energy content of the added water	j m ⁻²	new_energy
q^i_n	net water flux in soil layer i	m s ⁻¹	wfluxn(lrx)
q^i_r	resultant water flux between soil layers i and $i-1$	m s ⁻¹	wfluxr(lrx)
q^i_{src}	water flux from any in-layer source such as drip irrigation	m s ⁻¹	lay_source(lrx)
q^i_v	water vapor flux between soil layers i and $i-1$	m s ⁻¹	fluxv(lrx)
q^i_w	liquid water flux between soil layers i and $i-1$	m s ⁻¹	fluxw(lrx)
q_{rain}	rainfall (plus snowmelt) rate	m s ⁻¹	-
q_{rp}	representative peak intensity	m s ⁻¹	intenspeak
q_{sir}	surface irrigation application rate	m s ⁻¹	surface_rate
Q_{sno}	relative total energy of the existing snow layer	J m ⁻²	old_energy
R_a	extraterrestrial radiation	MJ m ⁻² day ⁻¹	ra
r_a	solar zenith angle at sunset	degrees	beamrise
r_{awc}	relative amount of available water content for the soil layer	unitless	awcr

r_e	ratio of the actual evaporation rate (e_a) to the potential evaporation rate (e_{mx})	unitless	evapratio
r_{ran}	random roughness of the soil surface	m	ranrough
R_{rn}	net radiation gain to the upper surface of the layer	$\text{J m}^{-2} \text{s}^{-1}$	rate_rad_net
R_n	net radiation	$\text{MJ m}^{-2} \text{day}^{-1}$	rn
r_{ref}	random roughness created by the last tillage operation	m	ref_ranrough
R_s	measured short wave (global) solar radiation	$\text{MJ m}^{-2} \text{day}^{-1}$	bweirr
R_{so}	clear sky short wave radiation	$\text{MJ m}^{-2} \text{day}^{-1}$	rso
$runoff$	amount of daily surface runoff	mm	bhzrun
S	any within layer water source	$\text{m}^3 \text{m}^{-3} \text{s}^{-1}$	lay_source
$snmelt$	daily snow melt	mm	bhzsmt
$snow$	amount of daily precipitation that falls as snow	mm	
S_w	degree of saturation	unitless	deg_sat
swc	amount of water in the soil profile on any given day	mm	swc
$swci$	initial amount of water in the soil profile	mm	lswc
T	temperature	$^{\circ}\text{C}$	airtemp
t	time	s	t
T'_l	new layer temperature at the end of the time step	$^{\circ}\text{C}$	tlay_end
T'_{sno}	daily average temperature of the amended snow layer	$^{\circ}\text{C}$	bhtsno
t_{3qd}	three quarter day length	s	64800
T_a	temperature of the layer above	$^{\circ}\text{C}$	tup_end
$\mathcal{J}a$	actual daily plant transpiration	mm day^{-1}	ahzpta
T_{air}	air temperature at that time of day	$^{\circ}\text{C}$	airtemp
T_{amp}	amplitude of the daily variation around the daily average air temperature	$^{\circ}\text{C}$	tamp

T_b	temperature of the layer below	°C	tdn_end
T_{daj}	adjusted mean daily air temperature	°C	tdavadj
T_{dav}	daily average air temperature	°C	t_air
T_{dew}	measured dew point temperature	°C	bwtdpt
t_{dl}	day length	s	lenday
T_{dmn}	daily minimum air temperature	°C	bwtdmn
T_{dmx}	daily maximum air temperature	°C	bwtdmx
T_{dwy}	adjusted dew point temperature	°C	tdewadj
t_{dy}	time of day	s	tday
t_{hd}	half day length	s	halfperiod
T_{dmn}^i	daily minimum soil temperatures for layer i	°C	bhtsmn(lay)
T_{dmx}^i	daily maximum soil temperatures for layer i	°C	bhtsmx(lay)
t_{ie}	irrigation end time	s	surface_end
t_{is}	irrigation start time	s	surface_start
T_l	temperature of the layer at the beginning of the time step	°C	tlay_beg
T_{mnj}	adjusted daily minimum air temperature	°C	tminadj
T_{mnk}	minimum daily air temperature	°K	tmink
T_{mxj}	adjusted daily maximum air temperature	°C	tmaxadj
T_{mxk}	maximum daily air temperature	°K	tmaxk
T_{dmn}^n	daily minimum air temperature for the next day	°C	airtminnext
$\mathcal{J}p$	potential daily plant transpiration	mm day ⁻¹	ahzptp
T_{dmx}^p	daily maximum air temperature from the previous day	°C	airtmaxprev
t_{qd}	one quarter day length	s	21600
t_{re}	time when the rain ends	s	rainend
t_{rise}	time of sunrise	s	sunrise

t_{rm}	“midpoint” of the rainfall event or when the peak intensity occurs	s	rainmid
t_{rs}	time when rain starts	s	rainstart
t_{se}	source end time	s	source_end
t_{set}	time of sunset	s	sunset
t_{sn}	time of solar noon with respect to the standard meridian time zone	s	sn
T_{sno}	temperature of the existing snow layer	°C	bhtsno
T_{soil}	temperature of the soil	°C	soiltemp
t_{ss}	source start time	s	source_start
T_{wat}	temperature of the water	°C	bhtsav
T_{wb}	wet bulb temperature	°C	t_wb
U_z	mean daily wind speed at height z_a	$m\ s^{-1}$	vel_wind
w	gravimetric water content	$Mg\ m^{-3}$	grav_wat
W_{at}	accumulated actual water use in the soil layers above the layer	mm	actwu
W_{ua}	actual plant water-uptake from the soil layer	$mm\ day^{-1}$	wua
w_{uc}	water use compensation parameter	unitless	wuc
w_{ud}	water use distribution by depth parameter	unitless	wud
W_{up}	potential plant water-uptake from the soil layer	$mm\ day^{-1}$	wup
x'_{sno}	new snow depth due to added snow or a change in frozen fraction	m	mmtom*bhzsnd
x'_{snw}	depth of water in the amended snow layer in liquid water equivalent	m	mmtom*bhzsno
x''_{sno}	depth of the snow layer adjusted for the change in frozen water fraction	m	mmtom*bhzsnd
x''_{snw}	depth of water in the snow layer after drainage in liquid water equivalent	m	mmtom*bhzsno
x_a	thickness of the layer above	m	-

x_{adw}	depth of added water	m	-
x_{asn}	thickness to be added to the existing snow layer	m	new_depth
x_{elv}	elevation of the site	m	bmzele
x_l^i	thickness of soil layer i	m	tlay(lrx)
x_l	thickness of the soil layer	m	mmtom*bszlyt, layth
x_{mlt}	liquid water that drains from the snow layer	m	mmtom*bhzsmt
x_{res}	thickness of the residue layer	m	res_depth
x_{rps}	total depth of rainfall (plus snowmelt) for the event	m	raindepth
x_{scr}	depth of in-layer source water applied	m	-
x_{sir}	depth of irrigation applied	m	mmtom*dirrig
x_{slp}	slope length	m	slopelength
x_{sno}	thickness of the snow layer	m	mmtom*bhzsnd
x_{snw}	total water content of the snow layer	m	mmtom*bhzsno
z	distance below the soil surface	m	depth
z^6	distance from the soil surface to midpoint of the surface layer	m	dist(1)
z_a	height of meteorological sensors for temperature, humidity, and radiation	m	loc_za
z_{aw}	standard meteorological height at the weather station	m	met_height
z_d	zero plane displacement	m	loc_zd
z_{damp}	damping depth, depth in the soil to which the temperature variation penetrates	m	zdamp
z_{dw}	zero plane displacement at the location of the meteorological measurements	m	awzdisp
z_{epd}	evaporation depth or depth to which evaporation occurs	m	epdp

z_l^i	depth to the midpoint of soil layer i from the soil surface	m	depth(lrx)
z_l	distance from the soil surface to the bottom of the soil layer	m	laydp
z_{olt}	height of any field outlet structure above the surface of the soil	m	bhzoutflow
z_{ov}	roughness length for vapor transfer	m	zo_v
z_{pmx}	maximum depth of ponded water where the surface is completely covered	m	pondmax
z_{pnd}	depth of ponded water	m	volw(5)
α	albedo (reflectance) of the surface		albt
Γ_{cl}	percent clay in the soil	%	per_clay
Γ_{sa}	percent sand in the soil	%	per_sand
Δ/γ	adjusted ratio of the slope of the saturation vapor pressure curve at mean air temperature	unitless	svpg
$(\Delta/\gamma)_0$	unadjusted ratio of the slope of the saturation vapor pressure curve at mean air temperature	unitless	svpg0
δ	declination of the sun	degrees	dec
Δt	time step	s	time_step
Δt_{b1}	time required for the layer to reach zero degrees C	s	time_brk_1
Δt_{b2}	time from the beginning of the time step when the layer is completely thawed	s	time_brk_2
Δt_{eot}	equation of time	s	e
Δz^i	distance between soil layers i and $i-1$	m	dist(lrx)
Θ	WEPP soil layer water content	m	st
θ	WEPS soil layer water content	$m^3 m^{-3}$	theta
θ_w^6	permanent wilting point water content of the soil surface layer	$m^3 m^{-3}$	thetaw(1)
θ_e	equivalent water content	unitless	thetae
θ_{es}	WEPS soil layer entrapped air reduced saturation water content	$m^3 m^{-3}$	thetes

θ_f	WEPS soil layer field capacity water content	$\text{m}^3 \text{m}^{-3}$	thetaf
Θ_{fc}	WEPP soil layer field capacity water content	m	fc
θ_i	volumetric soil water content of soil layer i	$\text{m}^3 \text{m}^{-3}$	theta(lrx)
θ_r^i	residual volumetric soil water content	$\text{m}^3 \text{m}^{-3}$	thetar(lrx)
θ_s^i	saturated volumetric soil water content	$\text{m}^3 \text{m}^{-3}$	thetas(lrx)
θ_l	volumetric water content of the layer	$\text{m}^3 \text{m}^{-3}$	vol_wat
θ_r	residual soil water content where hydraulic conductivity becomes zero	$\text{m}^3 \text{m}^{-3}$	thetar
Θ_{re}	soil layer readily evaporable water content	m	rew
θ_{rh80}	water content of the soil when the soil air is at 80% relative humidity	$\text{m}^3 \text{m}^{-3}$	theta80rh
θ_s	saturated volumetric soil water content	$\text{m}^3 \text{m}^{-3}$	thetas
θ^s	surface soil water content	$\text{m}^3 \text{m}^{-3}$	theta(0)
Θ_{te}	soil layer total evaporable water content	m	tew
Θ_{ul}	WEPP soil layer upper limit water content	m	ul
θ_w	WEPS soil layer wilting point water content	$\text{m}^3 \text{m}^{-3}$	thetaw
Θ_{wfe}	WEPP water available for evaporation in each layer	m	wfevp
λ	latent heat of vaporization	MJ kg^{-1}	vlh
λ_{loc}	local meridian	degrees	-dlong
λ_{bc}	Brooks and Corey pore size interaction parameter	unitless	lambda
λ^i	Brooks and Corey (1966) pore size interaction term	unitless	lambda(lrx)
λ_{st}	standard time zone meridian	degrees	-

ρ'_{sno}	average density of the snow layer after adjusting for frozen fraction	kg m ⁻³	snow_den
ρ''_{sno}	snow density adjusted for compaction	kg m ⁻³	snow_den
ρ'''_{sno}	snow density adjusted for settling	kg m ⁻³	snow_den
ρ''''_{sno}	snow density adjusted for the daily maximum air temperature	kg m ⁻³	snow_den
ρ_{air}	density of air	kg m ⁻³	arho
ρ_{asn}	density of new snow	kg m ⁻³	snow_den
ρ_b	bulk density of the soil layer	Mg m ⁻³	bsdblk
ρ_{ice}	density of ice	Mg m ⁻³	den_ice
ρ^i_v	water vapor density in the air of the soil layer <i>i</i>	kg m ⁻³	soilvapden(lrx)
ρ_{om}	density of organic material in the soil	Mg m ⁻³	den_organic
ρ_p	soil particle density	Mg m ⁻³	bsdpart
ρ_{qtz}	density of quartz	Mg m ⁻³	den_quartz
ρ_{res}	residue density	kg m ⁻³	res_bd
ρ_{sno}	snow density	kg m ⁻³	-
ρ_v	soil air vapor density	kg m ⁻³	soilvapden
ρ_w	density of water	kg m ⁻³	-
σ	Stephan-Boltzman constant	MJ m ⁻² day ⁻¹ K ⁻⁴	sbc
ϕ	latitude	degrees	bmalat
ϕ^6_{ae}	air entry potential of the soil surface layer	m	airentry(1)
ϕ_i	hydraulic potential of the soil layer <i>i</i>	m	swm(lrx)
Φ_{sa}	relative humidity of the air in the soil	unitless	soilrh
Φ_w	soil relative humidity at the permanent wilting point matric potential	unitless	relhumwilt
ψ	matric potential	m	potm
ψ_{ae}	Brooks and Corey air entry potential	m	airentry

ψ^i	matric potential of soil layer I	m	potm(lrx)
ψ_w	permanent wilting point matric potential	m	potwilt
ω_s	sunset hour angle	degrees	ws

*a dash (-) in this column indicates there is no variable name.

Management Submodel of WEPS

Contributors:

L.E. Wagner

F.A. Fox

Abstract

The Wind Erosion Prediction System (WEPS) is a process-based, daily time-step computer model that predicts soil erosion via the simulation of the physical processes controlling wind erosion. WEPS comprises five databases and several submodels that reflect the physical processes of erosion, soil water movement, plant growth, residue decomposition, dynamic soil properties, and management. This document describes the WEPS Management submodel which attempts to simulate the effects of typical cropping management practices, such as tillage, planting, harvesting, irrigation, or residue burning, at an operational level. Such management practices can affect the surface conditions, which in turn affect the wind erosion potential. A variety of land management operations are simulated by identifying the primary physical processes involved and representing each individual operation as a sequenced set of those processes. The process categories include: (1) surface modification (e.g., the creation or destruction of ridges and/or furrow dikes that form oriented surface roughness, change the surface random roughness, and destroy the soil crust); (2) mass manipulation within soil layers (e.g., the changes in the aggregate size distribution and soil porosity, the mixing of soil and residue among soil layers, and soil layer inversion); (3) biomass manipulation (e.g., burying and resurfacing of residue, clipping the standing residue, flattening the standing residue, killing the live crop biomass, and removing biomass); and (4) soil amendments (e.g., the application of residue/manure for cover, seeding or planting crops, and irrigation). The WEPS Management submodel simulates the major processes related to the most prevalent cultural practices used by producers and land managers that influence the susceptibility of a site to wind erosion.

Introduction

The development of the Wind Erosion Prediction System (WEPS) was started by USDA-Agricultural Research Service (ARS) scientists around 1985. The WEPS project was initiated in response to customer requests, primarily from the Soil Conservation Service (SCS), for improved wind erosion technology. WEPS was intended to replace the predominately empirical Wind Erosion Equation (Woodruff and Siddoway 1965) that was principally used by SCS at the time for estimates of field-scale soil loss caused by wind erosion. WEPS was to be the prediction tool for those who plan soil conservation systems, conduct environmental planning, or assess offsite impacts of wind erosion. SCS, now the National Soil Conservation System (NRCS), implemented WEPS in 2010 (Federal Register 2010) and uses it exclusively for cropland field wind erosion assessments, compliance checking, and for determining wind erosion estimates required for qualifying acceptance in some of their National Programs. WEPS incorporates improved technology for computing soil loss from agricultural fields by wind and provides new capabilities such as calculating the suspension loss, estimating the PM-10 emissions, and specifying the direction in which the soil leaves the field (Wagner 2013).

WEPS comprises several submodels that reflect different sets of physical processes: (a) Erosion (the entrainment, transport, and deposition of airborne particles); (b) Hydrology (the water movement within the soil); (c) Plant Growth (the development of the leaf, stem, and reproductive plant components); (d) Residue Decomposition (the decay of plant materials); (e) Soil (the surface soil conditions changed by daily weather conditions); and (f) Management (the simulation of applied cultural practices). These submodels are supported by five databases: soils, operations, plant growth/decomposition, wind barriers, and climate, including wind data. Figure 1 shows the basic structure of WEPS 1.0, including the interface user inputs, the submodels in the science code, and the databases.

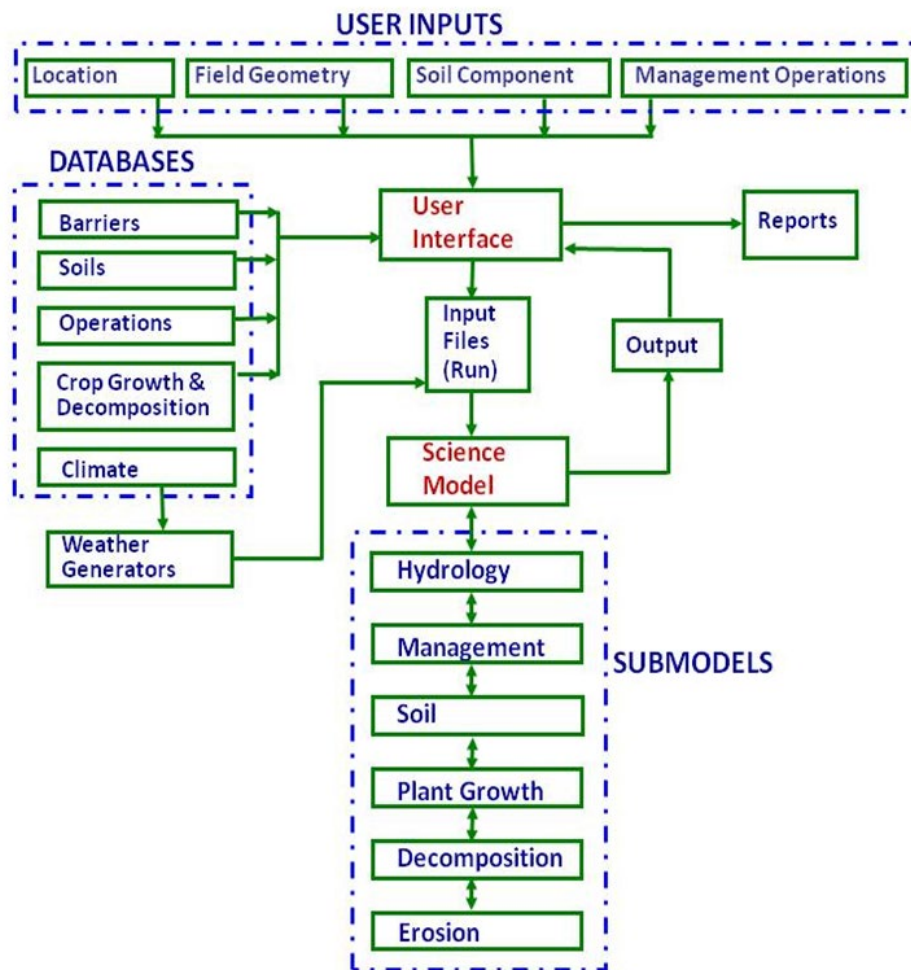


Figure 1. Schematic diagram of the WEPS 1.0 interface, science model submodels, and databases.

As a process-based planning tool, WEPS is expected to reflect the effects of various management practices that may affect a site's susceptibility to wind erosion. The diversity of these practices makes this task difficult, but WEPS must adequately simulate typical cultural practices to accurately assess their effects on the susceptibility to wind erosion. The Management submodel is assigned the task of handling the cultural practices

that affect the soil/surface state within WEPS, including primary and secondary tillage, cultivation, planting/seeding, and harvesting operations as well as irrigation, burning, and grazing practices. This submodel combines the efforts of prior researchers as described below.

Submodel Description

The Management submodel characterizes a variety of land management actions by identifying the primary physical processes involved in and representing each individual management operation as a sequenced set of those primary physical processes. Those processes include: (1) surface modification (the creation or destruction of ridges and/or dikes that form an oriented surface roughness, the changes in surface random roughness, and the destruction of the soil crust); (2) soil layer mass manipulation (the changes in the aggregate size distribution and soil porosity, the mixing of the soil and residue among soil layers, and soil layer inversion); (3) biomass manipulation (burying and resurfacing of residue, clipping the standing residue, flattening the standing residue, killing the live crop biomass, and biomass removal); and (4) soil amendments (the addition or removal of manure and residue, planting, and irrigation).

In accord with the WEPS design philosophy, the Management submodel simulates these processes on a physical basis, if possible, and incorporates the concepts of conservation of mass. It employs functional relationships developed from field and laboratory data of other published research, if available, using a minimum of parameters with readily available and/or attainable values. Some process representations were simplified due to a lack of knowledge about those processes. However, because of its inherent design, the WEPS Management submodel can be expanded and improved as new knowledge is gained about how physical processes affect the soil, surface, and biomass due to human initiated (management) events.

These processes are assumed to be independent of each other and are simulated sequentially. Each management operation is thus represented by an appropriate list of processes. The individual processes and their order of simulation describe each specific operation. The order of processes are specified to account for how an operation affects the “after-operation” state of the system; for example, for an operation that performs a soil tillage disturbance action and adds residue to the surface, one would obtain different after-operation results depending on whether the “add cover” process was specified before or after the “residue burial” process. Typical multi-tool and ganged multi-implement operations also can be described easily and fully by repeating the necessary processes for each tool (tillage) element that is a component of such operations. For example, a disk-ripper may have a front gang of disk blades, a middle gang of chisel shanks, and a back row of disk blades. Each of these tillage tool components can thus be described independently based on its effects on the soil, surface, and residue states in order of occurrence during the operation.

Each specific physical process represented by an operation is uniquely defined for that operation by the appropriate process equation and the assigned coefficients' values for that equation. Thus, if an operation breaks a portion of the surface crust and mixes the soil contents to some degree throughout the tillage zone, the associated equations for destroying the surface crust (Eq. 1) and mixing soil properties within the soil layers (Eq. 10) would be applied. The corresponding values of the coefficients assigned to the operation define the extent to which those equations modify the soil/surface state of the

system; e.g., ζ (the fraction of the crust removed based upon the surface area tilled) for Eq. 1 and μ (the mass mixing efficiency) for Eq. 10. The complete list of coefficient values for the pertinent process equations representing a specific operation, represent a management record for that operation. A collection of such operation records are referred to as an operation database for WEPS. NRCS has developed a set of operation records for WEPS where the assigned coefficient values for those operations have been derived from research data, similar operations, and best estimates from knowledgeable NRCS staff. However, the scope of this manuscript is to document only the process equations and not the derivation of the coefficient values for individual operations.

The list of management operations performed for a given management plan (the crop rotation/tillage sequence or the cyclical list of cultural practices) is specified in a management file. On the dates when operations are to be performed, the Management submodel will execute the routines implementing the process equations required to simulate the effects of those operations, based upon the specified process equations and coefficient values included in the management file.

Assumptions and Limitations

Several assumptions and limitations have been imposed on the Management submodel for the WEPS 1.0 release version 1.3.9, for reasons ranging from limiting the scope of the submodel to the inadequate knowledge of specific processes that may have a significant impact on the soil and/or surface under specific conditions. Some of these assumptions and limitations are expected to be relaxed in future releases as more relevant research data becomes available and user needs dictate. The current assumptions and limitations that affect the Management submodel are as follows:

1. The tillage depths are adjusted to the nearest soil layer boundary of the simulation. This ensures that the most recent tillage operation modifications on the soil state are adequately represented within the tilled soil layers (i.e., no averaging of soil properties occurs within a simulated soil layer due to a tillage depth that does not fall exactly on a soil layer boundary). Note that the number and thickness of the simulated soil layers used in WEPS are determined algorithmically by default and depend on the information about the usually coarser soil layer horizon that is typically provided as an input to the WEPS model. The soil layering routine follows the built-in rules that specify the general soil layering structure of the simulation (e.g., the default initial layer thicknesses, which increase by depth, the maximum and minimum allowable thicknesses for a layer, etc.). WEPS command line options are available for a user to influence the construction of the WEPS-simulated soil layer structure
2. In the Management submodel, the total water content of the soil within the current tillage zone is assumed to be unaffected by a tillage operation. The hydrology component of WEPS is expected to handle changes in the surface and soil layer water content. Thus, the usual rapid drying of the surface and soil within the tillage zone following the typical tillage operations is simulated in the hydrology module; however, the soil water content within the tillage zone can be redistributed due to the mixing of the soil among the tillage zone soil layers in the Management submodel.
3. The tillage depth alone is assumed to determine only which soil layers are directly affected by a tillage operation. The specific assigned processes for each operation determine the actual influence on the surface and within the soil tillage zone.

4. The effects of the tillage operations on the soil layers below the tillage depth are not currently considered; e.g., subsoil compaction below the tillage zone due to a tillage implement's mass.
5. No surface tillage "compaction" process is currently included in the WEPS Management submodel.
6. The tillage operations are currently assumed to not increase the soil aggregate sizes, e.g., the consolidation of aggregates, at this time. The consolidation of the soil aggregates in WEPS occurs only through the climatic effects of precipitation, wetting of the soil layers, and puddle formation on the surface prior to infiltration as simulated within the WEPS Soil submodel. Most of the tillage operations that generate large aggregates on the surface involve the breakdown of the consolidated soil, represented in WEPS as a distribution of "very large" aggregates that exist within the tillage zone prior to the tillage operation.
7. The effects of a management operation are assumed to be homogeneous. The effects of tractor tires will not be considered (except where they may knock down a significant proportion of the standing residue). Certain zone-related tillage operations, such as a row cultivator or strip tillage, are treated so that the result will be spatially averaged to determine the equivalent representative values that are assigned to the homogeneous region.
8. The dry stability and density of the aggregates in each layer are assumed to be unaffected by the tillage operations. This decision is based on analysis of the limited field data available. Future research may provide statistically significant effects that could then be modeled, but these properties can still change among the soil layers within the tillage zone due to the mixing of aggregates among these layers that is caused by tillage operations.

Physical Processes Modeled

In WEPS, spatial variability is handled through the use of subregions. Note that the first released version, WEPS 1.0, was limited to a single subregion. Hence, in each subregion, the submodel considers the soil mass, surface, and biomass properties to be homogeneous in the horizontal direction but variable in the vertical direction (the soil layers). The soil surface is considered to include various combinations of random roughness, ridges, or ridges and dikes. Live vegetation (crops) and decomposing biomass (crop residue) may exist in the soil and on the surface in standing and/or flat orientations.

The physical processes (actions) that most often modify the current state of the soil, surface, and biomass properties in WEPS have been identified. The processes have been formulated into equations that represent the effect of those actions upon the pertinent soil, surface, and biomass properties. A typical management operation will often perform several of these identified actions, so the effect of a management operation on the soil, surface, and biomass state is simulated as a sequential series of "step-change" processes. The processes modeled by the Management submodel are listed in Table 1 under the type of action they perform, and each process is described.

Table 1. Management processes of WEPS.

Action	Process	Description
Soil Surface Manipulation	Crust	Process of modifying the soil surface crust characteristics.
	Roughen	Process of modifying the random surface roughness.
	Ridge/Dike	Process of creating or destroying ridges and/or dikes (oriented surface roughness).
Soil Mass Manipulation	Crush	Process of applying forces to the soil that modifies the aggregate manipulation structure by breaking down soil aggregates.
	Loosen	Process of decreasing the soil bulk density and increasing the porosity (incorporation of air), or the inverse process of increasing the soil bulk density by removing air from the soil, e.g., compaction.
	Mix	Process of uniting or blending of soil layer properties, including biomass.
	Invert	Process of reversing the vertical order of occurrence of the soil layers within the current specified tillage zone.
Biomass Manipulation	Flatten	Process of converting standing biomass to flat biomass.
	Bury	Process of moving surface biomass into the soil.
	Re-surface	Process of bringing buried biomass to the surface.
	Change Standing Biomass Fall Rate	Process that adjusts the standing biomass fall rate to account for the accelerated change in standing residue due to roots being loosened or cut from the standing stalks due to tillage.
	Cut/Remove	Process of cutting standing biomass to a prescribed height and placing the cut material on the surface or, optionally, removing (harvesting) the cut material.
	Thin Population	Process of reducing the number of standing biomass stems or stalks by a fraction of the total or to a specified number per unit area and placing the thinned material on the surface or, optionally, removing (harvesting) it.
	Kill/Defoliate	Process of killing or defoliating live (or dead) biomass.

	Remove	Process of removing biomass from the system (harvest, grazing and burning).
	End Biomass Manipulation	Process that completes the transfer of the killed crop biomass to the residue decomposition pools. This is a WEPS-specific function to address a deficiency in the current model design that does not allow this process to occur automatically within the model.
Soil Amendments	Plant	Process of adding seeds/plants to the soil.
	Irrigate	Process of adding water on or into the soil.
	Add Biomass	Process of adding biomass (residue, manure, wood chips) to the surface and/or into the soil.

Soil Surface Manipulation

The soil surface is described within WEPS by random and oriented (the presence of ridges and dikes) roughness values, the fraction of the surface that is non-erodible (covered with rocks), and the fraction that is non-crust and crusted. The condition of the non-crust surface is described by the aggregate size distribution, the average aggregate density, and the dry aggregate stability values in the surface layer. In addition, properties describing the condition of the crusted surface, e.g., the crust thickness, density, and dry stability, as well as the amount of loose, erodible material on the crusted fraction of the surface are also maintained. The soil surface can be directly modified by an operation through any of the following processes.

Crust Process

Many field operations modify the soil surface and destroy all or part of the existing crust. This destruction is described by the equation:

$$Cr_f = (1 - \zeta)Cr_0 \quad [1]$$

where

Cr_f = fraction of the surface that is crusted after the operation,

Cr_0 = fraction of the surface that is crusted before the operation, and

ζ = fraction of the surface that is tilled by the field operation ($0 \leq \zeta \leq 1$).

Field implements are assumed to destroy the crust within the surface area tilled. Many field implements break all of the surface crust across the entire width of the tool and thus $\zeta = 1$. However, some operations do not till the entire surface or are designed or used in a way that only a portion of the surface is tilled ($\zeta < 1$), so some crust is left unbroken. Examples of some ζ operation parameter values as defined by NRCS are: a) a disk plow or tandem disk (1.0); b) a rotary bed cultivator where only the beds are tilled (0.85); c) a double disk opener no-till grain drill where only the portion around the opener slot is tilled (0.65); d) a strip till planter where only a strip is tilled where the seeds are placed in

the ground (0.3); and e) a wide row spacing double disk opener planter where even less surface area is tilled (0.15).

There are also instances where non-tillage operations may destroy a portion of the surface, such as a roller used to flatten residue or wheel traffic from a sprayer, fertilizer spreader, or harvester. Eq. 1 can be applied for those operations as well, however further research is necessary to determine their respective coefficients and determine if that type of breakage has the same effect as tillage on wind erosion.

Roughen Process

The random roughness of a surface within the Management submodel is represented in terms of the random roughness index of Allmaras et al. (1966). The process is defined by two parameters, a roughness flag and a roughness value. The flag determines whether the value will be used as the actual value (*Always use specified random roughness value*) or considered to be the nominal value (*Allow WEPS to auto-adjust random roughness value*). When the flag is set to represent the actual value, none of the adjustments for the soil type and the biomass quantity mentioned below are performed, and only the tillage fraction and intensity are applied. The adjustments for soil type and biomass quantity used in RUSLE2 (USDA 2013) were adopted later to increase commonality between the models.

When the flag is set to specify the nominal roughness value, the method and equations from RUSLE2 are applied. The nominal random roughness value, when assigned to an implement, RR_{impl} , in WEPS, is defined as the typical field value expected under a standard soil type (silt loam) that is composed of 15% clay and 65% silt and contains a very high soil biomass density (dry basis, greater than $44 \text{ kg ha}^{-1} \cdot \text{mm}^{-1}$) within the tillage zone (the depth of the soil disturbance), which includes both the buried residue and the roots. Therefore, the base RR_{impl} assigned to an operation tool is first adjusted for the soil type, RR_{s_adj} , which comes directly from the RUSLE2 model and then by the quantity of the residue within the tillage zone, RR_{b_adj} , which also comes directly from RUSLE2 but is converted to metric units. Therefore, the roughness values are higher for soils that are high in clay content and lower for soils that are high in sand content, according to the following relationship:

$$RR_{s_adj} = \begin{cases} 0.16(siltf)^{0.25} + 1.47(clayf)^{0.27} & \text{when } RR_{s_adj} > 0.6 \\ 0.6 & \end{cases} \quad [2]$$

where

RR_{s_adj} = RR adjustment factor for soil type,

$clayf$ = fraction of clay in soil, and

$siltf$ = fraction of silt in the soil.

The roughness values also increase with increasing quantities of buried biomass present at the time of the soil disturbance. Thus, the roughness values are also adjusted as a function of the biomass (buried residue and roots) within the depth of the soil disturbance using the following equation:

$$RR_{b_{adj}} = \begin{cases} RR_{impl} \cdot RR_{s_{adj}} & \text{when } RR_{impl} \cdot RR_{s_{adj}} < RR_{min} \\ RR_{min} + (RR_{impl} \cdot RR_{s_{adj}} - RR_{min}) (0.8(1 - \exp(-.5339.92 \cdot B_m)) + 0.2) & \text{otherwise} \end{cases} \quad [3]$$

where

$RR_{b_{adj}}$ = RR adj. for buried biomass (mm),

$RR_{s_{adj}}$ = RR adj. factor for soil type,

RR_{impl} = assigned nominal RR value for tillage operation (mm),

RR_{min} = 6.096 = minimum RR value (mm), and

B_m = buried biomass density (dry basis) within the soil tillage layer ($\text{kg m}^{-2} \text{mm}^{-1}$).

RR_{min} reflects the roughness value assumed for water erosion from unit plots and the value of 0.2 reflects the portion of the roughness value that is not affected by the soil biomass.

Most tillage tools cannot reduce the surface roughness to the value usually associated with the operation under all field surface roughness conditions. To account for this, a tillage intensity factor, λ , is assigned to each tillage operation (Alberts et al. 1995). If the pre-tillage random roughness, RR_0 , is greater than the roughness associated with an implement, RR_{impl} (after adjustment for the soil type and the quantity of residue in the tillage zone), the degree of change in the surface roughness is dependent on the value of the tillage intensity assigned to the operation tool. If the tillage operation does not modify the entire surface, the post-tillage random roughness is weighted accordingly.

$$RR_f = \begin{cases} \zeta RR_{b_{adj}} + (1 - \zeta) RR_0 & RR_{b_{adj}} \geq RR_0 \\ \zeta [\lambda RR_{b_{adj}} + (1 - \lambda) RR_0] + (1 - \zeta) RR_0 & RR_{b_{adj}} < RR_0 \end{cases} \quad [4]$$

where

RR_f = final tilled surface random roughness (mm),

RR_0 = pre-tillage surface random roughness (mm),

$RR_{b_{adj}}$ = implement-assigned roughness after adjustment for the soil type and biomass (mm),

λ = tillage intensity factor ($0 \leq \lambda \leq 1$), and

ζ = fraction of the surface tilled by the operation ($0 \leq \zeta \leq 1$).

Most NRCS-defined operations use the “Allow WEPS to auto-adjust random roughness value” setting option. Therefore, they will apply both the soil and biomass adjustment factors and use the λ and ζ values assigned to the implement along with the RR_{impl} value. Typical values for λ , ζ and RR_{impl} are: rototiller (1.0, 1.0, 10.2 mm); moldboard plow (1.0, 1.0, 48.2 mm); rodweeder (0.25, 1.0, 7.6 mm); and ridge till planter (0.5, 0.65, 10.2 mm). Thus, the rototiller and moldboard plow will achieve the nominal roughness, after adjustments for soil and buried biomass, under all initial surface roughness conditions, while the rodweeder and ridge till planter will not achieve the nominal roughness value, after adjustments for soil and buried biomass, if the original surface roughness is greater than the nominal roughness value.

Ridge and Dike Process

Oriented roughness is defined by uniform rows of ridges and furrows running in parallel lines, with the height being the distance from the bottom of the furrow to the top of the crest (Chepil and Milne 1941) and the spacing being commonly described as the distance between successive furrows or ridges. While Chepil and Woodruff (1954) asserted, “The degree of surface roughness depends on ... size, shape, and lateral frequency of clods, ripples, and ridges”, no researcher has performed more to quantify the degree of surface roughness provided by ridges than describe the height and spacing. To facilitate the utilization of future research and to acknowledge the use of beds (ridges with flat tops) in vegetable production in regions susceptible to wind erosion, the oriented roughness is described by the top width, height, and spacing of the ridge and the row direction within WEPS. If dikes exist in the furrows, they are assumed to be uniformly spaced with the same slope and top width as the ridges. Therefore, only the furrow dike height and spacing are required to define dikes within WEPS.

A ridge modification flag determines how an operation can influence the oriented roughness. Based on the flag value: a) a tillage tool can change the current surface configuration into the desired configuration with respect to the oriented roughness, regardless of the previous surface oriented roughness state (i.e., flag: Ridges/dikes set to specified values); b) the operation will modify the current oriented roughness based upon the depth of tillage specified (i.e., Ridges/dikes set, based on tillage depth); or c) the operation will not disturb the current oriented roughness, regardless of its value, as with row cultivation tools (i.e., Pre-existing ridges/dikes left unchanged). In cases where the tillage tool can only partially modify the current oriented roughness, past modelers (Sharpley and Williams 1990) estimated the effect based on the depth of the current tillage operation and the previous ridge forming operation. This parameterization violates the no lag state modeling approach used in this submodel, and therefore a linear estimation using only the ridge height and the tillage depth of the current operation and pre-tillage ridge height was developed.

$$\begin{aligned} \hat{R}_h &= R_{impl} & D_{act} &\geq R_h/2 \\ \hat{R}_h &= R_{impl} & D_{act} &< R_h/2 \text{ and } R_{impl} \geq 2(R_h/2 - D_{act}) \\ \hat{R}_h &= 2(R_h/2 - D_{act}) & D_{act} &< R_h/2 \text{ and } R_{impl} < 2(R_h/2 - D_{act}) \end{aligned} \quad [5]$$

where

\hat{R}_h = post tillage ridge height (mm),

R_h = pre tillage ridge height (mm),

R_{impl} = ridge height set by the implement (mm), and

D_{act} = actual tillage depth (mm).

Most NRCS-defined ridging operations use the “Ridges/dikes set to specified values” flag since it expects that the ridge height specified is desired by the operator and the tillage depth will be adjusted to achieve it. The operations that are not intended to modify ridges, either do not include this process, or have the flag set to “Pre-existing ridges/dikes left unchanged” such as planters that seed on an existing ridge bed. The operations that have the flag set to “Ridges/dikes set, based on tillage depth” are light tillage operations, like a harrow cultivator, that are not capable of tilling deep enough to remove tall ridges if used on such a surface condition.

Soil Mass Manipulation

Soil mass manipulation processes modify a series of stacked, parallel, homogeneous layers with a specified thickness. The conservation of mass principle was used to develop the following submodel processes that affect the soil layer properties (e.g., the layer thickness, bulk density, water content, aggregate size distribution, dry aggregate stability, aggregate density, and particle size distribution).

Crush Process

The aggregate size distribution at the soil surface provides the information necessary to determine the quantity of aggregates that are erodible in size and are available for direct emission and saltation, as well as the degree of shelter provided to these aggregates by larger aggregates. The aggregate size distribution below the surface is also of interest because emergency tillage operations used to control wind erosion fail if insufficient non-erodible aggregates are available to bring to the surface.

The aggregate size distributions are represented within WEPS as a 4-parameter modified log-normal distribution (Wagner and Ding 1994). The tillage-induced aggregate breakage is simulated within the Management submodel of WEPS with a Markov chain-based, two-parameter, stochastic model (Wagner and Ding 1993).

Currently, a simple two-parameter functional representation (Eq. 7) is used to represent the aggregate breakage process for a given operation tool and applied in Eq. 6. The tillage-induced aggregate breakage was also found to be dependent upon the soil type and water content at the time of tillage (Wagner et al. 1992, 1994, Wagner and Ding 1993). However, no water content and soil type functional relationships are employed in WEPS 1.0 because the tillage operations are simulated only on fixed dates regardless of soil water content and limited soil/tillage data were available to fully develop soil type relationships from the data. The aggregate breakage model can be summarized as follows in the context of the soil aggregate crushing process, as expressed by Wagner and Ding (1993):

“A soil aggregate is assumed to consist of many particles, with each having an extremely small volume and a unit mass. The soil particles can travel only downward from a larger aggregate size class to smaller aggregate size classes after each tillage pass (crushing of an aggregate). If a size class is called a “state”, then the transition of soil particles from one state to another can be treated as a completely random event. A probability matrix, $P[i,j]$, can be constructed for all possible transitions occurring in the soil when its aggregate size distribution (0 to $i-1$) (mass fractions across different size classes) shifts or transfers from $w[i]$ to $\hat{w}[k]_{(0 \text{ to } i-1)}$ size, after one crushing stage (tillage pass). $P[i,j]$, often called a transition matrix, maintains the properties of a Markov chain and does not change with the number of tillage passes performed but depends on the type of tillage and the specific soil conditions.”

Mathematically, the Markov chain-based crushing model is of the form:

$$\hat{w}[i]_{1 \times n} = w[i]_{(1 \times n)} P[i,j]_{(n \times n)} \quad [6]$$

where

$\hat{w}[i]$ = post-tillage array of the aggregate size class fractions,

$w[i]$ = pre-tillage array of the aggregate size class fractions,

$P[i,j]$ = transition matrix,
 i,j = indices for the soil aggregate size classes, and
 n = maximum number of the aggregate size classes.

The effectiveness of the model relies on how accurately the transition matrix, $P[i,j]$, can be estimated. The transition matrix, consisting of $p_{i,j}$ elements was represented by a binomial distribution using the p_i relationship below (Eq. 7). The specifics on how this was done are provided in detail by Wagner and Ding (1993). The most suitable two-parameter functional representation for p_i was found by Wagner and Ding (1993) to be:

$$p_i = \frac{1.0}{1.0 + \exp\left(-\alpha + \beta \frac{gmd_i}{gmd_{max}}\right)} \quad [7]$$

where

$i = 1,2,3,\dots,n,n+1$ (n =number of sieve cuts),
 gmd_i = geometric mean diameter of the aggregates in size class i (x_{i-1} to x_i),
 gmd_{max} = geometric mean diameter of the aggregates in the largest size class (x_n to x_{n+1}),
 α = aggregate size distribution breakage factor, and
 β = breakage intensity factor.

For a rotary sieve of n sieves, the x_0 and x_{n+1} are arbitrary minimum and maximum aggregate sizes assumed to exist in the data. The values used during model development analysis were 0.01 mm and 152.4 mm, respectively. These values also correspond to the x_0 and x_{n+1} values from a four-parameter “modified” lognormal function describing an aggregate size distribution.

Parameter α reflects the breakage of all soil aggregates regardless of size. As α decreases, the percentage of soil aggregates that are breaking increases. Parameter β reflects the unevenness of breakage among aggregates in different size classes. Large β values indicate that crushing mainly affects the large soil aggregates. Currently NRCS has chosen to only select and apply the limited α and β parameter values obtained by Wagner and Ding (1993) for other implements based upon their similarity to the tested implements. Some operation α and β crushing parameters are provided here from Wagner and Ding (1993) for reference: a) chisel plow (2.4, -2.0); b) disk harrow (4.3, 2.0); c) field cultivator (3.0, 1.8); and d) rotary tiller (1.5, 0.56). NRCS has assigned crushing parameter values for other operations based upon their similarity to the tillage operations evaluated by Wagner and Ding (1993).

Loosen Process

The loosening process is defined as the addition of air in the soil layer. This is represented as a change in the soil layer bulk density in the Management submodel by Eq. 8 and is taken directly from the EPIC model (Sharpley and Williams 1990). The reference settled bulk density, ρ_s , is determined using an interpolation of the published data, based on the soil texture and organic matter content (Rawls 1983). Applying the conservation of mass principle requires a corresponding change to the soil layer thickness as shown in Eq. 9.

$$\hat{\rho}_l = \rho_l - \left(\rho_l - \frac{2}{3}\rho_{sl}\right)\mu \quad [8]$$

where

$\hat{\rho}_l$ = post-tillage bulk density for layer l ,
 ρ_l = pre-tillage bulk density for layer l ,
 ρ_{sl} = settled bulk density for layer l , and
 μ = loosening intensity coefficient ($0 \leq \mu \leq 1.0$).

$$\hat{Z}_l = Z_l \frac{\rho_l}{\hat{\rho}_l} \quad [9]$$

where

\hat{Z}_l = post-tillage layer thickness for layer l (mm) and
 Z_l = pre-tillage layer thickness for layer l (mm).

Some typical NRCS defined operations have the following loosening parameter values: rototiller (0.7), moldboard plow (0.8), straight point chisel (0.85), and rodweeder (0.5).

Mix Process

The mixing process represents the uniting or blending of the soil layer properties among the layers that are within the depth of influence (tillage depth) and excludes surface constituents such as the crop residue and other non-soil elements. The mixing process uses a single mixing parameter, with values ranging from zero, for no mixing, to 1.0, for complete mixing, as described in the APEX, EPIC, and WEPP model documentation (Williams et al. 2008, Sharpley and Williams 1990, Alberts et al. 1995). Expressed on a mass basis, the equation becomes:

$$\hat{X}_l = (1 - \mu)X_l + \mu \left(\frac{\sum_{k=1}^m (\rho_k Z_k X_k)}{\sum_{k=1}^m (\rho_k Z_k)} \right) \quad [10]$$

where

\hat{X}_l = final mass concentration in layer l ,
 X_l, X_k = initial mass concentrations in layers l and k ,
 μ = mass mixing efficiency coefficient ($0 \leq \mu \leq 1.0$),
 $\rho_k Z_k$ = unit surface area mass of soil in layer k ,
 l, k = soil layer indices, and
 m = maximum number of soil layers.

Some typical NRCS defined operations have the following mixing parameter values: rototiller (0.9), moldboard plow (0.7), straight point chisel (0.37), and rodweeder (0.05).

Invert Process

The inversion process is the reversal of the vertical order of the soil layer properties within the working depth of the tillage tool. Thus, inversion is simply the reordering of the soil layer properties in the model where new values are assigned to each layer. Because the soil layer thicknesses are not re-ordered during this process, the soil layer properties are re-partitioned (averaged) into each layer.

Biomass Manipulation

The biomass manipulation processes describe the effects that the management operations have on the growing crop and the various biomass pools of a) residue age, b) location (standing, flat, or buried), and c) plant component (stems, leaves, and reproductive

components) maintained in the WEPS model. The biomass manipulation processes handled by the Management submodel are flatten, bury, re-surface, change standing biomass fall rate, cut/remove, thin population, kill/defoliate, and remove. The biomass manipulation processes are applied only to the fraction of the surface that is disturbed by the management operation, e.g., a tillage tool.

The processes of flattening, burying, re-surfacing, and changing the standing biomass fall rate, contain coefficients that depend on the toughness/size of the residue biomass being manipulated. The five toughness/size residue classes are a) fragile residue, b) moderately tough residue, c) non-fragile/large residue, d) woody residue, and e) small stones/gravel. Currently, there is no means within WEPS to convert a residue pool from one toughness/size class to another due to decomposition, etc. These five toughness/size residue classes and the accompanying flattening, burial, and re-surfacing coefficient values assigned to these processes for the individual operations match those used in RUSLE2 to achieve additional commonality between the ARS erosion models.

Flatten Process

Flattening is defined as the transfer of standing residue to flat residue (Wagner and Nelson 1995). This is a process that occurs for many operations. Even non-tillage operations often have wheel traffic that flattens a portion of the standing vegetation. This process is simulated simply by specifying the fraction of standing residue and/or crop biomass that is flattened by the operation. Typically, standing residue that becomes buried into the soil is handled by applying the flattening process prior to the burying process. This is different from the thinning process, which provides methods to directly specify a reduction in the plant population, and the standing material is either removed or left flat in the field. WEPS maintains separate plant component pools (leaves, stems, storage) that are represented for each plant location pool (standing, flat, buried), so each plant component from standing plants and residue that are flattened must be transferred to their corresponding flat component pools. Thus, the flat pools are increased, the standing pools are decreased, and the plant population and standing residue stem counts are decreased proportionally. Applying conservation of mass as shown by Wagner and Nelson (1995) yields:

$$\begin{aligned} FL_f &= FL_0 + ST_0\gamma\zeta \\ ST_f &= ST_0(1 - \gamma\zeta) \end{aligned} \quad [11]$$

where

FL_f = flat mass after the operation (stem, leaf, and store pools),

FL_0 = flat mass before the operation (stem, leaf, and store pools),

ST_f = standing mass after the operation (stem, leaf, and store pools),

ST_0 = standing mass before the operation (stem, leaf, and store pools),

γ = flattening coefficient ($0 \leq \gamma \leq 1$), and

ζ = fraction of surface that is tilled ($0 \leq \zeta \leq 1$).

Some typical NRCS defined operations have the following flattening parameter values: rototiller (1.0), moldboard plow (1.0), straight point chisel (0.6), and rodweeder (0.4).

Bury Process

The burying process is defined as the transfer of above-ground, flat biomass into the soil (Wagner and Nelson 1995). This process occurs with many tillage operations and is

simulated in WEPS by specifying the fraction of above ground residue (on a mass basis) that is buried. The Wagner and Nelson (1995) basic mass burial concepts are applied in Eq. 12. The actual burial of the surface residue, accounting for effects of both the speed and depth for all plant component pools (stem, leaf, storage), is computed from:

$$\begin{aligned} RES_{bf} &= RES_{b_0} + RES_{s_0}(B_{coef}D_{adj}S_{adj})\zeta \\ RES_{sf} &= RES_{s_0} + RES_{s_0}(B_{coef}D_{adj}S_{adj})\zeta \end{aligned} \quad [12]$$

where

RES_{bf} = buried biomass after the operation (stem, leaf, and store pools),
 RES_{b_0} = buried biomass before the operation (stem, leaf, and store pools),
 RES_{sf} = flat surface biomass after the operation (stem, leaf, and store pools),
 RES_{s_0} = flat surface biomass before the operation (stem, leaf, and store pools),
 B_{coef} = burial coefficient for a specified toughness/size residue class,
 S_{adj} = speed adjustment factor for the burial coefficient,
 D_{adj} = depth adjustment factor for the burial coefficient, and
 ζ = fraction of surface tilled ($0 \leq \zeta \leq 1$).

The burial coefficient is adjusted based on both the travel speed and depth selected for the operation relative to a nominal speed and tillage tool depth set for the operation. These speed and depth adjustments to the burial coefficient, as well as the available methods of redistribution of buried residue by depth, were conceived by the RUSLE2 developers (USDA 2013) as enhancements when they were incorporating the Wagner and Nelson (1995) mass flattening, burial, and resurfacing processes into RUSLE2 as part of a joint effort to improve commonality between the two ARS models. Derivation of these particular equations (Eqs. 13, 14, 15 and 16) are available in the RUSLE2 science document (USDA, 2013).

Biomass is distributed throughout the soil tillage zone based on the type of tillage tool used by the operation. Six types of burial by depth distribution processes are defined in WEPS and designated by a burial distribution flag: 0) uniform burial, 1) mixing plus inversion burial, 2) mixing burial, 3) inversion burial, 4) lifting, fracturing burial, and 5) compression burial. The nominal speed and depth assigned to an operation are the reference conditions and are assumed to be the manufacturer's recommended or normal operating depth for the implement, machine, or tool that performs the burial process. The effect of the operation depth or soil disturbance depth on the burial efficiency is computed using:

$$D_{adj} = \frac{[1 - (1 - \frac{D_{act}}{D_{max}})^{2.7}]}{[1 - (1 - \frac{D_{ref}}{D_{max}})^{2.7}]} \text{ for } D_{act} = \max[\min(D_{spec}, D_{max}), D_{min}] \quad [13]$$

where

D_{adj} = depth adjustment factor for burial coefficient,
 D_{spec} = specified tillage (soil disturbance) depth (mm),
 D_{act} = actual soil disturbance depth (mm),
 D_{ref} = nominal (reference) soil disturbance depth (mm),
 D_{max} = maximum soil disturbance depth (mm), and

D_{min} = minimum soil disturbance depth (mm).

Similarly, the effect of the speed on the surface residue burial is computed using:

$$S_{adj} = \frac{[0.6 + 0.4(S_{act}/S_{max})^{0.5}]}{[0.6 + 0.4(S_{ref}/S_{max})^{0.5}]} \text{ for } S_{act} = \max [\min(S_{spec}, S_{max}), S_{min}] \quad [14]$$

where

S_{adj} = speed adjustment factor for the burial coefficient,

S_{spec} = specified operation speed (m s⁻¹),

S_{act} = actual operation speed (m s⁻¹),

S_{ref} = nominal (reference) operation speed (m s⁻¹),

S_{max} = maximum operation speed (m s⁻¹), and

S_{min} = minimum operation speed (m s⁻¹).

The distribution of the buried residue into the tillage zone layers is defined by a cumulative mass distribution function for each type of residue burial. For most types, a function of the following form is used:

$$RES_{massfrac} = \left(\frac{D}{D_{act}} \right)^b \quad [15]$$

where

$RES_{massfrac}$ = fraction of the residue mass buried from the soil surface to depth D,

b = burial distribution exponent depending on the implement burial type,

D = depth in soil from the surface (mm), and

D_{act} = actual tillage depth (mm).

For a “uniform mixing” burial distribution implement type, the exponent b equals 1.0; for “mixing plus inversion and lifting, fracturing” types, b equals 0.5; and for “mixing and compression” types, b equals 0.3. For the “inversion” burial distribution implement type, the following equation is used:

$$\begin{aligned} RES_{massfrac} &= 0.28 \left\{ \exp \left[1.83 \left(\frac{D}{D_{act}} \right) \right] - 1 \right\} & \text{for } 0 \leq \frac{D}{D_{act}} \leq 0.6 \\ RES_{massfrac} &= 1 - 0.441 \left\{ \left[1 - \left(\frac{D}{D_{act}} \right) \right] / 0.4 \right\}^{1.4} & \text{for } 0.6 < \frac{D}{D_{act}} \leq 1.0 \end{aligned} \quad [16]$$

Some typical NRCS defined operations have the following burial parameter values: rototiller (0.9 using mixing burial distribution), moldboard plow (0.99 using inversion burial distribution), straight point chisel (0.76 using mixing plus inversion and lifting, fracturing burial distribution), and rodweeder (0.05 using uniform mixing burial distribution).

Resurface Process

Resurfacing is defined as the transfer of the buried biomass within the tillage zone back to the surface (Wagner and Nelson 1995). This process occurs with ground-engaging tillage operations and is most prevalent with chisel-style tools. It is not uncommon for one to end up with more residue on the surface after using one of these type of

implements if the original surface had little residue on the surface but contained a large amount of residue below the surface within the tillage zone. Specifying the fraction of below-ground residue within the tillage zone brought to the surface allows for the simulation of the process as outlined by Wagner and Nelson (1995). The fraction is uniformly applied to all soil layers in the tillage zone.

$$\begin{aligned} RES_{bf} &= RES_{b_0} - RES_{s_0}(L_{coef})\zeta \\ RES_{sf} &= RES_{s_0} + RES_{b_0}(L_{coef})\zeta \end{aligned} \quad [17]$$

where

RES_{bf} = buried biomass after the operation (stem, leaf, and storage pools),

RES_{b_0} = buried biomass before the operation (stem, leaf, and storage pools),

RES_{sf} = flat surface biomass after the operation (stem, leaf, and storage pools),

RES_{s_0} = flat surface biomass before the operation (stem, leaf, and storage pools),

L_{coef} = lift (resurface) coefficient for a specified toughness/size residue class, and

ζ = fraction of surface tilled ($0 \leq \zeta \leq 1$).

Some typical NRCS defined operations have the following resurfacing parameter values: rototiller (0.07), moldboard plow (0.01), straight point chisel (0.05), and rodweeder (0.05).

Change Standing Biomass Fall Rate Process

Most tillage operations that leave some residue standing will still affect the fall threshold and fall rate of the standing material due to the destruction of roots that anchor the standing residue in place. By providing a process to specify adjustments to the standing residue fall threshold and fall rate assigned to a residue pool, an acceleration of the decline in the standing residue can be simulated. Various fall rate adjustments are assigned to an operation based on the residue toughness/size class. A residue pool selection flag is used to specify which residue age pools are to have their fall rate modified.

This process was added to WEPS when NRCS observed that the model showed standing residue existing much longer than common field observations indicated. These were management rotations that involve undercutting (wide sweep, rodweeder for example) with little flattening but significant disturbance of the soil. Trying to compensate for this by increasing the amount of residue flattened by these operations would result in too little standing residue after the operation. The adjustment factor provides for a way to have a realistic standing residue amount immediately after the operation and a realistic absence of standing residue within a reasonable time interval following the operation.

$$\begin{aligned} TH_f &= TH_0(TH_{adj})\zeta \\ FR_f &= FR_0(FR_{adj})\zeta \end{aligned} \quad [18]$$

where

TH_f = threshold fall rate after the adjustment,

TH_0 = threshold fall rate assigned to the residue pool,

FR_f = fall rate after the adjustment,

FR_0 = fall rate after the adjustment assigned to residue pool,

TH_{adj} = threshold fall rate adjustment factor assigned to the operation,
 FR_{adj} = fall rate adjustment factor assigned to the operation (assigned by toughness/size residue class), and
 ζ = fraction of surface tilled ($0 \leq \zeta \leq 1$).

All numbers in the database were determined from WEPS model run testing with NRCS. NRCS inserted values and ran the model to compare with their field experience with those rotations. This is an example of a process that could benefit from additional field experiments to determine actual measured standing residue fall rates after tillage. An example of NRCS defined operations are the sweep plow implements employing this process. They have the following fall rate parameters (3.0, 2.5, 1.5, and 1.0) and threshold fall rate adjustment parameters (0.5, 0.6, 0.7, 0.8 and 1.0) assigned for the crop pool for each of the five toughness/size residue classes. The values are shown in most fragile to least fragile order. So, a fragile crop residue, like soybeans, would be assigned a value of 3.0 for the fall rate adjustment and 0.5 for the threshold fall rate if using one of these sweep plow implements.

Cut/Remove Processes

The cutting process simply changes the height of the standing biomass to a prescribed value. The biomass above the cutting height is either removed or added to the surface biomass pool, depending upon a cut flag value. The cut height can be specified as either an absolute or a relative value (fraction of total height) referenced from the ground surface or down from the current height of the biomass, depending on the specific “cut” process applied.

Thin Population Processes

Thinning is the process of reducing the plant and/or residue stem count. The manual pruning of plants is a common practice applied to vegetables crops. All thinned plant components are transferred to their corresponding flat pool components or removed as specified by the pool removal fraction coefficients. The degree of thinning can be specified by a specific desired plant population or as a fraction of the current plant population.

$$\begin{aligned} & \text{or} \\ & THINF_{remain} = (1.0 - THINF_{remove}) \\ & THINF_{remain} = \min \left(1.0, \frac{STEMPOP_{desired}}{STEMPOR_{current}} \right) \end{aligned} \quad [19]$$

where

$THINF_{remain}$ = fraction of the original population to remain,
 $THINF_{remove}$ = fraction of the original population to remove,
 $STEMPOP_{desired}$ = desired population, and
 $STEMPOR_{current}$ = current population.

Kill/Defoliate Process

The kill/defoliate process stops the growth of the biomass and transfers the crop biomass (roots, flat, or standing) to the corresponding categories in the residue biomass pools. The process may be initiated by tillage operations, the application of herbicides, or burning. The kill flag value can be set to specify that only annual plants or both annuals and perennials be killed. The kill/defoliate process also can be used for defoliating a growing

crop, e.g., the dropping of all standing crop leaf mass into the flat component of the crop pool (the flat component of the crop pool is a temporary storage pool for retaining the plant biomass from a growing crop until it is transferred to the flat residue pool for decomposition to begin). If the crop has sufficient reserve energy, it will regrow, otherwise it will die when defoliated. This is determined by a parameter in the crop growth record. If no crop is actively growing, this process does nothing. The current kill flag values and their definitions are:

$$\begin{aligned}
 KILL_{flag} = 0 &= \text{No crop killed} \\
 KILL_{flag} = 1 &= \text{Annual crop killed, perennial crop not killed} \\
 KILL_{flag} = 2 &= \text{All crop types killed} \\
 KILL_{flag} = 3 &= \text{Crop defoliation triggered}
 \end{aligned}
 \tag{20}$$

Removal Process

The remove process extracts biomass, either live crops and/or residue, from the site. This process is usually the result of harvest, grazing, or burning operations. The biomass amount, type, and position of the plant/residue are specified for removal by this process. The actual biomass pool variables available for fractional mass removal are the reproductive components (grain/fruit), leaves, stems, storage roots, and fibrous roots. Three remove-process flags specify the position of the biomass being removed (standing, flat, and buried locations), the pools selected for the biomass removal (crop, temporary crop, and residue decomposition pools), and the age of the material to be manipulated (crop, youngest residue, second youngest residue ... oldest residue). These flag value definitions are:

$$\begin{aligned}
 SelectPosition_{flag} = 1 &= \text{Standing and root components} \\
 SelectPosition_{flag} = 2 &= \text{Flat component} \\
 SelectPosition_{flag} = 3 &= \text{Standing, root and flat components} \\
 SelectPosition_{flag} = 4 &= \text{Buried component} \\
 SelectPosition_{flag} = 5 &= \text{Standing, root, and buried components} \\
 SelectPosition_{flag} = 6 &= \text{Flat and buried components} \\
 SelectPosition_{flag} = 7 &= \text{Standing, root, flat, and buried components} \\
 SelectPool_{flag} = 1 &= \text{Crop pool components} \\
 SelectPool_{flag} = 2 &= \text{Temporary pool components} \\
 SelectPool_{flag} = 3 &= \text{Crop and temporary pool components} \\
 SelectPool_{flag} = 4 &= \text{Residue pool components} \\
 SelectPool_{flag} = 5 &= \text{Crop and residue pool components} \\
 SelectPool_{flag} = 6 &= \text{Temporary and residue pool components} \\
 SelectPool_{flag} = 7 &= \text{Crop, temporary and residue pool components} \\
 SelectAge_{flag} = 0 &= \text{All ages} \\
 SelectAge_{flag} = 2 &= \text{Youngest residue age}
 \end{aligned}
 \tag{21}$$

End Biomass Manipulation Process

This process completes the transfer of the remaining biomass from a harvested or killed crop into the appropriate residue decomposition pool. The harvesting processes and the kill process will typically terminate the active growth of a growing crop; the crop biomass is then moved into the temporary crop pool where additional biomass

manipulation processes can still act on the crop material before it officially becomes crop residue within the WEPS model. It is normally specified as the last process in the harvesting and tillage operations that terminates the growth of a growing crop. This process is currently required for operations that kill growing crops in WEPS as decomposition can only occur in residue pools and not crop pools at this time in the model.

Soil Amendments

The soil amendment processes add material, e.g. water, seeds, plants, residue, etc. to the surface and/or within soil layers.

Plant Process

This process triggers the plant growth routines in WEPS to begin the simulation of the growth of a crop. The parameters (row spacing, plant population, and number of tillers per plant) and flags (type of planting and seed placement location) are specified, along with a complete crop growth and residue decomposition record for this process. The flag values are:

Irrigate Process

This process allows for the initiation and termination of scheduled irrigation events based

$PlantingType_{flag} = 0$ = Broadcast seeding

$PlantingType_{flag} = 1$ = Use implement ridge row spacing

$PlantingType_{flag} = 2$ = Use specified row spacing [22]

$SeedPlacement_{flag} = 0$ = Seed row placed in the furrow bottom

$SeedPlacement_{flag} = 2$ = Seed row placed on the ridge top

on a management-allowed depletion level. Based on the parameter values, the model can simulate a wide range of irrigation scenarios, including sprinkler, furrow, flood, and drip irrigation and their associated scheduling and application rate constraints. An irrigation type is specified by its maximum and minimum daily application depth, either the rate or the duration of application, the minimum number of days between applications, and the location of application as a distance above (+) or below (-) the soil surface. A single irrigation event can also be specified.

Add Biomass Process

This process provides the means to add additional crop residue biomass (or other material simulated as a crop residue) to the surface and/or into the soil. Typical non-crop residue materials such as manure, wood chips, and plastic covers can be simulated by setting the appropriate parameter values for standing residue stem count, height and mass, flat residue mass and residue toughness class, buried residue mass and burial depth, and buried root residue mass and burial depth.

Conclusions

The WEPS Management submodel attempts to combine published work from previous researchers to simulate the major processes related to the most prevalent cultural practices used by producers and land managers that influence the susceptibility of a site to wind erosion. The range of practices includes primary and secondary tillage, cultivation, planting/seeding, harvesting, and fertilization operations, as well as irrigation, burning, and grazing. The processes are simulated from a physical basis, if possible, and

incorporate the conservation of mass concepts. Because a goal of the submodel design was to use a minimum number of parameters with readily available and/or attainable values, the representations of some processes are simplified. The simulation of other processes was constrained simply by a lack of knowledge about those processes. The WEPS Management submodel can be expanded and improved as new knowledge is gained relating to the physical processes affecting the soil surface, soil mass, and biomass. Additionally, because WEPS represents a management operation as a sequence of physical processes, it not only allows for flexibility in how to describe specific existing operations but also allows for new implements and operations to be created and used easily within WEPS.

References

- Alberts, E.E., M.A. Nearing, M.A. Weltz, et al. 1995. Chapter 7. Soil component. *In* (Flanagan, D.C., and M.A. Nearing, eds.): USDA-Water Erosion Prediction Project (WEPP) Hillslope Profile and Watershed Model Documentation. NSERL Report No. 10, National Soil Erosion Research Laboratory, USDA-Agricultural Research Service, West Lafayette, Indiana.
- Allmaras, R.R., R.E. Burwell, W.E. Larson, et al. 1966. Total porosity and random roughness of the interrow zone as influenced by tillage. USDA Conservation Research Report 7.
- Chepil, W.S., and R.A. Milne. 1941. Wind erosion of soil in relation to roughness of surface. *Soil Science*. 52:417-433.
- Chepil, W.S., and N.P. Woodruff. 1954. Estimations of wind erodibility of field surfaces. *Journal of Soil Water Conservation*. 9:257-265, 285.
- Federal Register, 2010. Notice of implementation of the Wind Erosion Prediction System for soil erodibility system calculations for the Natural Resources Conservation Service. Federal Register 75, Number 234 (7 December 2010), 75961-75962. Print.
- Rawls, W.J. 1983. Estimating soil bulk density from particle size analysis and organic matter content. *Soil Science*. 134(2):123-125.
- Sharpley, A.N., and J.R. Williams, eds. 1990. EPIC--erosion/productivity impact calculator: 1. Model documentation. USDA Technical Bulletin Number 1768. 235 pp.
- USDA. 2013. Science Documentation, Revised Universal Soil Loss Equation, Version 2 (RUSLE2) (for the model with release date of May 20, 2008) USDA-Agricultural Research Service. Washington, D.C. Available at: https://www.ars.usda.gov/sp2UserFiles/Place/64080510/RUSLE/RUSLE2_Science_Doc.pdf. (Accessed August 10, 2020).
- Wagner, L.E. 2011. Overview of the management submodel in the wind erosion prediction system. *In* Proceedings International Symposium on Erosion and Landscape Evolution (ISELE), (18-21 September 2011, Anchorage, AK), ISELE Paper No. 11032. D.C. Flanagan, J.C. Ascough II, and J.L. Nieber (eds.). St. Joseph, MI: Society of Agricultural and Biological Engineers.
- Wagner, L.E. 2013. A history of wind erosion prediction models in the United States Department of Agriculture: The Wind Erosion Prediction System (WEPS). *Aeolian Research*. 10:9-24.
- Wagner, L.E., N.M. Ambe, and P. Barnes. 1992. Tillage-induced soil aggregate status as influenced by water content. *Transactions of the ASAE*. 35(2):499-504.
- Wagner, L.E., N.M. Ambe, and D. Ding. 1994. Estimating a proctor density curve from intrinsic soil properties. *Transactions of the ASAE*. 37(4):1121-1125.

- Wagner, L.E., and D. Ding. 1993. Stochastic modeling of tillage-induced aggregate breakage. *Transactions of the AASAE*. 36(4):1087-1092.
- Wagner, L.E., and D. Ding. 1994. Representing aggregate size distributions as modified lognormal distributions. *Transactions of the ASAE*. 37(3):815-821.
- Wagner, L.E., and F.A. Fox. 2001. Simulation of tillage and other management operations in WEPS. *In Soil Erosion Research for the 21st Century, Proceedings International Symposium (3-5 January 2001, Honolulu, HI, USA), 625-628*. Eds. J.C. Ascough II and D.C. Flanagan. St. Joseph, MI: American Society of Agricultural Engineers.
- Wagner, L.E., and R.G. Nelson. 1995. Mass reduction of standing and flat crop residues by selected tillage implements. *Transactions of the ASAE*. 38(2):419-427.
- Williams, J.W., R.C. Izaurralde, and E.M. Steglich. 2008. APEX, Agricultural Policy/Environmental eXtender Model, Theoretical Documentation, Version 0604, BREC Report # 2008-17. Blackland Research and Extension Center 720 East Blackland Road, Temple, Texas 76502. Available at: <https://blackland.tamu.edu/files/2012/10/the-apex-theoretical-documentation.pdf>. (Accessed August 10, 2020).
- Woodruff, N.P. and F.H. Siddoway. 1965. A wind erosion equation. *Soil Science Society of America Proceedings*. 29(5):602-608.

Soil Submodel of WEPS

Contributor:

L.J. Hagen

Abstract

The Soil submodel is one of several major science submodels included in the Wind Erosion Prediction System (WEPS). The objective of the Soil submodel is to simulate the soil temporal properties which control wind erodibility of soil on a daily basis in response to various driving processes including weather (precipitation, wetting, drying, freezing, thawing, and free-drying) and management (tillage, planting, harvesting, irrigation, etc.). The Soil submodel updates the relevant temporal variables by simulating the effects of these processes on ridge, furrow, and dike height; random roughness height; crust thickness; crust cover fraction; crust stability; loose erodible material on the crust; dry aggregate stability; aggregate size distribution; bulk density; and crust and aggregate density. A temporal variable to be updated is generally a function of more than one driving process, as well as intrinsic soil properties. Computational approaches as well as guiding equations that account for each soil property affecting wind erosion are presented. The development of the Soil submodel represents a new area in wind erosion research. In general, the variation in the temporal soil variables which control soil wind erodibility has not been widely investigated, so additional experimental research is ongoing for many of the topics addressed in this technical description. Updates and maintenance to this submodel will be necessary as new and more reliable data become available. The Soil submodel of WEPS is the only model that simulates the surface soil conditions that control erodibility for improved simulation of wind erosion.

Introduction

The Soil submodel is one of several major science submodels included in the Wind Erosion Prediction System (WEPS). The objective of the Soil submodel is to simulate the soil temporal properties which control wind erodibility of soil on a daily basis in response to various driving processes (Table 1). On days when wind erosion or management activities occur, the Erosion and Management submodels also may update some of the same soil temporal variables.

Table 1. Soil submodel variable and driving process matrix.

Temporal Variables	Surface Processes			Layer Processes		
	Rain	Sprinkler Irrigation	Snowmelt	Wet/dry	Freeze/thaw	Freeze/dry
Roughness:						
Ridge Height	X	X	X			
Dike Height	X	X	X			
Random	X	X	X			
Crust:						
Depth	X	X	X			
Cover Fraction	X	X	X			
Density	X	X	X			
Stability	X	X	X	X	X	X
Loose Mass	X	X	X			
Loose Cover	X	X	X			
Aggregates:						
Size Distribution	X	X	X	X	X	X
Dry Stability	X	X	X	X	X	X
Density	X	X	X	X	X	X
Layers:						
Bulk Density				X	X	X

The spatial domain affected by the Soil submodel consists of the entire simulation region whose boundaries are specified by the user. The simulation region is assumed to be homogeneous in the horizontal directions, but not in the vertical direction. The Soil submodel updates the relevant temporal variables in a series of soil layers by simulating the effects of both aggregation and deaggregation processes.

Symbols, definitions, and units used in this technical description are defined in the text and at the end of the chapter. The development of the Soil submodel represents a new area in wind erosion research. In general, the variation in the temporal soil variables which control soil wind erodibility has not been widely investigated, so additional experimental research is ongoing for many of the topics addressed in this technical

description. Updates and maintenance to this submodel will be necessary as new and more reliable data become available.

Soil Submodel Computation Scheme

In selecting a computation scheme, we considered several characteristics of the problem. First, the temporal variable to be updated is generally a function of more than one driving process as well as intrinsic soil properties. Unfortunately, temporal properties measured at a point in time are often the result of a combination of unknown prior processes. Moreover, researchers generally try to sort the field data and conduct laboratory experiments in order to determine the relationship between individual driving processes and a selected temporal soil variable. Two approaches were used in updating the soil erodibility variables.

For the first approach, a simple, typical case is illustrated in Figure 1, where the individual effects of process A and process B on ridge height are known. In the field, however, these driving processes, A and B, may occur in many combinations of sequences. An example is illustrated by the arrow sequence of Figure 1. Thus, the computation scheme must be able to accommodate the relationships which have been developed for single processes and combine them in a variety of sequences.

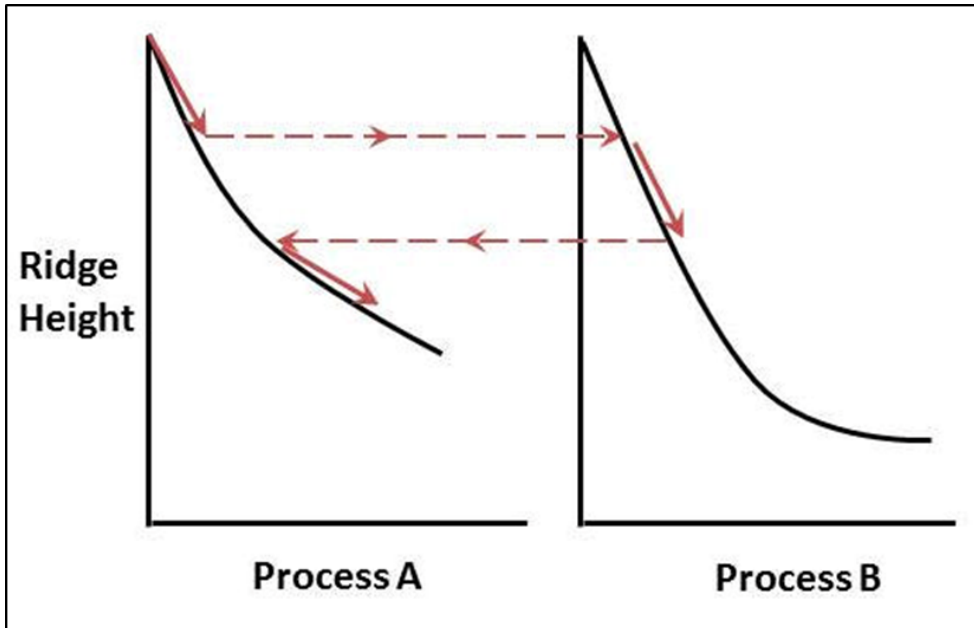


Figure 1. Typical example of temporal variable (e.g., ridge height) affected by two processes.

The approach used to update variables such as ridge height is illustrated in the following section. It was assumed that an explicit relationship (Eq. 1) is known from field data or other experiments.

$$Y = f(X_j) \quad [1]$$

where

Y = a dependent soil temporal variable, and
 X_j = an independent driving processes variable which changes Y .

Now, in principle, one can express X_j in terms of Y , i.e.:

$$X_j = f(Y) \quad [2]$$

Eq. 2 often can be derived from Eq. 1 algebraically. However, some solutions may not be analytic, so numerical values for X_j must be obtained using an iteration scheme. Further, note that Eq. 1 should be single-valued. In the event that a process is not single valued in Y , i.e., causes both aggregation and deaggregation under different conditions, it is useful to separate the effects into separate aggregation and deaggregation equations and calculate the effects successively.

Because the dependent Y variable can be changed by several processes, updating the Y on a daily basis requires two steps. First, an "equivalent" value for the independent variable must be calculated, i.e.:

$$X_{i,j} = f(Y_i) \quad [3]$$

where

$X_{i,j}$ = the current "equivalent" value which the j^{th} process would have, if it alone had caused the current value of the dependent variable Y_i ; where 'i' refers to the day.

The second step is then to update the dependent variable using the equation,

$$Y_{i+1} = f(X_{i,j} + \Delta X_j) \quad [4]$$

where

ΔX_j = the daily increment of the j^{th} driving force.

A second approach used to update some of the variables was to determine the average and standard deviation of a given variable from field measurements. Prediction equations were then developed to relate these results to intrinsic soil properties such as the sand, silt, and clay fractions.

Next, each temporal variable for each soil was given a non-dimensional range of zero to one, bounded by the average \pm two standard deviations. Over the non-dimensional range, processes' effects on individual variables were assigned. On a daily basis, the prior-day non-dimensional variables were calculated and processes for the current day were applied to update the non-dimensional variables. Finally, the non-dimensional updated variables were converted to dimensional values for use by other submodels. Except when soils were frozen, the preceding approach constrained the temporal variables within the limits bounded by the average \pm two standard deviations of the measured values.

Table 1 presents a matrix of the temporal soil variables that are updated by the Soil submodel and the driving processes that are currently considered in updating the temporal

variables. Note that furrow irrigation and biologically produced aggregation binding processes are not yet simulated.

Process Effects on Soil Temporal Properties

Ridge and Furrow Dike Height

Ridges and dikes are degraded by both precipitation and wind erosion. In addition, the degradation rate depends on the relative ridge height. Hence, before an update for daily precipitation is determined, the current height is used to calculate an apparent cumulative precipitation which could have produced that ridge height. Solving a modification of Eq. 6 for bare ridges gives:

$$CUMP = \left[\frac{1 - \frac{SZ_{rg-1}}{SZ_{rgo}}}{(0.034 CF1_{rg})} \right]^2 \quad [5]$$

where

$CUMP$ = cumulative depth of snowmelt, rainfall and sprinkler irrigation water (mm),

SZ_{rg-1} = prior day ridge height (mm),

SZ_{rgo} = initial ridge height after tillage (mm), and

$CF1_{rg}$ = correction factor for ridge scale.

Then, to update ridge height, an empirical equation developed by Lyles and Tatarko (1987) from field measurements was approximated, along with two empirical coefficients, as:

$$\frac{SZ_{rg}}{SZ_{rgo}} = 1 - 0.034[CUMP + DCUMP CF2_{cov}](1 - SV_{roc})^{(0.5)} (CF1_{rg}) \quad [6]$$

where

$DCUMP$ = daily depth of snowmelt, rainfall and sprinkler irrigation water in mm,

SZ_{rg} = updated ridge height (mm),

$CF2_{cov}$ = correction factor for biomass cover, and

SV_{roc} = surface layer soil volume of rock (fraction).

Ridges with various height/spacing ratios respond differently to precipitation. The ridges used to derive the response to precipitation in Eq. 5 ranged from 30 to 100 mm in height. Thus, the effect of scale for large ridges, such as lister ridges, was missing. An empirical correction factor for ridge scale was developed. Typical initial ridges (Lyles and Tatarko 1987) had the relation:

$$SX_{rg} = 4.17 SZ_{rgo} \quad [7]$$

where

SX_{rg} = ridge spacing (mm).

From geometric calculations, one can show that volume of soil which must be eroded to reach new height/spacing ratios is directly proportional to ridge height. To slow

degradation of large ridges and accelerate that of small ridges, a correction factor for ridge scale was estimated as:

$$CF1_{rg} = \left[\frac{348}{SX_{rg}} \right]^{0.3} \quad [8]$$

To slow degradation of ridges with biomass cover, a correction factor for biomass cover sheltering the soil surface is estimated as:

$$CF2_{cov} = 1 - 0.6 [BF_{scv} + (1 - BF_{scv})BF_{fcv}] \quad [9]$$

where

BF_{scv} = fraction of biomass standing cover, and

BF_{fcv} = fraction of biomass flat cover.

Eqs. 5 and 6 represent an implementation of Eqs. 3 and 4 respectively, to update ridge height.

Random Roughness

Random roughness is approximately the standard deviation of surface height as defined by Allmaras et al. (1966) of the soil and flat residue independent of the oriented roughness.

Random roughness can also be degraded by both precipitation and wind erosion. Similar to ridges, the degradation rate depends on relative roughness height. Hence, prior day random roughness height is used to calculate an apparent cumulative precipitation which could have produced that roughness. Solving a modified version of Eq. 13 for a bare surface gives:

$$CUMP = A_{rr} \left[-\ln \left(\frac{SZ_{rr-1}}{SZ_{rro}} \right) \right]^{C_{rr}} \quad [10]$$

where

SZ_{rr-1} = prior day random roughness (mm),

SZ_{rro} = random roughness after last tillage (Allmaras et al., 1966) (mm), and

A_{rr}, C_{rr} = regression coefficients.

$$A_{rr} = 91.08 + 765.8 SF_{sil} \quad [11]$$

$$C_{rr} = 0.53 + 4.66 SF_{san} - 3.8 SF_{san}^{1.5} - 1.22 SF_{san}^{0.5} \quad [12]$$

where

SF_{san} = soil fraction sand in first layer (kg kg^{-1}) and

SF_{sil} = soil fraction silt in first layer (kg kg^{-1}).

Reduction in random roughness height is predicted for bare soil (Potter 1990b, Zobeck and Onstad 1987), but Eq. 13 also includes empirical cover factors for biomass and rock:

$$\frac{SZ_{rr}}{SZ_{rr0}} = \exp [-\{(CUMP + (1 - SV_{roc}) CF2_{cov} DCUMP)/(A_{rr})\}^{C_{rr}}], \quad [13]$$

$$SZ_{rr} \geq 2.0$$

where

SZ_{rr} = updated random roughness, respectively, using Allmaras, et al. (1966) definition (mm), and

A_{rr}, C_{rr} = regression coefficients (personal communication, T. Zobeck).

Crust

The term 'crust' in WEPS refers to the near-surface consolidated zone which occurs after the addition of water to the surface or the puddling of surface soil when saturated. The equations which govern the changes in crust properties from addition of water will be presented in this section, and equations for the puddling effect will be included later in the layer process section.

Crust Thickness

The apparent precipitation based on crust thickness is:

$$CUMP = -\frac{\left\{ \ln \left(1 - \frac{SZ_{cr-1}}{7.6} \right) \right\}}{\{0.0705 - 0.0687 SF_{cla}^{0.146}\}}, \quad SZ_{cr-1} < 7.6 \quad [14]$$

where

SZ_{cr-1} = prior day crust thickness (mm), and

SF_{cla} = soil fraction clay in top layer.

The basic structure for simulation of crust thickness is based on that reported by Farres (1978) and data of Zobeck (personal communication). The initial surface condition is aggregated, and the crust thickness grows toward limits imposed by intrinsic soil properties. An estimate of the crust thickness when water additions exceed 10 mm is:

$$SZ_{cr} = 7.6 (1 - \exp[-(0.0705 - 0.0687 SF_{cla}^{0.146})(CUMP + DCUMP)]) \quad [15]$$

where

SZ_{cr} = updated crust thickness (mm).

Crust Cover Fraction

The apparent cumulative precipitation based on crust cover fraction is:

$$CUMP = -\frac{\ln(1 - SF_{cr-1})}{0.045}, \quad SF_{cr-1} < 1.0 \quad [16]$$

where

SF_{cr-1} = prior day crust cover.

An empirical surface crust cover fraction after rainfall was developed from a 3-year study at Big Spring, Texas (Zobeck and Popham 1992).

$$SF_{cr} = 1 - \exp[-0.045 (CUMP + DCUMP)], \quad [17]$$

$$CUMP + DCUMP > 10\text{mm}$$

where

SF_{cr} = soil fraction crust cover,

$DCUMP$ = daily snowmelt, sprinkler irrigation, and rainfall (mm), and

$CUMP$ = prior cumulative snowmelt, sprinkler irrigation, and rainfall (mm).

Crust Stability

Dry crust stability can be directly measured by passing saltating sand over a crusted soil tray. Then tray loss (kg m^{-2}) divided by saltation discharge (kg m^{-1}) gives the abrasion coefficient (m^{-1}). Experimental results show abrasion coefficients are linearly related to natural log of dry aggregate crushing energy (Hagen et al. 1992). Because it is practical to measure from small field samples, the natural log of crushing energy will be used as the measure of dry crust stability in WEPS.

Current data on crust stability show it may be less or close to that of the parent surface aggregates. Measured abrasion resistance on simulated crusts (Zobeck 1991) found abrasion rates similar to that predicted for aggregates. Hence, crust stability will be estimated as:

$$SE_{cr} = SE_{ag} \quad [18]$$

where

SE_{ag} = aggregate stability, $\ln(\text{J kg}^{-1})$ of crushing energy of top aggregate layer below crust (if present), and

SE_{cr} = crust stability, $\ln(\text{J kg}^{-1})$ of crushing energy.

Loose Erodible Material on Crust

The loose erodible material is defined as the single grains and water stable aggregates which occur on crusted surfaces after rainfall or sprinkler irrigation. Loose material on the crust was sampled using a vacuum system (Zobeck 1989). Simulated crusts using two rainfall intensities on 13 mineral soils were tested (Zobeck 1991). A prediction equation for maximum loose mass is:

$$SMX_{los} = 0.1 \exp \left[-0.57 + 0.22 \frac{SF_{san}}{SF_{cla}} + 7.0 SF_{cce} - SF_{om} \right] \quad [19]$$

with an upper limit of:

$$SMX_{los} < \frac{1}{-0.344 + \frac{0.352}{SF_{84}^2}} \quad [20]$$

where

SF_{cce} = soil fraction calcium carbonate equivalent (kg kg^{-1}),

SF_{om} = soil fraction organic matter (kg kg^{-1}),

SMX_{los} = maximum loose erodible material on crust (kg m^{-2}), and

SF_{84} = soil fraction less than 0.84 mm.

Eq. 19 is valid only when cumulative rainfall and sprinkler irrigation exceed 10 mm.

As precipitation accumulates, the loose material mass slowly decreases as (Zobeck and Popham 1992, Potter 1990a):

$$SM_{los} = SM_{los-1}(1 - 0.0053 DCUMSR) \quad [21]$$

where

SM_{los} = loose mass on surface crust (kg m^{-2}),
 SM_{los-1} = prior day loose mass on surface crust (kg m^{-2}),
 $DCUMSR$ = daily sprinkler irrigation and rainfall (mm).

Another process which acts to consolidate loose material is snowmelt. Snow does not melt uniformly over the field, so we estimate about 1.0 mm of melt may consolidate about 10 percent of the loose material. An approximation for this process is:

$$\frac{SM_{los}}{SM_{los-1}} = 1.0 - 0.1 HG_{snom}, \quad \frac{SM_{los}}{SM_{los-1}} > 0.1 \quad [22]$$

where

HG_{snom} = daily snowmelt (mm)

The cover fraction of loose, erodible soil on the crust is estimated from the mass of loose soil and the height of the surface roughness elements. The geometric mean diameter of the loose material was assumed to be 0.5 mm, and the bulk density as 1.2 Mg m^{-3} . For a smooth surface, the loose material was assumed to remain in a single layer until cover fraction was about 0.6 and then begin to overlap to give surface cover as:

$$SFX_{los} = [1.0 - \exp(-3.5 SM_{los}^{1.5})]CR_{los} \quad [23]$$

where

SFX_{los} = soil fraction cover of loose material on crust, and
 CR_{los} = correction coefficient for surface roughness.

In the presence of roughness elements, the wind tends to concentrate the loose material in sheltered areas and thus reduce the surface cover. From geometric analysis, we found a depth of loose material equal to 0.2 times the roughness height was needed to cover the roughness elements. For a rough surface, the loose surface cover coefficient was estimated as:

$$CR_{los} = \exp(-0.08 SZ^{0.5}), \quad CR_{los} \leq 1.0 \quad [24]$$

where

SZ = maximum of the ridge or 4 times random roughness height (mm).

Dry Aggregate Stability

Similar to crusts, crushing energy will be used as the measure of dry aggregate stability in WEPS. From sampling 10 soils periodically over 3 years (Skidmore and Layton 1992), the average aggregate stability was:

$$SEavg_{ag} = 0.83 + 15.7 SF_{cla} - 23.8 SF_{cla}^2, \quad SF_{cla} \leq 0.5 \quad [25]$$

with the estimate:

$$SEavg_{ag} = 2.73, SF_{cla} > 0.5 \quad [26]$$

where

$SEavg_{ag}$ = mean of natural log aggregate crushing energies, $\ln(\text{J g}^{-1})$.

The mean coefficient of variation (CV) averaged over all soils was 0.16.

Several processes affect the aggregate stability including freeze/thaw, freeze/dry, wet/dry, overburden pressure, and biological activity. Moreover, these processes may cause increases or decreases in stability depending upon soil and process conditions. We describe an approximate method to estimate dry aggregate stability. First, determine a maximum and a minimum aggregate stability for each soil as follows:

$$SEmax_{ag} = SEavg_{ag} + 2(0.16)SEavg_{ag} \quad [27]$$

$$SEmin_{ag} = SEavg_{ag} - 2(0.16)SEavg_{ag} \quad [28]$$

The soil aggregate and crust stabilities are modified by the layer processes as defined in Table 2.

Table 2. Decision matrix for soil layer processes and states.

Daily Processes Simulated	Final State	Soil Temperature (°C) *		
		Current Day		Prior Day
		Maximum Temperature	Minimum Temperature	Maximum
Wet	Unfrozen		≥ 0	≥ 0
Dry	Unfrozen		≥ 0	≥ 0
Wet + Freeze	Frozen	< 0		≥ 0
Dry + Freeze	Frozen	< 0		≥ 0
Thaw + Wet	Unfrozen	> 0		≤ 0
Thaw + Dry	Unfrozen	> 0		≤ 0
Freeze & Thaw + Wet	Unfrozen	> 0	< 0	≥ 0
Freeze & Thaw + Dry	Unfrozen	> 0	< 0	≥ 0
Wet while Frozen	Frozen	< 0		< 0
Dry while Frozen	Frozen	< 0		< 0

* Assumes minimum temperature in early A.M. and maximum temperature about 2 P.M.

The measured range of dry stabilities was related to the intrinsic soil properties using regression equations. However, the updating processes are applied to non-dimensional values in equations denoted by asterisks. For example, non-dimensional prior day stabilities (SE_{ag-1}^*) are estimated as:

$$SE_{ag-1}^* = \frac{(SE_{ag-1} - SE_{min_{ag}})}{(SE_{max_{ag}} - SE_{min_{ag}})} \quad [29]$$

In WEPS, wind-driven raindrop splash erosion is not determined, and erosion is simulated only for dry soils. Hence, when soil moisture is greater than wilting point, the simulated daily stability values (SE_{ag1}) are unmeasured, so stabilities that would increase to the measured dry stability upon drying are used.

A non-dimensional average prior day soil moisture ($HRwc_{-1}^*$) and the current day ($HRwc_1^*$) are also used in the updating processes.

$$HRwc_{-1}^* = \frac{HRwc_{-1} - HRwc_w}{HRwc_s - HRwc_w} \quad [30]$$

$$HRwc_1^* = \frac{HRwc_1 - HRwc_w}{HRwc_s - HRwc_w} \quad [31]$$

where

$HRwc_s$ = gravimetric water content at soil saturation (kg kg^{-1}) and

$HRwc_w$ = gravimetric water content at soil wilting~15 bar (kg kg^{-1}).

Updating stability with unfrozen wetting is simulated as:

$$SE_{ag1}^* = SE_{ag-1}^* + \frac{1.0001 - k4w (HRwc_1^*)}{1.0001 - k4w (HRwc_{-1}^*)}, \quad HRwc_1 > HRwc_{-1} \quad [32]$$

where

$k4w$ = coefficient for wetting (1.0)

Updating stability with unfrozen drying using the drying coefficient ($k4d$) is:

$$SE_{ag1}^* = SE_{ag-1}^* + k4d (HRwc_{-1}^* - HRwc_1^*), \quad HRwc_{-1}^* > HRwc_1^* \quad [33]$$

$$k4d = 0.6 (1.0 + 0.00333 SZ_{lyd}), \quad k4d \leq 1.0 \quad [34]$$

where

SZ_{lyd} = depth to bottom of a soil layer from surface (mm).

By making the drying coefficient ($k4d$) a function of depth, stability of aggregates near the surface may be decreased, while at other depths stability may be increased by a

wetting and drying cycle as illustrated in Figure 2. A partial cycle will, of course, result in smaller changes in stability than shown in Figure 2.

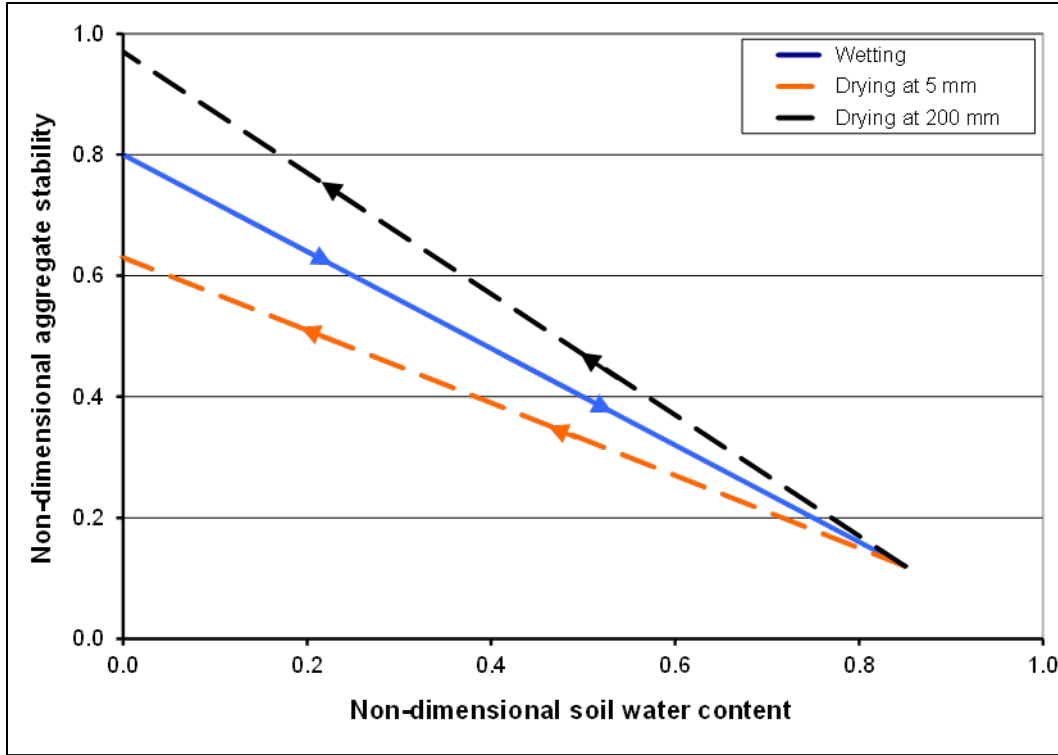


Figure 2. Simulated non-dimensional stability changes caused by wetting an aggregate with initial stability of 0.8 to 0.85 non-dimensional water content and then drying the aggregate to wilting point at two different soil depths.

Updating stability for freezing process is done in two steps. First, there is expansion and water migration to freezing layer using current day relative water content:

$$SE_{ag1/2}^* = SE_{ag-1}^* + \frac{1.0001 - k4w k4f (HRwc_1^*)}{1.0001 - k4w (HRwc_1^*)}, SE_{ag0} \geq 0. \quad [35]$$

Then solidifying (freezing):

$$SE_{ag1f}^* = SE_{ag1/2}^* + 0.5 + k4fs k4f (HRwc_1^*) \quad [36]$$

where

$k4fs$ = freezing solidification coefficient (4.25), and

$k4f$ = water migration and freezing expansion coefficient (1.4).

Updating stability for freezing/thawing process is done in several steps. First is expansion and water migration to freezing layer using prior day relative water content:

$$SE_{ag\ 1/2}^* = SE_{ag-1}^* + \frac{(1.0001 - k4w\ k4f\ (HRwc_{-1}^*))}{(1.0001 - k4w\ (HRwc_{-1}^*))}, \quad [37]$$

$$SE_{ag-1} \geq 0.0$$

Then solidifying (SE_{agf-1}) using prior day water content:

$$SE_{agf-1}^* = SE_{ag\ 1/2}^* + 0.5 + k4fs\ k4f\ (HRwc_{-1}^*) \quad [38]$$

The thawing process is also composed of two steps:
First, thaw:

$$SE_{ag\ 1/2}^* = SE_{agf-1}^* - 0.5 - k4fs\ k4f\ (HRwc_{-1}^*) \quad [39]$$

and then water migration and shrinkage using the after-thaw drying coefficient ($k4td$) is:

$$SE_{ag1}^* = SE_{ag\ 1/2}^* + k4td\ (k4f - 1.0)(HRwc_{-1}^*), \quad SE_{ag1}^* > 0.0 \quad [40]$$

$$k4td = 0.4 [1.0 + 0.00333 (SZ_{lyd})], \quad k4td \leq 0.667 \quad [41]$$

Alternatively, if thawing occurs at a high moisture content (i.e., $k4f\ (HRwc_{-1}^*) > 1.0$), then soil puddling is simulated instead of thawing as:

Change in relative stability caused by wetting while soil is frozen is simulated as:

$$SE_{ag1}^* = 0.999 - k4td\ (HRwc_{-1}^*), \quad SE_{ag1}^* > 0.0 \quad [42]$$

$$SE_{agf1}^* = SE_{agf-1}^* + k4fs\ k4f\ (HRwc_1^* - HRwc_{-1}^*), \quad SE_{agf1}^* \leq 10.0 \quad [43]$$

$$SE_{agf1}^* = SE_{agf-1}^* + k4fd\ k4f\ (HRwc_1^* - HRwc_{-1}^*), \quad SE_{agf-1}^* \geq 0.0 \quad [44]$$

Change in relative stability caused by drying while soil is frozen is simulated as:

The final step is to convert the non-dimensional stability to a quasi-stability or, if the soil is dry, to the real stability as:

$$SE_{ag} = SE_{ag1}^* (SE_{max\ ag} - SE_{min\ ag}) + SE_{min\ ag} \quad [45]$$

Non-dimensional prior day dry aggregate stabilities (SE_{-1}^*) and the current day (SE_{-1}) for non-frozen soil are also calculated for use in simulating changes in the aggregate size distribution as:

$$SE_{-1}^* = SE_{ag-1}^* + k4d\ (HRwc_{-1}^*), \quad SE_{-1}^* \leq 1.0 \quad [46]$$

$$SE_1^* = SE_{ag1}^* + k4d (HRwc_1^*), \quad SE_1^* \leq 1.0 \quad [47]$$

If soil is frozen, then:

$$SE_{-1}^* = SE_{ag-1}^*, \quad SE_{-1} \leq 10 \quad [48]$$

$$SE_1^* = SE_{ag1}^*, \quad SE_1 \leq 10 \quad [49]$$

Aggregate Size Distribution - ASD

Among the variables in the soil submodel, aggregate size distribution (ASD) is one of the most important. The ASD includes all sizes of aggregates as well as the loose individual soil particles. In addition to updating surface ASD, the Soil submodel must also update ASD in all other soil layers. It is important that the Soil submodel includes aggregation processes which increase ASD in the tillage zone. Otherwise, after a few iterations the deaggregation processes in the Soil and Management submodels only return a minimum value of ASD to the Erosion submodel.

The aggregate size distribution of field soils generally fits an abnormal log-normal distribution, which is defined by four parameters - a geometric mean diameter (SL_{agm}) and geometric standard deviation (SO_{ags}), coupled with upper (SL_{agx}) and lower (SL_{agn}) limit parameters. The lower limit is about 0.001 to 0.015 mm and varies as a function of soil intrinsic properties. The Soil and Management submodels must update the SL_{agm} , SO_{ags} , and SL_{agx} in response to the driving forces.

Similar to the representation of aggregate stability, aggregate mean geometric diameter was related to intrinsic soil properties. To begin, the average aggregate size fraction less than 0.84 mm diameter ($SF84_m$) was calculated using a regression equation (Fryrear et al. 1994) as:

$$SF84_m = 0.2909 + 0.31 SF_{san} + 0.17 SF_{sil} + 0.0033 \frac{SF_{san}}{SF_{cla}} - SF_{om} - 0.95 SF_{caco3}, \quad SF84_m \leq 1.0 \quad [50]$$

with the following limits:

$$SF_{om} \leq 0.03, \quad SF_{caco3} \leq 0.20, \quad SF_{cla} \leq 0.40, \quad \text{and} \quad SF_{san} / SF_{cla} \leq 40$$

The equation for $SF84_m$ was modified to provide higher erodible fraction (EF - fraction less than 0.84 mm) on sandy soils. Sand-clay ratio coefficient is increased from 0.0033 to 0.01 where sand fraction is greater than or equal to 0.15 and clay is less than or equal to 0.25. Otherwise the original equation is used. The use of the modified equation gives EF values that are more aligned with what has been observed in the field on sandy soils.

Over time, weathering and tillage cause variations in $SF84$, and the standard deviation is approximately:

$$SF84_{std} = (0.41 - 0.22 SF_{san})SF84_m \quad [51]$$

Next, a regression equation was developed for the geometric mean diameter as:

$$SL_{agm} = \exp(3.44 - 7.21 SF84_m) \quad [52]$$

Finally, maximum and minimum values for geometric mean aggregate diameters were estimated as:

$$SL_{min} = \exp[3.44 - 7.21 (SF84_m + 2 SF84_{std})], \quad SL_{min} \geq 0.025 \quad [53]$$

where

$$SL_{max} = \exp[3.44 - 7.21 (SF84_m - 2 SF84_{std})], \quad SL_{max} \leq 31.0 \quad [54]$$

SL_{min} = minimum value for geometric mean aggregate diameter (mm), and

SL_{max} = maximum value for geometric mean aggregate diameter (mm).

The parameter that is updated is the prior day non-dimensional aggregate geometric mean diameter defined as:

$$gmd_{-1}^* = \frac{SL_{agm-1} - SL_{min}}{SL_{max} - SL_{min}} \quad [55]$$

The processes that control aggregate stability, also affect aggregate size distribution. Hence, the non-dimensional aggregate stability is used to update the aggregate size distribution as follows:

When soil freezes ($SE_0^* < 1.0$ and $SE_1^* > 1.0$), the current day non-dimensional geometric mean diameter (gmd_1) is estimated as:

$$gmd_1 = gmd_{-1} + SE_1^*, \quad 1.0 \leq gmd_1 \leq 11.0 \quad [56]$$

When frozen soil thaws ($SE_{-1}^* > 1.0$ and $SE_1^* < 1.0$), or the soil is at maximum stability the update estimates gmd_1 based on SE_1^* as (Figure 3):

$$gmd_1 = 1.0 - \exp\left[-\left(\frac{SE_1^*}{c4p}\right)^2\right] \quad [57]$$

where

$c4p$ = coefficient (0.6).

When the soil is not frozen and stability is not changing ($SE_0^* = SE_1^*$), the gmd_1 moves slowly toward the average value (Figure 3) as:

$$gmd_1 = 0.2 \left[1.0 - \exp\left[-\left(\frac{SE_1^*}{c4p}\right)^2\right] \right] + 0.8 (gmd_{-1}) \quad [58]$$

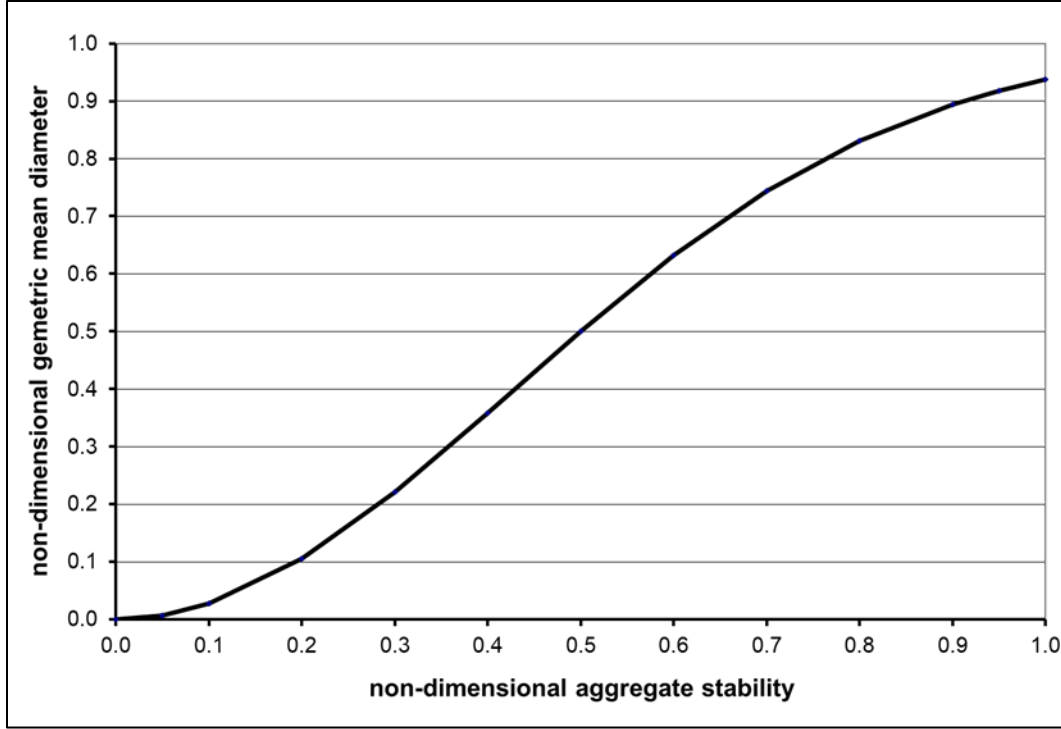


Figure 3. Plot of Eq. 58 illustrating estimated average gmd_1^* as a function of SE_1^* .

Cumulative rainfall generally decreases gmd of the surface layer of sandy soils (Zobeck and Popham 1990). Hence, when the soil is not frozen, but stability is changing ($SE_0^* \neq SE_1^*$), the gmd_1 moves toward average values using the following empirical steps:

$$gmd_{avg-1}^* = 1.0 - \exp \left[- \left(\frac{SE_{-1}^*}{c4p} \right)^2 \right] \quad [59]$$

$$slp_{-1} = \frac{gmd_{avg1}^* - gmd_{-1}^*}{SE_1^* - SE_{-1}^*} \quad [60]$$

$$gmd_{avg1}^* = 1.0 - \exp \left[- \left(\frac{SE_1^*}{c4p} \right)^2 \right] \quad [61]$$

The companion equation is given by:

$$slp_{avg} = \frac{gmd_{avg1}^* - gmd_{avg-1}^*}{SE_1^* - SE_{-1}^*} \quad [62]$$

Finally, the updated gmd_1 is:

$$gmd_1^* = gmd_{-1}^* + 0.5(slp_0 + slp_{avg})(SE_1^* - SE_{-1}^*) \quad [63]$$

and the dimensioned value is:

$$SL_{agm1} = gmd_1^*(SL_{max} - SL_{min}) + SL_{min}, \quad SL_{min} \leq unfrozen SL_{agm} \leq SL_{max} \quad [64]$$

At present, the SO_{ags} will be linked to SL_{agm} as:

$$SO_{(ags\ 1)} = 1.0 + \frac{1.0}{0.012448 + 0.002463 SL_{agm\ 1} + \frac{0.093467}{(SL_{agm\ 1}^{0.5})}} \quad [65]$$

Finally, SL_{agx} also will be linked to SL_{agm} and SO_{ags} as:

$$SL_{agx\ 1} = SL_{agm\ 1} SO_{ags\ 1}^{(1.52 SL_{agm\ 1})^{(-0.449)}} \quad [66]$$

Bulk Density

Bulk density is the mass per unit volume of soil. In the Soil submodel, the 'settled' bulk density (SD_{sblk}) that follows the initial after-tillage settling in any layer of mineral soil is estimated using the intrinsic properties of the soil layer as inputs to Rawls' (1983) prediction diagram.

Slow settling toward the settled bulk density is simulated on a daily basis as:

$$SD_{blk1} = SD_{blk-1} + 0.01(SD_{sblk} - SD_{blk-1}), \quad SD_{sblk} > SD_{blk-1} \quad [67]$$

where

SD_{blk1} = current day layer bulk density ($Mg\ m^{-3}$) and

SD_{blk-1} = layer bulk density on prior day ($Mg\ m^{-3}$).

The soil bulk density is further modified when water infiltration occurs in a given soil layer.

An initial value is assigned to a wet bulk density ($SD_{wblk\ 1}$) as:

$$SD_{wblk\ 1} = SD_{blk\ 1} \quad [68]$$

Then, for each 5 mm of water infiltration in a layer, a new wet bulk density is calculated as:

$$SD_{wblk(i+1)} = SD_{wblk(i)} + 0.75 \left[1.0 - \left(\frac{SD_{wblk(i)}}{0.97SD_{sblk}} \right)^{1.5} \right], \quad [69]$$

$$SD_{wblk(i)} 0.97SD_{sblk}$$

where the subscript i refers to the i^{th} iteration.

Finally, a weighted bulk density for the current day is calculated as a weighted average of the dry and wet bulk densities as:

$$SD_{blk1} = \frac{SD_{wblk}SZ_{wlyt} + SD_{blk}(SZ_{lyt} - SZ_{wlyt})}{SZ_{lyt}}, \quad [70]$$

$$SZ_{wlyt} \leq SZ_{lyt}$$

where

SZ_{wlyt} = wetted depth thickness in layer (mm), and

SZ_{lyt} = layer thickness (mm).

Crust and Aggregate Density

The crust and aggregate density are defined as the mass per unit volume of dry crust and single aggregates, respectively. In WEPS, the aggregate density is input as a constant:

$$SD_{ag} = 1.8 \quad [71]$$

where

SD_{ag} = Soil aggregate density (Mg m^{-3}).

As suggested by Zobeck (1991), the following equation is used for crust density:

$$SD_{cr} = 0.576 + 0.603 SD_{blk0} \quad [72]$$

where

SD_{blk0} = Soil bulk density of the top layer (Mg m^{-3}).

Conclusions

The Soil submodel of WEPS simulates the surface soil conditions that control erodibility and it is therefore critical for accurate simulation of soil loss by wind. Specifically, it simulates soil temporal properties which control wind erodibility of the soil on a daily basis in response to driving processes of time, weather, and management. The Soil submodel updates the relevant temporal variables by simulating the effects of these processes on ridge, furrow, and dike height; random roughness height; crust thickness, cover fraction, and stability; loose erodible material on the crust; dry aggregate stability;

aggregate size distribution; bulk density; and crust and aggregate density. Further research is needed that will provide an improved simulation of soil processes. Variation in the temporal soil properties which control soil wind erodibility throughout the year has also not been widely investigated, so additional experimental research is essential to better understand these processes. In particular, routines for simulating soil aggregation and crusting processes as well as processes for high organic soils need improved or developed.

References

- Allmaras, R.R., R.E. Burwell, W.E. Larson, and R.F. Holt. 1966. Total porosity and random roughness of the interrow zone as influenced by tillage. USDA Conservation Research Report 7.
- Farres, P. 1978. The Role of Time and Aggregate Size in the Crusting Process. *Earth Surface Processes*. 3:243-254.
- Fryrear, D.W., C.A. Krammes, D.L. Williamson, and T.M. Zobeck. 1994. Computing the wind erodible fraction of soils. *Journal of Soil and Water Conservation*. 49(2):183-188.
- Hagen, L.J., E.L. Skidmore, and A. Saleh. 1992. Wind erosion: Predictions of aggregate abrasion coefficients. *Transactions of the ASAE*. 35(6):1847-1850.
- Lyles, Leon and J. Tatarko. 1987. Precipitation Effects on Ridges Created by Grain Drills. *Journal of Soil and Water Conservation*. 42(4): 269-271.
- Potter, K.N. 1990a. Estimating wind-erodible materials on newly crusted soils. *Soil Science*.150(5):771-776.
- Potter, K.N. 1990b. Soil properties effect on random roughness decay by rainfall. *Transactions of the ASAE*. 33(6): 1889-1892.
- Rawls, W.J. 1983. Estimating Soil Bulk Density From Particle Size Analysis and Organic Matter Content. *Soil Science*. 135(2): 123-125.
- Skidmore, E.L. and J. Layton. 1992. Dry Soil Aggregate Stability as Influenced by Selected Soil Properties. *Soil Science Society of America Journal*. 56:557-561.
- Zobeck, T.M. 1989. Fast-Vac A vacuum system to rapidly sample loose granular material. *Transactions of the ASAE*. 32(4):1316-1318.
- Zobeck, T.M. 1991. Abrasion of crusted soils: influence of abrader flux and soil properties. *Soil Science Society of America Journal*. 55:1091-1097.
- Zobeck, T.M. and C.A. Onstad. 1987. Tillage and rainfall effects on random roughness: a review. *Soil and Tillage Research*. 9:1-20.
- Zobeck, T.M. and T.W. Popham. 1990. Dry aggregate size distribution of sandy soils as influenced by tillage and precipitation. *Soil Science Society of America Journal*. 54(1):198-204.
- Zobeck, T.M. and T.W. Popham. 1992. Influence of microrelief, aggregate size, and precipitation on soil crust properties. *Transactions of the ASAE*. 35(2):487-492.

Table 3. List of symbols for the Soil submodel of WEPS.

Symbol	Definition	Units
-1,1	subscripts indicating prior (-1) and current (1) day values	unitless
½	subscript denotes first step of a two-step soil updating process	unitless
*	asterisk in symbol denotes non-dimensional variable	unitless
A, B	undefined processes that update soil temporal properties	unitless
A_{rr}, C_{rr}	regression coefficients for random roughness	unitless
BF_{scv}	fraction of growing plant and residue biomass standing cover	m ² m ⁻²
BF_{fcv}	biomass fraction of flat cover	unitless
$c4p$	coefficient (0.6)	unitless
$CF2_{cov}$	correction factor for biomass cover	unitless
$CF1_{rg}$	correction factor for ridge scale	unitless
CR_{ios}	loose soil surface cover correction coefficient for roughness	unitless
$CUMP$	cumulative depth of snowmelt, rainfall, and sprinkler irrigation water	mm
$DCUMP$	daily total depth of snowmelt, rainfall and sprinkler irrigation water	mm
$DCUMSR$	daily total sprinkler irrigation and rainfall	mm
gmd	aggregate geometric mean diameter	mm
HG_{snom}	daily snowmelt	mm
$HRwc_a$	available soil water content	kg kg ⁻¹
$HRwc$	soil water content	kg kg ⁻¹
$HRwc^*$	non-dimensional soil water content	unitless
$HRwc_s$	soil water content at saturation	kg kg ⁻¹
$HRwc_w$	soil water content at wilting point (-1500 kPa)	kg kg ⁻¹
$k4_d$	coefficient for drying process as function of depth	unitless
$k4_f$	coefficient for water migration and expansion freezing (1.4)	unitless
$k4_{fs}$	coefficient for freezing and solidification (4.25)	unitless
$k4_{td}$	coefficient for thaw then dry as function of depth	unitless
$k4_w$	coefficient for updating stability during wetting	unitless
SD_{ag}	soil aggregate density	Mg m ⁻³
SD_{cr}	soil crust density	Mg m ⁻³
SD_{sblk}	settled bulk density of layer	Mg m ⁻³

<i>SD_{blk}</i>	soil bulk density	Mg m ⁻³
<i>SD_{blk 0}</i>	soil bulk density of top layer	Mg m ⁻³
<i>SD_{wblk}</i>	soil wet soil bulk density	Mg m ⁻³
<i>SE_{ag}</i>	aggregate stability crushing energy	ln(J kg ⁻¹)
<i>SE_{agf}</i>	aggregate stability crushing energy while frozen	ln(J kg ⁻¹)
<i>SE_{cr}</i>	crust stability crushing energy	ln(J kg ⁻¹)
<i>SE_{avg_{ag}}</i>	mean of natural log aggregate crushing energies	ln(J kg ⁻¹)
<i>SE_{max_{ag}}</i>	maximum of natural log aggregate crushing energies	ln(J kg ⁻¹)
<i>SE_{min_{ag}}</i>	minimum of natural log aggregate crushing energies	ln(J kg ⁻¹)
<i>SF₈₄</i>	current fraction < 0.84 mm diameter for a given soil	unitless
<i>SF_{84_m}</i>	average fraction < 0.84 mm diameter for given soil	unitless
<i>SF_{84_{std}}</i>	standard deviation of average fraction < 0.84 mm diameter	mm
<i>SF_{CaCO₃}</i>	soil fraction calcium carbonate	kg kg ⁻¹
<i>SF_{cce}</i>	soil fraction calcium carbonate equivalent	kg kg ⁻¹
<i>SF_{cla}</i>	soil fraction clay	kg kg ⁻¹
<i>SF_{cr}</i>	soil fraction crust cover	m ² m ⁻²
<i>SF_{om}</i>	soil fraction organic matter	kg kg ⁻¹
<i>SF_{san}</i>	soil fraction sand	kg kg ⁻¹
<i>SF_{sil}</i>	soil fraction silt	kg kg ⁻¹
<i>SFX_{los}</i>	maximum loose soil cover on crust	m ² m ⁻²
<i>SL_{agm}</i>	aggregate geometric mean diameter	mm
<i>SL_{agn}</i>	lower limit of abnormal log-normal aggregate size distribution	mm
<i>SL_{agx}</i>	maximum diameter of aggregate size distribution	mm
<i>SL_{max}</i>	maximum aggregate geometric mean diameter	mm
<i>SL_{min}</i>	minimum aggregate geometric mean diameter	mm
<i>slp</i>	daily change in gmd* per daily change in SE*	unitless
<i>slp_{avg}</i>	average daily change in gmd* per daily change in SE*	unitless
<i>SM_{los}</i>	loose, erodible mass on surface crust	kg m ⁻²
<i>SMX_{los}</i>	maximum loose, erodible mass on crust	kg m ⁻²
<i>SO_{ags}</i>	standard deviation of aggregate size distribution	unitless
<i>SV_{roc}</i>	soil layer volume of rock > 2.0 mm diameter	m ³ m ⁻³
<i>SX_{rg}</i>	ridge spacing	mm

SZ	maximum of ridge height or 4 times the random roughness	mm
SZ_{cr}	crust thickness	mm
SZ_{lyd}	depth to bottom of layer from surface	mm
SZ_{lyt}	layer thickness	mm
SZ_{wlyt}	wetted thickness in a layer	mm
SZ_{rg}	current ridge height	mm
SZ_{rgo}	initial ridge height after tillage	mm
SZ_{rr-1}, SZ_{rro}	current ($rr-1$) and initial (after tillage) (rro) random roughness	mm
ΔX_j	daily increment of the j^{th} driving force	unitless
X_j	an independent driving variable of the j^{th} process	unitless
X_{ij}	current value of the j^{th} process variable	unitless
Y	a dependent soil temporal variable	unitless

Crop Submodel of WEPS

Contributors:

F. Fox
A. Retta

Abstract

A plant growth submodel (dubbed Crop) was developed for the Wind Erosion Prediction System (WEPS). The model calculates daily production of roots, leaves, stems, and reproductive organ masses and leaf and stem areas as needed for simulating wind erosion. Plant growth variables are adjusted within the Crop submodel for suboptimal temperature conditions or lack of adequate water supplies to meet plant growth needs. The model was tested on data from 5 crops (corn, soybean, winter wheat, oats, and sorghum) grown at the Kansas State University Agronomy Farm in Manhattan, Kansas. Agreement between measured and simulated values was good for corn. The model is representative of the soybean growth trend and the relationship between total biomass and stem mass for soybean and winter wheat. The stem mass was under-predicted in relation to total biomass for oat and soybean. The use of a residue yield ratio resulted in an improved relationship between stem mass and total biomass at the end of the season for oat and soybean.

Introduction

The plant growth model (Crop) is one of the submodels in the Wind Erosion Prediction System (WEPS). The presence of live biomass on the soil surface influences the quantity of soil that can be removed by wind erosion. Biomass growth needs to be estimated throughout the growing season to account for live biomass cover. At harvest, an estimate of the amount of dead biomass remaining on the cropped surface is required for use by the Decomposition and other submodels of WEPS.

The Crop submodel was adapted from the Erosion Productivity Impact Calculator (EPIC) crop growth model (Williams et. al. 1989). EPIC simulates growth of many types of crops and other plant communities and has been validated for a variety of crops at different locations around the world. Additional capabilities and modifications have been developed and incorporated into the Crop submodel to meet the need for predicting effects of a growing crop on wind erosion. Some of the factors that affect wind erosion are the flexibility and arrangement of individual plant parts, distribution of plant parts by height, and number of plants per unit area (Shaw and Periera 1982). Leaves and stems have to be accounted for separately for several reasons: (1) on a per-unit-area basis, stems of young seedlings are roughly 10 times more effective than leaves in depleting wind energy, with the effectiveness of leaves increasing with plant growth (Hagen 1991, Armbrust and Bilbro, personal communication); (2) leaves are more sensitive to sandblast damage than are stems; and (3) leaves and stems decompose at different rates. Thus, one of the requirements of the Crop submodel is to give daily estimates of leaf and stem growth. In EPIC, leaf area index (LAI) is calculated directly, and no adjustments are made for differences in plant populations. The Crop submodel calculates leaf area per

plant, and thus, differences in plant cover resulting from differences in the number of live seedlings per unit area, so the effects on wind erosion can be properly evaluated.

Harvesting of grain crops removes the grain and returns the non-grain portion of the reproductive mass to the soil surface. In order to maintain an accurate mass balance, an estimate of the biomass (other than leaves and stems) that is left on the soil surface is needed. The Crop submodel is designed to (1) estimate daily biomass production; (2) partition biomass into fibrous root, storage root, leaf, stem, and reproductive mass pools (Table 1); (3) obtain estimates of leaf and stem area growth; and (4) calculate economic (grain or other yield) and noneconomic (chaff) parts at physiological maturity. Harvesting of non-grain crops removes reproductive material, leaves, stems, storage roots, or combinations of these plant parts. Plants may regrow after these kinds of harvest events depending on crop type and the availability of biomass reserves. The objective of this technical paper is to give a full description of the methods and approaches used in the Crop submodel to calculate crop-plant state variables. In the event our method of calculation differs from what EPIC used, the reason for doing so is discussed.

Table 1. Biomass pools used for tracking the plant growth state.

Pool	Pool Subdivisions	Pool Location
Reproductive	Standing	Above Ground
	Flat	
Leaf	Standing	
	Flat	
Stem	Standing	
	Flat	
Storage Root	Layer 1	Below Ground
	Layer ...	
	Layer n	
Fibrous Root	Layer 1	
	Layer ...	
	Layer n	

Although the WEPS submodel that simulates plant growth original modeled crop type plants exclusively, it has potential to model other plants not considered as crops. This submodel might, in the future, simulate growth for plants such as weeds or range plants; however, to maintain consistency with the WEPS literature, the submodel will retain the name “Crop Submodel” with the realization that other non-crop plants may be simulated with the submodel.

Submodel Description

Plant Growth Parameters

Plant growth parameters are a critical part of the Crop submodel and are considered to be constant for a given crop or plant. Many of the parameters were taken from EPIC (Williams et al. 1990b). Parameters for calculating leaf and stem areas and for partitioning aboveground biomass into leaf, stem, and reproductive masses were developed for soybean, corn, grain sorghum, winter wheat, oats, and rice (Retta and Armbrust 1995, Retta et al. 1995). Specific leaf area values for several crops are from van Keulen (1986). Crops for which measured parameters were lacking were assigned default values and adjusted until biomass amounts during the growing season matched the field experience of NRCS agronomists.

The plant growth parameter data file also contains stress-related parameters from the EPIC crop data file, several of which are given in EPIC as composite numbers, such as the 's-curve' frost damage parameter value for corn of 5.01. This type of definition limits the values that can be input and is non-standard; consequently, values were replaced by two separate parameters; -5.0 °C for the temperature and 0.01 as the frost damage factor.

EPIC classifies crops into 6 different types to account for their different responses to climate, soil nutrient status, and management. The Crop submodel assumes there is no nutrient stress, making some of the crop type classifications redundant. However, these classifications have been retained for compatibility purposes and to allow future Crop submodel versions to incorporate nutrient stress. Two additional crop types, Bi-annuals or Perennials with tuber dormancy type and Perennials with Staged Crown Release and Dormancy type, were added to account for growth habits not modeled by EPIC (Table 2).

Table 2. Crop types simulated in the WEPS Crop submodel.

Index	Description
1	Warm Season Legume (soybeans, etc.)
2	Cool Season Legume (peas, etc.)
3	Perennial Legume (alfalfa, etc.)
4	Spring Seeded and Warm Season Annuals (cotton, sunflowers, corn, etc.)
5	Cold Season Annuals (winter wheat, winter canola)
6	Perennials (pasture, etc.)
7	Bi-annuals or Perennials with Tuber Dormancy
8	Perennials with Staged Crown Release and Dormancy (Asparagus)

Phenological Development

Phenological development of the crop is based on the accumulation of heat units (HU, also known as growing-degree-days, GDD). The parameter file for the Crop submodel contains for each crop, the total HUs from planting to physiological maturity, the number of days to maturity, and a flag, which can be set to grow the crop using either. When the

flag is set to grow the crop using the number of days to maturity, the monthly average temperatures for the simulation location are used to determine the average number of heat units accumulating from the planting date through the number days to maturity. This heat unit accumulation is then used in place of the HUs to maturity specified in the parameter file. The specific algorithms are described in the Initialization of Plant Growth section. This method does not consider heat unit delay factors and is therefore not recommended for crop types that incorporate them. The parameter file also contains the relative HUs, or heat unit index (HUI), from planting to emergence and then to the start of leaf senescence. The Crop submodel uses similar procedures as EPIC for simulating annual or perennial plants and for winter or summer crops. Annual plants 'grow' from planting to the date when the accumulated HUs equal the potential HUs for the crop. For Cold Season Annuals such as winter wheat, HU accumulation (physiological development) is delayed until vernalization is complete, which is discussed later in this section. Perennial crops maintain their root systems throughout the year, accumulating biomass, which is available for the regrowth of the plant after complete leaf removal, killing or harvesting of the aboveground plant portion, or senescence. Some annual crops can also regrow if leaves are removed in early stages of plant growth. Plants start growing when the average daily air temperature exceeds the base temperature of the plant. Procedures described in the ALMANAC model (Kiniry et al. 1992) for simulating concurrent growth of two plant species (forage mixtures, range grass mixtures, weeds and crops, etc.) or removal of live biomass by grazing have not been incorporated into the Crop submodel at this time.

Heat Unit Index

The heat unit index is calculated daily using Eq. 1 and compared to the input values in the plant growth parameter file. A phenological event such as the beginning of senescence is reached when the calculated value of HUI reaches or exceeds the required HUI.

$$HUI^k = \frac{\sum_{i=1}^k HU^i}{THU_m} \quad [1]$$

where

k = days after planting,

HUI^k = heat unit index for day,

k, I = summation index of days after planting,

HU^i = heat units for day i ($^{\circ}C$), and

THU_m = total heat units required for the plant to reach physiological maturity ($^{\circ}C$).

For any single day, the heat units that accumulate are found by integrating a sinusoidal approximation of the daily temperature from midnight to midnight, between the base and optimum plant growth temperatures. It is assumed that the daily temperature minimum and maximum occur 12 hours apart. θ is the time of day in radians where the sinusoidal air temperature approximation is equal to the threshold temperature. Integration is done from the first crossing of daily temperature to above the threshold line until it passes below the threshold line again. This integration results in the following equation:

$$HU^i = F_{del}^i [f^i(T_{bas}) - f^i(T_{opt})]$$

$$f^i(x) = \begin{cases} 0, & x \geq T_{max}^i \\ T_{mean}^i - x, & x \leq T_{min}^i \\ \frac{(T_{mean}^i - x) \left(\frac{\pi}{2} - \theta^i\right) + T_{range}^i \cos(\theta^i)}{\pi}, & T_{min}^i < x < T_{max}^i \end{cases}$$

$$T_{mean}^i = \frac{T_{max}^i + T_{min}^i}{2}$$

$$T_{range}^i = \frac{T_{max}^i - T_{min}^i}{2}$$

$$\theta^i = \sin^{-1} \left(\frac{x - T_{mean}^i}{T_{range}^i} \right)$$

where

F_{del}^i = a heat unit delay factor on day i ,

T_{max}^i = daily maximum air temperature on day i (°C),

T_{min}^i = daily minimum air temperature on day i (°C),

T_{bas} = base plant growth temperature (°C),

T_{opt} = optimum plant growth temperature (°C),

T_{mean}^i = daily average air temperature on day i (°C), and

T_{range}^i = daily temperature range on day i (°C).

Heat Unit Delay Factor

Some species of Cool Season Legumes and Cold Season Annuals exhibit limited height development and will not begin the reproductive phase of growth until they have experienced cold temperatures for a sufficient period of time, a process known as vernalization. Ritchie (1991) modeled this behavior by discounting the heat units that accumulate prior to vernalization by a heat unit delay factor. This method was adapted to provide delayed phenological development for these crop types.

In Ritchie (1991), the degree of vernalization is directly related to the accumulation of vernalization units, a function of time and cool temperatures. The method also accounts for de-vernalization, which can occur if warming occurs before vernalization is complete. As adapted into the Crop submodel, the amount of vernalization units, which will occur in one day is found using:

$$VU^i = \begin{cases} 1.0, & 0 \leq T_{mean}^i \leq 7 \\ \frac{18 - T_{mean}^i}{11}, & 7 \leq T_{mean}^i \leq 18 \\ -0.5(T_{max}^i - 30), & T_{max}^i > 30 \text{ and } TVU^{i-1} < 10 \\ 0, & \text{all other conditions} \end{cases}$$

where

VU^i = vernalization units for day i , and

TVU^{i-1} = total vernalization units accumulated through day $i-1$, which is found using:

$$TVU^k = \sum_{i=1}^k VU^i \quad [4]$$

where

TVU^k = total vernalization units accumulated through day k , and

i = summation index of days after planting.

No delay is applied during the emergence period. The heat unit delay factor for day k can now be found using:

$$F_{del}^k = \begin{cases} 1, & HUI^{k-1} < HUI_e \\ 1 - K_{vrn}(50 - TVU^k), & HUI^{k-1} \geq HUI_e \end{cases} \quad [5]$$

where

K_{vrn} = a cultivar specific delay factor set as a plant growth parameter, and

HUI_e = heat unit index for emergence plant growth parameter.

For crops that do not have a vernalization delay, K_{vrn} is set to 0.

An initial assumption was made that plant height and root depth would use the same relative increase function. Unlike plant height, however, Cool Season Legumes and Cold Season Annuals develop as much as 50% or their root depth during this fall period (Weaver 1926), while their height development occurs after vernalization. To represent this, a heat unit index for root development with no delay factor applied is found (HUI_{rt}^k). Referring to Eq. 2, this is represented as:

$$HUI_{rt}^k = \frac{\sum_{i=1}^k [f^i(T_{bas}) - f^i(T_{opt})]}{THU_m} \quad [6]$$

where

HUI_{rt}^k = total root development heat units accumulated through day k , and

i = summation index of days after planting.

For Cool Season Legumes, Cold Season Annuals, and Perennials that experience re-growth, this index value may reach values greater than 1.

Initialization of Plant Growth

In WEPS, all plant growth is initiated by a management operation. When this occurs, a flag is set to indicate that a crop or plant is growing and that the plant growth submodel should now be executed. A plant growth initialization flag is also set, so that on the first

entry into the plant growth submodel, internal growth parameters are configured based on the parameter input set.

Seasonal Heat Unit Accumulation

When a crop input record specifies that the number of days to maturity is to be used to grow the crop, the monthly average temperatures for the simulation location are used to determine the number of heat units that would accumulate from the planting date through the number of days to maturity. The monthly average daily minimum and maximum temperature data from the climate location input file are placed in an array paired with the middle day of the month and a cubic spline interpolation (Press et al, 1986) applied to find values for each day of the month over a period of 2 years starting on January 1st. This allows for variable accumulations on crops that grow over the one-year boundary. These daily values are used to find the daily heat units, which are then summed from day of planting to the day of maturity. This sum is used for THU_m , the total heat units required for the plant to reach physiological maturity ($^{\circ}C$). This method does not work for crops whose maturity falls outside the bounds of this two-year interval.

Initial Mass for Emergence

All WEPS crops “grow” from an initial mass specified as an input parameter. If the initial mass is small in relation to the potential shoot mass, such as a seed, only one shoot will grow. If however the initial mass is large in relation to the potential shoot mass, such as a root stock planting, multiple shoots may grow. The number of shoots which will grow is initialized using:

$$N_{sh} = \frac{m_{irs}N_{pl}}{m_{0sh}} \quad [7]$$

where

N_{sh} = number of shoots which are being grown (shoots m^{-2}),

m_{irs} = initial mass for plant growth (mg plant $^{-1}$),

N_{pl} = number of plants which are being grown (plants m^{-2}), and

m_{0sh} = crop specific potential shoot mass (mg shoot $^{-1}$).

The mass that will be released from the initial storage is now found and the number of shoots adjusted if necessary, using:

$$\begin{cases} \left(\begin{array}{l} N'_{sh} = N_{pl} \\ M_{csrt} = m_{0srt}C_{mg2kg}N_{pl} \end{array} \right), & N_{sh} < N_{pl} \\ \left(\begin{array}{l} N'_{sh} = N_{mxsh}N_{pl} \\ M_{csrt} = m_{0sh}C_{mg2kg}N'_{sh} \end{array} \right), & N_{sh} > N_{mxsh}N_{pl} \\ \left(\begin{array}{l} N'_{sh} = N_{pl} \\ M_{csrt} = m_{0srt}C_{mg2kg}N_{pl} \end{array} \right), & else \end{cases} \quad [8]$$

where

N'_{sh} = adjusted number of shoots being grown (shoots m^{-2}),

M_{csrt} = total mass released from storage root biomass to grow shoots in the period from beginning to completion of emergence heat units (kg m^{-2}),

m_{0srt} = initial mass of storage root plant growth parameter (mg plant^{-1}),
 C_{mg2kg} = conversion from milligrams to kilograms ($10^{-6} \text{ kg mg}^{-1}$), and
 N_{mxsh} = maximum number of shoots per plant, which is a plant growth parameter (shoots plant^{-1}).

Initial Root Depth

The initial root depth is set to be equal to the crop specific initial growing depth parameter. Any planting depth set by the management operation is ignored, in order to prevent the use of a planting depth which would be too deep to allow the shoot to emerge. This was done to ensure that the shoot would always emerge within the WEPS model. It is assumed that the farmer would not intentionally make this mistake. Since it is not a goal of WEPS to simulate such conditions, it was determined best to not allow a WEPS user to accidentally or otherwise specify such a planting condition through the management operation. The initial storage root mass is also placed into the soil layer that intersects this initial root depth.

Emergence

Emergence is complete when the HUI equals the heat unit index for emergence (HUI_e) plant growth parameter. The Crop submodel does not account for effects of soil temperature, soil water, soil crusting, soil strength, seeding depth, soil removal, or deposition caused by wind erosion, which can influence germination, seedling emergence, survival, and growth. Emergence is modeled using a process of shoot growth, which is also used to model plant regrowth.

Shoot Growth

The process of shoot growth is modeled as the conversion of a specified amount of mass from the storage root, into a shoot consisting of fibrous root, stem, and leaf mass. When the mass of storage root available for shoot growth is less than the specified amount, the shoot created is smaller. When the mass of storage root available for shoot growth is greater than the specified mass, multiple shoots can be created or shoot growth can be initiated more frequently, depending on the plant type. Shoot elongation parameters are tuned so that the same shoot growth is used for initial plant growth from seed, where mass is usually much less than the species characteristic amount of storage mass released for regrowth from root storage. Regrowth from root storage only allocates root mass if the existing fibrous root mass of the plant is less than the mass of the shoot being grown. All shoot growth uses HUI_e to set the time required to go from shoot growth initiation to shoot growth completion. For germination from seed, initialization of a transplant placed in the field, or regrowth after complete defoliation, the heat unit index for the beginning of shoot growth (HUI_{sb}) is set to 0 and the heat unit index for the completion of shoot growth (HUI_{se}) is set to HUI_e . For spring shoot growth of winter annuals from crown storage, HUI_{sb} is set to the HUI on the day when all conditions for spring growth have been met, and $HUI_{se} = HUI_{sb} + HUI_e$.

The total mass released from storage root biomass in the period from beginning to completion of emergence heat units to grow shoots (M_{csrt} , kg m^{-2}) is set outside of the shoot growth routines. The methods vary depending on whether it is initial growth from seed, or some type of re-growth (see Re-growth Initiation Logic section). From this

value, the total mass to be used for complete growth of a single shoot (m_{csrt} , mg shoot⁻¹) is found using:

$$m_{csrt} = \frac{M_{csrt}}{N_{sh} C_{mg2kg}} \quad [9]$$

This storage mass is partially consumed to produce the energy required for growth, with the remaining mass becoming the shoot and root growth. Shoot and root growth are divided using:

$$\begin{aligned} m_{csh} &= m_{csrt} E_{cs} (1 - f_{rt}) \\ m_{cfrt} &= m_{csrt} E_{cs} f_{rt} \\ f_{rt} &= \begin{cases} 0.4, & M_{frt} \leq M_{sh} \\ 0, & M_{frt} > M_{sh} \end{cases} \end{aligned} \quad [10]$$

where

m_{csh} = single shoot mass grown when shoot growth is complete (mg shoot⁻¹),

m_{cfrt} = single shoot fibrous root mass grown when shoot growth is complete (mg shoot⁻¹),

E_{cs} = efficiency of conversion from storage mass to shoot mass (set to 0.7),

f_{rt} = fraction of mass that is allocated to fibrous root mass (set to 0.4),

M_{frt} = present mass of fibrous root (kg m⁻²) summed from the fibrous root mass by layer,
and

M_{sh} = present mass of shoots (kg m⁻²).

The addition of shoot and root mass occurs as an exponential function of the heat unit accumulation from growth initiation to completion of shoot growth. The mass increment added to the shoot and roots on any day is:

$$\begin{aligned} \Delta m_{sh} &= m_{csh} (f_{esi}^k - f_{esi}^{k-1}) \\ \Delta m_{frt} &= m_{cfrt} (f_{esi}^k - f_{esi}^{k-1}) \end{aligned} \quad [11]$$

where

Δm_{sh} = daily shoot mass increment (mg shoot⁻¹),

Δm_{frt} = daily fibrous root mass increment (mg shoot⁻¹),

f_{esi}^k = exponential shoot index for today, and

f_{esi}^{k-1} = exponential shoot index for yesterday.

The exponential function of heat unit accumulation is defined as:

$$\begin{aligned}
 f_{esi}^k &= \frac{e^{(p_s f_{si}^k)} - 1}{e^{(p_s)} - 1} \\
 f_{esi}^{k-1} &= \frac{e^{(p_s f_{si}^{k-1})} - 1}{e^{(p_s)} - 1} \\
 f_{si}^k &= \min\left(1, \frac{HUI^k - HUI_{sb}}{HUI_{se} - HUI_{sb}}\right) \\
 f_{si}^{k-1} &= \min\left(1, \frac{HUI^{k-1} - HUI_{sb}}{HUI_{se} - HUI_{sb}}\right)
 \end{aligned} \tag{12}$$

where

p_s = exponent parameter for the shoot index function (set to 2.0),

f_{si}^k = shoot index for today, and

f_{si}^{k-1} = shoot index for yesterday.

The increment of storage biomass needed for this day of shoot growth is found using:

$$\Delta m_{srt} = \frac{\Delta m_{sh} + \Delta m_{f_{rt}}}{E_{cs}} \tag{13}$$

where

Δm_{srt} = incremental amount of storage biomass required to grow the shoot today (mg shoot⁻¹).

The present amount of storage mass available to grow the shoot (m_{srt} , mg shoot⁻¹) is found:

$$m_{srt} = \frac{M_{srt}}{N_{sh} C_{mg2kg}} \tag{14}$$

where

M_{srt} = present mass of storage root available (kg m⁻²) summed from the storage root by layer.

If the storage amount needed is greater than the storage amount available, the shoot and root growth increments are adjusted:

$$f_{mr} = \begin{cases} \frac{m_{srt}}{\Delta m_{srt}}, & \Delta m_{srt} > m_{srt} \\ 1, & \Delta m_{srt} \leq m_{srt} \end{cases} \tag{15}$$

$$\begin{aligned}
 \Delta m'_{sh} &= \Delta m_{sh} f_{mr} \\
 \Delta m'_{f_{rt}} &= \Delta m_{f_{rt}} f_{mr} \\
 \Delta m'_{srt} &= \Delta m_{srt} f_{mr}
 \end{aligned}$$

where

f_{mr} = mass reduction factor,

$\Delta m'_{sh}$ = adjusted daily shoot mass increment (mg shoot⁻¹),

$\Delta m'_{frr}$ = adjusted daily fibrous root mass increment (mg shoot⁻¹), and

$\Delta m'_{srt}$ = adjusted incremental amount of storage biomass required to grow the shoot today (mg shoot⁻¹).

Shoot extension is considered to occur at the same rate as shoot mass increase. The shoot length when shoot growth is complete is used as a scaling factor. The shoot length at the end of yesterday is found using:

$$l_{ysh} = l_{csh} \left[\frac{\left(\frac{M_{sh}}{C_{mg2kg} N_{sh}} \right)}{m_{csh}} \right] \quad [16]$$

where

l_{ysh} = length of the shoot at the end of yesterday (m), and

l_{csh} = length of the shoot when shoot growth is complete (m).

Similarly, the shoot length at the end of today is found by adding the daily incremental shoot mass to the previous day shoot mass:

$$l_{sh} = l_{csh} \left[\frac{\left(\frac{M_{sh}}{C_{mg2kg} N_{sh}} \right) + \Delta m'_{sh}}{m_{csh}} \right] \quad [17]$$

where

l_{sh} = length of the shoot at the end of today (m).

The length of the shoot when shoot growth is complete is found using:

$$l_{csh} = \sqrt{\frac{a_{cst}}{r_{stal}}} \quad [18]$$

where

a_{cst} = shoot stem area when growth is complete (m² shoot⁻¹), and

r_{stal} = ratio of shoot diameter to length.

The shoot stem area when shoot growth completes is based on the plant stem area index (equation 68), using the shoot stem mass and plant population to find the stem area per shoot.:

$$a_{cst} = \sigma_a \left(m_{cst} C_{mg2kg} \left(\frac{N_{sh}}{N_{pl}} \right) \right)^{\sigma_b} \left(\frac{N_{pl}}{N_{sh}} \right) \quad [19]$$

where

σ_a and σ_b = coefficients relating plant stem area in square meters to plant stem mass in kilograms,

m_{cst} = shoot stem mass grown when shoot growth is complete (mg shoot⁻¹), and

N_{pl} = number of plants which are being grown per square meter (plants m⁻²).

The shoot stem mass grown when shoot growth is complete is found using:

$$m_{cst} = \frac{m_{csh}}{r_{lf2st} + 1} \quad [20]$$

where

r_{lf2st} = ratio of shoot leaf mass to shoot stem mass.

Shoot mass increments for the day are allocated between stem mass and leaf mass:

$$\begin{aligned} \Delta m_{st} &= \frac{\Delta m'_{sh}}{r_{lf2st} + 1} \\ \Delta m_{lf} &= \frac{\Delta m'_{sh} r_{lf2st}}{r_{lf2st} + 1} \end{aligned} \quad [21]$$

where

Δm_{st} = daily stem mass increment (mg shoot⁻¹), and

Δm_{lf} = daily leaf mass increment (mg shoot⁻¹).

Stem mass increments for the day are allocated between above ground and below ground mass using:

$$\begin{aligned} &\left(\begin{array}{l} \Delta m_{agst} = 0 \\ \Delta m_{bgst} = \Delta m_{st} \end{array} \right), \quad l_{sh} < z_{gp} \\ &\left(\begin{array}{l} \Delta m_{agst} = \Delta m_{st} \\ \Delta m_{bgst} = 0 \end{array} \right), \quad l_{ysh} \geq z_{gp} \\ &\left(\begin{array}{l} \Delta m_{agst} = \Delta m_{st} \left(\frac{l_{sh} - z_{gp}}{l_{sh} - l_{ysh}} \right) \\ \Delta m_{bgst} = \Delta m_{st} \left(\frac{z_{gp} - l_{ysh}}{l_{sh} - l_{ysh}} \right) \end{array} \right), \quad l_{ysh} < z_{gp} \text{ and } l_{sh} \geq z_{gp} \end{aligned} \quad [22]$$

where

Δm_{agst} = daily above ground stem mass increment (mg shoot⁻¹),

Δm_{bgst} = daily below ground stem mass increment (mg shoot⁻¹), and

z_{gp} = location of the shoot growing point (m), where a positive number indicates distance below ground and a negative number distance above ground.

If the length of the shoot when shoot growth is complete (l_{csh}) is ever less than the location of the shoot growing point (z_{gp}) then a warning is generated indicating the shoot will not break the soil surface. This can be caused by either a bad input parameter set or an improperly specified planting date for the crop at this location.

The daily mass increment to shoot growth is now converted to a mass per unit area basis before being adjusted and added to the mass pools that are used to track the state of the plant growth. The daily mass increment becomes:

$$\begin{aligned}\Delta M_{lf} &= \Delta m_{lf} C_{mg2kg} N_{sh} \\ \Delta M_{st} &= \Delta m_{agst} C_{mg2kg} N_{sh} \\ \Delta M_{rp} &= 0\end{aligned}\quad [23]$$

where

ΔM_{lf} = increase in leaf mass (kg m⁻²),

ΔM_{st} = increase in above ground stem mass (kg m⁻²),

ΔM_{rp} = increase in reproductive mass (kg m⁻²), and

ΔM_{rs} = increase in storage root mass (kg m⁻²).

These masses may be adjusted to match an input yield to residue ratio relationship, if that is defined for the crop being grown. That adjustment, which is done for both shoot growth and photosynthetic biomass production, is addressed in the Yield / Residue Ratio Adjustment section. Above ground stem mass and reproductive mass increments are divided between standing and flat pools using:

$$\begin{aligned}\Delta M_{sst} &= \Delta M_{st} f_{std} \\ \Delta M_{fst} &= \Delta M_{st} (1 - f_{std}) \\ \Delta M_{srp} &= \Delta M_{rp} f_{std} \\ \Delta M_{frp} &= \Delta M_{rp} (1 - f_{std}) \\ f_{std} &= \min\left(1, \frac{z_{mxht}}{x_{mxpd}}\right)\end{aligned}\quad [24]$$

where

ΔM_{sst} = increase in standing stem mass (kg m⁻²),

ΔM_{fst} = increase in flat stem mass (kg m⁻²),

ΔM_{srp} = increase in standing reproductive mass (kg m⁻²),

ΔM_{frp} = increase in flat reproductive mass (kg m⁻²),

f_{std} = fraction of mass that is considered to be standing,

z_{mxht} = maximum plant height (m), and

x_{mxd} = maximum plant diameter (m).

A special pool, which is a subset of the plant biomass pools called the shoot mass pool, is used to track shoot growth. This pool is not used in the overall mass balance since the mass is distributed into the other mass pools. Growth is added to the pool using:

$$M'_{sh} = M_{sh} + \Delta m_{sh} C_{mg2kg} N_{sh} \quad [25]$$

where

M_{sh} = shoot mass before growth is added (kg m^{-2}), and

M'_{sh} = shoot mass after growth is added (kg m^{-2}).

The above ground stem and reproductive mass pools are incremented using:

$$\begin{aligned} M'_{sst} &= M_{sst} + \Delta M_{sst} \\ M'_{fst} &= M_{fst} + \Delta M_{fst} \\ M'_{srp} &= M_{srp} + \Delta M_{srp} \\ M'_{frp} &= M_{frp} + \Delta M_{frp} \end{aligned} \quad [26]$$

where

M_{sst} = standing stem mass before growth is added (kg m^{-2}),

M'_{sst} = standing stem mass after shoot growth is added (kg m^{-2}),

M_{fst} = flat stem mass before growth is added (kg m^{-2}),

M'_{fst} = flat stem mass after shoot growth is added (kg m^{-2}),

M_{srp} = standing reproductive mass before growth is added (kg m^{-2}),

M'_{srp} = standing reproductive mass after shoot growth is added (kg m^{-2}),

M_{frp} = flat reproductive mass before growth is added (kg m^{-2}), and

M'_{frp} = flat reproductive mass after shoot growth is added (kg m^{-2}).

All leaf mass from growth is added to the standing leaf mass pool and is considered to be live leaf. The standing leaf mass pool can contain both live leaf and dead leaf mass. The fraction of leaf mass that is alive after adding shoot growth is found using:

$$f'_{ll} = \frac{f_{ll} M_{slf} + \Delta M_{lf}}{M_{slf} + \Delta M_{lf}} \quad [27]$$

where

f_{ll} = fraction of leaf mass that is alive before growth is added,

f'_{ll} = fraction of leaf mass that is alive after shoot growth is added, and

M_{slf} = standing leaf mass before growth is added (kg m^{-2}).

Growth is added to the standing leaf mass using:

$$M'_{slf} = M_{slf} + \Delta M_{lf} \quad [28]$$

where

M'_{slf} = standing leaf mass after shoot growth is added (kg m⁻²).

The plant height, which may also change as a result of shoot growth, is found using:

$$z'_{ht} = \min \left\{ \frac{z_{mxht} + z_{ht}}{2}, \max[z_{ht}, \max(0, (l_{sh} - z_{gp})f_{std})] \right\} \quad [29]$$

where

z_{ht} = plant height before shoot growth is added (m), and

z'_{ht} = plant height after shoot growth is added (m).

All below ground biomass is divided into mass pools that correspond to soil layering. Below ground stems extend from the below ground growing point to the soil surface and when elongation has reached the soil surface, the mass is uniformly distributed. Growth is added to each below ground stem mass pool using:

$$M'_{bgst}{}^i = M_{bgst}{}^i + \Delta m_{bgst} C_{mg2kg} N_{sh} f_{bgst}{}^i \quad [30]$$

where

$M_{bgst}{}^i$ = below ground stem mass in layer i before growth is added (kg m⁻²),

$M'_{bgst}{}^i$ = below ground stem mass in soil layer i after shoot growth is added (kg m⁻²), and

$f_{bgst}{}^i$ = fraction of below ground stem mass growth to be added to soil layer i .

The fraction of stem mass to be added to each soil layer is proportional to how much of the elongation during this time period occurred in each soil layer. The root depth may change depending on whether or not shoot growth is occurring with a seedling or an established plant. This is modeled using:

$$z'_{rt} = \max(z_{rt}, z_{gp} + l_{sh}) \quad [31]$$

where

z_{rt} = root depth before growth has been added (m), and

z'_{rt} = root depth after shoot growth has been added (m).

The fibrous root mass growth is distributed uniformly over the root depth attained after growth has been added each day. When shoot growth is completed over multiple days, the distribution of root mass is higher near the surface and lowest at the final root depth. This method should be revisited to get a proper distribution. With seedlings, the masses involved are small, however with transplants they could be significantly larger. Growth is added to each fibrous root mass pool using:

$$M_{f_{rt}}^i = M_{f_{rt}}^i + \Delta m_{f_{rt}} C_{mg2kg} N_{sh} f_{rt}^i \quad [32]$$

where

$M_{f_{rt}}^i$ = fibrous root mass in soil layer i before growth is added (kg m^{-2}),

$M_{f_{rt}}^i$ = fibrous root mass in soil layer i after shoot growth is added (kg m^{-2}), and

$f_{f_{rt}}^i$ = fraction of fibrous root mass growth to be added to soil layer i .

The fraction of fibrous root mass to be added to each soil layer is proportional to the ratio of the soil layer thickness to the root zone depth. The storage root mass used by shoot growth is removed from the storage root mass pools, starting with the top layer storage root mass pool and reducing each pool to zero mass until the full amount of storage root mass used by shoot growth has been removed from the pools. For each soil layer starting at the soil surface, this is done using:

$$\begin{aligned} M_{srt}^i &= M_{srt}^i - \Delta m_{srt} C_{mg2kg} N_{sh} \\ \left(\begin{array}{l} \Delta m_{srt}' = \frac{-M_{srt}^i}{C_{mg2kg} N_{sh}} \\ M_{srt}^i = 0 \end{array} \right), & \quad M_{srt}^i < 0 \\ \left(\begin{array}{l} \Delta m_{srt}' = 0 \\ M_{srt}^i = M_{srt}^i \end{array} \right), & \quad M_{srt}^i \geq 0 \end{aligned} \quad [33]$$

where

M_{srt}^i = storage root mass in soil layer i before mass used by shoot growth is removed (kg m^{-2}),

M_{srt}^i = trial storage root mass in soil layer i after mass used by shoot growth is removed (kg m^{-2}),

M_{srt}^i = final storage root mass in soil layer i after mass used by shoot growth is removed (kg m^{-2}), and

$\Delta m_{srt}'$ = adjusted storage root mass increment after storage root mass has been removed from this soil layer (mg shoot^{-1}).

Upon completion of shoot growth, the location of the growing point is adjusted to reflect how the plant would re-grow. The growing point is adjusted using:

$$z'_{gp} = -z_{rgp} \quad [34]$$

where

z'_{gp} = adjusted location of the shoot growing point (m), and

z_{rgp} = plant growth parameter for the location of the re-growth point after initial shoot growth is complete (m).

If the value of z_{rgp} is positive, it indicates that re-growth occurs above the soil surface while negative values indicate re-growth from below the soil surface.

Biomass Production

As shoot growth creates live leaf area, plant growth through photosynthetic carbon assimilation begins and continues as long as there is live leaf area to intercept solar radiation or heat unit accumulation reaches maturity. Live leaf area may be reduced at any stage of growth if freezing temperatures occur. The frost damage function from EPIC (Williams et al. 1990a) is adapted as follows: the temperature used for frost damage calculations is the daily minimum temperature of the soil surface layer, to account for the mitigating effect of a snow cover on temperature extremes. The insulating effect of snow on the soil surface temperature is simulated in the Hydrology submodel. The frost damage factor and the corresponding change in live leaf area are written as:

$$\left(\begin{array}{l} f_{fd} = \frac{|T_{dmn}^1|}{|T_{dmn}^1| + e^{(c_{afr} - c_{bfr})|T_{dmn}^1|}} \\ f_{ll}'' = f_{ll}'(1 - f_{fd}) \end{array} \right), \quad T_{dmn}^1 < -2 \quad [35]$$

$$\left(\begin{array}{l} f_{fd} = 0 \\ f_{ll}'' = f_{ll}' \end{array} \right), \quad T_{dmn}^1 \geq -2$$

where

f_{fd} = fraction of live leaf area killed by frost damage,

T_{dmn}^1 = daily minimum temperature of the surface soil layer (°C),

c_{afr} and c_{bfr} = coefficients for the temperature vs. frost damage sigmoid function, and

f_{ll}'' = fraction of leaf mass that is alive after frost damage has occurred.

The coefficients c_{afr} and c_{bfr} for the temperature vs. frost damage sigmoid function are found from plant growth parameters using:

$$c_{bfr} = \frac{\log^{-1}\left(\frac{|T_{fd}^1|}{f_{fd}^1} - |T_{fd}^1|\right) - \log^{-1}\left(\frac{|T_{fd}^2|}{f_{fd}^2} - |T_{fd}^2|\right)}{|T_{fd}^2| - |T_{fd}^1|} \quad [36]$$

$$c_{afr} = \log^{-1}\left(\frac{|T_{fd}^1|}{f_{fd}^1} - |T_{fd}^1|\right) + c_{bfr}|T_{fd}^1|$$

where

T_{fd}^1 = temperature where less frost damage occurs (°C),

f_{fd}^1 = fraction of leaf area which is killed when the daily minimum air temperature equals T_{fd}^1 ,

T_{fd}^2 = temperature where greater frost damage occurs (°C), and

f_{fd}^2 = fraction of leaf area which is killed when the daily minimum air temperature equals T_{fd}^2 .

Widely spaced crop plantings may not completely cover the soil area at plant maturity, making the standard leaf area index calculation less meaningful when determining the

solar radiation utilized by plant leaves. To account for this effect, growth calculations are done on a single plant basis. The leaf area available on a per plant basis is found using:

$$a_{lf} = \left(\frac{M'_{slf}}{N_{pl}} \right) A_{spl} f_{li}'' \quad [37]$$

where

a_{lf} = plant leaf area (m^2 plant⁻¹), and

A_{spl} = specific leaf area index plant growth parameter (m^2 kg⁻¹).

The area of the field occupied by the plant is found using:

$$a_{pl} = \begin{cases} \min(x_{row}, x_{mxpd}) \min\left(\frac{1}{N_{pl}x_{row}}, x_{mxpd}\right), & x_{row} > 0 \\ \min\left(\frac{\pi x_{pd} x_{mxpd}}{4}, \frac{1}{N_{pl}}\right), & x_{row} \leq 0 \end{cases} \quad [38]$$

where

a_{pl} = area of the field occupied by the plant (m^2 plant⁻¹),

x_{row} = spacing between rows of plants (m) with 0 or less indicating broadcast seeding,
and

x_{mxpd} = maximum plant diameter plant growth parameter (m).

The effective leaf area index (r_{elai}) is found using:

$$r_{elai} = \frac{a_{lf}}{a_{pl}} \quad [39]$$

For comparison and reporting purposes, the traditional closed canopy leaf area index (r_{tlai}) is found using:

$$r_{tlai} = a_{lf} N_{pl} \quad [40]$$

As was done in EPIC, shortwave radiation at the top of the canopy is multiplied by 0.5 to estimate the amount of photosynthetically active radiation. The amount of photosynthetically active radiation intercepted by the plant is calculated using the exponential function (Beer's law) for distribution of light within a canopy. The potential biomass produced daily is calculated by multiplying the intercepted light by the radiation use efficiency factor. A value of 0.65 for the extinction coefficient is used in EPIC for all crops. In the Crop submodel, the extinction coefficient is crop dependent (Jones 1992). The photosynthetically active radiation is found using:

$$R_{pa} = 0.5 R_{sw} (1 - e^{-c_{ext} r_{elai}}) \quad [41]$$

where

R_{pa} = photosynthetically active radiation (MJ m⁻²),

R_{sw} = short wave radiation at the top of the plant canopy (MJ m⁻²), and

c_{ext} = canopy light extinction coefficient plant growth parameter.

The potential daily biomass increase from photosynthesis for each plant is found using:

$$\Delta m_{pl} = \frac{a_{pl} E_{ru} R_{pa}}{C_{ha2m2}} \quad [42]$$

where

Δm_{pl} = potential daily biomass increment (kg plant⁻¹),

E_{ru} = radiation use efficiency plant growth parameter ((kg ha⁻¹)(MJ m⁻²)⁻¹), and

C_{ha2m2} = conversion from hectares to square meters (10000 m² ha⁻¹).

The potential daily biomass increment is adjusted to account for the effects of temperature and water stress on plant growth. Temperature stress as adapted from EPIC is found from:

$$f_{ts} = \left[\sin \left(\left(\frac{\pi}{2} \right) \frac{T_{mean} - T_{bas}}{T_{opt} - T_{bas}} \right) \right]^{\frac{1}{4}} \quad [43]$$

where

f_{ts} = temperature stress factor.

The original EPIC equation uses soil temperature while this equation uses air temperature. Soil temperature was not available when this equation was originally adapted. The original EPIC equation also used an exponent of 1 while this equation uses an exponent of 1/4 instead. This was added to reduce the temperature stress around the optimum temperature. In the future, soil temperature from the Hydrology submodel should be used here and the formula revised. The water stress factor is calculated as a ratio of actual to potential transpiration using the soil water content and evaporative demand in the Hydrology submodel. Unlike EPIC, no nutrient stress factors are included in the Crop submodel. The final level of growth stress and adjusted daily biomass increment are found with:

$$\Delta m'_{pl} = \Delta m_{pl} \min(f_{ts}, f_{ws}) \quad [44]$$

where

$\Delta m'_{pl}$ = adjusted daily biomass increment (kg plant⁻¹), and

f_{ws} = water stress factor.

Converting the adjusted daily biomass increment to mass per unit area is done using:

$$\Delta M_{tot} = \Delta m'_{pl} N_{pl} \quad [45]$$

where

ΔM_{tot} = adjusted daily biomass increment (kg m⁻²).

Partitioning of Biomass

Daily produced biomass is partitioned to below ground fibrous root and storage root, above ground standing and flat stems, standing and flat reproductive parts, and standing leaf masses. The fibrous root mass partitioning ratio adapted from EPIC to account for Cool Season Legumes, Cold Season Annuals, and Perennials whose root growth heat unit index can exceed 1 is calculated using:

$$P_{prt} = \max(0.05, (0.4 - 0.2)HUI_{rt}) \quad [46]$$

where

P_{prt} = fibrous root mass partitioning ratio.

The daily increment of fibrous root mass becomes:

$$\Delta M_{prt} = \Delta M_{tot} P_{prt} \quad [47]$$

where

ΔM_{prt} = daily increment of fibrous root mass (kg m⁻²).

The balance of daily converted biomass is allocated to aboveground biomass or storage root, which is subdivided further into leaf, stem, reproductive, and storage root masses. The leaf mass partitioning is calculated using:

$$P_{lf} = A_{lf} + \frac{B_{lf}}{1 + e^{-\frac{HUI - C_{lf}}{D_{lf}}}} \quad [48]$$

where

P_{lf} = leaf mass partitioning ratio, and

A_{lf} , B_{lf} , C_{lf} , D_{lf} = leaf mass partitioning plant growth parameters.

Reproductive mass partitioning is found using:

$$P_{rp} = A_{rp} + \frac{B_{rp}}{1 + e^{-\frac{HUI - C_{rp}}{D_{rp}}}} \quad [49]$$

where

P_{rp} = reproductive mass partitioning ratio, and

$A_{rp}, B_{rp}, C_{rp}, D_{rp}$ = reproductive mass partitioning plant growth parameters.

By definition, the sum of leaf and reproductive partitioning ratios is ≤ 1 and the sum of leaf, stem, and reproductive partitioning ratios are equal to 1, so the stem partitioning ratio is found using:

$$P_{st} = 1 - (P_{lf} + P_{rp}) \quad [50]$$

where

P_{st} = stem mass partitioning ratio.

As configured in the EPIC database, for typical annual field crops, aboveground biomass is partitioned only to leaf and stem masses before the onset of the reproductive phase, and after about 80% of the season has elapsed no biomass is allocated to leaves and stems. The daily increments of leaf, stem and reproductive mass are found using:

$$\begin{aligned} \Delta M_{lf} &= P_{lf}(\Delta M_{tot} - \Delta M_{frrt}) \\ \Delta M_{st} &= P_{st}(\Delta M_{tot} - \Delta M_{frrt}) \\ \Delta M_{rp} &= P_{rp}(\Delta M_{tot} - \Delta M_{frrt}) \end{aligned} \quad [51]$$

where

ΔM_{lf} = daily increment of leaf mass (kg m^{-2}),

ΔM_{st} = daily increment of stem mass (kg m^{-2}), and

ΔM_{rp} = daily increment of reproductive mass (kg m^{-2}).

For all crops that are capable of re-growth after losing all of their leaf mass (alfalfa, forage sorghum, and winter wheat are typical examples), some of the above ground mass partitioning is diverted to the storage root pool. This biomass pool is used for all shoot growth activity, as well as the economic yield for root crops. This diversion amount is specified by the three plant growth parameters: P_{lf2rs} , which is the fraction of the daily leaf mass increment diverted to storage root, P_{st2rs} , which is the fraction of the daily stem mass increment diverted to storage root, and P_{rp2rs} , which is the fraction of the daily reproductive mass increment diverted to storage root. For crops that produce tubers, P_{rp2rs} would be close to or equal to 1.

For Cool Season Legumes and Cold Season Annuals, frost damage may result in no living leaf mass for photosynthetic production of carbon assimilate when growth continues in the spring. For these crops, some additional assimilate biomass produced in the fall is diverted to the storage root pool, enabling shoot growth to create leaf area in the spring. This additional diversion of biomass is done by adjusting the diversion parameters when a freeze hardening process occurs. The method used in the Crop submodel is described by Ritchie (1991) where freeze hardening is a 2 stage process with the freeze hardening index, I_{fh} , going from 0 to 1 during stage 1, and going from 1 to 2 during stage 2. The diversion of assimilate is adjusted from the initial level to complete diversion as the freeze hardening index increases from 0 to 0.5 as follows:

$$\begin{aligned} & \left(\begin{array}{l} P'_{lf2rs} = P_{lf2rs} \\ P'_{st2rs} = P_{st2rs} \\ P'_{rp2rs} = P_{rp2rs} \end{array} \right) I_{fh} = 0 \\ & \left(\begin{array}{l} P'_{lf2rs} = P_{lf2rs} + 2I_{fh}(1 - P_{lf2rs}) \\ P'_{st2rs} = P_{st2rs} + 2I_{fh}(1 - P_{st2rs}) \\ P'_{rp2rs} = P_{rp2rs} + 2I_{fh}(1 - P_{rp2rs}) \end{array} \right) 0 < I_{fh} < 0.5 \\ & \left(\begin{array}{l} P'_{lf2rs} = 1 \\ P'_{st2rs} = 1 \\ P'_{rp2rs} = 1 \end{array} \right) I_{fh} \geq 0.5 \end{aligned} \quad [52]$$

where

P'_{lf2rs} = adjusted fraction of the daily leaf mass increment diverted to storage root,

P'_{st2rs} = adjusted fraction of the daily stem mass increment diverted to storage root, and

P'_{rp2rs} = adjusted fraction of the daily reproductive mass increment diverted to storage root.

For crops that do not produce tubers, the amount of assimilate stored in the storage root is limited to the amount required to grow 5 times the maximum number of shoots per plant. When the storage root reaches this capacity, all three diversion fractions are adjusted to zero.

Using the adjusted fractions of daily mass diversion, the daily increments of leaf, stem, and reproductive mass are adjusted with:

$$\begin{aligned} \Delta M'_{lf} &= \Delta M_{lf}(1 - P'_{lf2rs}) \\ \Delta M'_{st} &= \Delta M_{st}(1 - P'_{st2rs}) \\ \Delta M'_{rp} &= \Delta M_{rp}(1 - P'_{rp2rs}) \end{aligned} \quad [53]$$

where

$\Delta M'_{lf}$ = adjusted daily increment of leaf mass (kg m^{-2}),

$\Delta M'_{st}$ = adjusted daily increment of stem mass (kg m^{-2}), and

$\Delta M'_{rp}$ = adjusted daily increment of reproductive mass (kg m^{-2}).

The daily increment of storage root mass is found using:

$$\Delta M_{rs} = \Delta M_{lf}P'_{lf2rs} + \Delta M_{st}P'_{st2rs} + \Delta M_{rp}P'_{rp2rs} \quad [54]$$

where

ΔM_{rs} = daily increment of storage root mass (kg m⁻²).

Leaf Senescence

Senescence is the process in plants whereby, as plants grow toward maturity, living leaf mass dies and some of the leaf mass withers away, and some of the fibrous root mass dies and decomposes. The plant leaf mass, live leaf fractions, and fibrous root mass are adjusted for these losses before the daily incremental mass increase is added to the plant leaf mass. The senescence factors as adapted from EPIC (Ritchie 1991) are found using:

$$\begin{aligned} f_{frs} &= 0.98 \\ f_{lf} &= (f_{sen})^{0.125} \\ f_{lfw} &= (f_{sen})^{0.0625} \end{aligned} \quad [55]$$

where

f_{frs} = fibrous root mass daily senescence fraction,
 f_{lf} = live leaf mass daily senescence fraction, and
 f_{lfw} = total leaf mass daily senescence fraction.

The daily leaf mass loss from senescence (ΔM_{sen}) is found using:

$$\Delta M_{sen} = (1 - f_{lfw})M'_{slf} \quad [56]$$

The leaf mass and the fraction of live leaf are adjusted using:

$$\begin{aligned} M''_{slf} &= f_{lfw}M'_{slf} \\ f''_{ll} &= \frac{f_{lf}f'_{ll}}{1 + f'_{ll}(f_{lfw} - 1)} \end{aligned} \quad [57]$$

where

f''_{ll} = fraction of leaf mass that is alive after senescence and
 M''_{slf} = standing leaf mass after senescence (kg m⁻²).

Yield / Residue Ratio Adjustment

Yield to residue ratio relationships have been developed by NRCS for crop residue management and are used in the Revised Universal Soil Loss Equation, Version 2 (RUSLE2) (USDA 2013). NRCS requested that the use of these relationships be available for crops grown in WEPS. Use of this approach limits the ability of the model to reflect the full natural range of yield and residue variability caused by the timing of stress events. It also distorts the relationship between total and stem biomass during the growing season, since for many crops yield biomass only appears toward the end of the season. Configuration options are available to override the use of this ratio without modifying the plant growth records.

For most crops, the season total biomass must reach a certain level before any yield is produced. This is expressed in an equation of the form:

$$M_{res} = M_{yld}r_{resyld} + M_{0yld} \quad [58]$$

where

M_{res} = end of season residue mass (kg m^{-2}),

M_{yld} = end of season yield mass (kg m^{-2}),

M_{0yld} = end of season residue mass where yield goes to zero (kg m^{-2}), and

r_{resyld} = slope of the residue vs. yield line.

The daily increments of leaf, stem, reproductive, and storage root mass are adjusted to match the yield to residue ratio specified in the plant growth parameters, if it is defined (non-zero) for the crop being grown and the harvestable yield is some fraction of aboveground reproductive mass or below ground storage root mass. No adjustment is made if the harvestable yield consists of some fraction of leaves only, stems only, or the whole plant.

The expected reproductive or storage root mass increment for this day (ΔM_{rpry}) is found using:

$$\Delta M_{rpry} = \begin{cases} 0, & M_{tot} + \Delta M_{tot} \leq M_{0yld} \\ \frac{\Delta M_{tot} - (M_{0yld} - M_{tot})}{r_{resyld}f_{gr}}, & M_{tot} \leq M_{0yld} \\ \frac{\Delta M_{tot}}{r_{resyld}f_{gr}}, & M_{tot} > M_{0yld} \end{cases} \quad [59]$$

where

ΔM_{tot} = total above ground mass increment for this day (kg m^{-2}),

M_{tot} = total above ground plant mass before the increment is added (kg m^{-2}), and

f_{gr} = fraction of reproductive mass that is harvestable yield at maturity plant growth parameter.

For crops where the harvestable yield is a fraction of the aboveground reproductive mass, the total mass increment for this day is found from:

$$\Delta M_{tot} = \Delta M'_{lf} + \Delta M'_{st} + \Delta M'_{rp} - \Delta M_{sen} \quad [60]$$

and the total above ground plant mass before the increment is added is found using:

$$M_{tot} = \Delta M_{sen} + M'_{sst} + M''_{slf} + M'_{srp} + M'_{fst} + M_{flf} + M'_{frp} \quad [61]$$

where

M_{flf} = flat leaf mass before growth is added (kg m^{-2}).

The daily increments of mass are adjusted to maintain the specified residue to yield ratio using:

$$\begin{aligned} \Delta M''_{rp} &= \Delta M_{rpry} \\ \Delta M_{adt} &= \Delta M'_{lf} + \Delta M'_{st} + \Delta M'_{rp} - \Delta M''_{rp} \\ \left(\begin{array}{l} \Delta M''_{lf} = \Delta M'_{lf} \\ \Delta M''_{st} = \Delta M_{adt} - \Delta M'_{lf} \end{array} \right), & \quad \Delta M_{adt} > \Delta M'_{lf} \\ \left(\begin{array}{l} \Delta M''_{lf} = \Delta M_{adt} \\ \Delta M''_{st} = 0 \end{array} \right), & \quad \Delta M_{adt} \leq \Delta M'_{lf} \end{aligned} \quad [62]$$

where

$\Delta M''_{rp}$ = reproductive mass increment adjusted for residue to yield ratio (kg m⁻²),
 $\Delta M''_{lf}$ = leaf mass increment adjusted for residue to yield ratio (kg m⁻²), and
 $\Delta M''_{st}$ = stem mass increment adjusted for residue to yield ratio (kg m⁻²).

For crops where the harvestable yield is a fraction of the belowground storage root mass, the total mass increment for this day is found from:

$$\Delta M_{tot} = \Delta M'_{lf} + \Delta M'_{st} + \Delta M'_{rp} + \Delta M_{rs} - \Delta M_{sen} \quad [63]$$

and the total above ground plant mass before the increment is added is found using:

$$M_{tot} = M_{rs} + \Delta M_{sen} + M'_{sst} + M''_{slf} + M'_{srp} + M'_{fst} + M_{flf} + M'_{frp} \quad [64]$$

where

M_{rs} = storage root mass before growth is added (kg m⁻²).

The daily increments of mass are adjusted to maintain the specified residue to yield ratio using:

$$\begin{aligned} \Delta M'_{rs} &= \Delta M_{rpry} \\ \Delta M_{adt} &= \Delta M'_{lf} + \Delta M'_{st} + \Delta M'_{rp} + \Delta M_{rs} - \Delta M'_{rs} \\ \left(\begin{array}{l} \Delta M''_{lf} = \Delta M'_{lf} \\ \Delta M''_{rp} = \Delta M'_{rp} \\ \Delta M''_{st} = \Delta M_{adt} - \Delta M'_{lf} - \Delta M'_{rp} \end{array} \right), & \quad \Delta M_{adt} > \Delta M'_{lf} + \Delta M'_{rp} \end{aligned} \quad [65]$$

$$\left(\begin{array}{l} \Delta M''_{lf} = \Delta M'_{lf} \\ \Delta M''_{rp} = \Delta M_{adt} - \Delta M'_{lf} \\ \Delta M''_{st} = 0 \end{array} \right), \quad \begin{cases} \Delta M_{adt} \leq \Delta M'_{lf} + \Delta M'_{rp} \\ \Delta M_{adt} > \Delta M'_{lf} \end{cases}$$

$$\left(\begin{array}{l} \Delta M''_{lf} = \Delta M_{adt} \\ \Delta M''_{rp} = 0 \\ \Delta M''_{st} = 0 \end{array} \right), \quad \Delta M_{adt} \leq \Delta M'_{lf}$$

where

$\Delta M'_{rs}$ = storage root mass increment adjusted for residue to yield ratio (kg m⁻²).

The daily mass increments are added to the mass pools that are used to track the state of the plant. The added leaf mass increases the fraction of leaf mass that is alive as shown by:

$$M'''_{slf} = M''_{slf} + \Delta M''_{lf}$$

$$f'''_{ll} = \frac{f''_{ll} M''_{slf} + \Delta M''_{lf}}{M''_{slf} + \Delta M''_{lf}} \quad [66]$$

where

f'''_{ll} = fraction of leaf mass that is alive after photosynthetic growth is added, and

M'''_{slf} = standing leaf mass after photosynthetic growth is added (kg m⁻²).

Above ground stem mass and reproductive mass increments are divided between standing and flat pools using:

$$M''_{sst} = M'_{sst} + \Delta M''_{st} f'_{std}$$

$$M''_{fst} = M'_{fst} + \Delta M''_{st} (1 - f'_{std})$$

$$M''_{srp} = M'_{srp} + \Delta M''_{rp} f'_{std}$$

$$M''_{frp} = M'_{frp} + \Delta M''_{rp} (1 - f'_{std})$$

$$f'_{std} = \min \left(1, \frac{2z_{mxht}}{x_{mxpd}} \right) \quad [67]$$

where

M''_{sst} = standing stem mass after photosynthetic growth is added (kg m⁻²),

M''_{fst} = flat stem mass after photosynthetic growth is added (kg m⁻²),

M''_{srp} = standing reproductive mass after photosynthetic growth is added (kg m⁻²),

M''_{frp} = flat reproductive mass after photosynthetic growth is added (kg m⁻²), and

f'_{std} = fraction of mass that is considered to be standing for photosynthetic growth.

Stem Area Index and Stem Diameter

Stem area index is the ratio of the profile area (as viewed parallel to the ground surface) of the stem to the area of the ground surface that is populated by the stems. The stem area and stem weight relationship is linear for some crops but nonlinear for other crops (Retta and Armbrust 1995). The stem area index is found using:

$$r_{sai} = N_{pl} \sigma_a \left(\frac{M_{sst}''}{N_{pl}} \right)^{\sigma_b} \quad [68]$$

where

r_{sai} = stem area index.

A fixed stem diameter is one of the input plant growth parameters. The actual plant stem diameter may vary, depending on the growth conditions. For consistency throughout WEPS, when stems are cut, a representative stem diameter that is consistent with the plant height and stem area index is back calculated using:

$$x_{rsd} = \frac{r_{sai}}{N_{sh}' z_{ht}''} \quad [69]$$

where

x_{rsd} = representative stem diameter, and

z_{ht}'' = plant height after photosynthetic growth is added (m).

Plant Height

Plant height is estimated using a 2-parameter sigmoid function of heat units and parameters were obtained using plant height data. The potential daily height increment is found using:

$$\Delta z_{pht} = \min(z_{mxht}, z_{mxht} f_{ht}^i) - \min(z_{mxht}, z_{mxht} f_{ht}^{i-1})$$
$$f_{ht}^i = 0.01 + \frac{1}{1 + e^{\left(\frac{HUI^i - \beta_a}{\beta_b} \right)}} \quad [70]$$

where

Δz_{pht} = potential daily height increment (m), and

f_{ht}^i = plant height function for day i , β_a and β_b are plant height plant growth parameters.

The daily increment of height is found by adjusting the potential height for temperature stress and water stress as in:

$$\Delta z_{ht} = \Delta z_{pht} \min(f_{ts}, f_{ws}) \quad [71]$$

where

Δz_{ht} = stress adjusted daily height increment (m).

The new plant height is calculated using:

$$z''_{ht} = z'_{ht} + \Delta z_{ht} \quad [72]$$

Root Depth

Root depth is found using the same relative increase function as for plant height, modified to use the root depth heat unit accumulation shown in Eq. 6 resulting in:

$$\Delta z_{prt} = z_{mxrt} (f_{rt}^i - f_{rt}^{i-1})$$

$$f_{rt}^i = 0.01 + \frac{1}{1 + e^{\left(\frac{HUI_{rt}^i - \beta_a}{\beta_b}\right)}} \quad [73]$$

where

Δz_{prt} = potential daily root depth increment (m),

z_{mxrt} = maximum root depth (m), and

f_{rt}^i = root depth function for day i .

Rooting depth is not adjusted for temperature and water stress but is limited to the maximum depth of the soil profile. The new root depth is found using:

$$z''_{rt} = \min(z_{mxsd}, z'_{rt} + \Delta z_{prt}) \quad [74]$$

where

z''_{rt} = root depth after photosynthetic growth is added (m), and

z_{mxsd} = maximum depth of the soil profile (m).

Root Mass Distribution

Root mass distribution algorithms in the EPIC source code were difficult to interpret. Therefore, a relationship given by Jones et al. (1991) was used to distribute root mass in each soil layer. Jones et al. (1991) identified three general distribution patterns: Sunflower type - deep uniform root distribution; Corn and Soybean type - more roots toward the surface; Sorghum type - with roots concentrated close to the soil surface. The root distribution pattern type was not included in the plant growth parameter set, and the Corn and Soybean type is used for all crops. At present, root density by depth does not affect water uptake in WEPS. It does affect the amount of root mass that will be brought to the surface by tillage. As implemented, the root mass weighting factor for each soil layer by depth is set using:

$$w_{mrt}^i = \begin{cases} \left(1 - \frac{z_{sd}^i}{\omega_{mxd}}\right)^{\omega_{cg}}, & z_{sd}^i < \omega_{mxd} \\ 0, & z_{sd}^i \geq \omega_{mxd} \end{cases} \quad [75]$$

where

w_{mrt}^i = weighting factor for root mass distribution to soil layer i ,

z_{sd}^i = depth to the middle of layer i (m),

ω_{cg} = distribution type factor (set to 2 for all crops), and

ω_{mxd} = a maximum depth parameter (m), which is set using:

$$\omega_{mxd} = \max(3, z_{mxrt}) \quad [76]$$

Daily fibrous root mass increments are distributed over the current root depth using:

$$M_{frt}^{ni} = M_{frt}^i + \Delta M_{frt} \left(\frac{w_{mrt}^i}{\sigma_{frt}} \right) \quad [77]$$

$$\sigma_{frt} = \sum_{j=1}^{k_{rd}} w_{mrt}^j$$

where

M_{frt}^{ni} = fibrous root mass in soil layer i after photosynthetic growth is added (kg m^{-2}),

σ_{frt} = summation of weighting factors over the root depth, and

k_{rd} = index of the last soil layer where the root depth is greater than the depth to the middle of the layer.

Similarly, daily storage root mass increments are distributed over the upper one third of the current root depth using:

$$M_{srt}^{mi} = M_{srt}^i + \Delta M_{rs} \left(\frac{w_{mrt}^i}{\sigma_{srt}} \right) \quad [78]$$

$$\sigma_{srt} = \sum_{j=1}^{k_{sd}} w_{mrt}^j$$

where

M_{srt}^{mi} = storage root mass in soil layer i after photosynthetic growth is added (kg m^{-2}),

σ_{srt} = summation of weighting factors over the one third the root depth, and

k_{sd} = index of the last soil layer where one third the root depth is greater than the depth to the middle of the layer.

Harvestable Yield Fraction

The fraction of the reproductive mass, which is harvestable yield is removed at harvest and any remaining reproductive mass is left in the field as residue. For some crops, the fraction of harvestable reproductive mass yield is considered constant for the entire period of reproductive development as specified in the plant growth parameter. For others, the fraction of reproductive mass that is harvestable yield starts as zero and increases until, at maturity, it equals the fraction of reproductive mass, which is

harvestable yield as specified in the plant growth parameter. This increasing harvestable yield fraction is found using:

$$f_{igr}^k = f_{gr} \left(\frac{1}{1 + e^{\left(\frac{-(HUI^k - 0.64)}{0.05} \right)}} \right) \quad [79]$$

where

f_{igr}^k = increasing harvestable yield fraction on day k .

Re-growth Initiation Logic

If during the growth period a plant loses all of the living leaf area, either due to freeze kill or management actions, a shoot growth process may be triggered, allowing the plant to recover; the EPIC model did not have this functionality. For the purposes of re-growth, crops are divided into 3 classes, crops with tuber dormancy, winter annuals, and all others. The class of crops with tuber dormancy was created to prevent early re-growth of crops which store tuber mass in the storage root for harvest, such as beets, radishes, and potatoes. Future work should focus on extending the plant growth submodel to model the regrowth triggers and growth habits of these Bi-annuals and Perennials when they are commercially grown for seed. In addition to these classes, at least one of the partitioning parameters, P'_{lf2rs} , P'_{st2rs} , or P'_{rp2rs} must be non-zero, indicating that the crop is able to store and use mass for re-growth.

Winter Annuals

Winter annuals often lose all live leaf area during the over-winter period, requiring the re-growth of leaf area in the spring for photosynthetic growth to continue. Four conditions must be true before spring re-growth occurs: complete emergence, complete vernalization, sufficient spring warming, and sufficient de-hardening.

Completion of emergence shoot growth is signaled by the shifting of the plant growth point from the seed depth to the soil surface (see Shoot Growth section). This requires that the re-growth depth plant parameter (Z_{rgp}) for winter annuals have a value less than or equal to zero.

Complete vernalization has occurred if the total vernalization units for the plant (TVU) is greater than or equal to 50.

Spring warming is measured using a count of the number of days where the daily average air temperature exceeds the minimum plant growth temperature. The warm day count is divided in half for every day that the daily average air temperature is below the minimum plant growth temperature. Warming is considered to be sufficient when the warm day count is greater than or equal to 7 days or less as adjusted for the plant vernalization requirement as in:

$$N_{wd} \geq 7 \left(\frac{K_{vrn}}{0.04} \right) \quad [80]$$

where

N_{wd} = number of warm days.

De-hardening occurs when the daily maximum temperature exceeds 10 degrees C (Ritchie 1991). De-hardening is considered to be sufficient when the hardening index (I_{fh}) is less than or equal to 1.

When these four conditions have been met, the heat unit indices for the start and end of shoot growth are set, photosynthetic growth mass diversion fractions (P'_{lf2rs} , P'_{st2rs} , P'_{rp2rs}) are set to 0, and the freeze hardening index (I_{fh}) is set to 0. The heat unit indices set are:

$$HUI_{sb} = HUI^k \quad [81]$$

$$HUI_{se} = HUI^k + HUI_e$$

Summer Annuals, Perennials, and Crops without Tuber Dormancy

Summer Annuals, Perennials, and crops without tuber dormancy may experience complete leaf loss as a result of management operations, freeze damage, or attainment of physiological maturity for the current growth cycle. The methods used for this broad category of crops are, at best, approximations used to capture the gross features of plant re-growth. Six conditions must be true for re-growth to occur: (1) a negative living leaf mass trend, (2) living leaf mass below a threshold, (3) the number of consecutive warm days greater than or equal to seven, (4) complete emergence or a crop with staged crown release and a negative stem mass trend, (5) not yet physiologically mature or a perennial or a crop with staged crown release and day length is increasing, and (6) the re-growth leaf mass will exceed the present living leaf mass. This is expressed logically as:

if $\mu_{lf}^k < 0$ then

$$\left\{ \begin{array}{l} \text{if } f_{lf}^k M_{slf}^k < \frac{0.84 m_{irs} N_{pl} C_{mg2kg} r_{lf2st}}{r_{lf2st} + 1} \text{ then} \\ \left\{ \begin{array}{l} \text{if } N_{wd} \geq 7 \text{ then} \\ \left\{ \begin{array}{l} \text{if } \frac{THU^k}{THU_m} \geq HUI_e \text{ or } \left(\begin{array}{l} I_t = 8 \\ \text{and } \mu_{st}^k < 0 \end{array} \right) \text{ then} \\ \left\{ \begin{array}{l} \text{if } THU^k < THU_m \text{ or } I_t = 3 \text{ or } I_t = 6 \text{ or } \left(\begin{array}{l} I_t = 8 \\ \text{and } t_d^{k-1} < t_d^k \end{array} \right) \text{ then} \\ \left\{ \begin{array}{l} \text{if } f_{lf}^k M_{slf}^k < \Delta M_{plf} \text{ then} \\ \text{regrowth occurs} \end{array} \right. \end{array} \right. \end{array} \right. \end{array} \right. \quad [82]$$

where

μ_{lf}^k = living leaf mass trend at the beginning of the plant growth routines for day k,

THU^k = heat unit accumulation on day k (degree C),

t_d^{k-1} = day length for day k-1 (hours),

t_d^k = day length for day k (hours), and

ΔM_{plf} = potential re-growth leaf mass (kg m⁻²).

The living leaf mass trend is set at the beginning of the plant growth routines to reflect the effects of processes external to the plant growth submodel. It is also set at the end of the plant growth routines to reflect the effects of living leaf mass changes within the plant growth submodel. The living leaf mass trend is set at the beginning of the plant growth routines using:

$$\begin{aligned} \mu_{lf}^k &= \mu_{lf}^{(k-1)+}, & \left\{ \begin{array}{l} \mu_{lf} = 0 \\ \text{or } \left\{ \begin{array}{l} HUI^{k-1} \leq HUI_e \\ \text{and } I_t \neq 8 \end{array} \right. \end{array} \right. \\ \mu_{lf}^k &= \mu_{lf}, & \left\{ \begin{array}{l} \mu_{lf} \neq 0 \\ \text{and } \left\{ \begin{array}{l} HUI^{k-1} > HUI_e \\ \text{or } I_t = 8 \end{array} \right. \end{array} \right. \end{aligned} \quad [83]$$

$$\mu_{lf} = f_{ul}^k M_{slf}^k - f_{ul}^{m(k-1)} M_{slf}^{m(k-1)}$$

where

μ_{lf}^k = living leaf mass trend at the beginning of the plant growth routines for day k , and
 $\mu_{lf}^{(k-1)+}$ = living leaf mass trend at the end of the plant growth routines for day $k-1$.

The living leaf mass trend is set at the end of the plant growth routines using:

$$\begin{aligned} \mu_{lf}^{k+} &= \mu_{lf}^k, & \left\{ \begin{array}{l} \mu_{lf}^+ = 0 \\ \text{or } \left\{ \begin{array}{l} HUI^k \leq HUI_e \\ \text{and } I_t \neq 8 \end{array} \right. \end{array} \right. \\ \mu_{lf}^{k+} &= \mu_{lf}^+, & \left\{ \begin{array}{l} \mu_{lf}^+ \neq 0 \\ \text{and } \left\{ \begin{array}{l} HUI^k > HUI_e \\ \text{or } I_t = 8 \end{array} \right. \end{array} \right. \end{aligned} \quad [84]$$

$$\mu_{lf}^+ = f_{ul}^{mk} M_{slf}^{mk} - f_{ul}^k M_{slf}^k$$

where

μ_{lf}^{k+} = living leaf mass trend at the end of the plant growth routines for day k .

The stem mass is tracked similarly using:

$$\begin{aligned} \mu_{st}^k &= \mu_{st}^{(k-1)+}, & \left\{ \begin{array}{l} \mu_{st} = 0 \\ \text{or } \left\{ \begin{array}{l} HUI^{k-1} \leq HUI_e \\ \text{and } I_t \neq 8 \end{array} \right. \end{array} \right. \\ \mu_{st}^k &= \mu_{st}, & \left\{ \begin{array}{l} \mu_{st} \neq 0 \\ \text{and } \left\{ \begin{array}{l} HUI^{k-1} > HUI_e \\ \text{or } I_t = 8 \end{array} \right. \end{array} \right. \end{aligned} \quad [85]$$

$$\mu_{st} = M_{sst+}^k M_{fst}^k - M_{sst}^{m(k-1)} - M_{sst}^{m(k-1)}$$

where

μ_{st}^k = stem mass trend at the beginning of the plant growth routines for day k , and
 $\mu_{st}^{(k-1)+}$ = stem mass trend at the end of the plant growth routines for day $k-1$.

The stem mass trend is set at the end of the plant growth routines using:

$$\begin{aligned} \mu_{st}^{k+} &= \mu_{st}^k, & \begin{cases} \mu_{st}^+ = 0 \\ \text{or } \begin{cases} HUI^k \leq HUI_e \\ \text{and } I_t \neq 8 \end{cases} \end{cases} \\ \mu_{st}^{k+} &= \mu_{st}^+, & \begin{cases} \mu_{st}^+ \neq 0 \\ \text{and } \begin{cases} HUI^k > HUI_e \\ \text{or } I_t = 8 \end{cases} \end{cases} \end{aligned} \quad [86]$$

$$\mu_{st}^+ = M_{sst}^{mk} + M_{fst}^{mk} - M_{sst}^k - M_{fst}^k$$

where

μ_{st}^{k+} = stem mass trend at the end of the plant growth routines for day k .

The potential re-growth leaf mass is found using:

$$\Delta M_{plf} = \begin{cases} M_{slf} + \frac{0.42 \min(\Delta M_{prs}, M_{csrt}) r_{lf2st}}{r_{lf2st} + 1}, & z_{rgp} > 0 \\ \frac{0.42 \Delta M_{prs} r_{lf2st}}{r_{lf2st} + 1}, & z_{rgp} \leq 0 \end{cases} \quad [87]$$

where

ΔM_{prs} = storage root mass that can be released for re-growth (kg m^{-2}), found by converting the current storage root mass M_{srt} (kg m^{-2}) into the same units as m_{0srt} (mg plant^{-1}) and using it in Eqs. 6 and 7 in the place of m_{0srt} .

On the day that *regrowth occurs* (Eq. 81), the growth clock is reset and the shoot growth heat unit indices are set, any accumulated vernalization is removed, and the shoot growth routines are initialized. The growth clock is reset with:

$$THU^k = 0 \quad [88]$$

The shoot growth heat unit indices are set to:

$$\begin{aligned} HUI_{sb} &= 0 \\ HUI_{se} &= HUI_e \end{aligned} \quad [89]$$

Any accumulated vernalization is removed with:

$$TVU^k = 0 \quad [90]$$

Initialization of the shoot growth routines depends on whether the regrowth is occurring on the plant stem, from a crown, or below the soil surface. For crops re-growing from the soil surface or below, the existing above ground plant mass is moved into a residue pool. Shoot growth routines are initialized using:

$$\left(\begin{array}{l} M_{sh} = M_{sst} + M_{fst} + M_{slf} + M_{bgst} \\ M_{csrt} = \min(\Delta M_{prs}, M_{csrt}) \end{array} \right), \quad z_{rgp} > 0$$

$$\left(\begin{array}{l} M_{sh} = 0 \\ M_{csrt} = \Delta M_{prs} \\ M_{sst} = 0 \\ M_{slf} = 0 \\ M_{srp} = 0 \\ M_{fst} = 0 \\ M_{flf} = 0 \\ M_{frp} = 0 \\ M_{bgst} = 0 \\ f_{igr}^k = 0 \\ z_{ht} = 0 \end{array} \right), \quad z_{rgp} \leq 0 \quad [91]$$

Validation

Materials and methods

Data for soybean, corn, grain sorghum, winter wheat, and oats were used to test the accuracy of the Crop submodel in simulating biomass and organ growth of crop plants. All data contained detailed measurements of plant state variables taken at approximately weekly intervals. Data were obtained from experimental plots located at the Kansas State University Agronomy Farm in Manhattan, Kansas. Details of site and growth conditions for each crop are described elsewhere (Retta and Armbrust 1996) and total biomass and stem biomass data values digitized from the graphs in Retta et al. (1995) were used for comparison. For crops which were grown in multiple years, these were described as data from the crop year during which the crop experienced the least amount of water stress.

Simulations for each crop were made using WEPS. Weather data from the Kansas Automated Weather Network (Kansas State University 2014) station located at the Kansas State University Agronomy Farm was processed into equivalent Cligen and Windgen input files. Management files used the actual planting dates indicated for the crop years exhibiting the least amount of stress. For irrigated corn, the Irrigation Monitor process was specified. Plant growth records from the NRCS database were used without modification for a first set of simulations and then run with residue yield ratio methods disabled.

Results and Discussion

Measured and simulated stem and aboveground masses in grams per plant were compared for all crops (Figures 1 to 5). Field plant population data values for soybeans and wheat are given in Armbrust (1990). The field plant population for sorghum is assumed to be the same as that given in Armbrust and Bilbro (1993). No field plant population is available for corn and oats. When the plant populations from the plant growth records were used to convert simulated values from biomass per unit area to biomass per plant, field biomass values for oats were 2.8 times greater than simulated biomass measurements. One possible explanation is that plant population for the field data was less than the population specified in the plant growth record, resulting in significantly greater biomass per plant. With lower plant populations, oats would tiller resulting in multiple culms, so that the biomass per unit area could have been similar. The graph for oats shows the field data adjusted by this factor (Figure 1).

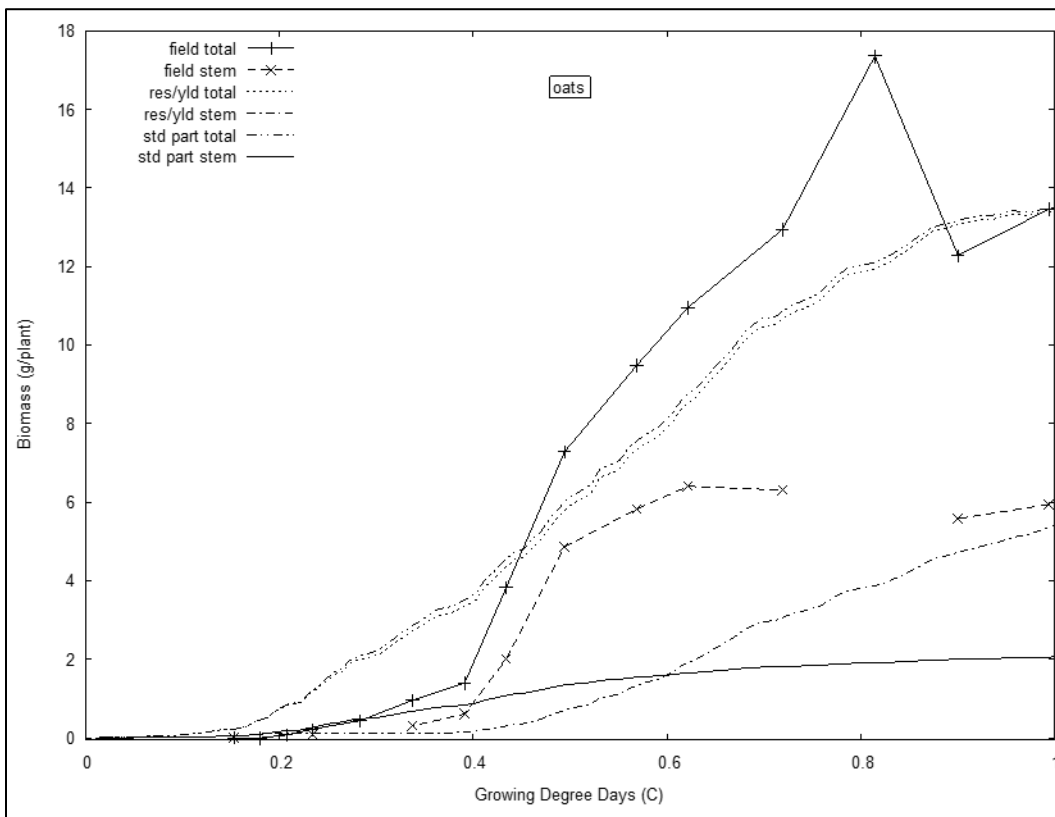


Figure 1. Comparison of measured oats total biomass and stem mass from Retta et al. (1995) (field total, field stem), with WEPS using a residue yield ratio (res/yld total, res/yld stem) and WEPS using standard partitioning (std part total, std part stem).

Part of the data used in the validation tests was also used to derive equations for partitioning aboveground biomass into leaf, stem, and reproductive masses (Retta et al. 1995), and all the data were used to derive the specific leaf and stem area values for each crop. Thus, there is some concern as to the validity of these tests, because an unbiased test of model accuracy can be obtained only by using data that were not used to develop model parameters. However, these tests may be less biased than they appear at first glance. The primary parameter for generating biomass in the model is the biomass

conversion efficiency factor (radiation use efficiency, RUE), which was obtained from the EPIC data base for each crop and not developed using these data. The partitioning and specific area parameters were applied to model-generated aboveground biomass, which was entirely independent of the data, and not on measured biomass. Thus, the bias, if any, may be considered of minor consequence.

In predicting the growth of corn (Figure 2), model performance was excellent with the growth pattern, partitioning, and total biomass all closely matching. Use of the residue yield ratio under predicted the stem biomass until the end of the season. This is to be expected based on the continuous adjustment of stem partitioning in the WEPS Crop submodel to meet the constraints of the required residue yield relationship.

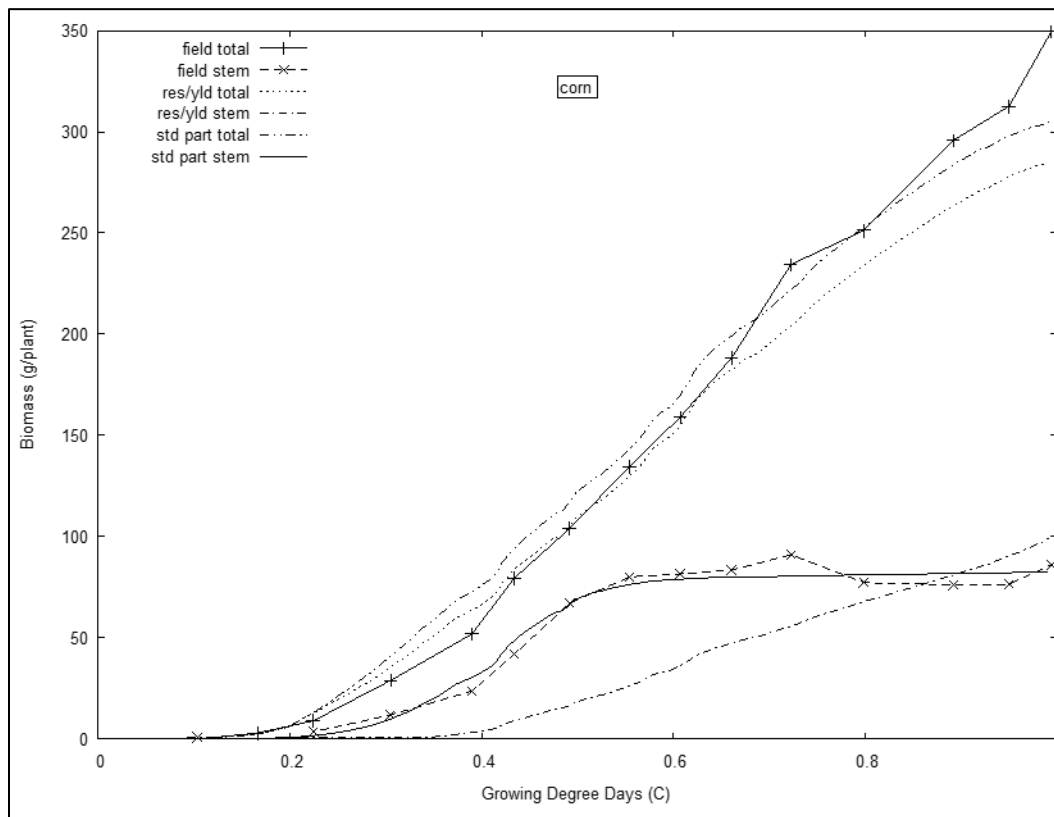


Figure 2. Comparison of measured corn total biomass and stem mass from Retta et al. (1995) (field total, field stem), with WEPS using a residue yield ratio (res/yld total, res/yld stem) and WEPS using standard partitioning (std part total, std part stem).

For oats, it would be possible to compare total biomass only if the plant population were known for the field data. It is clear (Figure 1) that WEPS does not predict the loss of leaf mass during senescence well. Using standard partitioning, it also under predicts the stem biomass in relation to the total biomass. Use of the residue yield ratio did closely predict the final relationship between total biomass and stem biomass, while under predicting stem biomass during the season.

With the growth of sorghum, WEPS did not predict the increase and loss of total biomass, which occurred three times during the growing season (Figure 3). It did

however predict the total biomass at the end of the season. The cause of the decreases and increases is not documented in either Retta and Armbrust (1995) or Retta et al. (1995). With the display of a smooth line through the data, it may be safe to assume that the authors attributed the decreases to sampling variability. Like for oats, WEPS again under-predicted the loss of leaf mass during senescence, under-predicted the stem mass in relation to total biomass using standard partitioning, and closely predicted the final relationship between total biomass and stem biomass when using the residue yield ratio.

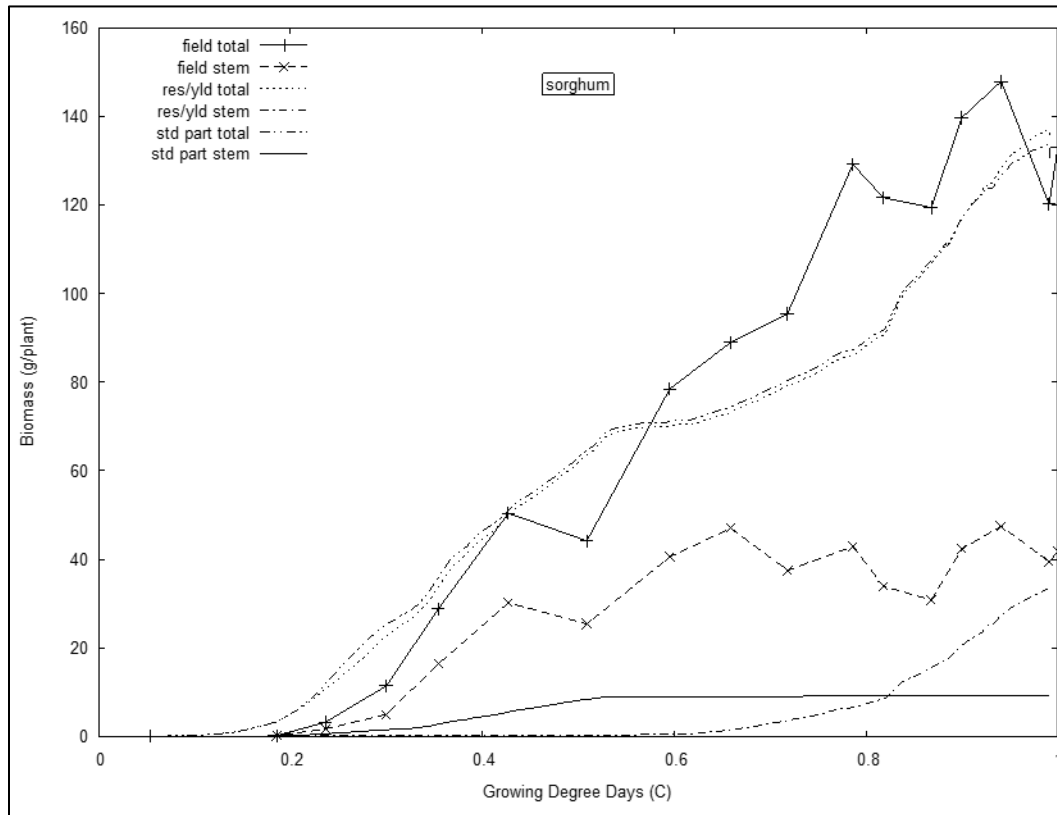


Figure 3. Comparison of measured sorghum total biomass and stem mass from Retta et al. (1995) (field total, field stem), with WEPS using a residue yield ratio (res/yld total, res/yld stem) and WEPS using standard partitioning (std part total, std part stem).

WEPS soybean simulations under-predict the total biomass by 18percent and the stem biomass by 13 percent (Figure 4). While total and stem biomass accumulation during the season follow the correct trend, WEPS does not capture the loss and increase of biomass which occurred during the season. As with sorghum, these decreases may only be due to experimental variability. When using the residue yield ratio, stem biomass is under-predicted with respect to total biomass until the end of the season, when it approaches the proportion indicated by the field data.

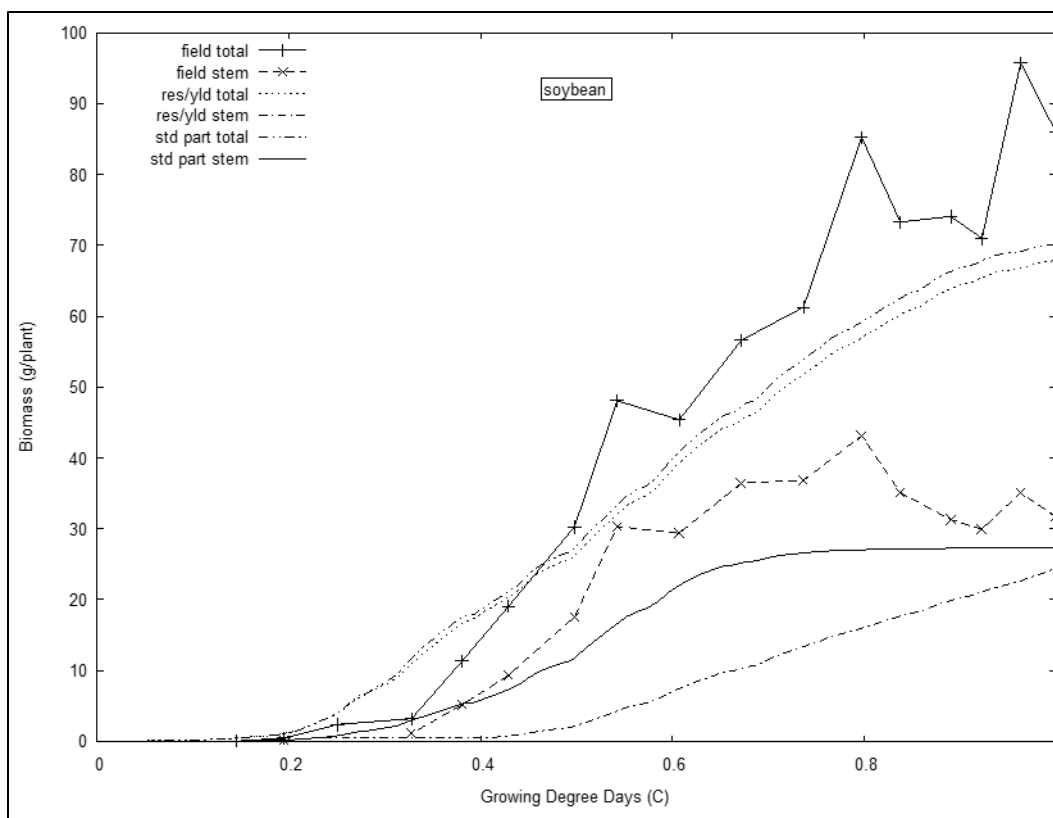


Figure 4. Comparison of measured soybean total biomass and stem mass from Retta et al. (1995) (field total, field stem), with WEPS using a residue yield ratio (res/yld total, res/yld stem) and WEPS using standard partitioning (std part total, std part stem).

WEPS simulations of winter wheat closely follow the total and stem biomass trend for the first half of the growing season (Figure 5). The sharp increase in biomass during the second half of the season is not captured so that the end of season biomass is under-predicted by 50 percent. It does capture the proportion of stem to total biomass.

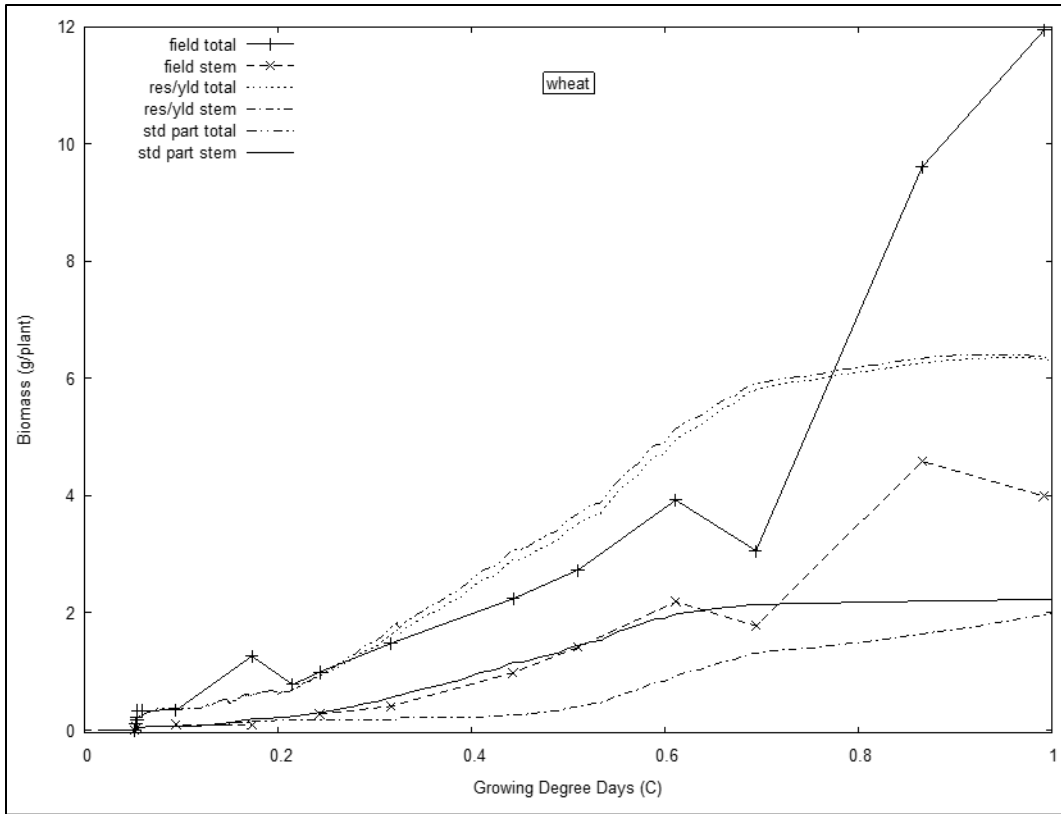


Figure 5. Comparison of measured wheat total biomass and stem mass from Retta et al. (1995) (field total, field stem), with WEPS using a residue yield ratio (res/yld total, res/yld stem) and WEPS using standard partitioning (std part total, std part stem).

Based on our limited testing, the Crop submodel of WEPS does well capturing the growth dynamics and biomass partitioning for some crops. For others, adjusting the input parameters using this and additional field data may improve the results. In general, the model performs better on summer annuals in capturing the season growth trends. Winter annuals are more problematic and may be better modeled with improved predictions of the stages of plant growth and the growth habit associated with each growth period. This work would also be enhanced by the acquisition of additional field data sets at varied locations, under different management practices, and which capture the degree of detail necessary to correctly partition biomass over the entire season, either from the literature or in new field experiments.

References

- Armbrust, D.V. 1990. Rapid measurement of crop canopy cover. *Agronomy Journal*. 82(6):1170-1171.
- Armbrust, D.V. and J.D. Bilbro. 1993. Predicting grain sorghum canopy structure for soil erosion modeling. *Agronomy Journal*. 85(3):664-668
- Hagen, L.J. 1991. A wind erosion prediction system to meet user needs. *Journal of Soil and Water Conservation*. 46:106-111.
- Jones, C.A., W.L. Blad, J.T. Ritchie, et al. 1991. Simulation of root growth. p. 91-123. In: *Modeling plant and soil systems*. J. Hanks and J. R. Ritchie (eds.). Agronomy Monograph Number 31.
- Jones, H.G. 1992. *Plant and microclimate*, 2nd edition. Cambridge, UK: Cambridge University Press.
- Kansas State University. 2014. Department of Agronomy Weather Data Library, <https://mesonet.k-state.edu/data/Historical-Hourly-Weather-Data.zip>. (Accessed August 7, 2020).
- Kiniry, J.R., J.R. Williams, P.W. Gassman, et al. 1992. A general, process-oriented model for two competing species. *Transactions of the ASAE* 35(3):801-810.
- Press, W.H., B.P. Flannery, S.A. Teukolsky, et al. 1986. *Numerical recipes, the art of scientific computing*. Cambridge University Press, Cambridge.
- Retta, A. and D.V. Armbrust. 1995. Estimation of leaf and stem area in the wind erosion prediction system (WEPS). *Agronomy Journal*. 87:93-98.
- Retta, A., D.V. Armbrust, and L.J. Hagen. 1996. Partitioning of biomass in the crop submodel of WEPS (Wind Erosion Prediction System). *Transactions of the American Society of Agricultural Engineers*. 39(1):145-151.
- Ritchie, J.T. 1991. Wheat Phasic development. In: Hanks, J. and Ritchie, J.T. (eds.). *Modeling plant and soil systems*. Agronomy Monograph 31.
- Shaw, R.H., and A.R. Periera. 1982. Aerodynamic roughness of a plant canopy: A numerical experiment. *Agricultural Meteorology*. 26:51-65.
- USDA. 2013. Science Documentation, Revised Universal Soil Loss Equation, Version 2 (RUSLE2) (for the model with release date of May 20, 2008) USDA-Agricultural Research Service. Washington, D.C. Available at: https://www.ars.usda.gov/sp2UserFiles/Place/64080510/RUSLE/RUSLE2_Science_Doc.pdf. (Accessed August 7, 2020).
- van Keulen, H. 1986. Plant data. p. 235-247. In H. van Keulen and J. Wolf (ed.). *Modeling of Agricultural Production: Weather, Soils and Crops*. Pudoc, Wageningen, the Netherlands.

Weaver, J.E., 1926. Root development of field crops. McGraw-Hill Book Company, Inc.

Williams, J.R., C.A. Jones, J.R. Kiniry, et al. 1989. The EPIC crop growth model. Transactions of the American Society of Agricultural Engineers. 32:497-511.

Williams, J.R., C.A. Jones, and P.T. Dyke. 1990a. The EPIC model. In EPIC--Erosion/Productivity Impact Calculator: 1. Model Documentation. eds. A. N. Sharply and J. R. Williams. U. S. Department of Agriculture Technical Bulletin Number 1768.

Williams, J.R., P.T. Dyke, W.W. Fuchs, et al. 1990b. EPIC--Erosion/Productivity Impact Calculator: 2. User Manual. A. N. Sharply and J. R. Williams (Ed.). U. S. Department of Agriculture Technical Bulletin Number 1768.

Table 3. List of symbols of the Crop submodel of WEPS.

Symbol	Definition	Units	Variable
a_{cst}	shoot stem area when growth is complete	$m^2 \text{ shoot}^{-1}$	end_stem_area
a_{lf}	plant leaf area	$m^2 \text{ shoot}^{-1}$	clfarea
A_{lf}	leaf mass partitioning plant growth parameter a	unitless	bc0alf
a_{pl}	area of the field occupied by the plant	$m^2 \text{ shoot}^{-1}$	parea
A_{rp}	reproductive mass partitioning plant growth parameter a	unitless	bc0arp
B_{lf}	leaf mass partitioning plant growth parameter b	unitless	bc0blf
B_{rp}	reproductive mass partitioning plant growth parameter b	unitless	bc0brp
C_{afr}	coefficient a for the temperature vs. frost damage S function	unitless	a_fr
C_{bfr}	coefficient b for the temperature vs. frost damage S function	unitless	b_fr
c_{ext}	canopy light extinction coefficient plant growth parameter	unitless	bc0ck
C_{ha2m2}	conversion from hectares to square meters	$10^4 m^2 ha^{-1}$	hatom2
C_{lf}	leaf mass partitioning plant growth parameter c	unitless	bc0clf
C_{mg2kg}	conversion from milligrams to kilograms	$10^{-6} kg mg^{-1}$	mgtokg
C_{rp}	reproductive mass partitioning plant growth parameter c	unitless	bc0crp
D_{lf}	leaf mass partitioning plant growth parameter d	unitless	bc0dlf
D_{rp}	reproductive mass partitioning plant growth parameter d	unitless	bc0drp
E_{cs}	efficiency of conversion from storage mass to shoot mass	unitless	be_stor
E_{ru}	radiation use efficiency plant growth parameter	$(kg ha^{-1})(MJ m^{-2})^{-1}$	bc0bceff
f_{bgst}^i	fraction of below ground stem mass growth to be added to layer i	unitless	frac_lay

f^{k-1}_{esi}	exponential shoot index for yesterday	unitless	fexp_huiy
f^{k-1}_{si}	shoot index for yesterday	unitless	shoot_huiy
f^k_{esi}	exponential shoot index for today	unitless	fexp_hui
f^k_{si}	shoot index for today	unitless	shoot_hui
f_{ll}	fraction of leaf mass that is alive after shoot growth is added	unitless	bcfliveleaf
f''_{ll}	fraction of leaf mass that is alive after frost damage has occurred	unitless	bcfliveleaf
f'_{ll}	fraction of leaf mass that is alive after senescence	unitless	bcfliveleaf
f'''_{ll}	fraction of leaf mass that is alive after photosynthetic growth is added	unitless	bcfliveleaf
f_{std}	fraction of mass that is considered to be standing for photosynthetic growth	unitless	stem_propor
f^1_{fd}	fraction of leaf area which is killed when the daily minimum air temperature equals $Tlfd$	unitless	cc0fd1
f^2_{fd}	fraction of leaf area which is killed when the daily minimum air temperature equals $Tlfd$	unitless	cc0fd2
f_{fd}	fraction of live leaf area killed by frost damage	unitless	frst
f_{frs}	fibrous root mass daily senescence fraction	unitless	ffr
f_{gr}	fraction of reproductive mass which is harvestable yield at maturity plant growth parameter	unitless	bcgrf
F^i_{del}	heat unit delay factor on day i	unitless	hu_delay
f^i_{frt}	fraction of fibrous root mass growth to be added to layer i	unitless	frac_lay
f^i_{ht}	plant height function for day I	unitless	huf
f^i_{rt}	root depth function for day i	unitless	prd
f^k_{igr}	increasing harvestable yield fraction on day k	unitless	bcgrainf
f_{lf}	live leaf mass daily senescence fraction	unitless	ffa
f_{lfw}	total leaf mass daily senescence fraction	unitless	ffw
f_{ll}	fraction of leaf mass that is alive before growth is added	unitless	bcfliveleaf

f_{mr}	mass reduction factor	unitless	red_mass_rat
f_{rt}	fraction of mass that is allocated to fibrous root mass	unitless	rootf
f_{std}	fraction of mass that is considered to be standing	unitless	stem_propor
f_{ts}	temperature stress factor	unitless	ts
f_{ws}	water stress factor	unitless	bhfwsf
HU^i	heat units for day i	°C	
HUI_e	heat unit index for emergence plant growth parameter	unitless	bc0hue
HU^k	heat unit index for day k	unitless	hui
HU_{rt}^k	heat unit index for root development (no delay factor applied)	unitless	bctrthucum
i	index of days after planting	unitless	bcdayap
I_{fh}	freeze hardening index	unitless	bcthardnx
k	days after planting	unitless	
k_{rd}	index of the last soil layer where the root depth is greater than the depth to the middle of the layer	unitless	irfiber
k_{sd}	index of the last soil layer where one third the root depth is greater than the depth to the middle of the layer	unitless	irstore
K_{vrn}	cultivar specific delay factor set as a plant growth parameter	unitless	bctverndel
l_{csh}	length of the shoot when shoot growth is complete	m	end_shoot_len
l_{sh}	length of the shoot at the end of today	m	bczshoot
l_{ysh}	length of the shoot at the end of yesterday	m	yesterday_len
M_{bgst}^i	below ground stem mass in layer i before growth is added	kg m ⁻²	bcmbgstemz
M'_{frp}	flat reproductive mass after shoot growth is added	kg m ⁻²	bcmflatstore
M''_{frp}	flat reproductive mass after photosynthetic growth is added	kg m ⁻²	bcmflatstore
M'_{fst}	flat stem mass after shoot growth is added	kg m ⁻²	bcmflatstem

M''_{fst}	flat stem mass after photosynthetic growth is added	kg m ⁻²	bcmflatstem
M^i_{bgst}	below ground stem mass in layer i after shoot growth is added	kg m ⁻²	bcmbgstemz
M^i_{frt}	fibrous root mass in layer i after shoot growth is added	kg m ⁻²	bcmrootfiberz
M''^i_{frt}	fibrous root mass in soil layer i after photosynthetic growth is added	kg m ⁻²	bcmrootstorez(i)
M^i_{srt}	trial storage root mass in layer i after mass used by shoot growth is removed	kg m ⁻²	bcmrootstorez
M''^i_{srt}	final storage root mass in layer i after mass used by shoot growth is removed	kg m ⁻²	bcmrootstorez
M''^i_{srt}	storage root mass in soil layer i after photosynthetic growth is added	kg m ⁻²	bcmrootstorez(i)
M'_{slf}	standing leaf mass after shoot growth is added	kg m ⁻²	bcmstandleaf
M''_{slf}	standing leaf mass after senescence	kg m ⁻²	bcmstandleaf
M'''_{slf}	standing leaf mass after photosynthetic growth is added	kg m ⁻²	bcmstandleaf
M'_{srp}	standing reproductive mass after shoot growth is added	kg m ⁻²	bcmstandstore
M''_{srp}	standing reproductive mass after photosynthetic growth is added	kg m ⁻²	bcmstandstore
M'_{sst}	standing stem mass after shoot growth is added	kg m ⁻²	bcmstandstem
M''_{sst}	standing stem mass after photosynthetic growth is added	kg m ⁻²	bcmstandstem
m^{0sh}	crop specific potential shoot mass	mg shoot ⁻¹	bc0shoot
m^{0srt}	initial mass of storage root plant growth parameter	mg plant ⁻¹	bc0storeinit
M^{0yld}	end of season residue mass where yield goes to zero	kg m ⁻²	bcrestid_int
m^{cfrt}	single shoot fibrous root mass grown when shoot growth is complete	mg shoot ⁻¹	end_root_mass
m^{csh}	single shoot mass grown when shoot growth is complete	mg shoot ⁻¹	end_shoot_mass
M^{csrt}	total mass released from storage root biomass to grow shoots in the period	kg m ⁻²	bcmtotshoot

	from beginning to completion of emergence heat units		
m^{cst}	shoot stem mass grown when shoot growth is complete	mg shoot ⁻¹	-
M^{lf}	flat leaf mass before growth is added	kg m ⁻²	bcmflatleaf
M^{rtp}	flat reproductive mass before growth is added	kg m ⁻²	bcmflatstore
M^{prt}	present mass of fibrous root	kg m ⁻²	f_root_sum
M^{fst}	flat stem mass before growth is added	kg m ⁻²	bcmflatstem
M_{frit}^i	fibrous root mass in layer i before growth is added	kg m ⁻²	bcmrootfiberz
m_{irs}	initial mass for plant growth	mg plant ⁻¹	bc0storeinit
M_{srt}^i	storage root mass in layer i before mass used by shoot growth is removed	kg m ⁻²	bcmrootstorez
M_{res}	end of season residue mass	kg m ⁻²	
M_{rs}	storage root mass before growth is added	kg m ⁻²	drswt
M_{sh}	present mass of shoots	kg m ⁻²	bcmshoot
M_{slf}	standing leaf mass before growth is added	kg m ⁻²	bcmstandleaf
M_{srp}	standing reproductive mass before growth is added	kg m ⁻²	bcmstandstore
M_{srt}	present mass of storage root available	kg m ⁻²	avail_mass
M_{sst}	standing stem mass before growth is added	kg m ⁻²	bcmstandstem
M_{tot}	total above ground plant mass before the increment is added	kg m ⁻²	temp_tot
M_{yld}	end of season yield mass	kg m ⁻²	
N'_{sh}	adjusted number of shoots being grown	shoots m ⁻²	bcdstm
N_{mxsh}	maximum number of shoots per plant, plant growth parameter	shoots plant ⁻¹	bcdmaxshoot
N_{pl}	number of plants which are being grown	plants m ⁻²	bcdpop
N_{sh}	number of shoots which are being grown	shoots m ⁻²	bcdstm
N_{wd}	number of warm days	unitless	bctwarmdays
$P'_{l/2rs}$	adjusted fraction of the daily leaf mass increment diverted to storage root	unitless	adjleaf2stor

P'_{rp2rs}	adjusted fraction of the daily reproductive mass increment diverted to storage root	unitless	adjstor2stor
P'_{st2rs}	adjusted fraction of the daily stem mass increment diverted to storage root	unitless	adjstem2stor
P_{frt}	fibrous root mass partitioning ratio	unitless	p_rw
P_{lf}	leaf mass partitioning ratio	unitless	p_lf
P_{lf2rs}	fraction of the daily leaf mass increment diverted to storage root	unitless	bcfleaf2stor
P_{rp}	reproductive mass partitioning ratio	unitless	
P_{rp2rs}	fraction of the daily reproductive mass increment diverted to storage root	unitless	bcfstor2stor
P_{st}	stem mass partitioning ratio	unitless	p_st
P_{st2rs}	fraction of the daily stem mass increment diverted to storage root	unitless	bcfstem2stor
r_{elai}	effective leaf area index	unitless	eff_lai
r_{lf2st}	ratio of shoot leaf to shoot stem mass	mg shoot ⁻¹	bcfleafstem
R_{pa}	photosynthetically active radiation	MJ m ⁻²	apar
r_{resyld}	slope of the residue vs. yield line	unitless	bcyld_coef
r_{sai}	stem area index	unitless	bcrsai
r_{stal}	ratio of shoot diameter to length	unitless	bcfshoot
R_{sw}	short wave radiation at the top of the plant canopy	MJ m ⁻²	bweirr
r_{tlai}	traditional closed canopy leaf area index	unitless	trad_lai
$T^{l dmn}$	daily minimum temperature of the surface soil layer	°C	bhtsmn(1)
$T^{l fd}$	temperature where less frost damage occurs	°C	bc0fd1
$T^{2 fd}$	temperature where greater frost damage occurs	°C	bc0fd2
T_{bas}	base plant growth temperature	°C	bctmin
THU^k	heat unit accumulation on day k	°C	bcthucum
THU_m	total heat units required for the plant to reach physiological maturity	°C	bethum
T_{max}^i	daily maximum air temperature on day i	°C	bwt dmx
T_{mean}^i	daily average air temperature on day i	°C	tmean

T_{min}^i	daily minimum air temperature on day i	°C	bwtadmin
T_{range}^i	daily temperature range on day i	°C	range
t_d^{k-1}	day length for day $k-1$	hours	hrlty
t_d^k	day length for day k	hours	hrlt
T_{opt}	optimum crop/plant growth temperature	°C	bctopt
TVU^{i-1}	total vernalization units accumulated through day $i-1$	unitless	betchillucum
VU^i	vernalization units for day i	unitless	relvern
w_{mrt}^i	weighting factor for root mass distribution to soil layer i	unitless	wfl(i)
x_{mxpd}	maximum plant diameter plant growth parameter	m	bc0diammax
x_{row}	spacing between rows of plants with 0 or less indicating broadcast seeding	m	bcxrow
x_{rsd}	representative stem diameter	mm	bcxstmrep
z'_{gp}	adjusted location of the shoot growing point	m	bczgrowpt
z'_{ht}	plant height after shoot growth is added	m	bczht
z''_{ht}	plant height after photosynthetic growth is added	m	bczht
z'_{rt}	root depth after shoot growth has been added	m	bczrtd
z''_{rt}	root depth after photosynthetic growth is added	m	bczrtd
z_{gp}	location of the shoot growing point	m	bczgrowpt
z_{ht}	plant height before shoot growth is added	m	bczht
z^i_{sd}	depth to the middle of layer i	m	za(i)
z_{mxht}	maximum plant height	m	bczmx
z_{mxrt}	maximum root depth	m	bczmrt
z_{mxsd}	maximum depth of the soil profile	m	-
z_{rgp}	plant growth parameter for the location of the re-growth point after initial shoot growth is complete	m	bczloc_regrow
z_{rt}	root depth before growth has been added	m	bczrtd

β_a	plant height plant growth parameter a	unitless	bc0aht
β_b	plant height plant growth parameter b	unitless	bc0bht
$\Delta m'_{frt}$	adjusted daily fibrous root mass increment	mg shoot ⁻¹	d_root_mass
$\Delta M''_{lf}$	leaf mass increment adjusted for residue to yield ratio	kg m ⁻²	dlfwt
$\Delta M''_{rp}$	reproductive mass increment adjusted for residue to yield ratio	kg m ⁻²	drpwt
$\Delta M'_{rs}$	storage root mass increment adjusted for residue to yield ratio	kg m ⁻²	drswt
$\Delta m'_{sh}$	adjusted daily shoot mass increment	mg shoot ⁻¹	d_shoot_mass
$\Delta m'_{srt}$	the adjusted incremental amount of storage biomass required to grow the shoot today	mg shoot ⁻¹	d_s_root_mass
$\Delta M''_{st}$	stem mass increment adjusted for residue to yield ratio	kg m ⁻²	dstwt
Δm_{agst}	daily above ground stem mass increment	mg shoot ⁻¹	ag_stem
Δm_{bgst}	daily below ground stem mass increment	mg shoot ⁻¹	bg_stem
ΔM_{frp}	increase in flat reproductive mass	kg m ⁻²	
Δm_{frt}	daily fibrous root mass increment	mg shoot ⁻¹	d_root_mass
ΔM_{frt}	daily increment of fibrous root mass	kg m ⁻²	drfwt
ΔM_{fst}	increase in flat stem mass	kg m ⁻²	flat_stem
Δm_{lf}	daily leaf mass increment	mg shoot ⁻¹	d_leaf_mass
ΔM_{lf}	increase in leaf mass	kg m ⁻²	dlfwt
ΔM_{lf}	daily increment of leaf mass	kg m ⁻²	dlfwt
Δm_{pl}	potential daily biomass increment	kg plant ⁻¹	pddm
ΔM_{plf}	potential re-growth leaf mass	kg m ⁻²	pot_leaf_mass
ΔM_{prs}	storage root mass which can be released for re-growth	kg m ⁻²	root_store_rel
ΔM_{rp}	daily increment of reproductive mass	kg m ⁻²	drpwt
ΔM_{rpry}	expected reproductive or storage root mass increment for this day	unitless	store_mass
ΔM_{rs}	daily increment of storage root mass	kg m ⁻²	drswt
ΔM_{sen}	daily leaf mass loss from senescence	unitless	lost_mass

Δm_{sh}	daily shoot mass increment	mg shoot ⁻¹	d_shoot_mass
ΔM_{srp}	increase in standing reproductive mass	kg m ⁻²	
Δm_{srt}	incremental amount of storage biomass required to grow the shoot today	mg shoot ⁻¹	d_s_root_mass
ΔM_{sst}	increase in standing stem mass	kg m ⁻²	stand_stem
Δm_{st}	daily stem mass increment	mg shoot ⁻¹	d_stem_mass
ΔM_{st}	daily increment of stem mass	kg m ⁻²	dstwt
ΔM_{tot}	adjusted daily biomass increment	kg m ⁻²	ddm
ΔM_{tot}	total above ground mass increment for this day	kg m ⁻²	ddm_res_yld
Δz_{ht}	stess adjusted daily height increment	m	dht
Δz_{pht}	potential daily height increment	m	pdht
Δz_{prt}	potential daily root depth increment	m	
$\mu^{(k-1)+}_{lf}$	living leaf mass trend at the end of the plant growth routines for day $k-1$	unitless	bcleafareatrend
$\mu^{(k-1)+}_{st}$	stem mass trend at the end of the plant growth routines for day $k-1$	unitless	bcstemmasstrend
μ^{k+}_{lf}	living leaf mass trend at the end of the plant growth routines for day k	unitless	bcleafareatrend
μ^{k+}_{st}	stem mass trend at the end of the plant growth routines for day k	unitless	bcstemmasstrend
μ^k_{lf}	living leaf mass trend at the beginning of the plant growth routines for day k	unitless	bcleafareatrend
μ^k_{st}	stem mass trend at the beginning of the plant growth routines for day k	unitless	bcstemmasstrend
σ_a	coefficient a relating plant stem area to plant stem mass	unitless	bc0ssa
σ_b	coefficient b relating plant stem area to plant stem mass	unitless	bc0ssb
σ_{rt}	summation of weighting factors over the root depth	unitless	wffiber
σ_{srt}	summation of weighting factors over the one third the root depth	unitless	wfstore
ω_{cg}	distribution type factor (set to 2 for all crops)	unitless	wcg
ω_{mxd}	maximum depth parameter	m	wmaxd

Residue Decomposition Submodel of WEPS

Contributors:

S.J. van Donk
J.L. Steiner
H.H. Schomberg
F.A. Fox

Abstract

The Residue Decomposition submodel of the Wind Erosion Prediction System (WEPS) simulates the decrease in crop residue biomass due to microbial activity. The decomposition process is modeled as a first-order reaction with temperature and moisture as driving variables. Decomposition is a function of decomposition days; under optimum temperature and moisture conditions, one decomposition day per day is accumulated, but only a fraction of a decomposition day is accumulated if less than optimum conditions occur. Biomass remaining after harvest is partitioned between standing, flat, and buried position pools. Residue from different crops may have different properties and decompose at different rates. Therefore, each event that creates residue places it into one of five unique age pools. After harvest, any residue biomass remaining from a previous crop is moved down one age pool and residue from the just harvested crop is moved into the first age pool. The fifth age pool accumulates remaining biomass from the oldest crop(s). Standing residue losses not only result from microbial activity, but also from physical forces. Transfer of crop residue from the standing biomass position pool will reduce stem population and standing biomass. A daily estimate of the standing stem population is required to evaluate the vertical stem area that the wind encounters. This area is quantified by the stem area index, which is calculated from standing stem number, stem height, and stem diameter. It affects aerodynamic resistance and, ultimately, wind erosion. Stems start to fall after reaching a threshold of cumulative decomposition days after harvest. Both standing and flat crop residue provide cover to the soil surface, protecting it against wind erosion. Soil cover from flat residue is calculated from flat residue mass. Tillage may alter the amount of residue in the different position pools. The WEPS Residue Decomposition model was compared and contrasted with other residue decomposition models and five simulation scenarios were created to illustrate its functionality. The Residue Decomposition submodel of WEPS is the only model that simulates the residue decomposition as it affects erodibility for improved simulation of wind erosion.

Introduction

Land used for production agriculture can be damaged by erosion of soil by wind if it is managed poorly. Post-harvest crop residue reduces wind erosion potential, but its effect is dependent on the type and amount of residue and its orientation to the soil surface (Siddoway et al. 1965, Hagen and Armbrust 1994, Hagen 1996). While agricultural management operations often greatly affect the amount and orientation of crop residue remaining on the surface, natural processes influenced by climate also slowly and continually cause stems to fall and residue to decompose (Steiner et al. 1994, Steiner et

al. 1999), resulting in a slow and continual decrease in the level of wind erosion protection.

The Residue Decomposition submodel of the Wind Erosion Prediction System (WEPS) simulates the effect of natural processes on changes in crop residue and is described below. WEPS simulates the wind erosion potential of an agricultural field by tracking the state of that field as modified over time, using submodels for management operations, hydrology, crop growth, soil properties, and residue decomposition. Daily erosion amounts are then calculated from that daily state of the field. The decomposition of residue varies significantly with climate and must be considered to evaluate the erosion potential based on location and management practices.

Much of the data used to develop and calibrate the WEPS crop Residue Decomposition submodel came from Steiner et al. (1994), Schomberg and Steiner (1997), and Steiner et al. (1999). Steiner et al. (1994) monitored standing stem persistence of four small grain crops (winter wheat, spring wheat, winter barley, and spring oat) for 14 months at the Conservation and Production Research Laboratory in Bushland, Texas. They developed an equation to predict standing stem number over time, based on precipitation and temperature. Steiner et al. (1999) monitored crop residue biomass for the same four small grain crops at the same location in order to quantify crop residue decomposition as affected by irrigation, initial residue biomass, and initial N concentration in standing biomass. Schomberg and Steiner (1997) estimated crop residue decomposition coefficients for five crops (alfalfa, corn, grain sorghum, winter wheat, and spring wheat) using substrate-induced respiration.

Model Overview

The crop Residue Decomposition submodel of WEPS simulates the decrease in crop residue biomass. The decomposition process is modeled as a first-order reaction with temperature and moisture as driving variables since these are the principal environmental variables affecting the microbial activity responsible for decomposition. The model assumes decomposition is a function of decomposition days. Under optimum temperature and moisture conditions, one decomposition day is accumulated per day, but only a fraction of a decomposition day is accumulated if conditions are less than optimum. Biomass remaining after harvest is partitioned between standing, flat, and buried residue position pools, and the model calculates belowground biomass (buried and root) decomposition for each soil layer.

Residue from different crops may have different properties and decompose at different rates. Therefore, each event that kills plant biomass places residue into a unique age pool. The model accounts for crop residue from sequential harvests in five separate age pools.

Standing residue biomass losses result not only from microbial activity, but also from physical forces. The transfer of crop residue from the standing biomass pool will reduce both stem population and standing biomass. Stems start to fall after reaching a threshold of cumulative decomposition days since harvest (Steiner et al. 1994). The surface wind is affected by the vertical stem area that the wind encounters. This is quantified by the stem area index (SAI) (Hagen and Armbrust 1994), which is calculated from standing stem number, stem height, and stem diameter. Stem area index decreases proportionally with decreasing standing stem number. The stem area index affects aerodynamic resistance and, ultimately, wind erosion. We assumed that for standing stems in the early stages of

decay, biomass loss from microbial activity has little effect on the external dimensions and therefore SAI (stems fall down before decay results in changes in stem diameter and length). Further research is needed to clarify this assumption.

Both standing and flat crop residue provide cover to the soil surface, thus protecting it against wind erosion. Percent soil cover from standing residue is typically small and is calculated from stem number and stem diameter. Percent soil cover from flat residue is calculated from flat residue mass. Tillage may alter the amount of residue in the different position pools.

Decomposition

The general decomposition equation is a simple first-order rate loss equation (Steiner et al. 1999):

$$M_t = M_0 \exp^{-k CDD} \quad [1]$$

where

M_t = present biomass (kg m^{-2}) in the standing, flat, or buried position pools,

M_0 = initial biomass (kg m^{-2}),

k = a crop-specific rate constant ($\text{kg kg}^{-1} \text{day}^{-1}$), and

CDD = cumulative decomposition days (day), a weighted-time variable calculated from functions of temperature and moisture.

WEPS uses the same k -value for the standing, flat, and buried residue pools. This does not mean, however, that these pools decompose at the same rate; the k -value is only one factor determining the decomposition rate. The other factor is the CDD (Eq. 1): the different pools are exposed to different moisture and temperature conditions that result in different rates of decomposition, as will be discussed later.

For most crops, only stems are left after harvest, but in some situations, residue also includes leaves and reproductive material (e.g., chaff, awns). Stroo et al. (1989) showed that the decomposition rate for reproductive material is closer to that of stems than that of leaves. Thus, we assumed relative decomposition values for stems, reproductive material, and leaves of k , $1.5k$, and $3k$, respectively. Root mass is assumed to decompose at the same rate as stems.

Residue from different crops or applied residue (bedding manure for example) may have different properties and decompose at different rates. Examples of slowly decomposing residue are corn and sorghum ($k = 0.01 \text{ kg kg}^{-1} \text{day}^{-1}$). Alfalfa residue decomposes much faster ($k = 0.05 \text{ kg kg}^{-1} \text{day}^{-1}$, Figure 1). Schomberg and Steiner (1997) and Steiner et al. (1999) present and discuss k -values for a number of crops.

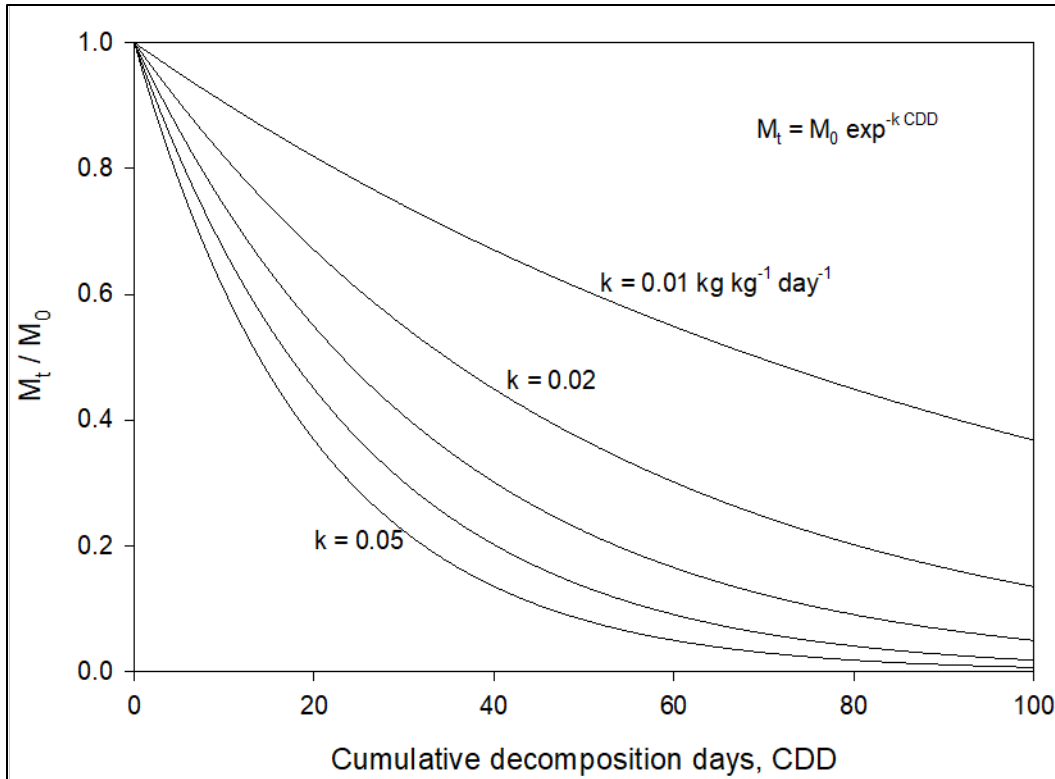


Figure 1. Residue decomposition at five different rates.

Because residue from different crops may decompose at different rates, each event that kills plant biomass (or applies residue) places residue into a unique age pool. The model accounts for crop residue from sequential harvests (or applied residue) in five separate age pools. Biomass from the most recently harvested crop will be in pool one, biomass from the previous crop in pool two, and so on. After harvest, any residue biomass remaining from a previous crop is moved down one pool.

The age pool with the oldest residue (pool five) may include residue from more than one crop if decomposition is very slow. The k -value for pool five will be that of the “newest” of these old crops. Typically, by the time residue moves into the fifth pool, the amount is small enough that combining it with residue from older crops with different decomposition rates will have little effect on total residue mass and cover.

Our experience with a wide variety of management rotations used by the USDA Natural Resources Conservation Service (NRCS) led us to expand the number of age pools from three to five, as some types of management scenarios, and the techniques used to model them, result in multiple residue creation events in a single year, in some cases resulting in most of the residue residing in the final age pool. For some special scenarios in irrigated or more humid areas, where decomposition of residue generated by multiple harvests and weed killing operations in a single year is simulated, increasing the number of age pools beyond five may be necessary to prevent residue in the fifth pool from becoming the dominate amount of residue in the simulation.

The original program designers were concerned with the memory footprint associated with a larger number of age pools. This should not be an issue with modern computer

systems but could be significant as simulations are conducted on a larger spatial scale, e.g. for an entire state, with simulations for a large series of fields instead of just one field. Alternate implementations, using dynamic allocation of age pools when residue is created and consolidation of age pools when residue amounts in pools are small, have been considered but not yet implemented.

To summarize the different pools, the model keeps track of five age pools and three position pools (standing, flat, and buried). Within each of the standing, flat, and buried residue position pools, the model distinguishes between stems, leaves, reproductive, and root material.

Optimum moisture and temperature conditions result in the accumulation of one decomposition day for each day of the simulation. When moisture or temperature limit the rate of decomposition, the minimum of the moisture and temperature functions is used to accumulate a fraction of a decomposition day. Biomass loss is calculated using the numeric form of Eq. 1 as follows:

$$M_t = M_{t-1} (1 - k DD) \quad [2]$$

where

M_{t-1} = biomass (kg m^{-2}) on the previous day, and
 DD = decomposition day:

$$DD = \text{MIN}(TF, MF) \quad [3]$$

where

TF = a temperature function, and
 MF = a moisture function.

Thus, if moisture and temperature are optimum for decomposition on a given day, a k of 0.01, for example, results in a 1% reduction of stem mass on that day. TF and MF range between 0 and 1 and depend on residue placement (standing, flat, or buried). For standing residue, the moisture function is (Steiner et al. 1994):

$$MF_s = P/4 + 0.4 MF_{s,t-1} \quad [4]$$

where

$MF_{s,t-1}$ = moisture function for standing residue on the previous day.

$MF_s = 1$ if the right-hand side of Eq. 4 exceeds 1. The moisture function is based on precipitation P (mm), with 4 mm of precipitation considered to saturate the standing residue. MF_s decreases by 60% each day following a wetting event (Schomberg et al. 1996). After more than 4 dry days in a row, $MF_s = 0$ (Figure 2).

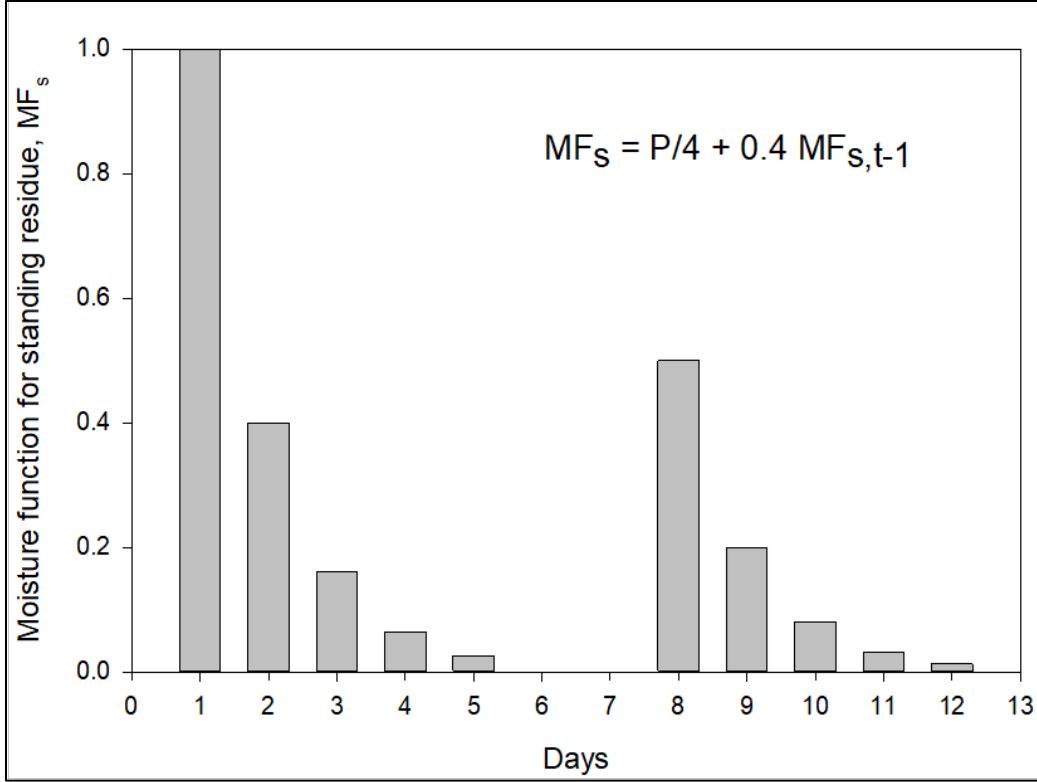


Figure 2. Behavior of the moisture function for standing residue if precipitation were equal to or greater than 4 mm on day 1, equal to 2 mm on day 8, and all other days were dry (after van Donk et al. 2008).

The decomposition of flat residue is influenced by both precipitation and soil moisture at the soil surface. The maximum of either the above estimate of MF_s or a function MF_f that considers the flat residue to be in equilibrium with the soil surface is used. MF_f is calculated from the soil water content at the soil surface at noon, θ_{surf} , and the optimum water content for decomposition. The water content at field capacity of the upper soil layer, $\theta_{fc, 1}$, is considered to be the optimum water content:

$$MF_f = \frac{\theta_{surf}}{\theta_{fc,1}} \quad [5]$$

Water content values are provided by the WEPS Hydrology submodel. If flat leaves are present in the crop pool (as modeled by the WEPS Crop submodel), e.g. as a result of defoliation, they will be decomposed in the same manner as flat residue.

For buried residue, the model contains a moisture function for each soil layer:

$$MF_{b,i} = \frac{\theta_i}{\theta_{fc,i}} \quad [6]$$

where

θ_i = water content of layer i and

$\theta_{fc, i}$ = water content at field capacity of layer i .

The temperature function is calculated similarly to a function describing the influence of temperature on photosynthesis (Taylor and Sexton 1972) and used by Stroo et al. (1989) and Steiner et al. (1999) for residue decomposition:

$$TF = \frac{2(T - T_b)^2(T_o - T_b)^2 - (T - T_b)^4}{(T_o - T_b)^4} \quad [7]$$

where

T = temperature (°C),

T_o = optimum temperature for decomposition (32 °C), and

T_b = a base temperature (0 °C) below which no decomposition occurs (see Figure 3).

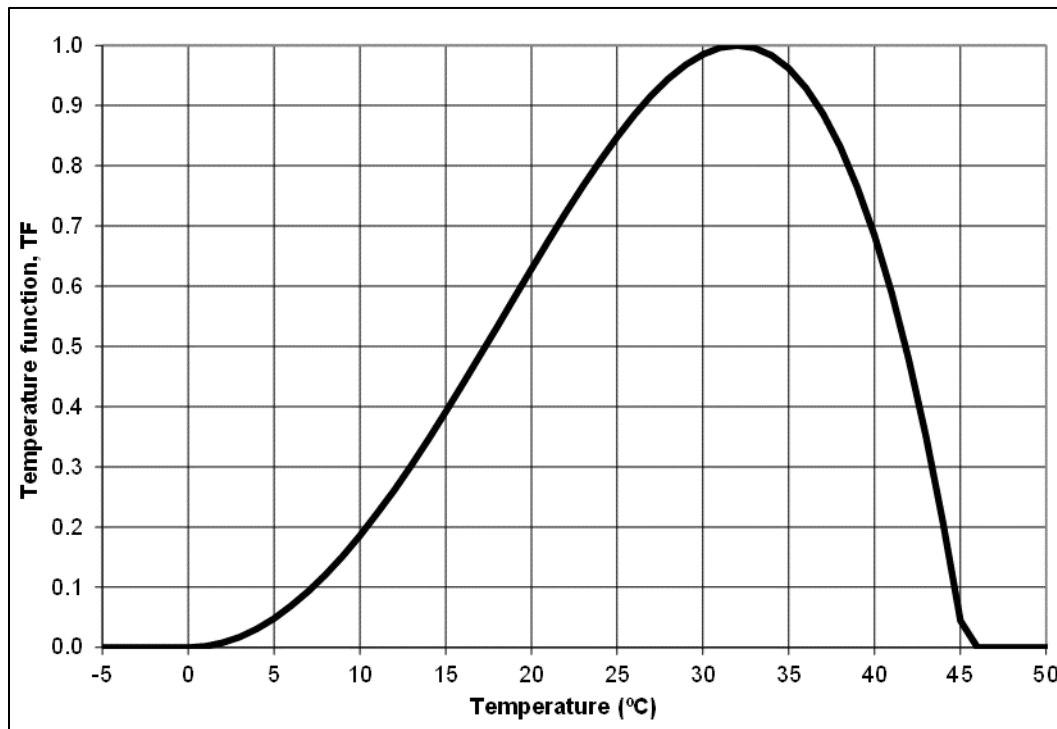


Figure 3. Plot of the temperature function, TF (Equation 7) with $T_b = 0$ °C and $T_o = 32$ °C (after van Donk et al. 2008).

TF is not allowed to become negative. For standing and flat residue, TF is calculated as the average of two TF values: one calculated using daily maximum air temperature and a second using daily minimum air temperature. For belowground residue, the model uses daily average soil temperature by layer.

Decline in Stem Population and Standing Biomass

Standing residue losses due to physical forces such as wind, snow, and gravity are modeled with a stem fall threshold and a stem fall rate. Standing residue losses due to tillage or wheel traffic are modeled with processes in the WEPS Management submodel

which redistribute standing stems to both the flat and buried residue position pools and may decrease the stem fall threshold and increase the stem fall rate of remaining standing stems. A daily estimate of the standing stem population is required to evaluate stem area index and its influence on aerodynamic resistance and, ultimately, wind erosion.

Stems are allowed to fall only after a threshold of cumulative decomposition days since harvest has been reached; for example, a threshold of 20 decomposition days means that standing stalks begin to fall 20 days after harvest if moisture and temperature conditions are optimum for decomposition during these 20 days. If conditions are not optimum, the number of days that stalks remain standing increases. The threshold depends on crop type. Steiner et al. (1994) present and discuss threshold values for several crops.

After reaching the threshold, the change in stem number is calculated similarly to the loss in biomass (Eq. 2):

$$N_t = N_{t-1} [1 - k_{stem} \text{MIN}(TF, MF_s)] \quad [8]$$

where

N_t = number of stems standing on day t (# m⁻²),

N_{t-1} = number of stems standing on the previous day (# m⁻²), and

k_{stem} = a crop-specific rate constant (# #⁻¹ day⁻¹) (Steiner et al. 1994).

For example, under optimum conditions, 10% of all standing stems fall in one day if $k_{stem} = 0.10$. Steiner et al. (1994) present and discuss k_{stem} values for several crops. Falling stems cause standing mass to be transferred to the flat mass pool.

The standing residue provides a vertical area that has a direct influence on wind speed. Stem area index (SAI, m² m⁻²) decreases proportionally with stem number. For the five age pools, SAI is estimated by:

$$SAI = \sum_{i=1}^5 N_i h_i D_i \quad [9]$$

where

h_i = stem height (m) of standing residue in age pool i, and

D_i = stem diameter (m) of standing residue in age pool i (Figure 4).

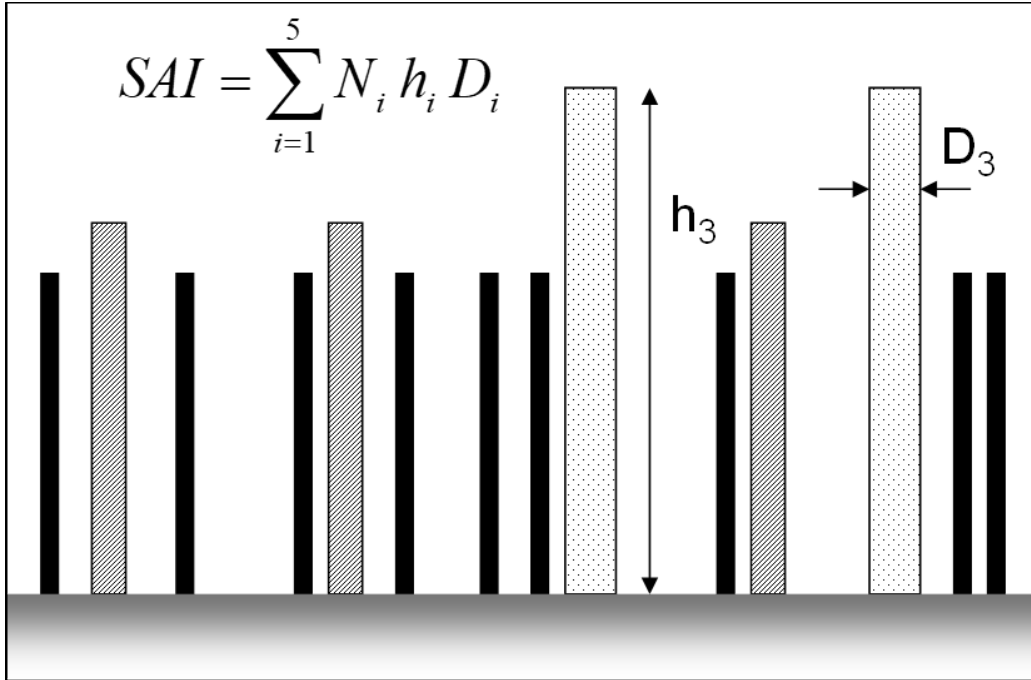


Figure 4. Calculation of stem area index (SAI) from number of stems per m^2 (N), stem height (h), and stem diameter (D) for residue in a maximum of five age pools (only three age pools in this illustration).

Soil Cover

Both standing and flat crop residue provide cover to the soil surface. Soil cover from standing residue is typically small. However, standing residue is important for reducing air velocity near the soil surface, shading the soil surface from light, and protecting the soil surface from slanting rainfall. For the five age pools, soil cover from standing residue is estimated as:

$$C_s = \sum_{i=1}^5 \pi (D_i/2)^2 N_i \quad [10]$$

where

C_s = standing residue cover ($m^2 m^{-2}$) (Figure 5).

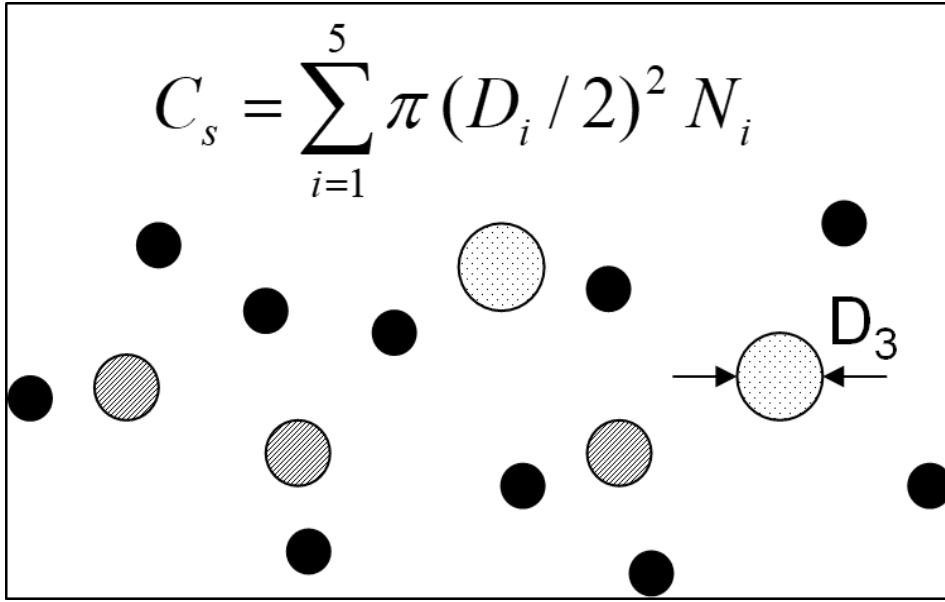


Figure 5. Calculation of standing residue cover (C_s) from stem diameter (D) and number of stems per m^2 (N) for residue in a maximum of five age pools (only three age pools in this illustration).

Soil cover from flat residue mass is predicted by an equation developed by Gregory (1982) and used by Steiner et al. (2000):

$$C_f = 1 - \exp^{-b M_f} \quad [11]$$

where

C_f = flat residue cover ($m^2 m^{-2}$),

b = a crop-specific coefficient ($m^2 kg^{-1}$), and

M_f = flat residue mass ($kg m^{-2}$) (Figure 6).

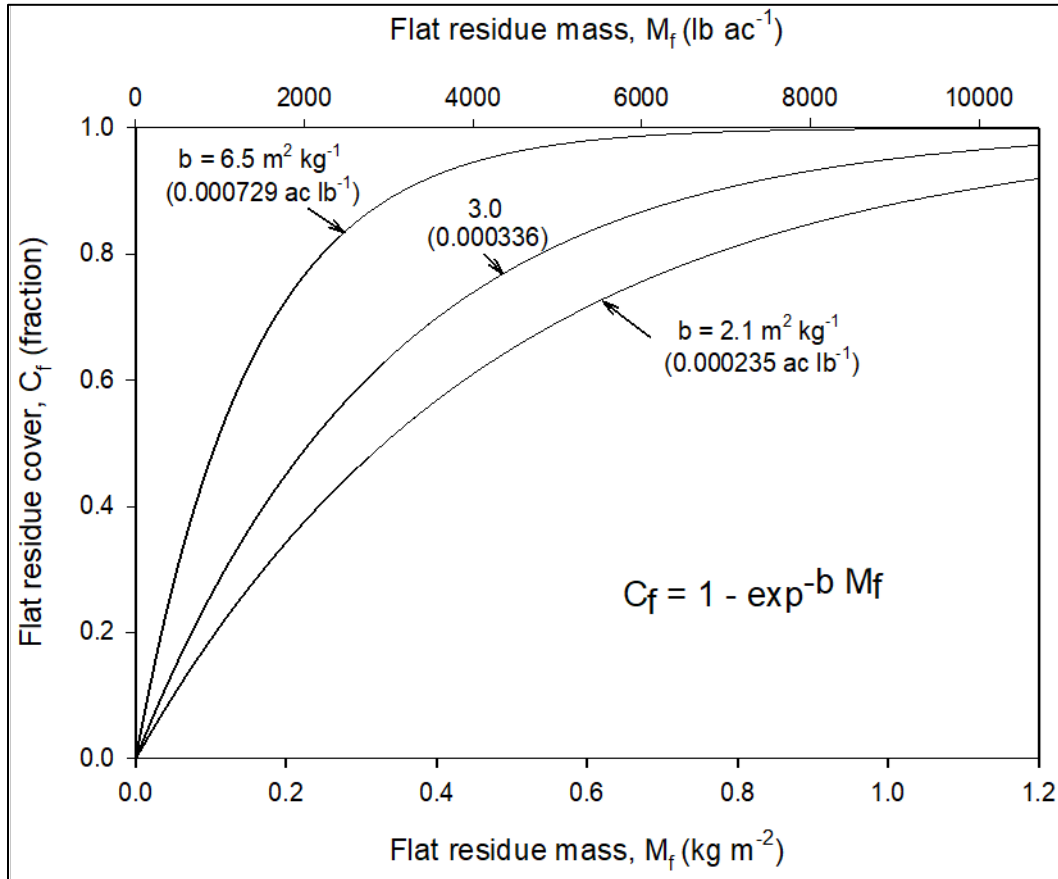


Figure 6. Relationship between flat residue mass and the cover provided by this flat residue for three different values of the mass to cover factor b . WEPS uses $b = 6.5 \text{ m}^2 \text{ kg}^{-1}$ for wheat, barley, oats, rye, and triticale; $b = 3.0 \text{ m}^2 \text{ kg}^{-1}$ for corn, sorghum, and millet; and $b = 2.1 \text{ m}^2 \text{ kg}^{-1}$ for cotton and sunflower (after van Donk et al. 2008).

Residue from crops such as cotton and sunflower ($b = 2.1 \text{ m}^2 \text{ kg}^{-1}$) does not provide much cover per unit mass, whereas wheat residue provides much more cover ($b = 6.5 \text{ m}^2 \text{ kg}^{-1}$). Total flat cover from the five age pools is calculated, taking into account overlap among the five age pools. Total (standing plus flat) residue cover is computed by adding total standing residue cover and total flat residue cover.

Changes Due to Tillage Operations

After tillage, the distribution of residue will change between standing, flat, and buried components depending on the tillage implement. The WEPS Management submodel updates current biomass for each position pool (standing, flat, and buried) in each of the five age pools. Soil surface cover and SAI are then updated from the amount of biomass remaining in the flat and standing pools.

Comparison with Other Models

Other erosion models such as the Water Erosion Prediction Project (WEPP) (Flanagan and Nearing 1995) and the Revised Universal Soil Loss Equation, Version 2 (RUSLE2)

(USDA-ARS 2013) also include residue decomposition submodels. All three (WEPS, WEPP, RUSLE2) are more or less based on the same science. One unique feature of the WEPS Residue Decomposition submodel is the simulation of stem area index, which is needed to predict wind speed near the soil surface, a factor that is very important for wind erosion prediction as described earlier. Some differences between the Residue Decomposition submodel in WEPS, WEPP, and RUSLE2 are discussed below.

WEPP simulates decomposition of residue for cropland and rangeland ecosystems in separate submodels. WEPS does not simulate residue in rangeland systems. WEPP includes a separate prediction of residue cover for rill and interrill areas. When ridges and furrows are present, decomposition of residue on ridges and in furrows is accounted for separately. WEPP has different k-values for above-ground vs. buried residue; in WEPS they are the same. WEPP uses three age pools as opposed to five in WEPS. For stem fall, WEPP does not use a threshold; stems can start falling immediately after harvest. Also, the rate of stem fall is controlled by a constant factor that can be adjusted by the user to account for local climate conditions. It is not based on decomposition days (moisture, temperature) as it is in WEPS.

RUSLE2 uses long-term average monthly climate inputs as opposed to WEPS and WEPP which use stochastically generated daily weather data. This creates the potential for very different results, even if RUSLE2 would use the same equations as WEPS and/or WEPP. For the moisture function, RUSLE2 uses an equation similar to Eq. 4. This equation is not only used for standing, but also for flat and buried residue. However, the decomposition coefficient (k-value) for standing residue is assumed to be 30 percent of that for flat and buried residue. Similar to WEPP, RUSLE2 has no threshold of decomposition days that needs to be reached before stems fall. RUSLE2 uses the same temperature function as WEPS and WEPP (Eq. 7), but with a value of 8 °C for T_b . Again, the fact that RUSLE2 uses long-term average monthly temperature data will likely cause this equation to give results different from WEPS.

The amount of residue on the soil surface may affect the rate of residue decomposition. In the Agricultural Production Systems Simulator (APSIM) model (Keating et al. 2003), a 'contact factor' discounts decomposition according to the amount of residue. Where a large amount of surface residue is present, overall rates of decomposition will be lower. It is assumed that the residue in immediate contact with the soil decomposes more rapidly than that on top. Thorburn et al. (2001) have investigated the importance of this contact factor for sugarcane systems that involve large amounts of surface residue (up to 20 t/ha). WEPS does not account for the effect of residue amount on decomposition rate. It is typically used to simulate dryland agriculture scenarios in semi-arid regions, where residue amounts are usually much less than 20 t/ha.

Some processes are not (explicitly) simulated in WEPS. It simulates stem fall as described earlier, but not explicitly in response to mechanical forces such as high winds and snow storms, which may be important, especially in climates such as that of the northern U.S. (van Donk et al. 2008). Also, WEPS does not simulate the migration of unanchored (loose) residue caused by wind or runoff. This migration and 'bunching' of residue will change the mass-to-cover relationship (Eq. 11) and may affect susceptibility to erosion (van Donk et al. 2008). We do not know of other models that simulate stem fall triggered by wind and/or snow, and migration of loose residue.

Simulations

Five simulation scenarios were created to illustrate the functionality of the WEPS residue decomposition model (Table 1). Locations were selected to show how the model responds to the main drivers of decomposition: temperature and moisture. No-till crop management rotations, typical for the location, were used to illustrate the persistence of standing residue. The Wisconsin rotation was the only rotation with tillage, immediately before corn planting and after corn harvest, with no-till following wheat and soybeans. All scenarios included winter wheat for cross-location comparison (Table 1). Each simulation was run for 50 rotation cycles in order to obtain stable long-term averages. Thus, a one-year rotation was run for 50 years and a two-year rotation for 100 years. Crop yields were adjusted to match average county yields obtained from the USDA, National Agricultural Statistics Service. Soils were selected to be similar among all five locations and the selected soils were verified, against satellite imagery and the county soil survey (websoilsurvey.nrcs.usda.gov), to be under cultivation.

Table 1. Five simulation scenarios used to illustrate the functionality of the WEPS residue decomposition model where **Precip.** is average annual precipitation, **Temp.** is average annual temperature, and **Yrs.** is years in crop rotation.

State	County	Precip.	Temp.	Soil	Rotation	Yrs.
		(mm)	(°C)			
Arkansas	Johnson	1161	15.5	Nella Fine Sandy Loam	Winter Wheat, Soybean	1
Oklahoma	Cimarron	422	13	Gruver Loam	Winter Wheat, Fallow, Sorghum	2
South Dakota	Perkins	345	6.9	Parchin Fine Sandy Loam	Winter Wheat, Millet	2
Wisconsin	Trempealeau	831	8	Port Byron Silt Loam	Corn, Winter Wheat, Soybean	2
Colorado	Washington	378	9.6	Weld Silt Loam	Winter Wheat Fallow	2

There are significant instantaneous increases in residue when a crop is harvested (Figures 7 and 8) or weeds are killed with an herbicide (Figure 8), moving the just-harvested or just-killed biomass from pools accounted for in the Crop submodel into the first residue decomposition age pool. Little decomposition occurs in the winter, increasing in the spring with increasing temperatures. While the rotations are no-till, the seeding operation

does disturb the soil surface, resulting in a reduction in standing residue. This is clearly seen in Figures 7 (October) and 8 (September of year 2) when the wheat is planted. This planting operation knocks down and buries some of the residue resulting in a decrease in standing residue, an increase in buried (below ground) residue, and little change in flat residue (Figure 7).

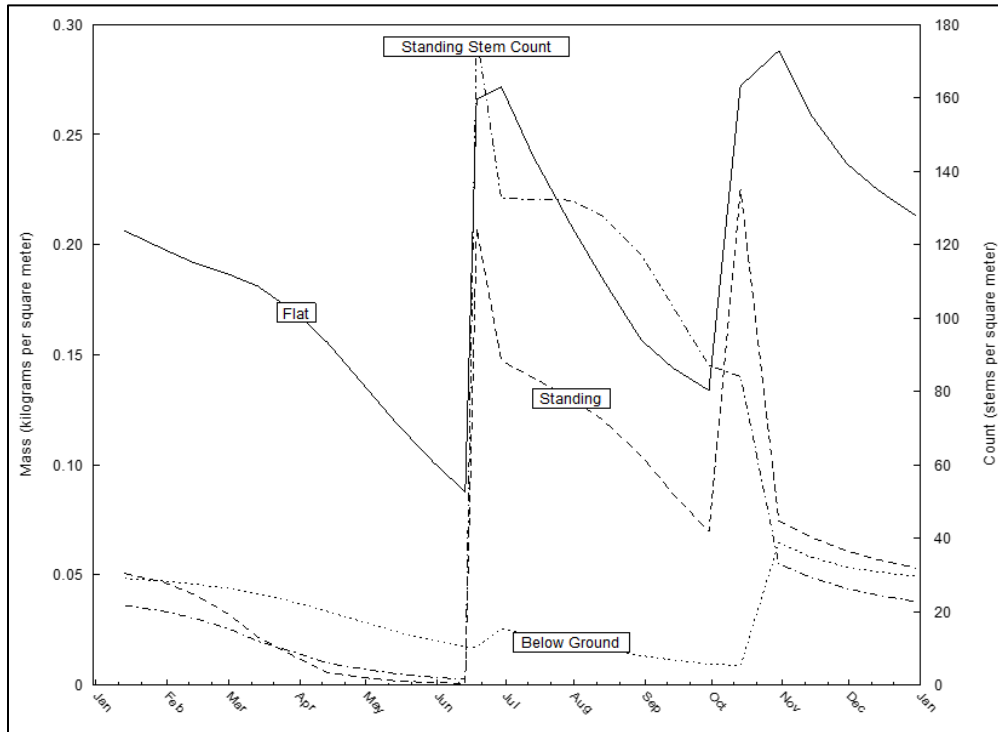


Figure 7. One-year Arkansas winter wheat-soybean crop rotation: simulation of crop residue mass (standing, flat, and below-ground) and the number of standing stems. Wheat harvest is on 6/15, soybean planting on 6/20, soybean harvest on 10/1, and wheat drilling on 10/15. Values are averages of 50 simulations.

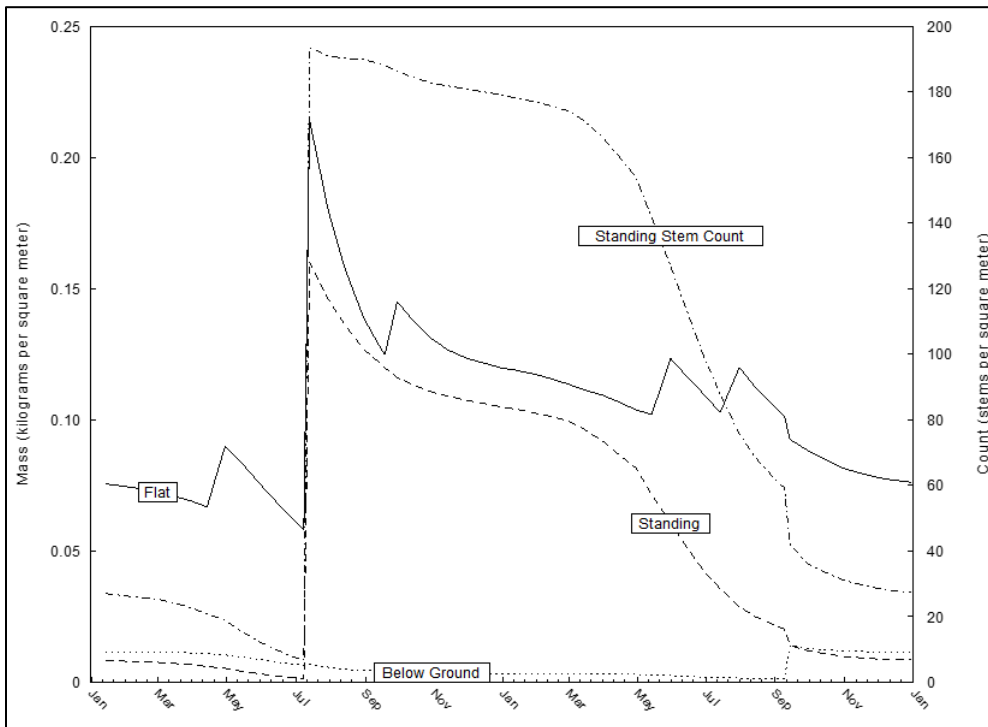


Figure 8. Two-year Colorado winter wheat-fallow crop rotation: simulation of crop residue mass (standing, flat, and below-ground) and the number of standing stems. Weed spraying is on 4/15 and 9/20 of year 1, and on 5/15 and 7/15 of year 2. Wheat harvest is on 7/10 of year 1 and wheat drilling on 9/10 of year 2. Values are averages of 50 simulations.

Decomposition days (Eqs. 1-3) accumulate more slowly in dry, cool regions and more rapidly in wet, warm regions, as expected (Figures 9-11). Decomposition days accumulate slowly for standing residue (Figure 9), more rapidly for flat residue (Figure 10), and most rapidly for below-ground residue (Figure 11), as generally standing residue is driest and below ground residue wettest (Eqs. 4-6).

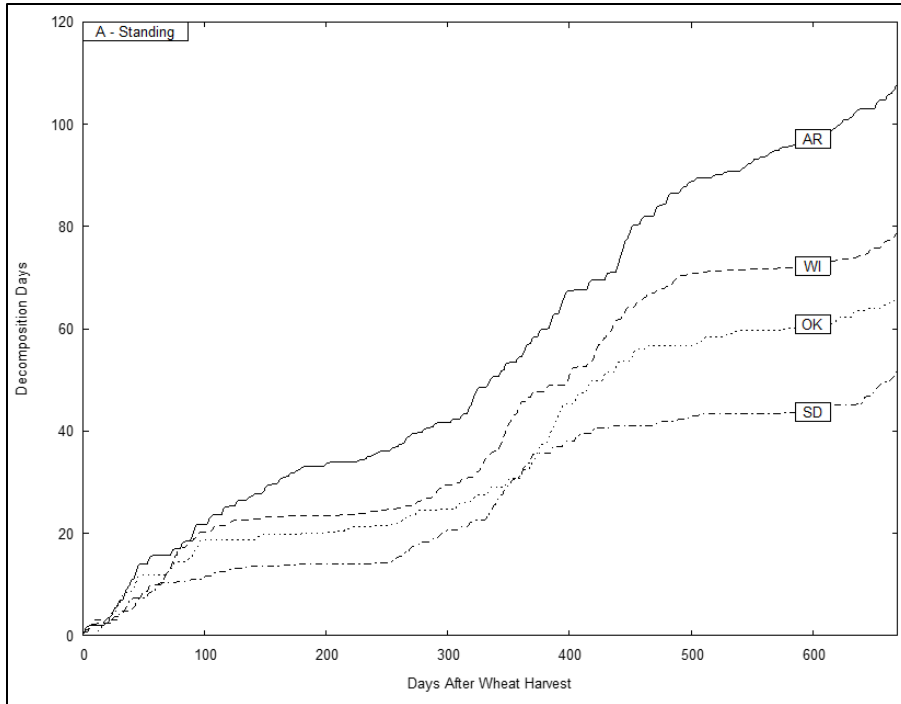


Figure 9. Decomposition day accumulation at four locations (in Arkansas, Wisconsin, Oklahoma, and South Dakota) for standing crop residue. Curves are medians of 50 simulations.

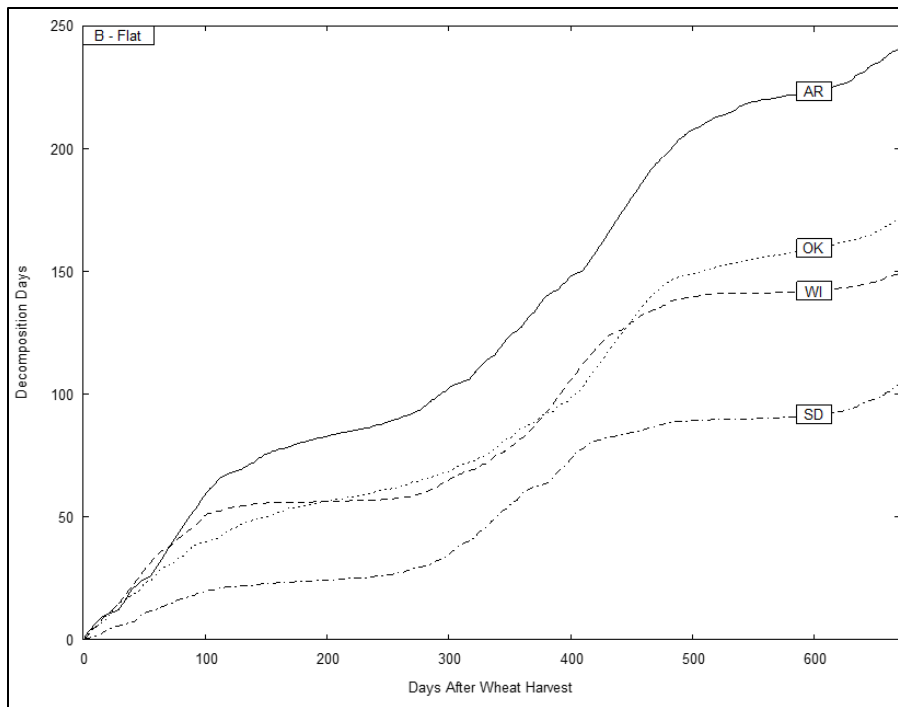


Figure 10. Decomposition day accumulation at four locations (in Arkansas, Wisconsin, Oklahoma, and South Dakota) for flat crop residue. Curves are medians of 50 simulations.

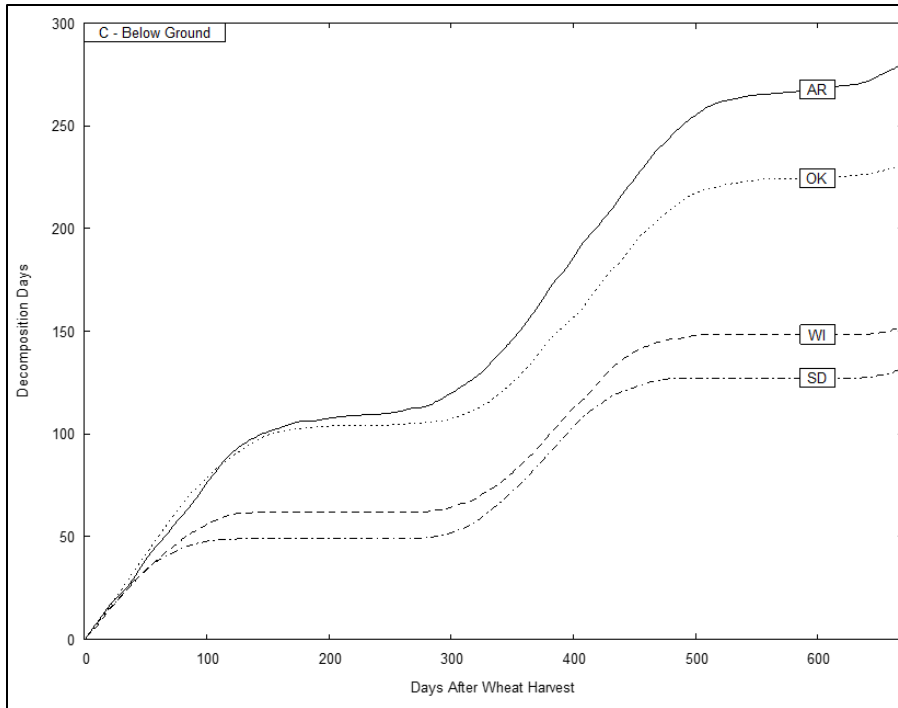


Figure 11. Decomposition day accumulation at four locations (in Arkansas, Wisconsin, Oklahoma, and South Dakota) for crop residue 45-59 mm below-ground. Curves are medians of 50 simulations.

Figure 9 shows a comparison of standing residue decomposition days across four of the locations; wheat residue decomposition days accumulate fastest in Arkansas (warm, wet), followed by Wisconsin (cool, wet), Oklahoma (warm, dry) and South Dakota (cool, dry). For flat residue, decomposition day accumulation is greater for Oklahoma than for Wisconsin (Figure 10); moisture is less of a limitation for flat residue than it is for standing residue. Moisture is even less of a limitation with the below-ground accumulation of decomposition days (Figure 11), where Oklahoma (warm, dry) becomes very similar to Arkansas (warm, wet) and Wisconsin (cool, wet) becomes very similar to South Dakota (cool, dry). This is best explained by the moderating effect of the soil to preserve enough moisture for decomposition, even at the relatively shallow depth of 45-59 mm, making temperature the more dominant factor.

A comparison of the relative rate of decomposition between standing, flat, and below ground residue at one location further illustrates the importance of the simulation of moisture status on residue decomposition (Figure 12). Decomposition day accumulation is lower for standing residue given that the stems dry quickly after a precipitation event (Eq. 4; Figure 2). The soil surface dries more slowly, especially when the effect of residue on evaporation is considered, so decomposition accumulation is higher for flat residue. Lastly, within the soil itself, moisture retention is even higher, resulting in the highest accumulation rate of decomposition days.

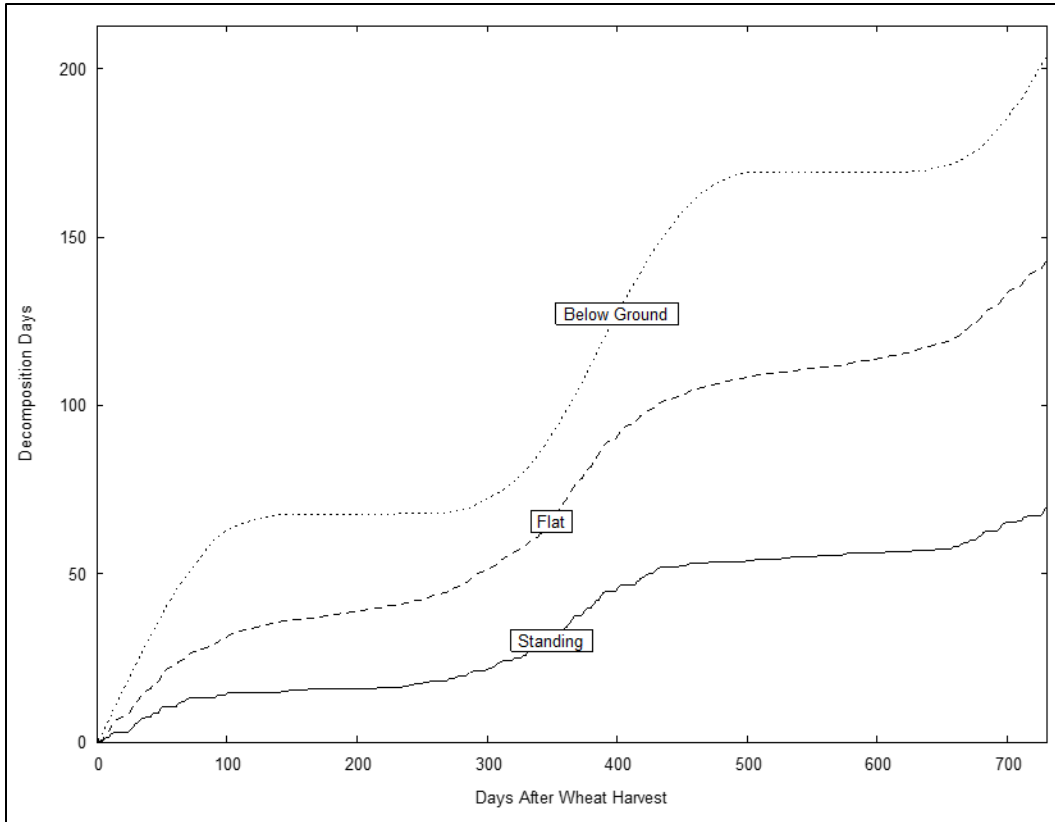


Figure 12. Decomposition day accumulation for standing, flat and below-ground residue for the two-year Colorado winter wheat-fallow rotation. Curves are medians of 50 simulations.

The use of five residue age pools to simulate residue amounts through their decomposition cycle is illustrated for the Colorado simulation (Figure 13). The small amounts of weed residue created when herbicide is applied move the wheat residue into pool 5 fairly quickly, where it is added to any other residue that remains. The amount of other residue in pool 5 is small compared to the amount of wheat residue added. By comparison, when weed residue is added to pool 5, the amount of other residue is relatively large compared to the amount being added. While these simulations show decomposition rates generally follow expected results, field studies are needed to validate the Residue Decomposition submodel.

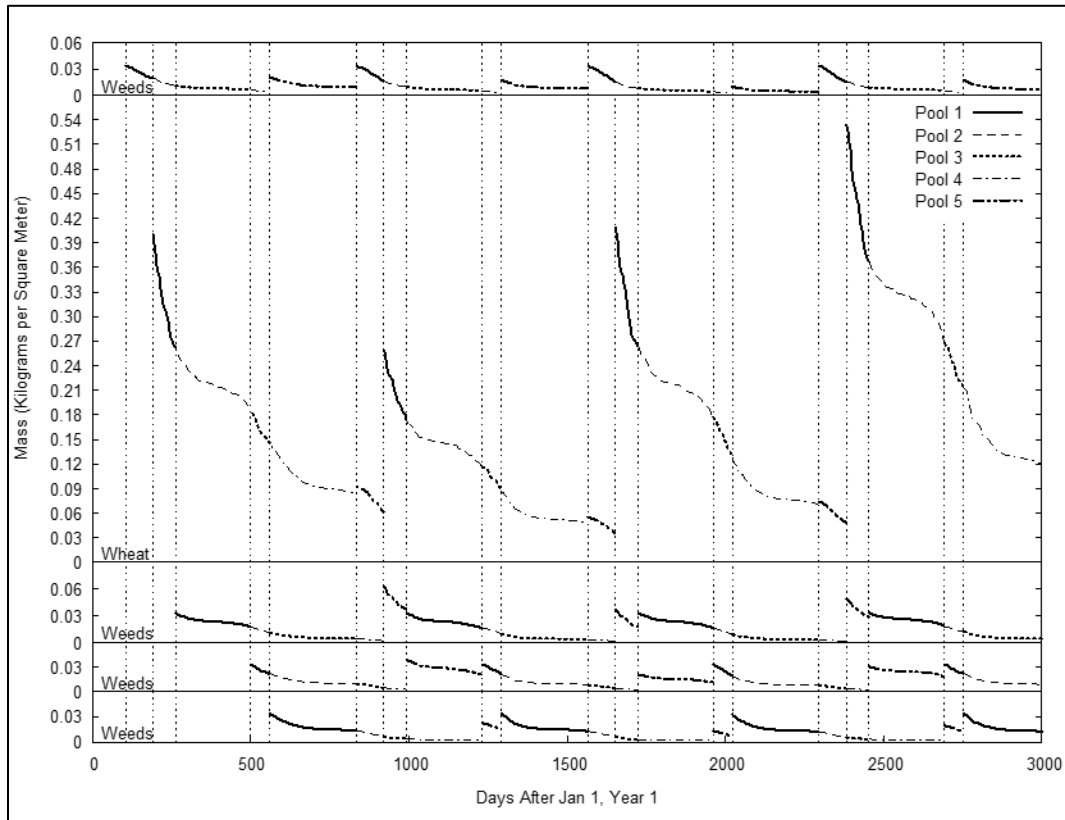


Figure 13. Decrease in residue mass with time; illustration of the five residue age pools the model uses to simulate residue amounts for the two-year Colorado winter wheat-fallow rotation. Weeds are sprayed (killed) on day 105 and the killed weed biomass is moved into residue pool 1. Wheat is harvested on day 191, the wheat residue is moved into pool 1, and the weed biomass that was in pool 1 is moved into pool 2. On day 263, weeds are again sprayed; this biomass goes into pool 1, the wheat residue goes into pool 2, and the weed residue from the first spraying goes into pool 3.

Conclusions

The Residue Decomposition submodel for WEPS supports estimating the wind erosion protection available from crop residue by simulating the decrease in residue biomass and standing stem count due to the effects of biological decomposition in response to climatic conditions. Because residue from multiple years of cropping may be present, and the age and crop type of residue is a factor in decomposition, the submodel uses five age pools. The decomposition rate and protective effect are also a function of the plant parts, so the submodel simulates leaf, stem, and reproductive masses separately. The location of the residue also affects the decomposition rate and protective effect and is manipulated by management operations, so the geometric positions (standing, flat, and buried by soil layer) also are simulated separately. By combining all the standing residue age pools and all the flat residue age pools, the end result is an estimate of the protection against wind erosion provided by crop residue at any time during the crop rotation cycle.

References

- Flanagan, D.C. and M.A. Nearing (editors). 1995. USDA-Water Erosion Prediction Project (WEPP) Hillslope Profile and Watershed Model Documentation, and WEPP Version 95.7 Computer Model. NSERL Report No. 10, National Soil Erosion Research Laboratory, USDA-Agricultural Research Service, West Lafayette, Indiana. 298 pp.
- Gregory, J.M. 1982. Soil cover prediction with various amounts and types of residue. *Transactions of the ASAE*. 25: 1333-1337.
- Hagen, L.J. Crop residue effects on aerodynamic processes and wind erosion. *Theoretical Applied Climatology*. 54:39-46, 1996.
- Hagen, L.J. and D.V. Armbrust. 1994. Plant canopy effects on wind erosion saltation. *Transactions of the ASAE*. 37(2): 461-465.
- Keating, B.A. et al. 2003. An overview of APSIM, a model designed for farming systems simulation. *European Journal of Agronomy*. 18: 267-288.
- Schomberg, H.H., and J.L. Steiner. 1997. Estimating crop residue decomposition coefficients using substrate-induced respiration. *Soil Biology and Biochemistry*. 29(7): 1089-1097.
- Schomberg, H.H., J.L. Steiner, S.R. Evett, and A.P. Moulin. 1996. Climatic influence on residue decomposition prediction in the Wind Erosion Prediction System. *Theoretical Applied Climatology*. 54(1-2): 5-16
- Siddoway, F.H., W.S. Chepil, and D.V. Armbrust. 1965. Effect of kind, amount, and placement of residue on wind erosion control. *Transactions of the ASAE*. 8(3):327-331.
- Steiner, J.L., H.H. Schomberg, C.L. Douglas, Jr., and A.L. Black. 1994. Standing stem persistence in no-tillage small-grain fields. *Agronomy Journal*. 86:76-81.
- Steiner, J.L., H.H. Schomberg, P.W. Unger, and J. Cresap. 1999. Crop residue decomposition in no-tillage small-grain fields. *Soil Science Society of America Journal*. 63: 1817-1824.
- Steiner, J.L., H.H. Schomberg, P.W. Unger, and J. Cresap. 2000. Biomass and residue cover relationships of fresh and decomposing small grain residue. *Soil Science Society of America Journal*. 64: 2109-2114.
- Stroo, H.F., K.L. Bristow, L.F. Elliott, R.I. Papendick, and G.S. Campbell. 1989. Predicting rates of wheat residue decomposition. *Soil Science Society of America Journal*. 53: 91-99.
- Taylor, S.E. and O.J. Sexton. 1972. Some implications of leaf tearing in musacea. *Ecology*. 53: 143-149.
- Thorburn, P.J., M.E. Probert, and F.A. Robertson. 2001. Modelling decomposition of sugarcane surface residues with APSIM-Residue. *Field Crops Research*. 70: 223-232.

USDA-ARS. 2013. Science Documentation, Revised Universal Soil Loss Equation, Version 2 (RUSLE2) (for the model with release date of May 20, 2008) USDA-Agricultural Research Service. Washington, D.C. Available at: https://www.ars.usda.gov/sp2UserFiles/Place/64080510/RUSLE/RUSLE2_Science_Doc.pdf. (Accessed August 10, 2020).

van Donk, S.J., S.D. Merrill, D.L. Tanaka, and J.M. Krupinsky. 2008. Crop residue in North Dakota: measured and simulated by the Wind Erosion Prediction System. *Transactions of the ASABE*. 51(5): 1623-1632.

Inputs and Command Line Arguments for WEPS

Contributor:

L.E. Wagner

Abstract

The Wind Erosion Prediction System (WEPS) was designed for ease of use that includes simple inputs wherever possible. The inputs required for the WEPS science model are contained in five files. Specific file formats and variables are required for the master WEPS Run input file, the WEPS Soil Initial Field Conditions (IFC) file containing both the intrinsic soil properties and the initial values for the temporal soil and surface properties, the Management/Crop Rotation file consisting of the management operations and their dates, and two climate (CLIGEN and WINDGEN) generated output files consisting of the daily climatic and hourly wind parameters. The master input file is the WEPS Run file, which specifies the filenames for the Soil IFC file, the Management/Crop Rotation file, the two climate files (CLIGEN and WINDGEN generator output formatted), as well as the location information, simulation region dimensions, and wind barrier information if any are present. In addition, all WEPS command line arguments are fully described. WEPS inputs and command line arguments are simplified within the user interface wherever feasible for minimal user supplied inputs.

Introduction

This chapter presents the inputs required for the WEPS science model. It outlines the file formats and variables required for the WEPS Run file, the WEPS Soil Initial Field Conditions (IFC) file and the Management/Crop Rotation file, as well as the climate (CLIGEN and WINDGEN) files. The master input file is the WEPS Run file, which specifies: (a) the Soil IFC file containing both the intrinsic soil properties and the initial values for the temporal soil and surface properties; (b) the Management/Crop Rotation file; (c) the two climate files (CLIGEN and WINDGEN generator output formatted); and (d) the location information, simulation region dimensions and any wind barrier information. In addition, specific command line arguments for WEPS are also briefly described that affect the required WEPS inputs in some cases.

WEPS Run File

The WEPS Run file (`weps.run`) is the master input file used by WEPS. It specifies the simulation region dimensions and orientation, the accounting region dimensions for outputs, the location and properties for any wind barriers described for the simulation, as well as the climate files (both CLIGEN and WINDGEN), the WEPS Soil IFC file, and the Management/Crop Rotation file. It also includes some additional parameters that are reserved for use by the WEPS graphical user interface but are not required for the WEPS science model. Although this section documents the file format sufficiently for someone to create and edit a WEPS Run file manually, it is strongly encouraged that users create WEPS Run files automatically through the WEPS interface to ensure that the resulting file meets the requirements of the WEPS science model.

The format of the WEPS Run file consists of comment lines (some of the WEPS science model comment lines (lines that begin with a # character) store data used by the WEPS interface so those particular lines are not comment lines for the WEPS interface), which is indicated by a # character at the beginning of the line, and other lines that contain the data. The comment lines are ignored by the WEPS science model when reading in the numerical and textual data used by the science model. Special comment lines used by the WEPS science model are identified below. The WEPS interface generates and includes these comments by default to make the file more readable for users viewing the input file. Some data lines consist of multiple values that are separated by white space or spaces, which will be specifically identified below. In addition, there are other lines with multiple values that are separated by the pipe character, (|), whose values are written out by the WEPS interface and read and used by the WEPS interface when restoring the inputs from a previous WEPS run within the interface.

An example WEPS Run file is provided below and parsed into specific line sections to document the file format, present the order of the input parameters listed with their definitions, and provide additional parameter information as required.

1. The first four lines of a standard WEPS Run file are typically comment lines generated by the WEPS interface.

```
#VERSION=1.05
#----- WEPS SIMULATION RUN FILE -----
# Note: Lines beginning with '#' are comment lines.
#       Lines beginning with '# RFD' are comments used by the interface.
```

As specified in these four lines, the first comment line includes the WEPS Run file version number. If the WEPS Run file format changes, then the version number will reflect that change. This allows the WEPS science model and the WEPS interface to know which version is being used and read that file format, if currently supported, or to generate an error message to the user if the WEPS Run file version has been deprecated. The information provided above in the four comment lines are produced by the current WEPS interface (version 1.3.9). In addition, lines immediately following the “# RFD” comment lines signify that data immediately following are specifically used by the current WEPS interface but may also be used for informational purposes by the science model. These are identified individually below.

The “User” information is specified in the next five lines. This is primarily informational data requested by the Natural Resources Conservation Service (NRCS) for the user to track the individual WEPS runs made. They were specifically tailored for NRCS use with the WEPS interface but can be used by any user as desired. This input data were originally skipped by the science model but is now read to provide for future science model output as necessary. The actual text or values are not required for an WEPS simulation run to be made with the WEPS science model and the values may be omitted if manually creating the weps.run file, but at least one “|” character must be present on the 5th line for the WEPS science model to correctly read the file. However, for the WEPS interface, the lines must exist and all five “|” characters are required on the 5th line for the WEPS interface to correctly read and interpret the optional parameter text for the first three parameters “RFD-FarmID, RFD-TractId and RFD-FieldId” and the remaining three parameter values which are required by the interface.

```

# --USER INFORMATION
#   RFD-UserName
Joe Smith
#   RFD-FarmId RFD-TractId RFD-FieldId RFD-runtypedisp RFD-RotationYears RFD-CycleCount
FmID | TID | FldID | NRCS | 2 | 50

```

The “UserName” is the identified user for the simulation run. It is typically used by NRCS to provide the client’s name. In the example above, “Joe Smith” is specified. The current WEPS interface now restricts this input field to 65 characters, although the science model will read in up to 256 characters. The “FarmId”, “TractId”, “FieldId”, “runtypedisp”, “RotationYears”, and “CycleCount” variables are specified in the next line, separated by the pipe, “|” character. The “FarmId”, “TractId” and “FieldId” are input fields made available in the WEPS user interface for NRCS which signifies information they use for filing and indexing information on their clients. These values can be any alphanumeric values, except the “|” character. The total line length cannot be greater than 256 characters containing all six variables in the science model. To ensure that this constraint is not exceeded, the WEPS interface now restricts the “FarmId”, “TractId”, and “FieldId” to 65, 10, and 10 characters respectively. Currently, only the “CycleCount” value is extracted by the science model. However, it is only made available for debugging purposes (the science model computes the number of cycles directly from the start and end simulation dates provided later in the WEPS Run file and does not use the value specified here in the Run file, which is only used by the WEPS interface). The other variables on this line are currently ignored by the science model. The “runtypedisp” is the WEPS run mode specified in the WEPS user interface. There is a specific NRCS run mode, which defines how WEPS is run for official NRCS WEPS simulations. It enforces some constraints on the inputs for NRCS use and guarantees that the WEPS interface generated reports are consistent. There are two other run modes defined and used by the current WEPS interface, “Date” mode and “Cycle” mode, so "Date" and "Cycle" are also valid "runtypedisp" values that could exist on this line. The “Date” mode allows the user to explicitly specify the starting and ending dates for a simulation, and the “Cycle” mode allows the user to specify exactly how many cycles (number of times a management/crop rotation is “cycled” within a simulation) are desired for the WEPS run. For example, a two-year crop rotation cycled 20 times will cause WEPS to simulate a total of 40 years, e.g., 20 years per individual year in the crop rotation. This field is only accessed by the WEPS user interface at this time and not used by the WEPS science model at all. The “RotationYears” is the length of a single cycle for the crop rotation sequence specified in the management/crop rotation file later in the WEPS Run file. It is required to be an integer value. This value is included here for the WEPS interface and is not used directly by the WEPS science model. The science model determines this value directly when reading in the contents of the WEPS management/crop rotation file. For example, a continuous corn rotation would have a value of “1” rotation year while a wheat-fallow or a corn-bean rotation would have a value of “2”, etc. The “CycleCount” is the number of cycles of a management/crop rotation practice will be simulated within WEPS. By default, the NRCS mode enforces a fixed number of cycles (currently 50) for all official NRCS WEPS runs by the WEPS interface. This allows for consistency in comparisons between WEPS runs for NRCS and provides a certain level of accuracy to be attained for all their WEPS runs. It is required to be an integer value. This value is provided here for the WEPS interface and is currently read and printed by the WEPS science model for debugging purposes. The science model calculates this value directly from the start and end simulation dates provided later in the WEPS Run file.

2. The next line consists of another WEPS interface parameter that is read but currently ignored by the WEPS science model. This line is read by the science model and sets this line's content to the "userloc" variable. This required line does not contain the information defined for the WEPS science model's "userloc" variable, but since it is not currently used within the WEPS science model, it is not causing an error. Note that this information is used by the WEPS GUI interface and will likely be rectified in a future release of the science model. It defines the type of GIS map and coordinate system used within the WEPS interface GIS mapping system.

```
# RFD-Site
FIPS:US-KS-069
```

3. The following lines describe the site information:

```
# --SITE INFORMATION
# Signed Latitude
+38.00
# Signed Longitude
-100.66
# RFD-Elevation(meters)
801.0
# RFD-ClimateFlag|RFD-cligen.station
nracs|cligen|+37.783;-100.333|14|1522|CIMARRON|801.0
# RFD-WindFlag|RFD-windgen.station
nracs|interpolated|+37.738;-100.438
```

The first two lines specify the latitude and longitude values in decimal degrees for the selected site. A positive value is assumed to be the northern and eastern hemispheres respectively. These values are assumed to be the center (centroid) of the simulation region specified and are used to estimate the season changes in the daylength. The values are expected to be floating point numbers and the sign of the value determines the hemispheres. The third line contains the estimated elevation in meters for the simulation site above mean sea level. It defaults to the value provided in the CLIGEN file when the WEPS user interface is used to create a WEPS run, but the user can override that value if desired. It is used to estimate the air density change by elevation within the WEPS science model. The value is expected to be a floating-point number. The last two lines define the CLIGEN and WINDGEN station information used by the WEPS interface. The WEPS science model currently does not use any of the information from these two input lines. The values are separated by the “|” symbol. The WEPS science model simply reads these two lines in as text and assigns them to the "awclsn" and "awwisn" character variables. The first field value signifies the type of method used for selecting the weather stations within the WEPS user interface. The displayed values in this example, “nracs”, mean that only the approved NRCS methods, which are dependent upon location, are available for selecting the weather stations for use with the simulation. The flag value in the second field on the first line, “cligen”, signifies that only the nearest station could be selected for this site location. The flag value in the second field on the second line, “interpolated” signifies that an interpolation method used three nearby stations for developing the station statistical parameters used in generating the WINDGEN input file. The third values, separated by semicolons, specify the latitude and longitude values for the selected or interpolated stations. The values are specified in decimal degrees with positive (+) values denoting the northern and eastern hemispheres respectively and the negative (-) values the southern and western hemispheres. The (+) sign is not required to denote a positive value. The fourth and fifth values shown on the first line indicate the “State ID” code number and the “Station ID” code number for the CLIGEN station. The

“Station ID” code numbers are unique identifiers within each “State ID”. The sixth value shown on the first line indicates the CLIGEN station name selected. The seventh field value shown on the first line indicates the elevation of the selected CLIGEN station in meters, which is a floating-point value. Similarly, if a WINDGEN station had been selected rather than an interpolated station, a unique “Windgen Station ID” number would be displayed in the fourth field (no separate “State ID” codes are used for WINDGEN stations). The fifth and sixth fields would then display the WINDGEN country and state abbreviations with the seventh field displaying the WINDGEN station name. For this case, see the example below.

```
# RFD-WindFlag|RFD-windgen.station  
nracs|windgen|+38.28333;-104.51667|724640|US|CO|PUEBLO MEMORIAL (AW)
```

4. The following 3 input lines provide the science model with the start and stop dates and the time step for the simulation.

```
# --SIMULATION PERIOD  
# RFD-StartDate(day month year)  
01 01 01  
# RFD-EndDate(day month year)  
31 12 50  
# RFD-TimeSteps(per day)  
24
```

Although any date can be specified for the start and end dates for the science model, there are some constraints that currently limit the acceptable values under certain conditions. The start date (i.e., StartDate) must be January 1st if the climate files generated from the CLIGEN and WINDGEN generators are used, since they start with that date and the WEPS science model does not search the climate files for the specified starting date within them. Although alternative climate files can be created that can begin on a different day, it must match the start date specified in the WEPS Run file. Testing in this configuration has been limited.

In addition, the end date (i.e., EndDate) is typically the end of a calendar year, December 31, with the year usually being a multiple of the rotation length of the specified management/crop rotation file. For example, if a 3-year rotation file with a start year of 2000 and a rotation cycle length of 4 is used, then a single cycle would equate to an end year of 2012, 2 cycles would end in year 2016, etc. This requirement is needed because some of the WEPS science model reports expect to have equivalent time lengths to compute the correct average values for selected time periods during a management/crop rotation cycle. The WEPS interface enforces such consistency by having the user specify the number of cycles, in CYCLE mode, or for NRCS mode where the number of cycles is fixed (currently set to 50 cycles). However, if one is not interested in those summarization reports, any ending date can be specified.

Note that the WEPS science model determines the cycle length (length of a management/crop rotation sequence) from the management/crop rotation file and determines the number of cycles that will be run in the simulation by taking the total number of simulation years and dividing it by the cycle length.

The time step parameter was originally intended to allow flexibility in the base daily time interval that the WEPS erosion simulation would run. However, WEPS has since standardized on a daily interval (24 hours) for wind data input. Thus, this value should

always be set to 24 because WEPS has had limited testing with any other time interval settings.

5. The next five input lines consist of file/path names for the climate files, soil file, and management/crop rotation file used by the WEPS science model. If no file path is specified, the files are expected to exist in the current WEP Run directory that also contains the WEPS Run file.

```
# --RUN FILE FILENAMES (INPUT)
#   RFD-climate file
cli_gen.cli
#   RFD-wind file
interpolated.win
#   RFD-sub-daily file
none
#   RFD-SoilFile
Loam_NA_100_L.ifc
#   RFD-ManagementFile
Sorghum,Grain;MT,CMZ19.man
```

Note that the default CLIGEN climate filename when using the CLIGEN generator is “cli_gen.cli”. Similarly, the default WINDGEN climate filename when using the WINDGEN generator is “wind_gen.win”. If an interpolated windgen file is generated through the WEPS interface, the filename is “interpolated.win”. If manually or externally created climate files are used, then those filenames would appear here instead of these default filenames with the corresponding “.cli” and “.win” file extensions.

Note also that there is an option for a sub-daily (i.e., sub-hourly) WINDGEN file that can contain additional wind data on a time step less than an hour (an hourly time step is the time step of a standard WINDGEN file). However, that input option has not been tested extensively with WEPS and may not work as expected. A value of “none” causes the WEPS science model to ignore this line.

6. Obsolete WEPS science model output option flags in the weps.run file. The first line was for a simulation output file that is no longer generated, so that line is read but no longer used. The second line “RFD-ReportForm” line was intended to supply options which specified additional, non-default reports from the WEPS science model, which is not used. The third line “RFD-OutputPeriod” was used to set the frequency of non-default output from the WEPS Erosion submodel code, which is also no longer used. However, even though these inputs are no longer used in the WEPS science model, they are still required as place holders when the data is read from the WEPS run file.

```
# --WEPS OUTPUT OPTIONS
#   RFD-OutputFile
null
#   RFD-ReportForm
0 0 0 0 0 0
#   RFD-OutputPeriod
2
```

7. The next two lines consist of 6 integer option values which determine whether additional submodel detail and debug level output files are generated from the WEPS science model. The order of the values refers to the following WEPS submodels: 1) Hydrology; 2) Soil; 3) Management; 4) Crop; 5) Decomposition; and 6) Erosion. A value of 0 (zero) means no additional output is generated for that submodel.

Increasing values mean that increasingly detailed output is generated in additional report files for the respective submodels. Some submodels have several levels of output available and some submodels have only one or none available for detail and/or debug reports. Currently, the following filenames listed in Table 1 are opened if the corresponding SubmodelOutput or DebugOutput option is set to the specified value.

```
# RFD-SubmodelOutput
0 0 0 0 0 0
# RFD-DebugOutput
0 0 0 0 0 0
```

Table 2. WEPS submodel output filenames and flags for various levels of output.

Filename	Submodel Output (S) or Debug Output (D) Parameter	SubmodelOutput or Debug Output Parameter Value
manage.out	Management (S)	1
hydro.out	Hydrology (S)	1, 3, 5 or 7
hlayers.out	Hydrology (S)	1, 3, 5 or 7
water.out	Hydrology (S)	2, 3, 6 or 7
surfwat.out	Hydrology (S)	2, 3, 6 or 7
weather.out	Hydrology (S)	2, 3, 6 or 7
temp.out	Hydrology (S)	4, 5, 6 or 7
decomp.out	Decomposition (S)	1 or 3
bio1.btmp	Decomposition (S)	1 or 3
dabove.out	Decomposition (S)	1 or 3
decXX.btmp*	Decomposition (S)	2 or 3
dbelow.out	Decomposition (S)	2 or 3
crop.out	Crop (S)	>0
shoot.out	Crop (S)	>0
inpt.out	Crop (S)	>0
allcrop.prn	Crop (S)	>1
soilsurf.out	Soil (S)	1
soillay.out	Soil (S)	1
erosion.out	Erosion (S)	>0
eeegt.out	Erosion (S)	>0

eros.tmp	Erosion (S)	>0
daily_erod.out	Erosion (S)	1 (1st bit set)
daily_egr.out	Erosion (S)	2 (2nd bit set)
subdaily_emit.out	Erosion (S)	4 (3rd bit set)
plot.out	Hydrology (S), Soil(S), Management (S) Decomposition (S), and Erosion (S)	>0
hdebug.out	Hydrology (D)	1
sdebug.out	Soil (D)	1
tdebug.out	Management (D)	1
cdebug.out	Crop (D)	1
ddebug.out	Decomposition (D)	1

*XX refers to the biomass age pool number.

- The WEPS simulation region is defined as the rectangular area that the simulation will be performed on. The orientation (degrees clockwise from North, with North = 0) and the opposite corners of the rectangular simulation region are specified as the origin (X_1, Y_1) and x-length and y-length (X_2, Y_2) coordinates in meters (all of these are real values). Although not specifically required in WEPS, the (X_1, Y_1) coordinate has historically been set to (0.0,0.0) and the (X_2, Y_2) coordinate containing only positive values. Other coordinate orientations for the simulation region have not been tested and it is probably prudent that the user follow these recommendations.

The “RFD-Scales” parameter was originally used by the WEPS interface but is no longer used. The input line is still required though for a valid current WEPS run input file.

```
# --SIMULATION REGION INFORMATION
#   RFD-RegionAngle(degrees clockwise from North)
0
#   Origin coordinates of simulation region (meters)
0.0 0.0
#   RFD-XLength(meters)  RFD-YLength(meters)
804.7 804.7
#   RFD-Scales(place holder line - needed for older versions of WEPS)
5.5 5.5
```

- The following input lines specify the coordinates for the Accounting Region which is defined as the region for which WEPS output is to be provided. The coordinates must match the coordinates for the simulation region in the current version of WEPS (1.3.9)

```
#   RFD-AccNo
1
#   Accounting region coordinates (meters)
0.0 0.0
804.7 804.7
```

10. Specifies the WEPS subregion which is a constant when WEPS expands to multiple subregions. The current version of WEPS (1.3.9) is limited to a single subregion, so the "RFD-SubregionNo" value must be "1" here and the coordinates must also match the coordinates specified earlier for the simulation and accounting regions.

```
# RFD-SubregionNo
1
# Subregion region coordinates (meters)
0.0 0.0
804.7 804.7
```

11. The next line specifies the average slope of the simulation site, as a floating-point number, within the WEPS science model. By default, the value is obtained from the soil input file. The ability to override that value in the main WEPS interface was provided at the request of NRCS who wanted the ability to override it without providing their users direct edit capability of the soil input file parameters. If the value is negative, but greater than or equal to -1.5, it will use the soil input file parameter value. If the value is less than -1.5, it will assume that no runoff from the field is normally expected, set the slope to 0.0 and default the minimum depression storage value to 0.5 m depth. All values greater than or equal to 0.0 will replace the parameter value listed in the soil input file. The options available on the interface screen correspond to: a) "Override Soil Slope" which allows the user to specify a value greater than or equal to zero to be used; b) "Use Soils Slope from the Soils Database" where the value is set to -1 in the WEPS run file; c) "Level Basin, No Runoff" where the value is set to -2.0 in the WEPS run file; and d) some common default slope values which a user can select without manual entry, which will override the value in the soil input file.

```
# RFD-AverageSlope(ratio m/m)
-1
```

12. The next line refers to barrier information. The first line specifies the number of barriers. If the value is zero, then the next 6 lines are merely placeholders that the science model expects to be in the current weps.run file. If the value is greater than zero, then WEPS expects these six lines to be repeated that many times, once for each barrier.

```
# RFD-BarrierNo
0
```

13. The next 6 lines are default placeholders if zero barriers are specified.

```
0.0 0.0
0.0 0.0
none
0.0
0.0
0.0
```

14. Here is an example of valid barrier parameters if the number of barriers specified is greater than zero. These lines are repeated for each specified barrier. The comment line generally describes the following parameters. The first two lines are the end point X,Y coordinates of a line transect in meters (the barrier location is specified as a line transect with a fixed width). The type of barrier (name associated with the barrier) is listed in the third line. The average height of the barrier in meters is specified in the fourth line. The width of the barrier in meters is specified in the fifth line. The sixth line is the average optical porosity through the entire width of the barrier and is specified as a decimal fraction. All six input lines are repeated for each barrier specified.

```

# RFD-BarrierN coordinates (meters) | type | height (meters) | width (meters) |
porosity
0 804.7
804.7 819.98
Trees 3row conifer estb
10.668
15.2755092
0.4

```

Note that the WEPS interface currently restricts the placement of barriers on the simulation site (field) borders and must be the full length of the border. Therefore, a maximum of four barriers is allowed at this time.

15. The following lines that include the "Shape" and "Radius" fields are used only by the WEPS interface to keep track of the site shape options. Neither parameter is currently used by the WEPS science model, so these two lines are read but ignored.

The shape for a simulation region is currently defined as a rectangular shape (including a square), which is used by the WEPS science model. However, to more easily provide NRCS users the ability to apply the model to other physical shapes, such as circular and half-circular fields, the interface now lists several non-rectangular options. These non-rectangular shapes are then converted to a rectangular shape of the same area for use in the WEPS science model. The shape options are: (a) rectangle; (b) square; (c) circle; (d) eastern half-circle; (e) western half-circle; (f) southern half-circle; (g) northern half-circle; (h) northeast quarter-circle; (i) southeast quarter-circle; (j) southwest quarter-circle; and (k) northwest quarter-circle.

When a circle or partial circle has been selected, the radius of the circle is specified on the 2nd line in meters. This allows the interface to re-display the selected non-rectangular shape and size (radius) appropriately if the WEPS Run file is reloaded into the WEPS interface. When the interface outputs a new WEPS Run file, it will use the radius value specified for non-rectangular shapes to determine the representative rectangular region coordinates (length and width values). The radius value is ignored by the interface for rectangular and square site selections and the length and width values are used, which are specified earlier within the WEPS Run file and previously discussed.

```

# --CIRCULAR FIELD INFORMATION
# Note: These fields are not used by the weps simulation.
#       The shape and radius values are used by the user
#       interface to approximate a rectangular field. They
#       are included here so the reports can display the
#       correct field shape.
#
# RFD-Shape
rectangle
# RFD-Radius
454

```

16. The next input line consists of the water erosion loss estimate, which is only used for the "Soil Quality Index" calculation in the WEPS science model. It is not used in the estimates for wind erosion. The value is in units of kg m⁻².

```

# RFD-WaterErosionLoss
0.00

```

17. The “soil rock fragments” is listed in the last input line and refers to the volume fraction of rocks in the surface layer. Since this value can change significantly over many years as a result of tillage and erosion, NRCS requested that this parameter be made accessible in the main interface screen to override the default value in the soil record, if necessary. A value of -1.0 tells the WEPS science model to use the value in the soil database record. This value is converted to an area fraction to provide estimates of the non-erodible surface fraction.

18.

```
#   RFD-SoilRockFragments
0.0
#----- END OF SIMULATION RUN FILE -----
```

WEPS Soil IFC File

The WEPS Soil Initial Field Conditions (IFC) file (soilfilename.ifc) contains the soil and surface initial condition parameters used by WEPS. It specifies the soil taxonomic order, the initial soil surface condition excluding vegetation and the soil layer information. Both temporal (i.e., vary over time) and intrinsic (i.e., remain constant during the simulation unless mixing between soil layers occurs) soil parameters are input into the WEPS science model from the Soil IFC file. The Soil IFC file’s location and name are specified in the WEPS Run file. Some parameters listed are not required for the WEPS science model but are included to indicate the source of the data and the taxonomic information about the soil record. This information is used by the WEPS interface, for reporting and information purposes. Although the file format is adequately documented within the file for the user to create and edit a WEPS Soil IFC file manually, the user is strongly encouraged to create WEPS Soil IFC files through the WEPS interface since the interface checks for invalid inputs (e.g., out of range values). This will ensure that the WEPS Soil IFC files meet the requirements of the WEPS science model.

The format of the WEPS Soil IFC file consists of comment lines, which begin with a # character followed by input lines that contain the data. The comment lines are ignored by the WEPS science model when reading in the data. The WEPS interface generates and includes some comments by default to make the file more readable for users viewing the WEPS Soil IFC file, however, they are not always 100% accurate in their description of the following input lines. The generated comment lines are provided for general reference only along with the data input lines in the example soil IFC file.

Some data lines consist of multiple values, separated by white space(s), specifically for soil layer parameters, which will be identified below. There are additional comments that may exist at the bottom of the WEPS Soil IFC file that specifies which parameters may have been estimated by the interface, if missing or out of range, in the NRCS SSURGO database record used to create the Soil IFC file. The NRCS SSURGO database is the primary source for most WEPS Soil IFC file data.

Note that the soil interface (tabular) screen is accessible through the WEPS interface. It has been designed to function as a standalone viewer (as primarily used in WEPS and exclusively so for NRCS users) and, if enabled through the WEPS interface configuration settings, as a soil record editor. The user can start from an existing Soil IFC file to modify or create a new record or create a new record from scratch. In addition, there is a feature in the Soil interface that allows a minimum set of parameters to be specified and

the remainder to be estimated to create a complete Soil IFC record. This process is described in detail at the end of this section.

The first group of 5 input lines in the IFC file contains informational data listed in Table 2. None of this information is required for the WEPS science model to operate but is used in some output reports for informational purposes. They are also used within the WEPS interface for soil record identification purposes. The next group of 5 input lines (lines 6-10) in the IFC file contains most of the surface soil data parameters listed in Table 3. Two parameters, dike height and dike spacing, are missing. Therefore, these two parameters cannot currently be set from within an IFC file. Table 4 lists the 42 (lines 11-52) soil layer properties. Many soil properties can be estimated if missing from the NRCS SSURGO soil database record with the estimation equations listed as necessary. The list of minimum required soil properties is provided in Table 5.

Table 3. Informational soil data provided in the WEPS Soil IFC file.

Line	Input Item	Data Type	Description
1	Version Number	string	Version of WEPS Soil IFC file. The current version is 1.0.
2	Soil ID	string	Coded concatenated taxonomic information which includes the NRCS soil survey ID, NRCS map unit symbol, soil component name, soil component percent, USDA surface texture class, state and county soil exists in and the NRCS soil survey name the soil record refers to.
3	Local Phase	string	Lists the local soil phase if known, otherwise defaults to “unknown”.
4	Soil Order	string	Lists the official NRCS soil order class the soil belongs to.
5	Soil Loss Tolerance	integer	Defined by NRCS as the maximum amount of erosion at which the quality of a soil as a medium for plant growth can be maintained. Its value can range from 1 to 5 with units of (tons ⁻¹ ac ⁻¹ yr ⁻¹).

Table 4. Surface soil data provided in the WEPS Soil IFC file.

Line	Input Item	Data Type	Units	Absolute Range (Typical values)	Description
6	Dry soil albedo	float	unitless	0.0 – 1.0 (0.05 – 0.25)	Ratio of incident short-wave (solar) radiation reflected by the less than 2 mm soil fraction on the soil surface.
7	Slope gradient	float	m·m ⁻¹	0.0 – 0.999 (0.0 – 0.3)	Difference in elevation between two points on the overall field surface.
8	Surface rock fragment cover	float	m ² ·m ⁻²	0.0 - 1.0 (0.0 - 0.5)	Fraction of surface area covered by rock greater than 2.0 mm in diameter (m ² m ⁻²).
9	Depth to bedrock	float	mm	≥0.0	Depth to the bedrock layer (mm). If not available, a default value of 99990 is used.
10	Depth to root restrictive layer	float	mm	≥0.0	Depth to the first root restrictive soil layer (mm). If not available, a default value of 99990 is used.
34	Crust thickness	float	mm	0.0– 23.0 (0.0 – 10.0)	Average thickness of the consolidated zone in the surface layer. The default value is 0.01.
35	Crust density	float	Mg·m ⁻³	0.6 – 2.0 (0.8 – 1.6)	Density of the soil crust. The value currently defaults to the surface layer aggregate density value (line 32).
36	Crust stability	float	ln (J kg ⁻¹)	0.1 – 7.0 (0.3 – 5.0)	Mean of the natural log of crust crushing energies. The default value is set to the surface layer aggregate stability value (line 33).
37	Crust surface fraction	float	m ² ·m ⁻²	0.0 – 1.0	Surface area fraction covered with consolidated soil. The default is 0.0.
38	Mass of LEM (loose erodible material)	float	kg·m ⁻²	0.0 – 3.0 (0.0 – 1.0)	Mass of loose, saltation size, erodible soil material on surface crust area. The default is set to 0.0.

39	Fraction of LEM	float	m ² ·m ⁻²	0.0 – 1.0 (0.0 – 0.5)	Cover fraction of loose, saltation size, erodible material on surface crust area. Value cannot exceed the fraction of surface crust cover area (line 37). The default value is 0.0.
40	RR (Random Roughness)	float	mm	1.0 – 70.0 (2.0 – 10.0)	Value defined as the standard deviation of the elevation from a plane of a random soil surface, including any flat biomass adjusted as suggested by Allmaras et. al. (1967).
41	Ridge orientation	float	degrees	0.0 – 180.0	Direction of tillage ridge, clockwise from true north. The default is 0.0.
42	Ridge height	float	mm	0.0 – 500.0 (0.0 – 300.0)	Height of soil ridges from the bottom of the furrow to the top of the ridge. The default is 0.0.
43	Ridge spacing	float	mm	10.0 – 2000.0 (60.0 – 1000.0)	Spacing between ridge tops. The default is 10.0.
44	Ridge width	float	mm	10.0 – 4000.0 (100.0 – 2000.0)	Width of ridge tops (bed top width). The default is 10.0.
N/A	Dike height	float	mm	0.0 – 500.0 (0.0 – 300.0)	Height of soil dike ridges from the bottom of the furrow to the top of the dike ridge. The default value is 0.0. This parameter is currently missing in the Soil IFC file.
N/A	Dike spacing	float	mm	0.0 – 2000.0 (0.0 – 1000.0)	Spacing between soil dike ridges. The default value is 0.0. This parameter is currently missing in the Soil IFC file.

Table 5. Soil layer data provided in the WEPS Soil IFC file.

Line	Input Item	Data Type*	Units	Absolute Range (Typical Range)	Description
11	Number soil layers	integer		≥ 1	Number of soil layers specified in the soil record.
12	Soil layer thickness	float (array)	mm	>0.0	Thickness of each soil layer (mm)
13	Sand	float (array)	kg kg ⁻¹	0.0 – 1.0	Mass fraction of mineral particles of equivalent size (0.05 to 2.0 mm) of the less than 2.0 mm soil fraction of the bulk soil.
14	Silt	float (array)	kg kg ⁻¹	0.0 – 1.0	Mass fraction of mineral particles of equivalent size (0.002 to 0.05 mm) of the less than 2.0 mm soil fraction of the bulk soil.
15	Clay	float (array)	kg kg ⁻¹	0.0 – 1.0	Mass fraction of mineral particles of equivalent size (<0.002 mm) of the less than 2.0 mm soil fraction of the bulk soil.
16	Rock fragments	float (array)	m ³ m ⁻³	0.0 – 1.0	Volume fraction of the layer occupied by the 2.0 mm or larger (20 mm or larger for wood fragments) on a whole soil basis.
17	Very coarse sand	float (array)	kg kg ⁻¹	0.0 – 1.0	Mass fraction of mineral particles of equivalent size (1.0 to 2.0 mm) of the less than 2.0 mm soil fraction of the bulk soil.
18	Coarse sand	float (array)	kg kg ⁻¹	0.0 – 1.0	Mass fraction of mineral particles of equivalent size (0.5 to 1.0 mm) of the less than 2.0 mm soil fraction of the bulk soil.
19	Medium sand	float (array)	kg kg ⁻¹	0.0 – 1.0	Mass fraction of mineral particles of equivalent size (0.2 to 0.5 mm) of the less

					than 2.0 mm soil fraction of the bulk soil.
20	Fine sand	float (array)	kg kg ⁻¹	0.0 – 1.0	Mass fraction of mineral particles of equivalent size (0.1 to 0.2 mm) of the less than 2.0 mm soil fraction of the bulk soil.
21	Very fine sand	float (array)	kg kg ⁻¹	0.0 – 1.0	Mass fraction of mineral particles of equivalent size (0.05 to 0.1 mm) of the less than 2.0 mm soil fraction of the bulk soil.
22	Bulk density (1/3 bar)	float (array)	Mg m ⁻³	>0.0 – 10.0 (0.8 – 1.6)	Oven dry weight of the less than 2 mm soil material per unit volume of soil at a tension of 1/3 bar.
23	Organic matter	float (array)	kg kg ⁻¹	0.0 – 1.0 (0.0005 – 0.05)	Mass fraction amount by weight of decomposed plant and animal residue of the less than 2 mm soil fraction of the bulk soil.
24	Soil pH	float (array)	unitless	1.0 – 14.0 (4.0 - 9.0)	Negative logarithm to base 10 of the hydrogen ion activity of the soil by the 1:1 soil:water ratio method. It is a numerical expression of the relative acidity or alkalinity of a soil.
25	CaCO ₃	float (array)	kg kg ⁻¹	0.0 - 1.0 (0.0 – 0.3)	Calcium carbonate equivalent of carbonate (CO ₃) in the soil expressed as CaCO ₃ as a mass fraction of the < 2 mm size fraction of the bulk soil.
26	CEC	float (array)	meq 100g ⁻¹	0.0 – 400.0	Cation exchange capacity.
27	Linear extensibility	float (array)	m ³ m ⁻³	0.0 – 30.0	Linear extensibility is the volume difference of natural soil fabric at 1/3 or 1/10 bar water content and oven dryness. The volume change is reported as a percentage change for the whole soil.
28	GMD	float (array)	mm	0.03 – 30.0 (0.1 – 15.0)	Soil geometric mean diameter of the modified log-normal

					description of the aggregate size distribution.
29	GSD	float (array)	unitless	1.0 – 20.0 (4.0 – 15.0)	Soil geometric standard deviation of the modified log-normal description of the aggregate size distribution.
30	Maximum agg size	float (array)	mm	1.0 – 1000.0 (2.0 – 100.0)	Maximum size geometric diameter of the modified log-normal description of the aggregate size distribution.
31	Minimum agg size	float (array)	mm	0.001 - 5.0 (0.006 - 0.020)	Minimum size geometric diameter of the modified log-normal description of the aggregate size distribution.
32	Aggregate density	float (array)	Mg·m ⁻³	0.6 – 2.5 (0.8 – 2.0)	Mean density of aggregates.
33	Aggregate stability	float (array)	ln (J kg ⁻¹)	0.1 – 7.0 (0.5 – 5.0)	Aggregate stability is the mean of the natural log of the aggregate crushing energies.
45	Bulk density (initial)	float (array)	Mg·m ⁻³	>0.0 – 10.0 (0.8 – 1.6)	Oven dry weight of the less than 2 mm soil material per unit volume of soil at initial soil water content.
46	SWCi	float (array)	m ³ m ⁻³	Varies with soil texture	Initial soil water content.
47	SWCsat	float (array)	m ³ m ⁻³	Varies with soil texture	Saturated soil water content (when all soil pores are filled with water, i.e. zero soil water matric potential).
48	SWCfc	float (array)	m ³ m ⁻³	Varies with soil texture	SWC field capacity is amount of soil water retained at 1/3 bar (33 kPa) expressed as a fraction of the less than 2 mm, oven dry soil by volume.
49	SWCwp	float (array)	m ³ m ⁻³	Varies with soil texture	SWC wilting point is the amount of soil water retained at 15 bar (1500 kPa) expressed as a fraction of the less than 2 mm, oven dry soil by volume.
50	Soil CB	float (array)	unitless	0.1917 – 27.027	Soil CB is the power of Campbell's model of soil water characteristic curve.

51	Air entry potential	float (array)	J kg ⁻¹	-17.91 – 0.0	Potential at which the largest water filled pores start to drain and hence gas flow can be observed.
52	Saturated hydraulic conductivity	float (array)	m s ⁻¹	0.0 – 0.001	Amount of water that would move vertically through a unit area of saturated soil in a unit time under a unit hydraulic gradient.

*All array values refer to the soil layers.

Table 6. Minimum soil data required for estimating all other properties in a WEPS Soil initial field conditions (IFC) record.

Soil Table				
Input Item	Data Type*	Units	Absolute Range (Typical Values)	Description
Number soil layers	Integer	unitless	≥1	Number of soil layers specified in the soil record.
Soil layer thickness	float (array)	mm	>0.0	Thickness of each soil layer (mm)
Organic matter	float (array)	kg kg ⁻¹	0.0 - 1.0 (0.0005 - 0.05)	Mass fraction amount by weight of decomposed plant and animal residue of the less than 2 mm soil fraction of the bulk soil.
Sand	float (array)	kg kg ⁻¹	0.0 - 1.0	Mass fraction of mineral particles of equivalent size (0.05 to 2.0 mm) of the less than 2.0 mm soil fraction of the bulk soil.
Clay	float (array)	kg kg ⁻¹	0.0 - 1.0	Mass fraction of mineral particles of equivalent size (<0.002 mm) of the less than 2.0 mm soil fraction of the bulk soil.
Very fine sand	float (array)	kg kg ⁻¹	0.0 - 1.0	Mass fraction of mineral particles in equivalent diameter size range (0.05 to 0.1 mm) of the less than 2.0 mm soil fraction of the bulk soil.
Bulk density (1/3 bar)	float (array)	Mg m ⁻³	>0.0 - 10.0 (0.8 - 1.6)	Oven dry weight of the less than 2 mm soil material per unit volume of soil at a tension of 1/3 bar.

CaCO ₃	float (array)	kg kg ⁻¹	0.0 - 1.0 (0.0 - 0.3)	Calcium carbonate equivalent is the carbonate (CO ₃) in the soil expressed as CaCO ₃ and is the mass fraction of the < 2 mm size fraction of the bulk soil.
-------------------	------------------	---------------------	--------------------------	--

*All array values refer to the soil layers.

Input lines from an example IFC file are provided below along with the one-line comment fields generated from the WEPS user interface when creating the file from an NRCS SSURGO data record. A very brief description of the individual inputs is provided. Additional detailed information for all the input parameters listed in this file is provided in Tables 2, 3, and 4. Note that the numbers in Tables 2, 3, and 4 represent the input line number in the IFC file and can be used to reference the same input soil-related parameters in the three tables.

1. The first line of the IFC file lists the version number.
Version: 1.0
2. Soil Identification (ID) information extracted from the NRCS SSURGO database record. This line consists of the soil identification string, which is a concatenated list separated by dashes "-", which includes the NRCS Soil Survey ID, the Map Unit Symbol, the soil component name, the soil component percent, the surface texture class based upon the USDA system for particle size, the State, the county and the Soil Survey Area Name the soil record refers to.
Soil ID
TX011-Gr-Tascosa-100-GR_L-Texas-Armstrong County-Armstrong County, Texas
3. Soil phase if known. Otherwise this is populated with the string "unknown".
Local Phase
unknown
4. Taxonomic Soil Order. If unknown, it is populated with the string "unknown".
Soil Order
Mollisols
5. Soil Loss Tolerance for the soil.
Soil Loss Tolerance (tons/acre/year)
1
6. Surface soil albedo (fraction). The absolute range is 0.0 to 1.0, with a typical range of 0.05 to 0.25. If it is unavailable, it is estimated using the methods of Baumer (1990) and Post, et al (2000).
Dry soil albedo (fraction)
0.230
7. Slope gradient (m/m). If no value is available in the SSURGO record a value of 0.01 is used. The parameter should have been previously set in the WEPS Run file. If so, then the following applies: (a) a previous slope value < -1.5 from the WEPS Run file implies a level basin field condition with no runoff expected. The slope value is then set to 0.0, the depressional storage is set to 0.5 m and the value in the IFC file is ignored; (b) a previous slope value <0.0 and >-1.5 set in the WEPS Run file means

that the value in the IFC file is read in and used (if that value happens to be negative for some reason, then it is set to a value of 0.01); and (c) if the previous value is >0.0 from the WEPS Run file, then that value is used and the value in the IFC file is ignored.

```
# Slope gradient (fraction)
0.180
```

8. Surface rock fragment cover is input on the next line. It is estimated using the surface layer fragment volume from the NRCS SSURGO database.

```
# Surface fragment cover or surface layer fragments (area fraction)
0.0
```

9. Observed depth to the top of the bedrock layer (mm), if present, is specified on the next line. A default value of 99990 is used if the value is not provided in the NRCS SSURGO database.

```
# Depth to bedrock (mm)
99990
```

10. Depth to the upper boundary of a restrictive layer (mm), if present. A default value of 99990 is used if the value is not provided in the NRCS SSURGO database.

```
# Depth to root restricting layer (mm)
99990
```

The Soil IFC file contains 11 additional surface properties which are listed within the layer properties below (line numbers 34 – 44) and are explicitly mentioned where they exist in a properly formatted Soil IFC file. These additional surface properties are documented in Table 3.

11. The number of soil layers in the soil record. This is typically determined by the number of soil horizons for which soil properties are reported in the NRCS SSURGO database. It is not necessarily the total number of soil layers used by WEPS because WEPS usually is configured to define the soil layers according to a pre-determined scheme. The following WEPS science model command line arguments (-L # and -l #) specify how the original soil layers are split within WEPS. The -L option specifies the minimum soil layer thickness to scale layer splitting (mm). The -l option specifies the rate of soil layer thickness increase with depth (%) for layer splitting in percent increase of layer thickness. The default values are -L2 and -l25, thus the surface layer is set to the first value (2 mm) and each succeeding layer is increased by 25%. Soil properties from the original soil layers are mapped into these new layers based on their overlap. When two original soil layers intersect one of the new soil layers, the new soil layer uses properties which are a weighted average of the two original soil layer property values. This means that the layers in the soil record are usually split after WEPS reads the WEPS IFC file to meet those requirements. There is no combining of the soil layers specified in the soil record by WEPS. At least one soil layer is required.

```
# Number of layers
3
```

All subsequent soil layer properties are specified for each layer on the same line separated by white space (spaces) with the surface layer value first and the subsequent deeper layer values following in order by depth.

12. Thickness of each soil layer. Required input for each layer specified (not estimated).

```
# Layer thickness (mm)
200      310      1010
```

The next three input lines specify the sand, silt, and clay particle size mass fractions of each soil layer. Each is the mass fraction of the mineral particles of the specified size range (Table 4) for the < 2.0 mm portion of the whole soil. The values of all three must sum to 1.0 for each layer. Required input for each layer specified (not estimated).

13. Sand mass fraction for each soil layer.

```
# Sand fraction
0.453    0.453    0.453
```

14. Silt mass fraction for each soil layer (if data is estimated using the Soil Viewer/Editor or obtained from the NRCS NASIS database, this value is computed using the sand and clay fraction values so that the sum of the three fractions equals 1.0).

```
# Silt fraction
0.432    0.432    0.432
```

15. Clay mass fraction for each soil layer.

```
# Clay fraction
0.115    0.115    0.115
```

16. Rock fragments for each layer, which is defined as the volume fraction of the layer occupied by the > 2.0 mm (> 20 mm for wood fragments) on a whole soil basis ($\text{m}^3 \text{m}^{-3}$). The surface layer fraction (1st value) can be overridden if the appropriate value is set in the WEPS Run file. If no value is available in the NRCS SSURGO database, it is set to 0.0. The WEPS GUI asks for this information as the surface cover fraction of rocks on a cover basis ($\text{m}^2 \text{m}^{-2}$) because users relate to that value better than the volume fraction. WEPS assumes that they are the equivalent units in this case for the surface layer.

```
# Rock fragments
0.220    0.400    0.390
```

The next five input lines consist of the sand fractions by layer. Each are defined as a size range of mineral particles (see Table 4 for specific size ranges) in equivalent diameter as a mass fraction of the less than 2.0 mm soil fraction of the bulk soil. The sum of the sand fractions for each layer must equal the total sand fraction for the layer listed earlier in the IFC file (input line 13).

17. Very coarse sand mass fraction by layer.

```
# Sand fraction very coarse
0.045    0.045    0.045
```

18. Coarse sand mass fraction by layer.

```
# Sand fraction coarse
0.061    0.061    0.061
```

19. Medium sand mass fraction by layer.

```
# Sand fraction medium
0.081    0.081    0.081
```

20. Fine sand mass fraction by layer.

```
# Sand fraction fine
0.139    0.139    0.139
```

21. Very fine sand mass fraction by layer.

Sand fraction very fine
0.127 0.127 0.127

22. 1/3 bar bulk density value by layer. Required input for each layer (not estimated).

Bulk Density (1/3 bar) (Mg/m³)
1.530 1.530 1.530

23. Organic matter content by layer. Required input by layer (not estimated).

Organic matter (kg/kg)
0.0200 0.0055 0.0055

24. Soil pH by layer.

Soil PH (0-14)
8.20 8.20 8.20

25. Calcium carbonate equivalent by layer. Required input by layer (not estimated).

Calcium carbonate equivalent (CaCO₃)
0.06 0.18 0.40

26. Cation exchange capacity (CEC) by layer. Estimated with the following equation:

$$\text{CEC} = \text{clay} * 0.5 + \text{om} * 2.0 \quad [1]$$

where

clay = the clay content in percent, and

om = the organic matter in percent.

Cation exchange capacity (CEC) (meq/100g)
6.00 6.00 6.00

27. Linear extensibility by layer. Estimated by NRCS Soil Survey Staff (1996) method.

Linear extensibility
1.500 1.500 1.500

The next four input lines contain the parameters required for a 4-parameter modified log-normal description of the soil aggregate size distribution for each layer. The initial values are estimated using the given equations. The four parameters are:

- a. Aggregate Geometric Mean Diameter
- b. Aggregate Geometric Standard Deviation
- c. Maximum Aggregate Size
- d. Minimum Aggregate Size

28. Aggregate geometric mean diameter by layer. This is defined as the soil geometric mean diameter of the modified log-normal equation representing the aggregate size distribution. The value is estimated by:

$$\text{agg_gmd} = \exp(1.343 - 2.235 * \text{sand} - 1.226 * \text{silt} - 0.0238 * \text{sand/clay} + 33.6 * \text{om} + 6.85 * \text{CaCO}_3) * (1.0 + 0.006 * \text{bottom of layer depth}) \quad [2]$$

where

agg_gmd = geometric mean diameter (mm),

sand = fraction of sand (0.05-2 mm) in the layer,

silt = fraction of silt (0.002-0.05 mm) in the layer,
 clay = fraction of clay (< 0.002 mm) in the layer,
 om = fraction of organic matter in the layer, and
 CaCO₃ = equivalent calcium carbonate (kg kg⁻¹), and
 bottom of layer depth = depth to the bottom of the layer being considered (mm).

```
# Aggregate geometric mean diameter (mm)
4.848      12.505      30.000
```

29. Aggregate geometric standard deviation by layer. This is defined as the soil geometric standard deviation of the modified log-normal equation representing the aggregate size distribution. The value is estimated as:

$$\text{agg_gsd} = 1.0 / (0.0203 + 0.00193(\text{agg_gmd}) + 0.074 / (\text{agg_gmd})^{0.5}) \quad [3]$$

where

agg_gsd = geometric standard deviation (mm/mm), and

agg_gmd = geometric mean diameter (mm).

```
# Aggregate geometric standard deviation
14.962      14.351      9.671
```

30. Maximum aggregate size by layer. This is defined as the upper size limit of the modified log-normal equation representing the aggregate size distribution. The value is estimated by:

$$\text{agg_max_size} = (\text{agg_gsd})^p * (\text{aggr. gmd}) + 0.84 \quad [4]$$

where

$$p = 1.52 * (\text{agg_gsd})^{-0.449}$$

agg_gsd = geometric standard deviation (mm/mm), and

agg_gmd = the geometric mean diameter (mm).

```
# Maximum aggregate size (mm)
36.703      45.998      63.446
```

31. Minimum aggregate size by layer. This is defined as the lower size limit of the modified log-normal equation representing the aggregate size distribution. The value assigned by default for the minimum aggregate size is 0.01.

```
# Minimum aggregate size (mm)
0.010      0.010      0.010
```

32. Aggregate density values for each layer. This is estimated, if not available in the NRCS SSURGO database, using the method of Rawls (1983) where:

$$\text{agg_density} = 2.0 \quad \text{when bottom_of_layer_depth} > 300 \text{ mm}$$

otherwise, [5]

$$\text{agg_density} = 2.01 * ((0.72 + 0.00092 * \text{bottom_of_layer_depth})$$

where

agg_density = average density of aggregates (Mg m⁻³)

bottom_of_layer_depth = depth to bottom of layer (mm).

```
# Aggregate density (Mg/m^3)
1.800      1.800      1.800
```

33. Dry aggregate stability values for each layer. This is defined as the mean of the natural log of the aggregate crushing energies. It is estimated, if not available in the NRCS SSURGO database, where:

$$\text{dry_agg_stability} = 0.83 + 15.7 * \text{clay} - 23.8 * \text{clay}^2 \quad [6]$$

where

dry_agg_stability = stability of dry aggregates ($\ln(\text{J m}^{-2})$), and
clay = fraction of clay content.

```
# Aggregate stability (ln(J/m^2))
2.321      2.321      2.321
```

The next 11 lines (line numbers 34 – 44) contain the remainder of the surface properties that exist in a WEPS Soil IFC file as specified with the current file format. The first six lines six lines (lines 34 – 39) define the surface crust properties, if a crust exists.

34. Crust thickness.

```
# Crust thickness (mm)
0.010
```

35. Crust density.

```
# Crust density (Mg/m^3)
1.800
```

36. Crust dry stability is the natural log of the average crust crushing energy.

```
# Crust stability (ln(J/m^2))
2.32
```

37. Crust surface cover fraction is the fraction of the surface covered with a crust.

```
# Crust surface fraction (m^2/m^2)
0.00
```

38. Mass of loose erodible material (LEM) residing on the crusted portion of the surface.

```
# Mass of loose material on crust (kg/m^2)
0.00
```

39. Cover fraction of LEM on the crusted portion of the surface.

```
# Fraction of loose material on crust (m^2/m^2)
0.00
```

40. Surface random roughness value as defined by Allmaras et. al. (1967). The default value is set to 4.0.

```
# Random roughness (mm)
4.00
```

The following four input lines (Lines 41 – 44) define the oriented roughness of the surface. The ridge orientation is the direction of the tillage ridge, clockwise from true north. The ridge height is the height of soil ridges from the bottom of the furrow

to the top of the ridge. Ridge spacing is the spacing between ridge tops. The ridge width is the width of the ridge top (i.e., bed width). Note that dike height and dike spacing are not included in the IFC file (accidentally left out of the file specification). WEPS currently initializes both variables to zero. They can be initialized to alternative values by using a special management operation configured to run only once and be set to the first date of the simulation.

41. Ridge orientation.

```
# Ridge orientation (deg)
0.00
```

42. Ridge height.

```
# Ridge height (mm)
0.00
```

43. Ridge spacing.

```
# Spacing between ridge tops (mm)
10.00
```

44. Ridge width.

```
# Ridge width (mm)
10.00
```

45. Initial bulk density value by layer at the current water content. This is a required input by layer (values are not estimated). Note the comment line being written into the file by the WEPS interface immediately prior to the initial layer bulk density parameter values incorrectly mentions (1/3 bar) for the water content value of these bulk density values. The initial layer water content values are provided on the following line (46), which can be 1/3 bar, but are not by default.

```
# Initial Bulk Density (1/3 bar) (Mg/m^3)
1.530 1.530 1.530
```

46. Initial soil water content for each layer. The initial value defaults to:

$$wc_i = 0.5 * (wc_{fc} + wc_{wp}) \quad [7]$$

where

wc_i = initial soil water content value ($m^3 m^{-3}$) at beginning of simulation,

wc_{fc} = soil water content value at field capacity ($m^3 m^{-3}$), and

wc_{wp} = soil water content value at wilting point ($m^3 m^{-3}$).

```
# Initial soil water content (m^3/m^3)
0.140 0.086 0.090
```

47. Saturated water content for each layer. It is estimated using Saxton's method (1986) and is based upon soil texture.

```
# Saturation soil water content (m^3/m^3)
0.434 0.434 0.434
```

48. Field capacity water content for each layer. It is estimated using Saxton's method (1986) and is based upon soil texture.

```
# Field capacity water content (m^3/m^3)
0.202 0.130 0.136
```

49. Wilting point water content for each layer. It is estimated using Saxton's method (1986) and is based upon soil texture.

```
# Wilting point water content (m^3/m^3)
0.078      0.043      0.045
```

50. Soil CB value by layer. It is estimated using Saxton's method (1986) and is based upon soil texture.

```
# Soil CB value (exponent to Campbell's SWRC)
4.256      4.256      4.256
```

51. Air entry potential by layer. It is estimated using Saxton's method (1986) and is based upon soil texture.

```
# Air entry potential (J/kg)
-2.514     -2.514     -2.514
```

52. Saturated hydraulic conductivity by layer. It is estimated using Saxton's method (1986) and is based upon soil texture.

```
# Saturated hydraulic conductivity (m/s)
9.0E-6     9.0E-6     2.8E-5
```

Additional comments are included at the end of the IFC file in a "Notes" section when the WEPS interface creates the file based upon the selected soil record from the NRCS SSURGO database. Examples of typical information generated are provided here.

```
# Notes:
## INFORMATION: Tabular Version: 8
## WARNING: Local Phase (localphase) is missing. Null value was substituted with
'unknown'.
## WARNING: Bedrock Depth (bedrockDepth) is missing. Null value was substituted
with '9999.0'.
## WARNING: Impermeable/Restrictive Depth (resdept_r_min) is missing. Null value
was substituted with '9999.0'.
## WARNING: Aggregate geometric mean diameter (mm) adjusted: old value 140.6782
new value 30.0
```

Minimum required soil inputs (estimating all other soil properties)

If there is a need to create a new WEPS Soil IFC record and one does not know the majority of the soil property values contained in an IFC file, the user can create a new IFC record by specifying a minimum list of soil parameters within the IFC editor and it will estimate the remaining parameters to create a complete Soil IFC record. The list of minimum soil parameters is identified in Table 5. Once the "Estimate" button is selected in the Soil IFC editor, the table views displays all the soil parameters and the user can modify the values as necessary. Note that the estimate feature and the editing capabilities of the IFC editor can be disabled through WEPS interface configuration settings if so desired.

WEPS Management/Crop Rotation File

The WEPS Management/Crop Rotation file (manfilename.man) contains the date ordered list of management operations and when crops are planted and harvested, along with the necessary parameter values describing the operations and how to simulate the growing of crops for the selected rotation cycle. The ".man" filename extension is short for "management" and is the expected extension for all WEPS Management/Crop Rotation

files. The Management/Crop Rotation file's location and name are specified in the WEPS Run file. It consists of some parameters that are not required for the WEPS science model but are included to indicate the source of the data and information about the management file record. This information is used by the WEPS interface for reporting and information purposes. Although the file format is adequately documented for the user to create and edit a WEPS Management/Crop Rotation file manually, it is strongly encouraged for the user to create these files through the WEPS interface using the WEPS Management/Crop Rotation Editor (MCREW). This will ensure that the WEPS Management/Crop Rotation files meet the input requirements of the WEPS science model.

The format of the WEPS Management/Crop Rotation file consists of comment lines, which begin with a # character and other input lines that contain the data. The comment lines are, in general, ignored by the WEPS science model when reading in the data. The WEPS interface generates and includes some comment lines by default to make the WEPS Management/Crop Rotation file somewhat more readable for users viewing it; however, these comments may not be fully accurate in their descriptions.

The WEPS Management/Crop Rotation file format is a little different than the format specified for the previously discussed input files (i.e., the WEPS Run file and the WEPS Soil IFC file). This was required because the order and number of the inputs (operations and parameters) vary widely from file to file, depending upon the management/crop rotation being simulated. Tables 6-11 list the full selection of management operation processes available in WEPS. These processes are selected and correctly ordered to best represent the real-world effects of the operation on the soil, surface, and vegetation state within the WEPS simulation model. Each process may contain a list of parameters that describe the degree to which that effect occurs within the simulation. For many common parameters among the processes, several operation level (Table 6) and group processes (Table 7) have also been defined so that these parameters can be shared and not be repeatedly specified as input into the model if their values are not changing between processes.

Table 7. Operation level parameters used in WEPS.

Code	Operation Name	Parameter Name	Variable Name	Type	Units	Parameter Definition
00	Initialization	Operation note	sop_notes0	string	N/A	Text information regarding operation.
01	Direction and Speed	Operation speed	ospeed	float	m s ⁻¹	Operation travel speed.
		Operation direction	odirect	float	degrees	Travel direction clockwise from true north.

		Standard speed	ostdspeed	float	m s ⁻¹	Speed at which some of the physical processes, like residue burial efficiency, have coefficients specified. In WEPS, many of these coefficients are then adjusted internally based on travel speed, as well as other parameters.
		Minimum speed	ominspeed	float	m s ⁻¹	Minimum operation travel speed. This value determines the lower limit at which WEPS will adjust certain process-specific parameters that are influenced by speed.
		Maximum speed	omaxspeed	float	m s ⁻¹	Maximum operation travel speed. Value determines the upper limit at which WEPS will adjust certain process-specific parameters that are influenced by speed.
		Operation notes	op_notes1	string	N/A	Text information regarding operation.
02	Others	Operation notes	op_notes2	string	N/A	Text information regarding operation.
03	Energy STIR Direction and Speed	Energy per unit area	oenergyarea	float	l ha ⁻¹	Diesel energy units (in liters) consumed per unit area covered.

Stir	ostir	float	unitless	Soil Tillage Intensity Rating (STIR) value assigned to the operation.
Operation speed	ospeed	float	m s ⁻¹	Operation travel speed.
Operation direction	odirect	float	degrees	Travel direction clockwise from north.
Standard speed	ostdspeed	float	m s ⁻¹	Speed at which some of the physical processes, like residue burial efficiency, have coefficients specified. In WEPS, many of these coefficients are then adjusted internally based upon travel speed, as well as other parameters.
Minimum speed	ominspeed	float	m s ⁻¹	Minimum operation travel speed. This value determines the lower limit at which WEPS will adjust certain process-specific parameters that are influenced by speed.
Maximum speed	omaxspeed	float	m s ⁻¹	Maximum operation travel speed. This value determines the upper limit at which WEPS will adjust certain process-specific parameters that are influenced by speed.

		Operation notes	op_notes3	string	N/A	Text information regarding operation.
		Fuel	ofuel	string		Parameter currently not used.
04	Energy STIR Others	Energy per unit area	oenergyarea	float	l ha ⁻¹	Diesel energy units (in liters) consumed per unit area covered.
		Stir	ostir	float	unitless	STIR value assigned to the operation.
		Operation notes	op_notes4	string	N/A	Text information regarding operation.
		Fuel	ofuel	string	N/A	Parameter currently not used.

Table 7. Group level parameters used in WEPS.

Code	Operation Name	Parameter Name	Variable Name	Type	Units	Parameter Definition
00	Initialization	Operation note	sop_notes0	string	N/A	Text information regarding operation
01	Direction and Speed	Operation speed	ospeed	float	m s ⁻¹	Operation travel speed
		Operation direction	odirect	float	degrees	Travel direction clockwise from true north
		Standard speed	ostdspeed	float	m s ⁻¹	Speed at which some of the physical processes, like residue burial efficiency, have coefficients specified. In WEPS, many of these coefficients are then adjusted internally based on travel speed, as well as other parameters

		Minimum speed	ominspeed	float	m s ⁻¹	Minimum operation travel speed. This value determines the lower limit at which WEPS will adjust certain process-specific parameters that are influenced by speed
		Maximum speed	omaxspeed	float	m s ⁻¹	Maximum operation travel speed. This value determines the upper limit at which WEPS will adjust certain process-specific parameters that are influenced by speed
		Operation notes	op_notes1	string	N/A	Text information regarding operation
02	Others	Operation notes	op_notes2	string	N/A	Text information regarding operation
03	Energy STIR Direction and Speed	Energy per unit area	oenergyarea	float	l ha ⁻¹	Diesel energy units (in liters) consumed per unit area covered
		Stir	ostir	float	unitless	Soil Tillage Intensity Rating (STIR) value assigned to the operation
		Operation speed	ospeed	float	m s ⁻¹	Operation travel speed
		Operation direction	odirect	float	degrees	Travel direction clockwise from north
		Standard speed	ostdspeed	float	m s ⁻¹	Speed at which some of the physical processes, like residue burial efficiency, have coefficients specified. In WEPS, many of these coefficients are then

						adjusted internally based upon travel speed, as well as other parameters
		Minimum speed	ominspeed	float	m s ⁻¹	Minimum operation travel speed. This value determines the lower limit at which WEPS will adjust certain process-specific parameters that are influenced by speed
		Maximum speed	omaxspeed	float	m s ⁻¹	Maximum operation travel speed. This value determines the upper limit at which WEPS will adjust certain process-specific parameters that are influenced by speed
		Operation notes	op_notes3	string	N/A	Text information regarding operation
		Fuel	ofuel	string		Parameter currently not used
04	Energy STIR Others	Energy per unit area	oenergyarea	float	l ha ⁻¹	Diesel energy units (in liters) consumed per unit area covered
		Stir	ostir	float	unitless	STIR value assigned to the operation
		Operation notes	op_notes4	string	N/A	Text information regarding operation
		Fuel	ofuel	string	N/A	Parameter currently not used

In addition to typical operation processes used to describe things like tillage and cultivation events, there are additional plant growth parameters that are required for planting or seeding operation processes. These plant growth parameters are included in such processes so that they are input into the model for simulating the growth of such plants in response to such things as water availability and air temperature. Included in

these plant growth records are also the residue decomposition parameters, which are used to simulate the decomposition of residue after the growing crop has been terminated.

The definition of an operation consists of an ordered list of parameters that are grouped under an operation, group, or process name. If an operation also includes the process of planting, drilling, transplanting, etc., of a crop, then that operation will also include the relevant crop parameters for the assigned crop. A complete list of the "Operation" database record parameters is provided through an XST file displaying the relevant content of the operation record defining XML files in Supplement A: Operation record parameter definitions, prompts, and display options (Table 8). Likewise, the complete list of the Crop database parameters is provided through another XST file displaying the relevant content of the crop record defining XML files in Supplement B: Crop record parameter definitions, prompts, and display options (Table 9).

WEPS Operation Level Processes

An operation line (operation level process) is labeled with a code letter of "O" followed by a number and then followed by a text string which is the name of the operation. This will be followed by lines that contain parameters that apply to the operation. For example, the direction and speed of travel are specified by the parameters "Operation direction" and "Operation speed" for tillage operations. Each operation will contain a single operation level process first in its definition. The name of the operation is read by the science model and used in the result reports. There are several types of valid operation lines defined for WEPS operations, each of which have a unique identification number (ID).

All the valid operation lines are listed and defined here. Note that some operation processes have been designated as obsolete and are noted below. All of the listed processes are still fully functional in the WEPS science model, but the code supporting them may be removed in the future. All currently maintained operation records have been updated to not use any obsolete processes and any new operations should not use them, but some old WEPS management files that have not been updated may still contain operations that use them. Thus, they are fully documented here.

O 00: Initialization

The "Initialization" operation line represents a special type of operation. It is intended to be used when one needs to initialize a WEPS simulation run in a special manner. Therefore, any operation defined with an "Initialization" operation line will only be executed once, during the initialization cycle, and will not be repeated like other normal operations. This type of operation will usually only be created and used by researchers or for special WEPS uses. There is only one parameter included with this operation line, which is defined in Table 6.

O 01: Direction and Speed

In many management events, like tillage operations, the speed of the operation and/or the direction in which the operation is performed on the field can influence the degree to which it impacts the physical state of the soil, surface, and vegetation. These types of management events will be defined with the "Direction and Speed" operation line. The six parameters assigned to this operation line is defined in Table 6.

O 02: Others

Management events that are not influenced by speed of operation or direction of travel will use this operation line. Examples would be most grain-harvest, herbicide-spraying, baling, burning, and irrigation operations. There is only one parameter included with this operation line, which is defined in Table 6.

O 03: Energy STIR Direction and Speed

The “O 03” operation line supersedes the “O 01” coded operation line defined above. It includes three additional parameters to support the “Soil Quality Index”, “Energy STIR (Soil Tillage Intensity Rating)”, and fuel usage calculations used by NRCS. The nine parameters assigned to this operation line are defined in Table 6.

O 04: Energy STIR Others

The “O 04” operation line supersedes the “O 02” coded operation line defined above. It includes three additional parameters to support the “Soil Quality Index”, “Energy STIR”, and fuel usage calculations used by NRCS. The four parameters assigned to this operation are defined in Table 6.

WEPS Group Level Processes

The “group” lines (group level processes) consist of parameters that are shared among other processes and thus are required to be initialized prior to the simulation of these processes within WEPS. There are currently four types of valid group level processes defined in WEPS, each of which have a unique identification number (ID). All the valid group lines are listed and defined here:

G 01: Tillage

Many tillage operations perform several physical processes as they modify the soil and surface condition (e.g., loosening the soil, mixing soil properties within the tillage zone, burial of residue, etc.). All physical processes require some information that is common among them. These shared parameter values, like tillage depth, surface area disturbed, etc., have been grouped together into a single “group” line so that they don’t have to be specified repeatedly as parameters for each individual process that needs them. This allows one to conveniently make a single change to a shared parameter listed in a “group” line and have it impact all the succeeding processes that require it. But it also requires ensuring that any process line that requires a shared parameter has the appropriate “group” line specified before that “process” line in the definition file of that operation. Often, a tillage operation may contain multiple tillage tool components on a single implement (e.g., disk gang, followed by a row of chisel shanks) or consist of several individual implements, one behind the other (e.g., a springtooth harrow with a straight tine drag harrow behind it). These types of tillage operations/implements can be represented as a single operation in WEPS by specifying the physical processes each tillage tool component performs on the soil/surface/vegetation. Often, this is done by specifying a Tillage “group” line, followed by the appropriate “process” lines to represent the tillage/residue burial effects of the individual tillage tool components. Thus, multiple “Tillage group” lines, followed immediately by several “process” lines, will be used to represent multi-tool and multi-implement tillage operations in WEPS. The six parameters assigned to this “group” line are defined in Table 7.

G 02: Biomass Manipulation

The “Biomass Manipulation” group contains a shared parameter that is required by many WEPS processes that simulate the manipulation of biomass (e.g., the removal of biomass, flattening of standing residue, etc.). This “group” line is commonly used for operations that do not affect (till) the soil, where the shared parameters dealing with tillage depth in the “Tillage” group are not required. Examples of operations that would use this “group” line are harvesting and spraying operations. There is only one parameter included with this “group” line, which is defined in Table 7.

G 03: Crop Name

The “Crop Name” group consists of a single parameter, the name of a crop being planted or transplanted. It is required by the planting/seeding and transplanting processes. That parameter is listed in Table 7.

G 04: Add Material to Field

The “Add Material to Field” group consists of a single parameter, the name of the residue, manure, water, etc. type being applied. It is required by the “Add Residue” and “Set Residue” processes. That parameter is listed in Table 7.

WEPS Process Level Processes

The “process” lines (process level processes) define the physical processes exerted on the soil, surface, and/or vegetation by an operation. These “process” lines are listed in the order they are to be applied in the simulation of that operation. The entire list of “process” lines is given here. Their respective parameters are listed in Table 8.

P 01: Break Crust

If this process is specified, it means that the operation will physically destroy any crust on the soil surface. No process-level parameters are required for the simulation of this effect in WEPS. It does require a shared, group-level parameter that specifies the fraction of the surface area to which this effect applies.

P 02: Random Roughness

This process will simulate an operation’s effect on the random roughness of the surface. Two parameters are defined for this process, which are listed in Table 10.

P 03: Oriented Roughness (ridges only)

This process is obsolete and no longer used.

P 04: Oriented Roughness (dikes only)

This process is obsolete and no longer used.

P 05: Ridges and Dikes

This process will simulate an operation's effect on oriented roughness of the surface. Six parameters are defined for this process, which are listed in Table 10.

P 11: Aggregate Crushing

This process will simulate the breakage of aggregates due to tillage operations. Two parameters are defined for this process, which are listed in Table 11.

P 12: Soil Loosening

This process simulates the loosening of the soil, e.g., reduces the bulk density in response to tillage operations. This process inherently affects the thickness of the affected layers. There is a single parameter defined for this process, which is listed in Table 11.

P 13: Soil Layer Mixing

This process simulates the mixing of soil layers due to tillage operations. There is a single parameter defined for this process, which is listed in Table 11.

P 14: Soil Layer Inversion

This process specifies that the current tillage tool inverts the soil layers within the specified tillage zone. This process has no specific parameter values.

P 24: Flatten Standing Biomass

This process specifies the degree to which standing crops and/or residue are flattened. Six parameters are defined for this process, which are listed in Table 12. There are flattening coefficients specified for each type of residue, on its toughness/size. The five types of residue classes are:

- Fragile - Residue that is easily broken down (e.g., soybean residue)
- Moderately tough - Similar to size and toughness of wheat residue
- Non-fragile/large - Similar to size and toughness of corn residue
- Woody - Similar to size and toughness of woody brush residue
- Small stones/gravel - Non-decomposing material

P 25: Bury Flat Biomass

This process specifies distribution and the degree to which crops and/or residue are buried. Six parameters are defined for this process, which are listed in Table 12. There are burial coefficients specified for each type of residue, based on its toughness/size. The five types of residue classes are specified under "Flatten Standing Biomass." The burial distribution pattern by depth is specified based upon the "Bury Biomass Flag" values. The five types of burial distribution patterns are:

- Uniform - Biomass is buried uniformly by depth
- Mixing and inversion - Biomass is inverted and mixed during burial
- Mixing - More biomass is buried near the soil surface
- Inversion - Biomass buried at bottom of tillage zone

Lifting, fracturing - Biomass buried similar to a chisel plow

P 26: Resurface Buried Biomass

This process specifies the degree to which buried residue are brought back to the surface. Five parameters are defined for this process, which are listed in Table 12. There are re-surfacing coefficients specified for each type of residue, based on its toughness/size. The five types of residue classes are specified under “Flatten Standing Biomass”.

P 30: Defoliate Growing Crop (Obsolete Process – replaced with P31)

This process causes all crop leaves to be transferred from the standing crop pool to the flat temporary pool, after which they are transferred to the flat residue pool by P 40. One parameter is defined for this process, which is listed in Table 12.

P 31: Kill or Defoliate Growing Crop

This process will cause some or all the biomass of a growing crop to be killed depending on the setting. One parameter is defined for this process, which is listed in Table 12. Any killed biomass is moved to temporary pools, which are transferred to residue pools by P 40.

P 32: Cut/Remove Biomass to Height (Obsolete Process – replaced with P 42)

This process cuts the specified standing biomass (crop and residue if present) to the specified height. This process is also a harvest process if components of the cut material are removed from the field as specified by the removal parameter values. Five parameters are defined for this process, which are listed in Table 12. Based upon the “Cut Biomass Flag” setting, the cut height is measured from the ground up or from the top of the crop down.

P 33: Cut/Remove Biomass by Fraction (Obsolete Process – replaced with P 43)

This process cuts the specified standing biomass (crop and residue if present) to a fraction of the crop height. This process is also a harvest process if components of the cut material are removed from the field as specified by the removal parameter values. Four parameters are defined for this process, which are listed in Table 12.

P 34: Change Standing Biomass Fall Rate

This process allows an operation to modify the fall rate of decay for standing residue stalks. The purpose is to simulate the effects of undercutting the supporting roots, which decreases the ability of residue stalks to remain standing over time. Eleven parameters are defined for this process, which are listed in Table 12.

P 37: Thin Biomass to Population (Obsolete Process – replaced with P 47)

This process reduces the crop plant population to the specified value. This process is also a harvest process if components of the thinned plants are removed from the field as specified by the removal parameter values. Four parameters are defined for this process, which are listed in Table 12.

P 38: Thin Biomass by Fraction (Obsolete Process – replaced with P 48)

This process reduces the crop plant population by the specified value. This process is also a harvest process if components of the thinned plants are removed from the field as specified by the removal parameter values. Four parameters are defined for this process, which are listed in Table 12.

P 40: End Crop Biomass Manipulation

This process is required after all crop-related biomass manipulation processes have been completed, for WEPS to correctly account for changes in vegetation pools within the simulation. There are no parameters associated with this process line.

P 42: Cut/Remove Biomass to Height (flags)

This process cuts the specified standing biomass (crop and residue if present) to the specified height. This process is also a harvest process if components of the cut material are removed from the field as specified by the removal parameter values. Nine parameters are defined for this process, which are listed in Table 12. Based upon the “Cut Biomass Flag” setting, the cut height is measured from the ground up or from the top of the crop down. It replaces the P 32 process and includes additional flags that determine whether the harvested material and crop maturity warnings get reported as well as whether this process’s results are used during a yield calibration run.

P 43: Cut/Remove Biomass by Fraction (flags)

This process cuts the specified standing biomass (crop and residue if present) to a fraction of the crop height. This process is also a harvest process if components of the cut material are removed from the field as specified by the removal parameter values. Eight parameters are defined for this process, which are listed in Table 12. It replaces the P 33 process and includes additional flags that determine whether the harvested material and crop maturity warnings get reported as well as whether this process’s results are used during a yield calibration run.

P 47: Thin Biomass to Population (flags)

This process reduces the crop plant population to the specified value. This process is also a harvest process if components of the thinned plants are removed from the field as specified by the removal parameter values. Eight parameters are defined for this process, which are listed in 8. It replaces the P 37 process and includes additional flags that determine whether the harvested material and crop maturity warnings get reported as well as whether this process’s results are used during a yield calibration run.

P 48: Thin Biomass by Fraction (flags)

This process reduces the crop plant population by the specified value. This process is also a harvest process if components of the thinned plants are removed from the field as specified by the removal parameter values. Eight parameters are defined for this process, which are listed in Table 12. It replaces the P 38 process and includes additional flags

that determine whether the harvested material and crop maturity warnings get reported as well as whether this process's results are used during a yield calibration run.

P 50: Set Crop Residue Amounts

Sets the crop residue amounts (flat, standing, and buried) and thus can be used in an "O 0" initialization operation since it resets all the variables to the specified values. This is in contrast to the P 65 "Add Crop Residue" process which just changes the quantities relative to the current values. Nine parameters are defined for this process, which are listed in Table 12. Ten additional crop decomposition parameters are also used.

P 51: Seeding Configuration

This process is included in planting/seeding/transplant operations. Specific parameters determine the type of planting being conducted, row spacing used or broadcast seeding, and whether the seeds are placed in the furrow or in the ridge. These three parameters are listed in Table 12. All remaining process parameters consist of the crop database record parameters. They are documented fully in the crop database section and only the name, type of data and the order they appear in the Management/Crop Rotation file are provided here.

P 61: Remove Plant/Residue Material

Removes plant and/or residue material from the field. Specific parameter values determine the plant/residue location(s) the biomass is removed from (standing, roots, buried, flat). Seven parameters are defined for this process, which are listed in Table 12.

P 62: Remove (by age pool) Plant/Residue Material

Remove plant and/or residue material based upon the selected biomass age pool(s) available in WEPS. Ten parameters are defined for this process, which are listed in Table 12.

P 65 – Add Crop Residue Amounts

This process allows the addition of crop residue to the field. This process not only simulates the typical flat residue additions but can also be used to add standing and buried residue. Nine parameters are defined for this process, which are listed in Table 12. Ten additional crop decomposition parameters are also used.

P 66 – Add Manure Residue Amount

Allows the addition of manure to a field. Since manure is simulated as a residue, it contains specific parameters to allow the addition of manure and the process converts it to an equivalent residue that provides similar cover benefits for erosion control and appropriate decomposition rates. Eleven parameters are defined for this process, which are listed in Table 13. Ten additional crop decomposition parameters are also used.

P 71: Irrigation (Obsolete) (Obsolete Process – replaced with P 72, 73, and 74)

This process simulates the application of water. It specifies the application method and depth of water applied. Two parameters are defined for this process, which are listed in Table 13.

P 72: Monitor Irrigation

This process simulates the application of water. It simulates applying water via flood, sprinkler, and below ground drip irrigation. It can apply a fixed amount on a schedule or in response to plant needs based upon soil water content. It can also reflect resource limitations so that only a maximum amount of water can be applied during a specified interval. All of these can be simulated based upon specific parameter settings associated with this operation. Eight parameters are defined for this process, which are listed in Table 13. Of the two, rate and duration, only one needs to be specified. The other will then be derived by the science model.

P 73: Single Irrigation

This process simulates the application of water for a single day. The amount, type of irrigation, etc., can be specified based upon the parameters associated with this process. Four parameters are defined for this process, which are listed in Table 13. Of the two, rate and duration, only one needs to be specified. The other will then be derived by the science model.

P 74: Terminate Irrigation Monitor

This process concludes the “Irrigation Monitor” process. Thus, no more water will be applied with the “Irrigation Monitor” process after this process is initiated. There are no parameters associated with this process line.

An example WEPS Management/Crop Rotation file is used here for discussion of the file format. The contents of other WEPS Management/Crop Rotation files may be very different in content, due to the selection of different operations, number of operations specified, crops grown, and the length of the rotation cycle. This ASCII file format is controlled by the XML file listed in Supplement C: Man_fileformat.xml.

1. The first line in the file consists of the WEPS Management/Crop Rotation file version. It is used by the WEPS science model to determine which version of the file is being read to ensure it correctly reads in all the specified parameters. The current version number is 1.5.

```
Version: 1.5
```

2. The second line consist of the asterisk character “*” followed by the keyword “START” and the number one “1” following it. The asterisk and keyword are used by the WEPS science model to signify the beginning of the management rotation file contents. The “1” signifies that the rotation cycle listed in this management file is one year in length.

```
*START 1
```

- The next four lines in this file begin with an “N.” This signifies that line contents consist of Notes, i.e., information regarding the WEPS Management/Crop Rotation file itself. In this case, the original rotation file was developed in RUSLE2 (a water erosion model used by NRCS) and then converted to the WEPS management rotation file format on the date specified using version 1.1 of the “SKEL” conversion routine (SKEL is short for skeleton, which is what the rotation file is called when it is stripped of the specific processes and parameters used to define it for RUSLE2 or WEPS). The final note line informs the user that the management file was updated on the specified date to use the most current crop and operation records for WEPS.

```
N Originating Program: RUSLE2
N Skel Format Version: 1.1
N This management file was originally converted from the NRCS standard XML
format on - Wed May 09 09:53:41 CDT 2007
N This management file was updated to contain the most current crop and
operation records for WEPS on - Wed May 05 15:05:47 CDT 2010
```

- This line consists of a comment, signified by the sharp character (#), and followed by several dashes. It signifies the start of an operation’s list of processes and parameters. It is inserted automatically by MCREW to make it easier to distinguish the beginning of the next operation in the file when a user is viewing it manually.

```
#-----
```

- This line starts with a “D” signifying a “Date” line. The date follows it on this line using the dd/mm/yy date format. Note that the year is the year within the rotation cycle. This is the date within the rotation file that the next operation listed is used in the simulation.

```
D 15/04/01
```

- This line begins with an “O” which signifies that this is the operation to be simulated on the date specified on the previous line. The “03” is the operation level group ID, which signifies which group parameters are to be included with this operation on the subsequent lines. The number and type of shared operation level group parameters vary depending upon the operation level group ID defined for the operation. There are currently 4 different operation level group IDs defined. They are listed in Table 6 with their respective parameters.

Everything following the operation level group ID is the operation name string. Note that spaces can be included in the operation name.

```
O 03 Sweep plow, wider than 40 in
```

- This line, which begins with a plus sign (+), signifies that this line is a continuation of the previous line, and in this case, lists the parameter values for the operation level shared parameters designated for the “03” operation level group. The parameters for this operation level group are: energyarea, stir, speed, direction, standard speed, minimum speed, and maximum speed. See Table 6 for a full description of all operation level group parameters and Supplement A (Table 8) for the entire order of the variables on this line.

```
+ 7.4831395 7.8 2.2351363 0.0 2.2351363 1.5645955 2.9056773
```

8. The following seven lines that begin with a “T” signifies that these lines are “Text” lines that consist of the notes regarding this operation, “Sweep plow, wider than 40 in”. Often, they provide information on the reason the operation was created and what the operation is expected to simulate.

```
T Stubble Mulch blade plow, Sweeps or V-blades 40+ wide. Noble is a brand
name
T Run shallow to undercut stubble and weeds, thus killing weeds but leaving
stubble upright. 12-18-01 DTL
T 10-26-06 MAS
T
T Added a flattening to the file for fallow application. This flattens any
weed growth (fragile only) completely and
T leaves the standing residue to go through the normal flattening. This keeps
the model from showing additional
T standing residue when there never is any from the small summer fallow
weeds. MAS 11-19-09
```

9. This line starts with a “G” signifying that this is a group process containing a list of shared parameters. The “01” indicates the specific group process and the string following the group process code is the group name, “Tillage” in this case.

```
G 01 Tillage
```

10. This line, which begins with a plus sign (+), signifies that this is a continuation of the previous process, a group 01 process in this instance. The shared parameters listed on this line are: depth, intensity, area affected, standard depth, minimum depth, and maximum depth which are defined in Table 7. See Table 7 for a full description of all group level parameters and Supplement A (Table 8) for the entire order of the variables on this line.

```
+ 76.20015 0.5 1.0 76.20015 50.800102 127.00026
```

11. This line starts with a “P” signifying that this is a process line, which happens to not include any process specific parameters. It does use a “group” parameter, “area affected”, which is provided by the previous “G 01” group lines above.

```
P 01 Break Crust
```

12. This line starts with a “P” signifying that this is a process line. The process specific parameters are provided on the next line below.

```
P 02 Random Roughness
```

13. This line, which begins with a plus sign (+), signifies that this line is a continuation of the previous line, and in this case, lists the parameter values for the “Random Roughness” process specific parameters. Those parameters are: random roughness flag and nominal random roughness value, which are defined in Table 10. See Table 10 for a full description of all process level parameters and Supplement A (Table 8) for the entire order of the variables on this line.

```
+ 1 10.160021
```

14. This line starts with a “P” signifying that this is a process line. The process specific parameters are listed on the following line: ridge flag, ridge height, ridge spacing, ridge width, dike height, and dike spacing, which are defined in Table 10. See Table

10 for a full description of all process level parameters and Supplement A (Table 8) for the entire order of the variables on this line.

```
P 05 Ridges and Dikes
+ 1 50.800102 1524.003 101.600204 0.0 0.0
```

15. This line starts with a “P” signifying that this is a process line. The process specific parameters are listed on the following line: aggregate size distribution factor and crushing intensity factor, which are defined in Table 11. See Table 11 for a full description of all process level parameters and Supplement A (Table 8) for the entire order of the variables on this line.

```
P 11 Aggregate Crushing
+ 2.4 -2.0
```

16. This line starts with a “P” signifying that this is a process line. The process specific parameter is listed on the following line: loosening intensity coefficient, which is defined in Table 11. See Table 11 for a full description of all process level parameters and Supplement A (Table 8) for the entire order of the variables on this line.

```
P 12 Soil Loosening
+ 0.7
```

17. This line starts with a “P” signifying that this is a process line. The process specific parameter is listed on the following line: mass mixing efficiency coefficient, which is defined in Table 11. See Table 11 for a full description of all process level parameters and Supplement A (Table 8) for the entire order of the variables on this line.

```
P 13 Soil Layer Mixing
+ 0.25
```

18. This line starts with a “P” signifying that this is a process line. The process specific parameters are listed on the following line: flatten biomass flag, mass flattened (fragile residue), mass flattened (moderately tough residue), mass flattened (non-fragile/large residue), mass flattened (woody residue), and mass flattened (small stones/gravel), which are defined in Table 12. See Table 12 for a full description of all process level parameters and Supplement A (Table 8) for the entire order of the variables on this line.

```
P 24 Flatten Standing Biomass
+ 1 1 0 0 0 0
```

19. This line starts with a “P” signifying that this is a process line. The process specific parameter is listed on the following line: kill flag, which is defined in Table 12. See Table 12 for a full description of all process level parameters and Supplement A (Table 8) for the entire order of the variables on this line.

```
P 31 Kill or Defoliate Growing Crop
+ 2
```

20. This line starts with a “P” signifying that this is a process line, which happens to not include any process specific parameters.

P 40 End crop Biomass Manipulation

21. This line starts with a “P” signifying that this is a process line. The process specific parameters are listed on the following line: flatten biomass flag, mass flattened (fragile residue), mass flattened (moderately tough residue), mass flattened (non-fragile/large residue), mass flattened (woody residue), and mass flattened (small stones/gravel), which are defined in Table 12. See Table 12 for a full description of all process level parameters and Supplement A (Table 8) for the entire order of the variables on this line. Note that this process was also specified previously (line 19 above).

```
P 24 Flatten Standing Biomass
+ 0 0.4 0.25 0.15 0.15 1.0
```

22. This line starts with a “P” signifying that this is a process line. The process specific parameters are listed on the following line: burial biomass flag, mass buried (fragile residue), mass buried (moderately tough residue), mass buried (non-fragile/large residue), mass buried (woody residue), and mass buried (small stones/gravel), which are defined in Table 12. See Table 12 for a full description of all process level parameters and Supplement A (Table 8) for the entire order of the variables on this line.

```
P 25 Bury Flat Biomass
+ 1 0.50 0.15 0.1 0.05 0.25
```

23. This line starts with a “P” signifying that this is a process line. The process specific parameters are listed on the following line: mass resurfaced (fragile residue), mass resurfaced (moderately tough residue), mass resurfaced (non-fragile/large residue), mass resurfaced (woody residue), and mass resurfaced (small stones/gravel), which are defined in Table 12. See Table 12 for a full description of all process level parameters and Supplement A (Table 8) for the entire order of the variables on this line.

```
P 26 Resurface Biomass
+ 0.02 0.03 0.05 0.07 0.02
```

24. This line starts with a “P” signifying that this is a process line. The process specific parameters are listed on the following two lines: selected biomass pool type, standing biomass fall rate multiplier (fragile residue), standing biomass fall rate multiplier (moderately tough residue), standing biomass fall rate multiplier (non-fragile/large residue), standing biomass fall rate multiplier (woody residue), standing biomass fall rate multiplier (small stones/gravel), standing biomass fall rate threshold (fragile residue), standing biomass fall rate threshold (moderately tough residue), standing biomass fall rate threshold (non-fragile/large residue), standing biomass fall rate threshold (woody residue), and standing biomass fall rate threshold (small stones/gravel), which are defined in Table 12. See Table 12 for a full description of all process level parameters and Supplement A (Table 8) for the entire order of the variables on this line.

```
P 34 Change Standing Biomass Fall Rate
+ 7 3.0 2.5 2.0 1.5 1.0
```

+ 0.5 0.6 0.7 0.8 1.0

25. The next group of lines consists of the soil, surface, and biomass manipulation processes defined for the next operation and the date it will be used in the simulation.

```
#-----  
D 20/05/01  
O 03 Planter, ridge till  
+ 5.799433 10.56 2.2351363 0.0 2.2351363 1.5645955 2.9056773  
T RUSLE:6/7/01 DTL This is a planter on 30 in sp where 65% of the area is  
tilled with a 4 in ridge. MAS 8/8/07  
T G2 was added into file in front of the flattening (P24), burial (P25), and  
resurfacing (P26) factors because the area affected is less than 1.0 and  
T the RUSLE values were normalized to 1.0. This change will emulate the  
correct residue changes based on the method set forth in RUSLE.  
T RUSLE's factors have been reduced based on the area affected.  
T The stalk fall rate factor (P34) was moved ahead of the new (G2) factor to  
set the fall rate to the less than 1.0 area affected. 8/8/07 MAS  
G 01 Tillage  
+ 63.500126 0.5 .65 63.500126 50.800102 101.600204  
P 01 Break Crust  
P 02 Random Roughness  
+ 1 10.160021  
P 05 Ridges and Dikes  
+ 1 101.600204 762.0015 558.8011 0.0 0.0  
P 11 Aggregate Crushing  
+ 2.8 0.75  
P 12 Soil Loosening  
+ 0.75  
P 13 Soil Layer Mixing  
+ 0.35  
P 34 Change Standing Biomass Fall Rate  
+ 7 3.0 2.5 2.0 1.5 1.0  
+ 0.5 0.6 0.7 0.8 1.0  
G 02 Biomass Manipulation  
+ 1.0  
P 24 Flatten Standing Biomass  
+ 0 .3 .25 .2 0.1 1.0  
P 25 Bury Flat Biomass  
+ 1 .15 .12 .09 .078 .114  
P 26 Resurface Buried Biomass  
+ .01 .01 .01 .02 .01
```

26. Since this operation is a planting operation, it consists of additional group and process lines. This line starts with a “G” signifying that this is a group process containing a list of shared parameters. The “03” indicates the specific group process and the string following the group process code is the group name, “Crop Name” in this case. The crop name follows on the next “+” line

```
G 03 Crop Name  
+ Sorghum, grain
```

27. This line starts with a “P” signifying that this is a process line. The process specific parameters are listed on the following lines: type of planting, crop row spacing, and seed placement, which are defined in Table 13. Additional crop record parameters follow this line. See Table 13 for a full description of all process level parameters and Supplement A (Table 8) for the entire order of the variables on this line

```
P 51 Seeding Configuration  
+ 1 0.0 2
```

28. These two lines are the first of the crop record parameters included by this planting process: plant population per unit area, maximum number of tillers (stems) per plant,

crop growth parameters selection flag, target harvestable yield, biomass adjustment factor, yield/biomass ratio adjustment factor, and yield component specification flag, and on the second line contains the text string listing the units for harvestable yield. See Supplement A (Table 8) for the entire order of the variables on this line.

+ 24.71149331554106 3 1 64 1 1 0
+ bu/ac

29. The remaining crop record parameters are included in the following lines (these parameters are more completely defined later in this document and Supplement A: Table 8):

Line 1: Moisture content (%) for reporting yield, harvestable yield conversion factor (kg m⁻² to specified yield display units), crop type (integer value denoting type of crop grown, perennials, warm or cool season legumes, etc.), grain (seed) fraction of reproductive biomass component, light extinction coefficient, and ratio of heat units (start of senescence/total).

Line 2: Maximum crop height (m), starting depth of growing point (m), maximum root depth (m), minimum temperature for plant growth (°C), optimal temperature for plant growth (°C), crop maturity measurement method (integer value: 0 = matures in days specified; 1 = matures in heat units specified), time of uninterrupted growth to maturity (days), and growing degree days to maturity (°C day).

Line 3: Upper frost damage threshold temperature (°C), lower frost damage threshold temperature (°C), damage at upper frost damage threshold temperature (fraction), damage at lower frost damage threshold temperature (fraction), thermal delay coefficient of vernalization (unitless), and biomass conversion efficiency (t ha⁻¹ MJ m⁻²).

Line 4: Leaf fraction coefficient a (unitless), leaf fraction coefficient b (unitless), leaf fraction coefficient c (unitless), leaf fraction coefficient d (unitless), reproductive mass coefficient a (unitless), reproductive mass coefficient b (unitless), reproductive mass coefficient c (unitless), and reproductive mass coefficient d (unitless).

Line 5: Crop height curve shape coefficient a (unitless), crop height curve shape coefficient b (unitless), stem silhouette area coefficient a (unitless), stem silhouette area b (unitless), specific leaf area (m² kg⁻¹), heat units ratio to emergence (unitless), transplant or seed flag (0 = plant emerges in specified heat units; 1 = transplanted crop placed in the field), and maximum growth diameter of a single plant (m).

Line 6: Planted mass dry weight (mg/plant), root storage mass required for each regrowth shoot (mg/shoot), ratio of leaf mass/stem mass in shoot (unitless), ratio of shoot diameter to shoot length at full extension (unitless), fraction of leaf mass partitioning diverted to root store, fraction of stem mass partitioning diverted to root store, fraction of standing store mass partitioning diverted to root store, and residue size/toughness class (integer value: 1 = fragile, very small residue; 2 = moderately tough short residue; 3 = non-fragile, medium residue; 4 = woody, large residue; 5 = gravel, rock).

Line 7: Decomposition rate for standing stalks (kg kg⁻¹ day⁻¹), decomposition rate for surface residue (kg kg⁻¹ day⁻¹), decomposition rate for buried crop residue (kg kg⁻¹ day⁻¹), decomposition rate for roots (kg kg⁻¹ day⁻¹), decomposition (fall) rate for standing stalks

(# stems # stems⁻¹ day⁻¹), average stem diameter (m), decomposition days threshold when stems begin to fall (days), and cover factor coefficient for mass to cover conversion (unitless).

Line 8: Residue evaporation suppression multiplier coefficient a (unitless), Residue evaporation suppression multiplier coefficient b (unitless), residue to yield ratio (kg kg⁻¹), regrowth location above (+) or below the surface (-) in meters, and three currently unused parameters.

See Supplement C: man_fileformat.xml for the entire order of the variables on these lines.

```
+ 14 162.2 4 0.8 0.8 0.8
+ 1.5000000000000002 0.025 1.5240185 10 27.5 0 125 1300
+ -5 -15 0.01 0.95 0 35
+ -0.0302 0.99 0.5 -0.065 -0.018 1.015 0.5224 0.039
+ 0.3728 -0.065 0.03985145 0.42 19.2 0.05 0 0.7010057909174031
+ 30.303029999999996 30.303029999999996 3 0.03 0.1 0.1 0 3
+ 0.01 0.01 0.01 0.01 0.153 0.01 20 2.9797485
+ -1.20379 0.604887 0.8988 0.038108904 0 0.0 0.0 0.0
```

30. This line contains the crop notes, if any. These lines begin with a “T”.

```
T Enter crop notes here.
```

31. The next operation is listed here. Specific operation, group and process lines and their parameters can be determined from Tables 5-7, 10-12 and Supplement A (Table 8) similar to what was demonstrated for previous operations above in this example.

```
#-----
D 25/06/01
O 03 Cultivator, row - 1st pass ridge till
+ 5.799433 17.55 2.2351363 0.0 1.7881091 1.5645955 2.9056773
T 8/4/06 MAS from RUSLE
T G2 was added into file in front of the flattening (P24), burial (P25), and
resurfacing (P26) factors because the area affected is less than 1.0 and
T the RUSLE values were normalized to 1.0. This change will emulate the
correct residue changes based on the method set forth in RUSLE2.
T RUSLE2's factors have been reduced based on the area affected.
T The stalk fall rate factor (P34) was moved ahead of the new (G2) factor to
set the fall rate to less than 1.0 area affected. 8/8/07 MAS
G 01 Tillage
+ 63.50013 .75 0.85 63.500134 50.800102 101.600204
P 01 Break Crust
P 02 Random Roughness
+ 1 17.780035
P 05 Ridges and Dikes
+ 1 101.600204 762.0015 152.4003 0.0 0.0
P 11 Aggregate Crushing
+ 3.0 1.0
P 12 Soil Loosening
+ 0.75
P 13 Soil Layer Mixing
+ .6
P 34 Change Standing Biomass Fall Rate
+ 4 3.0 2.5 2.0 1.5 1.0
+ 0.5 0.6 0.7 0.8 1.0
G 02 Biomass Manipulation
+ 1.0
P 24 Flatten Standing Biomass
+ 14 0.8 .7 .7 0.1 1.0
P 25 Bury Flat Biomass
+ 1 .43 .34 .26 .22 .32
P 26 Resurface Buried Biomass
```

+ 0.04 0.045 .05 .22 0.04

32. The next operation is listed here, which is a harvest operation. Specific operation, group, and process lines and their parameters can be determined from Tables 5-7, 10-12 and Supplement A (Table 8) similar to what was demonstrated for previous operations above in this example.

```
#-----  
D 10/10/01  
O 04 Harvest, killing crop 50pct standing stubble  
+ 14.311503 .15  
T ARS record - filename is: Harvest Wheat - grain (combine cutterbar  
header).oprn  
T This operation record is designed to represent actual field harvesting  
operation  
T of removing the grain from small grain crops with a cutterbar head on a  
combine.  
T This harvesting operation record removes all the reproductive component of  
a crop above the  
T cutting height. Typically this is specified as the "yield" component in the  
crop record.  
T The non-harvested crop plant material above the specified cut height  
becomes flat residue.  
T The remaining above ground crop material below the specified cut height  
becomes standing residue.  
T Nov 02, 2005 Created - Larry Wagner  
T Detailed info regarding this operation record:  
T This harvest record specifies the actual cut height dependent upon the  
height  
T of the crop. The cut height is specified as a fraction of the crop height.  
T Added 0.2 for the flattening of the combine and tire traffic for hauling  
grain.  
T MAS 1-18-07  
T The harvesting operation could also have an effect on the "standing stalk"  
T fall rate and fall threshold values. The default "biomass pool" flag  
parameter  
T is set to "No adjustments applied" so that no "stalk residue decay rate  
change" will occur.  
T However, this flag value can be changed along with the default parameter  
values  
T to change the "stalk residue decay processes".  
G 02 Biomass Manipulation  
+ 1.0  
P 31 Kill or Defoliate Growing Crop  
+ 2  
P 43 Cut/Remove Biomass by Fraction (flags)  
+ 1 1 0 1 0.2 1 0 0  
P 34 Change Standing Biomass Fall Rate  
+ 0 1.0 1.0 1.0 1.0 1.0  
+ 1.0 1.0 1.0 1.0 1.0  
P 40 End crop Biomass Manipulation  
P 24 Flatten Standing Biomass  
+ 0 0.2 0.2 0.15 0.2 1
```

33. The final lines in the WEPS management/crop rotation file consist of the following: (a) a comment line containing a few dashes; (b) a line beginning with an asterisk, "*", followed by the word "END", to signify the end of this specific management/crop rotation sequence; and (c) another line beginning with an asterisk, "*", followed by the letters "EOF" signifying the end of file or end of the WEPS management/crop rotation file.

```
#-----  
*END  
*EOF
```

Table 10. Process level parameters used in WEPS (Part 1: Soil Surface Manipulation).

Code	Process Name	Parameter Name	Variable Name	Type	Units	Parameter Definition
01	Break Crust	N/A				If included within the operation's definition, it breaks (removes) any existing crust based upon the spatial area (listed by the appropriate "group") as affected by that operation.
02	Random Roughness	RR flag	rroughflag	integer		Specifies how an operation affects random roughness (RR). A value of zero allows the operation to always set the RR to the specified value. A value of 1 will allow WEPS to auto-adjust the RR value based upon other parameters.
		Nominal RR	rrough	float	mm	If the RR flag = 0, then this value is the Allmaras RR for the surface after using this tillage tool. If the RR flag = 1, then this is to be the typical Allmaras RR expected on a silt loam soil with lots of buried residue present. Internally, WEPS will use the shared group parameter value for tillage intensity, as well as soil type and residue quantity to determine the surface RR created by the tillage tool. In general, a high tillage intensity value will mean that the "Nominal RR" value will not be affected much by the pre-tillage surface roughness. A low tillage

intensity would affect the final RR. In general, a sandier soil will result in a lower RR value, and a soil with more clay will create a higher RR value. Because most field operations are performed with less residue than specified for the “Nominal RR” value, the resulting surface roughness will be less than the specified value.

05	Ridges and Dikes	Ridge flag	rdgflag	integer		Tillage operations will: a) leave existing ridges alone (Ridge flag = 0); b) create a specified ridged and/or diked surface, regardless of pre-existing surface conditions (Ridge flag = 1); or c) create a specific ridged and/or diked surface based upon tillage depth (Ridge flag = 2).
		Ridge height	rdghit	float	mm	Ridge height from the top of the ridge to the bottom of the furrow.
		Ridge spacing	rdgspac	float	mm	Ridge spacing parallel across the top of two adjacent ridges.
		Ridge top width	rdgwidth	float	mm	Ridge width across the top of the ridge.
		Dike height	dkhit	float	mm	Dike height from the top of the dike to the bottom of the furrow.
		Dike spacing	dkspac	float	mm	Dike spacing from dike top to dike top down the furrow.

Table 11. Process level parameters used in WEPS (Part 2: Soil Mass Manipulation).

Code	Process Name	Parameter Name	Variable Name	Type	Units	Parameter Definition
01	Break Crust	N/A				If included within the operation's definition, it breaks (removes) any existing crust based upon the spatial area (listed by the appropriate "group") as affected by that operation.
02	Random Roughness	RR flag	rroughflag	integer		Specifies how an operation affects random roughness (RR). A value of zero allows the operation to always set the RR to the specified value. A value of 1 will allow WEPS to auto-adjust the RR value based upon other parameters.
		Nominal RR	rrough	float	mm	If the RR flag = 0, then this value is the Allmaras RR that the surface will have after using this tillage tool. If the RR flag = 1, then this is to be the typical Allmaras RR expected on a silt loam soil with lots of buried residue present. Internally, WEPS will use the shared group parameter value for tillage intensity, as well as soil type and residue quantity to determine the surface RR created by the tillage tool. In general, a high tillage intensity value will mean that the "Nominal RR" value will not be affected

much by the pre-tillage surface roughness. A low tillage intensity would affect the final RR. In general, a sandier soil will result in a lower RR value, and a soil with more clay will create a higher RR value. Because most field operations are performed with less residue than specified for the “Nominal RR” value, the resulting surface roughness will be less than the specified value.

05	Ridges and Dikes	Ridge flag	rdgflag	integer		Tillage operations will: a) leave existing ridges alone (Ridge flag = 0); b) create a specified ridged and/or diked surface, regardless of pre-existing surface conditions (Ridge flag = 1); or c) create a specific ridged and/or diked surface based upon tillage depth (Ridge flag = 2).
		Ridge height	rdghit	float	mm	Ridge height from the top of the ridge to the bottom of the furrow.
		Ridge spacing	rdgspac	float	mm	Ridge spacing parallel across the top of two adjacent ridges.
		Ridge top width	rdgwidth	float	mm	Ridge width across the top of the ridge.
		Dike height	dkhit	float	mm	Dike height from the top of the dike to the bottom of the furrow.
		Dike spacing	dkspac	float	mm	Dike spacing from dike top to dike top down the furrow.

Table 82. Process level parameters used in WEPS (Part 3: Biomass Manipulation).

Code	Process Name	Parameter Name	Variable Name	Type	Units	Parameter Definition
24	Flatten Standing Biomass	Flatten Biomass Flag	fbioflagvt	integer	unitless	Specifies the type of material that is flattened: 1- Flatten crop and residue. 2- Flatten crop only. 3-Flatten residue only.
		Mass flattened (fragile residue)	massflatvt1	float	unitless	Fraction of “fragile residue” flattened.
		Mass flattened (moderately tough residue)	massflatvt2	float	unitless	Fraction of “moderately tough residue” flattened.
		Mass flattened (non-fragile /large residue)	massflatvt3	float	unitless	Fraction of “non-fragile/large residue” flattened.
		Mass flattened (woody residue)	massflatvt4	float	unitless	Fraction of “woody residue” flattened.
		Mass flattened (small stones/gravel)	massflatvt5	float	unitless	Fraction of “small stones/gravel” flattened.
25	Bury Flat Biomass	Burial Biomass Flag	burydist	integer	unitless	Specifies the type of burial distribution: 0- Compression burial distribution. 1- Inversion burial distribution. 2- Lifting, fracturing

						burial distribution. 3- Mixing and inversion
						burial distribution. 4- Mixing burial distribution. 5- Uniform burial distribution
		Mass buried (fragile residue)	massburyvt1	float	unitless	Fraction of "fragile residue" buried.
		Mass buried (moderately tough residue)	massburyvt2	float	unitless	Fraction of "moderately tough residue" buried.
		Mass buried (non-fragile /large residue)	massburyvt3	float	unitless	Fraction of "non-fragile/large residue" buried.
		Mass buried (woody residue)	massburyvt4	float	unitless	Fraction of "woody residue" buried.
		Mass buried (small stones /gravel)	massburyvt5	float	unitless	Fraction of "small stones/gravel" buried.
26	Resurface Buried Biomass	Mass resurfaced (fragile residue)	massresurvt1	float	unitless	Fraction of "fragile residue" resurfaced.
		Mass resurfaced (moderately tough residue)	massresurvt2	float	unitless	Fraction of "moderately tough residue" resurfaced.
		Mass resurfaced (non-fragile /large residue)	massresurvt3	float	unitless	Fraction of "non-fragile/large residue" resurfaced.

		Mass resurfaced (woody residue)	massresurvt4	float	unitless	Fraction of “woody residue” resurfaced.
		Mass resurfaced (small stones /gravel)	massresurvt5	float	unitless	Fraction of “small stones/gravel” resurfaced.
30	Defoliate Growing Crop	Defoliate flag		integer		The valid values are: 0-No defoliation occurs. 1-Crop defoliated.
31	Kill or Defoliate Growing Crop	Kill Flag	kilflag	integer	unitless	Specifies type of crop killed and/or defoliated. The valid values are: 0-All crops are killed. 1-Annual crop killed, perennial crop regrows. 2-Crop defoliated. 3-No crop killed.
32	Cut/Remove Biomass to Height	Cut Biomass Flag	cutflag	integer	unitless	Values assigned to determine how cut is specified: 0-Cut Value = Height of standing stubble remaining. 1-Cut Value = Length standing stalks removed.
		Cut Value	cutvalh	float	mm	Cut depth or height based upon “Cut Biomass Flag” value.

		Cut Yield Removed	cyldrmh	float	fraction	Fraction of yield biomass removed, remaining material goes to flat.
		Cut Plant Removed	cplrmh	float	fraction	Fraction of plant (crop) biomass removed, remaining material goes to flat.
		Cut Standing Residue Removed	cstrmh	float	fraction	Fraction of residue biomass removed, remaining material goes to flat.
33	Cut/Remove Biomass by Fraction	Plant Height Removed	cutvalf	float	fraction	Fraction of plant height cut.
		Cut Yield Removed	cyldrmf	float	fraction	Fraction of cut yield biomass removed, remaining cut goes to flat.
		Cut Plant Removed	cplrmf	float	fraction	Fraction of plant (crop) cut biomass removed, remaining cut material goes to flat.
		Cut Standing Residue Removed	cstrmf	float	fraction	Fraction of residue cut biomass removed, remaining cut material goes to flat.

34	Change Standing Biomass Fall Rate	Select biomass pool type	frselpool	integer	unitless	Values assigned to determine what standing biomass fall rate is changed: 0-Crop. 1-Crop and Residue. 2-Crop and Temporary. 3-Crop, Temporary and Residue. 4-No adjustments applied. 5-Residue. 6-Temporary. 7-Temporary and Residue.
			ratemultvt1	float	unitless	Standing Biomass Fall Rate Multiplier (fragile residue)
			ratemultvt2	float	unitless	Standing Biomass Fall Rate Multiplier (moderately tough residue)
			ratemultvt3	float	unitless	Standing Biomass Fall Rate Multiplier (non-fragile/large residue)
			ratemultvt4	float	unitless	Standing Biomass Fall Rate Multiplier (woody residue)
			ratemultvt5	float	unitless	Standing Biomass Fall Rate Multiplier (small stones/gravel)

			threshmultvt1	float	unitless	Standing Biomass Fall Rate Threshold (fragile residue)
			threshmultvt2	float	unitless	Standing Biomass Fall Rate Threshold (moderately tough residue)
			threshmultvt3	float	unitless	Standing Biomass Fall Rate Threshold (non-fragile/large residue)
			threshmultvt4	float	unitless	Standing Biomass Fall Rate Threshold (woody residue)
			threshmultvt5	float	unitless	Standing Biomass Fall Rate Threshold (small stones/gravel)
37	Thin Biomass to Population	Thinning Value	thinvalp	float	# m ⁻²	Absolute amount of thinning performed.
		Thinned Yield Removed	tyldrmp	float	fraction	Fraction of thinned yield removed, remaining thinned material goes to flat.
		Thinned Plant Removed	tplrmp	float	fraction	Fraction of thinned plant (crop) removed, remaining thinned material goes to flat.

		Thinned Standing Residue	tstrmp	float	fraction	Fraction of thinned standing residue removed, remaining thinned material goes to flat.
38	Thin Biomass by Fraction	Thinning Value	thinvalf	float	fraction	Fraction of standing biomass flattened, remaining thinned material goes to flat.
		Thinned Yield Removed	tyldrmf	float	fraction	Fraction of yield removed, remaining thinned material goes to flat.
		Thinned Plant Removed	tplrmf	float	fraction	Fraction of plant (crop) removed, remaining thinned material goes to flat.
		Thinned Standing Residue	tstrmf	float	fraction	Fraction of standing residue removed, remaining thinned material goes to flat.
40	End Crop Biomass Manipulation	N/A				No specific parameter for this process.
42	Cut/Remove Biomass to Height (flags)	Report Harvest	harv_report_flg	integer	unitless	Value specifies whether harvest yield is reported: 0- No Report. 1- Report.

Use Harvest in Calibration	harv_calib_flg	integer	unitless	Value specifies whether harvest operation is used in a yield calibration run: 0-Do not Use. 1-Use for Calibration.
Harvest Units	harv_unit_flg	integer	unitless	Value specifies what harvest units are used: 0-Use Units in Crop Record. 1-Use mass/area Units
Crop Maturity Warnings	mature_warn_flg	integer	unitless	Value specifies whether crop maturity warnings are displayed: 0-No Warnings. 1-Warnings.
Cut Biomass Flag	cutflag	integer	unitless	Specific values assigned to determine how cut is specified: 0-Cut Value = Height of standing stubble remaining. 1-Cut Value = Length standing stalks removed.
Cut Value	cutvalh	float	mm	Cut depth or height based upon "Cut Biomass Flag" value.
Cut Yield Removed	cyldrmh	float	fraction	Fraction of yield biomass removed, remaining cut

						material goes to flat.
		Cut Plant Removed	cplrmh	float	fraction	Fraction of plant (crop) biomass removed, remaining cut material goes to flat.
		Cut Standing Residue Removed	cstrmh	float	fraction	Fraction of residue biomass removed, remaining cut material goes to flat.
43	Cut/Remove Biomass by Fraction (flags)	Report Harvest	harv_report_flg	integer	unitless	Value specifies whether harvest yield is reported: 0-No Report. 1-Report.
		Use Harvest in Calibration	harv_calib_flg	integer	unitless	Value specifies whether harvest operation is used in a yield calibration run: 0-Do not Use. 1-Use for Calibration.
		Harvest Units	harv_unit_flg	integer	unitless	Value specifies what harvest units are used: 0-Use Units in Crop Record. 1-Use mass/area Units.
		Crop Maturity Warnings	mature_warn_flg	integer	unitless	Value specifies whether crop maturity warnings are displayed: 0-No Warnings. 1-Warnings.

		Plant Height Removed	cutvalf	float	fraction	Fraction of plant height cut.
		Cut Yield Removed	cyldrmf	float	fraction	Fraction of cut yield biomass removed, remaining cut goes to flat.
		Cut Plant Removed	cplrmh	float	fraction	Fraction of plant (crop) cut biomass removed, remaining cut material goes to flat.
		Cut Standing Residue Removed	cstrmh	float	fraction	Fraction of residue cut biomass removed, remaining cut material goes to flat.
47	Thin Biomass to Population (flags)	Report Harvest	harv_report_flg	integer	unitless	Value specifies whether harvest yield is reported: 0-No Report. 1-Report.
		Use Harvest in Calibration	harv_calib_flg	integer	unitless	Value specifies whether harvest operation is used in a yield calibration run: 0-Do not Use. 1-Use for Calibration
		Harvest Units	harv_unit_flg	integer	unitless	Value specifies what harvest units are used: 0-Use Units in Crop Record. 1-Use mass/area Units.

		Crop Maturity Warnings	mature_warn_flg	integer	unitless	Value specifies whether crop maturity warnings are displayed: 0-No Warnings. 1-Warnings.
		Thinning Value	thinvalp	float	# · m ⁻²	Absolute amount of thinning performed.
		Thinned Yield Removed	tyldrmp	float	fraction	Fraction of thinned yield removed, remaining thinned material goes to flat.
		Thinned Plant Removed	tplrmp	float	fraction	Fraction of thinned plant (crop) removed, remaining thinned material goes to flat.
		Thinned Standing Residue	tstrmp	float	fraction	Fraction of thinned standing residue removed, remaining thinned material goes to flat.
48	Thin Biomass by Fraction (flags)	Report Harvest	harv_report_flg	integer	unitless	Value specifies whether harvest yield is reported: 0-No Report. 1-Report.
		Use Harvest in Calibration	harv_calib_flg	integer	unitless	Value specifies whether harvest operation is used in a yield calibration run:

				0-Do not Use. 1-Use for Calibration
Harvest Units	harv_unit_flg	integer	unitless	Value specifies what harvest units are used: 0-Use Units in Crop Record. 1-Use mass/area Units.
Crop Maturity Warnings	mature_warn_flg	integer	unitless	Value specifies whether crop maturity warnings are displayed: 0-No Warnings. 1-Warnings.
Thinning Value	thinvalf	float	fraction	Fraction of standing biomass flattened, remaining thinned material goes to flat.
Thinned Yield Removed	tyldrmf	float	fraction	Fraction of yield removed, remaining thinned material goes to flat.
Thinned Plant Removed	tplrmf	float	fraction	Fraction of plant (crop) removed, remaining thinned material goes to flat.
Thinned Standing Residue	tstrmf	float	fraction	Fraction of standing residue removed, remaining thinned

						material goes to flat.
61	Remove Plant/Residue Material	Select plant/residue material	selpos	integer	unitless	Value specifies type of biomass selected: 0-Standing with Roots. 1-Flat. 2-Standing with Roots and Flat. 3-Buried. 4- Standing with Roots and Buried. 5-Flat and Buried. 6- Standing with Roots, Flat and Buried.
		Select biomass pool type	selpool	integer	unitless	Specifies type biomass pool (biomass type): 0-Crop. 1-Temporary. 2-Crop and Temporary. 3-Residue. 4-Crop and Residue. 5-Temporary and Residue. 6-Crop, Temporary and Residue.
		Grain (fruit) Removed	rstore	float	fraction	Fraction of grain removed.
		Leaf Removed	rleaf	float	fraction	Fraction of leaves removed.
		Stem Removed	rstem	float	fraction	Fraction of stems removed.
		Storage Root Removed	rrootstore	float	fraction	Fraction of storage roots removed.

		Fibrous Roots Removed	rootfiber	float	fraction	Fraction of fibrous roots removed.
62	Remove (by age pool) Plant/Residue Material	Report Harvest	harv_report_flg	integer	unitless	Specifies whether harvest yield is reported: 0-No Report. 1- Report.
		Use Harvest in Calibration	harv_calib_flg	integer	unitless	Specifies whether harvest operation is used in a yield calibration run: 0-Do not Use. 1-Use for Calibration.
		Harvest Units	harv_unit_flg	integer	unitless	Specifies what harvest units are used: 0-Use Units in Crop Record. 1-Use mass/area Units.
		Crop Maturity Warnings	mature_warn_flg	integer	unitless	Specifies whether crop maturity warnings are displayed: 0-No Warnings. 1-Warnings.
		Select biomass pool type	selpos	integer	unitless	Specifies type biomass pool (biomass type): 0-Crop. 1-Temporary. 2-Crop and Temporary. 3-Residue. 4-Crop and Residue. 5-Temporary and Residue. 6-Crop,

Temporary and Residue.

Select residue age pool type	selpool	integer	unitless	Specifies residue age pool type: 0-All age pools. 1-Youngest age pool.
Grain (fruit) Removed	rstore	float	fraction	Fraction of grain removed.
Leaf Removed	rleaf	float	fraction	Fraction of leaves removed.
Stem Removed	rstem	float	fraction	Fraction of stems removed.
Storage Root Removed	rrootstore	float	fraction	Fraction of storage roots removed.
Fibrous Roots Removed	rrootfiber	float	fraction	Fraction of fibrous roots removed.

Table 93. Process level parameters used in WEPS (Part 4: Soil Amendments).

Code	Process Name	Parameter Name	Variable Name	Type	Units	Parameter Definition
50	Set Crop Residue Amounts	# Standing Residue Stems	numst	float	# m ⁻²	Set number of standing residue stems per unit area.
		Standing Residue Height	rstandht	float	m	Set height of standing residue stems.
		Standing Residue Mass	rstandmass	float	kg m ⁻²	Set mass of standing residue stems.

		Flat Surface Residue Mass	rflatmass	float	kg m ⁻²	Set mass of flat residue per unit area.
		Residue size/toughness class	rbc	integer	unitless	Set residue size/toughness class for residue.
		Buried Residue Mass	rburiedmass	float	kg m ⁻²	Set mass of buried residue.
		Buried Residue Depth	rburieddepth	float	mm	Set maximum depth of buried residue.
		Root Residue Mass	rrootmass	float	kg m ⁻²	Set mass of root residue per unit area.
		Root Residue Depth	rrootdepth	float	mm	Set maximum depth of root residue. 10 additional crop residue decomposition parameters
51	Seeding Configuration	Type of Planting	rowflag	integer	unitless	Specifies the type of planting operation: 0-Broadcast Planting. 1-Use Implement Ridge Spacing. 2-Use Specified Row Spacing.
		Crop Row Spacing	rowspac	float	mm	Row spacing to use, if “Type of Planting” value is set to use the specified row spacing, otherwise this value is ignored.
		Seed Placement (ridge/furrow)	rowridge	integer	unitless	Specifies whether the seed is planted in the furrow or in the ridge:

						0-Seed row placed in bottom of furrow. 1-Seed row placed on ridge top. Additional parameters contained in the "crop" database record.
65	Add Crop Residue Amounts	# Standing Residue Stems	numst	float	# m ⁻²	Number of standing residue stems added per unit area.
		Standing Residue Height	rstandht	float	m	Height of added standing residue stems.
		Standing Residue Mass	rstandmass	float	kg m ⁻²	Mass of added standing residue stems.
		Flat Surface Residue Mass	rflatmass	float	kg m ⁻²	Mass of flat residue added per unit area.
		Residue size/toughness class	rbc	integer	unitless	Residue size/toughness class of added residue.
		Buried Residue Mass	rburiedmass	float	kg m ⁻²	Mass of added buried residue.
		Buried Residue Depth	rburieddepth	float	mm	Maximum depth of added buried residue.
		Root Residue Mass	rrootmass	float	kg m ⁻²	Mass of added root residue per unit area.
		Root Residue Depth	rrootdepth	float	mm	Maximum depth of added root residue. 10 additional crop residue decomposition parameters

66	Add Manure Residue Amount	# Standing Residue Stems	M_numst	float	# m ⁻²	Number of standing residue (manure) stems added per unit area.
		Standing Residue Height	M_rstandht	float	m	Height of added standing residue (manure) stems.
		Standing Residue Mass	M_rstandmass	float	kg m ⁻²	Mass of added standing residue (manure) stems.
		Flat Surface Residue Mass	M_rflatmass	float	kg m ⁻²	Mass of flat residue (manure) added per unit area.
		Residue size/toughness class	rbc	integer	unitless	Residue size/toughness class of added residue.
		Buried Manure Mass	M_rbuiedmass	float	kg m ⁻²	Mass of added buried manure.
		Buried Manure Depth	M_rbuireddepth	float	mm	Maximum depth of added buried manure.
		Root Residue Mass	M_rrootmass	float	kg m ⁻²	Mass of added root residue (manure) per unit area.
		Root Residue Depth	M_rrootdepth	float	mm	Maximum depth of added root residue (manure).
		Total Manure Applied	manure_total_mass	float	kg m ⁻²	Total mass per unit area of manure applied.
		Total manure buried	manure_buried_ratio	float	fraction	Fraction of total mass of manure that is buried. 10 additional crop residue decomposition parameters

71	Irrigation (Obsolete)	Irrigation Application Method	irrtype	integer	unitless	Value represents the type of irrigation application method used: 0-Sprinkler. 1-Other.
		Depth of Water Applied	irrdepth	float	mm	Amount of water applied.
72	Monitor Irrigation	Set Irrigation Monitoring Status	irrmonflag	integer	unitless	Specifies whether irrigation is turned on or off: 0-Turn off irrigation monitoring. 1-Turn on irrigation monitoring.
		Maximum daily depth of water applied	irrmaxapp	float	mm	Maximum daily amount of water applied.
		Rate of water application	irrrate	float	mm hr ⁻¹	Rate at which irrigation water is applied.
		Duration of maximum daily depth water application	irrduration	float	hr	Duration for which maximum amount of daily irrigation water is applied.
		Application height (+ above) (- below) soil surface	irrapploc	float	mm	Height (+ value) above surface or depth (- value) below surface that water is applied.
		Minimum irrigation application depth	irrminapp	float	mm	Minimum amount of irrigation water applied.
		Management allowed	irrmad	float	unitless	Amount of soil water depletion allowed. Zero

		depletion (0 to 1)				means no water depletion and 1.0 means complete water depletion (wilting point).
		Minimum days between irrigations	irrminint	float	days	Minimum days between irrigation applications.
73	Single Irrigation	Depth of water applied	irrdepth	float	mm	Amount of irrigation water to apply.
		Rate of water application	irrrate	float	mm hr ⁻¹	Rate at which irrigation water is applied.
		Duration of water application	irrduration	float	hr	Duration for which irrigation water is applied.
		Application height (+ above)(- below) soil surface	irrapoloc	float	mm	Height (+ value) above surface or depth (- value) below surface that water is applied.
74	Terminate Irrigation Monitor					N/A

WEPS CLIGEN generated File

The weather information used by WEPS is usually generated from stochastic climate generators. CLIGEN is used to generate most of the typical daily weather variables such as max, min, and dew point temperatures, solar radiation, precipitation, etc. A standard CLIGEN generated daily output file (version 5.110 and greater) is the file format used to provide these weather input variables to WEPS, regardless of the source of the data, e.g. generated or historical. This filename is provided to the WEPS science model from within the "WEPS Run" file. The standard CLIGEN output file contains some header information followed by the generated daily data. The header information consists of the following information: (a) information about the CLIGEN station used to generate the file; (b) the command line used along with the command line arguments to generate the file (see Table 14 for the complete list of command line arguments); and (c) some monthly average information. Earlier versions of CLIGEN used different header formats with fewer header lines. For a user creating a CLIGEN format input file from historical data, WEPS uses specific information from the header lines as noted below. The specific

line by line information is fully described in here in an example CLIGEN generated output file:

1. CLIGEN generator version number. This number should be greater than or equal to 5.110 if using this file format description to create the file.

```
5.30001
```

2. Output of CLIGEN parameters (isim, itemp, and igcode) values. The isim variable specifies the simulation the CLIGEN simulation mode where "1" means a continuous storm simulation and a "2" means a single storm simulation. The itemp variable specifies whether breakpoint data is used where a "0" means no breakpoint data used and a "1" means that breakpoint data is used. The igcode variable specifies the evapotranspiration equation to use where a "0" means that wind information exists and to use the Penman ET equation and a "1" means no wind information exists and to use the Priestly-Taylor ET equation. This line is read in as a text string and ignored by WEPS. This line should not exceed 128 characters in length.

```
1 0 0
```

3. CLIGEN station statistical database record used to generate the file. It also includes the CLIGEN version number and some command line arguments used during its generation (-r specifies the random see value and -I specifies the interpolation method used with a value of 3 preserving the averages). This information is read as a text string and ignored by WEPS. This line should not exceed 128 characters in length.

```
Station: TRINIDAD CAA HOEHNE CO          CLIGEN VER. 5.30001 -r: 0 -
I: 3
```

4. These two lines consist of a text header line and a data line. The data line consists of the latitude in degrees and a positive value denotes the northern hemisphere, longitude in degrees with a negative value denoting the western hemisphere, elevation (meters), and number of years of data used to develop the CLIGEN database record. In addition, it includes the beginning year used in the daily output file and the number of years of daily simulated data in the file. It also includes the complete command line, including command line arguments (see Table 14), used to generate this CLIGEN output file. Note that the second line is wrapped here and displays as three lines but is really a single long line in the CLIGEN output file. These lines are read in as text strings and ignored by WEPS. These lines should each not exceed 128 characters in length.

```
Latitude Longitude Elevation (m) Obs. Years Beginning year Years simulated
Command Line:
 37.25 -104.33      1752          45          1          50
-S5 -s8434 -
iC:\ProgramData\USDA\WEPS\Databases\db/cligen/upd_US_cligen_stations.par -t5
-I3 -F -b01 -y50 -oC:\Users\wagner\Documents\WEPS
Files\Runs\testrun2_override_0.03_3.wjr\cli_gen.cli
```

5. These two lines consist of a text header line and a data line. The data line consists of the 12 monthly average maximum temperatures in degrees Celsius. January's value is in the first column and December's value is in the last column. While the text line is read but not used, the numerical values line is used by WEPS

```

Observed monthly ave max temperature (C)
 8.3 10.3 13.4 18.5 23.3 29.1 31.4 30.3 26.5 20.9 13.2  9.0

```

- These two lines consist of a text header line and a data line. The data line consists of the 12 monthly average minimum temperatures in degrees Celsius. January's value is in the first column and December's value is in the last column. While the text line is read but not used, the numerical values line is used by WEPS.

```

Observed monthly ave min temperature (C)
-8.2 -6.5 -3.9  1.3  6.5 11.7 14.9 13.9  9.5  3.1 -3.7 -7.5

```

- These two lines consist of a text header line and a data line. The data line consists of the 12 monthly average solar radiation values in Langley's/day. January's value is in the first column and December's value is in the last column. These lines are read in as text strings and ignored by WEPS. These lines should each not exceed 128 characters in length.

```

Observed monthly ave solar radiation (Langleys/day)
242.0 316.0 438.0 516.0 542.0 602.0 589.0 507.0 471.0 354.0 445.0 224.0

```

- These two lines consist of a text header line and a data line. The data line consists of the 12 monthly average precipitation values in mm. January's value is in the first column and December's value is in the last column. While the text line is read but not used, the numerical values line is used by WEPS.

```

Observed monthly ave precipitation (mm)
 9.6 11.2 18.9 23.1 44.7 36.1 49.8 50.4 25.7 20.2 16.5 13.1

```

- The remaining content of a CLIGEN generated file consists of the simulated daily values for the length of the simulation. Here are the two remaining header lines and example first and last lines of the daily data. The data lines consist of: (a) the date (day, month, and year in the first three columns), (b) the precipitation amount in millimeters that occurred on that day along with the duration in hours that the precipitation occurred, the time to peak in minutes, and the intensity of precipitation at peak precipitation if it occurs on that day (these values should be zero if no precipitation occurred on that day); (c) maximum and minimum daily temperature in degrees C; (d) solar radiation received on that day in Langley's/day; (e) average daily wind speed in m/s and its direction in degrees clockwise from true north; and (f) the last column contains the dew point temperature in degrees C. Note that the daily wind information available in CLIGEN is not used in WEPS.

```

da mo year  prcp  dur   tp      ip  tmax  tmin  rad  w-vl  w-dir  tdew
          (mm)  (h)          (C)   (C)  (l/d) (m/s) (Deg)  (C)
  1  1    1    0.0  0.00 0.00  0.00 -1.1 -11.8 176.  5.1  296. -14.1
[...]
31 12   50    0.0  0.00 0.00  0.00 -2.1 -15.6 198.  8.4  354. -20.8

```

CLIGEN stochastically generates (simulates) daily weather data from summary statistics. Simulation is always initiated on the first day of a year and produced in multiples of one full calendar year. The simulated weather is generated via command line arguments of the generator with the desired options and flags specified (Table 14).

Command line usage is:

```
cligen -S# -s# -i dbfile -o outfile -b# -y# -f -F -H -r# -t# -I# -v -V -h -? -O
```

Make sure there are no spaces between each flag and its parameter. If command line arguments are omitted, CLIGEN will interactively request the required information. An example command line is shown here:

```
Cligen -S14 -s4695 -iupd_US_cligen_stations.par -t5 -I3 -F -b01 -y100 -oliberal.cli
```

This directs CLIGEN to search in the wind database ‘upd_US_cligen_stations.par’ for the station with state ID 14 (Kansas), station code 4695 (Liberal), generate 100 years of daily weather data with starting year 1, using the interpolation method that preserves monthly means, and write the generated data to the file ‘liberal.cli’.

Table 14. Command line arguments for CLIGEN version 5.3.

Option	Description
S#	Valid state ID
s#	Valid station ID
i dbfile	Weather database (input) file
o outfile	Output file
b#	Beginning simulation year
y#	Number of years to simulate (generate)
f	Old WEPS record format
F	Overwrite output file if it exists
H	Omit header output
r#	Random number seed
t#	Simulation type: 4=single storm, 5=multiple years
I#	Interpolation method: 0= none (default), 1=linear, 2=Fourier, 3= interpolation preserving monthly means
v or V	Verbose option: generate additional information
h or ?	Display command line arguments and exit program
O filename	Use observed data

WEPS WINDGEN Generated File

The second weather information file used by WEPS is the WINDGEN generated file that provides hourly wind speed and daily direction information. Real hourly wind data can be used by WEPS, but it must be made available in the WINDGEN generator output file format. This filename is provided to the WEPS science model within the "WEPS Run" file. The WINDGEN file format consists of seven header lines that begin with the sharp character (#) to signify that they are comment lines followed by the data lines that consist of the hourly wind and daily wind direction for each day on a single line. The specific line by line information is fully described here in an example WINDGEN generated output file. The valid command line arguments for WINDGEN are listed in Table 15.

1. WINDGEN version and revision number. Earlier versions of WINDGEN used different data formats for the daily data. A user creating a WINDGEN format input file from historical data must include "WIND_GEN4" on this data line to correctly use a file created using the format described here.

```
# WIND_GEN4 $Revision: 1.1 $ Hourly values per day output
```

2. WINDGEN statistical database record name and location. This line is read in as a text string and ignored by WEPS. This line should not exceed 80 characters in length.

```
# station: 724640 PUEBLO MEMORIAL(AW), CO US
```

3. Station latitude and longitude location in degrees, minutes, and Hemisphere. This line is read in as a text string and ignored by WEPS. This line should not exceed 80 characters in length.

```
# lat: 38deg 17min N lon: 104deg 31min W
```

4. Period of record used to develop the station database record. The date format is: yyyyymmdd-yyyyymmdd. Also, the elevation of the station site is recorded in meters above mean sea level. This line is read in as a text string and ignored by WEPS. This line should not exceed 80 characters in length.

```
# period: 19540101-20001231 el:1439m
```

5. The next three comment header lines describe the remaining data lines. The columns are day, month, year, and wind direction for the day in degrees clockwise from north, followed by the 24 average hourly wind speeds in m/s, beginning with 1 am and ending with 12 pm (1 to 24 hrs.). Some columns are removed to allow the example rows to display in a single line. These lines are read in as text string and ignored by WEPS. These lines should each not exceed 80 characters in length.

```
# day mo year dir hr1 hr2 hr3 hr4 hr5 hr6 [...] hr20 hr21 hr22 hr23  
hr24
```

```
#          deg m/s m/s m/s m/s m/s m/s [...] m/s m/s m/s m/s  
m/s
```

```
# -----  
--
```

6. The individual data lines, representing a single simulated day's daily wind direction in degrees clockwise from north, and the 24-hourly wind values. Some columns are removed to allow the example rows to display in a single line.

```
1 1 1 157.5 0.9 0.0 0.0 0.0 1.3 [...] 2.2 1.8 1.5
```

```
[...]
31 12 50 22.5 1.1 0.0 0.0 0.0 1.6 [...] 2.8 2.3 1.8
```

7. WINDGEN version and revision number. Earlier versions of WINDGEN used different data formats for the daily data. A user creating a WINDGEN format input file from historical data must include “WIND_GEN4” on this data line to correctly use a file created using the format described here.

```
# WIND_GEN4 $Revision: 1.1 $ Hourly values per day output
```

8. WINDGEN statistical database record name and location. This line is read in as a text string and ignored by WEPS. This line should not exceed 80 characters in length.

```
# station: 724640 PUEBLO MEMORIAL(AW), CO US
```

9. Station latitude and longitude location in degrees, minutes, and hemisphere. This line is read in as a text string and ignored by WEPS. This line should not exceed 80 characters in length.

```
# lat: 38deg 17min N lon: 104deg 31min W
```

10. Period of record used to develop the station database record. The date format is: yyyyymmdd-yyyyymmdd. Also, the elevation of the station site is recorded in meters above mean sea level. This line is read in as a text string and ignored by WEPS. This line should not exceed 80 characters in length.

```
# period: 19540101-20001231 el:1439m
```

11. The next three comment header lines describe the remaining data lines. The columns are day, month, year, and wind direction for the day in degrees clockwise from north, followed by the 24 average hourly wind speeds in m/s, beginning with 1am and ending with 12 pm (1 to 24 hrs.). Some columns are removed to allow the example rows to display in a single line. These lines are read in as text string and ignored by WEPS. These lines should each not exceed 80 characters in length.

```
# day mo year dir hr1 hr2 hr3 hr4 hr5 hr6 [...] hr20 hr21 hr22 hr23
hr24
# deg m/s m/s m/s m/s m/s m/s [...] m/s m/s m/s m/s
m/s
# -----
--
```

12. The individual data lines, representing a single simulated day’s daily wind direction in degrees clockwise from north, and the 24-hourly wind values. Some columns are removed to allow the example rows to display in a single line.

```
1 1 1 157.5 0.9 0.0 0.0 0.0 1.3 [...] 2.2 1.8 1.5
[...]
31 12 50 22.5 1.1 0.0 0.0 0.0 1.6 [...] 2.8 2.3 1.8
```

WINDGEN stochastically generates (simulates) hourly wind data from summary statistics. Wind simulation is always initiated on the first day of a year and produced in multiples of one full calendar year. Leap years are accounted for. Only the -s option is

required. The simulated hourly wind is generated via command line arguments of the generator with the desired options and flags specified (Table 15).

Command line usage:

```
wind_gen4 -D -V -v -h -l -f dbfile -o outfile -s # -x # -r # -b # -y # -u # -d # -?
```

Note: spaces are optional between each flag and its parameter.

Two command line examples are shown here:

```
wind_gen4 -s 724515 -o GardenCity.out
```

This directs WINDGEN to search in the default wind database (wind_gen.wdb) for the station with station code 724515 (Garden City, Kansas), generate 1 year of daily wind data, and write it to the file ‘GardenCity.out’.

```
wind_gen4 -s 724515 -f ks.wdb -b 1980 -y 30 -o GardenCity.out
```

This directs WINDGEN to search in the wind database ‘ks.wdb’ for the station with station code 724515 (Garden City, Kansas), generate 30 years of daily wind data with a starting year of 1980, and write it to the file ‘GardenCity.out’.

Table 10. Command line arguments for WINDGEN version 4.

Option	Default value	Description
D		Debug flag: additional output is generated for debugging purposes
V		Display WINDGEN version only and exit program
v		Verbose option: generate additional information. This option would typically be used in situations where a corrupted wind database was suspected because of possibly erroneous output data being observed.
h		Do not generate a heading (title) for the output
l		Generate long (additional) output; currently only generates additional column headings but no data
f dbfile	wind_gen.wdb	Wind database (input) file
o outfile	screen display	Output file; The default output (screen display) is used if this option is not specified.

s #		Valid station code (WBAN number); this option is REQUIRED
x #		Station database index number (an index number for the station code specified with the -s option) to obtain faster access to the desired database record information.
r #	54321	Random number seed
b #	1	Beginning simulation year
y #	1	Number of years to simulate (generate)
u #	6	Storm duration length in hours (24 or less)
d #	5	Number of days to build storms from (7 or less)
?		Display command line arguments and exit program

WEPS Command line arguments

The WEPS program contains a number of command line arguments that allow the user to modify the behavior of WEPS for specific situations and give the user additional control over how it simulates specific processes. Some of the arguments have been added to allow the developers to better debug code changes and evaluate new features added to the model. A complete listing and brief description of all the command line arguments (Table 16) can be obtained by executing the following command line:

```
weps.exe -h (Windows systems)
```

or

```
weps -h (Linux systems)
```

The following is the entire list of WEPS command line arguments with complete descriptions of the arguments and any parameters that they may have. Note that no spaces are allowed between the command line argument and any parameters the arguments may have. Any text strings, such as filenames, must be enclosed in quotes if there are spaces in those text parameters.

-? and -h

Both of these two flags will generate a complete listing of all WEPS command line parameters with brief descriptions of them.

-c#

Specifies whether WEPS will compute the NRCS Soil Conditioning Index for the simulation and generate the "sci_energy.out" and "stir_energy.out" files. An argument parameter of "0" specifies no SCI output and a value of "1" (the default) specifies that the SCI be computed, and the appropriate files be generated.

- C#
Specifies if WEPS is to be run in “Yield Calibration” mode or not. A parameter value of “0” (the default) will not run WEPS in calibration mode. Any positive value will run WEPS in calibration mode with the specified value being the maximum number of iterations it will attempt during the calibration process. The “Yield Calibration” mode does a simple bisection iteration process to determine the proper biomass adjustment value to apply to selected crop(s) to meet the target yield(s) desired. Once the target yields are met (within $\pm 5\%$), WEPS will perform one more simulation in non-calibration mode using the previously determined biomass adjustment parameters for the selected crops.
- f#.#
Specifies the amount of freeze damage to leaves that can occur. The parameter must be specified as a fraction (≥ 0.0 and ≤ 1.0) of total leaf mass present at the time. The default is “0.0”
- E#
Specifies whether wind and/or water erosion is simulated in the WEPS run or not. A parameter value of “0” will not execute the either erosion submodel. A value of “1” (the default) will run the wind erosion submodel. A value of “2” will run only the Water Erosion Prediction Program’s (WEPP) water erosion submodel (Flanagan, et al, 2001). A value of “3” will run both the wind and water erosion submodel code.
- g#
Specifies whether the crop submodel’s growth stress functions are enabled within WEPS. A parameter value of “0” means no stress functions are applied. A value of “1” means only the water stress function is applied. A value of “2” means only the temperature stress function is applied. A value of “3” (the default) means both the water and temperature stress functions are applied.
- G#.#
Specifies the maximum level of water stress allowed (≥ 0.0 and ≤ 1.0). A value of “0.0” (the default) means that the maximum water stress is allowed to occur. A value of “1.0” means that no water stress is allowed to occur.
- I#
Specifies whether an initial warmup cycle is run prior to the simulation. A value of “0” means no initialization is done. A positive value means that number of management cycles will be run during the initialization step. A value of “1” is the default.
- L#
Specifies the soil layer thickness (mm) to scale layer splitting internally in WEPS (no decimals are allowed for this parameter). The default value is “2”.
- I#
Specifies the rate of soil layer thickness increase (%) with depth for soil layer splitting (no decimals are allowed for this parameter). The default value is “25”.
- O#
Specifies the internal WEPS simulation day to generate a standalone erosion (SWEEP) input file. This argument requires a positive value as an argument when used.

- oDD/MM/YYYY
Specifies the simulation date (DD/MM/YYYY format) to generate a standalone erosion (SWEEP) input file. This argument requires a valid simulation date when used. The month and day values must always be specified with 2 digits. The year value can be specified with 1, 2, 3, or 4 digits.
- p#
Specifies whether soil puddling with saturation occurs above freezing. A value of “0” disables this functionality. A value of “1” (the default) enables it.
- Ppath
Specifies the WEPS project run directory. The directory path must be enclosed in quotes if there are any spaces or special characters in the directory name. The “-P” can be omitted only if there are no other command line arguments specified.
- r#
Specifies the winter annual root depth growth option. A value of “0” means the depth grows at the same rate as the above ground height of the plant. A value of “1” (the default) means the depth grows based upon the fall season heat units.
- R#
Specifies what level of debug messages are dumped to the screen (stdout). A value of “0” (the default) means that no debug messages are sent to the screen. Any positive value specifies the maximum level at which debug messages are sent to the screen, e.g., a value of “1” specifies only the first level of debug messages are sent to the screen, a value of “2” means both level 1 and level 2 debug message are sent, etc.
- s#
Specifies the soil IFC file format to input. A value of “0” (the default) means the new (current) format is input. A value of “1” means the old (obsolete) format which is missing the slope input value is used.
- S#
Specifies how the 1/3 bar and 15 bar soil water content values are determined and set. A value of “0” means that the input values for both 1/3 and 15 bars are provided in volumetric units. A value of “1” means the input value for 1/3 bar is in volumetric units and the 15 bar is in gravimetric units. A value of “2” means the input values for both 1/3 and 15 bars are provided in gravimetric units. A value of “3” means a texture-based calculation is used to set both the 1/3 bar and 15 bar values. A value of “4” (the default) means that Walter Rawls texture-based method is used for all relevant properties, e.g., the soil water retention curve, bulk density parameters, and saturated hydraulic conductivity are estimated using the texture-based calculation.
- t#
Specifies whether the “Confidence Interval” is reported on a crop/management rotation basis for mean annual wind erosion (ci.out). A value of “0” (the default) means that no confidence interval report is generated. A value of “1” means that the confidence interval report is generated. A value of “2” (not implemented) means that the confidence interval value will limit the run length of the simulation.
- T#
Specifies whether the effect of planting to moisture with a deep furrow drill on plant available soil water is simulated. A value of “0” (the default) means that there is no deep furrow effect applied. A value of “1” means that the deep furrow

effect is applied. For a full description of the deep furrow effect, see the chapter: “Hydrology Submodel of WEPS” in the WEPS Technical Documentation.

- u#
Specifies whether resurfacing of buried roots is simulated or not. A value of “0” means that no resurfacing of roots is simulated. A value of “1” (the default) means that buried roots are resurfaced.
- w#
Specifies the weighting method used for soil layer conductivity and water flow. A value of “0” (the default) means the arithmetic mean (equal weighting) between the two adjacent layers is used. A value of “1” means that the layer thickness is used for proportional weighting. A value of “2” means an internodal method using the Darcian mean is used.
- W#
Specifies which hydrology and infiltration method is used within WEPS. A value of “0” (the default) uses Darcian flow dynamics for hydrology and infiltration. A value of “1” means WEPP hydrology (soil water balance and Green-Ampt infiltration) is used. A value of “2” means WEPP hydrology (soil water balance and Green-Ampt infiltration) is used with WEPP runoff calculations.
- X#.#
Specifies the maximum wind speed to cap the input values to in m/s. For example, “-X25.0” would limit the maximum wind speed to 25.0 m/s.
- Z#
Specifies the maximum number of simulation cycles to run while in “Yield Calibration” mode. A value of “0” (the default) means to use all cycles specified for a normal WEPS run in the calibration phase. A positive integer value means to limit the number of cycles to the specified value, if less than the number of cycles desired for the simulation run itself.

Table 16. WEPS command line arguments help screen list as generated with the “-h” option.

```
WEPS 1.0
Release: development
Built on: Tue Jul 12 18:00:54 MDT 2016
Compiled with: gfortran_64
Compiled flags: optimize

Date of WEPS Run: Jul 22, 2016 14:45:05

Valid command line options:
-?  Display this help screen
-h  Display this help screen
-c  Soil Conditioning Index output
    0 = no output
    1 = create soil-conditioning.out file (default)
-C  WEPS crop calibration mode
    0 = Do not run crop calibration (default)
    # = Run crop calibration # interation max
-f  Specify leaf freeze damaged mass loss fraction
```

Specify -f0.85 to make 85% of freeze damaged mass disappear

- E Simulate "\"erosion\" in WEPS run
 - 0 = Do not run any erosion submodel
 - 1 = Run the erosion submodel (default)
 - 2 = Run only WEPP erosion submodel
 - 3 = Run WEPS and WEPP erosion submodels
- g Application of growth stress functions
 - 0 = no growth stress function applied
 - 1 = water stress function applied
 - 2 = temperature stress function applied
 - 3 = both stress functions applied
- G Maximum level of water stress allowed
 - G0.00 allows maximum water stress to occur
 - G1.00 does not allow any water stress
- I Specify if initialization is done and if so, the # loops
 - 0 = No initialization
 - 1 = Runs one management cycle (default)
 - 2 = Runs x management cycles
- L Specify soil layer thickness to scale layer splitting (mm)
 - Specify -L2 for layer splitting to use 2 mm (no decimals)
- l Specify rate of soil layer thickness increase with depth
 - for layer splitting in percent increase of layer thickness.
 - Specify -150 to inc. 50 percent for each layer (no decimals)
- O Generate stand alone erosion input file on simulation day
 - Specify -O2932 to output file on simulation day 2932
- o Generate stand alone erosion input file on DD/MM/YY
 - Specify -o020901 to output file on day 2 month 9 year 1
 - Day and month must be 2 digits, Year can be 1 to 4 digits
- p Select soil puddling with saturation all above freezing
 - 0 = disable
 - 1 = enable
- P Specify path to WEPS project run directory
 - Must be specified if other command line switches are used
 - Specifying only the path without the "\"-P\" option only works if no other command line switches are specified.
 - e.g: "\"weps path_to_weps.run_file\""
- r Select winter annual root depth growth option
 - 0 = depth grows at same rate as height
 - 1 = depth grows with fall heat units
- R WEPS debug messages dumped to screen
 - 0 = no debug messages sent to screen
 - 1 = 1st level debug messages sent to screen
 - 2 = 1st and 2nd level debug messages sent to screen
 - 3 = 1st, 2nd, and 3rd level debug messages sent to screen
- s Specify soil ifc file input format type
 - 0 = new format (default)
 - 1 = old format (slope set in weps.run)
- S Vary type of value input for 1/3 bar, 15 bar water
 - 0 = 1/3bar(vol) 15bar(vol)
 - 1 = 1/3bar(vol) 15bar(grav)
 - 2 = 1/3bar(grav) 15bar(grav)
 - 3 = use texture based calc
 - 4 = use Rawls texture for full properties (default)
 - Override 1/3bar, 15bar, bulk density w/ texture estimate
- t Confidence Interval on Rotation Mean Annual Erosion

0 = no confidence interval calc (default)
 1 = confidence interval reported
 2 = used to limit run length (not implem)
 -T Deep Furrow Effect on Transpiration Depth
 0 = no deep furrow effect (default)
 1 = deep furrow affects transpiration
 -u Resurfacing buried roots
 0 = no resurfacing of buried roots
 1 = resurface buried roots (default)
 -w Specify method of weighting for layer conductivity and flow
 0 = arithmetic mean 0.5 method (default)
 1 = layer thickness proportional weighted
 2 = internodal method, darcian mean
 -W Specify hydrology calculation method used
 0 = darcian flow (default)
 1 = Green-Ampt infil., simple drainage
 2 = Green-Ampt infil., WEPP runoff
 -X Specify maximum wind speed cap (m/s)
 Specify -X25.0 to limit input wind speeds to a max of 25
 m/s
 -Y Optional functional Yield/residue ratio
 0 = Use full staged biomass partitioning
 1 = Use partitioned Yield/residue ratio (default)
 -Z Specify maximum number of cycles to run while calibrating
 0 = Use all cycles (default)

Default options are set to:

-c1 -C0 -E1 -f0.00 -g3 -G0.00 -I1 -L2 -l25 -O(no file) -o(no
 file) -p1 -P./ -r1 -R0 -S4 -s0 -T0 -t0 -u1 -w0 -W0 -X 0.0 -Y1 -Z0

References

- Allmaras, R.R., R.E. Burwell, and R.F. Holt. 1967. Plow-Layer Porosity and Surface Roughness from Tillage as Affected by Initial Porosity and Soil Moisture at Tillage Time1. *Soil Science Society of America Journal*. 31:550-556.
- Baumer, O.W. 1990. Prediction of soil hydraulic parameters. IN: WEPP Data Files for Indiana. SCS National Soil Survey Laboratory, Lincoln, NE.
- Flanagan, D.C., J.C. Ascough II, M.A. Nearing, and J.M. Laflen. 2001. Chapter 7: The Water Erosion Prediction Project (WEPP) Model. *In Landscape Erosion and Evolution Modeling*, R.S. Harmon and W.W. Doe III, eds. Kluwer Academic Publishers, Norwell, MA. 51 pp.
- Post, D.F., A. Fimbres, A.D. Matthias, E.E. Sano, L. Accioly, A.K. Batchily, and L.G. Ferreira. 2000. Predicting soil albedo from color value and spectral reflectance data. *Soil Science Society of America Journal*. 64:1027-1034.
- Rawls, W.J. 1983. Estimating soil bulk density from particle size analysis and organic matter content. *Soil Science*. 135(2):123-125.
- Saxton, K.E., W.J. Rawls, J.S. Romberger, and R. I. Papendick. 1986. Estimating generalized soil-water characteristics from texture. *Soil Science Society of America Journal*. 50(4):1031-1036.
- Soil Survey Staff. 1996. Soil survey laboratory method manual. Soil Survey Investigations Report Number 42, Version 3.0. USDA-NRCS, Washington, DC.

Supplement A: Operation record parameter definitions, prompts, and display options.

Table 8. An XST formatted display of the operation parameters and properties.

Code	Id	Name	Param Prompt	Action Name	Param Type	Param Display	Param Unit	Conversion Factor	Alternative Units	Param Choices
O	0	Initialization	Initialization Operation Notes	op_notes0	string	E,T				
O	1	Direction and Speed	Speed	ospeed	float	E,N	m s ⁻¹	value * 2.237	mph	
O	1	Direction and Speed	Direction from North	odirect	float	E,N	deg.			
O	1	Direction and Speed	Standard Speed	ostdspeed	float	E,N	m s ⁻¹	value * 2.237	mph	
O	1	Direction and Speed	Minimum Speed	ominspeed	float	E,N	m s ⁻¹	value * 2.237	mph	
O	1	Direction and Speed	Maximum Speed	omaxspeed	float	E,N	m s ⁻¹	value * 2.237	mph	
O	1	Direction and Speed	Tillage Operation Notes	op_notes1	string	E,T				
O	2	Others	Other Operation Notes	op_notes2	string	E,T				
O	3	Energy STIR Direction Speed	Diesel Energy (in fuel) per Area	oenergyarea	float	E,N	l ha ⁻¹	value * 0.106907	gal/acre	
O	3	Energy STIR Direction Speed	Soil Tillage intensity Rating	ostir	float	E,N				

O	3	Energy STIR Direction Speed	Speed	ospeed	float	E,N	m s ⁻¹	value * 2.237	mph
O	3	Energy STIR Direction Speed	Direction from North	odirect	float	E,N	Deg.		
O	3	Energy STIR Direction Speed	Standard Speed	ostdspeed	float	E,N	m s ⁻¹	value * 2.237	mph
O	3	Energy STIR Direction Speed	Minimum Speed	ominspeed	float	E,N	m s ⁻¹	value * 2.237	mph
O	3	Energy STIR Direction Speed	Maximum Speed	omaxspeed	float	E,N	m s ⁻¹	value * 2.237	mph
O	3	Energy STIR Direction Speed	Tillage Operation Notes	op_notes3	string	E,T			
O	3	Energy STIR Direction Speed	Fuel	ofuel	string	E,F			
O	4	Energy STIR Others	Diesel Energy per Area	oenergyarea	float	E,N	l ha ⁻¹	value * 0.106907	gal/acre
O	4	Energy STIR Others	Soil Tillage intensity Rating	ostir	float	E,N			
O	4	Energy STIR Others	Other Operation Notes	op_notes4	string	E,T			
O	4	Energy STIR Others	Fuel	ofuel	string	E,F			

G	1	Tillage	Actual Depth	gtdepth	float		mm	value * 0.03937	in	
G	1	Tillage	Intensity	gtilint	float		fraction			
G	1	Tillage	Area Affected	gtilArea	float		fraction			
G	1	Tillage	Standard Depth	gtstddepth	float		mm	value * 0.03937	in	
G	1	Tillage	Minimum Depth	gtmindepth	float		mm	value * 0.03937	in	
G	1	Tillage	Maximum Depth	gtmaxdepth	float		mm	value * 0.03937	in	
G	2	Biomass Manipulation	Area Affected	gbioarea	float		fraction			
G	3	Crop Name	Crop Name	gcropname	string	E,S				
G	4	Add Material to Field	Material Name	gamdname	string	E,S				
P	2	Random Roughness	Random Roughness Flag	rroughflag	int	E,C				0:Always use specified random roughness value 1:Allow WEPS to auto-adjust random roughness value
P	2	Random Roughness	Nominal Random Roughness	rrough	float	E,N	mm	value * 0.03937	in	
P	5	Ridges and Dikes	Ridge Flag	rdgflag	int	E,C				0:Pre-existing ridges/dikes left unchanged

										1:Ridges/dikes set to specified values
										2:Ridges/dikes set, based on tillage depth
P	5	Ridges and Dikes	Ridge Height	rdghit	float	E,N	mm	value * 0.03937	in	
P	5	Ridges and Dikes	Ridge Spacing	rdgspac	float	E,N	mm	value * 0.03937	in	
P	5	Ridges and Dikes	Ridge Top Width	rdgwidth	float	E,N	mm	value * 0.03937	in	
P	5	Ridges and Dikes	Dike Height	dkhit	float	E,N	mm	value * 0.03937	in	
P	5	Ridges and Dikes	Dike Spacing	dkspac	float	E,N	mm	value * 0.03937	in	
P	11	Aggregate Crushing	Aggregate Size Distribution Factor	asdf	float	E,N				
P	11	Aggregate Crushing	Crushing Intensity Factor	crif	float	E,N				
P	12	Soil Loosening	Soil Loosening	soilos	float	E,N	fraction			
P	13	Soil Layer Mixing	Layer Mixing	laymix	float	E,N	fraction			
P	24	Flatten Standing Biomass	Flatten Biomass Flag	fbioflagvt	int	E,C				0:Flatten crop and residue

								1:Flatten crop only
								14:Flatten residue only
P	24	Flatten Standing Biomass	Mass flattened (fragile residue)	massflatvt1	float	E,N	fraction	
P	24	Flatten Standing Biomass	Mass flattened (moderately tough residue)	massflatvt2	float	E,N	fraction	
P	24	Flatten Standing Biomass	Mass flattened (non-fragile/large residue)	massflatvt3	float	E,N	fraction	
P	24	Flatten Standing Biomass	Mass flattened (woody residue)	massflatvt4	float	E,N	fraction	
P	24	Flatten Standing Biomass	Mass flattened (small stones/gravel)	massflatvt5	float	E,N	fraction	
P	25	Bury Flat Biomass						
P	25	Bury Flat Biomass	Bury Biomass Flag	burydist	int	E,C		0:Uniform burial distribution
								1:Mixing and inversion burial distribution
								2:Mixing burial distribution

3:Inversion burial
distribution

4:Lifting,
fracturing burial
distribution

5:Compression
burial
distribution

P	25	Bury Flat Biomass	Mass Buried (fragile residue)	massburyvt1	float	E,N	fraction
P	25	Bury Flat Biomass	Mass Buried (moderately tough residue)	massburyvt2	float	E,N	fraction
P	25	Bury Flat Biomass	Mass Buried (non-fragile/large residue)	massburyvt3	float	E,N	fraction
P	25	Bury Flat Biomass	Mass Buried (woody residue)	massburyvt4	float	E,N	fraction
P	25	Bury Flat Biomass	Mass Buried (small stones/gravel)	massburyvt5	float	E,N	fraction
P	26	Resurface Buried Biomass	Mass Resurfaced (fragile residue)	massresurvt1	float	E,N	fraction
P	26	Resurface Buried Biomass	Mass Resurfaced (moderately tough residue)	massresurvt2	float	E,N	fraction

P	26	Resurface Buried Biomass	Mass Resurfaced (non-fragile/large residue)	massresurvt3	float	E,N	fraction	
P	26	Resurface Buried Biomass	Mass Resurfaced (woody residue)	massresurvt4	float	E,N	fraction	
P	26	Resurface Buried Biomass	Mass Resurfaced (small stones/gravel)	massresurvt5	float	E,N	fraction	
P	30		Defoliate Flag	defoliateflag	int	E,C		1:Crop defoliated 0:Crop not defoliated
P	31	Kill or Defoliate Growing Crop	Kill/Defoliate Flag	kilflag	int	E,C		1:Annual crop killed, perennial crop regrows 2:All crop types are killed 3:Crop defoliated 0:No crop killed
P	32	Cut/Remove Biomass to Height	Cut Biomass Flag	cutflag	int	E,C		0:Cut Value = Height of standing stubble remaining 1:Cut Value = Length of standing plant stalks removed

P	32	Cut/Remove Biomass to Height	Cut Value	cutvalh	float	E,N	mm	value * 0.03937	in
P	32	Cut/Remove Biomass to Height	Cut Yield Removed	cyldrmh	float	E,N	fraction		
P	32	Cut/Remove Biomass to Height	Cut Plant Removed	cplrmh	float	E,N	fraction		
P	32	Cut/Remove Biomass to Height	Cut Standing Residue Removed	cstrmh	float	E,N	fraction		
P	33	Cut/Remove Biomass by Fraction							
P	33	Cut/Remove Biomass by Fraction	Plant Height Removed	cutvalf	float	E,N	fraction		
P	33	Cut/Remove Biomass by Fraction							
P	33	Cut/Remove Biomass by Fraction	Cut Yield Removed	cyldrmf	float	E,N	fraction		
P	33	Cut/Remove Biomass by Fraction							
P	33	Cut/Remove Biomass by Fraction	Cut Plant Removed	cplrmf	float	E,N	fraction		

P	33	Cut/Remove Biomass by Fraction						
P	33	Cut/Remove Biomass by Fraction	Cut Standing Residue Removed	cstrmf	float	E,N	fraction	
P	34	Change Standing Biomass Fall Rate				E,C		
P	34	Change Standing Biomass Fall Rate	Select biomass pool type	frselpool	int			1: Crop 2: Temporary 3: Crop and Temporary 4: Residue 5: Crop and Residue 6: Temporary and Residue 7: Crop, Temporary and Residue 0: No adjustments applied
P	34	Change Standing Biomass Fall Rate	Standing Biomass Fall Rate	ratemultvt1	float	E,N	multiplier	

		Biomass Fall Rate	Rate Multiplier (fragile residue)				
P	34	Change Standing Biomass Fall Rate	Standing Biomass Fall Rate Multiplier (moderately tough residue)	ratemultvt2	float	E,N	multiplier
P	34	Change Standing Biomass Fall Rate	Standing Biomass Fall Rate Multiplier (non-fragile/large residue)	ratemultvt3	float	E,N	multiplier
P	34	Change Standing Biomass Fall Rate	Standing Biomass Fall Rate Multiplier (woody residue)	ratemultvt4	float	E,N	multiplier
P	34	Change Standing Biomass Fall Rate	Standing Biomass Fall Rate Multiplier (small stones/gravel)	ratemultvt5	float	E,N	multiplier
P	34	Change Standing Biomass Fall Rate	Standing Biomass Fall Threshold Multiplier (fragile residue)	threshmultvt1	float	E,N	multiplier
P	34	Change Standing Biomass Fall Rate	Standing Biomass Fall Threshold Multiplier (moderately tough residue)	threshmultvt2	float	E,N	multiplier

P	34	Change Standing Biomass Fall Rate	Standing Biomass Fall Threshold Multiplier (non-fragile/large residue)	threshmultvt3	float	E,N	multiplier		
P	34	Change Standing Biomass Fall Rate	Standing Biomass Fall Threshold Multiplier (woody residue)	threshmultvt4	float	E,N	multiplier		
P	34	Change Standing Biomass Fall Rate	Standing Biomass Fall Threshold Multiplier (small stones/gravel)	threshmultvt5	float	E,N	multiplier		
P	37		Thinning Value	thinvalp	float	E,N	# m ⁻²	value * 0.0929	# ft ⁻²
P	37		Thinned Yield Removed	tyldrmp	float	E,N	fraction		
P	37		Thinned Plant Removed	tplrmp	float	E,N	fraction		
P	37		Thinned Standing Residue Removed	tstrmp	float	E,N	fraction		
P	38	Thin Biomass by Fraction	Thinning Value	thinvalf	float	E,N	fraction		
P	38	Thin Biomass by Fraction	Thinned Yield Removed	tyldrmf	float	E,N	fraction		

P	38	Thin Biomass by Fraction	Thinned Plant Removed	tplrmf	float	E,N	fraction	
P	38	Thin Biomass by Fraction	Thinned Standing Residue Removed	tstrmf	float	E,N	fraction	
P	42	Cut/Remove Biomass to Height (flags)	Report Harvest	harv_report_flg	int	E,C		0:No Report 1:Report
P	42	Cut/Remove Biomass to Height (flags)	Use Harvest in Calibration	harv_calib_flg	int	E,C		0:Do not Use 1:Use for Calibration
P	42	Cut/Remove Biomass to Height (flags)	Harvest Units	harv_unit_flg	int	E,C		0:Use Units in Crop 1:Use mass/area Units
P	42	Cut/Remove Biomass to Height (flags)	Crop Maturity Warnings	mature_warn_flg	int	E,C		0:No Warnings 1:Warnings
P	42	Cut/Remove Biomass to Height (flags)	Cut Biomass Flag		cutflag	E,C	int	0:Cut Value = Height of standing stubble remaining 1:Cut Value = Length of

standing plant stalks removed

P	42	Cut/Remove Biomass to Height (flags)	Cut Value	cutvalh	float	E,N	mm	value * 0.03937	in	
P	42	Cut/Remove Biomass to Height (flags)	Cut Yield Removed	cyldrmh	float	E,N	fraction			
P	42	Cut/Remove Biomass to Height (flags)	Cut Plant Removed	cplrmh	float	E,N	fraction			
P	42	Cut/Remove Biomass to Height (flags)	Cut Standing Residue Removed	cstrmh	float	E,N	fraction			
P	43	Cut/Remove Biomass by Fraction (flags)	Report Harvest	harv_report_flg	int	E,C				0:No Report
P	43	Cut/Remove Biomass by Fraction (flags)	Use Harvest in Calibration	harv_calib_flg	int	E,C				1:Report 0:Do not Use
P	43	Cut/Remove Biomass by Fraction (flags)	Harvest Units	harv_unit_flg	int	E,C				1:Use for Calibration

								0:Use Units in Crop
								1:Use mass/area Units
P	43	Cut/Remove Biomass by Fraction (flags)	Crop Maturity Warnings	mature_warn_flg	int	E,C		0:No Warnings
								1:Warnings
P	43	Cut/Remove Biomass by Fraction (flags)	Plant Height Removed	cutvalf	float	E,N	fraction	
P	43	Cut/Remove Biomass by Fraction (flags)	Cut Yield Removed	cyldrmf	float	E,N	fraction	
P	43	Cut/Remove Biomass by Fraction (flags)	Cut Plant Removed	cplrmf	float	E,N	fraction	
P	43	Cut/Remove Biomass by Fraction (flags)	Cut Standing Residue Removed	cstrmf	float	E,N	fraction	
P	47	Thin Biomass to Population (flags)	Report Harvest	harv_report_flg	int	E,C		0:No Report
								1:Report

P	47	Thin Biomass to Population (flags)	Use Harvest in Calibration	harv_calib_flg	int	E,C				0:Do not Use 1:Use for Calibration
P	47	Thin Biomass to Population (flags)	Harvest Units	harv_unit_flg	int	E,C				0:Use Units in Crop 1:Use mass/area Units
P	47	Thin Biomass to Population (flags)	Crop Maturity Warnings	mature_warn_flg	int	E,C				0:No Warnings 1:Warnings
P	47	Thin Biomass to Population (flags)	Thinning Value	thinvalp	float	E,N	# m ⁻²	value * 0.0929	# ft ²	
P	47	Thin Biomass to Population (flags)	Thinned Yield Removed	tyldrmp	float	E,N	fraction			
P	47	Thin Biomass to Population (flags)	Thinned Plant Removed	tplrmp	float	E,N	fraction			
P	47	Thin Biomass to Population (flags)	Thinned Standing Residue Removed	tstrmp	float	E,N	fraction			
P	48	Thin Biomass by Fraction (flags)	Report Harvest	harv_report_flg	int	E,C				0:No Report

P	48	Thin Biomass by Fraction (flags)	Use Harvest in Calibration	harv_calib_flg	int	E,C		1:Report 0:Do not Use
P	48	Thin Biomass by Fraction (flags)	Harvest Units	harv_unit_flg	int	E,C		1:Use for Calibration 0:Use Units in Crop
P	48	Thin Biomass by Fraction (flags)	Crop Maturity Warnings	mature_warn_flg	int	E,C		1:Use mass/area Units 0:No Warnings
P	48	Thin Biomass by Fraction (flags)	Thinning Value	thinvalf	float	E,N	fraction	1:Warnings
P	48	Thin Biomass by Fraction (flags)	Thinned Yield Removed	tyldrmf	float	E,N	fraction	
P	48	Thin Biomass by Fraction (flags)	Thinned Plant Removed	tplrmf	float	E,N	fraction	
P	48	Thin Biomass by Fraction (flags)	Thinned Standing Residue Removed	tstrmf	float	E,N	fraction	

P	50	Set Crop Residue Amounts	Number of Standing Residue Stems	numst	float	E,N	# m ⁻²	value * 0.0929	# ft ²	
P	50	Set Crop Residue Amounts	Standing Residue Height	rstandht	float	E,N	m	value * 39.37	in	
P	50	Set Crop Residue Amounts	Standing Residue Mass	rstandmass	float	E,N	kg m ⁻²	value * 8921.8	lb acre ⁻¹	
P	50	Set Crop Residue Amounts	Flat Surface Residue Mass	rflatmass	float	E,N	kg m ⁻²	value * 8921.8	lb acre ⁻¹	
P	50	Set Crop Residue Amounts	Residue size/toughness class	rbc	int	E,C				1:Fragile, very small residue, e.g. soybeans 2:Moderately tough, short residue, e.g. wheat 3:Non-fragile, medium residue, e.g. corn 4:Woody, large residue 5:Gravel, rock
P	50	Set Crop Residue Amounts	Buried Residue Mass	buriedmass	float	E,N	kg m ⁻²	value * 8921.8	lb acre ⁻¹	

P	50	Set Crop Residue Amounts	Buried Residue Depth	rburieddepth	float	E,N	mm	value * 0.03937	in
P	50	Set Crop Residue Amounts	Root Residue Mass	rrootmass	float	E,N	kg m ⁻²	value * 8921.8	lb acre ⁻¹
P	50	Set Crop Residue Amounts	Root Residue Depth	rrootdepth	float	E,N	mm	value * 0.03937	in
P	50	Set Crop Residue Amounts	decomposition rate for standing stalks	standdk	float	E,N	kg kg ⁻¹ day ⁻¹		
P	50	Set Crop Residue Amounts	decomposition rate for surface residue	surfdk	float	E,N	kg kg ⁻¹ day ⁻¹		
P	50	Set Crop Residue Amounts	decomposition rate for buried crop residue	burieddk	float	E,N	kg kg ⁻¹ day ⁻¹		
P	50	Set Crop Residue Amounts	decomposition rate for roots	rootdk	float	E,N	kg kg ⁻¹ day ⁻¹		
P	50	Set Crop Residue Amounts	decomposition (fall) rate for standing stalks	stemnodk	float	E,N	# #day ⁻¹		
P	50	Set Crop Residue Amounts	average stem diameter	stemdia	float	E,N	m	value * 39.3696	in
P	50	Set Crop Residue Amounts	decomposition days threshold when stems begin to fall	threddys	float	E,N	day		

P	50	Set Crop Residue Amounts	cover factor coefficient(mass to cover)	covfact	float	E,N	m ⁻² kg ⁻¹	value * 0.00011209	
P	50	Set Crop Residue Amounts	Residue Evaporation Suppression multiplier coefficient a	resevapa	float	E,N			
P	50	Set Crop Residue Amounts	Residue Evaporation Suppression exponent coefficient b	resevapb	float	E,N			
P	50	Set Crop Residue Amounts		crop_notes	string	E,T			
P	51	Seeding Configuration							
P	51	Seeding Configuration	Type of planting	rowflag	int	E,C			0:Broadcast Planting 1:Use Implement Ridge Spacing 2:Use Specified Row Spacing
P	51	Seeding Configuration	Crop row spacing	rowspac	float	E,N	mm	value * 0.03937	in
P	51	Seeding Configuration	Seed placement (ridge/furrow)	rowridge	int	E,C			0:Seed row placed in furrow bottom 2:Seed row placed on ridge top

P	51	Seeding Configuration	Plant population	plantpop	float	E,N	# m ⁻²	value * 4046.7	# acre ⁻¹	
P	51	Seeding Configuration	Maximum number of tillers (stems) per plant	dmaxshoot	float	E,N	# plant ⁻¹			
P	51	Seeding Configuration	Crop growth parameters selection	cbaflag	int	E,C				0:Grow crop using baseline parameters 1:Use given biomass and ratio adjustment factors
P	51	Seeding Configuration	Target Harvestable yield	tgtyield	float	E,N				
P	51	Seeding Configuration	Biomass adjustment factor	cbafact	float	E,N				
P	51	Seeding Configuration	Yield/biomass ratio adjustment factor	cyrafact	float	E,N				
P	51	Seeding Configuration	Yield component specification	hyldflag	int	E,C				0:Yield is all of reproductive mass (grain+) 1:Yield is fraction of reproductive mass (grain) 2:Yield is all or fraction of aboveground biomass

									3:Yield is all or fraction of the leaf mass
									4:Yield is all fraction of the stem mass
P	51	Seeding Configuration	Units harvestable yield is reported in	hyldunits	string	E,S			
P	51	Seeding Configuration	Moisture content yield is reported	hyldwater	float	E,N	percent		
P	51	Seeding Configuration	Harvestable yield conversion factor (kg/m ² to displayed units)	hyconfact	float	E,N			
P	51	Seeding Configuration	Crop Type	idc	int	E,C			1:Warm season legume (soybeans, etc.) 2:Cool season legume (peas, etc.) 3:Perennial Legume (alfalfa, etc.) 4:Spring Seeded and Warm Season Annuals (cotton, sunflowers, corn, etc.)

5: Cold Season
Annuals (winter
wheat, winter
canola)

6: Perennials
(pasture, etc.)

7: Bi-annuals or
Perennials with
Tuber
Dormancy

8: Perennials with
Staged Crown
Release and
Dormancy
(Asparagus)

P	51	Seeding Configuration	Grain (seed) fraction of reproductive biomass component	grf	float	E,N	fraction		
P	51	Seeding Configuration	light extinction coefficient	ck	float	E,N			
P	51	Seeding Configuration	Ratio of heat units (start of senescence/total)	hui0	float	E,N	fraction		
P	51	Seeding Configuration	maximum crop height	hmx	float	E,N	m	value *	ft
								3.2808	
P	51	Seeding Configuration	Starting depth of growing point	growdepth	float	E,N	m	value *	inches
								39.3696	
P	51	Seeding Configuration	maximum root depth	rdmx	float	E,N	m	value *	ft
								3.2808	

P	51	Seeding Configuration	minimum temperature for plant growth	tbas	float	E,N	deg C	value * 1.8 + 32	degree F	
P	51	Seeding Configuration	optimal temperature for plant growth	topt	float	E,N	deg C	value * 1.8 + 32	degree F	
P	51	Seeding Configuration	Crop maturity measurement method	thudf	int	E,C				0: Crop matures on average in Days shown 1: Crop Matures in Heat Units shown
P	51	Seeding Configuration	time of uninterrupted growth to maturity	dtm	int	E,N	days			
P	51	Seeding Configuration	Growing degree to maturity	thum	float	E,N	deg C day	value * 1.8	deg F day	
P	51	Seeding Configuration	Upper frost damage threshold temperature	frsx1	float	E,N	deg C	value * 1.8 + 32	degree F	
P	51	Seeding Configuration	Lower frost damage threshold temperature	frsx2	float	E,N	deg C	value * 1.8 + 32	degree F	
P	51	Seeding Configuration	Damage at upper frost damage threshold temperature	frsy1	float	E,N	fraction			

P	51	Seeding Configuration	Damage at lower frost damage threshold temperature	frsy2	float	E,N	fraction
P	51	Seeding Configuration	Thermal delay co-efficient pre- vernalization	verndel	float	E,N	
P	51	Seeding Configuration	Biomass Conversion Efficiency	bceff	float	E,N	(t ha ⁻¹) MJ ⁻¹ m ⁻²
P	51	Seeding Configuration	leaf fraction coefficient a	a_lf	float	E,N	
P	51	Seeding Configuration	leaf fraction coefficient b	b_lf	float	E,N	
P	51	Seeding Configuration	leaf fraction coefficient c	c_lf	float	E,N	
P	51	Seeding Configuration	leaf fraction coefficient d	d_lf	float	E,N	
P	51	Seeding Configuration	reproductive mass coefficient a	a_rp	float	E,N	
P	51	Seeding Configuration	reproductive mass coefficient b	b_rp	float	E,N	
P	51	Seeding Configuration	reproductive mass coefficient c	c_rp	float	E,N	
P	51	Seeding Configuration	reproductive mass coefficient d	d_rp	float	E,N	

P	51	Seeding Configuration	crop height curve shape coefficient a	a_ht	float	E,N			
P	51	Seeding Configuration	crop height curve shape coefficient b	b_ht	float	E,N			
P	51	Seeding Configuration	Specific stem silhouette area	ssaa	float	E,N			
P	51	Seeding Configuration	Specific stem silhouette area exponent	ssab	float	E,N			
P	51	Seeding Configuration	specific leaf area	sla	float	E,N	m ² kg ⁻¹		
P	51	Seeding Configuration	Heat units ratio to emergence	huie	float	E,N			
P	51	Seeding Configuration	Transplant or Seed flag	transf	int	E,C			1:Transplants placed in field (mass immediately divided into leaf, stem, roots) 0:plant shoots emerge in the required heat units to emergence
P	51	Seeding Configuration	maximum growth diameter of a single plant	diammax	float	E,N	m	value * 3.281	ft
P	51	Seeding Configuration	planted mass,dry weight	storeinit	float	E,N	mg plant ⁻¹		

P	51	Seeding Configuration	Root storage mass required for each regrowth shoot	mshoot	float	E,N	mg shoot ⁻¹	
P	51	Seeding Configuration	ratio of leaf mass/stem mass in shoot	leafstem	float	E,N		
P	51	Seeding Configuration	ratio of shoot diameter to shoot length at full extension	fshoot	float	E,N		
P	51	Seeding Configuration	fraction of leaf mass partitioning diverted to root store	leaf2stor	float	E,N	fraction	
P	51	Seeding Configuration	fraction of stem mass partitioning diverted to root store	stem2stor	float	E,N	fraction	
P	51	Seeding Configuration	fraction standing mass partitioning diverted to root store	stor2stor	float	E,N	fraction	
P	51	Seeding Configuration	Residue size/toughness class	rbc	int	E,C		1:Fragile, very small residue, e.g. soybeans 2:Moderately tough, short

residue, e.g.
wheat

3:Non-fragile,
medium residue,
e.g. corn

4:Woody, large
residue

5:Gravel, rock

P	51	Seeding Configuration	decomposition rate for standing stalks	standdk	float	E,N			
P	51	Seeding Configuration	decomposition rate for surface residue	surfdk	float	E,N			
P	51	Seeding Configuration	decomposition rate for buried crop residue	burieddk	float	E,N			
P	51	Seeding Configuration	decomposition rate for roots	rootdk	float	E,N			
P	51	Seeding Configuration	decomposition (fall) rate for standing stalks	stemnodk	float	E,N			
P	51	Seeding Configuration	average stem diameter	stemdia	float	E,N	m	value * 39.3696	in
P	51	Seeding Configuration	decomposition days threshold when stems begin to fall	threddys	float	E,N			

P	51	Seeding Configuration	cover factor coefficient(mass to cover)	covfact	float	E,N		value *	0.00011209
P	51	Seeding Configuration	Residue Evaporation Suppression multiplier coefficient a	resevapa	float	E,N			
P	51	Seeding Configuration	Residue Evaporation Suppression exponent coefficient b	resevapb	float	E,N			
P	51	Seeding Configuration	Residue:Yield ratio	yield_coefficient	float	E,N	kg kg ⁻¹		
P	51	Seeding Configuration	Residue:Yield intercept	residue_intercept	float	E,N	kg m ⁻²	value *	8921.8 lb ac ⁻¹
P	51	Seeding Configuration	Location of regrowth (height)	regrow_location	float	E,N	m	value *	39.3696 in
P	51	Seeding Configuration	Not Used	noparam3	float	H,N			
P	51	Seeding Configuration	Not Used	noparam2	float	H,N			
P	51	Seeding Configuration	Not Used	noparam1	float	E,N			
P	51	Seeding Configuration	Crop Record Notes	crop_notes	string	E,T			

P	61	Remove Plant/Residue Material					
P	61	Remove Plant/Residue Material	Select plant/residue material	selpos	int	E,C	1:Standing with Roots 2:Flat 3:Standing with Roots and Flat 4:Buried 5:Standing with Roots and Buried 6:Flat and Buried 7:Standing with Roots, Flat and Buried
P	61	Remove Plant/Residue Material	Select biomass pool type	selpool	int	E,C	1:Crop 2:Temporary 3:Crop and Temporary 4:Residue 5:Crop and Residue 6:Temporary and Residue

								7: Crop, Temporary and Residue
P	61	Remove Plant/Residue Material	Grain (fruit) Removed	rstore	float	E,N	fraction	
P	61	Remove Plant/Residue Material	Leaf Removed	rleaf	float	E,N	fraction	
P	61	Remove Plant/Residue Material	Stem Removed	rstem	float	E,N	fraction	
P	61	Remove Plant/Residue Material	Storage Root Removed	rrootstore	float	E,N	fraction	
P	61	Remove Plant/Residue Material	Fibrous Roots Removed	rrootfiber	float	E,N	fraction	
P	62	Remove (by age pool) Plant/Residue Material	Report Harvest	harv_report_flg	int	E,C		0: No Report
P	62	Remove (by age pool) Plant/Residue Material	Use Harvest in Calibration	harv_calib_flg	int	E,C		1: Report 0: Do not Use
								1: Use for Calibration

P	62	Remove (by age pool) Plant/Residue Material	Harvest Units	harv_unit_flg	int	E,C	0:Use Units in Crop
							1:Use mass/area Units
P	62	Remove (by age pool) Plant/Residue Material	Crop Maturity Warnings	mature_warn_flg	int	E,C	0:No Warnings
							1:Warnings
P	62	Remove (by age pool) Plant/Residue Material	Select plant/residue material	selpos	int	E,C	1:Standing with Roots
							2:Flat
							3:Standing with Roots and Flat
							4:Buried
							5:Standing with Roots and Buried
							6:Flat and Buried
							7:Standing with Roots, Flat and Buried
P	62	Remove (by age pool) Plant/Residue Material	Select biomass pool type	selpool	int	E,C	1:Crop

										2:Temporary
										3:Crop and Temporary
										4:Residue
										5:Crop and Residue
										6:Temporary and Residue
										7:Crop, Temporary and Residue
P	62	Remove (by age pool) Plant/Residue Material	Select residue age pool type	selagepool	int	E,C				0:All age pools
										2:Youngest age pool
P	62	Remove (by age pool) Plant/Residue Material	Fibrous Roots Removed	rrootfiber	float	E,N	fraction			
P	65	Add Crop Residue Amounts	Number of Standing Residue Stems	numst	float	E,N	# m ⁻²	value * 0.0929		# ft ⁻²
P	65	Add Crop Residue Amounts	Standing Residue Height	rstandht	float	E,N	m	value * 39.37		in
P	65	Add Crop Residue Amounts	Standing Residue Mass	rstandmass	float	E,N	kg m ⁻²	value * 8921.8		lb acre ⁻¹

P	65	Add Crop Residue Amounts	Flat Surface Residue Mass	rflatmass	float	E,N	kg m ⁻²	value * 8921.8	lb acre ⁻¹
P	65	Add Crop Residue Amounts	Residue size/toughness class	rbc	int	E,C			1:Fragile, very small residue, e.g. soybeans 2:Moderately tough, short residue, e.g. wheat 3:Non-fragile, medium residue, e.g. corn 4:Woody, large residue 5:Gravel, rock
P	65	Add Crop Residue Amounts	Buried Residue Mass	rburiedmass	float	E,N	kg m ⁻²	value * 8921.8	lb acre ⁻¹
P	65	Add Crop Residue Amounts	Buried Residue Depth	rburieddepth	float	E,N	mm	value * 0.03937	in
P	65	Add Crop Residue Amounts	Root Residue Mass	rrootmass	float	E,N	kg m ⁻²	value * 8921.8	lb acre ⁻¹
P	65	Add Crop Residue Amounts	Root Residue Depth	rrootdepth	float	E,N	mm	value * 0.03937	in

P	65	Add Crop Residue Amounts	decomposition rate for standing stalks	standdk	float	E,N	kg kg ⁻¹ day ⁻¹		
P	65	Add Crop Residue Amounts	decomposition rate for surface residue	surfdk	float	E,N	kg kg ⁻¹ day ⁻¹		
P	65	Add Crop Residue Amounts	decomposition rate for buried crop residue	burieddk	float	E,N	kg kg ⁻¹ day ⁻¹		
P	65	Add Crop Residue Amounts	decomposition rate for roots	rootdk	float	E,N	kg kg ⁻¹ day ⁻¹		
P	65	Add Crop Residue Amounts	decomposition (fall) rate for standing stalks	stemnodk	float	E,N	# #day ⁻¹		
P	65	Add Crop Residue Amounts	average stem diameter	stemdia	float	E,N	m	value * 39.3696	in
P	65	Add Crop Residue Amounts	decomposition days threshold when stems begin to fall	thrddys	float	E,N	day		
P	65	Add Crop Residue Amounts	cover factor coefficient(mass to cover)	covfact	float	E,N	m ² kg ⁻¹	value*0.000 11209	cov=1-exp(-covfact*(lbs acre ⁻¹))
P	65	Add Crop Residue Amounts	Residue Evaporation Suppression multiplier coefficient a	resevapa	float	E,N			

P	65	Add Crop Residue Amounts	Residue Evaporation Suppression exponent coefficient b	resevapb	float	E,N			
P	66	Add Manure Residue Amount	Number of Standing Residue (manure) Stems	M_numst	float	H,N	# m ⁻²	value * 0.0929	# ft ²
P	66	Add Manure Residue Amount	Standing Residue (manure) Height	M_rstandht	float	H,N	m	value * 39.37	in
P	66	Add Manure Residue Amount	Standing Residue (manure) Mass	M_rstandmass	float	H,N	kg m ⁻²	value * 8921.8	lb acre ⁻¹
P	66	Add Manure Residue Amount	Flat Surface Residue (manure) Mass	M_rflatmass	float	E,N	kg m ⁻²	value * 8921.8	lb acre ⁻¹
P	66	Add Manure Residue Amount	Residue size/toughness class	rbc	int	E,C			1:Fragile, very small residue, e.g. soybeans 2:Moderately tough, short residue, e.g. wheat 3:Non-fragile, medium residue, e.g. corn 4:Woody, large residue 5:Gravel, rock

P	66	Add Manure Residue Amount	Buried Manure Mass	M_rburiedmass	float	E,N	kg m ⁻²	value * 8921.8	lb acre ⁻¹
P	66	Add Manure Residue Amount	Buried Manure Depth	M_rburieddepth	float	E,N	mm	value * 0.03937	in
P	66	Add Manure Residue Amount	Root Residue (manure) Mass	M_rrootmass	float	H,N	kg m ⁻²	value * 8921.8	lb acre ⁻¹
P	66	Add Manure Residue Amount	Root Residue (manure) Depth	M_rrootdepth	float	H,N	mm	value * 0.03937	in
P	66	Add Manure Residue Amount	Total Manure Applied	manure_total_mass	float	E,N	kg m ⁻²	value * 8921.8	lb acre ⁻¹
P	66	Add Manure Residue Amount	Fraction of total manure buried	manure_buried_ratio	float	E,N	fraction		
P	66	Add Manure Residue Amount	decomposition rate for standing stalks	standdk	float	E,N	kg kg ⁻¹ day ⁻¹		
P	66	Add Manure Residue Amount	decomposition rate for surface residue	surfdk	float	E,N	kg kg ⁻¹ day ⁻¹		
P	66	Add Manure Residue Amount	decomposition rate for buried crop residue	burieddk	float	E,N	kg kg ⁻¹ day ⁻¹		
P	66	Add Manure Residue Amount	decomposition rate for roots	rootdk	float	E,N	kg kg ⁻¹ day ⁻¹		

P	66	Add Manure Residue Amount	decomposition (fall) rate for standing stalks	stemnodk	float	E,N	# #day ⁻¹		
P	66	Add Manure Residue Amount	average stem diameter	stemdia	float	E,N	m	value * 39.3696	in
P	66	Add Manure Residue Amount	decomposition days threshold when stems begin to fall	thrdays	float	E,N	day		
P	66	Add Manure Residue Amount	cover factor coefficient (mass to cover)	covfact	float	E,N	m ² kg ⁻¹	value * 0.00011209	cov=1-exp(-covfact*(lbs acre ⁻¹))
P	66	Add Manure Residue Amount	Residue Evaporation Suppression multiplier coefficient a	resevapa	float	E,N			
P	66	Add Manure Residue Amount	Residue Evaporation Suppression exponent coefficient b	resevapb	float	E,N			
P	66	Add Manure Residue Amount		crop_notes	string	E,T			
P	71		Irrigation Application Method	irrtype	int	E,C			1:Sprinkler 2:Other

P	71	Depth of water applied	irrdepth	float	E,N	mm	value * 0.03937	in	
P	72	Set Irrigation Monitoring Status	irrmonflag	int	E,C				0:Turn off Irrigation Monitoring 1:Turn on Irrigation Monitoring
P	72	Maximum daily depth of water applied	irrmaxapp	float	E,N	mm	value * 0.03937	in	
P	72	Rate of water application	irrrate	float	H,N	mm hr ⁻¹	value * 0.03937	in hr ⁻¹	
P	72	Duration of maximum daily depth water application	irrduration	float	E,N	hours			
P	72	Application height (+ above) (- below) soil surface	irrapoloc	float	E,N	mm	value * 0.03937	in	
P	72	Minimum irrigation application depth	irrminapp	float	E,N	mm	value * 0.03937	in	
P	72	Management allowed depletion (0 to 1)	irrmad	float	E,N				

P	72		Minimum days between irrigations	irrminint	float	E,N	days		
P	73	Single Irrigation	Depth of water applied	irrdepth	float	E,N	mm	value * 0.03937	in
P	73	Single Irrigation	Rate of water application	irrrate	float	H,N	mm hr ⁻¹	value * 0.03937	in hr ⁻¹
P	73	Single Irrigation	Duration of water application	irrduration	float	E,N	hours		
P	73	Single Irrigation	Application height (+ above) (- below) soil surface	irrapplc	float	E,N	mm	value * 0.03937	in

Supplement B: Crop record parameter definitions, prompts, and display options.

Table 9. An XST formatted display of the crop parameters and properties.

Categories	Param Prompt	Param Name	Param Type	Param Display	Param Unit	Conversion Factor	Alternate Units	Parameter Choices
Shoot	Crop Type	idc	int	E,C	unitless			1:Warm season legume (soybeans, etc.) 2:Cool season legume (peas, etc.) 3:Perennial Legume (alfalfa, etc.) 4:Spring Seeded and Warm Season Annuals (cotton, sunflowers, corn, etc.) 5:Cold Season Annuals (winter wheat, winter canola) 6:Perennials (pasture,etc.) 7:Bi-annuals or Perennials with Tuber Dormancy 8:Perennials with Staged Crown Release and Dormancy (Asparagus)
	Transplant or Seed flag	transf	int	E,C	unitless			0:Seeds planted in field 1:Transplants planted in field (mass immediately divided into leaf, stem, roots)
	Plant population	plantpop	float	E,N	# m ⁻²	value * 4046.7	# acre ⁻¹	
	Maximum number of shoots per plant	dmaxshoot	float	E,N	# plant ⁻¹			

	Starting depth of growing point	growdepth	float	E,N	m	value * 39.3696	inches	
	Location of regrowth (height)	regrow_location	float	E,N	m	value * 39.3696	in	
	Planted mass,dry weight	storeinit	float	E,N	mg plant ⁻¹	value * 0.000035274	ounce plant ⁻¹	
	Root storage mass required for each regrowth shoot	mshoot	float	E,N	mg shoot ⁻¹	value * 0.000035274	ounce plant ⁻¹	
	Ratio of leaf mass/stem mass in shoot	leafstem	float	E,N	unitless			
	Ratio of stem diameter to stem length	fshoot	float	E,N	unitless			
	Heat unit index at emergence	huie	float	E,N	unitless			
Growth	Crop maturity measurement method	thudf	int	E,C	unitless			0:Crop matures on average in Days shown 1:Crop Matures in Heat Units
	Days to maturity	dtm	int	E,N	days			
	Heat units to maturity	thum	float	E,N	degree C day	value * 1.8	deg F day	

	Heat unit index at start of senescence	hui0	float	E,N	fraction		
	Minimum temperature for plant growth	tbas	float	E,N	degree C	value * 1.8 + 32	degree F
	Optimum temperature for plant growth	topt	float	E,N	degree C	value * 1.8 + 32	degree F
Geometry	Maximum growth diameter of a single plant	diammax	float	E,N	m	value * 3.281	ft
	Stem silhouette area coefficient a	ssaa	float	E,N	unitless		
	Stem silhouette area coefficient b	sab	float	E,N	unitless		
	Specific leaf area	sla	float	E,N	m ² kg ⁻¹		
	Light extinction coefficient	ck	float	E,N	unitless		
	Biomass Conversion Efficiency	bceff	float	E,N	(t ha ⁻¹) (MJ m ²) ⁻¹		
Partitioning	Leaf fraction coefficient a	a_lf	float	E,N	unitless		

Leaf fraction coefficient b	b_lf	float	E,N	unitless		
Leaf fraction coefficient c	c_lf	float	E,N	unitless		
Leaf fraction coefficient d	d_lf	float	E,N	unitless		
Reproductive mass coefficient a	a_rp	float	E,N	unitless		
Reproductive mass coefficient b	b_rp	float	E,N	unitless		
Reproductive mass coefficient c	c_rp	float	E,N	unitless		
Reproductive mass coefficient d	d_rp	float	E,N	unitless		
Residue:Yield ratio	yield_coefficient	float	E,N	kg kg ⁻¹		lb/lb
Residue:Yield intercept	residue_intercept	float	E,N	kg m ⁻²	value * 8921.8	lb acre ⁻¹
Fraction of leaf mass partitioning diverted to root storage	leaf2stor	float	E,N	fraction		

	Fraction of stem mass partitioning diverted to root storage	stem2stor	float	E,N	fraction		
	Fraction of reproductive mass partitioning diverted to root storage	stor2stor	float	E,N	fraction		
	Maximum root depth	rdmx	float	E,N	m	value * 3.2808	ft
	Maximum crop height	hmx	float	E,N	m	value * 3.2808	ft
	Crop height coefficient a	a_ht	float	E,N	unitless		
	Crop height coefficient b	b_ht	float	E,N	unitless		
Cold	Higher temperature	frsx1	float	E,N	degree C	value * 1.8 + 32	deg F
	Reduction in green leaf area at higher temperature	frsy1	float	E,N	fraction		
	Lower temperature	frsx2	float	E,N	degree C	value * 1.8 + 32	deg F
	Reduction in green leaf area at lower temperature	frsy2	float	E,N	fraction		

	Thermal delay coefficient pre-vernalization	verndel	float	E,N	unitless	
Harvest	Which plant component is (partially) harvested?	hyldflag	int	E,C	unitless	0:constant fraction of reproductive mass (grain+) 1:increasing fraction of reproductive mass 2:all or fraction of aboveground 3:all or fraction of the leaf mass 4:all or fraction of the stem mass 5:all or fraction of underground mass
	Harvested fraction of plant component (grain fraction etc.)	grf	float	E,N	fraction	
	Units for reporting harvested yield	hyldunits	string	E,S	unitless	
	Moisture content for reporting harvested yield	hyldwater	float	E,N	%	

	Harvested yield conversion factor (kg m ⁻² to units shown)	hyconfact	float	E,N	unitless	
Decomposition	Residue size/toughness class	rbc	int	E,C	unitless	1:Fragile, very small residue, e.g. soybeans 2:Moderately tough, short residue, e.g. wheat 3:Non-fragile, medium residue, e.g. corn 4:Woody, large residue 5:Gravel, rock
	Decomp days after which stems begin to fall	threddys	float	E,N	day	
	Fall rate for standing stalks	stemnodk	float	E,N	# #day ⁻¹	
	Decomp rate for standing stalks	standdk	float	E,N	kg kg ⁻¹ day ⁻¹	lb lb ⁻¹ day ⁻¹
	Decomp rate for surface (flat) stalks	surfdk	float	E,N	kg kg ⁻¹ day ⁻¹	lb lb ⁻¹ day ⁻¹
	Decomp rate for buried stalks	burieddk	float	E,N	kg kg ⁻¹ day ⁻¹	lb lb ⁻¹ day ⁻¹
	Decomp rate for roots	rootdk	float	E,N	kg kg ⁻¹ day ⁻¹	lb lb ⁻¹ day ⁻¹

	Stalk diameter	stemdia	float	E,N	m	value * 39.3696	inches
	Mass to cover factor	covfact	float	E,N	m ⁻² kg ⁻¹	value * 0.00011209	acres lb ⁻¹
	Residue Evaporation Suppression multiplier coefficient a	resevapa	float	E,N	unitless		
	Residue Evaporation Suppression exponent coefficient b	resevapb	float	E,N	unitless		
Calibration	Crop growth calibration selection	cbaflag	int	E,C	unitless		0: Crop NOT selected for calibration 1: Select Crop for calibration to match target yield
	Target harvested yield	tgtyield	float	E,N	unitless		
	Biomass adjustment factor	cbafact	float	E,N			
	Yield/biomass ratio adjustment factor	cyrafact	float	E,N			
	Not Used	noparam3	float	H,N	unitless		
	Not Used	noparam2	float	H,N	unitless		

	Not Used	noparam1	float	H,N	unitless
Crop Notes	Crop Record Notes	crop_notes	string	E,T	unitless

Supplement C: The “man_fileformat.xml” file.

The following are the contents of the “man_fileformat.xml” file containing an XML description, which fully describes the ASCII file format used by the WEPS Management/Crop Rotation file. This file is used by the WEPS interface to create WEPS Management/Crop Rotation files as well as for reading them into the interface. Thus, it fully defines the ASCII WEPS Management/Crop Rotation file format and can be considered the definitive reference for that file format as currently used in WEPS version 1.3.9.

```
<?xml version="1.0"?>
<!--<?xml-stylesheet type="text/xsl" href="operation_defn.xsl"?-->
<!DOCTYPE manfileformat SYSTEM "man_fileformat.dtd">

<!--
<!ENTITY manfileformat (operationformat*)>
<!ELEMENT operationformat (actionformat*) >
<!ENTITY % identityDTD SYSTEM "identity.dtd">
%identityDTD;
<!ELEMENT actionformat (identity, paramformat *)>
<!ELEMENT paramformat (paramname*)>
<!ELEMENT paramname (#PCDATA)>
-->
<manfileformat >
  <actionformat>
    <identity>
      <code>O</code>
      <id>00</id>
    </identity>
    <paramformatline symbol="T">
      <paramname>op_notes0</paramname>
    </paramformatline>
  </actionformat>
  <actionformat>
    <identity>
      <code>O</code>
      <id>01</id>
    </identity>
    <paramformatline symbol="+">
      <paramname>ospeed</paramname>
      <paramname>odirect</paramname>
      <paramname>ostdspeed</paramname>
      <paramname>ominspeed</paramname>
      <paramname>omaxspeed</paramname>
    </paramformatline>
    <paramformatline symbol="T">
      <paramname>op_notes1</paramname>
    </paramformatline>
  </actionformat>
</manfileformat >
```

```

</actionformat>

<actionformat>
  <identity>
    <code>O</code>
    <id>02</id>
  </identity>
  <paramformatline symbol="T">
    <paramname>op_notes2</paramname>
  </paramformatline>
</actionformat>
<actionformat>
  <identity>
    <code>O</code>
    <id>03</id>
  </identity>
  <paramformatline symbol="+">
    <paramname>oenergyarea</paramname>
    <paramname>ostir</paramname>
    <paramname>ospeed</paramname>
    <paramname>odirect</paramname>
    <paramname>ostdspeed</paramname>
    <paramname>ominspeed</paramname>
    <paramname>omaxspeed</paramname>
  </paramformatline>
  <paramformatline symbol="T">
    <paramname>op_notes3</paramname>
  </paramformatline>
  <paramformatline symbol="+">
    <paramname>ofuel</paramname>
  </paramformatline>
</actionformat>

<actionformat>
  <identity>
    <code>O</code>
    <id>04</id>
  </identity>
  <paramformatline symbol="+">
    <paramname>oenergyarea</paramname>
    <paramname>ostir</paramname>
  </paramformatline>
  <paramformatline symbol="T">
    <paramname>op_notes4</paramname>
  </paramformatline>
  <paramformatline symbol="+">
    <paramname>ofuel</paramname>
  </paramformatline>
</actionformat>

<actionformat>

```

```

    <identity>
      <code>G</code>
      <id>01</id>
    </identity>
    <paramformatline symbol="+">
      <paramname>gtdepth</paramname>
      <paramname>gtlint</paramname>
      <paramname>gtilArea</paramname>
      <paramname>gtstddepth</paramname>
      <paramname>gtmindepth</paramname>
      <paramname>gtmaxdepth</paramname>
    </paramformatline>
  </actionformat>

<actionformat>
  <identity>
    <code>G</code>
    <id>02</id>
  </identity>
  <paramformatline symbol="+">
    <paramname>gbioarea</paramname>
  </paramformatline>
</actionformat>

<actionformat>
  <identity>
    <code>G</code>
    <id>03</id>
  </identity>
  <paramformatline symbol="+">
    <paramname>gcropname</paramname>
  </paramformatline>
</actionformat>

<actionformat>
  <identity>
    <code>G</code>
    <id>04</id>
  </identity>
  <paramformatline symbol="+">
    <paramname>gamdname</paramname>
  </paramformatline>
</actionformat>

<actionformat>
  <identity>
    <code>P</code>
    <id>01</id>
  </identity>
</actionformat>

```

```
<actionformat>
  <identity>
    <code>P</code>
    <id>02</id>
  </identity>
  <paramformatline symbol="+">
    <paramname>rroughflag</paramname>
    <paramname>rrough</paramname>
  </paramformatline>
</actionformat>
```

```
<actionformat>
  <identity>
    <code>P</code>
    <id>03</id>
  </identity>
  <paramformatline symbol="+">
    <paramname>rrough3</paramname>
  </paramformatline>
</actionformat>
```

```
<actionformat>
  <identity>
    <code>P</code>
    <id>04</id>
  </identity>
  <paramformatline symbol="+">
    <paramname>rrough4</paramname>
  </paramformatline>
</actionformat>
```

```
<actionformat>
  <identity>
    <code>P</code>
    <id>05</id>
  </identity>
  <paramformatline symbol="+">
    <paramname>rdgflag</paramname>
    <paramname>rdghit</paramname>
    <paramname>rdgspac</paramname>
    <paramname>rdgwidth</paramname>
    <paramname>dkhit</paramname>
    <paramname>dkspac</paramname>
  </paramformatline>
</actionformat>
```

```
<actionformat>
  <identity>
    <code>P</code>
    <id>11</id>
```

```

        </identity>
        <paramformatline symbol="+">
            <paramname>asdf</paramname>
            <paramname>crif</paramname>
        </paramformatline>
    </actionformat>

<actionformat>
    <identity>
        <code>P</code>
        <id>12</id>
    </identity>
    <paramformatline symbol="+">
        <paramname>soilos</paramname>
    </paramformatline>
</actionformat>

<actionformat>
    <identity>
        <code>P</code>
        <id>13</id>
    </identity>
    <paramformatline symbol="+">
        <paramname>laymix</paramname>
    </paramformatline>
</actionformat>

<actionformat>
    <identity>
        <code>P</code>
        <id>14</id>
    </identity>
</actionformat>

<actionformat>
    <identity>
        <code>P</code>
        <id>24</id>
    </identity>
    <paramformatline symbol="+">
        <paramname>fbioflagvt</paramname>
        <paramname>massflatvt1</paramname>
        <paramname>massflatvt2</paramname>
        <paramname>massflatvt3</paramname>
        <paramname>massflatvt4</paramname>
        <paramname>massflatvt5</paramname>
    </paramformatline>
</actionformat>

<actionformat>
    <identity>

```

```

        <code>P</code>
        <id>25</id>
    </identity>
    <paramformatline symbol="+">
        <paramname>burydist</paramname>
        <paramname>massburyvt1</paramname>
        <paramname>massburyvt2</paramname>
        <paramname>massburyvt3</paramname>
        <paramname>massburyvt4</paramname>
        <paramname>massburyvt5</paramname>
    </paramformatline>
</actionformat>

<actionformat>
    <identity>
        <code>P</code>
        <id>26</id>
    </identity>
    <paramformatline symbol="+">
        <paramname>massresurvt1</paramname>
        <paramname>massresurvt2</paramname>
        <paramname>massresurvt3</paramname>
        <paramname>massresurvt4</paramname>
        <paramname>massresurvt5</paramname>
    </paramformatline>
</actionformat>

<actionformat>
    <identity>
        <code>P</code>
        <id>31</id>
    </identity>
    <paramformatline symbol="+">
        <paramname>kilflag</paramname>
    </paramformatline>
</actionformat>

<actionformat>
    <identity>
        <code>P</code>
        <id>32</id>
    </identity>
    <paramformatline symbol="+">
        <paramname>cutflag</paramname>
        <paramname>cutvalh</paramname>
        <paramname>cyldrmh</paramname>
        <paramname>cplrmh</paramname>
        <paramname>cstrmh</paramname>
    </paramformatline>
</actionformat>

```

```

<actionformat>
  <identity>
    <code>P</code>
    <id>33</id>
  </identity>
  <paramformatline symbol="+">
    <paramname>cutvalf</paramname>
    <paramname>cyldrmf</paramname>
    <paramname>cplrmf</paramname>
    <paramname>cstrmf</paramname>
  </paramformatline>
</actionformat>

```

```

<actionformat>
  <identity>
    <code>P</code>
    <id>34</id>
  </identity>
  <paramformatline symbol="+">
    <paramname>frselpool</paramname>
    <paramname>ratemultvt1</paramname>
    <paramname>ratemultvt2</paramname>
    <paramname>ratemultvt3</paramname>
    <paramname>ratemultvt4</paramname>
    <paramname>ratemultvt5</paramname>
  </paramformatline>
  <paramformatline symbol="+">
    <paramname>threshmultvt1</paramname>
    <paramname>threshmultvt2</paramname>
    <paramname>threshmultvt3</paramname>
    <paramname>threshmultvt4</paramname>
    <paramname>threshmultvt5</paramname>
  </paramformatline>
</actionformat>

```

```

<actionformat>
  <identity>
    <code>P</code>
    <id>37</id>
  </identity>
  <paramformatline symbol="+">
    <paramname>thinvalp</paramname>
    <paramname>tyldrmp</paramname>
    <paramname>tplrmp</paramname>
    <paramname>tstrmp</paramname>
  </paramformatline>
</actionformat>

```

```

<actionformat>
  <identity>
    <code>P</code>
    <id>38</id>
  </identity>

```

```

</identity>
<paramformatline symbol="+">
  <paramname>thinalf</paramname>
  <paramname>tyldrmf</paramname>
  <paramname>tplrmf</paramname>
  <paramname>tstrmf</paramname>
</paramformatline>
</actionformat>

<actionformat>
  <identity>
    <code>P</code>
    <id>40</id>
  </identity>
</actionformat>

<actionformat>
  <identity>
    <code>P</code>
    <id>42</id>
  </identity>
  <paramformatline symbol="+">
    <paramname>harv_report_flg</paramname>
    <paramname>harv_calib_flg</paramname>
    <paramname>harv_unit_flg</paramname>
    <paramname>mature_warn_flg</paramname>
    <paramname>cutflag</paramname>
    <paramname>cutvalh</paramname>
    <paramname>cyldrmh</paramname>
    <paramname>cplrmh</paramname>
    <paramname>estrnh</paramname>
  </paramformatline>
</actionformat>

<actionformat>
  <identity>
    <code>P</code>
    <id>43</id>
  </identity>
  <paramformatline symbol="+">
    <paramname>harv_report_flg</paramname>
    <paramname>harv_calib_flg</paramname>
    <paramname>harv_unit_flg</paramname>
    <paramname>mature_warn_flg</paramname>
    <paramname>cutvalf</paramname>
    <paramname>cyldrmf</paramname>
    <paramname>cplrmf</paramname>
    <paramname>estrmf</paramname>
  </paramformatline>
</actionformat>

```

```
<actionformat>
  <identity>
    <code>P</code>
    <id>47</id>
  </identity>
  <paramformatline symbol="+">
    <paramname>harv_report_flg</paramname>
    <paramname>harv_calib_flg</paramname>
    <paramname>harv_unit_flg</paramname>
    <paramname>mature_warn_flg</paramname>
    <paramname>thINVALP</paramname>
    <paramname>tyldRMP</paramname>
    <paramname>tplrmp</paramname>
    <paramname>tstrmp</paramname>
  </paramformatline>
</actionformat>
```

```
<actionformat>
  <identity>
    <code>P</code>
    <id>48</id>
  </identity>
  <paramformatline symbol="+">
    <paramname>harv_report_flg</paramname>
    <paramname>harv_calib_flg</paramname>
    <paramname>harv_unit_flg</paramname>
    <paramname>mature_warn_flg</paramname>
    <paramname>thINVALF</paramname>
    <paramname>tyldRMF</paramname>
    <paramname>tplrmf</paramname>
    <paramname>tstrmf</paramname>
  </paramformatline>
</actionformat>
```

```
<actionformat>
  <identity>
    <code>P</code>
    <id>50</id>
  </identity>
  <paramformatline symbol="+">
    <paramname>numst</paramname>
    <paramname>rstandht</paramname>
    <paramname>rstandmass</paramname>
    <paramname>rflatmass</paramname>
    <paramname>rbc</paramname>
  </paramformatline>
  <paramformatline symbol="+">
    <paramname>rburiedmass</paramname>
    <paramname>rburieddepth</paramname>
    <paramname>rootmass</paramname>
    <paramname>rootdepth</paramname>
  </paramformatline>
```

```

</paramformatline>
<paramformatline symbol="+">
    <paramname>standdk</paramname>
    <paramname>surfdk</paramname>
    <paramname>burieddk</paramname>
    <paramname>rootdk</paramname>
    <paramname>stemnodk</paramname>
    <paramname>stemdia</paramname>
    <paramname>thrddys</paramname>
    <paramname>covfact</paramname>
</paramformatline>
<paramformatline symbol="+">
    <paramname>resevapa</paramname>
    <paramname>resevapb</paramname>
</paramformatline>
<paramformatline symbol="T">
    <paramname>crop_notes</paramname>
</paramformatline>
</actionformat>

<actionformat>
    <identity>
        <code>P</code>
        <id>51</id>
    </identity>
    <paramformatline symbol="+">
        <paramname>rowflag</paramname>
        <paramname>rowspac</paramname>
        <paramname>rowridge</paramname>
    </paramformatline>
    <paramformatline symbol="+">
        <paramname>plantpop</paramname>
        <paramname>dmaxshoot</paramname>
        <paramname>cbaflag</paramname>
        <paramname>tgyield</paramname>
        <paramname>cbafact</paramname>
        <paramname>cyrafact</paramname>
        <paramname>hyldflag</paramname>
    </paramformatline>
    <paramformatline symbol="+">
        <paramname>hyldunits</paramname>
    </paramformatline>
    <paramformatline symbol="+">
        <paramname>hyldwater</paramname>
        <paramname>hyconfact</paramname>
        <paramname>idc</paramname>
        <paramname>grf</paramname>
        <paramname>ck</paramname>
        <paramname>hui0</paramname>
    </paramformatline>
    <paramformatline symbol="+">

```

```

    <paramname>hmx</paramname>
    <paramname>growdepth</paramname>
    <paramname>rdmx</paramname>
    <paramname>tbas</paramname>
    <paramname>topt</paramname>
    <paramname>thudf</paramname>
    <paramname>dtm</paramname>
    <paramname>thum</paramname>
</paramformatline>
<paramformatline symbol="+">
    <paramname>frsx1</paramname>
    <paramname>frsx2</paramname>
    <paramname>frsy1</paramname>
    <paramname>frsy2</paramname>
    <paramname>verndel</paramname>
    <paramname>bceff</paramname>
</paramformatline>
<paramformatline symbol="+">
    <paramname>a_lf</paramname>
    <paramname>b_lf</paramname>
    <paramname>c_lf</paramname>
    <paramname>d_lf</paramname>
    <paramname>a_rp</paramname>
    <paramname>b_rp</paramname>
    <paramname>c_rp</paramname>
    <paramname>d_rp</paramname>
</paramformatline>
<paramformatline symbol="+">
    <paramname>a_ht</paramname>
    <paramname>b_ht</paramname>
    <paramname>ssaa</paramname>
    <paramname>ssab</paramname>
    <paramname>sla</paramname>
    <paramname>huie</paramname>
    <paramname>transf</paramname>
    <paramname>diammax</paramname>
</paramformatline>
<paramformatline symbol="+">
    <paramname>storeinit</paramname>
    <paramname>mshoot</paramname>
    <paramname>leafstem</paramname>
    <paramname>fshoot</paramname>
    <paramname>leaf2stor</paramname>
    <paramname>stem2stor</paramname>
    <paramname>stor2stor</paramname>
    <paramname>rbc</paramname>
</paramformatline>
<paramformatline symbol="+">
    <paramname>standdk</paramname>
    <paramname>surfdk</paramname>
    <paramname>burieddk</paramname>

```

```

        <paramname>rootdk</paramname>
        <paramname>stemnodk</paramname>
        <paramname>stemdia</paramname>
        <paramname>thrddys</paramname>
        <paramname>covfact</paramname>
    </paramformatline>
    <paramformatline symbol="+">
        <paramname>resevapa</paramname>
        <paramname>resevapb</paramname>
        <paramname>yield_coefficient</paramname>
        <paramname>residue_intercept</paramname>
        <paramname>regrow_location</paramname>
        <paramname>noparam3</paramname>
        <paramname>noparam2</paramname>
        <paramname>noparam1</paramname>
    </paramformatline>
    <paramformatline symbol="T">
        <paramname>crop_notes</paramname>
    </paramformatline>
</actionformat>

<actionformat>
    <identity>
        <code>P</code>
        <id>61</id>
    </identity>
    <paramformatline symbol="+">
        <paramname>selpos</paramname>
        <paramname>selpool</paramname>
        <paramname>rstore</paramname>
        <paramname>rleaf</paramname>
        <paramname>rstem</paramname>
        <paramname>rrootstore</paramname>
        <paramname>rrootfiber</paramname>
    </paramformatline>

</actionformat>

<actionformat>
    <identity>
        <code>P</code>
        <id>62</id>
    </identity>
    <paramformatline symbol="+">
        <paramname>harv_report_flg</paramname>
        <paramname>harv_calib_flg</paramname>
        <paramname>harv_unit_flg</paramname>
        <paramname>mature_warn_flg</paramname>
        <paramname>selpos</paramname>
        <paramname>selpool</paramname>
        <paramname>selagepool</paramname>
    </paramformatline>

```

```
<paramname>rstore</paramname>
<paramname>rleaf</paramname>
<paramname>rstem</paramname>
<paramname>rootstore</paramname>
<paramname>rootfiber</paramname>
</paramformatline>
```

```
</actionformat>
```

```
<actionformat>
```

```
<identity>
<code>P</code>
<id>65</id>
</identity>
<paramformatline symbol="+">
<paramname>numst</paramname>
<paramname>rstandht</paramname>
<paramname>rstandmass</paramname>
<paramname>rflatmass</paramname>
<paramname>rbc</paramname>
</paramformatline>
<paramformatline symbol="+">
<paramname>rburiedmass</paramname>
<paramname>rburieddepth</paramname>
<paramname>rrootmass</paramname>
<paramname>rrootdepth</paramname>
</paramformatline>
<paramformatline symbol="+">
<paramname>standdk</paramname>
<paramname>surfdk</paramname>
<paramname>burieddk</paramname>
<paramname>rootdk</paramname>
<paramname>stemnodk</paramname>
<paramname>stemdia</paramname>
<paramname>thrddys</paramname>
<paramname>covfact</paramname>
</paramformatline>
<paramformatline symbol="+">
<paramname>resevapa</paramname>
<paramname>resevapb</paramname>
</paramformatline>
<paramformatline symbol="T">
<paramname>crop_notes</paramname>
</paramformatline>
```

```
</actionformat>
```

```
<actionformat> <!-- New process for handling manure like RUSLE2 -->
```

```
<identity>
<code>P</code>
<id>66</id>
</identity>
```

```

<paramformatline symbol="+">
  <paramname>M_numst</paramname>
  <paramname>M_rstandht</paramname>
  <paramname>M_rstandmass</paramname>
  <paramname>M_rflatmass</paramname>
  <paramname>rbc</paramname>
</paramformatline>
<paramformatline symbol="+">
  <paramname>M_rburiedmass</paramname>
  <paramname>M_rburieddepth</paramname>
  <paramname>M_rootmass</paramname>
  <paramname>M_rootdepth</paramname>
</paramformatline>

<paramformatline symbol="+">
  <paramname>manure_total_mass</paramname>
  <paramname>manure_buried_ratio</paramname>
</paramformatline>

<paramformatline symbol="+">
  <paramname>standdk</paramname>
  <paramname>surfdk</paramname>
  <paramname>burieddk</paramname>
  <paramname>rootdk</paramname>
  <paramname>stemnodk</paramname>
  <paramname>stemdia</paramname>
  <paramname>thrddys</paramname>
  <paramname>covfact</paramname>
</paramformatline>
<paramformatline symbol="+">
  <paramname>resevapa</paramname>
  <paramname>resevapb</paramname>
</paramformatline>
<paramformatline symbol="T">
  <paramname>crop_notes</paramname>
</paramformatline>
</actionformat>

<actionformat>
  <identity>
    <code>P</code>
    <id>71</id>
  </identity>
  <paramformatline symbol="+">
    <paramname>irrtype</paramname>
    <paramname>irrdepth</paramname>
  </paramformatline>
</actionformat>

<actionformat>
  <identity>

```

```
        <code>P</code>
        <id>72</id>
    </identity>
    <paramformatline symbol="+">
        <paramname>irrmonflag</paramname>
        <paramname>irrmaxapp</paramname>
        <paramname>irrrate</paramname>
        <paramname>irrduration</paramname>
        <paramname>irrapploc</paramname>
        <paramname>irrminapp</paramname>
        <paramname>irrmad</paramname>
        <paramname>irrminint</paramname>
    </paramformatline>
</actionformat>

<actionformat>
    <identity>
        <code>P</code>
        <id>73</id>
    </identity>
    <paramformatline symbol="+">
        <paramname>irrdepth</paramname>
        <paramname>irrrate</paramname>
        <paramname>irrduration</paramname>
        <paramname>irrapploc</paramname>
    </paramformatline>
</actionformat>

<actionformat>
    <identity>
        <code>P</code>
        <id>74</id>
    </identity>
</actionformat>
</manfileformat>
```

Single Storm Applications of WEPS and the Single-event Wind Erosion Evaluation Program (SWEEP)

Contributor:

J. Tatarko

Abstract

The Wind Erosion Prediction System (WEPS) model can be used to predict soil loss by wind for single wind-storm events (e.g., a single day). Single-storm applications of WEPS are often used by wind erosion researchers to study wind erosion processes in detail as well as by land managers who wish to predict the amounts and direction of soil loss given specific known surface and wind conditions (e.g., highway construction managers). Single-event wind erosion simulations can be run on the command line as the standalone Erosion submodel of WEPS or through a graphical user interface known as the Single-event Wind Erosion Evaluation Program (SWEEP). A variety of inputs describing the field geometries, vegetation characteristics, soil and surface properties, and wind parameters for the site are inputs to the simulation of single storm wind erosion events. Single storm use of WEPS through SWEEP is a unique tool for special applications of wind erosion simulation technology.

Introduction

The Wind Erosion Prediction System (WEPS) model simulates hydrology, plant growth, decomposition, land management, and soil surface erodibility to estimate soil wind erosion loss as affected by stochastically simulated local weather (Hagen 2004). The purpose of the full WEPS model is to simulate changes in field conditions as a result of management and weather to estimate wind erosion. WEPS simulates these processes on a daily basis, and a typical run can simulate up to 50 years per crop in a rotation. If one desires to simulate only a single storm with field surface conditions that are mostly static using a single distribution of subdaily winds for the day, the full WEPS model is unnecessary.

The simulation of a single wind erosion storm (i.e., event) is often desired by researchers or managers who have measured data and want to input those data to study the model response to changes in surface conditions (Feng and Sharratt 2009). The standalone erosion model also provides detailed outputs not readily available through the full WEPS model interface.

Another use of a single-storm application of WEPS is to predict the likelihood and severity of an erosion event. For example, managers of disturbed lands such as a construction site likely know the planned surface configuration of the site over a period of time. The probability of an event can be determined based upon those surface conditions. If an event is likely, the technology can be used to simulate various control strategies to reduce or control soil loss and dust emissions.

To simulate single erosion events of one day or less, only the standalone Erosion submodel can be employed, either through an interface program or the command line; refer to the chapter on the Erosion submodel for a complete technical description. A program known as the Single-event Wind Erosion Evaluation Program (SWEEP) allows a simple method to input the simulation area description, surface conditions, and winds. After a completed run, the output results are displayed in tabular and graphical detail. The SWEEP model consists of the standalone WEPS Erosion submodel combined with a user-friendly graphical interface to simulate soil loss and dust emissions for a single wind-storm event (i.e., one day or less). Users typically run the model through the interface, for which template input files can be developed and selected, or inputs can be manually entered. See the SWEEP user manual for information on how to select, modify, and save input files within the interface. The SWEEP model and user manual are available as part of the WEPS download at: www.ars.usda.gov/services/software/software.htm.

Determination of Erosion Threshold

A unique feature of the SWEEP is its ability to determine the likelihood of an erosion event occurring for a given location and defined surface conditions. The SWEEP interface has been configured to use the weather file from the WEPS WINDGEN wind database for a specified location with the surface conditions to calculate: (1) the threshold wind speed at a 10 m height (m s^{-1}) at which erosion begins based on the given surface conditions (soil and biomass) for all 16 cardinal directions; (2) the percentage of winds coming from each of the 16 cardinal directions for each month that exceeds the threshold wind speed for that direction and month; (3) the frequency of wind (%) coming from the specified direction for each month; and (4) the frequency of any wind (%) regardless of direction, exceeding the threshold wind speed from any direction for each month. The threshold wind speed is determined by increasing the wind speed by 1 m s^{-1} increments for each hour of the day, beginning with 6 m s^{-1} , until erosion is detected. The incremental wind speed at which erosion first occurs is reported as the threshold wind speed. The other parameters are then calculated and reported in table format through the SWEEP interface.

To determine the threshold parameters, click the 'Run' menu on the SWEEP interface, then 'Threshold Run' (Ctrl-H) or the "Threshold Run" toolbar button. This opens a window that allows the user to select a WINDGEN wind station for which to calculate the wind speed threshold at which erosion will occur as well as other wind parameters by direction and month. Once a station is selected, clicking the 'Run' button in the station selection window generates a table that displays the following information by month and direction (see Figure 1). The SWEEP is the only option for performing this type of analysis for wind erosion.

	N-0	NNE-22	NE-45	ENE-67	E-90	ESE-112	SE-135	SSE-157	S-180	SSW-202	SW-225	WSW-247	W-270	WNW-292	NW-315	NNW-337	Total
Threshold (m/s)	9.0	9.0	9.0	9.0	9.0	9.0	9.0	9.0	9.0	9.0	9.0	9.0	9.0	9.0	9.0	9.0	9.0
Winds > Thresh (%)	4.35	2.35	0.55	1.75	9.55	4.95	0.85	3.10	9.35	18.40	22.50	26.15	9.90	8.50	13.10	15.70	
Dir Prob (%)	6.10	2.50	1.90	1.70	4.30	4.00	4.50	5.80	11.60	10.00	10.30	8.00	5.30	3.80	4.80	5.60	90.20
Thresh Prob (%)	0.27	0.06	0.01	0.03	0.41	0.20	0.04	0.18	1.08	1.84	2.32	2.09	0.52	0.32	0.63	0.88	10.88

Figure 1. An example of the wind generator station display table showing threshold parameters for March in Saguache County, Colorado.

Standalone Erosion Submodel

The WEPS Erosion submodel (tsterode.exe) also can be operated as a standalone model to simulate erosion for a single storm (i.e., one day or less). Input parameters that must be provided for the day include the field and barrier dimensions as well as biomass, soil, hydrology, and wind parameters. Wind speed can be entered either as Weibull distribution parameters or listed as average wind speeds for each time period throughout the day. Valid command line options for the standalone Erosion submodel are listed below.

Command Line Options

Usage: tsterode -? -h -i"input_filename" -x# -y# -t# -T# -u -d# -E

Valid command line options:

-? or -h Display the available command line options.

-i"input_filename" Specify input filename. The input filename must be specified and listed before the -Einp, -Erod, -Egrd, and -Emit options. Quotes are required if spaces are a part of the filename.

-x# -y# Number of grid lines in x and y directions (min. = 3; max. = 500). The submodel calculates the loss/deposition over a series of individual, equal-sized grid cells representing the entire simulation region. The more grid lines, the smaller the area in each grid cell for the same size simulation region. The recommended total number of grid lines in each direction is 30 for a field without a barrier and 60 for a field with a barrier (these are the maximum values used by WEPS). Increasing the number of grid cells increases the accuracy of the soil loss/deposition estimates and increases the run time. If not specified, the number of grid lines and thus the number of grid cells is automatically calculated within the model. This is based upon whether there are any wind barriers specified (quadrupling the total number of cells), the physical size of the simulation region (x and y dimensions) as well as the ratio of the x and y dimensions specified. This is the method used within WEPS.

-t# Interval for surface updating in seconds (min. = 60 seconds; max. = 86400 seconds). This is used to specify a fixed surface updating interval and is primarily for testing and evaluation purposes. This allows one to override the default variable updating time interval code used within WEPS. By default, the erosion code contains an update

loop dependent upon the number of time intervals/day and an inner loop that allows more frequent surface updating to occur, based upon the intensity of the erosion occurring and thus the rate at which the surface is changing. The interval must be evenly divisible into both the number of time intervals/day and 24 (hours in a day). If these conditions are not met, the program aborts with an error message. The default is -t900. If this option is not specified, then the auto-surface variable updating time interval code used within WEPS is applied.

-T3 Minimum erosive wind speed (m s^{-1}).

-u Disables erosion surface updating.

-d# Set read input file debug flag. Writes (echos) the input file parameters to stdin (displayed on the screen).

-Einp Writes the input file to "input_filename.einp." This is useful for debugging. The "input_filename" is the same name as the input filename with an ".einp" extension and will be created in the same directory specified for the input filename.

-Erod Output erosion summary (kg m^{-2}) (positive values represent soil loss and negative values represent soil deposition). The one-line output in the file contains the values for total loss, saltation plus creep, suspension, PM10, and the input filename. The "-Erod" option requires that the input file (-i "input_filename") be specified as a command line argument before the "-Erod" option; e.g., tsterode -"input_filename.ext" -Erod. The "input_filename" in the erosion summary is the same name as the input filename with a ".erod" extension and will be created in the same directory specified for the input filename.

-Egrd Output grid summary results (kg m^{-2}) (positive values represent soil loss and negative values represent soil deposition). The "-Egrd" option requires that the input file (-i"input_filename") be specified as a command line argument before the "-Egrd" option; e.g., tsterode -i "input_filename.ext" -Egrd

The "input_filename" in the grid summary is the same name as the input filename with an ".egr" extension and will be created in the same directory specified for the input filename.

-Esgrd Output all grid cell values for selected grid cell variables (e.g., RR, ridge ht, friction velocity, etc.) as well as the standard erosion results for each subdaily period. Each "period" is identified by the "yy mm dd hr variable_name_title" prior to the grid cell values. The "-Esgrd" option requires that the input file (-i"input_filename") be specified as a command line argument before the "-Esgrd" option; e.g., tsterode -i "input_filename.ext" -Esgrd

The "input_filename" in the grid summary is the same name as the input filename with a ".sgrd" extension and will be created in the same directory specified for the input filename.

-Emit Output hourly erosion results (kg m^{-2}) (positive values represent soil loss and negative values represent soil deposition). The "-Emit" option requires that the input file

(-i"input_filename") be specified as a command line argument before the "-Emit" option; e.g., tsterode -iinput_filename.ext -Emit

The "input_filename" in the hourly erosion results is the same name as the input filename with a ".emit" extension and will be created in the same directory specified for the input filename.

-Eplt Enable printing of a file that can be used to plot various data. The data are appended to the file for each run.

Note that these command line options cannot be specified when the Erosion submodel is run through the WEPS interface.

The standalone Erosion submodel input file contains comments (indicated by # in column one) that describe each line of input data to aid in checking and modifying input data, which follows the comments. Specific definitions of these parameters are documented within the comment lines of the input file. An example of an input file is given in Example 1.

The output file from the stand-alone Erosion submodel is shown in Example 2. The file contains a listing of the inputs to the submodel, followed by the generated results labeled 'OUTPUT FROM ERODOUT.FOR'. This section lists the amount of total, suspension, and PM10 leaving each boundary and field grid cell. At the bottom of the file is the field average of each of these grid cells.

Below are the definitions of the variables in the output file (these variable definitions are not included as comments within the output file). See the SWEEP user manual for more details on the use of the model.

ntstep - Number of time steps for the simulation
am0eif - EROSION "initialization" flag. Must be set to .TRUE. for standalone erosion runs
nsubr - Number of subregions
nacctr - Number of accounting regions
nbr - Number of barriers
am0efl - EROSION "print" flag
amasim - Orientation of the simulation region (deg clockwise from north)
amxsim - Dimensions of the simulation region listing the lower left and upper right corners as (x1,y1) (x2,y2) in meters
SAI - Growing crop stem area index ($m^2 m^{-2}$)
LAI - Growing crop leaf area index ($m^2 m^{-2}$)
nslay - Number of soil layers
layer depth - Depth of each layer
b.density - The oven-dry weight of the <2 mm soil material per unit volume of soil at a tension of 1/3 bar ($Mg m^{-3}$)
Vfsand - Mineral particles 0.05 to 0.1 mm in equivalent diameter as a weight fraction of the <2.0 mm fraction ($kg kg^{-1}$)
sand - Mineral particles 0.05 to 2.0 mm in equivalent diameter as a weight fraction of the <2.0 mm fraction ($kg kg^{-1}$)
silt - Mineral particles 0.002 to 0.05 mm in equivalent diameter as a weight fraction of the <2.0 mm fraction ($kg kg^{-1}$)

clay - Mineral particles less than 0.002 mm in equivalent diameter as a weight fraction of the <2.0 mm fraction (kg kg^{-1})
 rock vol - The volume fraction of the layer occupied by the 2.0 mm or larger (20 mm or larger for wood fragments) on a whole soil basis ($\text{m}^3 \text{m}^{-3}$)
 AgD - The aggregate density for (Mg m^{-3})
 AgS - Mean of natural log of aggregate crushing energies ($\ln(\text{J kg}^{-1})$)
 GMD - Soil aggregate geometric mean diameter of the modified log-normal distribution (mm)
 GMDmn - Upper limit of the modified log-normal aggregate size distribution (mm)
 GMDmx - Lower limit of the modified log-normal aggregate size distribution (mm)
 GSD - Soil aggregate geometric standard deviation of the modified log-normal distribution (dimensionless)
 Cr frac mass - Fraction of surface covered with consolidated soil, as opposed to aggregated soil ($\text{m}^2 \text{m}^{-2}$)
 mass LOS - Mass of the loose, saltation-size soil on the surface soil crusted area (kg m^{-2})
 LOS frac. - Fraction of total soil surface area covered with loose material on the crust ($\text{m}^2 \text{m}^{-2}$)
 LOS, density - The density of the soil crust (Mg m^{-3})
 LOS stability - Mean of natural log of crust crushing energies ($\ln(\text{J kg}^{-1})$)
 RR - The standard deviation of elevation from a plane of a random soil surface, including any flat biomass adjusted as suggested by Allmaras et. al. (1966) (mm)
 Rg ht - The height of soil ridges from bottom of furrow to top of ridge (mm)
 width - Width of the top of the ridge (i.e., bed width) (mm)
 spacing - Spacing between ridge tops (mm)
 orient. - Direction of the tillage ridge, clockwise from true north (degrees)
 dike spacing - Spacing between dikes within the furrow (mm)
 ahrwc0 - Surface layer water content (Mg Mg^{-1})
 anemht - Anemometer height (m)
 awwzo - Aerodynamic roughness at anemometer site (mm)
 wzoflg - Flag to denote location of z_o (aerodynamic roughness)
 (flag = 0 - at weather station location - z_o is a constant)
 (flag = 1 - on field location - z_o varies based on field surface)
 wind dir - Wind direction for the event (deg clockwise from north)
 max wind speed - Maximum wind speed for the event (m s^{-1})
 egt - Amount passing the border grid cells - total (kg m^{-1}) or amount leaving all interior field grid cells - total (kg m^{-2}); these will be separated to different variables and units in upcoming versions
 egtss - Amount passing the border grid cells as Suspension (kg m^{-1}) or amount leaving all interior field grid cells - suspension (kg m^{-2}); these will be separated to different variables and units in upcoming versions
 egt10 - Amount passing the border grid cells as PM10 (kg m^{-1}) or amount leaving all interior field grid cells - PM10 (kg m^{-2}); these will be separated to different variables and units in upcoming versions

References

Feng, G., and B. Sharratt. 2009. Evaluation of the SWEEP model during high wind on the Columbia Plateau. *Earth Surface Process and Landforms*. 34, 1461-1468.

Hagen, L.J. 2004. Evaluation of the Wind Erosion Prediction System (WEPS) erosion submodel on cropland fields. *Environmental Modelling and Software*. 19(2):171-176.

Example 1. Example stand-alone erosion input file.

```
*****
#   erod_template.in   Template INPUT DATA FILE
#                       Updated January 2006 - LEW
*****
#
#   +++ PURPOSE +++
#
#   Input file for standalone erosion submodel program (tsterode)
#
#   All lines beginning with # are assumed to
#   be comment lines and are skipped.
#
#   +++ DEFINITIONS +++
#
#   All comments prior to each line of data input
#   in this template input file have the following format:
#
#   Variable_Name, Var_type, Text Definition
#
#   where Var_type is: I = integer L = logical R = real
#
#
# +++ DEBUG STUFF +++
#
#   debugflg - debug flag for providing different levels of debug info
#               currently useful to debug/check input file data format
#
#               value of 0 will print no debug information
#               value of 1 will print out and number all input file
lines
#               value of 2 will print out and number all data input
lines
#               value of 3 will do both 1 and 2
#
#   0
#
#
# +++ INIT STUFF +++
#
#   am0eif, L, EROSION "initialization" flag
#               Must be set to .TRUE. for standalone erosion runs
#   .TRUE.
#
#   am0eifl, I, EROSION "print" flag
#               NOTE: Not sure if all of these have yet been replaced by
#               "tsterode" cmdline options. Regardless, this flag
#               should be considered deprecated in this file. -
LEW
#               Range: 0 to 6
#               0 = print input, no output
#               1 = print input, standard output
#               2 = print input, 1 line output
#               3 = used in WEPS to print input, then create file
"emit.out"
#               containing hourly suspended emission rates
#   4 = used in standalone to print input, then create file
"emit.out"
#               containing hourly suspended emission rates
#               5 = not used at present
#               6 = print input, detail output each step using calls
#               to sb1out and sb2out
```

```

1
#
# +++ SIMULATION REGION +++
#
#   amxsim(x,y), R, Simulation Region diagonal coordinates (meters)
#   Input (x,y) coordinates in this form: x1,y1 x2,y2
#   Typical Range: 10.0 to 1600.0
#
#           NOTE: Accounting region and subregion coordinates
#           must also be set to the same values
#
#   0.0, 0.0 1000.0, 200.0
#
#
#   amasim, R, Simulation Region orientation angle (degrees from north)
#   0.0
#
# +++ ACCOUNTING REGIONS +++
#
#   nacctr, I, Number of accounting regions (must always be 1 for now)
#   1
#
#   amxar(x,y,a), R, Accounting Region diagonal coordinates (meters)
#   Input (x,y) coordinates in this form: x1,y1 x2,y2
#   for each Accounting Region specified (nacctr)
#
#           NOTE: Accounting region coordinate values must
#           match simulation region coordinates above
#
#   0.0, 0.0 1000.0, 200.0
#
# +++ BARRIERS +++
#
#   nbr, I, Number of barriers (0-5)
#   2
#
#   NOTE: Remaining BARRIER inputs are repeated for each barrier
#   specified
#           If no barriers specified (nbr=0), then no BARRIER inputs will
#           be listed here.
#
#   amxbr(x,y,b), R, Barrier linear coordinates (meters)
#   Input (x,y) coordinates in this form: x1,y1 x2,y2
#   for each barrier specified (nbr)
#   0.0, 0.0 0.0, 200.0
#
#   amzbr(b), R, Barrier height (meters)
#   ampbr(b), R, Barrier porosity (m^2/m^2)
#   amxbrw(b), R, Barrier width (meters)
#
#   0.2 0.5 15.0
#
#           Repeat previous two input lines for each additional barrier
#
#           Barrier #2 coordinates (x1,y1) (x2,y2)
#   0.0, 0.0 1000.0, 0.0
#           Barrier #2 height, porosity and width
#   0.2 0.5 15.0
#
# +++ SUBREGION REGIONS +++
#

```

```

#   nsubr, I, Number of subregions (1-5)
#       NOTE: Currently not fully tested for multiple subregions
#           Only use value of 1
#
#   1
#
#   NOTE: Remaining SUBREGION inputs (BIOMASS, SOIL, and HYDROLOGY;
#   ie, variables defined by subregion) are repeated for "nsubr"
#   subregions specified
#
#   amxsr(x,y,s), R, Subregion diagonal coordinates (m)
#       Input (x,y) coordinates in this form: x1,y1 x2,y2
#       for each subregion specified (subr)
#
#       NOTE: Since only one subregion is currently
supported,
#           subregion coordinate values must match
#           Simulation Region coordinates above
#
#   0.0, 0.0 1000.0, 200.0
#
#   +++ BIOMASS +++
#
#   adzht_ave(s), R, Height of standing residue (meters)
#       WEPS-generated input files will provide
#       "SAI weighted" average residue height
#       across all residue pools.
#       Typical Range: 0.0 to 3.0
#   0.21
#
#   aczht(s), R, Average height of growing crop (meters)
#   0.0
#
#   acrsai(s), R, Growing crop stem area index (m2/m2)
#       Typical Range: 0.0 to 3.0
#   acrlai(s), R, Growing crop leaf area index (m2/m2)
#       Typical Range: 0.0 to 8.0
#   0.0 0.0
#
#   adrsaitot(s), R, Residue stem area index (m2/m2)
#   adrlaitot(s), R, Residue leaf area index (m2/m2)
#       WEPS generated input files will provide
#       total "SAI" and "LAI" values
#       across all residue pools.
#   0.02 0.00
#
#   acxrow(s), R, Growing crop row spacing (meters)
#       Use value of 0.0 if not planted in rows;
#       e.g., broadcast seeded
#   ac0rg(s), I, Specify seed location (0 = furrow, 1 = ridge)
#       Value doesn't matter if no ridges exist
#   0.3, 0
#
#   abffcv(s), R, Flat biomass cover (m2/m2)
#   0.0
#
#   +++ SOIL +++
#
#   nslay(s), I, (s1layr.inc) Number of soil layers (1-100)
#       NOTE: Only surface soil layer necessary

```

```

1
#
# NOTE: Remaining SOIL inputs are repeated on each input line
#       for each layer specified
#
# aszlyt(l,s), R, Thickness (mm)
1000.0
#
# asdblkl(s), R, Bulk density of soil layer (Mg/m^3)
#       Typical Range: >0.0 to 10.0
1.8
# asfsan(l,s), R, Fraction of sand content in soil layer (Mg/Mg)
#       Range: 0.0 to 1.0 (sand + silt + clay = 1.0)
0.90
# asfvfs(l,s), R, Fraction of very fine sand in soil layer (Mg/Mg)
#       Range: 0.0 to 1.0 (fraction of total soil < 2.0 mm)
0.21
# asfsil(l,s), R, Fraction of silt content in soil layer (Mg/Mg)
#       Range: 0.0 to 1.0 (sand + silt + clay = 1.0)
0.08
# asfcla(l,s), R, Fraction of clay content in soil layer (Mg/Mg)
#       Range: 0.0 to 1.0 (sand + silt + clay = 1.0)
0.02
#
# asvroc(l,s), R, Rock volume in soil layer (m^3/m^3)
#       Range: 0.0 to 1.0
0.30
#
# asdagd(l,s), R, Average aggregate density of soil layer (Mg/m^3)
#       Typical Range: 0.5 to 2.5
1.8
# aseags(l,s), R, Average dry aggregate stability of soil layer
#       [ln(J/kg)]
#       Typical Range: 0.1 to 7.0
2.50
#
# ----- Size distribution of soil aggregates -----
#       GMD - Geometric Mean Diameter of aggregates
#       GSD - Geometric Mean Standard Deviation of aggregates
#
# aslagm(l,s), R, GMD of aggregate sizes in soil layer (mm)
#       Typical Range: 0.03 to 30.0
0.47
# aslagn(l,s), R, Minimum aggregate size in soil layer (mm)
#       Typical Range: 0.001 to 5.0
0.043
# aslagx(l,s), R, Maximum aggregate size in soil layer (mm)
#       Typical Range: 1.0 to 1000.0
89.8
# as0ags(l,s), R, GSD of aggregate sizes in soil layer (mm/mm)
#       Typical Range: 1.0 to 40.0
12.0
#
# +++ SOIL SURFACE +++
#
# asfcr(s), R, Surface crust fraction (m^2/m^2)
#       Range: 0.0 to 1.0
# aszcr(s), R, Surface crust thickness (mm)
#       Typical Range: 0.0 to 23.0
# asflos(s), R, Fraction of crusted surface with loose material on
# top of crust
#       (m^2/m^2)
#       Range: 0.0 to 1.0

```

```

#   asmlos(s), R, Mass of loose material on top of crust (kg/m^2)
#       Typical Range: 0.0 to 3.0
#   asdcr(s), R, Density of soil crust (Mg/m^3)
#       Typical Range: 0.6 to 2.0
#   asecr(s), R, Dry crust stability [ln(J/kg)]
#       Typical Range: 0.0 to 7.0
0.6 7.0 0.2 0.4 0.1 1.0
#
#   aslrr(s), R, Allmaras random roughness (mm)
#       Typical Range: 1.0 to 60.0
5.0
#   aszrgh(s), R, Ridge height (mm)
#       Typical Range: 0.0 to 500.0
#   asxrgs(s), R, Ridge spacing (mm)
#       Typical Range: 0.0 to 2000.0
#   asxrgw(s), R, Ridge width (mm)
#       Typical Range: 0.0 to 4000.0
#   asxrgo(s), R, Ridge orientation (degrees)
#       Range: 0.0 to 179.99
#       NOTE: If no ridges, then specify 0.0 for height, width
and spacing
0.0 0.0 0.0 0
#   asxdks(s), R, Dike spacing (mm)
#       Typical Range: 0.0 to 1000.0
#       NOTE: If no dikes, then specify 0.0
0.0
#
#   +++ HYDROLOGY +++
#
#   ahzsnd(s), R, Snow depth (mm)
#       Typical Range: 0.0 to 1000.0
0.0
#
#   ahrwcw(l,s), R, Wilting point water content of soil layer (Mg/Mg)
#       Typical Range: 0.0 to 0.25
0.077
#
#   ahrwca(l,s), R, Current water content of soil layer (Mg/Mg)
#       Typical Range: 0.0 to 0.50
0.0
#
#   ahrwc0(h,s), R, Surface layer water content (Mg/Mg)
#       Typical Range: 0.0 to 0.50
#       NOTE: The near surface water content is specified on
an
#       hourly basis. We read in the hourly water
content
#       on two lines, with 12 values in each line.
0.0 0.0 0.0 0.0 0.0 0.0 0.0 0.0 0.0 0.0 0.0 0.0
0.0 0.0 0.0 0.0 0.0 0.0 0.0 0.0 0.0 0.0 0.0 0.0
#
#
# NOTE: This is the end of the SUBREGION variables
#
#   +++ WEATHER +++
#
#   awdair, R, Air density (kg/m^3)
#       Typical Range: 0.7 to 1.5
1.2
#
#   awadir, R, Wind direction (degrees) measured clockwise from North
#       Typical Range: 0.0 to 359.9

```

```

270.0
#
#   ntstep, I, Number of intervals/day to run EROSION
#           Range: 24 to 96
#
#           NOTE:  ntstep = 24 means hourly updates
#                  ntstep = 48 means 30 minute updating
#                  ntstep = 96 means 15 minute updating
24
#
#   anemht, R  anemometer height (m)
#           Typical Range: 0.5 to 30.0
#   awzso, R  aerodynamic roughness at anemometer site (mm)
#           Typical Range: 0.5 to 2000.0
#   wzoflg, I (global variable) zo location flag
#           (flag = 0 - at weather station location - zo is a
constant)
#           (flag = 1 - on field location - zo varies based on field
surface)
10.0, 10.00 0
#
#   wflg, I, Wind/Weibull flag
#           (0 - read in Weibull parameters, 1 - read in wind speeds)
1
#
# NOTE: This is only present when (wflg=0)
#   wfcalm, R, Fraction of time winds are calm (hr/hr)
#           Range: 0.0 to 1.0
#   wuc, R, Weibull "c" factor (m/s)
#           Typical Range: >0.0 to 30.0
#   w0k, R, Weibull "k" factor
#           Typical Range: 1.0 to 3.0
# 0.217 7.125 2.971 <--- Example data line for wind expressed as
Weibull parameters
#
# NOTE: The remaining data is only present when (wflg=1)
#   awu(i), R, Wind speed for (ntstep) intervals (m/s)
#           Typical Range: 0.0 to 30.0
#
#           NOTE: We can read multiple lines with 6 values per line
#                 Wind data should be AVERAGES for the period.
#                 Hourly averages will often under estimate wind
erosion.
#                 30 minute averages or shorter time interval is
more suitable.
8.181 4.068 4.068 4.426 5.052 5.052
4.739 4.292 4.515 3.353 3.621 2.280
5.275 6.750 7.242 7.868 9.835 13.814
17.211 12.651 11.712 12.964 10.014 8.583
#
#
# *****
#   NOTE:  Not necessary to modify any information below this line
#          unless one is interested in generating a "plot.out" file.
# *****
#
#   + + + DATA TO PLOT + + +
#
#   "xplot" flag for writing variables to file 'tsterode.eplt'.
#   -1 = write nothing
#   0 = write erosion variables;
#   Actual variables listed below are only written if flagged with a 1
#

```

```

#     NOTE: This flag is deprecated. Tsterode cmdline options
determine
#           if this file is created and/or data appended to it.
#
#
#     Next are 2 lines per variable:
#     1st line: flag (0=don't write, 1=do write) and variable
description
#     2nd line: this info is used as a header in 'plot.out'
#           place header within first 12 positions of the line
#
# xin(i), R, (field length)
#     1
#     Length(m)
# abzht, R, (biomass ht.(m))
#     1
#     bio_ht(m)
# abrsai, R (stem area index)
#     1
#     stem_area
# abrlai(s), R, Biomass leaf area index (m^2/m^2)
#     1
#     lai_area
# abffcv, R, (biomass flat fraction cover)
#     0
#     flat_cov
# asfvfs(1,s), R, (soil fraction very fine sand in layer 1)
#     0
#     vfsand
# asfsan(1,s), R, (soil fraction sand in layer 1)
#     1
#     sand
# asfsil(1,s), R (soil fraction silt in layer 1)
#     0
#     silt
# asfcla(1,s), R (soil fraction clay in layer 1)
#     0
#     clay
# asvoc(1,s), R (soil volume roc in layer 1)(m^3/m^3)
#     0
#     rock_vol
# aseags(1,s), R (soil aggregate stability) (ln J/m^3)
#     0
#     ag_stab
# aslagm(1,s), R (soil aggregate geom. mean dia.) (mm)
#     0
#     ag_gmd
# aslagn(1,s), R (soil aggregate min. dia.) (mm)
#     0
#     ag_min
# aslagx(1,s), R (soil aggregate max. dia.) (mm)
#     0
#     ag_max
# as0ags(1,s), R (soil aggregate geo. std. dev.)
#     0
#     ag_std
# asfcr(s), R, (s1surf.inc) Surface crust fraction (m^2/m^2)
#     0
#     crust_cv
# aszcr(s), R, (s1surf.inc) Surface crust thickness (mm)
#     0
#     crust_z(mm)

```

```

#   asflos(s), R, (slsurf.inc) Fraction of loose material on surface
(m^2/m^2)
0
  los_cv
#   asmlos(s), R, (slsurf.inc) Mass of loose material on crust (kg/m^2)
0
  los(kg/m^2)
#   asdcr(s), R, (slsurf.inc) Soil crust density (Mg/m^3)
0
  cr_den(Mg/m^3)
#   asecr(s), R, (slsurf.inc) Soil crust stability ln(J/kg)
0
  cr_se
#   aslrr(s), R, (slsgeo.inc) Allmaras random roughness (mm)
0
  rr(mm)
#   aszrgh(s), R, (slsgeo.inc) Ridge height (mm)
0
  z_rgh(mm)
#   asxrgs(s), R, (slsgeo.inc) Ridge spacing (mm)
0
  x_rgs(mm)
#   asxrgw(s), R, (slsgeo.inc) Ridge width (mm)
0
  x_rgw(mm)
#   asxrgo(s), R, (slsgeo.inc) Ridge orientation (deg)
0
  a_rgo(deg)
#

```

Example 2. Example standalone erosion output file.

```
REPORT OF INPUTS (read by erodin.for)

+++ Control Flags, etc. +++

ntstep  am0eif  nsubr  nacctr  nbr  am0efl
  48      T      1      1      0      1

+++ SIMULATION REGION +++

orientation and dimensions of sim region
amasim(deg)  amxsim - (x1,y1) (x2,y2)
  0.00      0.00      0.00  276.00  276.00

+++ ACCOUNTING REGIONS +++

nacctr - number of accounting regions
  1
accounting region dimensions (x1,y1) (x2,y2)
  0.00      0.00  276.00  276.00

+++ BARRIERS +++

  no barriers

+++ SUBREGIONS +++

nsubr - number of subregions
  1
subregion dimensions (x1,y1) (x2,y2)
  0.00      0.00  276.00  276.00

***** Subregion 1 *****

+++ BIOMASS +++

Biomass ht, SAI,   LAI,  flat cover
  0.000  0.000  0.000  0.000

+++ SOIL +++

nslay - number of soil layers
  3

layer depth b.density vfsand  sand  silt  clay  rock vol
  1  230.00  1.05  0.14  0.22  0.71  0.08  0.00
  2  680.00  1.05  0.14  0.22  0.71  0.08  0.00
  3  610.00  1.05  0.14  0.22  0.71  0.08  0.00

layer  AgD  AgS  GMD  GMDmn  GMDmx  GSD
  1  1.87  1.00  1.64  0.01  36.73  15.13
  2  2.00  1.87  7.68  0.01  41.79  16.17
  3  2.00  1.87  30.00  0.01  70.96  9.98

Cr frac mass LOS frac.LOS, density stability
  0.00  0.00  0.00  1.87  1.87

  RR,  Rg ht,  width, spacing, orient., dike spacing
  1.50  0.00  0.00  0.00  0.00  0.00

+++ HYDROLOGY +++

Snow depth (mm)
0.00000000E+00

layer  wilting and actual water contents
  1  0.05  0.02
  2  0.05  0.02
  3  0.05  0.02
```

Hourly water contents - ahrwc0
 0.02 0.02 0.02 0.02 0.02 0.02
 0.02 0.02 0.02 0.02 0.02 0.02
 0.02 0.02 0.02 0.02 0.02 0.02
 0.02 0.02 0.02 0.02 0.02 0.02

+++ WEATHER +++

anemht awwzo wzoflg
 2.00000000 25.0000000 1
 wind dir (deg) and max wind speed (m/s)
 250.00 11.86

Wind speeds (m/s) - 48 intervals
 0.00 0.00 0.00 0.00 0.00 1.19
 2.76 3.47 4.00 4.44 4.84 5.20
 5.54 5.87 6.20 6.53 6.86 7.20
 7.56 7.95 8.39 8.91 9.57 10.64
 11.86 10.02 9.21 8.64 8.16 7.75
 7.38 7.03 6.69 6.36 6.04 5.71
 5.37 5.02 4.64 4.23 3.75 3.15
 2.24 0.00 0.00 0.00 0.00 0.00

END OF INPUTS

OUTPUT FROM ERODOUT.FOR

Total grid size: (31 , 31) Inner grid size: (29 , 29)

Passing Border Grid Cells - Total egt (kg/m)
 top (i=1,imax-1,j=jmax) bottom(i=1,imax-1,j=0) right(i=imax,j=1,jmax-1)
 left(i=0,j=1,jmax-1)
 0.72 1.98 3.58 5.51 7.90 10.63 13.56 16.56
 19.55 22.35 24.57 26.02 26.87 27.36 27.64 27.79
 27.88 27.92 27.95 27.96 27.97 27.98 27.98 27.98
 27.98 27.98 27.98 27.98 27.98 27.98
 0.00 0.00 0.00 0.00 0.00 0.00 0.00 0.00
 0.00 0.00 0.00 0.00 0.00 0.00 0.00 0.00
 0.00 0.00 0.00 0.00 0.00 0.00 0.00 0.00
 13.93 37.80 59.60 70.80 74.85 76.21 76.66 76.81
 76.86 76.87 76.88 76.88 76.88 76.88 76.88 76.88
 76.88 76.88 76.88 76.88 76.88 76.88 76.88 76.88
 76.88 76.88 76.88 76.88 76.88 76.88
 0.00 0.00 0.00 0.00 0.00 0.00 0.00 0.00
 0.00 0.00 0.00 0.00 0.00 0.00 0.00 0.00
 0.00 0.00 0.00 0.00 0.00 0.00 0.00 0.00

Passing Border Grid Cells - Suspension egtss (kg/m)
 top (i=1,imax-1,j=jmax) bottom (i=1,imax-1,j=0) right (i=imax,j=1,jmax-1) left
 (i=0,j=1,jmax-1)
 0.21 0.72 1.65 3.09 5.03 7.52 10.57 14.18
 18.34 23.03 28.15 33.59 39.21 44.95 50.76 56.59
 62.45 68.32 74.20 80.08 85.96 91.85 97.73 103.61
 109.50 115.38 121.26 127.15 133.03
 0.00 0.00 0.00 0.00 0.00 0.00 0.00 0.00
 0.00 0.00 0.00 0.00 0.00 0.00 0.00 0.00
 0.00 0.00 0.00 0.00 0.00 0.00 0.00 0.00
 0.00 0.00 0.00 0.00 0.00 0.00 0.00 0.00
 10.00 33.70 67.44 105.62 144.28 181.22 215.22 245.57
 271.88 294.03 312.14 326.54 337.67 346.04 352.18 356.56
 359.62 361.70 363.09 364.00 364.58 364.95 365.17 365.31
 365.39 365.44 365.46 365.48 365.49
 0.00 0.00 0.00 0.00 0.00 0.00 0.00 0.00
 0.00 0.00 0.00 0.00 0.00 0.00 0.00 0.00
 0.00 0.00 0.00 0.00 0.00 0.00 0.00 0.00
 0.00 0.00 0.00 0.00 0.00 0.00 0.00 0.00

Passing Border Grid Cells - PM10 egt10 (kg/m)

top (i=1,imax-1,j=jmax) bottom (i=1,imax-1,j=0) right (i=imax,j=1,jmax-1) left (i=0,j=1,jmax-1)

0.0046	0.0193	0.0473	0.0912	0.1488	0.2196	0.3027	0.3977
0.5039	0.6207	0.7463	0.8784	1.0145	1.1531	1.2931	1.4338
1.5750	1.7164	1.8579	1.9995	2.1412	2.2828	2.4245	2.5662
2.7079	2.8496	2.9913	3.1329	3.2746			
0.0000	0.0000	0.0000	0.0000	0.0000	0.0000	0.0000	0.0000
0.0000	0.0000	0.0000	0.0000	0.0000	0.0000	0.0000	0.0000
0.0000	0.0000	0.0000	0.0000	0.0000	0.0000	0.0000	0.0000
0.0000	0.0000	0.0000	0.0000	0.0000	0.0000	0.0000	0.0000
0.3050	0.9706	1.8304	2.7605	3.6919	4.5786	5.3937	6.1209
6.7510	7.2814	7.7153	8.0603	8.3271	8.5281	8.6755	8.7810
8.8547	8.9051	8.9387	8.9607	8.9748	8.9836	8.9891	8.9924
8.9944	8.9956	8.9963	8.9966	8.9969			
0.0000	0.0000	0.0000	0.0000	0.0000	0.0000	0.0000	0.0000
0.0000	0.0000	0.0000	0.0000	0.0000	0.0000	0.0000	0.0000
0.0000	0.0000	0.0000	0.0000	0.0000	0.0000	0.0000	0.0000
0.0000	0.0000	0.0000	0.0000	0.0000	0.0000	0.0000	0.0000

Leaving Field Grid Cells - Total egt (kg/m^2)

-0.27	-0.51	-0.73	-0.97	-1.25	-1.51	-1.73	-1.91
-2.06	-2.16	-2.12	-1.99	-1.87	-1.80	-1.75	-1.73
1.72	-1.71	-1.70	-1.70	-1.70	-1.70	-1.70	-1.70
1.70	-1.70	-1.70	-1.70	-1.70	-1.70	-1.70	-1.70
-0.27	-0.51	-0.73	-0.97	-1.25	-1.51	-1.73	-1.91
-2.06	-2.16	-2.12	-1.99	-1.87	-1.80	-1.75	-1.73
1.72	-1.71	-1.70	-1.70	-1.70	-1.70	-1.70	-1.70
1.70	-1.70	-1.70	-1.70	-1.70	-1.70	-1.70	-1.70
-0.27	-0.51	-0.73	-0.97	-1.25	-1.51	-1.73	-1.91
-2.06	-2.16	-2.12	-1.99	-1.87	-1.80	-1.75	-1.73
1.72	-1.71	-1.70	-1.70	-1.70	-1.70	-1.70	-1.70
1.70	-1.70	-1.70	-1.70	-1.70	-1.70	-1.70	-1.70
-0.27	-0.51	-0.73	-0.97	-1.25	-1.51	-1.73	-1.91
-2.06	-2.16	-2.12	-1.99	-1.87	-1.80	-1.75	-1.73
1.72	-1.71	-1.70	-1.70	-1.70	-1.70	-1.70	-1.70
1.70	-1.70	-1.70	-1.70	-1.70	-1.70	-1.70	-1.70
-0.27	-0.51	-0.73	-0.97	-1.25	-1.51	-1.73	-1.91
-2.06	-2.16	-2.12	-1.99	-1.87	-1.80	-1.75	-1.73
1.72	-1.71	-1.70	-1.70	-1.70	-1.70	-1.70	-1.70
1.70	-1.70	-1.70	-1.70	-1.70	-1.70	-1.70	-1.70
-0.27	-0.51	-0.73	-0.97	-1.25	-1.51	-1.73	-1.91
-2.06	-2.16	-2.12	-1.99	-1.87	-1.80	-1.75	-1.73
1.72	-1.71	-1.70	-1.70	-1.70	-1.70	-1.70	-1.70
1.70	-1.70	-1.70	-1.70	-1.70	-1.70	-1.70	-1.70
-0.27	-0.51	-0.73	-0.97	-1.25	-1.51	-1.73	-1.91
-2.06	-2.16	-2.12	-1.99	-1.87	-1.80	-1.75	-1.73
1.72	-1.71	-1.70	-1.70	-1.70	-1.70	-1.70	-1.70
1.70	-1.70	-1.70	-1.70	-1.70	-1.70	-1.70	-1.70
-0.27	-0.51	-0.73	-0.97	-1.25	-1.51	-1.73	-1.91
-2.06	-2.16	-2.12	-1.99	-1.87	-1.80	-1.75	-1.73
1.72	-1.71	-1.70	-1.70	-1.70	-1.70	-1.70	-1.70
1.70	-1.70	-1.70	-1.70	-1.70	-1.70	-1.70	-1.70
-0.27	-0.51	-0.73	-0.97	-1.25	-1.51	-1.73	-1.91
-2.06	-2.16	-2.12	-1.99	-1.87	-1.80	-1.75	-1.73
1.72	-1.71	-1.70	-1.70	-1.70	-1.70	-1.70	-1.70
1.70	-1.70	-1.70	-1.70	-1.70	-1.70	-1.70	-1.70
-0.27	-0.51	-0.73	-0.97	-1.25	-1.51	-1.73	-1.91
-2.06	-2.16	-2.12	-1.99	-1.87	-1.80	-1.75	-1.73
1.72	-1.71	-1.70	-1.70	-1.70	-1.70	-1.70	-1.70
1.70	-1.70	-1.70	-1.70	-1.70	-1.70	-1.70	-1.70
-0.27	-0.51	-0.73	-0.97	-1.25	-1.51	-1.73	-1.91
-2.06	-2.16	-2.12	-1.99	-1.87	-1.80	-1.75	-1.73
1.72	-1.71	-1.70	-1.70	-1.70	-1.70	-1.70	-1.70
1.70	-1.70	-1.70	-1.70	-1.70	-1.70	-1.70	-1.70
-0.27	-0.51	-0.73	-0.97	-1.25	-1.51	-1.73	-1.91
-2.06	-2.16	-2.12	-1.99	-1.87	-1.80	-1.75	-1.73
1.72	-1.71	-1.70	-1.70	-1.70	-1.70	-1.70	-1.70
1.70	-1.70	-1.70	-1.70	-1.70	-1.70	-1.70	-1.70

Future Work and Uses of WEPS

Contributor:

L.E. Wagner

Abstract

The Wind Erosion Prediction System (WEPS) has many potential uses beyond its current capabilities, especially if specific enhancements are made to the science model and/or its interface. The primary enhancements anticipated include: (a) multiple subregion support to simulate different soils and/or management practices (like strip cropping) within a single field; (b) representing terrain elevation effects on hilly fields; (c) providing for the simultaneous growth of multiple crops at one time, allowing for inter-seeding of crops and multiple species to be grown at once such as range land and pasture vegetation; (d) extending the model to simulate wind erosion on rangelands and soils high in organic matter; (e) allowing simulation of complex field shapes to better represent more field shapes accurately; (f) integrating both wind and water erosion simulations within the same modelling framework and utilizing a common user interface for both erosion simulations; and (g) create a web-enabled interface with remote access to databases for inputs to allow easier access for users. In addition, several potential coding modifications are possible to speed up simulations, especially for multiple subregion simulations and refining the ability to simulate erosion accurately in regions where erosion inputs are changing rapidly, e.g., by implementing an automated gridding system. Future expansions of the WEPS model will provide for more accurate simulations and more diverse uses than presently available for improved conservation planning.

Introduction

In addition to the normal fixes, improvements, and updates required by any production software package, researchers and users have identified desired improvements and changes to WEPS, both in the science of the model and its interfaces. Most of these improvements extend WEPS into additional wind erosion application areas, but some are intended to expand WEPS into other areas, such as cover crop planting/killing dates and incorporation of a water erosion model into the WEPS framework. Major users of WEPS, such as the Natural Resources Conservation Service (NRCS), have identified items to address deficiencies and limitations in the model's core domain of simulating wind erosion on cultivated agricultural lands, and non-agriculture users have recommended other changes according to their needs for wind erosion assessments in specific occupations (mining, military training, road construction, land developments, etc.). WEPS developers also have identified areas in which improvement could provide significant gains in runtime, usability, or increased accuracy of simulated results.

Future Enhancements

Several items that have been identified by ARS and NRCS to address WEPS deficiencies in traditional cultivated agricultural applications and to extend its applicability to non-cultivated agricultural applications (pasture and rangelands) are listed below.

1. Expand WEPS to work on a multiple-subregion basis to simulate wind erosion under non-homogeneous site conditions. Different soil types and management practices applied to different regions of a field would be more accurately represented within WEPS as separate subregions in which surface conditions are allowed to differ from those in other subregions. For example, multiple subregions would allow WEPS to simulate strip cropping practices correctly, thus improving its ability to simulate wind erosion more accurately. Because strip cropping alone is a common practice, NRCS has voiced strong support for this enhancement.

Multiple-subregion capability also includes the ability to specify sinks, or areas that do not contribute to wind erosion but do collect wind-blown particulates, such as ponds, waterways, road ditches, and barrow pits. A variety of sinks would likely be provided, including: (a) unlimited sinks (ponds, rivers, lakes, etc.) that would be able to trap all saltation and creep particulates that enter these areas; (b) limited sinks that would have a maximum trapping capacity that, if reached, would no longer behave as a sink, such as road ditches and waterways; and (c) variable sinks with trapping properties that change over time, such as growing vegetative wind barriers and trap strips. Wind barriers also could be fully represented as separate subregion areas, if desired, that can grow and thus not only change their barrier properties seasonally but also accumulate and report deposited airborne particulates within the barrier area according to appropriate trapping characteristics.

A version of the model has been extended to support multiple subregions, but it has had only limited testing. Providing a complete end-user version of WEPS with multiple-subregion capability requires an interface that allows users to easily provide additional inputs and display new outputs available from the enhanced model.

2. Add the effects of terrain elevation on surface wind speed within WEPS. This enhancement would allow WEPS to represent the effects of non-homogeneity in elevation of agricultural field surfaces (e.g., hills, knolls, valleys, swales). Such changes in elevation cause increased or decreased surface wind speeds surface winds. Terrain elevation often influences where wind erosion initiates within a field, so being able to reflect the change in surface winds as a result of terrain elevation would allow WEPS to identify locations with higher potential for wind erosion emissions, thus allowing site-specific management practices to reduce wind erosion susceptibility for the entire field at a lower cost compared with treating the entire field.

Multiple-subregion and terrain enhancements provide additional synergistic benefits; for example, a knoll sometimes consists of a more erodible soil and is more exposed to higher winds because of the relative increase in elevation compared with the surrounding area. Thus, both the multiple-subregion and terrain elevation enhancements should mean WEPS can better simulate knolls and estimate erosion susceptibility and loss from them. In addition, the site-specific practices that could be applied to help control wind erosion initiated on a knoll could be simulated more realistically, thus providing more accurate results.

Enhancing WEPS ability to simulate plant growth based on phenology should improve the model's ability to represent the growth stages during the life cycle of a plant more accurately. Current work is progressing on the Universal Plant Growth Model (UPGM), which allows users to change plant growth characteristics based on

phenology and addresses other deficiencies in the current plant growth model in WEPS (McMaster et al. 2014). UPGM allows crops that grow differently in the fall than they do in the spring, such as winter wheat, to be characterized more accurately through independent parameterization of multiple growth stages. UPGM also provides new modules for seedling emergence and canopy height, ultimately improving simulation of a plant during its entire life cycle. Although not critical to WEPS as a wind erosion model, UPGM is able to simulate nutrient stresses, so soil fertility and applied nutrient rates could be fully incorporated into WEPS. This may be important if either the Root Zone Water Quality Model (RZWQM) or the Water Erosion Prediction Program (WEPP) is included within the WEPS framework, and runoff water and/or seepage water past the root zone could include nutrient level estimates in that lost water.

3. Enable WEPS to simulate inter-seeding of crops. This functionality could be improved if WEPS simulated the simultaneous growth of competing, multiple plant species, which would provide WEPS with the added ability to better simulate the planting of another crop before harvesting the previous crop (a scenario not easily simulated in the current release of WEPS), correctly represent additional cropping scenarios (e.g., inter-seeding and relay cropping), and simulate the multispecies mixtures of plants commonly found in rangelands and pastures. This feature could also help evaluate weed pressure effects on a growing crop. When these plants exhibit different growth behaviors and compete unequally for scarce resources such as water, light interception, and nutrients, WEPS often will not accurately reflect the overall growth conditions of such a site if growth is simulated with a single surrogate plant growth record.
4. Improve WEPS ability to simulate soils high in organic matter. Such soils are known as Histosols and have >20% organic matter. Such soils under agricultural production are very susceptible to wind erosion because the density of the organic material is significantly smaller than wind-erodible-sized particles on more common mineral-based soils. NRCS desires this feature in WEPS because critical agricultural regions within the United States contain organic soils and experience high wind erosion rates (Robertson et al. 1978, Lucas 1982, Parent et al. 1982, Mokma 1992, Riksen and De Graaff 2001, Campbell et al. 2002, Ilniki and Zeitz 2003). Native simulations of organic soils require: (a) a Hydrology submodel that can simulate water movement in organic soils, and (b) a modified Erosion submodel that can account for the difference in particle densities between mineral-based and organic soils. Initial basic field and laboratory work, including wind tunnel studies (Kohake et al. 2009), have been conducted, and more studies are ongoing to address specific deficiencies in simulating wind erosion on organic soils in WEPS. An additional objective of such studies is determining the necessary parameters and coefficients to allow WEPS to reflect erosion processes correctly on these soils. Significant effort remains necessary to fully incorporate this new research into WEPS, and modifications to the current Hydrology submodel, or possibly an alternative organic soil specific submodel, may need to be added to or created for WEPS because the current Hydrology submodel assumes a mineral soil in its water balance relationships.
5. Modify WEPS to simulate complex field shapes. WEPS can simulate only rectangular areas, so all non-rectangular fields, such as center pivot circles, are represented as rectangular fields of equivalent area. This restricts the model's ability

to correctly represent the effects of barriers along the borders of irregularly shaped and circular fields.

6. Include in WEPS a revised and enhanced automated grid mesh system that increases the grid density where greater erosion simulation detail is needed, generally where a transition in surface conditions occurs. WEPS currently grids a field into smaller cell areas, using a fixed rectangular based automated gridding system, so it can simulate and report where within a field different particulate flux levels exist as well as where erosion and deposition are occurring. Enhancing the automated gridding system to provide a denser grid in specific regions of the field would allow better accounting in regions with wind gradients, such as near barriers, terrain elevation effects (when this feature is added), and changes in soil, vegetation, or cropping practices, such as subregion boundaries, occur. One approach to consider is using non-rectangular grid cells (e.g., triangular), which could allow easier implementation of variable grid cell sizes.
7. Integrate wind and water erosion science into one user model. WEPS and the Water Erosion Prediction Project (WEPP) models have many similar features (e.g., both are process-based, run on a primary daily time step simulation, use the same CLIGEN climate generator for meteorological inputs, feature similar plant growth, decomposition, and management routines, and contain the same Hydrology submodel; Savabi et al., 1995). NRCS has expressed a desire for these two ARS models to contain as much similar science as possible. Work has progressed in the science code to facilitate a much greater degree of commonality where feasible. Besides having a common hydrology component, the differences in the infiltration and runoff components recently have been resolved, and the base water erosion submodel (Fox et al. 2011) has been incorporated into the WEPS framework. Additional science model issues yet to be resolved are related to the winter routines, which simulate the accumulation and melting of snow and the subsequent re-freezing, infiltration, and runoff of that melted snow. The two models currently represent these processes differently. Some issues that have not been looked at yet include the addition of unique WEPP-specific inputs such as tile drainage and terrace channels description parameters.
8. A common interface for both WEPS and WEPP is desired. NRCS has frequently requested that WEPP and WEPS have a common interface to eliminate redundant entry of common inputs, obtain the same results for same conditions/processes (for example, the same residue cover values as it decays over time), and reduce training costs. Because both models have many similar user inputs, such as weather and management (date-ordered list of tillage and cropping practices), a common interface is a reasonable request. For a user who needs both wind and water erosion results, it is desirable to consolidate these inputs into a single consistent user interface. Work is progressing slowly to assimilate as many of the common user interface elements as possible into the two models' current interfaces and to eventually produce a common interface for both models.
9. Create a web-enabled WEPS user interface and provide access to the required database elements through internet services. NRCS also has requested that the WEPS standalone application become a web application; e.g., an application that can be initiated from within a web browser and not require an explicit installation of the application or its required databases. This desire to web enable WEPS is driven by

NRCS's need to reduce maintenance and support costs associated with the standalone WEPS program, which is currently installed on thousands of the agency's PCs. WEPS already accesses necessary soil data through the NRCS Soil Data Mart service, but similar services are required for climate, barrier, and management rotation template data. In addition, the planned multi-subregion version of WEPS needs polygon soil and field boundary data, requiring modifications to the current soil database service connection. NRCS is working to provide a complete service for WEPS that will execute the climate generators as well as the WEPS science model and return the run results to the user. The current WEPS interface is coded in Java, so the option exists to make it a Java web-start application without rewriting much of the core interface and still provide full model functionality to the user. This is being investigated for feasibility.

10. Parallelize the WEPS multiple-subregion FORTRAN science code so that multiple parts (individual subregions, submodels, etc.) of the code can be executed simultaneously on separate CPU threads. This will allow more complex WEPS simulation runs, such as multiple-subregion scenarios, to still complete wind erosion runs within NRCS time constraints. Most modern personal computers contain several processor cores that can take advantage of parallelized code, so the benefits will not require new hardware to be realized. If successful, even more parallelization could be performed on the code for additional runtime benefits.
11. Develop a version of WEPS to simulate wind erosion on rangelands in addition to cultivated croplands. Conditions unique to rangeland, some of which would need to be simulated quite differently in WEPS, have been discussed. Specifically, the need to simulate the effects of spatially sparse vegetative cover is required. One promising approach to this problem is outlined by Okin (2008). Additional improvements to the plant growth submodel are also likely required to better reflect the actual growth of multiple species of plants typically found on rangeland and pastures. These issues should be adequately addressed if UPGM and the multiple plant species competition enhancement are included in WEPS as previously discussed.

Work is progressing on many of these items with varying levels of effort. WEPS also has been modified and incorporated into regional air quality dispersion models, including the Multiscale Climate and Chemistry Model (MCCM) by Diaz et al. (2010), and the more recent AIRPACT-3 model in the Pacific Northwest (Chung et al. 2013, Gao et al. 2013). Likewise, a standalone version of the WEPS wind Erosion submodel has been created with a separate user interface, which has been named the Single-event Wind Erosion Evaluation Program (SWEEP) (USDA-ARS 2008). This tool has been found useful for construction and land use managers to apply to construction areas and disturbed sites to evaluate specific wind erosion mitigation practices and determine a site's risk of generating dust emissions. Significant potential is envisioned for SWEEP if the interface is revamped and tailored to the specific needs of non-agricultural customers. SWEEP can also serve as an effective teaching tool for those who want to understand erosion processes during a storm event using its wide range of graphical outputs.

References

- Campbell, D.R., C. Lavoie, and L. Rochefort. 2002. Wind erosion and surface stability in abandoned milled peatlands. *Canadian Journal of Soil Science*. 82:85–95.
- Chung, S.H., F.L. Herron-Thorpe, B.K. Lamb, T.M. VanReken, J.K. Vaughan, J. Gao, L.E. Wagner, and F. Fox. 2013. Application of the wind erosion prediction system in the AIRPACT regional air quality modeling framework. *Transactions of the ASABE*. 56(2):625-641.
- Diaz, E.N., Tatarko, J., Jazcilevich, A.D., Garcia, A.R., Caetano, E. and Ruiz-Suarez, L.G. 2010. A modeling study of aeolian erosion enhanced by surface wind confluences over Mexico City. *Aeolian Research*. 2:143-157.
- Fox, F.A, J.R. Frankenburger, D.C. Flanagan and L.E. Wagner. 2011. Integrating WEPP into the WEPS infrastructure. International Symposium on Erosion and Landscape Evolution. Anchorage, AK. American Society of Agricultural and Biological Engineers. ISELE paper number 11142. Available at: <https://topsoil.nserl.purdue.edu/~flanagan/isele2011/presentations/11142-Fox.pdf>. (Accessed August 10, 2020).
- Gao, J., L.E. Wagner, F. Fox, S.H. Chung, J.K. Vaughan, and B.K. Lamb. 2013. Spatial application of WEPS for estimating wind erosion in the Pacific Northwest. *Transactions of the ASABE*. 6(2):613-624.
- Ilniki, P., and J. Zeitz. 2003. Chapter 2: Irreversible loss of organic soil functions after reclamation. In: L.E. Parent and P. Ilnicki. (eds). *Organic soils and peat materials for sustainable agriculture*, 15-32. CRC Press, Boca Raton, FL.
- Kohake, D.J., L.J. Hagen, and E.L. Skidmore. 2009. Wind erodibility of organic soils. *Soil Science Society of America Journal*. 74:250–257.
- Lucas, R.E. 1982. *Organic soils (Histosols): Formation, distribution, physical and chemical properties and management for crop production*. Res. Rep. 435. Michigan State University Agricultural Experiment Station and Cooperative Extension Service. East Lansing. 77 pp.
- McMaster, G.S, J.C. Ascough II, D.A. Edmunds, L.E. Wagner, F.A. Fox, K.C. DeJonge and N.C. Hansen. 2014. Simulating unstressed crop development and growth using the unified plant growth model (UPGM). *Environmental Modeling & Assessment*. 19:407-424. doi: 10.1007/s10666-014-9402-x.
- Mokma, D.L. 1992. Effect of tillage and climate on temporal soil properties of wind-erodible organic and sandy soils in Michigan. *Field Study Final Rep*. Michigan State University. East Lansing. 44 pp.
- Okin, G. S. 2008. A new model of wind erosion in the presence of vegetation. *Journal of Geophysical Research-Earth Surface*, 113:F02S10. doi: 10.1029/2007JF000758
- Parent, L.E., J.A. Millette, and G.R. Mehuys. 1982. Subsidence and erosion of a Histosol. *Soil Science Society of America Journal*. 46:404–408.

Riksen, M.J.P.M., and J. De Graaff. 2001. On-site and off-site effects of wind erosion on European light soils. *Land Degradation and Development*. 12:1–11.

Robertson, L.S., H.C. Price, D.D. Warncke, and D.L. Mokma. 1978. Wind erosion: A major problem of organic soil. File 3221. Cooperative Extension Service, Michigan State University. East Lansing.

Savabi, M.R., Skaggs, R.W., Onstad, C.A. 1995. Chapter 6, Subsurface Hydrology. In: D.C. Flanagan, M.A. Nearing (Eds.) *USDA Water Erosion Prediction Project (WEPP) Hillslope Profile and Watershed Model Documentation*. s.l.: NSERL Report No. 10, National Soil Erosion Research Laboratory, USDA Agricultural Research Service, West Lafayette, Indiana, pp. 6.1–6.14.

USDA-ARS. 2008. User's Manual: single-event wind erosion evaluation program (SWEEP). Available as a part of the WEPS installation package at: <https://ars.usda.gov/services/software/download.htm?softwareid=415&modecode=54-30-05-20>. (Accessed August 10, 2020).

Appendix A: Contributing Authors and Affiliations

A.A. Durar, Former Research Assistant
USDA-ARS, Wind Erosion Research Unit
Manhattan, Kansas

F.A. Fox, Information Technology Applications Specialist
USDA-ARS, Rangeland Resources and Systems Research Unit
Fort Collins, Colorado

L.J. Hagen, Agricultural Engineer (Retired)
USDA-ARS, Wind Erosion Research Unit
Manhattan, Kansas

A. Retta, Former Post-Doc Soil Scientist (Retired)
USDA-ARS, Wind Erosion Research Unit
Manhattan, Kansas

H.H. Schomberg, Ecologist
USDA-ARS, Sustainable Agricultural Systems Laboratory
Beltsville, Maryland

E.L. Skidmore, Soil Scientist (Retired)
USDA-ARS, Wind Erosion Research Unit
Manhattan, Kansas

M.A. Sporcic, Conservation Agronomist (Retired)
USDA-NRCS, Central National Technology Support Center
Fort Worth, Texas

J.L. Steiner, Soil Scientist (Retired)
USDA-ARS, Grazinglands Research Laboratory
El Reno, Oklahoma

J. Tatarko, Soil Scientist
USDA-ARS, Rangeland Resources and Systems Research Unit
Fort Collins, Colorado

S.J. van Donk, Senior Agronomist
Iteris, Incorporated
Grand Forks, North Dakota

L.E. Wagner, Agricultural Engineer
USDA-ARS, Rangeland Resources and Systems Research Unit
Fort Collins, Colorado

Appendix B: WEPS Related Peer-Reviewed Publications

Updated August 2020

General WEPS

1. Seo, I.W., Lim, C.S., Yang, J.E., Lee, S.P., Jung, H.G., Lee, K.S., and Chung, D.Y. 2020. An overview of applicability of WEQ, RWEQ, and WEPS models for prediction of wind erosion in lands. *Korean Journal of Agricultural Science* 47:381-394. doi: 10.7744/kjoas.2020
2. Tatarko, J., Wagner, L.E. and Fox, F.A. 2019. The Wind Erosion Prediction System and its use in conservation planning. *In* O. Wendroth, R.J. Lascano, L. Ma, eds., *Bridging Among Disciplines by Synthesizing Soil and Plant Processes*, *Adv. Agric. Syst. Model.* 8:71-101. ASA, CSSA, and SSSA, Madison, WI. doi: 10.2134/advagriscystmodel8.2017.0021
3. Wagner, L.E. 2013. A history of wind erosion prediction models in the United States Department of Agriculture: The Wind Erosion Prediction System (WEPS). *Aeolian Research.* 10:9-24.
4. Hagen, L.J. 1991. A Wind Erosion Prediction System to meet user needs. *Journal of Soil and Water Conservation.* 46(2):106-111.

Validations of WEPS

1. Pi, H and B. Sharratt. 2019. Threshold friction velocity influenced by the crust cover of soils in the Columbia Plateau. *Soil Science Society of America Journal.* 83(1): 232-241. doi: 10.2136/sssaj2018.06.0230
2. Pi, H., and B. Sharratt. 2017. Evaluation of the RWEQ and SWEEP in simulating soil and PM10 loss from a portable wind tunnel. *Soil and Tillage Research.* 170:94-103.
3. Zhang, J., C. Zhang, C. Chang, R. Wang, and G. Liu. 2017. Comparison of wind erosion based on measurements and SWEEP simulation: A case study in Kangbao County, Hebei Province, China. *Soil and Tillage Research.* 165:169-180.
4. Pi, H., B. Sharratt, G. Feng, J. Lei, X. Li, and Z. Zheng. 2016. Validation of SWEEP for creep, saltation, and suspension in a desert–oasis ecotone. *Aeolian Research.* 20:157-168.
5. Liu, B., J. Qu, Q. Niu, and Q. Han. 2014. Comparison of measured wind tunnel and SWEEP simulated soil losses. *Geomorphology.* 207:23-29.

6. Pi, H., G.G. Feng, and B.S. Sharratt. 2014. Performance of the SWEEP model affected by estimates of threshold friction velocity. *Transactions of the ASABE*. 57:1675-1685.
7. Pi, H., B.S. Sharratt, G. Feng, and X. Zhang. 2014. Comparison of measured and simulated friction velocity and threshold friction velocity using SWEEP. *Soil Science*. 179:393-402.
8. Pi H, Feng G, Sharratt BS, Li X, Zheng Z. 2014. Validation of SWEEP for contrasting agricultural land use types in the Tarim Basin. *Soil Science*. 179:433-445.
9. Hagen, L.J., R.S. Van Pelt, and B.S. Sharratt. 2010. Estimating the saltation and suspension components from field wind erosion. *Aeolian Research*. 1:147-153.
10. Feng, G., and B.S. Sharratt. 2009. Evaluation of the SWEEP model during high winds on the Columbia Plateau. *Earth Surface Processes and Landforms*. 34:1461-1468.
11. van Donk, S.J., S.D. Merrill, D.L. Tanaka, and J.M. Krupinsky. 2008. Crop residue in North Dakota: measured and simulated by the Wind Erosion Prediction System. *Transactions of the ASABE*. 51(5): 1623-1632.
12. Buschiazzo, D.E., and T.M. Zobeck. 2008. Validation of WEQ, RWEQ and WEPS wind erosion for different arable land management systems in the Argentinean Pampas. *Earth Surface Processes and Landforms*. 33:1839–1850.
13. Feng, G., and B.S. Sharratt. 2007. Validation of WEPS for soil and PM10 loss from agricultural fields on the Columbia Plateau of the United States. *Earth Surface Processes and Landforms*. 32:743-753.
14. Visser, S.M., G. Sterk, and D. Karsenberg. 2005. Wind erosion modeling in a Sahelian Environment. *Environmental Modelling and Software*. 20(1):69-84.
15. Funk, R., E.L. Skidmore, and L.J. Hagen. 2004. Comparison of wind erosion measurements in Germany with simulated soil losses by WEPS. *Environmental Modelling and Software*. 19(2):177-183.
16. Hagen, L.J. 2004. Evaluation of the Wind Erosion Prediction System (WEPS) erosion submodel on cropland fields. *Environmental Modelling and Software*. 19(2):171-176.
17. van Donk, S.J., and E.L. Skidmore. 2003. Measurement and simulation of wind erosion, roughness degradation and residue decomposition on an agricultural field. *Earth Surface Processes and Landforms* 28(11):1243-1258.

18. Fryrear, D.W., J.E. Stout, L.J. Hagen, and E.D. Vories. 1991. Wind erosion: Field measurement and analysis. *Transactions of the ASAE*. 34(1):155-160.

Applications of WEPS

1. Pi, H., Huggins, D.R., Abatzoglou, J.T., and Sharratt, B. 2020. Modeling soil wind erosion from agroecological classes of the Pacific Northwest in response to current climate. *Journal of Geophysical Research: Atmospheres*, 125, e2019JD031104. doi: 10.1029/2019JD031104
2. Pi, H., B. Sharratt, J. Lei. 2019. Wind erosion and dust emissions in central Asia: Spatiotemporal simulations in a typical dust year. *Earth Surface Processes and Landforms*. 44(2):521-534.
3. Pi, H., D.R. Huggins, B. Sharratt. 2019. Dry aggregate stability of soils influenced by crop rotation, soil amendment, and tillage in the Columbia Plateau. *Aeolian Research*. 40:65-73.
4. Rakkar, M.K., H. Blanco-Canqui, J. Tatarko. 2019. Prediction of soil wind erosion potential under different corn residue management scenarios. *Geoderma*. 353:25-34.
5. Jianga, Y., Y. Gaoa, Z. Dong, B. Liu, L. Zhao. 2018. Simulations of wind erosion along the Qinghai-Tibet Railway in north-central Tibet. *Aeolian Research*. 32:192-201.
6. Pi, H., B. Sharratt, J. Lei. 2018. Wind erosion and dust emissions in central Asia: spatiotemporal simulations in a typical dust year. *Earth Surface Processes and Landforms*. 44:521–534. doi: 10.1002/esp.4514
7. Li, J., T. Kandakji, J.A. Lee, J. Tatarko, J. Blackwell III, T.E. Gill, J. Collins. 2018. Blowing dust and highway safety in the southwestern United States: Characteristics of dust emission “hotspots” and management implications. *Science of the Total Environment*. 621:1023-1032.
8. He, X., D.R. Presley, J. Tatarko, H. and Blanco-Canqui. 2017. Crop residue harvest impacts wind erodibility and simulated loss in the Central Great Plains. *Global Change Biology and Bioenergy*. 10:213-226.
9. Nerger, R., R. Funk, E. Cordsen, and N. Fohrer. 2017. Application of a modeling approach to designate soil and soil organic carbon loss to wind erosion on long-term monitoring sites (BDF) in Northern Germany. *Aeolian Research*. 25:135-147.

10. Liu, B., L.E. Wagner, D. Ning, J. Qu. 2017. Estimation of wind erosion from construction of a railway in arid Northwest China. *International Soil and Water Conservation Research*. 5:102-108.
11. Chen, L., H. Zhao, W. Wang, Z. Bai, Z. Wang, F. Sun, L. Hou, G. Liu, M. Shi, Y. Miao. 2017. Effect of windblown dust from local and regional sources on the air quality of the central district in Jinan, China. *Atmospheric Research*. 185:44-52.
12. Blanco-Canqui, H., J. Tatarko, A.L. Stalker, T.M. Shaver, and S.J. van Donk. 2016. Impacts of Corn Residue Grazing and Baling on Wind Erosion Potential in a Semiarid Environment. *Soil Science Society of America Journal*. 80:1027-1037.
13. Tatarko, J., S.J. van Donk, J.A. Ascough II, and D.G. Walker. 2016. Application of the WEPS and SWEEP models to non-agricultural disturbed lands. *Heliyon*. 2: e00215.
14. Behbahani, A.M. 2015. Hazard and risk assessment of wind erosion and dust emissions in Denmark - a simulation and modelling approach. PhD Thesis, University of Basel. Basel, Switzerland. Available at: <https://edoc.unibas.ch/38575/> (Accessed August 10, 2020).
15. Cao, Y, and L. Chen. 2015. Analysis of a Typical Sand-dust Pollution Accident on March 9, 2013 in Tianjin Based on SWEEP Model. *Journal of Desert Research*. 6: 1644-1651.
16. Nelson, R., J. Tatarko, and J.C. Ascough II. 2015. Soil erosion and organic matter variations for central Great Plains cropping systems under residue removal. *Transactions of the ASABE*. 58(2): 415-427.
17. Sharratt, B.S., J. Tatarko, J. Abatzoglou, F. Fox, and D. Huggins. 2015. Implications of climate change on wind erosion of agricultural lands in the Columbia Plateau. *Weather and Climate Extremes*. 10:20-31.
18. Shi, M. and L. Chen. 2015. Estimation of the Soil Loss in Typical Days from Agricultural Land in Jinan Based on SWEEP Model. *Environmental Science & Technology*. 8:200-205.
19. Zobeck, T.M., J.L. Steiner, D.E. Stott, S. Duke, P.J. Starks, D.N. Moriasi, and D.L. Karlen. 2015. Soil quality index comparison using Fort Cobb Oklahoma watershed-scale land management data. *Soil Science Society of America Journal*. 79(1):224-238. doi: 10.2136/sssaj2014.06.0257.
20. Chen, L., H. Zhao, B. Han, and Z. Bai. 2014. Combined use of WEPS and Models-3/CMAQ for simulating wind erosion source emission and its environmental impact. *Science of the Total Environment*. 466–467:762–769.

21. Jia, Q., N. Al-Ansari, and S. Knutsson. 2014. Modeling of Wind Erosion of the Aitik Tailings Dam Using SWEEP Model. *Engineering*. 6(7):355-364. doi: 10.4236/eng.2014.67038
22. Li, J., G.S. Okin, J. Tatarko, N.P. Webb, and J.E. Herrick. 2014. Consistency of wind erosion assessments across land use and land cover types: a critical analysis. *Aeolian Research*. 15:253-260.
23. Chung, S.H., F.L. Herron-Thorpe, B.K. Lamb, T.M. VanReken, J.K. Vaughan, J. Gao, L.E. Wagner, and F. Fox. 2013. Application of the wind erosion prediction system in the AIRPACT regional air quality modeling framework. *Transactions of the ASABE*. 56(2):625-641.
24. Gao, J., L.E. Wagner, F. Fox, S.H. Chung, J.K. Vaughan, and B.K. Lamb. 2013. Spatial application of WEPS for estimating wind erosion in the Pacific Northwest. *Transactions of the ASABE*. 6(2):613-624.
25. Muth, D.J. and K.M. Bryden. 2013. An integrated model for assessment of sustainable agricultural residue removal limits for bioenergy systems. *Environmental Modelling and Software*. 39:50-69.
26. Maurer, T. and H.H. Gerke. 2011. Modelling Aeolian sediment transport during initial soil development on an artificial catchment using WEPS and aerial images. *Soil & Tillage Research*. 117:148–162.
27. U.S. Department of Energy; Perlack, R.D., Eaton, L.M., Turhollow, A.F. Jr., Langholtz, M.H., Brandt, C.C., Downing, M.E., Graham, R.L., Wright, L.L., Kavkewitz, J.M., Shamey, A.M., Nelson, R.G., Stokes, B.J., Rooney, W.L., Muth, D.J. Jr., Hess, J.R., Abodeely, J.M., Hellwinckel, C., De La Torre Ugarte, D., Yoder, D.C., Lyon, J.P., Rials, T.G., Volk, T.A., Buchholz, T.S., Abrahamson, L.P., Anex, R.P., Voigt, T.B., Berguson, W., Riemenschneider, D.E., Karlen, D., Johnson, J. M.F., Mitchell, R.B., Vogel, K.P., Richard, E.P. Jr., Tatarko, J., Wagner, L.E., Skog, K.E., Lebow, P.K., Dykstra, D.P., Buford, M.A., Miles, P.D., Scott, D.A., Perdue, J.H., Rummer, R.B., Barbour, J., Stanturf, J.A., McKeever, D.B., Zalesny, R.S. Jr., Gee, E.A., Cassidy, P.D., and Lightle, D. 2011. U.S. Billion-ton Update: Biomass Supply for a Bioenergy and Bioproducts Industry. *Agricultural and Biosystems Engineering Technical Reports and White Papers*. Paper 16. Available at: https://lib.dr.iastate.edu/abe_eng_reports/16. (Accessed August 10, 2020).
28. Diaz, E.N., Tatarko, J., Jazcilevich, A.D., Garcia, A.R., Caetano, E., and Ruiz-Suarez, L.G. 2010. A modeling study of Aeolian erosion enhanced by surface wind confluences over Mexico City. *Aeolian Research*. 2:143-157.

29. Hagen, L.J., P.R. Schroeder, and L. Thai. 2009. Estimated particle emissions by wind erosion from the Indiana Harbor Combined Disposal Facility. *Practice Periodical of Hazardous, Toxic, and Radioactive Waste Management*. 13(1):20-28.
30. Feng, G. and B. Sharratt. 2007. Scaling from field to region for wind erosion prediction using the Wind Erosion Prediction System and geographical information systems. *Journal of Soil and Water Conservation*. 62(5):321-328.
31. Visser, S.M., L. Stroosnijder, W.J. Chardon. 2005. Nutrient losses by wind and water, measurements and modeling. *CATENA*. 63(1):1-22.
32. Coen, G.M., J. Tatarko, T.C. Martin, K.R. Cannon, T.W. Goddard, and N.J. Sweetland. 2004. A method for using WEPS to map wind erosion risk of Alberta soils. *Environmental Modelling and Software*. 19(2):185-189.

Weather Generator

1. van Donk, S.J., C. Liao and E.L. Skidmore. 2008. Using temporally limited wind data in the Wind Erosion Prediction System. *Transactions of the ASAE*. 51(5):1585-1590.
2. Hagen, L.J. 2007. Ratios of erosive wind energies on dry days and all days in the western United States. *Transactions of the ASABE*. 50(6):1981-1986.
3. van Donk, S.J., L.E. Wagner, E.L. Skidmore, and J. Tatarko. 2005. Comparison of the Weibull Model with measured wind speed distributions for stochastic wind generation. *Transactions of the ASAE*. 48(2):503-510.
4. Skidmore, E.L. and J. Tatarko. 1990. Stochastic wind simulation for erosion modeling. *Transactions of the ASAE*. 33(6):1893-1899.
5. Richardson, C.W. 1981. Stochastic simulation of daily precipitation, temperature and solar radiation. *Water Resources Research*. 17(1):182-190.

Hydrology Submodel

1. Saxton, K.E. and W.J. Rawls. 2006. Soil water characteristic estimates by texture and organic matter for hydrologic solutions. *Soil Science Society of America Journal*. 70:1569-1578.
2. Durar, A.A., J.L. Steiner, S.R. Evett, and E.L. Skidmore. 1995. Measured and simulated surface soil drying. *Agronomy Journal*. 87(2):235-144.

3. Durar, A.A. 1991. Simulation of soil-water dynamics for wind erosion modeling. Ph.D. Dissertation. Kansas State Univ., Manhattan, Kansas (Dissertation Abstract. 91-28491).

Soil Submodel

1. Zobeck, T.M., M. Baddock, R.S. Van Pelt, J. Tatarko, and V. Acosta-Martinez. 2013. Soil property effects on wind erosion of organic soils. *Aeolian Research*. 10:43-51.
2. Kohake, D.J., L.J. Hagen, and E.L. Skidmore. 2010. Wind erodibility of organic soils. *Soil Science Society of America Journal*. 74(1):250-257.
3. Kohake, D.J. 2003. Wind erodibility of organic soils. M.S. thesis. Kansas State University, Manhattan.
4. Zobeck, T.M., T.W. Popham, E.L. Skidmore, J.A. Lamb, S.D. Merrill, M.J. Lindstrom, D.L. Mokma, and R.E. Yoder. 2003. Aggregate-mean diameter and wind-erodible soil predictions using dry aggregate-size distributions. *Soil Science Society of America Journal*. 67:425-436.
5. Tatarko, J. 2001. Soil aggregation and wind erosion: Processes and measurements. *Annals of Arid Zone*. 40(3): 251-263.
6. Zobeck, T.M. and T.W. Popham. 2001. Cropping and Tillage Effects on Soil Roughness Indexes. *Transactions of the ASAE*. 44(6):1527-1536.
7. Merrill, S.D., A.L. Black, D.W. Fryrear, A. Saleh, T.M. Zobeck, A.D. Halvorson, and D.L. Tanaka. 1999. Soil wind erosion hazard of spring wheat-fallow as affected by long-term climate and tillage. *Soil Science Society of America Journal*. 63(6):1768-1777.
8. Zobeck, T.M. and T.W. Popham. 1997. Modification of the wind erosion roughness index by rainfall. *Soil and Tillage Research*. 42(1-2):47-61.
9. Hagen, L.J., B. Schroeder, and E.L. Skidmore. 1995. A vertical soil crushing-energy meter. *Transactions of the ASAE*. 38(3):711-715.
10. Fryrear, D.W., C.A. Krammes, D.L. Williamson, and T.M. Zobeck. 1994. Computing the wind erodible fraction of soils. *Journal of Soil and Water Conservation*. 49(2):183-188.
11. Layton, J.B., E.L. Skidmore, and C.A. Thompson. 1994. Winter-associated changes in dry-soil aggregation as influenced by management. *Soil Science Society of America Journal*. 57:1568-1572.

12. Merrill, S.D., A.L. Black, and T.M. Zobeck. 1994. Overwinter changes in dry aggregate size distribution influencing wind erodibility in a spring wheat-summer fallow cropping system. *Minnesota Academy of Science Journal*. 59(2):27-36.
13. Saleh, A. 1994. Measuring and predicting ridge orientation effect on soil surface roughness. *Soil Science Society of America Journal*. 58(4):1228-1230.
14. Wagner, L.E. and D.J. Ding. 1994. Representing aggregate size distributions as modified lognormal distributions. *Transactions of the ASAE*. 37(3):815-821.
15. Saleh, A. 1993. Soil aggregate and crust density prediction. *Soil Science Society of America Journal*. 57:524-526.
16. Saleh, A. 1993. Soil roughness measurement: Chain Method. *Journal of Soil and Water Conservation*. 48(6):527-529.
17. Skidmore, E.L. and J.B. Layton. 1992. Dry soil-aggregate stability as influenced by selected soil properties. *Soil Science Society of America Journal*. 56:557-561.
18. Zobeck, T.M. and T.W. Popham 1992. Influence of microrelief, aggregate size, and precipitation on soil crust properties. *Transactions of the ASAE*. 35(2):487-492.
19. Wagner, L.E. and Y. Yu. 1991. Digitization of profile meter photographs. *Transactions of the ASAE*. 34(2):412-416.
20. Zobeck, T.M. 1991. Abrasion of crusted soils: Influence of abrader flux and soil properties. *Soil Science Society of America Journal*. 55(4):1091-1097.
21. Zobeck, T.M. 1991. Soil properties affecting wind erosion. *Journal of Soil and Water Conservation*. 46(2):112-118.
22. Zobeck, T.M. and T.W. Popham. 1991. Influence of abrader flux and soil properties. *Soil Science Society of America Journal*. 55(4):1091-1097.
23. Potter, K.N. 1990. Estimating wind-erodible materials on newly crusted soils. *Soil Science* 150(5):771-776.
24. Potter, K.N. 1990. Soil properties' effect on random roughness decay by rainfall. *Transactions of the ASAE*. 33(6):1889-1892.
25. Potter, K.N., and T.M. Zobeck. 1990. Estimation of soil microrelief. *Transactions of the ASAE*. 33(1):156-161.

26. Potter, K.N., T.M. Zobeck, and L.J. Hagen. 1990. A microrelief index to estimate soil erodibility by wind. *Transactions of the ASAE*. 33(1):151-155.
27. Zobeck, T.M. and T.W. Popham. 1990. Dry aggregate size distribution of sandy soils as influenced by tillage and precipitation. *Soil Science Society of America Journal*. 54(1):197-204.
28. Zobeck, T.M. 1989. Fast-Vac - A vacuum system to rapidly sample loose granular material. *Transactions of the ASAE*. 32(4):1316-1318.
29. Lyles, L. and J. Tatarko. 1988. Soil wind erodibility index in seven north central states. *Transactions of the ASAE*. 31(5):1396-1399.
30. Hagen, L.J., E.L. Skidmore, and D.W. Fryrear. 1987. Using two sieves to characterize dry soil aggregate size distribution. *Transactions of the ASAE*. 30(1):162-165.
31. Lyles, L. and J. Tatarko. 1987. Precipitation effects on ridges created by grain drills. *Journal of Soil and Water Conservation*. 42(4):269-271.
32. Zobeck, T.M., and D.W. Fryrear. 1986. Chemical and physical characteristics of windblown sediment, I. Quantities and physical characteristics. *Transactions of the ASAE*. 29(4):1032-1036.
33. Zobeck, T.M., and D.W. Fryrear. 1986. Chemical and physical characteristics of windblown sediment, II. Chemical Characteristics and total soil and nutrient discharge. *Transactions of the ASAE*. 29(4):1037-1041.

Plant Growth Submodel

1. McMaster, G.S., D.A. Edmunds, R. Marquez, S.D. Haley, G.W. Buchleiter, P.F. Byrne, T.R. Green, R.H. Erskine, N.P. Lighthart, H. Kipka, F.A. Fox, L.E. Wagner, and J. Tatarko, M. Moragues, J.C. Ascough II. 2019. Winter wheat phenology simulations improve when adding responses to water stress. *Agronomy Journal*. 111:1–11. (Published on-line). doi: 10.2134/agronj2018.09.0615
2. Armbrust, D.V. and A. Retta. 2000. Wind sandblast damage to growing vegetation. *Annals of Arid Zone*. 39(3):273-284.
3. Retta, A., D.V. Armbrust, L.J. Hagen, and E.L. Skidmore. 2000. Leaf and stem area relationships to masses and their height distributions in native grasses. *Agronomy Journal*. 92(2):225-230.
4. Armbrust, D.V. and J.D. Bilbro, Jr. 1997. Relating plant canopy characteristics to soil transport capacity by wind. *Agronomy Journal*. 89:157-162.

5. Retta, A., D.V. Armbrust, and L.J. Hagen. 1996. Partitioning biomass in the crop submodel of WEPS (Wind Erosion Prediction System). *Transactions of the ASAE*. 39(1):145-151.
6. Retta, A. and D.V. Armbrust. 1995. Estimation of leaf and stem area in the Wind Erosion Prediction System (WEPS). *Agronomy Journal*. 87:93-98.
7. Bilbro, J.D. and D.W. Fryrear. 1994. Wind erosion losses as related to plant silhouette and soil cover. *Agronomy Journal*. 86(3):550-553.
8. Hagen, L.J. and D.V. Armbrust. 1994. Plant canopy effects on wind erosion saltation. *Transactions of the ASAE*. 37(2):461-465.
9. Armbrust, D.V. and J.D. Bilbro. 1993. Predicting grain sorghum canopy structure for soil erosion modeling. *Agronomy Journal*. 85(3):664-668.
10. Bilbro, J.D. 1992. Sunflower dry matter production and plant structural relationships for wind erosion modeling. *Journal of Soil and Water Conservation*. 47(2):194-197.
11. Skidmore, E.L. and R.G. Nelson. 1992. Small-grain equivalent of mixed vegetation for wind erosion control and prediction. *Agronomy Journal*. 83(1):98-101.
12. Bilbro, J.D. 1991. Relationships of cotton dry matter production and plant structural characteristics for wind erosion modeling. *Journal of Soil and Water Conservation*. 46(5):381-384.
13. Bilbro, J.D. and D.W. Fryrear. 1991. Pearl millet versus gin trash mulches for increasing soil water and cotton yields in a semiarid region. *Journal of Soil and Water Conservation*. 46(1):66-69.
14. Bilbro, J.D., J.D. Undersander, D.W. Fryrear, and C.M. Lester. 1991. A survey of lignin, cellulose, and acid detergent fiber ash contents of several plants and implications for wind erosion control. *Journal of Soil and Water Conservation*. 46(4):314-316.
15. Armbrust, D.V. 1990. Rapid measurement of crop canopy cover. *Agronomy Journal*. 82:1170-1171.
16. van de Ven, T.A.M., D.W. Fryrear, and W.P. Span. 1989. Vegetation characteristics and soil loss by wind. *Journal of Soil and Water Conservation*. 44:347-349.

17. Bilbro, J.D., and D.W. Fryrear. 1988. Annual herbaceous wind barriers for protecting crops and soils and managing snowfall. *Agriculture Ecosystems and Environment*. 22/23:149-161.
18. Lyles, L. and B.E. Allison. 1976. Wind erosion: The protective role of simulated standing stubble. *Transactions of the ASAE*. 19(1):61-64.

Residue Decomposition Submodel

1. van Donk, S.J., S.D. Merrill, D.L. Tanaka, and J.M. Krupinsky. 2008. Crop residue in North Dakota: measured and simulated by the Wind Erosion Prediction System. *Transactions of the ASAE*. 51(5):1623-1632.
2. Hagen, L.J. 1996. Crop residue effects on aerodynamic processes and wind erosion. *Theoretical and Applied Climatology*. 54:39-46.
3. Schomberg, H.H., J.L. Steiner, S.R. Evett, and A.P. Moulin. 1996. Climatic influence on residue decomposition prediction in the Wind Erosion Prediction System. *Theoretical and Applied Climatology*. 54:5-16.
4. Schomberg, H.H., J.L. Steiner, and P.W. Unger. 1994. Decomposition and nitrogen dynamics of crop residues: Residue quality and water effects. *Soil Science Society of America Journal*. 58:372-381.
5. Steiner, J.L., H.H. Schomberg, C.L. Douglas, Jr., and A.L. Black. 1994. Standing stem persistence in no-tillage small-grain fields. *Agronomy Journal*. 86:76-81.
6. Steiner, J.L., H.H. Schomberg, and J.E. Morrison. 1994. Residue decomposition and redistribution. *In* B.A. Stewart and W.C. Moldenhauer, eds., *Crop Residue Management to Reduce Erosion and Improve Soil Quality in the Southern Great Plains*, USDA-ARS Conservation Research Report 37.

Management Submodel

1. Wagner, L.E. and F.A. Fox. 2013. The Management Submodel of the Wind Erosion Prediction System. *Applied Engineering in Agriculture*. 29(3):361-372.
2. Hagen, L.J. 1999. Development of a tillage system to prevent soil pulverization and wind erosion. *Scientific Papers of the Agricultural University of Poznan, Poland*. 1:15-57.
3. Wagner, L.E. and R.G. Nelson. 1995. Mass reduction of standing and flat residues by selected tillage implements. *Transactions of the ASAE*. 38(2):419-427.

4. Unger, P. and E.L. Skidmore. 1994. Conservation tillage in the southern Great Plains. *In* R.M. Carter, ed., *Conservation Tillage in Temperate Agroecosystems*. Chapter 14, pp. 329-356. Lewis Publishers. Boca Raton, FL.
5. Wagner, L.E., N.M. Ambe, and D.J. Ding. 1994. Estimating a proctor density curve from intrinsic soil properties. *Transactions of the ASAE*. 37(3):1121-1125.
6. Wagner, L.E. and D.J. Ding. 1993. Stochastic modeling of tillage-induced aggregate breakage. *Transactions of the ASAE*. 36(4):1087-1092.
7. Wagner, L.E., N.M. Ambe, and P. Barnes. 1992. Tillage-induced soil aggregate status as influenced by water content. *Transactions of the ASAE*. 35(2):499-504.

Erosion Submodel

1. Tatarko, J., M. Kucharski, H. Li, H. Li. 2020. PM2.5 and PM10 emissions by abrasion of agricultural soils. *Soil & Tillage Research*. 200:104601.
2. Gonzales, H.B., M.E. Casada, L.J. Hagen, J. Tatarko, R.G. Maghirang, C.J. Barden. 2018. Porosity and drag determination of a single row vegetative barrier (*Maclura pomifera*). *Trans. ASABE*. 61(2): 641-652.
3. Gonzales, H.B., J. Tatarko, M.E. Casada, R.G. Maghirang, L.J. Hagen, C.J. Barden. 2018. Dust reduction efficiency of a single-row vegetative barrier (*Maclura pomifera*). *Trans. ASABE*, 61: 1907-1914.
4. Gonzales, H.B. 2015. Aerodynamics of wind erosion and particle collection through vegetative controls. PhD Dissertation, Kansas State University, Manhattan, Kansas. Available at: <https://hdl.handle.net/2097/20382>. (Accessed August 10, 2020).
5. Li, H., J. Tatarko, M. Kucharski, and Z. Dong. 2015. PM2.5 and PM10 emission from agricultural soils by wind erosion. *Aeolian Research*. 19:171-182.
6. Hagen, L.J. and M.E. Casada. 2013. Effect of canopy leaf distribution on sand transport and abrasion energy. *Aeolian Research*. 10:37-42.
7. Hagen, L.J. 2008. Updating soil surface conditions during wind erosion events using the Wind Erosion Prediction System (WEPS). *Transactions of the ASABE*. 51(1):129-137.
8. Hagen, L.J., S. van Pelt, T.M. Zobeck, and A. Retta. 2007. Dust deposition near an eroding source field. *Earth Surface Processes and Landforms*. 32(2):281-289.

9. Hagen, L.J. 2004. Fine particulates (PM10 and PM2.5) generated by breakage of mobile aggregates during simulated wind erosion. *Transactions of the ASABE*. 47(1):108-112.
10. Vigiak, O., G. Sterk, A. Warren, and L.J. Hagen. 2003. Spatial modeling of wind speed around windbreaks. *CATENA*. 52(3-4):273-288.
11. Hagen, L.J. 2001. Processes of soil erosion by wind. *Annals of Arid Zone*. 40(3):233-250.
12. van Donk, S.J. and E.L. Skidmore. 2001. Field experiments for evaluating wind erosion models. *Annals of Arid Zone*. 40(3):281-302.
13. Hagen, L.J., L.E. Wagner, and E.L. Skidmore. 1999. Analytical solutions and sensitivity analyses for sediment transport in WEPS. *Transactions of the ASAE*. 42(6):1715-1721
14. Hagen, L.J. and D.E. James. 1998. The PM-10 production potential of soils in the Las Vegas Valley of Nevada. *In* S. Basacca, S. Lilligren and K. Newell, eds., *Dust Aerosol, Loess Soils and Global Change*. Washington State Univ. College of Agriculture and Home Economics, Misc. Pub. No. MISC0190, Pullman, WA, pp.45-48.
15. Mirzamostafa, N., L.J. Hagen, L.L. Stone, and E.L. Skidmore. 1998. Soil aggregate and texture effects on suspension components from wind erosion. *Soil Science Society of America Journal*. 62:1351-1361.
16. Zobeck, T.M. and T.W. Popham. 1998. Wind erosion roughness index response to observation spacing and measurement distance. *Soil & Till. Research*. 45:311-324.
17. Zobeck, T.M. and T.W. Popham. 1997. Modification of the wind erosion roughness index by rainfall. *Soil & Tillage Research*. 42:47-61.
18. Stetler, L.D. and K.E. Saxton. 1996. Wind erosion and PM10 emissions from agricultural fields on the Columbia Plateau. *Earth Surface Processes and Landforms*. 21:673-685.
19. Larney, F.J., M.S. Bullock, S.M. McGinn, and D.W. Fryrear. 1995. Quantifying wind erosion on summer fallow in southern Alberta. *Journal of Soil and Water Conservation*. 50(1):91-95.
20. Skidmore, E.L. 1994. Wind erosion. *In* R. Lal, ed., *Soil Erosion Research Methods*, 2nd ed., Soil and Water Conservation Society, Ankeny, IA. pp. 265-293.

21. Skidmore, E.L., L.J. Hagen, D.V. Armbrust, A.A. Durar, D.W. Fryrear, K.N. Potter, L.E. Wagner, and T.M. Zobeck. 1994. Methods for investigating basic processes and conditions affecting wind erosion. *In* R. Lal, ed., *Soil Erosion Research. Methods*, 2nd ed., Soil and Water Conservation. Society, Ankeny, IA. pp. 295-330.
22. Fryrear, D.W. and A. Saleh. 1993. Field wind erosion: Vertical distribution. *Soil Science* 155(4):294-300.
23. Fryrear, D.W. 1992. Measured wind erosion of agricultural lands. *A&WMA Transactions of the Series*, ISSN 1040-8177, No. 22 1:433-439.
24. Hagen, L.J. and D.V. Armbrust. 1992. Aerodynamic roughness and saltation trapping efficiency of tillage ridges. *Transactions of the ASAE*. 35(4):1179-1184.
25. Hagen, L.J., E.L. Skidmore, and A. Saleh. 1992. Wind erosion: Predictions of aggregate abrasion coefficients. *Transactions of the ASAE*. 35(6):1847-1850.
26. Hagen, L.J. 1991. Wind erosion mechanics: Abrasion of aggregated soil. *Transactions of the ASAE*. 34(4):831-837.
27. Vories, E.D. and D.W. Fryrear. 1991. Vertical distribution of wind-eroded soil over a smooth, bare field. *Transactions of the ASAE*. 34(4):1763-1768.
28. Stout, J. 1990. Wind erosion within a simple field. *Transactions of the ASAE*. 33(5):1597-1600.
29. Stout, J.E., and D.W. Fryrear. 1989. Performance of a windblown-particle sampler. *Transactions of the ASAE*. 32(6):2041-2045.
30. Hagen, L.J., E.L. Skidmore, and J.B. Layton. 1988. Wind erosion abrasion: Effects of aggregate moisture. *Transactions of the ASAE*. 31(3):725-728.
31. Fryrear, D.W. 1987. Ridging reduces wind damage to cotton. *Applied Agricultural Research*. 1(5):311-314.
32. Zobeck, T.M. and C.A. Onstad. 1987. Tillage and rainfall effects on random roughness: A review. *Soil & Tillage Research*. 9:1-20.
33. Fryrear, D.W. 1986. A field dust sampler. *Journal of Soil and Water Conservation*. 41(2):117-120.

In accordance with Federal civil rights law and U.S. Department of Agriculture (USDA) civil rights regulations and policies, the USDA, its Agencies, offices, and employees, and institutions participating in or administering USDA programs are prohibited from discriminating based on race, color, national origin, religion, sex, gender identity (including gender expression), sexual orientation, disability, age, marital status, family/parental status, income derived from a public assistance program, political beliefs, or reprisal or retaliation for prior civil rights activity, in any program or activity conducted or funded by USDA (not all bases apply to all programs). Remedies and complaint filing deadlines vary by program or incident.

Persons with disabilities who require alternative means of communication for program information (e.g., Braille, large print, audiotape, American Sign Language, etc.) should contact the responsible Agency or USDA's TARGET Center at (202) 720-2600 (voice and TTY) or contact USDA through the Federal Relay Service at (800) 877-8339. Additionally, program information may be made available in languages other than English.

To file a program discrimination complaint, complete the USDA Program Discrimination Complaint Form, AD-3027, found online at [How to File a Program Discrimination Complaint](#) and at any USDA office or write a letter addressed to USDA and provide in the letter all of the information requested in the form. To request a copy of the complaint form, call (866) 632-9992. Submit your completed form or letter to USDA by: (1) mail: U.S. Department of Agriculture, Office of the Assistant Secretary for Civil Rights, 1400 Independence Avenue, SW, Washington, D.C. 20250-9410; (2) fax: (202) 690-7442; or (3) email: program.intake@usda.gov.

USDA is an equal opportunity provider, employer, and lender.

Use of commercial and trade names does not imply approval or constitute endorsement by USDA.